emc²

18–23 August 2024

4th european mineralogical conference • Dublin, Ireland

# PROGRAMME AND ABSTRACTS

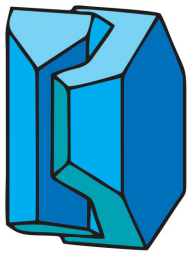

Mineralogical Society of the UK and Ireland

Trinity College Dublin
Coláiste na Tríonóide, Baile Átha Cliath
The University of Dublin

Academic Open Access Publishing
since 1996

Geological Survey
Suirbhéireacht Gheolaíochta
Ireland | Éireann

*An Roinn Comhshaoil, Aeráide agus Cumarsáide*
Department of the Environment, Climate and Communications

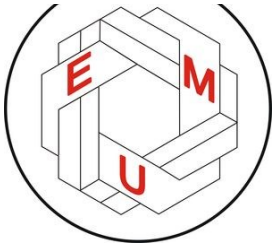

Mineralogical Society
of the UK and Ireland

**CONTENTS**


WELCOME 4
Programme at a Glance (1) 5
Programme at a Glance (2) 7
Sponsors 9
Oral Programme
- Monday, 19th August 11
- Tuesday 20th August 24
- Thursday 22nd August 34
- Friday 23rd August 44

Poster Session A 53
Poster Session B 60
Plenary Lecture Abstracts 66
Public Lecture Abstract 70
Abstracts
- Session 1 71
- Session 2
- Session 3 114
- Session 4 134
- Session 5 142
- Session 6 159
- Session 7 173
- Session 8 185
- Session 9 200
- Session 10 220
- Session 11 233
- Session 12 240
- Session 13 263
- Session 14 274
- Session 16 288
- Session 17 317
- Session 18/19 322
- Session 20 338
- Session 21/23 350
- Session 22 361
- Session 24 373
- Session 25 382
- Session 26/28 394
- Session 27 414
- Session 29 433
- Session 31 448
- Session 32 469
- Session 33 481
- Session 34 492
- Session 35/36 502
- Session 37 517
- Session 38 525

## WELCOME

We are delighted to welcome all delegates, in-person and remote, to Dublin for this the fourth edition of the European Mineralogical Conference (EMC 2024). We hope that we can live up to the high standards set in Frankfurt, Rimini and Cracow.

Thanks to your enthusiasm and willingness to participate, we have a jam-packed programme for you to enjoy. We have sessions numbering up to 38, we have four plenary lectures and a public lecture to which all conference delegates are invited.

In addition, we have an ice-breaker reception and conference banquet to look forward to.

You should have received a copy of the 'Joining Instructions'. If not, it is available from the Conference Staff at registration/help desk. This should answer most if not all of the questions you may have. If it does not, please let conference staff/convenors know.

Our international team of volunteers will be identifiable by their t-shirts. They will be mostly responsible for running the hybrid aspect of our meeting ensuring that our remote participants have a rewarding conference experience.

From the perspective of the Mineralogical Society of the UK and Ireland, our President, Sally Gibson will be present at the conference to greet you. In addition, editors of two of our journals: Roger Mitchell (*Mineralogical Magazine*) and Jon Lloyd (*Geo-Bio Interfaces*) are also going to be in attendance. Make sure to say hello!

Finally, I encourage all delegates to visit the booths of our sponsors/exhibitors and engage with their representatives. Our conference could not run without their support and attendance.

Again, welcome to Baile Atha Cliath (Dublin). Tá súil againn go mbainfidh sibh taitneamh as do bhfuair gcuairt (we hope you enjoy your visit).

**David Chew, Emma Tomlinson**
Trinity College, Dublin

**Russell Rajendra, Kevin Murphy**
Mineralogical Society

**Maciej Jaranowski**
Polish Academy of Sciences, Kraków

## PROGRAMME AT A GLANCE 1

### MONDAY 19TH AUGUST

| Session No. | Session Title | Room |
|---|---|---|
| Session 31: | The Testimony of the Minerals: A Celebration of Edward S. Grew at 80 | Room 1 |
| Session 2: | The Petrology of Accessory Minerals: from the Ubiquitous to the Exotic | Room 2 |
| Session 12: | Understanding the geology and formation of ore deposits - new constraints on the enrichment processes of metals | Room 3 |
| Session 16: | Mineralogy and circular economy | Room 4 |
| Session 27: | All change: subsolidus, melting, volatile and redox reactions in the upper mantle | Room 5 |
| Session 22: | Biominerals and environment | Room 6 |
| Session 20: | Archaeometry: Geoscience-based approaches for studying the human past | Room 7 |
| Session 24 | Volatiles and metals in volcanic systems: constraining their behaviour and processes between magma, gas emissions, and primary ore deposits | Room 7 |

### TUESDAY 20TH AUGUST

| Session No. | Session Title | Room |
|---|---|---|
| Session 1: | Apatite - an accessory mineral with a big footprint in geochemical, environmental, and biological processes | Room 1 |
| Session 26/28: | Origin and composition of $CO_2$-bearing fluids and melts as transport agents between mantle and crust | Room 2 |
| Session 6: | Structure-properties relationships of framework, layered and related minerals | Room 3 |
| Session 31: *continued* | The Testimony of the Minerals: A Celebration of Edward S. Grew at 80 | Room 4 |
| Session 32: | The future of mineralogy, petrology, geochemistry and cosmochemistry - New informatics approaches to harnessing the multidimensionality of complex Earth and planetary systems | Room 4 |
| Session 18/19: | Characterization of gem materials and their geographical/geological origin | Room 5 |
| Session12: | Understanding the geology and formation of ore deposits - new constraints on the enrichment processes of metals | Room 6 |
| Session 5: | Spectroscopic approaches for crystallochemical characterization of minerals and mineral behavior under ambient and non-ambient conditions: application for Earth and Planetary exploration | Room 6 |
| Session 21/23: | Microbial biomineralization/microbes transforming metals | Room 7 |
| Session 16 *continued*: | Mineralogy and circular economy | Room 7 |

**Tuesday, 7.00 pm, Lecture Theatre 1 – Burke**

**Public Lecture: Perspectives on the Energy Transition – Everything starts with a rock**

Dr Karen Hanghøj, Director, British Geological Survey

## THURSDAY 22ND AUGUST

| Session No. | Session Title | Room |
|---|---|---|
| Session 11: | Platinum group elements and minerals | Room 1 |
| Session 7: | Recent challenges and advances in theoretical and experimental mineral physics | Room 1 |
| Session 10: | The role of mafic and ultramafic rocks in carbon capture and storage | Room 2 |
| Session 4: | Partial Melting in Continental Settings | Room 2 |
| Session 25: | One drop at a time: fluid, melt and multiphase inclusions as tools to understand geological processes | Room 3 |
| Session 17: | Innovation and challenges in process mineralogy, geometallurgy and supporting analytical techniques | Room 3 |
| Session 34: | Exploring solar system evolution using meteorites and returned samples | Room 4 |
| Session 26/28 *continued*: | Origin and composition of $CO_2$-bearing fluids and melts as transport agents between mantle and crust | Room 4 |
| Session 14: | Atypical critical metal ores and ore deposits | Room 5 |
| Session 8: | Medical mineralogy and hazardous natural materials. State of the art and future trends | Room 6 |

**Thursday, 7.30-11.00 pm, Croke Park Hogan Banqueting Suite**

**Conference Banquet**

## FRIDAY 23RD AUGUST

| Session No. | Session Title | Room |
|---|---|---|
| Session 3: | Multi-mineral petrochronology of metamorphism and deformation: linking grain-scale processes to lithosphere dynamics | Room 1 |
| Session 29: | Water in the deep (and not so deep) Earth | Room 2 |
| Session 33: | New Minerals, nomenclature, and classification | Room 3 |
| Session 37: | General | Room 3 |
| Session 9: | Crystallisation of carbonates: Mechanisms, kinetics, methods, case studies, and novel applications | Room 4 |
| Session 35/36: | Geoscience outreach in museums and beyond | Room 5 |
| Session 13: | Micro- and nano-mineralogy of critical metals | Room 6 |
| Session 38: | Chemical evolution of sediments and igneous rocks and their implications on Earth's ocean, crust and mantle | Room 6 |

## PROGRAMME AT A GLANCE 2

| Session No. | Session Title | Room |
|---|---|---|
| Session 1: | Apatite - an accessory mineral with a big footprint in geochemical, environmental, and biological processes | Room 4, Tuesday |
| Session 2: | The Petrology of Accessory Minerals: from the Ubiquitous to the Exotic | Room 2, Monday |
| Session 3: | Multi-mineral petrochronology of metamorphism and deformation: linking grain-scale processes to lithosphere dynamics | Room 1, Friday |
| Session 4: | Partial Melting in Continental Settings | Room 2, Thursday |
| Session 5: | Spectroscopic approaches for crystallochemical characterization of minerals and mineral behavior under ambient and non-ambient conditions: application for Earth and Planetary exploration | Room 6, Tuesday |
| Session 6: | Structure-properties relationships of framework, layered and related minerals | Room 3, Tuesday |
| Session 7: | Recent challenges and advances in theoretical and experimental mineral physics | Room 1, Thursday |
| Session 8 | Medical mineralogy and hazardous natural materials. State of the art and future trends | Room 6, Thursday |
| Session 9: | Crystallisation of carbonates: Mechanisms, kinetics, methods, case studies, and novel applications | Room 4, Friday |
| Session 10: | The role of mafic and ultramafic rocks in carbon capture and storage | Room 2, Thursday |
| Session 11: | Platinum group elements and minerals | Room 1, Thursday |
| Session 12: | Understanding the geology and formation of ore deposits – new constraints of the enrichment processes of metals | Room 3, Monday<br>Room 6, Tuesday |
| Session 13: | Micro- and nano-mineralogy of critical metals | Room 6, Friday |
| Session 14: | Atypical critical metal ores and ore deposits | Room 5, Thursday |
| Session 16: | Mineralogy and circular economy | Room 4, Monday<br>Room 7, Tuesday |
| Session 17: | Innovation and challenges in process mineralogy, geometallurgy and supporting analytical techniques | Room 3, Thursday |

| | | |
|---|---|---|
| Session 18/19: | Characterization of gem materials and their geographical/geological origin | Room 5, Tuesday |
| Session 20: | Archaeometry: Geoscience-based approaches for studying the human past | Room 7, Monday |
| Session 21/23: | Microbial biomineralization/microbes transforming metals | Room 7, Tuesday |
| Session 22: | Biominerals and environment | Room 6, Monday |
| Session 24 | Volatiles and metals in volcanic systems: constraining their behaviour and processes between magma, gas emissions, and primary ore deposits | Room 7, Monday |
| Session 25: | One drop at a time: fluid, melt and multiphase inclusions as tools to understand geological processes | Room 3, Thursday |
| Session 26/28: | Origin and composition of $CO_2$-bearing fluids and melts as transport agents between mantle and crust | Room 2, Tuesday<br>Room 4, Thursday |
| Session 27: | All change: subsolidus, melting, volatile and redox reactions in the upper mantle | Room 5, Monday |
| Session 29: | Water in the deep (and not so deep) Earth | Room 2, Friday |
| Session 31: | The Testimony of the Minerals: A Celebration of Edward S. Grew at 80 | Room 1, Monday<br>Room 4, Tuesday |
| Session 32: | 32. The future of mineralogy, petrology, geochemistry and cosmochemistry - New informatics approaches to harnessing the multidimensionality of complex Earth and planetary systems | Room 4, Tuesday |
| Session 33: | New Minerals, nomenclature, and classification | Room 3, Friday |
| Session 34: | Exploring solar system evolution using meteorites and returned samples | Room 4, Thursday |
| Session 35/36: | Geoscience outreach in museums and beyond | Room 5, Friday |
| Session 37: | General | Room 3, Friday |
| Session 38: | Chemical evolution of sediments and igneous rocks and their implications on Earth's ocean, crust and mantle | Room 6, Friday |

# MDPI – Pioneer in Open Access Publishing

MDPI is a publisher of fully peer-reviewed, open access journals with a focus on robust and rapid editorial processes.

Our aim is to ensure that high-quality research is verified and made available to the research community as quickly as possible.

Today, MDPI is a leader in open access publishing with more than 430 journals across all research disciplines. Every article is published under a Creative Commons Attribution License.

mdpi.com

MDPI

Meet us at our booth #3

Sponsoring Journals

minerals

applied sciences

crystals

geosciences

OUR SOLUTIONS
YOUR RESULTS

Enabling you to accurately analyse and characterise materials down to the nanoscale level more rapidly, by combining superior detection and analysis instruments with software platforms that interpret the resulting data in the context of your research.

EDS EBSD MICROSCOPY WDS BEX

OXFORD INSTRUMENTS

The Mineralogical Society of the UK and Ireland
https://www.minersoc.org/

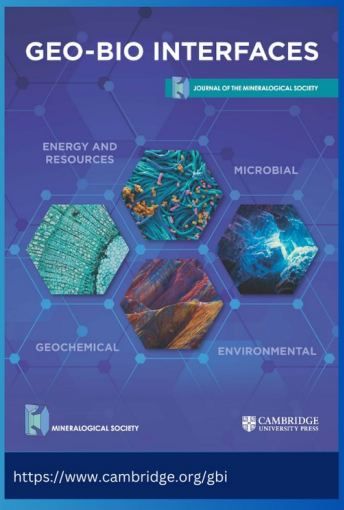

New open access journal for 2024

CAMBRIDGE UNIVERSITY PRESS

Springer

Our business is publishing

We are offering a variety of topical book-series that fit your expertise.

Feel free to browse our program

Have an idea or questions about publishing books?

Feel free to visit us at the meeting or send an email. Let's discuss how we can support your publishing goals!:

- Qiao Shu: *Qiao.Shu@springernature.com*
- Annett Buettner: *Annett.Buettner@springer.com*

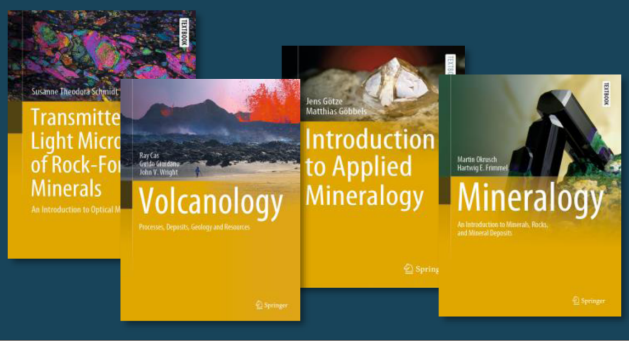


TESCAN

Visit New Website dedicated to Automated Mineralogy

info.tescan.com/natural-resources

Continue here

Elemental Scientific

TELEDYNE PHOTON MACHINES

iCRAG
SFI RESEARCH CENTRE IN APPLIED GEOSCIENCES

Geological Survey
Suirbhéireacht Gheolaíochta
Ireland | Éireann

*An Roinn Comhshaoil, Aeráide agus Cumarsáide*
Department of the Environment, Climate and Communications

Agilent
Trusted Answers

ThermoFisher SCIENTIFIC

| Monday, 19th August | | |
|---|---|---|
| **Lecture Theatre 1 – Burke** | | |
| | | |
| 08.15-08.30 | **Introduction and Welcome** | D. Chew, E. Tomlinson |
| 08.30–09.20 | **PLENARY LECTURE**<br>What's so special about Mössbauer spectroscopy anyway? | C. McCammon |
| 09.20-09.25 | Exhibitor Announcement - MDPI | |
| 09.25-09.30 | Exhibitor Announcement – Agilent | |
| 09.30–09.35 | Exhibitor Announcement – Cambridge University Press | |

| **Lecture Theatre 1 - Burke** | | |
|---|---|---|
| **Session 31. The Testimony of the Minerals: A Celebration of Edward S. Grew at 80** | | |
| Session Chairs: Bob Hazen, Barb Dutrow, Gerhard Franz and Jesse Walters | | |
| 09.40–10.20<br>KEYNOTE | Data-driven discovery in mineralogy: Mineral evolution, mineral ecology, and Edward Grew's legacy | Hazen, Robert M. |
| 10.20-10.40 | Titanium in ultra-high-pressure rocks: Implications of the new minerals wenjiite, $Ti_5Si_3$, maurogemmiite, $Ti_{10}Fe_3O_3$, paulrobinsonite, $Ti_8Fe_4O_2$, and TiFe | Grew, E.*, Xiong, F., Mugnaioli, E., Xu, X., Yang, J., Wirth, R., Franke, P. and Yates, M. |
| 10.40-11.00 | Magnesioqingheiite, a new member of the alluaudite supergroup of minerals | Cámara, F., Chopin, C. and Deldicque, D. |
| 11.00-11.40 | **BREAK** | |
| 11.40-12.00 | $Fe^{3+}GeO_6H_5$ and $Fe^{3+}SnO_6H_5$: hints of novel H behaviour in perovskite-related structures | Welch, M.D., Najorka, J. and Kleppe A.K. |
| 12.00-12.20 | 3D electron diffraction for the crystallo-chemical characterization of micrometric and sub-micrometric mineral phases in mantle inclusions | Mugnaioli, E., Grew, E., Wirth, R., Ferrero, S., Lorenzon, S., Borriello, R., Xiong, F., Xu, X., Yang, J. and Borghini A. |
| 12.20-12.40 | Eudialyte decomposition and the formation of a cuspidine-wöhlerite skarn associated with the Sierra La Vasca complex, Mexico. | Mitchell, R.H. and Rodriguez Vega, A. |
| 12.40-13.00 | Extreme chemical disequilibrium patterns in hydrothermal vein minerals – a case study from Columbian emeralds | Franz, G., Khomenko, V., Schiperski, F., Gernert, U. and Nissen, J. |
| 13.00-14.00 | **LUNCH** | |

| Lecture Theatre 1 – Burke | | |
|---|---|---|
| **Session 31. The Testimony of the Minerals: A Celebration of Edward S. Grew at 80** | | |
| 14.00-14.40 | Mechanisms of uranium incorporation into garnet | Marschall, H.R., Ackermann, C., Millonig, L.J., Kutzschbach, M., Walters, J.B., Schmidt, A., Woodland, A.B. and Hezel D.C. |
| 14.40-15.00 | Garnet in low-temperature metamorphic rocks: far from simple, far from cubic | Cesare, B., Mugnaioli, E., Tacchetto, T., Lorenzon, S., Biagioni, C., Nestola, F., Campomenosi, N. and Della Ventura, G. |
| 15.00-15.20 | A Single-Crystal UV/Vis Spectroscopic Investigation of $^{VIII}Fe^{2+} + {}^{VI}Fe^{3+} \rightarrow {}^{VIII}Fe^{3+} + {}^{VI}Fe^{2+}$ Intervalence Charge Transfer in Aluminosilicate Garnets | Geiger, C.A. and Taran, M.N. |
| 15.20-16.00 | **BREAK** | |
| 16.00–16.20 | Boron-rich fluids in a highly evolved niobium-yttrium-fluorine (NYF) type pegmatite | Anderson, A.J., Scott, M., Wise, M.A. and Boucher, B.M. |
| 16.20–16.40 | Bond-valence constraints for tourmalines with Li and various X-site occupancy | Bačík P. and Ertl, A. |
| 16.40–17.00 | On the limitation of Li in tourmalines with Na and vacancies at the X site | Ertl, A. and Bačík P. |

| Lecture Theatre 2 – Davis | | |
|---|---|---|
| **Session 2. The Petrology of Accessory Minerals: from the Ubiquitous to the Exotic** | | |
| Session Chairs: Callum J Hetherington, Ewa Slaby, Bartosz Budzyń | | |
| 09.40–10.20 KEYNOTE | Exotic radio-minerals in the geological disposal of radioactive waste | Corkhill, C.L., Mottram, L. M., Friskney A. A., Harding L., Kvashnina K., Bazarkina E. F. and Hyatt N.C. |
| 10.20-10.40 | Titanite as a petrogenetic indicator of the magmatic and post-magmatic evolution – Closepet Batholith (Dharwar craton, southern India) | Gmochowska, W., Słaby, E., Gumsley, A., Anczkiewicz, R., Kozub-Budzyń, G.A. and Bhattacharya, S. |
| 10.40-11.00 | Super- and Subsolidus Processes in the Rolvsnes Granodiorite, W Norway, Recorded by Titanite | Drivenes, K., Buisman, I., Coint, N., Huyskens, M, Knies, J, Larsen, R.B. and Sørensen, B.E. |
| 11.00-11.40 | **BREAK** | |
| 11.40-12.00 | Two types of titanites in the Precambrian granitoids of southern Lithuania, East European Craton | Demina, O., Šiliauskas, L., Skridlaitė, G. and Næraa, T. |
| 12.00-12.20 | Bahalda Pluton of Singhbhum Craton (eastern India) - Archean crust undisturbed for three billion years | Gumsley, A., Słaby, E., Dey, S., Chew, D., Gmochowska, W., Wudarska, A., Gumsley, A.P., Szopa, K., Krzykawski, T., Marciniak-Maliszewska, B. and Drakou, F. |
| 12.20-12.40 | Modern-style cold subduction in the Proterozoic: Insights from detrital rutile analysis | Lueder, M., Hermann, J., Pereira, I., Tamblyn, R. and Rubatto, D. |
| 12.40-13.40 | **LUNCH** | |

| Lecture Theatre 2 – Davis | | |
|---|---|---|
| **Session 2. The Petrology of Accessory Minerals: from the Ubiquitous to the Exotic** | | |
| 13.40-14.00 | Crystal mush formed and remobilized within 1 Ma: insights from glomerocryst-loaded silicic laccoliths | Pietranik, A., Słodczyk, E., Pańczyk, M., Schaltegger, U. and Senger, M. |
| 14.00-14.20 | New features on the use of apatite as a petrogenetic indicator in mafic layered intrusions | Kieffer, M.A., Dare, S.A.S., Namur, O. and Mansur E.T. |
| 14.20-14.40 | Lu-Hf, Sm-Nd and U-Pb isotopic decoupling in phosphates from the Central African Copperbelt | Vincent, V.I., Torremans, K., Chew, D.M., Subarkah, D. , Fisher, C.M., Gilbert, S., Farkas, J., Drakou, F. , Doran, A.L., Collins, A.S., Stacey, J., and Hitzman, M. |
| 14.40-15.00 | The geochemical signature and trace-element remobilisation in the Prakovce-Zimná Voda REE-U-Au quartz-vein hydrothermal mineralisation developed in exocontact of rare metal granites, Western Carpathians, Slovakia | Ondrejka, M., Uher, P., Ferenc, Š., Majzlan, J., Bačík, P., Molnárová, A. and Števko, M. |
| 15.00-15.20 | REE mineral assemblage in REE-fluorite masses from Kråkmo pegmatite, Tysfjord-Hamarøy area, Norway | Škoda, R. |
| 15.20-16.00 | **BREAK** | |
| 16.00-16.20 | Nb-Ta minerals in granitic pegmatites: tracers of magmatic to hydrothermal evolution (Western Carpathians, Slovakia) | Uher, P., Ondrejka, M., Bačík, P., Broska, I., Števko, M., Georgiev, S. and Kurylo, S. |
| 16.20-16.40 | Fluorine and bismuth-bearing accessory minerals indicate magma evolution in rare element pegmatites in Embu County, Kenya | Muriungi, N., Büttner, S.H., Glodny, J. and Harder, S. (REMOTE) |

| Lecture Theatre 3 – Synge | | |
|---|---|---|
| **Session 12. Understanding the geology and formation of ore deposits - new constraints on the enrichment processes of metals** | | |
| Session Chairs: Maximilian Korges, Philip Rieger, Hilde Koch, Malte Junge | | |
| 09.40–10.20 KEYNOTE | CARBONATITES: A Key Resource for REE | Giebel, R.J. |
| 10.20-10.40 | Precious and base metal sources and enrichment processes in a proto-arc VMS system | Belgrano, T.M. Milton, J.A., Diamond, L.W., Wolf, R.C. and Teagle, D.A.H |
| 10.40-11.00 | Prerequisites for large SMS deposits along slow-spread mid-ocean ridges: implications for the Polish contract area at the MAR (26–33°N) | Ciążela, J., Kozłowska-Roman, A., Tomczak, M., Elsherif, E., Woźniak, W. and Wojtulek, P. |
| 11.00-11.40 | **BREAK** | |
| 11.40-12.00 | Ore resources on Mars: comparative study of 16 martian meteorites | Fitt, M., Ciążela, J., Mojzsis, S., Lazarov, M., Junge, M., Kaliwooda, M., Jokubauskas, P., Szczęśniewicz, M., Pańczyk, M. and Lei, Ch. |
| 12.00-12.20 | Mineral chemistry and texture of metasomatic mica in halos around the Leinster spodumene pegmatites, Ireland | Geiger, E.J., Brodbeck, M., Menuge J.F. and Nazari-Dehkordi, T. |
| 12.20-12.40 | The Partitioning of Lithium between Granitic Minerals and Melts | Horányi, B., Gaillard, F., Gion A.M., Gloaguen É., Melleton J. and Plunder A. |
| 12.40-13.00 | Examining relationship between Organic matter-rich Cenomanian-Turonian limestones and base metals in the Kebbouch South Pb-Zn deposit (Diapirs zone, Northern Tunisia): insight from LA-ICP-MS trace elements analysis | Jaballah, S., Jemmali, N., Mc Clenaghan, S., Rddad, L. and Henchiri M. (REMOTE) |
| 13.00-14.00 | **LUNCH** | |

| Lecture Theatre 3 – Synge | | |
|---|---|---|
| **Session 12. Understanding the geology and formation of ore deposits - new constraints on the enrichment processes of metals** | | |
| 14.00-14.20 | The role of trisulfur radical ion in the transport of molybdenum by hydrothermal fluids | Kokh, M.A., Wilke, M., Klemme S. and Pokrovski G.S. |
| 14.20-14.40 | Critical raw materials contents in Fe-Mn crusts from Canary Island Seamount Province: controls of the mineralogy and environment. | Marino, E., González, F.J., Medialdea, T., Somoza, L., Lobato, A.B., Reyes, J. and Bellido, E. |
| 14.40-15.00 | The Geyer SW tin skarn deposit, Erzgebirge, Germany: mineral chemistry records changing fluid/rock ratios and metal fluxes | Meyer, N., Burisch, M., Gutzmer, J. and Markl, G. |
| 15.00-15.20 | Overprinting of primary magmatic signature by fluid-driven processes in a F-bearing system: The Mueilha granite (Central Eastern Desert, Egypt) | Michaud, J. A-S, Holtz, F., Kontak, D. J., Goldmann, S., Abu El-Rus, M. |
| 15.20-15.40 | Exploring Critical Element Enrichment Pathways in Black Shales: A Case Study of Türisalu Formation in Estonia | Ndiaye, M., Kallaste, T., Graul, S. and Hints, R. |
| 15.40-16.00 | **BREAK** | |

| Lecture Theatre 4 – Emmett | | |
|---|---|---|
| **Session 16. Mineralogy and circular economy** | | |
| Session Chairs: Daniel Vollprecht, Cyrill Grengg, Mario Tribaudino | | |
| 09.40–10.20 KEYNOTE | The potential of Mineralogy in Circular Economy | Pavese A. |
| 10.20-10.40 | Waelza slag as potential Fe source – a geometallurgical case study to convert waste to resource | Gronen, L., Gondorf, C., Gürsel, G., Feldrappe, V. and Weitkämper, L. |
| 10.40-11.00 | Investigation of a Lithium-Ion-Battery Recycling Slag | Gantz, C., Neumann, A., Roggendorf, H. and Stöber, S. |
| 11.00-11.40 | **BREAK** | |
| 11.40-12.00 | Material/Substance flow analysis of biomass ash in the United Kingdom | Chen, D.T. and Stagemann, J.A. |
| 12.00-12.20 | Why is Raman spectroscopy not used for characterizing MSWI Bottom Ash? – A comparative study of different analytical methods | Kremlicka, T., Demschar, P. and Sedlazeck, K.P. |
| 12.20-12.40 | Reactivity of Municipal Solid Waste Fly Ash into Magnesium Phosphate Cement | Bernasconi, D., Viani, A., Zárybnická, L., Das, G., Bordignon, S., Borfecchia, E., Caviglia, C., Destefanis, E., Gobetto, R. and Pavese, A. |
| 12.40-13.00 | Sustainable binders for soil stabilisation of pavement roads based on recycling of wood biomass ash, municipal and solid waste incineration ash and concrete demolition waste | Pandolfi Balbi, E., Comodi, P., Fastelli, M., Zucchini, A., Cambi, C., Corradini, A., Mantovani, L., Cerni, G., Bou Farhat, H. and Snellings, R. |
| 13.00-14.00 | **LUNCH** | |

| Lecture Theatre 4 – Emmett | | |
|---|---|---|
| **Session 16. Mineralogy and circular economy** | | |
| 14.00-14.20 | Reactive binder components for building materials by thermochemical upcycling of mineral wastes and by-products | Steindl, F., Grengg, C., Rudic, O., Radinger, S., Hussein, A., Weisser, K., Krammer, A., Doschek-Held, K., Ratz, B., Steiner, S., Gatschlhofer, C. and Mittermayr, F. |
| 14.20-14.40 | Resource Optimization in Ceramics: Integrating MMVF Waste for Sustainable Glaze Innovations | Sisti, M., Andreola, F., Barbieri, L., Guidetti, D., Gualtieri, A.F., Fantini, R., Colombo, F. and Arletti, R. |
| 14.40-15.00 | A circular approach in reusing sludges from water potabilization and urban wastewater treatment plants through alkaline activation | Clausi, M., Cofano, V., Medini, M., Occhipinti, R. and Pinto, D. |
| 15.00-15.20 | Recycling detoxified asbestos-cement in several industrial applications: Towards an end of the “asbestos problem”! | Capitani, G., Bernasconi, A., Bianchi, A., Bizjan, B., Conconi, R., Ferrario, S., Ferrini, S., Lavagna, L., Marian, M., Mauri, M., Dalpiaz, M., Pavese, M., Squitieri, L., Tarantino, S.C., Vergani, F. and Viti, C. |
| 15.20-15.40 | Mineral wastes – key players to reach resource efficiency and $CO_2$ neutrality in construction industry | Grengg, C., Rudic, O., Steindl, F., Raic, S., Hussein, A., Radinger, S., Ratz, B., Zögl, I. and Mittermayr, F. |
| 15.40-16.20 | **BREAK** | |

| **Lecture Theatre 5 – O'Cadhain** | | |
|---|---|---|
| **Session 27. All change: subsolidus, melting, volatile and redox reactions in the upper mantle** | | |
| Session Chairs: Emma Tomlinson, Caterina Melai, Michele Rinaldi | | |
| 09.40–10.20 KEYNOTE | The continental subduction factory as a precursor to long-term volatile storage in the lithosphere | Aulbach, S. |
| 10.20-10.40 | The redox state of marble-cake mantle: clues from deeply recycled C-bearing crustal materials | Malaspina, N., Langenhorst, F., Pollok, K., Cerantola, V., Murri, M., Longa, C., Bersani, D. and Montanini A. |
| 10.40-11.00 | Crustal recycling into the mantle: evidence from HSE and Os isotope compositions of Ligurian garnet pyroxenites (N Apennine, Italy) | Montanini, A., Luguet, A., Van Acken and T.R. |
| 11.00-11.40 | **BREAK** | |
| 11.40-12.00 | Insights into molecular hydrogen solubility in $SiO_2$ polymorphs from redox-buffered experiments at subduction conditions | Toffolo, L., Tumiati, S., Confortini, G., and Fumagalli P. |
| 12.00-12.20 | Volatile storage and melting processes in the thermal boundary layer and lower lithosphere beneath continents | Foley, S.F., Chen, C.F., Ezad, I.S. and Jacob, D.E. |
| 12.20-12.40 | A new machine learning single-crystal barometer and thermometer for peridotitic garnet | O'Sullivan, G.J., Janney, P.E., Higgins, O. and Tomlinson, E. |
| 12.40-13.40 | **LUNCH** | |

| Lecture Theatre 5 – O'Cadhain | | |
|---|---|---|
| **Session 27. All change: subsolidus, melting, volatile and redox reactions in the upper mantle** | | |
| 13.40-14.00 | Oxidation state and metasomatism of the lithospheric mantle beneath Letlhakane, Botswana: Insights into effects of metasomatism on the Re-Os system | Rakipov, A., Woodland, A.B., Heckel, C. and Luguet, A. |
| 14.00-14.20 | Slip system-controlled segregation of minor and trace elements in olivine low-angle grain boundaries | Dimitriou, D., Reddy, S., Evans, K., Fougerouse, D., Saxey, D. and Tacchetto, T. |
| 14.20-14.40 | Quantifying the melting conditions of Archean mantle peridotites | Kaekane, J.B., Hoare, B.C. and Tomlinson, E.L. |
| 14.40-15.00 | The melting behaviour of fertile and depleted peridotite at high pressures | Melai, C., Walter, M.J., Yang, J., Rinaldi, M. and Tomlinson, E. |
| 15.00-15.20 | Petrogenesis and indicator mineral chemistry of the K-richterite- and leucite-bearing diamondiferous Kareevlei Kaapvaal lamproite | Qashani, Z., Hashibi, S., Howarth G. H., Janney, P. E., le Roux, P. and Robey, J. |
| 15.20-16.00 | **BREAK** | |
| 16.00–16.20 | The origin of melilitites: an experimental study | Poli, S. and Melluso, L. |
| 16.20–16.40 | Olivine in ultramafic lamprophyres from the Delitzsch carbonatite complex, Saxony, records metasomatic activity in the Central European lithospheric mantle | Hellers, M., Bussweiler, Y., Kühle, T., Wombacher, F., Möckel, F. and Münker, C. |
| 16.40–17.00 | $^{182}W$, $^{142}Nd$, and Pb isotopes indicate entrainment of Hadean recycled crust within the Deccan-Réunion plume | Pakulla, J.J., Tusch, J., Hasenstab-Dübeler, E., Ravindran, A., Jansen, M.W., Leitzke, F.P., Gadpallu, P., Duraiswami, R.A. and Münker, C. |

| Lecture Theatre 6 – Swift | | |
|---|---|---|
| **Session 22. Biominerals and environment** | | |
| Session Chairs: Giovanni De Giudici, Juraj Majzlan | | |
| 09.40–10.20 KEYNOTE | Investigating the physical basis of biomineralization: New insights from polysaccharides | Dove, P.M., Knight, B.M., McCutchin, C.A., Edgar, K.J. and De Yoreo, J.J. |
| 10.20-10.40 | Determination of Great Barrier Reef Ca–C–O mineralogy and trace element systematics using synchrotron X-ray techniques | Missen, O.P., Mills, S.J., Villalobos-Portillo, E.E. and Castillo-Michel, H. (REMOTE) |
| 10.40-11.00 | Durability assessment of microbially-induced calcite precipitation | La Bella, M., Noiriel, C., Schroer, L., Cnudde, V. and Naillon, A. |
| 11.00-11.20 | Copper oxidation zone at Ľubietová (Slovakia) as a combination of ore weathering and biologically-induced mineralization | Majzlan, J.M., Chovan, M., Števko, M., Jeleň, S., Milovská, S. and Milovský, R. |
| 11.20-11.40 | Bioremediation: learning from bio-geo processes in extreme environments | Onnis, P., Kirk, R., Rehmanji M., Falagan, C., Ramos, V., Jennings, E., Newsome, L., Gandy, C., Jarvis, A., Rollinson, G., Medas., D., De Giudici, G. and Hudson-Edwards, K.A. |
| 12.00-12.20 | **BREAK** | |

| Lecture Theatre 7 – Beckett | | |
|---|---|---|
| **Session 20. Archaeometry: Geoscience-based approaches for studying the human past** | | |
| Session Chairs: Sabine Klein, Thomas Rose, Katrin Westner | | |
| 09.40–10.20 KEYNOTE | Trading Egyptian blue – on material provenance and processing | Rodler-Rørbo, A. |
| 10.20-10.40 | Costa Rican gold and copper ore deposits and their potential significance for local pre-Columbian metal artwork production | Westner, K.J., Klein, S., Gassmann, G., Alvarado, G.E., Schäfer, S. and Welk, E. |
| 10.40-11.00 | Improved classification of a large lithic find inventory using pXRF | Burri, T., Eggenberger, U. and Widmer, A.-B. REMOTE |
| 11.00-11.40 | **BREAK** | |
| 11.40-12.00 | Stones and pigments made by Raimondo di Sangro: New findings in Eighteenth Century Naples | Tempesta G., Monno A., de Ceglia F.P., Maraschi A., Rigante E.C.L. and Calvano C.D. |
| 12.00-12.20 | Material analysis of Egyptian and Egyptianising scarabs by XRF and Raman spectroscopy | Aspiotis, S., Bonnerot, O. and Mascia, L. |
| 12.20-12.40 | Weathering of the tuffeau building materials under the microscope. Focus on gypsum | Naumenko-Dèzes, M.O., Beck, K., Wille, G. and Kloppmann, W. |
| 12.40-13.40 | **LUNCH** | |
| 13.40-14.00 | Thermal decomposition of dolomite: Raman spectroscopy as a thermometric tool for the analysis of carbonates in mortar binders | Zöllner, M.T., Dariz, P., Riedel, J. and Schmid, T. |
| 14.00-14.20 | A new digital data infrastructure to make Pb isotope data fit for the future | Rose, T., Greifelt, T., Westner, K. J., Hornschuch, A., Hsu, Y.-K., Wiethoff, H. and Klein, S. |

| Lecture Theatre 7 – Beckett | | |
|---|---|---|
| **Session 24. Volatiles and metals in volcanic systems: constraining their behaviour and processes between magma, gas emissions, and primary ore deposits** | | |
| Session chair: Michael Stock | | |
| 14.00-14.20 | The effect of pressure on sulfur stability in silicate melts | Thomas, R.W. and Wood, B.J. |
| 14.20-14.40 | The effect of water on chlorine solubility in basalts | Rusiecka, Monika, K.* and Wood, B. J. |
| 14.40-15.00 | Speciation equilibria of $H_2O$, HCl, and NaCl in low-density magmatic-hydrothermal fluids | Salomone, F. and Dolejš, D. |
| 15.00-15.20 | The Volatility of Hg at Magmatic Temperatures | Boulliung, J., Wood, B.J. and Mather, T.A. |
| 15.20-16.00 | **BREAK** | |
| 16.00–16.20 | Decoding the $H_2O$ degassing mechanism as a trigger for the explosive eruption of the Lower Laacher See phonolite | Marks, P.L. and Nowak, M. |
| 16.20–16.40 | On the paragenesis of quartz and native copper in the continental flood basalts of Western Volyn (Ukraine) | Batsevych, N.V., Naumko, I.M., Vovk, O.P., Beletska, Yu.A. and Triska, N.T. (REMOTE) |

| Tuesday, 20th August | | |
|---|---|---|
| **Lecture Theatre 1 – Burke** | | |
| 08.25 | Announcements | D. Chew, E. Tomlinson |
| 08.30–09.20 | PLENARY LECTURE<br>Natural Quasicrystals - Novel State of Matter, Open State of Mind | L. Bindi |
| 09.20-09.25 | Exhibitor Announcement – European Journal of Mineralogy | |
| 09.25-09.30 | Exhibitor Announcement – Springer | |
| 09.30–09.35 | Exhibitor Announcement – iCRAG | |

| **Lecture Theatre 1 – Burke** | | |
|---|---|---|
| **Session 1. Apatite - an accessory mineral with a big footprint in geochemical, environmental, and biological processes** | | |
| Session Chairs: David Chew, Alicja Wudarska, Bartosz Puzio | | |
| 09.40-10.00 | Contaminant metal desorption induced by apatite additions to a contaminated sediment | Kaplan, D.I. and Knox, A.S. |
| 10.00-10.20 | Facts and myths about the environmental role of hydroxylpyromorphite $Pb_5(PO_4)_3OH$ | Manecki, M. |
| 10.20-10.40 | Thermodynamic sublattice model for the solid-solution aqueous-solution equilibria in the apatite system $(Ca,Sr)_5[(P,V)O_4]_3(OH,F)$ | Kersten, M. and Kulik, D.A. |
| 10.40-11.00 | Exploring iodine-containing apatite: synthesis, characterization, and environmental implications | Puzio, B. |
| 11.00-11.40 | **BREAK** | |
| 11.40-12.00 | Sequestration of arsenic from aqueous solutions by lead apatites precipitation strategy | Stępień, E. and Manecki, M. |
| 12.00-12.20 | REE recovery from apatite-rich rock containing accessory monazite | Staszel, K., Manecki, M. and Majka, J. |
| 12.20-12.40 | Bat guano-derived hydroxylapatite: an overlooked testimony of past biological activity and a sink of metals in cave environments | Galliano, Y., Bellatreccia, F., Bruxelles, L., De Waele, J. and Carbone, C. |
| 12.40-13.00 | Oxygen isotope study of fluorapatite in conodonts – insights from chemical analyses | Wudarska, A., Wiedenbeck, M., Männik, P., Lepland, A., Hints, O., Wilke, F.D.H., Emsbo, P., Couffignal, F. and Scicchitano, M.R. |
| 13.00-14.00 | **LUNCH** | |

| Lecture Theatre 1 – Burke | | |
|---|---|---|
| **Session 1. Apatite - an accessory mineral with a big footprint in geochemical, environmental, and biological processes** | | |
| 14.00-14.20 | Effects of Phosphorus Concentration on Apatite Trace Element Partitioning and the Formation of Immiscible Phosphorus Rich Melts in the Lower Crust | Manselle, P.A., Foley, S. and Shcheka, S.S. |
| 14.20-14.40 | In-situ laser ablation Lu-Hf apatite geochronology: applications to date mafic intrusions and detrital apatite | Kharkongor, M.B., Glorie, S., Mulder, J., Dare, S., Abersteiner, A., Kirkland, C. and Bedoya, A. |
| 14.40-15.00 | Insights into the tectonometamorphic evolution of the Norwegian Caledonides and Fennoscandia from apatite petrochronology | Piraquive, A., Machado, J.P., Huyskens, M., Redfield, T.F., Schönenberger, J., Jakob, J. and Knies, J. |
| 15.00-15.20 | Pb mobility in Apatite: Exploring chemical influences and its potential for nano-scale petrochronology | Ullah, M., Klötzli, U., Černok, A., Khubab, M. and Goudarzi, M. |
| ~~15.20-16.00 KEYNOTE~~ | ~~Crystal Structure, the foundation for apatite's many and varied uses~~ | ~~Rakovan, J.~~ |
| 16.00-16.20 | **BREAK** | |

| Lecture Theatre 2 – Davis | | |
|---|---|---|
| **Session 26/28. Origin and composition of $CO_2$-bearing fluids and melts as transport agents between mantle and crust** | | |
| Session Chairs: Antonio Acosta-Vigil, Melanie J. Sieber, Luca Toffolo, Jesse Walters | | |
| 09.40–10.00 | Hydrocarbons in the Ivittuut cryolite body, SW Greenland | Szreter, A., Finch, A.A. and Friis, H. |
| 10.00–10.20 | Co-existing fenitizing fluids and carbonatite melts derived from ultramafic lamprophyres | Ezad, I.S., Chattopadhyay, S., Shcheka, S.S., Foley, S.F. and Tuimati, S. |
| 10.20-10.40 | The distribution and generation of Archean to Recent carbonatites | Gibson, S.A., McKenzie, D. and Lebedev, S. |
| 10.40-11.20 KEYNOTE | Distribution of hydrous carbonate liquid in dunite: an experimental study | Fumagalli, P., Capizzi, L., Ildefonse, B., Tumiati S. and Poli S. |
| 11.20-11.40 | **BREAK** | |
| 12.00-12.20 | Bromine partitioning between olivine, orthopyroxene and silicate melt at MORB and OIB source conditions | Joachim-Mrosko, B., Clay, P., Pawley, A., Burgess, R., Ballentine, C.J. and Busemann, H. |
| 12.20-12.40 | Boron isotope fractionation in subducted oceanic crust | Xu, J.D., Marschall, H.R., Gerdes, A., Schmidt, A. and John, T. |
| 12.40-13.00 | Sources of sulphur in pyrite-rich eclogite and omphacitite xenoliths from the Navajo Volcanic Field (USA) | Pohlner, J.E., Aulbach, S., Stern, R.A., Schulze, D.J. and Helmstaedt, H. |

| | | |
|---|---|---|
| 13.00-14.00 | **LUNCH** | |
| 14.00-14.20 | The speciation of sulfur in silicate melts between 1250 and 1050°C | Gorojovsky, L.R. and Wood, B. J. |
| 14.20-14.40 | A key role for paragonite mica in the recycling of volatiles and fluid-mobile elements in subduction zones | De Hoog, J.C.M., Harris, B.H. and Halama, R. |
| 14.40-15.00 | Fluid mobile elements and volatile behaviour during serpentinite dehydration | Asetre, J.H., Alard, O., Ezad, I.S. and Foley, S.F. |
| 15.00-15.40 KEYNOTE | Redox dehydration in subduction zones | Padrón-Navarta, J.A. |
| 15.40 | **BREAK** | |

| Lecture Theatre 3 – Synge | | |
|---|---|---|
| **Session 6. Structure-properties relationships of framework, layered and related minerals** | | |
| Session Chairs: Georgia Cametti, Michael Fischer, Paolo Lotti | | |
| 09.40–10.20 KEYNOTE | The interdependence of structure and redox properties of clay minerals | Neumann, A. |
| 10.20-10.40 | Isotopic fractionation during Sr adsorption on clay minerals: comparison between theoretical calculations and macroscopic experimental data | Blanchard, M., Ferrage, E., Dazas, B., Tertre, E., Isnard, E. and Savoye, S. |
| 10.40-11.00 | Insights from single-crystal X-ray diffuse scattering on disorder in framework and layered minerals | Lepore, G.O., Schmidt, E.M., Morana, M., Minelli, A. and Margheri, S. |
| 11.00-11.20 | **BREAK** | |
| 11.40-12.00 | Exploring pyrochlores: incorporation of Tl and Pb in synthetic microlite and elsmoreite | Margheri, S., Morana, M., Taddei, A., Checchia, S., Goudjil, M., Bindi, L., d'Acapito, F. and Lepore, G.O. |
| 12.00-12.20 | Temperature dependence of elastic properties and damage of natural and man-made silica materials during heating and cooling - From quartz sandstones to silica refractories | Pabst, W., Gregorová, E. and Kotrbová L. |
| 12.20-12.40 | Thermoelastic properties of paracelsian-related danburite and hurlbutite | Münchhalfen, M. and Schreuer, J. |
| 12.40-13.00 | Structure-properties relationships of flexible framework materials | Ross, N.L. |
| 13.00-14.20 | **LUNCH** | |
| 14.00-14.20 | Zeolite for an effective solar protection: understanding the stability unravelling the structure | Arletti, R., Fantini, R., Fischer, M., Brauer, J., Cavalli, R., Argenziano, M. and Mino, L. |
| 14.20-14.40 | Secondary and authigenic phase formation in the 50-year-old tuff from Surtsey (Iceland) | Montesano, G., Rispoli, C., Petrosino, P. and Cappelletti, P. (REMOTE) |

| Lecture Theatre 4 – Emmett | | |
|---|---|---|
| **Session 31. The Testimony of the Minerals: A Celebration of Edward S. Grew at 80 (continued)** | | |
| Session Chairs: Bob Hazen, Barb Dutrow, Gerhard Franz and Jesse Walters | | |
| 09.40–10.00 | Metamorphic and detrital tourmaline in the Archean meta-turbidites of the Beartooth Mountains, MT-WY, USA: Evidence for lithologically diverse Mesoarchean crust | Henry, D.J., Mogk, D.W., Mueller, P.A., Loocke, M. and Dutrow, B.L. |
| 10.00–10.20 | Chromium-bearing tourmalines from the Jack Hills, Western Australia: Implications for Cr mobility | Dutrow, B.L., Henry, D.J., Cavosie, A.J., Valley, J.W. and Loocke, M. |
| 10.20-10.40 | New insights into the origin and metamorphic evolution of the Waldheim prismatine granulite (Saxon Granulite Complex) from pseudosection modeling, B isotopes and nanogranitoids | Rötzler, J., Grew, E.S., Ferrero, S., Borghini, A., Meixner, A., Wilke, M. and Yates, M.G. |
| 10.40-11.00 | A potentially new tourmaline with tetrahedrally coordinated boron | Cempírek, J., Skřápková, L. and Jonsson, E. |
| 11.00-11.20 | CLOSING REMARKS | |
| 11.20 | **BREAK** | |

| Lecture Theatre 4 – Emmett | | |
|---|---|---|
| **Session 32. The future of mineralogy, petrology, geochemistry and cosmochemistry - New informatics approaches to harnessing the multidimensionality of complex Earth and planetary systems** | | |
| Session Chairs: Shaunna Morrison, Anirudh Prabhu, Robert Hazen, Marko Bermanec | | |
| 12.00-12.40 KEYNOTE | Minerals as a case study of a bounded (as opposed to open-ended) evolutionary system – **Mineralogical Society Hallimond Lecture** | Hazen, Robert M. |
| 12.40-13.40 | **LUNCH** | |
| 13.40-14.00 | A data sharing ecosystem for everyday datasets | Hezel, D.C. |
| 14.00-14.20 | Factors of development of lithodynamic processes in the coastal zone of the north-western Black Sea region (Ukraine) | Melnyk E.V., Granova A.K. and Volynska V.O. (REMOTE) |
| 14.20-15.00 KEYNOTE | Predicting unknown mineral occurrences with Mineral Association Analysis and improving our understanding of mineralogy | Prabhu, A., Morrison, S.M., Eleish, A., Fox, P., Golden, J., Downs, R.T., Perry, S., Burns, P.C., Ralph, J. and Hazen R.M. |
| 15.00-15.20 | Using Machine Learning for automatic rock classification | Tamanna, Tamanna, Hezel, D.C., Srivastava, N. and Faber, J. |
| 15.20-15.40 | MinPlot 2.0: A new tool for formula recalculation, visualization, and comparison of large mineral compositional datasets | Walters, J.B. and Gies, N. |
| 15.40 | **BREAK** | |

| **Lecture Theatre 5 – O'Cadhain** | | |
|---|---|---|
| **Session 18/19. Characterisation of gem materials and their geographic/geological origin** | | |
| Session Chairs: Alessandra Costanzo, Isabella Pignatelli, Lee Groat, Giovanna Agrosí | | |
| 09.40–10.00 | Growth history of a multicoloured tourmaline crystal from the Mavuco gem deposit (Alto Ligoña pegmatite district, NE Mozambique) | Altieri, A., Pezzotta, F., Skogby, H., Hålenius, U. and Bosi, F. |
| 10.00–10.20 | Detecting instability of opal: insights from infrared spectroscopy | Chauviré, B., Mevellec, J.-Y., Fereire, J., Thomas, P.S. and Fritsch E. |
| 10.20-10.40 | Trace element composition as indicator of prehnite genesis in igneous rocks from Vis Island, Croatia | Topalović, E., Čobić, A., Paradžik, A., Fiket, Ž., Petrinec, Z., Kniewald, G. and Bermanec, V. |
| 10.40-11.00 | Baltic Amber Inclusions: a multi-analytical approach to their characterization | Costanzo, A., Bojarski, B., Kosior, M., Klikowicz, A. and Cipriani, M. |
| 11.00-11.40 | **BREAK** | |
| 11.40-12.00 | The southern Canadian Cordillera – a new gem district? | Groat, L.A. |
| 12.00-12.40 KEYNOTE | Why I study Diamonds | Harris, J.W. |
| 12.40-13.40 | **LUNCH** | |
| 13.40-14.00 | Diffusivity of Al vacancies in corundum | Jollands, M.C. |
| 14.00-14.20 | Partially crystalline silica varieties in gemmology: The case study of the blue Andean opal | Monico S., Marinoni N., Gatta G.D., Adamo I., Prosperi L., Mácová P. and Ševčík R. |
| 14.20-14.40 | Crystallogenetic features of topaz and beryl from chamber pegmatites of Volyn (Ukrainian shield): elements of similarity and differences | Naumko, I.M., Vovk, O.P. and Nedbailo D.R. (REMOTE) |

| Lecture Theatre 6 – Swift | | |
|---|---|---|
| **Session 12. Understanding the geology and formation of ore deposits - new constraints on the enrichment processes of metals (continued)** | | |
| Session Chairs: Maximilian Korges, Philip Rieger, Hilde Koch, Malte Junge | | |
| 09.40–10.00 | Lithostratigraphic controls on the mineralizing system at the Stonepark Zn-Pb deposit, SW Ireland | Rieger, P., Hitzman, M.W., Susin, V., Holdstock, M., Dunlevy, E. and Melo, A. |
| 10.00–10.20 | Critical-Ireland: Using Irish mafic intrusions as a natural laboratory to understand PGE mineralising processes | Stock, M.J., Beckwith, J., Geifman, E., Morrison, A., Bretagne, E., Carter, E., Cooper, M., Holness, M.B., Andersen, J.C. Ø., Huber, C. and Chew D.M. |
| 10.20-10.40 | Revived interest in dismissed historical Cu-Fe-Zn deposits in the Northern Apennine ophiolites (Italy) | Tagliacollo, L., Bonadiman, C., Saccani, E., Bianchini, G., Brombin, V. and Tassinari, R. |
| 10.40-11.00 | Constraining REE enrichment in alkaline-silicate magmatic systems using new thermodynamic models | Weller, O.M., Holland, T.J.B., Soderman, C.R., Green, E.C.R., Powell, R., Beard, C.D. and Riel, N. |
| 11.00-11.20 | Tracing the fluid and metal sources of the polymetallic mineralization in the Cyclades, Greece, by a multi-isotope study of hydrothermal barite | Wind, S.C., Schneider, D.A., Hannington, M.D. and Fietzke, J. |
| 11.20 | **BREAK** | |

| Lecture Theatre 6 – Swift | | |
|---|---|---|
| **Session 5. Spectroscopic approaches for crystallochemical characterization of minerals and mineral behavior under ambient and non-ambient conditions: application for Earth and Planetary exploration** | | |
| Session chairs: Giovanni B. Andreozzi, Stylianos Aspiotis, Lisa Baratelli, Simone Bernardini, Gioacchino Tempesta | | |
| 12.00-12.20 | The electrical conductivity in riebeckite, $Na_2Fe^{2+}_3Fe^{3+}_2Si_8O_{22}(OH)_2$, and geophysical implication | Bernardini, S., Della Ventura, G. and Mihailova, B. |
| 12.20-12.40 | Developing new web based software for analysing and interpreting spectroscopy in Earth and Environmental Sciences | Byrne, J.M. |
| 12.40-13.00 | From rocks to wastes: Tracing the fate of chromium in nickel mining areas | Delina, R.E.G., Perez, J.P.H., Prieur, D., Scheinost, A.C., Bazarkina, E.F., Kvashnina K.O. and Benning, L.G. |
| 13.00-13.20 | Tc and Pu retention by magnetite – Combining experimental and theoretical techniques | Katheras, A.S., Zimmermann, T., Karalis, K., Krack, M., Scheinost, A.C. and Churakov, S.V. |
| 13.20-14.20 | **LUNCH** | |
| 14.00-14.40 KEYNOTE | Raman spectroscopy to study mineral host-inclusion systems: when experiments meet ab initio simulations | Murri, M., Prencipe, M., Mihailova, B., Angel, R.J. and Alvaro M. |
| 14.40-15.00 | Identification of ferrous hydroxychlorides in rocks and inclusions - hibbingite (γ-$Fe_2(OH)_3Cl$) versus parahibbingite (β-$Fe_2(OH)_3Cl$) | Koděra, P., Majzlan, J., Pollok K., Kiefer, S., Šimko, F., Scholtzová, E., Luptáková, J. and Cawthorn, G. |
| 15.00-15.20 | Spectroscopic and minero-petrological investigation of boninites from Cyprus as potential analogues of Mercury lavas | Landi, A.I., Carli, C., Capaccioni, F., Maturilli, A., Helbert, J., Alemanno, G. and Pratesi, G. |
| 15.20-15.40 | Impact of crystal-to-glass ratio and acquisition geometry on the reflectance spectra of synthetic Nakhlitic rocks. | Pisello, A., Fastelli, M., Baroni, M., Schmitt, B., Beck, P., Zucchini, A., Petrelli, M., Comodi, P. and Perugini, D. |
| 15.40-16.00 | Investigating Uranium in Mineral Systems using M4,5-edge X-ray Adsorption Spectroscopy | Shaw, S, Waters, C, Neill, TS, Morris, K, Baker, ML, Mosselmans, FW, Igatyev, K |
| 16.00 | **BREAK** | |

| Lecture Theatre 7 – Beckett | | |
|---|---|---|
| **Session 21/23. Microbial biomineralization/microbes transforming metals** | | |
| Session Chairs: Casey Bryce, John Moreau, Gerhard Franz | | |
| 09.40–10.20 KEYNOTE | Microbial reduction of metals: mechanisms, environmental implications, and biotechnological applications | Kimber, R.L., Egan Morriss, C., Byrd, N. and Lloyd, J.R. |
| 10.20-10.40 | Phototrophic iron oxidation under complex geochemical conditions | Bryce, C., Nikeleit, V., Byrne, J. and Kappler, A. |
| 10.40-11.00 | A new way for microorganisms mediated by minerals to capture solar energy | Lu, A.H. |
| 11.00-11.40 | **BREAK** | |
| 11.40-12.00 | Geochemical and microbiological reactions controlling siderite in redox active soils | Chen, Z., Perez, J.P.H., Trivedi, C.B., Stammeier, J.A., Gislason, S.R. and Benning, L.G. |
| 12.00-12.20 | On the occurrence of Carboniferous MnFe-oxide stromatolites from the Merdani Formation (Merzouga, Morocco) | Bernardini, S., Abbassi, A., Della Ventura, G., Cipollari, P., Boukili, B., Cavallo, A., Sodo, A. and Cosentino, D. |
| 12.20-12.40 | Geochemical and Microbiological Contribution to Speciation and Mineralogy of Antimony in Subsurface Environment | Kwon, M.J., Zhang, Y., Jang Y., Park, S., Boyanov, M.I., O'Loughlin E.J. and Kenneth, K.M. |
| 12.40-13.00 | Microbial interactions with nuclear waste glass | Thorpe, C.L., Crawford, R., Manifold, G., Boothman, C., Morris, K., Lloyd, J.R., Corkhill, C.L. and Hand, R.J. |
| 13.00-14.00 | **LUNCH** | |

| Lecture Theatre 7 – Beckett | | |
|---|---|---|
| **Session 16. Mineralogy and circular economy (continued)** | | |
| Session Chairs: Daniel Vollprecht, Cyrill Grengg, Mario Tribaudino | | |
| 14.00-14.20 | Nano- to microscale weathering of thallium in ore deposits | Đorđević, T., Kolitsch, U., Stöger-Pollach, M., Schwarz, S. and Majzlan, J. |
| 14.20-14.40 | MinerAll - A new tool for characterizing the utilization potential of mine tailings | Kärenlampi, K., Markkanen, M., Jooshaki, M., Salvador, D., Rama, M. and Kauppila T. |
| 14.40-15.00 | Exploring the use of magnetite to recover critical metals from waste | O'Neill, K.E.B., Biswakarma, J., Crane, R.and Byrne, J.M. |
| 15.00-15.20 | The potential of recycling eggshell waste calcite for the sustainable capture of rare earth elements | Rateau R., Maddin M., Szucs A., Terribili L., Drost K., Guyett. and Rodriguez-Blanco J.D. |
| 15.20-15.40 | A comparison between a flux and TEOS based synthesis of zircon-hafnon solid solutions | Neumann, A., Kahlenberg, V., Lerche, I., Stöber, S. and Pöllmann, H. |
| 15.40 | **BREAK** | |

| Thursday, 22nd August | | |
|---|---|---|
| **Lecture Theatre 1 – Burke** | | |
| 08.25 | Announcements | D. Chew, E. Tomlinson |
| 08.30–09.20 | PLENARY LECTURE<br>Deciphering functional group controls on $CaCO_3$ nucleation using sulfated glycomaterials and insights for natural systems | Dove, P.M.*, Knight, B.M., Mondal, R., Vaissier Welborn, V., Gallagher, C.M.B., Schulz, M., Edgar, K.J. and De Yoreo, J.J. |
| 09.20-09.25 | Exhibitor Announcement – ESI | |
| 09.25-09.30 | Exhibitor Announcement – Teledyne | |
| 09.30–09.35 | Exhibitor Announcement – Oxford Instruments | |

| Lecture Theatre 1 - Burke | | |
|---|---|---|
| **Session 11. Platinum group elements and minerals** | | |
| Session Chairs: Anna Vymazalova, Jussi Liipo | | |
| 09.40–10.20<br>KEYNOTE | Characterisation of PGEs in Minerals Using X-ray Absorption Spectroscopy | Filimonova, O.N., Bikondoa, O., Kutyrev, A., Vymazalova, A. and Wermeille, D. |
| 10.20-10.40 | Platinum-group minerals from Norilsk – a tribute to S.F. Sluzhenikin | Vymazalová, A., Kozlov, V.V., Laufek F., Antsiferova T. and Stanley, C. |
| 10.40-11.20 | **BREAK** | |
| 11.20-11.40 | Platinum-group minerals of the Freetown Intrusion, Sierra Leone | Bowles, J.F.W. and Suárez, S. |
| 11.40-12.00 | Platinum-group minerals and gold particles from the Elbe, Germany | Junge, M., Goldmann, S. and Wotruba, H. |
| 12.00-12.20 | Chemistry in 3D: Deep Learning Fusion of X-ray Datasets for Characterisation of Platinum Group Element Enriched Chromitite | Divers M., Einsle J.F., Dobson K.J., O'Driscoll B., Butcher A.R. and Jolis E.M. |
| 12.20-12.40 | The crystal structures of Pd-Ni arsenides: majakite (PdNiAs) and menshikovite ($Pd_3Ni_2As_3$) | Laufek, F., Vymazalová, A., Chareev, D.A., Grokhovskaya, T.L., Kozlov, V.V. and Plášil, J. |

| Lecture Theatre 1 - Burke | | |
|---|---|---|
| **Session 7. Recent challenges and advances in theoretical and experimental mineral physics** | | |
| Session Chairs: Paola Comodi; Jun Tsuchiya | | |
| 13.40-14.20 KEYNOTE | Single crystals at high-pressures and high-temperatures: constraining planetary interiors | Boffa Ballaran, T., Criniti, G., Kurnosov, A. and Glazyrin, K. |
| 14.20-14.40 | Phase evolution and thermal behavior of hydrous Fe sulfate minerals: coquimbite $AlFe_3(SO_4)_6(H_2O)_{18}$, römerite $Fe^{2+}Fe^{3+}{}_2(SO_4)4(H_2O)_{14}$ and aluminocopiapite $Al^{3+}{}_2/3Fe^{3+}{}_4(SO_4)6(OH)_2(H_2O)_20$ | Abdulina, V., Borisov, A., Siidra, O. and Holzheid, A. |
| 14.40-15.00 | Is newer always better? Not for quartz! | Angel, R.J., Casati, N.P.M., Morana, M., Nestola, F. and Alvaro M. |
| 15.00-15.20 | Sound velocity of metals at megabar pressures, and implications for the Earth's Inner Core | Ohtani, E., Ikuta, D., Fukui, H., Ishikawa, D., Sakamaki, T. and Baron, A.Q.R. |
| 15.20-15.40 | Quantitative mineralogical analysis of drill cuttings by calibrated SEM-EDS mapping and lithofacies classification | Fialips, C.I., Olivier, M., Turpain, M., Pedelabat Lartigau, M., Mouret, N., Bacque, M., Martinez, L. and Teinturier, S. |
| 15.40-16.20 | **BREAK** | |
| 16.20-16.40 | High-pressure elastic behaviour and structural re-arrangement in monazite-type minerals | Lotti, P., Pagliaro, F., Comboni, D., Battiston, T. and Gatta, G.D. |
| 16.40-17.00 | Accurate structure geometry of *P*2/*n* omphacite at variable pressures | Baratelli, L., Merlini, M., Nestola, F., Joseph, B. and Cámara, F. |
| 17.00-17.20 | The phase transitions of $CaSiO_3$ perovskite at extreme conditions | Thomson, A.R., Crichton, W.A., Huang, R., Rosenthal, A. and Brodholt, J.P. |

| Lecture Theatre 2 – Davis | | |
|---|---|---|
| **Session 10. The role of ultramafic rocks in carbon capture and storage** | | |
| Session Chairs: Nadia Malaspina, Andrea Rielli, Alicja Lacinska | | |
| 09.40–10.20 KEYNOTE | Carbon Capture and Mineral Storage: Italy as natural laboratory for its application | Boschi, C., Baneschi I., Castellari, I., Dini, A., Ganci F., Marieni C., Sigfússon B., Snaebjornsdottir S., Trumpy E. and Rielli A. |
| 10.20-10.40 | Geological storage of $CO_2$ in Anatolian ophiolites: Reaction experiments between fluids and ultramafic rock suites at 25-100℃ and 1-125 Bar | Ünal Ercan, H., Gülmez, F., Göçmengil, G., Topkafa, M, Ündül, Ö and Deveci, İ |
| 10.40-11.00 | A mineralogical and geochemical approach to evaluate the redox capacity of basaltic glass and crystals via experiments | Pierozzi, A., Rateau, R., Orlando, A., Borrini, D., Tassi, F. and Rodriguez Blanco, J.D. |
| 11.00-11.40 | **BREAK** | |
| 11.40-12.00 | The potential of Kenyan basalts for carbon sequestration via enhanced rock weathering and geological sequestration with in-situ mineralization | Santos, R.M., Khalidy, R., Basimalla, J., Roobroeck, D., Collinson, J.D., Manga, M. and Marangu, M. |
| 12.00-12.20 | Boosting of the water-mediated mineral carbonation by microwave chemistry | D'Alessio, D., Corti, M., Campione, M., Capitani, G., Lucotti, A., Yivlialin, R., Tommasini, M., Bussetti, G. and Malaspina, N. |
| 12.20-12.40 | Investigation of early signs of mineral weathering through tea bag experiments | Khalidy, R., Jariwala, H., Chiang, Y.W. and Santos, R.M. |
| 12.40-13.40 | **LUNCH** | |

| Lecture Theatre 2 – Davis | | |
|---|---|---|
| **Session 4. Partial Melting in Continental Settings** | | |
| Session Chair: Owen Weller | | |
| 13.40-14.20 KEYNOTE | Partial melting in the continental crust: thermal & chemical consequences of melting reactions and melt–rock interaction | Schorn, S. |
| 14.20-14.40 | A reappraisal of granite emplacement mechanisms, temperatures and time-scales using thermal aureoles: A case study at Ballachulish and Strontian (UK) | Sudholz, Z.J., Copley, A. and Weller O.M. |
| 14.40-15.00 | The evolution of the lower continental crust constrained through high-precision HFSE systematics | Emo, R.B., Münker, C., Pakulla, J.J., Downes, H. and Murphy D.T. |
| 15.00-15.20 | Bimodal Miocene volcanism in the Hegau region (SW Germany) by differentiation of primitive melilititic to nephelinitic magmas towards evolved nosean phonolites | Binder, T., Marks, M.A.W., Friedrichsen, B.-E., Walter, B.F., Wenzel, T. and Markl, G. |
| 15.20-15.40 | Nephelinites from the Northern Tanzania Divergence Zone | Schmitt, F. H., Marks, M. A. W. and Markl, G. |
| 15.40-16.00 | Petrogenesis of mid-Neoproterozoic, ferroan to magnesian charnockites from the Madurai block, India: Constraints from U-Pb geochronology, geochemistry, and geochemical modelling | Kumar, T.A. and Sarkar, T. (REMOTE) |
| 16.00 | **BREAK** | |

| Lecture Theatre 3 – Synge | | |
|---|---|---|
| **Session 25. One drop at a time: fluid, melt and multiphase inclusions as tools to understand geological processes** | | |
| Session Chairs: Silvio Ferrero, Jannick Ingrin, Alessia Borghini, Rosario Esposito, Marta Berkesi | | |
| 09.40–10.20 KEYNOTE | Sulphur speciation in magmatic fluids: facts and artefacts | Farsang, S. and Zajacz, Z. |
| 10.20-10.40 | Vibrational properties of oxidized sulfur species in hydrothermal fluids from ab initio molecular dynamics simulations and Raman spectroscopy | Jahn, S. and Schmidt, C. |
| 10.40-11.00 | Unraveling metasomatic agent in the upper mantle xenoliths – via 3D Raman mapping of complex inclusions: a case study from the Styrian Basin (W-Carpathian Pannonian Region) | Myovela, J.L., Aradi, L.E., Spránitz, T., Hegedűs, M., Taracsák Z., Konečný, P., Kovács, J. and Berkesi, M. |
| 11.00-11.40 | **BREAK** | |
| 11.40-12.00 | Halogen impact on Raman water bands at high pressure and the implications for salinity estimations in fluid inclusions | Grützner, T. and Bureau, H. |
| 12.00-12.20 | The origin of deep $CO_2$-rich fluids in the Pannonian Basin: combined stable isotope study on fluid inclusions and dissolved gases in groundwaters | Spránitz, T., Lange, T.P, Hencz, M., Porkoláb, K., Kővágó, Á., Gelencsér, O., Créon, L., Palcsu, L., Tóth, Á., Erőss, E., Rouchon, V., Szabó, Cs., Kovács, I.J., Török, K. and Berkesi, M. |
| 12.20-12.40 | Pfaffenbergite and “phase 430” new minerals in crystallized melt inclusions | Lorenzon, S., Ferrero, S., Borriello, R., Mugnaioli, E., Borghini, A., Fuchs, R., Wirth, R., Schreiber, A. and Grew, E.S. |
| 12.40-13.40 | **LUNCH** | |
| 13.40-14.00 | The evolution of large ilmenite-hosted melt inclusions: evidence of spinodal and binodal dissociation of kimberlitic carbonated silicate melt | Büttner, S.H., Marima, E. and Rocholl, A. |
| 14.00-14.20 | Innovative methodology for exploration of marine hydrocarbon deposits according to geological predictive criteria and mineralogical-thermobarogeochemical prospecting signs (using the example of the Black Sea) | Yanko, V., Naumko, I., Kadurin, V., Zinchuk, I., Dikol, O. and Kadurin, S. |

| Lecture Theatre 3 – Synge | | |
|---|---|---|
| **Session 17. Innovation and challenges in process mineralogy, geometallurgy and supporting analytical techniques** | | |
| Session Chairs: Patrick Krolop, Marek Dosbaba, Dominique Brising | | |
| 14.20-14.40 | Tailor Made High throughput Infrastructure for Synchrotron X-Ray Diffraction Measurement of Mineralogical Samples | Chang, C.S.T., Stenman, J., Casati, N., Grünzweig, C. and Wagner, M. |
| 14.40-15.00 | Understanding the impact of platy morphology on the floatability of gangue minerals from X-ray diffraction patterns: A talc case study | Dodoo, D., Webster, N A.S., Forbes, L., Usher, S.P., Scales, P.J. and Stickland, A.D. |
| 15.00-15.20 | Automated mineralogy as a part of complex analytical workflows | Dosbaba, M. |
| 15.20-15.40 | Analytical Advancements in Mining: High-Throughput Synchrotron Radiation X-Ray Powder Diffraction for Sustainable Efficiency | Stenman, J., Kortelainen, L., Chang, C.S.T., Casati, N., Grünzweig C. and Wagner, M. |

| Lecture Theatre 4 - Emmett | | |
|---|---|---|
| **Session 34. Exploring Solar System evolution using meteorites and returned samples** | | |
| Session Chairs: Martin Lee, Beverley Tkalcec | | |
| 09.40–10.20 KEYNOTE | Applying Correlative Microscopy in Solar System Science | Daly, L. |
| 10.20-10.40 | 3D electron diffraction and nanotexture analysis of impactites | Gemmi, M., Parlanti, P., Mugnaioli, E., Campanale, F., Folco L. and Veron M. |
| 10.40-11.00 | The functional chemistry of Ryugu organic matter investigated by high spatial resolution electron energy loss spectroscopy | Vollmer, C., Lier, J., Kepaptsoglou, D., Mosberg, A. B. and Ramasse Q. M. |
| 11.00-11.40 | **BREAK** | |
| 11.40-12.00 | Rare-earth element distribution in particles from asteroid Bennu measured by high-energy synchrotron X-ray fluorescence | Tkalcec, B., DePauw, E., Bazi, B., Vekemans, B., Tack, P., Baert, T., Herthogs, J., Vincze, L., Falkenberg, G., Garrevoet, J., Di Michiel, M., Burghammer, M., Connolly Jr., H. C., Lauretta, D. S. and Brenker, F. E. |
| 12.00-12.20 | Water/rock interaction within primitive asteroids explored using the Solar System's oldest calcite, aragonite, and dolomite | Lee, M.R. and Griffin, S. |
| 12.20-12.40 | Expanded Insights into Martian Mineralogy: Updated Analysis of Gale Crater's Mineral Composition via CheMin Crystal Chemical Investigations | Morrison, S.M., Downs, R.T., Bristow, T.F., Rampe, E.B., Blake, D.F., Vaniman, D.T. Achilles, C.N., Hazen, R.M., Eleish, A., Prabhu, A., Ming, D.W., Yen, A,S., Treiman, A.H., Morris, R.V., Chipera, S.J., Craig, P.I., Tu, V.M., Meusburger, J.M., Castle, N., Sarrazin, P.C. and Des Marais, D.J. |
| 12.40-13.40 | **LUNCH** | |

| Lecture Theatre 4 - Emmett | | |
|---|---|---|
| **Session 26/28. Origin and composition of $CO_2$-bearing fluids and melts as transport agents between mantle and crust** | | |
| Session Chairs: Antonio Acosta-Vigil, Melanie J. Sieber, Luca Toffolo, Jesse Walters | | |
| 13.40-14.00 | Recycled Carbonate-Bearing Silicate Sediments in the Sources of Circum-Mediterranean K-Rich Lavas: Evidence from Mg-Zn Isotopic Decoupling | Shu, Z.T., Liu,S-A., Prelević, D., Wang, Y., Foley, S.F., Cvetković, V. and Li, S. |
| 14.00-14.20 | Reaction experiments constrain the products of crust-mantle interaction during the subduction of the continental crust | Borghini, A., Borghini, G., Ferrero, S. and Toffolo, L. |
| 14.20-14.40 | Quantification of global $H_2O$ transport capacity in subduction zones by hydrous phases and nominally anhydrous minerals | Gies, N.B., Hermann, J. and Konrad-Schmolke, M. |
| 14.40-15.00 | Investigating the diffusion of noble gases in the polymorphs of $SiO_2$: the decisive role of the structure | Figowy, S., Mohn, C.E. and Caracas, R. |
| 15.20-16.00 | Formation of hydrocarbons favored by high pressure at subduction zone conditions | Daniel, I., Huang, J. and Sverjensky D.A. |
| 15.20-16.00 KEYNOTE | The migration of methane-hydrogen-rich fluids may trigger seismic failure in subduction zones at forearc depths | Giuntoli F., Menegon L., Siron G., Cognigni F., Leroux L., Compagnoni R., Rossi M. and Vitale Brovarone A. |
| 16.00 | **BREAK** | |

| **Lecture Theatre 5 – O'Cadhain** | | |
|---|---|---|
| **Session 14. Atypical critical metal ores and ore deposits** | | |
| Session Chairs: Sean McClenaghan, Vladimir Khomenko, Daria Chernysh, Iryna Lunova (remote) | | |
| 09.40–10.00 | Maghemite, a new key player to consider in the study of Ni-Co laterite deposits | Domínguez-Carretero, D., Proenza, J.A., Villanova-de-Benavent, C. and Galí, S. (REMOTE) |
| 10.00-10.20 | REE potential in sedimentary apatite: Delve deeper with microanalytics | Graul, S., Monchal, V., Rateau, R., Joosu, L., Moilanen, M., Ndiaye, M. and Hints, R. |
| 10.20-10.40 | Graphitic sedimentary marbles and Sc-V-Y-REE bearing trace element minerals in carbonatite veins, The Aird, Scotland | Heptinstall, E.A, Parnell, J., Schito, A., Boyce, A.J. Armstrong, J.G.T., Muirhead. and Still, J. |
| 10.40-11.00 | Genthelvite from Be-polymetallic ores of Perga deposit, NW Ukraine: Crystal chemistry, zonation and evolution during metasomatic events | Khomenko, V., Kurzbach, M. and Nissen, J. |
| 11.00-11.40 | **BREAK** | |
| 11.40-12.00 | Interactions of carbonatitic fluids with crustal wall rocks: A field-based study of Ondurakorume, NW Namibia | Ladisic, A., Marks, M.A.W., Walter, B.F., Giebel, R.J., Markl, G. |
| 12.00-12.20 | Crystallochemical features of feldspars from Perga deposit (Ukraine) | Lunova, I.M., Lunov, Ye.S., Khomenko, V.M. and Nissen, J. (REMOTE) |
| 12.20-12.40 | The distribution of lithium pegmatites in Eastern Europe and Northern Asia | Naumenko, O. and Dèzes, M. (REMOTE) |
| 12.40-13.00 | Kaolin diapirs of the Ukrainian shield - potential resource of titanium mineral deposits | Komliev, O.O., Remezova, O.O., Spytsia, R.O., Okholina, T.V., Vasylenko, S.P. and Komlieva, M.O. (REMOTE) |
| 13.00-14.00 | **LUNCH** | |
| 14.00-14.40 KEYNOTE | Crustal wall-rock assimilation and metasomatism caused by carbonatites – key processes for HFSE enrichment? | Walter, B.F., Marks, M.A.W., Giebel, R.J. and Markl, G. |
| 14.40-15.00 | Germanium in sphalerite, but how and why? Atomistic simulations have an answer | Haghi, A. and Jahn, S. (REMOTE) |

| Lecture Theatre 6 – Swift | | |
|---|---|---|
| **Session 8. Medical mineralogy and hazardous natural materials. State of the art and future trends** | | |
| Session Chairs: Alessandro F. Gualtieri, Alessandro Pacella, Jasmine Rita Petriglieri | | |
| 09.40–10.20 KEYNOTE | Mesothelioma and asbestos-induced carcinogenesis | Felley-Bosco, Emanuela |
| 10.20-10.40 | Slag dust from Kabwe (Zambia) - one of the most polluted places on Earth: mineralogy and contaminant bioaccessibility | Ettler, V., Mihaljevic, M., Drahota, P., Kribek B. and Nyambe, I. |
| 10.40-11.00 | Health effects of cristobalite dusts: comparison of their physico-chemical and mineralogical features in different occupational settings | Di Benedetto, F., Belluso, E., Capella, S., Ardit, M., Baroni, T. and Capacci, F. |
| 11.00-11.40 | **BREAK** | |
| 11.40-12.00 | Simulations of temperature-driven release of arsenic from minerals and phases related to wildfires | Tuhý, M., Ettler, V., Rohovec, J., Matoušková, Š. and Drahota, P. |
| 12.00-12.20 | Effects of Simulated Lung Fluids (SLFs) on zeolite fibres through real-time SC-XRD investigations | Giordani, M., Cametti, G. and Mattioli, M. |
| 12.20-12.40 | Geological occurrence, morphological characterisation, and toxicological evaluation of erionite in New Zealand | Patel, J.P., Brook, M.S, Scarfi, S., Mirata, S., Almonti, V., Hamilton, A., Kah, M. and Gualtieri, A.F. |
| 12.40-13.40 | **LUNCH** | |

| | | |
|---|---|---|
| 13.40-14.00 | Surveying airborne fibrous zeolite deposition on leaf surfaces around sedimentary and volcanic zeolitic outcrops in New Zealand | Fan, W., Dirks, N, K ., Hamilton, A ., Patel, P. J. and Salmond, A. J. |
| 14.00-14.20 | A Mobile Sampling Method for Monitoring Vehicle-Induced Dispersion of Elongate Mineral Particles from Unsealed Gravel Roads | Chen, S., Dirks, K., Costello, S., Chen, G. and Salmond, J. |
| 14.20-14.40 | Correlating dissolution kinetics, surface alterations, and chemical reactivity: new insights into the mechanisms of mineral fibre toxicity | Di Carlo, M.C., Ballirano, P., Bloise, A., Campopiano, A., Fantauzzi, M., Montereali, M.R., Nardi, E., Petriglieri, J.R., Rossi, A., Tomatis, M., Turci, F. and Pacella, A. |

| Friday, 23rd August | | |
|---|---|---|
| **Lecture Theatre 1 – Burke** | | |
| 08.25 | **Announcements** | D. Chew, E. Tomlinson |
| 08.30–09.20 | PLENARY LECTURE<br>Ultramafic geosystems: a source of metallic elements to the environment | Kierczak, J.R. |
| 09.20-09.25 | Exhibitor Announcement – Tescan | |
| 09.25-09.30 | Exhibitor Announcement – Geological Survey of Ireland | |
| 09.30–09.35 | Exhibitor Announcement – Thermo Scientific | |

| **Lecture Theatre 1 – Burke** | | |
|---|---|---|
| **Session 3. Multi-mineral petrochronology of metamorphism and deformation: linking grain-scale processes to lithosphere dynamics** | | |
| Session Chairs: Stefania Corvó, Mattia Bonazzi, Hugo van Schrojenstein Lantman, Aratz Beranoaguirre | | |
| 09.40–10.20<br>KEYNOTE | Nanorocks in zircon from metamorphic rocks: a new frontier in the investigation of melt evolution | Tedeschi, M., Ferrero, S., Wunder, B., Hermann, J., Borghini, A., Pettke, T., Lanari, P., Paiva-Silva, P., Rubatto, D., Van Schijndel, V., Tollan, P. and O'Brien, P.J. |
| 10.20-10.40 | Multi-method geochronology (Lu–Hf, Rb–Sr and U–Pb) to unravel the evolution of complex metamorphic terranes | Bedoya, A., Glorie, S., Hand, M., Kirkland, C.L., Kelsey, D.E., He, X.F. and Kharkongor, M.B. |
| 10.40-11.00 | Raman spectroscopy as a tool to measure stress-induced deformation in garnet | Gilio, M., Toffol, G., Pennacchioni, G., Campomenosi, N., Mihailova, B. and Alvaro M. |
| 11.00-11.20 | **BREAK** | |
| 11.40-12.00 | Applying U-Pb calcite direct dating by LA-ICP-MS mapping to investigate shallow crustal deformation histories in Ireland | Monchal, V., Drost, K. and Chew, D. |
| 12.00-12.20 | Decoupled behaviour of $^{40}Ar$ and $^{87}Sr/^{86}Sr$ during deformation of metamorphic white mica in a high-pressure marble | Barnes, C.J., Zack, T., Bukała, M., Dubosq, R., Camacho, A., Gerdes, A. and Rösel, D. |
| 12.20-12.40 | Coupling apatite and zircon petrochronology to reveal (U)HP to retrograde metamorphic evolutions of eclogites from the Scandinavian Caledonides | Jaranowski, M., Budzyń, B., Barnes, C., Majka, J., Sláma, J., Kozub-Budzyń G.A., Roddatis, V., Wirth, R., Schreiber, A. and Kośmińska K. |
| 12.40-13.40 | **LUNCH** | |

| Lecture Theatre 1 – Burke | | |
|---|---|---|
| **Session 3. Multi-mineral petrochronology of metamorphism and deformation: linking grain-scale processes to lithosphere dynamics** | | |
| 13.40-14.00 | How is a polyepisodic magmatic and metamorphic history recorded in zircon (Aar and Gotthard units, central Alpine basement) | Schaltegger, U., Noroña, E., Ulyanov A., Berger, A., Abrecht, J., Spikings R. and Wiederkehr, M. |
| 14.00-14.20 | Dating metamorphism and metasomatism in the mantle | Kotková, J., Čopjaková, R., Millonig, L.J., Marschall, H., Gerdes, A., Kutzschbach, M. |
| 14.20-14.40 | Stabilization hiatus of the North China Craton revealed by microsampling garnet geochronology on single xenoliths | Du, K.Y., Cheng, H. and Yang, R.Y. |
| 14.40-15.00 | Petrochronology reveals extremely slow cooling of granulites in the Dniester–Bouh Domain, Ukrainian Shield | Shumlyanskyy, L., Wilde, S.A., Johnson, T., Alfing J., Jourdan, F., Lisna, I.M., Stepanyuk, L.M. |
| 15.00-15.20 | Shear zone petrochronology | Villa, I.M. (REMOTE) |
| 15.20 | **BREAK** | |

| Lecture Theatre 2 – Davis | | |
|---|---|---|
| **Session 29. Water in the deep (and not so deep) Earth** | | |
| Session Chairs: Sylvie Demouchy, Davide Novella, Michael Jollands | | |
| 09.40–10.20 KEYNOTE | H storage and speciation within the deep Earth | Bolfan-Casanova, N. |
| 10.20-10.40 | Latest advances in hydrogen analysis in Nominally Anhydrous Minerals and Diamonds with ERDA | Bureau, H., Khodja, H. and Estève I. |
| 10.40-11.00 | Hydrogen defect evolution in natural diamonds and implications for the preservation of primordial hydrogen | Day, M.C., Pamato, M.G., Jollands, M.C., Novella, D., Nestola, F. and Dovesi, R. |
| 11.00-11.20 | **BREAK** | |
| 11.40-12.00 | The spectroscopy of hydride in perovskites | Palfey, W.R., Hwang, S.J., Goddard, W.A. III and Rossman, G.R. |
| 12.00-12.20 | High resolution transmission electron microscopy of a defect in hydrous forsterite | Miyajima, N., Purevjav, N. and Withers, A.C. (REMOTE) |
| 12.20-12.40 | The coesite-stishovite transition of hydrous, Al-bearing $SiO_2$: An in situ synchrotron X-ray study | Koch-Müller, M., Lathe, C., Wunder B., Appelt, O., Bhat, S., Farla, R., Roddatis, V., Schreiber, A. and Wirth, R. |

| | | |
|---|---|---|
| 12.40-13.00 | **LUNCH** | |
| 13.40-14.00 | Spin transition links water and ferric iron in Earth's lower mantle | Buchen, J.B., Pardo, O.S., Dobrosavljevic, V.V., Sturhahn, W., Ishii, T., Chariton, S., Greenberg, E., Toellner, T.S. and Jackson, J.M. |
| 14.00-14.20 | Water partitioning between nominally anhydrous minerals and hydrous minerals, and the role of water in subducting slabs | Ohtani, E. and Ishii, I. |
| 14.20-14.40 | The importance of carbon to the formation and composition of silicates during mantle metasomatism | Rinaldi, M.R., Mikhail, S., Sverjensky, D.A. and Kalita, J. |
| 14.40-15.00 | Phase relations in the system MgO-$CO_2$-$H_2O$: dehydration of brucite and melting of brucite and magnesite in subduction zones | Sieber, M.J., Reichmann, H-J, Farla, R. and Koch-Müller, M. |
| 15.00-15.20 | Using quartz to constrain the formation conditions of pegmatites | Bermanec, M., Pettke, T. and Hermann J., Nils Gies |
| 15.20 | **BREAK** | |

| Lecture Theatre 3 – Synge | | |
|---|---|---|
| **Session 33. New Minerals, nomenclature, and classification** | | |
| 09.40–10.20 KEYNOTE | Mineral species and mineral substances according to the IMA-CNMNC | Bosi, F. |
| 10.20-10.40 | Two new super-reduced phases from Luobusa chromitite: jianmuite, $ZrTi^{4+}Ti^{3+}5Al_3O_{16}$, and a $Ti^{3+}$-rich calcium amphibole, $\square Ca2(Mg_2Ti^{3+}_3)(Si_5Al_3)O_{22}(OH)_2$ | Borriello, R., Xiong, F., Ma, C., Lorenzon, S., Mugnaioli, E., Yang, J., Xu, X. and Grew, E.S. |
| 10.40-11.00 | Crystal chemistry of Belgian ardennites | Depret, M., Hatert, F., Blondieau, M., Puccio, S., Dal Bo, F., Erambert, M. and Bomal, F. |
| 11.00-11.40 | **BREAK** | |
| 11.40-12.00 | "Ferroåkermanite" - a potentially new mineral from kirschsteinite-bearing paralava from Hatrurim Complex, Israel | Juroszek, R., Krüger, B., Galuskin, E. and Vapnik Ye. |
| 12.00-12.20 | Crystal chemistry and nomenclature of the triphylite group of phosphates | Hatert, F., Lyalina, L.M. and Selivanova, E.A. |
| 12.20-12.40 | New data for undescribed uranyl minerals supporting the CURIES database | Olds, Travis A., Spano, Tyler L., McDonnell, Marshall, Smith, Robert, Niedziela, Jennifer L., Miskowiec, Andrew, Kapsimalis, Roger, and Shields, Ashley E. |
| 12.40-13.20 | **LUNCH** | |
| 13.20-13.40 | Cr - analogue of hydrocalumite – a potentially new mineral from the Negev Desert, Hatrurim Complex, Israel | Skrzyńska, K., Stachowicz, M., Juroszek, R., Pakhomova, A., Galuskina, I., Vapnik, Y., and Galuskin, E. |
| 13.40-14.00 | The puzzle of an allanite-like epidote mineral from Malmkärra, Sweden: Toward the new (OH)-analogue of dollaseite-(Ce) | Taddei, A., Bindi, L., Bonazzi, P., Casey, P., Förster, H.-J., Holtstam, D. and Karlsson, A. |

| Lecture Theatre 3 – Synge | | |
|---|---|---|
| **Session 37. General** | | |
| Session Chairs: D. Chew, E. Tomlinson | | |
| 14.00-14.20 | Sulphide to sulphate reactions: sulphur degassing and its effects on platinum group mineral enrichment, Rum layered intrusion, NW Scotland | Pentland, K., Einsle, J.F. and Divers, M. |
| 14.20-14.40 | Age and evolution of the Raibl carbonate-hosted Zn-Pb deposit (NE Italy) | Velicogna M., Beltrame M., Barago N., De Min, A., Lenaz, D., Nimis, P., Chiaradia, M., Venier, M., Chelle-Michou, C. and Tavazzani, L. |
| 14.40-15.00 | Cation and anion ordering in synthetic lepidolites and lithian muscovites: Influence of the OH/F and Li/Al ratios on the mica formation studied by NMR spectroscopy and X-ray diffraction | Fechtelkord, M., Marler, B. and Sulcek, L. |
| 15.00-15.20 | New pathway to enhance crop and vegetable yield and quality through the infrared emissive characteristics of minerals | Du, Y.F., Ding, H. and Lu, A.H. |
| 15.20-15.40 | Investigation of Microscale Pores in Terrestrial Mineral Coatings and Their Photoreactive Traits | Ge, X., Ding, H.R., Wang, C.Q. and Lu, A.H. |
| 15.40 | **BREAK** | |

| Lecture Theatre 4 – Emmett | | |
|---|---|---|
| **Session 9. Crystallisation of carbonates: Mechanisms, kinetics, methods, case studies, and novel applications** | | |
| Session Chairs: Remi Rateau, Gabrielle Stockmann, Juan Diego Rodriguez-Blanco | | |
| 09.40–10.20 KEYNOTE | Tracing Fluids in the Early Solar System Using Carbonates | King, A. J., Schofield, P. F. and Russell, S.S. |
| 10.20-10.40 | Carbonation hardening of cements produced from recycled concrete fines | Neubauer, J., Villmow, S. and Mielkau, A. |
| 10.40-11.00 | Utilising mining waste materials for carbon sequestration: A novel laboratory method assessing enhanced weathering potential in an arctic climate | Mouchos, E., Pearce, S., Shiimi, R., Savage, W., Buckley, L., Lim, C., Brussee, O. and Ronne, E. |
| 11.00-11.40 | **BREAK** | |
| 11.40-12.00 | Crystallisation of Carbonates to Make Anthropogenic 'Rocks' | MacDonald, J.M. |
| 12.00-12.20 | Uncovering the Mineralogy and Metal Concentrations in Metal Processing Wastes: A data-driven microstructural approach | Hilderman, R.X., Einsel, J.F. and MacDonald, J.M. |
| 12.20-12.40 | Accelerated Carbonation from Aqueous Ca/Mg Hydroxide Systems to Hazardous Waste Incinerator Residues | Wehrung, Quentin, Pastero, Linda, Bernasconi, Davide, Cotellucci, Andrea, Bruno, Marco, Destefanis, Enrico, Caviglia, Caterina, Cavagna, Simona and Pavese, Alessandro |
| 12.40-13.40 | **LUNCH** | |
| 13.40-14.00 | On the growth of ikaite ($CaCO_3x6H_2O$) in the presence of phosphate | Strohm, S.B., Saldi, G.D., Mavromatis, V., Schmahl, W.W., Jordan, G. |
| 14.00-14.20 | Transformation of ikaite into less hydrated $CaCO_3$ minerals – from in-situ observations of tufa columns, Ikka Fjord and IceLab-RAMAN experiments | Stockmann, G.J., Peternell, M., Konrad-Schmolke, M. and Rasmussen M.B. |
| 14.20-14.40 | The Key Role of Sulfate in the Conversion of Aragonite into Calcite | Forjanes, P., Astilleros, J.M. and Fernández-Díaz L. |
| 15.20 | **BREAK** | |

| Lecture Theatre 5 – O'Cadhain | | |
|---|---|---|
| **Session 35/36. Geoscience outreach in museums and beyond** | | |
| Session Chairs: Mike Rumsey, Bastian Joachim-Mrosko, Melanie Kaliwoda | | |
| 09.40–10.20 KEYNOTE | More than cool curiosities: using social media for mineral science communication to engage on geoscience topics | Anderson, E.B. |
| 10.20-10.40 | Geo-education in Colombia enhanced by student chapters | Cramer, T.H., Bonilla-Perez, A. and Sanchez Novoa, D.F.C. |
| 10.40-11.00 | Crystal magic – Fascinating tourmaline crystals with fantastic inner worlds 20 years of optimization of a successful traveling exhibition | Rustemeyer, Paul |
| 11.00-11.40 | **BREAK** | |
| 11.40-12.00 | Guided tours and projects for children and young people at the Museum Mineralogia Munich on the topic of "How was the moon actually formed and what can we learn from meteorites? | Kaliwoda, M., Junge, M., Hentschel, F. and Schmahl, W.W. |
| 12.00-12.20 | Roots of removal: Kenyan basalt rock and mineral sculpture art and the carbon removals odyssey – The Mutuma Marangu Sculpture and Art Collection's "TMMSAC" "RoR BRAMSA Movement" Exhibition | Marangu, M., Collinson, J.D., Blackbourn, G., Roobroeck, D., Manga, M., Kimani, F., Santos, R.M., Motondi Oroo, G.,, Kenyanya Oendo, P., Okeyo Mbera, R., Tabule Ogao, J.A., Kombo, C.D., Ong'esa, E. (REMOTE) |
| 12.20-12.40 | 'Finding the Smoking Gun: A cross-museum survey of pyrite | Royce, K. |
| 12.40-13.40 | **LUNCH** | |
| 13.40-14.00 | An extensive powder diffraction study of 'hydrocerussite-type' mineral specimens in museum collections from the Mendip Hills area, Somerset, UK | Rumsey, M.S. and Najorka, J. |
| 14.00-14.20 | Seeking a Specific Mineral for Research? An Introduction to Mineral Specimen Data Infrastructure and MinExt for Darwin Core | Walcott, R.C. and Norton, B. |
| 14.20-14.40 | GeoSpecify, a Collection Management Platform for Geological Objects | Beach, J. H., Burri, T. and Fitzsimons, G. |
| 14.40-15.00 | Count Vargas Bedemar, J.W. v. Goethe and the Mineralogical Collection in Jena | Kreher-Hartmann, B. |

| Lecture Theatre 6 – Swift | | |
|---|---|---|
| **Session 13. Micro- and nano-mineralogy of critical metals** | | |
| Session Chairs: José María González Jiménez, Malte Junge, | | |
| 09.40–10.00 KEYNOTE | High resolution mineralogy and petrography of Mn-oxyhydroxides from Caribbean Ni-Co laterite deposits | Villanova-de-Benavent, C., Nieto, F., Domènech, C., Domínguez-Carretero, D., Galí, S and Proenza, J.A. |
| 10.00-10.20 | Understanding the origine and formation process of goethite framboids in Cretaceous sedimentary rocks by nanoscale analysis | Ohfuji, H., Konishi, S. and Yamamoto, K. |
| 10.20-10.40 | Nanoscale characterization of (Ca-REE) fluorcarbonates | Conconi, R., Capitani, G. Gentile, P. and Fumagalli, P. |
| 10.40-11.00 | A FIB-HRTEM investigation of (Co-Ni-Cu)-rich Fe sulfides in basic rocks from the internal zones of the Betic Cordillera | Ferreira, A. R., González-Jiménez, J.M., Yesares, L., Blanco-Quintero, I. F., Piña, R., Gervilla, F. |
| 11.00-11.40 | **BREAK** | |
| 11.40-12.00 | Nanomaterials as agents for critical metal transfer in magmatic and hydrothermal ore systems | González-Jiménez, J.M., Schettino, E., Cano, N., González-Pérez, I., Ferreira, A., Yesares, L., Marchesi, C., Camprubí, A., Thomas N. Kerestedjian, Gervilla, F. |
| 12.00-12.20 | Dual mineralogical sitting of the critical metals Nb-Ta-Sn-W in rutile | Bermejo-López, D., González-Jiménez, J.M., Ortega, L., Castiñeiras, P., Crespo, E. |
| 12.20-12.40 | Microstructures of the Platinum Group Mineral nuggets in the Finnish Lapland | Soukka, T., Tuisku, P., Moilanen, M., Jaskari M., Ranta, J-P |
| 12.40 | **LUNCH** | |

| Lecture Theatre 6 – Swift | | |
|---|---|---|
| **Session 38. Chemical evolution of sediments and igneous rocks and their implications on Earth's ocean, crust, and mantle** | | |
| Session Chairs: Josua J. Pakulla, Jaganmoy Jodder | | |
| 13.40-14.20 KEYNOTE | Aleutian Arc Initiation: Tectonic and climatic implications | Hoernle, K., Jicha, B., Portnyagin, M., Hauff, F., Höfig, T., Yogodzinski, G., Timm, C., Guillong, M., Berndt, C., Savelyev, D., Bezard, R., Baranov, B. |
| 14.20-14.40 | Palaeozoic continental growth: The Köli Nappe Complex, Swedish Caledonides: Iapetus Ocean arc magmatism, rifting and accretion to Baltica | Cuthbert, S.J., Ziemniak, G. and Walczak K., Carter, I. |
| 14.40-15.00 | Constraints on Iceland mantle sources from μ182W, Sr-Pb isotopes and trace elements | Kallnik, N., Armstrong, C., Pakulla, J., Halldórsson, S.A., Fischer-Gödde, M., Hasenstab-Dübeler, E., Münker, C. |
| 15.00-15.20 | Significance of W isotope anomalies in early Earth rocks | Münker, C., Fischer-Gödde, M. , Tusch, J. and Hoffmann, J.E. |
| 15.20-15.40 | Mechanisms of pyrite formation in marine sediments and implications for isotope fractionation in the presence of trace elements | Rabone, J., Blanchard, M., Aufort, J. and Le Pape, P. |
| 15.40 | **BREAK** | |

# POSTER SESSION A

| | | |
|---|---|---|
| **Session 1: Apatite - an accessory mineral with a big footprint in geochemical, environmental, and biological processes** | | |
| 1 | Geochemistry and U-Pb isotopic characteristics of apatite from the Loch Roag xenolith suite | Badenszki, E., Buczko, D., Matusiak-Małek, M., Upton B.G.J. and Daly, J.S. |
| 2 | Potential of mineralogical characterization for improvement of calcium phosphate cements and their hydration | Goetz-Neunhoeffer, F. and Hurle, K. |
| 3 | Apatite as a provenance indicator for I-, S- and A-type granites and mafic intrusions | Kieffer, M.A., Dare, S.A.S. and Gendron, M. |
| 4 | Controlled calcium phosphate precipitation via vapor diffusion sitting drop methodology in bacterial cellulose template | Navarro-Zabarburú, Isabel, Zavaleta, Amparo Iris, Calderón-Toledo, Susana and Alvarez-Lloret, Pedro REMOTE |
| 5 | Raman spectroscopic analysis of the As-bearing apatite supergroup minerals from pyrometamorphic xenoliths of the Upper Chegem Caldera, Russia | Środek, D., Dulski, M., and Balin, K. |
| **Session 2: The Petrology of Accessory Minerals: from the Ubiquitous to the Exotic** | | |
| 6 | Mineralogy and petrography of Fe-Mn phosphates from the Varuträsk pegmatite, Sweden | Depret, M., Hatert, F., Bomal, F., Langhof, J. and Holtstam D. |
| 7 | Precipitation of Aluminum phosphate sulphates minerals: an experimental challenge for an environmental question | Galán-Abellán, A.B., Fernández-Barrenechea, J. and Mateo-Martí, E. |
| 8 | Titanite breakdown to rutile during the albitization of a granitoid: Natural observations and experimental results | Gumsley, A., Harlov, D., Juroszek, R., Marciniak-Maliszewska, B., Jokubauskas, P. and Gerdjikov, I. |
| 9 | Accessory zircon as an petrogenetic indicator in granitoid rocks of the Vepor pluton (Fabova hoľa, Western Carpathians, Slovakia) | Molnárová A., Ondrejka M., Putiš M. and Nemec O. |
| 10 | Garnet and vesuvianite – geochronological tools for U-Pb dating of skarns deposits | Stifeeva, M.V., Salnikova, E.B. and Kotov A.B. |
| 11 | Geological-paleooceanographic models of early Oligocene (Maikop) sedimentation in the Crimean-Caucasian segment of the Paratethys | Kokhan, O.M., Hnidets V.P., Hryhorchuk, K.H., Rever, A.O. |
| 12 | Accessory minerals as fingerprints of complex processes in volcanogenic massive sulphide systems | Volkmann, R., Van Schijndel, V., Codeço, M.S., Relvas, J.M.R.S. and Gleeson, S.A. |
| 13 | Apatite texture characteristics in the Per Geijer Iron Oxide-Apatite-REE deposit, Sweden | Zanderink, B.B.G., Krolop, P., Miles A-J. and Seifert T. |

| | | |
|---|---|---|
| 14 | Fluorine-enriched skarn association: an evidence for fluid/rock interaction during pegmatite emplacement | Vassileva, R.D., Georgieva, S., Grozdev, V., Cempírek, J. and Škoda R. |
| 15 | Trace-element signatures of rare-metal accessory mineralization in Smilovene area pegmatites, Sredna Gora Mountain, Bulgaria | Georgieva S., Vassileva R.D., Grozdev V., Cempírek J., Škoda R. and Stefanova E. |
| 16 | Monazite-(Ce) as a product of experimentally induced hydrothermal transformation of chevkinite-(Ce) | Urbanik , K.M., Bagiński, B. , Macdonald, R., Harlov, D.E. |
| 17 | Hexavalent Cr removal by carbonates and iron oxyhydroxides minerals in the presence the absence of organic chelating agents | Maftei, A.M., Lupu, A., Bulai, G., Rateau, R., Rodriguez Blanco, J.D. and Brinza L. |
| **Session 5: Spectroscopic approaches for crystallochemical characterization of minerals and mineral behavior under ambient and non-ambient conditions: application for Earth and Planetary exploration** | | |
| 18 | Cation order in omphacitic clinopyroxenes: implications for Raman elastic geothermobarometry | Baratelli, L., Cámara, F., Mihailova, B., Murri, M. and Alvaro, M. |
| 19 | Ultra-Thin Sections - Illuminating the Spectra of Highly Opaque Minerals | Funaro, E.J., Palfey, W.R., Park, A., Schlom, D.G., and Rossman G.R. |
| 20 | Raman Spectroscopy as an important tool for the study of lunar, Martian and other meteorites and for the collection of new Raman databases for future space missions | Kaliwoda, M., Zuncke, J. and Drozdovsky, I. |
| 21 | Basaltic glasses in the lower mantle: trace elements as markers of local structure changes | Kovalskii, G., Rosa, A.D., Mathon, O., Morgenroth, W., Morard, G., Pennacchioni, L., Wilke, M. |
| 22 | Hydrothermal reduction of hematite to magnetite by molecular hydrogen | Ostertag-Henning, C. and Plümper, O. |
| 23 | Elasticity of dolomite-ankerite solid solutions | Pennacchioni, L., Speziale, S. and Winkler, B. |
| 24 | Spectroscopic feature on gem quality topaz from different localities after E-beam treatment | Tempesta, G., Elettivo G.S., Vadrucci, M. and Agrosì, G. |
| **Session 6: Structure-properties relationships of framework, layered and related minerals** | | |
| 25 | Pressure-driven crystal structure and fluids interaction in erionite-group zeolites | Battiston, T., Lotti, P., Comboni, D. and Gatta, G.D. |
| 26 | Adsorption of chlorinated ethenes in hydrophobic zeolites studied by molecular simulations | Fischer, M. |
| 27 | Atomistic modelling of the Tschermak and di-trioctahedral substitutions in chlorite | Françoise, M., Dubacq, B., Bourdelle, F. and Verlaguet, A. |
| 28 | A multi-method, in situ temperature-dependent investigation of the taranakite-francoanellite phase transition | Galliano, Y., Bellatreccia, F., Campomenosi, N. and Carbone, C. |

| | | |
|---|---|---|
| 29 | Evolution of Young's modulus and changes in phase composition of kaolins and CaO-$Al_2O_3$-$SiO_2$ ceramics during heating and sintering | Gregorová, E., Pabst, W. and Šimonová, P. |
| **Session 12: Understanding the geology and formation of ore deposits - new constraints on the enrichment processes of metals** | | |
| 30 | Ore Minerals and Metal Migration within the Oceanic Crust of the Central Sudetic Ophiolite, Poland | Elsherif E.A., Ciążela, J., Wojtulek, P., Strauß, H., Kuhn, Th., Pańczyk, M., Woźniak, W., Fitt, M., Stawikowski, W., Kukula, A. and Łuszczek, K. |
| 31 | Mineral chemistry of hydrothermal biotite from Na-Ca-K-silicate alteration associated with the Elatsite porphyry copper deposit, Bulgaria | Georgieva, H., Nedialkov, R., Stefanova, E. and Milenkov, G. |
| 32 | Mineralogical and chemical characterization of tungstenite | Goldmann, S., Wegorzewski, A.V. and Fuchs, S. |
| 33 | Paragenetic sequence and mineral chemistry of the scheelite skarn deposit of Monleón (Salamanca, NW Spain) | Posado-De Castro, J., Timón-Sánchez, S.M., Fernández-Fernández, A., Llorens-González, T., Díez-Montes, A. and Sánchez-García, T. |
| 34 | Tetrahedrite group minerals and their weathering products from Chamrousse, Belledonne Range, Western Alps, France | Skrzyńska, K. and Müller, H. |
| 35 | Major and trace element composition of tourmaline in the Kaustinen Li-pegmatites: implications for melt origin and evolution | Tvauri, A.V., Kalliomäki, H., Law, K.A., Ranta, E. and Rämö, O.T. |
| **Session 16: Mineralogy and circular economy** | | |
| 36 | 13X Zeolite for Rare Earth Elements separation: evaluation of the selectivity and structural characterization | Colombo, F., Fantini, R., Di Renzo, F., Confalonieri, G., Sobczyk, M., Malavasi, G., Malferrari, D., and Arletti R. |
| 37 | Sustainable Solutions: Utilizing Extractive Waste in Ceramic Tile Production | Fantini, R., Bernini, M., Conte, S., Zanelli, C., Dondi, M., Gualtieri, A.F. and Arletti, R. |
| 38 | Preliminary results of the effect of nano Mg-Al layered double hydroxides (LDHs) on chemical and physical properties of cement paste | Fastelli, M., Vivani, R., Sassi, P., Speranzini, E., Schoubben, A., Di Michele, A., Zucchini, A., Mortaro, F. and Comodi, P. |
| 39 | Quantitative mineralogy and potential recovery of metal(loid)s from copper metallurgical slag | Lichovník, M., Ettler, V., Aiglsperger, T., Kříbek, B. and Mapani, B. |

| | | |
|---|---|---|
| 40 | Forgotten wastes in coastal areas – tackling risks through mineralogy | Onnis, P., Ramos, V., Riley, A.L., Gandy, C., Jennings, E., Nannoni, A., Rollinson, G.K., Burke, I., Byrne, P.A., Crane, R., Jarvis, A., Mayes, W.M. and Hudson-Edwards, K.A. |
| 41 | Wood biomass ash: a possible alternative to free lime and cement as stabilizing agent in clayey subgrade of road pavement | Pandolfi Balbi, E., Corradini, A., Cambi, C., Fastelli, M., Cerni, G., Cotana, F., Zucchini, A. and Comodi, P. |
| 42 | Mechanisms of metallurgical slag dissolution deciphered from contact and non-contact bioleaching experiments | Potysz, A. |
| 43 | Mineral characterization of the mining residues from the Golpejas mine (Spain): Implications for processing | San Cipriano-Mata, A., Llorens-González, T., Fernández-Fernández, A., Timón-Sánchez, S.M., Díez-Montes, A., Sánchez-García, T., López-Moro, F.J., Menéndez-Aguado, J.M. and Medina-Pierres, J. |
| 44 | Resource Optimization in Ceramics: Integrating MMVF Waste for Sustainable Glaze Innovations | Sisti, M., Andreola, F., Barbieri, L., Guidetti, D., Gualtieri, A.F., Fantini, R., Colombo, F. and Arletti, R. |
| 45 | Bottom ashes from MSWI in/and ceramics: a higher value reuse of waste | Bernasconi, A., Mantovani, L. and Tribaudino, M. |
| 46 | Properties of low sulfur leached spodumene as supplementary cementitious material in ordinary portland cement | Woskowski, J., Neumann, A. and Stöber, S. |
| **Session 18/19: Characterization of gem materials and their geographical/geological origin** | | |
| 47 | Crystal chemistry of tourmalines from Mozambican pegmatites | Bomal, F., Hatert, F., Philippo, S. and Guennou, M. |
| 48 | "Aquafire" beryl from Brazil: inclusions used as a tool to define a new variety of aquamarine | Costanzo, A., Laurs, B., Campos-Venuti, M., Cipriani, M. |
| 49 | Causes of colour changes in tourmalines from different pegmatite provinces after e-beam irradiation and thermal treatments | Rizzo, F., Tempesta, G., Bosi, F., Vadrucci, M., Skogby, H. and Agrosì, G. |
| 50 | Bohemian garnet from the Dolní Olešnice deposit and its enigmatic source | Škoda, R., Čopjaková, R., Štefanová, M., Millonig, L.J., Kotková, J. and Gerdes, A. |
| 51 | Light elements in gem quality topaz from different localities | Tempesta, G., Elettivo, G.S. and Agrosì, G. |
| 52 | Microdiamonds from the Zelenyi Yar Neogene placer (the Ukrainian Shield) | Vyshnevskyi, O.A., Kvasnytsya, V.M., Wirth, R., Schreiber, A. and Pavlyuk, V.M. |

| | | |
|---|---|---|
| 53 | Study of color mechanisms in natural and treated elbaite crystals | Luppi, R., Pezzotta, F., Skogby, H., Hålenius, U., Altieri, A., Tempesta, G., Vadrucci, M., Sejkora, J., and Bosi F. |
| **Session 20: Archaeometry: Geoscience-based approaches for studying the human past** | | |
| 54 | The study of alabaster art objects in the cultural heritage of Ukraine using isotopic analysis methods | Naumenko, U., Dezes, M., Borniak, U., Lipinska, A. and Kloppmann, W. |
| 55 | Shipshape and Bristol fashion: Characterising the corrosion of the SS Great Britain | Rothwell, K.A., Grahamslaw, N., Grigg, A.R.C. and Byrne, J.M. |
| 56 | Archaeometric study of the stone tesserae from the "A grandi fiori" mosaic in the archaeological site of Casignana (Reggio Calabria, Italy) | Barca, D., Zicarelli, M.A., La Russa, M.F., Musella, M., Randazzo, L., Ricca M. and Rovella, N. |
| 57 | Characterization of chert by X-ray diffraction, infrared and Raman spectroscopy to identify Moganite | De Uribe-Zorita, M., Álvarez-Lloret, P., and Marcos, C. |
| **Session 21/23: Microbial biomineralization/microbes transforming metal** | | |
| 58 | Bi-Te-S biomineralization in the Volyn biota (Ukraine) | Franz, G., Wirth, R., Schreiber, A. and Khomenko, V. |
| 59 | Conundrum of anhydrite formation at surface conditions | Wehmann, N., Lenting, C., Stawski, T.M. , Agudo Jácome, L., Heim, C. and Jahn, S. |
| 60 | Nanoscale biosignatures in native copper from the Wadi Tayin dunite, Oman | Tenuta, S., Evans, K.A., Reddy, S.R., Rickard, W.D.A. and Saxey, D.W. |
| 61 | Metabolically-versatile Hg methylators: their implications and origins | Moreau, J.W., Lin, H., Gionfriddo, C.M., Moody, E.R.R. and Williams, T.A. |
| **Session 22: Biominerals and environment** | | |
| 62 | Skeletal disorder in laying hens: a study at macro and microscale of hen bone structure and composition | Cappelli, C., Rodríguez-Navarro, A.B., Álvarez-Lloret, P., Enrich, T., Duclos, M.J. and Gautron, J. |
| 63 | Heavy Metal Adsorption from Mining Tailings Leachate Using Shell-Based Adsorbent: Characterization and Kinetic/Isotherm Studies | Fernández-González, A., Ayala-Espina, J. and Fernández-Pérez, B. |
| 64 | High concentrations of $Mg^{2+}$ decelerates the abiotic decomposition of ATP at elevated temperatures | Moeller, C., Testemale, D., Kokh, M., Schmidt, C., Guyot, F. and Wilke, M. |
| 65 | The fate of Arsenic in the Carletti Spring System (Viterbo, Italy): a XAS speciation study | Montegrossi, G.*, Venturi, S., Baroni, T., Casentini, B., Fazi, S., Costagliola, P., Rimondi, V., Piacentini, A., Mazzoni, C., Di Benedetto, F. |

| | | |
|---|---|---|
| 66 | Rare Earth Elements concentration in riverbed biominerals: Potential tool for Bio-Based Extraction | Sedda, L., Naitza, S., Fancello, D., Medas, D., Musu, E., Onnis, P., Podda, F. and De Giudici, G. |
| 67 | Mineralogical controls on the persistence and preservation of DNA | Singh, V.V., Kimber, R.L., Kumar, N., and Kraemer, S.M. |
| 68 | Bioprospecting for Sustainable Mineral Management in Arsenic-Rich Environments | Tomlinson, N.O., Schofield, P.F., Jungblut, A.D., Hodson, M.E. and Santos, A.L. |
| **Session 24: Volatiles and metals in volcanic systems: constraining their behaviour and processes between magma, gas emissions, and primary ore deposits** | | |
| 69 | Petro-geochemical and environmental significance of SO2 emissions during a basaltic eruption in Central America: the case-study of the December 29th, 2013 eruption of the San Miguel volcano, El Salvador | Hernández De la Cruz, A., Gimeno, D., Conde Jacobo, V., Olmos Guevara, R., Barahona Escoto, F., Hernández Martínez, M. and Novembre, D. |
| 70 | Control of effusive and explosive eruptions of Ciomadul volcano: constraints by apatite composition | Hajdu Krisztina, Lukács Réka, Popa Razvan-Gabriel, Allaz Julien Marius, Pánczél-Oelberg Emese, Cserép Barbara, Bachmann Olivier, Pál-Molnár Elemér, Seghedi Ioan and Harangi Szabolcs |
| 71 | Potentially harmful elements released by volcanic ash of the 2021 Tajogaite eruption (Cumbre Vieja, La Palma Island, Spain): Implications for human health | Ruggieri, F., Forte, G., Bocca, B., Casentini, B., Petrangeli, A.B., Salatino, A. and Gimeno, D. |
| **Session 26/28: Volatiles and metals in volcanic systems: constraining their behaviour and processes between magma, gas emissions, and primary ore deposits** | | |
| 72 | Unravelling the redox conditions during deserpentinization through sulphide mineral assemblages | Cristóbal, L.S., Padrón-Navarta, J.A. and Garrido, C.J. |
| 73 | Decompression-driven crystallization of carbonate-silicate melts trapped in garnet in orogenic peridotite (NW Bohemian Massif) | Haifler, J., Kotková, J. and Čopjaková, R. |
| 74 | High-pressure metasomatism and carbonation of metaserpentinites during deformation at the subduction interface | López Sánchez-Vizcaíno, V., Padrón-Navarta, J.A., Menzel, M.D. and Garrido, C.J. |
| **Session 27: All change: subsolidus, melting, volatile and redox reactions in the upper mantle** | | |
| 75 | Sheared peridotites: linking deformation and hydrous metasomatism to the onset of craton destabilization | Heckel, C., Woodland, A.B., Gibson, S.A., Linckens, J., Withers, A.C., Seitz, H.-M. and Ludwig, T. |
| 76 | Complex metasomatic history and exhumation-driven refertilization of subcontinental lithospheric mantle beneath Central Europe | Kubeš, M., Čopjaková, R., Kotková, J., Ackerman, L., Haifler, J. and Škoda, R. |

| | | |
|---|---|---|
| 77 | The thickness of the Archean Kaapvaal cratonic lithosphere at 1.6 Ga | Qashani, Z., O'Sullivan, G.J., Janney, P.E. and Tomlinson E.L. |
| 78 | An improved thermodynamic model for the melting evolution of a peridotite up to 12 GPa | Rinaldi, M.R., Green, E.C.R., Melai, C. and Tomlinson, E.L. |
| 79 | Compositional effects of komatiite-peridotite reaction | Tomlinson, E.L., Rinaldi, M. and Melai, C. |
| **Session 31: The Testimony of the Minerals: A Celebration of Edward S. Grew at 80** | | |
| 80 | Rubinite from Hatrurim Complex, Israel | Galuskin, E.V., Galuskina, I.O., Kusz, J. and Vapnik, Ye. |
| 81 | Niobium garnets | Galuskina, I.O., Galuskin, E.V. and Vapnik, Ye. |
| 82 | Coesite and florencite hidden in garnet and revealed by micro-Raman spectroscopy | Ghignone, S., Borghini, A., Boero, F., Prencipe, M., Bruno, M., Gilio, M., Scaramuzzo, E., Manzotti, P. |
| 83 | Garnet, not always the archetypal cubic mineral | Lorenzon, S., Mugnaioli, E., Biagioni, C., Nestola, F. and Cesare, B. |
| **Session 32: The future of mineralogy, petrology, geochemistry and cosmochemistry - New informatics approaches to harnessing the multidimensionality of complex Earth and planetary systems** | | |
| 84 | mineralML: Leveraging Machine Learning for Probabilistic Classification in Earth and Planetary Minerals | Shi, S., Wieser, P., Toth, N., Antoshechkina, P. and Lehnert, K. |
| 85 | Using average mineral properties to study trends through mineral evolution | Bermanec, M.*, Hazen, Robert M. and Ma, Xiaogang |
| 86 | Lithodynamic processes on the north-western shelf of the Black Sea of Ukraine | Granova, A.K., Melnik, E.V. and Volynska, V.O. |
| 87 | Characterizing Earth's biosignatures via mineral network analysis | Morrison, S.M., Prabhu, A., Hazen, R.M., Wong, M.L. and Eleish, A. |
| 88 | The German National Research Data Infrastructure for the Earth System Sciences (NFDI4Earth) | Bernard, L., Braesicke, P., Bertelmann, R., Frickenhaus, S., Gödde, H., Keßler, C., Lorenz, S., Mahecha, M., Marschall, H.R., Hezel, D.C., Nage, W.E., Reichstein, M., Sester, M., Thiemann, H., Weiland, C., Wytzisk-Arens, A., Xu, J.D.*, NFDI Consortium Earth System Sciences |
| 89 | Geochemical Modelling Beyond Mars – from Asteroid Belt to Kuiper Belt | Yoosefdoost, A., Bakhshoodeh, R. and Santos, R.M. |

# POSTER SESSION B

| | | |
|---|---|---|
| **Session 3: Multi-mineral petrochronology of metamorphism and deformation: linking grain-scale processes to lithosphere dynamics** | | |
| 1 | Ultrafast geological processes on the grain scale | Angel, R.J., Campomensoi, N., Gilio, M., Morana, M. and Alvaro M. |
| 2 | Potentiality of titanite petrochronological tool in the metacarbonate system | Bonazzi, M., Simonetti, M., Maino, M. and Langone, A. |
| 3 | Coupled petrochronology on monazite and titanite to unravel the evolution of shear zones from mid- to low continental crust (Ivrea-Verbano Zone; Italy). | Corvò, S., Maino M., Bonazzi, M., Simonetti M., Montemagni, C., Zanchetta, S., Piazolo, S., Langone, A. |
| 4 | The stiffening of the elastic tensor of quartz and its effect on strain-stress relationship. Implications for elastic geobarometry | Gilio, M., Angel, R.J.* and Alvaro, M. |
| 5 | Hybrid veins and heterogeneous deformation in the Saih Hatat window, Oman belt: a possible record of fossil episodic tremors and slow slip events | Petroccia, A., Giuntoli, F., Callegari, I. and Viola, G. |
| 6 | Typical spinifex structures of Archean komatiite metabasalts of the Sur greenstone structure, Middle Dnieper, Ukrainian shield | Reshetnyk, M., Sukach, V. and Starokadomsky, D. |
| 7 | Early Paleozoic Andean-type evolution recorded in the Dunhuang block (NW China): insights from petro-structural, geochronological and metamorphic P–T constraints | Soldner, J., Jiang, Y.D., Štípská, P., Schulmann, K., Yuan, C. and Anczkiewicz, R. |
| 8 | Multi-method approach for deciphering the growth mechanisms of non-typical textures in Archaean garnet | van Schijndel, V., Cutts, K., Stevens, G., Hoffmann, G., Ohl, M., Ji, Y. and Plümper, O. |
| 9 | Residual stress mapping in diopside as tool to reconstruct seismogenic faulting in the lower crust | Van Schrojenstein Lantman, H.W. and Menegon, L. |
| **Session 4: Partial Melting in Continental Settings** | | |
| 10 | High- to Ultrahigh-Temperature Evolution and partial melting of the Central Adirondack Highlands Gneiss Complex (New York State, US) | Ferrero, S., Nicoli, Gautier, Darling, R., Yakymchuk, C., Wannhoff, I. and Gresky, K. |
| 11 | Early Paleoproterozoic high-K granites of the Bastar craton formed by reworking of TTGs: Insights from phase equilibria and trace element modeling | Padmaja, J.*, Sarkar, T., Dasgupta, S. |
| 12 | Mantle lithology of Cenozoic continental basalts in Central Asia: Constraints from olivine chemistry and whole-rock Mo-B isotopes | Zhang, Y.Y., Sun, M. and Yuan, C. |
| **Session 7: Recent challenges and advances in theoretical and experimental mineral physics** | | |
| 13 | Hazard and risk sensing in dating by optimized isotopic diversity and quantifications | Akai, R. |

| | | |
|---|---|---|
| 14 | First-principles investigations of antigorite polysomatism under pressure | Tsuchiya, J., Mizoguchi, T., Inoue, S. and Thompson, E.C. |
| 15 | Cation disorder and Fe-content in ankerite: their effect on its mineral physics | Zucchini, A.*, Boffa Ballaran, T., Masotta, M., Pennacchioni, L., McCammon, C., Fastelli, M., Comboni, D., Hanfland, M., Frondini, F., Comodi, P. |
| 16 | HP-HT behaviour of Jamesonite: A combined Single-Crystal Synchrotron X-ray Diffraction and Raman spectroscopy study | Comodi, P., Fastelli, M., Pennacchioni, L., Balic-Zunic, T., Hanfland, M. and Zucchini, A. |
| **Session 8: Medical mineralogy and hazardous natural materials. State of the art and future trends** | | |
| 17 | Transforming waste into resource: Synthesis of tobermorite from crystalline silica | Bernini, M., Galamini, G., Fantini, R., Malferrari, D. and Gualtieri, A.F. |
| 18 | Understanding Asbestos in Calabria: Assessing Mineralogy and Geochemistry with Insights into Groundwater Quality and Secondary Airborne Exposure Risks | Bloise, A.*, Fuoco, I., Vespasiano, G., Pacella, A., Villella, S., Piersante, C.1, Malvasi, G., Campopiano, A., Ballirano, P., Bruno, M.R., Bruni, B.M., Sinopoli, F., Di Carlo, M.C. and Apollaro, C. |
| 19 | Geo-inspired nanotubes for Alzheimer's Disease treatment by low dose radiotherapy: preliminary results | D'Alessio, D., Secchi, V., Campione, M., Malaspina, N. and Monguzzi, A. |
| 20 | Arsenic bioaccessibility in environmentally significant arsenic mineral(oid)s | Drahota, P., Ettler, V. and Košek, F. |
| 21 | Study of the mineral fibres associated to the clay from Gomsiqe-Puka (Albania) | Gualtieri, A.F. and Mugnaioli, E. |
| 22 | A new approach to quantitatively assess the asbestos-like morphology of mineral fibres | Petriglieri, J.R., Barale, L., De Giuli, C, Tomatis, M., Belluso, E., Campopiano, A., Piana, F., Pacella, A. and Turci, F. |
| **Session 9: Crystallisation of carbonates: Mechanisms, kinetics, methods, case studies, and novel applications** | | |
| 23 | Pseudomorphism and Porosity Formation during the Conversion of Gypsum Single Crystals into Strontianite via intermediate Celestine | Forjanes, P. and Benning, L.G. |
| 24 | $CO_2$-hardening of slag-based bricks – a novel approach of direct carbon usage | Gronen, L., Schieferstein, E., Prokein, M., Hoffmanns, D., Feldrappe, V. and Fusswinkel, T. |
| 25 | Heterogeneous lithification across a legacy coastal slag bank: the creation of new sedimentary rock from anthropogenic material | Hilderman, R.X., MacDonald, J.M., Griffin, S., Slaymark, C., Einsel, J.F., and Monaghan, A. |
| 26 | The effect of organic chelating agents on the kinetic of amorphous calcium carbonates formation and transformation: a facile in situ and real-time monitoring and off-line particles characterization | Ignat, M., Rodriguez Blanco, J.D. and Brinza, L. |

| | | |
|---|---|---|
| 27 | Immobilisation of chromium in magnesium carbonate minerals | Lacinska, A.M., Bateman, K., Chenery, S., Kemp, S.J., Liddy, T., Rushton, J.C., Saha, D. and Schroeder, S.L.M. |
| 28 | Alteration of siderite ($FeCO_3$) in the presence of multi-component rare earth element (REE) aqueous solution at hydrothermal conditions (50-205°C) | Maddin, M., Rateau, R., Szucs, A.M., Terribili, L., and Rodriguez-Blanco, J.D. |
| 29 | Key insights into CDR standards requirements supporting MRV methods | Savage, W., Mouchos, E., Shiimi, R., Pearce, S., Buckley, L., Štyriaková, D., Šuba, J., Kraljić, D., Prekopova, M., Pike, D. and Kurt, Z. |
| 30 | Calcimetry as a reliable method for monitoring soil inorganic carbon stocks: a parametric assessment of its reliability and interferences | Silva, J.M.P., Khalidy, R. and Santos, R.M. |
| 31 | Transient epitaxial overgrowths in the $CaCO_3$-$REECO_3OH$ system formed during pseudomorphic mineral replacement processes | Szucs, A.M., and Rodriguez-Blanco, J.D. |
| 32 | Novel kinetic and mechanistic findings into the fluorite-fluocerite-bastnasite transformation reaction | Terribili, L. and Rodriguez-Blanco, J.D. |
| 33 | Crystallisation of $CaCO_3$ polymorphs in the presence of microplastic glitter particles | Zubovic, K.P., Horvath, A., Brien, M.D., Rateau, R., Guyett, P., and Rodriguez-Blanco, J.D. |
| **Session 10: The role of ultramafic rocks in carbon capture and storage** | | |
| 34 | The fate of nickel during ex-situ mineral carbonation of serpentinized peridotites | Cieślik, B., Kierczak, J., Lacinska, M.A., Bateman, K., and Pietranik, A. |
| 35 | Insights into incipient carbonation phases of synthetic Mg- and Ni-serpentine end members | Corti, M., D'Alessio, D., Campione, M., Capitani, G., Murri, M. and Malaspina, N. |
| 36 | Effect of carbon on thermoelastic properties of $(Fe, Mg)_2SiO_4$-olivine under upper mantle *P-T* conditions | Gholamimahmoodabadi, Z., Mondal, R. and Chatterjee, S. |
| 37 | $CO_2$-negative Mg-binders based on olivine for carbon capture and storage | Neubauer, J., Goetz-Neunhoeffer, F., Franke, S., Rafalski, F. and Bellmann, F. |
| 38 | Understanding and replicating natural basalt carbonation: the case study of Sverrejfellet Volcano (Svalbard, Norway) | Pierozzi, A., Faulkner, N., and Rodriguez Blanco, J.D. |
| 39 | Assessing carbon dioxide storage potential in Swedish and Finnish mine waste | Rees, E., Warlo, M., Crafoord, E. and Bark, G. |
| 40 | Metal mobility during serpentinite carbonation: evaluating recovery potential and environmental impact | Rielli, A., Dini, A., Baneschi, I., Ricci, L., Brugger, J., Etschmann, B. and Chiara, B. |
| **Session 11: Platinum group elements and minerals** | | |
| 41 | Experimental study of kotulskite solid solution | Kamenský, J., Vymazalová, A., Laufek, F. and Tuhý, M. |
| **Session 13: Micro- and nano-mineralogy of critical metals** | | |

| | | |
|---|---|---|
| 42 | Nanomineralogy of Fe-rich sphalerite from the Santa Lucía Zn-Pb deposit (nothwest Cuba) | Gervilla, F., Pérez-Vizcaíno, P., González-Jiménez, J.M. and González-Pérez, I. |
| 43 | Mineralogy of Sn, W, Sc and Ga in ores of Ozernovskoe epithermal Au-Te-Se deposit, Kamchatka, Russia | Kozlov, V.V., Vymazalova, A., Skilskaya, E.D. and Kudaeva, Sh.S. |
| 44 | The replacement of pyrrhotite into pyrite-marcasite seen at the nanoscale | Yesares, L., González-Jiménez, J.M., Blanco-Quintero, I.F., Ferreira, A.R., González-Pérez, I., Gervilla, F. |
| 45 | Critical metals in laterites, bauxites and red muds: concentration and distribution | Laita, E., Yuste, A., and Bauluz, B. |
| **Session 14: Atypical critical metal ores and ore deposits** | | |
| 46 | Copper, Uranium and REE Mineralisation in an Exhumed Oil Reservoir, Southwest Orkney, Scotland | Heptinstall, E.A., Parnell, J., Armstrong, J.G.T., Schito, A. and Akinsanpe, T.O |
| 47 | Rare Earth Element Distribution in Tošići-Dujići Bauxite Deposit: Insights from BCR Sequential Extraction | Topalović, E., Čobić, A., Fiket, Ž. and Tomašić, N. |
| 48 | Preliminary Results of an Antimony Geochemical Study, Longford-Down terrane | Cooper, M.R., Patton, M.A.G., McNulty, K., Murrells, A., Hollis, S. and Torvela, T. |
| 49 | Typical features of the chemical composition of columbites from Perha metasomatites, North-West of Ukrainian Shield | Chernysh, D.S., Khomenko, V.M., and Nissen, J. |
| **Session 17: Innovation and challenges in process mineralogy, geometallurgy and supporting analytical techniques** | | |
| 50 | Improved XRD specimen preparation method for accurate morphological quantification of platy gangue minerals: A case study of talc | Dodoo, D., Webster, N.A.S., Huang, S., Owen, N., Forbes, L., Usher, S.P. and Stickland, D. |
| **Session 25: One drop at a time: fluid, melt and multiphase inclusions as tools to understand geological processes** | | |
| 51 | Immiscible fluids and melts trapped in garnet from pyroxenite-veined garnet peridotites related to metasomatism by basaltic melts | Čopjaková, R., Kubeš, M., Talacko, J. and Kotková, J. |
| 52 | A protocol to interpret magmatic processes recorded by melt inclusions | Esposito, R. |
| 53 | TEM study of a lower mantle mineral inclusion suite in a super-deep diamond | Ogunjobi, C., Singerling, S., Schreiber, A., Bulanova, G. and Brenker, F.E. |
| 54 | Confocal μ-XANES as a tool to analyse Fe oxidation state in heterogeneous samples: The case of melt inclusions in olivine from Hekla volcano | Wilke, M., Botcharnikov, R., Garrevoet, J., Portnyagin, M., Klimm, K., Krasheninnikov, S., Almeev, R., Moune, S. and Falkenberg, G. |
| 56 | Hydrogen concentrations and petrophysical properties of an exceptionally fresh tectonically exhumed oceanic mantle lithosphere sliver | Demouchy, S., Barou, F., Ishikawa, A., Gardés E., and Tommasi, A. |
| 57 | SpecXY – an open-source tool for working with spatial spectroscopic data | Gies, Nils B., Hermann, Jörg and Lanari, Pierre |

| | | |
|---|---|---|
| 58 | Three dimensional distribution of hydrogen distribution in corundum resolved using photoluminescence lifetime imaging | Jollands, M.C., Jones, D.J. and Jin, S. |
| 50 | Water in the continental lithosphere: insights from inclusions in diamonds | Curtolo, A.*, Novella, D., Bolfan-Casanova, N., Day, M.C., Pamato, M.G., Nestola, F. and Harris, J.W. |
| **Session 33: New Minerals, nomenclature, and classification** | | |
| 60 | Zoning in cassiterite: Sectors or twins? | Drivenes, K., Sørensen, B.E., Antao, S., Brownscombe, W., Debuhr, S.R., Spratt, J. and Thomas, R. |
| 61 | End-member Hunter: A computer algorithm for assigning proper end-member formulae to minerals from their empirical formulae | Haifler, J. |
| 62 | Allanite-(Y) from the Åskagen, Sweden | Skřápková, L., Cempírek, J. and Škoda, R. |
| **Session 34: Exploring Solar System evolution using meteorites and returned samples.** | | |
| 63 | Micro-mineralogical characterization of two Ryugu particles by advanced FIB-SEM, TEM and electron diffraction | Borriello, R., Ferrari, M., Folco, L., Mugnaioli, E. and Masotta, M. |
| 64 | Relict of an unknown process in the pre planetary nebula? Petrological & geochemical analysis of Inver-zoned Chondrules | Joseph, F., Drozdovsky, I., Junge, M., Brau, J., Kaliwoda, M. |
| 65 | The microstructure of dolomite from asteroid Ryugu characterised by transmission electron microscopy and transmission Kikuchi diffraction | Lee, M.R., Griffin, S., Daly, L. and Fujiya, W. |
| 66 | Transmission electron microscopy of the fine-grained matrix in the observed meteorite fall Winchcombe | Lier, J., Vollmer, C., Risthaus, L., Kepaptsoglou, D., Ramasse, Q.M., Mosberg, A.B., El Hajraoui, K., Bays, C.L., Schofield, P.F., King, A.J. |
| **Session 35/36: Geoscience Outreach in Museums and Beyond** | | |
| 67 | The historical Ungemach mineral collection at the University of Liège | Hatert, F., Bouvy, A. and Warin, R. |
| 68 | The role of natural history museums for the public awareness of the need of raw materials | Junge, M., Kaliwoda, M., Hentschel, F. and Schmahl, W.W. |
| 69 | An Investigation of Material Changes Occurring within Mineral Collections | Royce, K. |
| 70 | Early 19th Century mineral collection: Robert Jameson's last stand | Walcott, R.C. |
| 71 | Alexearlite (Hg2+3(MoO4)S2): A new mineral with a novel chemistry and structure | Emproto, C., Olds, T.A., Kampf, A.R. and Ma, C. |
| **Session 37: General** | | |
| 72 | The role of volatile elements in cancrinites from the Larvik Complex, Norway | Dehousse, C.*, Hatert, F., Friis, H. and Dal Bo, F. |
| 73 | STRUPLO-24, a new version of the crystal-structure drawing program | Fischer, R.X. and Messner, T. |

| | | |
|---|---|---|
| 74 | Chemical composition of calcite of veinlets-impregnation mineralization of rock complexes of the Silesian cover of the northwestern part of the Ukrainian Carpathians | Zankovuch, H.O., Naumko, I.M., Kokhan, O.M., Matviishyn, Z.H. |
| **Session 38: Chemical evolution of sediments and igneous rocks and their implications on Earth's ocean, crust, and mantle** | | |
| 75 | Geochemistry of the pre-Variscan Pedrógão Grande S-type granitic pluton, central Portugal | Andrade, L., Carvalho, P.C.S. and Santos, J.F. |
| 76 | Missing late veneer constrained by short-lived isotopes in the earliest rock record of South America | Leitzke, F.P., Pakulla, J.J., Tusch, J., Ravindran, A., Barbosa, R.G., Zincone, S.A., Hellers, M., Martins, A.A., Spreafico, R.R., Yang, R., Wombacher, F., Barbosa, J.S.F., Münker, C. |
| 77 | Sulfur concentration and isotope composition in the (ultra)mafic rocks of the Central Sudetic Ophiolite, Poland | Woźniak W., Elsheriff E., Ciążela J. and Strauß, H. |

## What's so special about Mössbauer spectroscopy anyway?

McCammon, C.A.[1]

[1]Bayerisches Geoinstitut, University of Bayreuth, catherine.mccammon@uni-bayreuth.de

---

At first glance Mössbauer spectroscopy might not appear to be one of the most powerful techniques in the mineralogy toolbox. Measurements can take hours or even days and only a few elements are practical to use. But one of them is iron, which is not only the most abundant element in Earth but also the only major element with multiple electronic configurations (oxidation and spin state). Whatever randomness led our universe to possess not only a Mössbauer effect but also a convenient parent and nuclear properties for 57Fe was a lucky break for us indeed. Its unique properties have allowed us to explore new realms in both time and space. The presentation will showcase results already achieved and provide a tantalizing glimpse of discoveries yet to come.

## Natural Quasicrystals - Novel State of Matter, Open State of Mind

Bindi, L.

[1]Department of Earth Sciences, University of Florence, Italy, email: luca.bindi@unifi.it

Quasicrystals, materials characterized by a quasiperiodic distribution of atoms arranged in a pattern violating the crystallographic symmetry rules that apply to ordinary (periodic) crystals, are a wonderful example of how being too uncritical of conventional wisdom may hinder research and progress in understanding the marvels of this world and beyond.

In her book *Purity and Danger* (first published in 1966), the anthropologist Mary Douglas introduced the notion that humans tend to assign and interpret objects and situations around them to well-organized cognitive structures. She contended that the older people become, the more confidence they place in these established structures. As a result, when an individual encounters facts or tendencies that do not fit in any of the established structure, they tend to ignore them. This is what happened about 40 years ago when the first synthetic quasicrystal was discovered [1] and about 15 years ago when the first quasicrystalline material was found in the mineral kingdom [2]. Both discoveries were greeted with scepticism to maintain the *integrity* of the system. Furthermore, at least for natural materials, this scepticism was fuelled by the fact that only few occurrences of these materials were reported. Does that mean that these exotic materials must be extremely rare in the Universe?

During the talk, the author will guide the audience on a cosmic-scale excursion going from presolar materials to grains from a placer-deposit from a remote tundra, through nuclear test debris to recently formed fulgurites. Several arguments will be presented for recognising that quasicrystals may prove to be among the most ubiquitous minerals in the Universe and, perhaps, that the quasicrystalline state could be pervasive in any material subjected to fast cooling.

Natural quasicrystals are probably the tip of an iceberg of novel materials. Our ability to discover new solids is limited only by the human imagination. The hope is that soon we will discover many new classes of novel materials that have yet to be envisioned. Mineralogy can continue to surprise us and have a profound impact on other disciplines, including cosmochemistry, condensed matter physics, solid state chemistry and materials engineering.

*References:*

[1] Shechtman D et al. (1984) Phys Rev Lett 53:1951-1953
[2] Bindi L et al. (2009) Science 324:1306-1309

## The onset of biological crystallization: Tuning the timing and placement of mineral nucleation

Dove, P.M.[1,2,3], Knight, B.M. [1,2], McCutchin, C.A.[2], Edgar, K.J.[2,4], and De Yoreo, J.J.[5,6]

[1] Department of Geosciences, Virginia Tech, Blacksburg, VA 24061, USA

[2] Department of Chemistry, Virginia Tech, Blacksburg, VA 24061, USA

[3] Department of Materials Science and Engineering, Virginia Tech, Blacksburg, VA 24061, USA

[4] Department of Sustainable Biomaterials, Macromolecules Innovation Institute, GlycoMIP Materials Innovation Platform, Virginia Tech, Blacksburg, VA 24061, USA

[5] Physical Sciences Division, Physical and Computational Sciences Directorate, Pacific Northwest National Laboratory, Richland, WA 99352 USA

[6] Department of Materials Science and Engineering, University of Washington, Seattle, WA 98195, USA

---

With the emergence of biological crystallization, the chemical machinery of living organisms has honed the ability to control mineral nucleation and growth over geological time. The resulting biomineral products confer advantages for ecological success by serving as structural supporters, filters, grinders, gravity or magnetic sensors, and more. For thousands of years, humans have regarded these remarkable mineral-organic biocomposites with a combination of awe and curiosity.

The organic matrix is at the heart of forming these biomaterials. This macromolecular mixture of proteins, polysaccharides, proteoglycans, and lipids presents commonalities that regulate mineral nucleation and growth processes. Previous studies indicate their diverse roles, which include concentrating precursor ions and providing substrates that determine the location and preferred orientation of nucleated crystals while also directing the polymorphs that form. While these investigations provide considerable insight, we lack a comprehensive understanding of how biochemistry preferentially enables directed crystallization.

Our approach to deciphering the roles of macromolecules in controlling mineralization is to ask how their active functional groups modify the thermodynamics and kinetics of crystal nucleation. Of particular interest is how macromolecule activity varies with the degree of substitution and local configurations of these groups (e.g., $COO^-$, $SO_3^-$). By viewing activity as an energetic landscape, we are working to establish a mechanistic understanding of how macromolecule structure and composition modulate biological mineralization.

This presentation will highlight findings from our recent collaborations with sustainable biopolymer chemists. Using advances in biopolymer synthesis, we prepare polysaccharides with tailored (and characterized) compositions and use them in quantitative nucleation studies to resolve the energetic landscape on mineral nucleation. In small steps toward a comprehensive understanding of biological crystallization, we show how macromolecule composition and functional group regioposition can tune the kinetics of calcite and $SiO_2$(am) nucleation through systematic shifts in the kinetic and thermodynamic barriers.

References:

[1] Knight BM et al. (2023) Biomacromolecules 24: 1078-1102
[2] Knight BM et al. (2024) Crystal Growth and Design DOI 10.1021/acs.cgd.4c00602
[3] McCutchin CA et al. (in press) Biomacromolecules

## Ultramafic geosystems: a source of metallic elements to the environment

Kierczak, J.R.[1]

[1]University of Wrocław, Institute of Geological Sciences, Pl. M. Borna 9, 50-204Wrocław, Poland, e-mail: jakub.kierczak@uwr.edu.pl

Ultramafic geosystems (rocks and associated soils) are a natural phenomenon where elevated metallic elements content (especially Ni, Cr, and Co) is not the result of pollution but rather a peculiar geochemical background. The concentration of these metallic elements oversteps legislative limits established for maximum allowable concentrations of metals in polluted soils [1]. However, the ultramafic soils are natural and they should not be remediated, but rather protected and treated with caution.

Ultramafic soils, although referred to by one name regardless of what parent material they are formed of, show a range of compositions reflecting either peridotite or serpentinite bedrock. Likewise, the mobility of metallic elements in ultramafic soils also depends on the mineral composition of parent rocks. This is particularly true for nickel. Mineralogy comes to the rescue in explaining this phenomenon because, the main nickel-bearing phase in peridotites, is olivine, while in serpentinites these are serpentine and magnetite group minerals. As olivine is less stable than serpentine and magnetite and weathers faster in soil environments, it is expected that the nickel will be more mobile in soils that were formed on rocks characterized by a lower degree of serpentinization [2]. On the other hand, chromium is found in the structure of weathering-resistant spinel group minerals in both peridotites and serpentinites and is not easily mobilized regardless of the parent material. However, the same behavior is not observed in plant composition. Unexpectedly, the plants growing on the serpentinite contain higher nickel concentrations than those growing on the peridotite parent material. This surprising behavior is also controlled by the chemical and mineral composition of the parent rocks. Soil developed on peridotite contains higher concentrations of available magnesium (as a result of olivine weathering) than soil on serpentinite. Magnesium is more readily taken up by plants than nickel resulting in a lower uptake of the latter despite its higher concentrations in the soil [3].

Ultramafic rocks are well known as potent sinks for $CO_2$, this is because they weather easily and release magnesium and calcium that bind $CO_2$ to form carbonates. However, as magnesium is released so is nickel and other metallic elements, and their fate is not well recognized. The experiments performed so far show that the type of ultramafic rock and the pressure and temperature conditions determine if the metallic elements are leached during weathering or if they are bound in carbonates or other secondary phases. In this context, one of the challenges for future research is to determine the optimal conditions for the mineral carbonation process, not only to bind $CO_2$ without polluting the environment with metals but also to extract them as additional resources.

*References:*

[1] Kierczak et al. (2021) Sci Total Environ 755: 142620
[2] Kierczak et al. (2016) Geoderma 268: 78-91
[3] Pędziwiatr et al. (2018) Plant Soil 423: 339-362

## PUBLIC LECTURE: Perspectives on the Energy Transition - Everything starts with a rock

Dr Karen Hanghøj

Director, British Geological Survey

---

To reduce carbon emissions and mitigate their impact on Earth's climate we need to transition to renewable and low-emission energy sources. Society however faces many challenges to achieve this energy transition, such as how to use natural resources responsibly and sustainably, manage environmental change and be resilient to environmental hazards. This has to be done while taking commercial and societal imperatives into account, so that public and political support for the transition can be sustained.

Emerging clean energy technologies (including those that harness the wind, sun and hydrogen) and mobility technologies (e.g. batteries for self-driving vehicles) create a strong demand for raw materials, including metals such as copper and lithium. These 'critical' metals are sourced from rocks and minerals but the demand for them will dramatically exceed their current global production in the next decades. The potential scarcity and critical importance of these materials might negatively impact on the energy transition, and the supply to the consumer. Sustainable and responsible sourcing of these raw materials (metals) is thus going to be important on a global level in the decades ahead.

We need to design smarter solutions for the sustainable extraction, processing, repairing and recycling of 'critical' metals from both primary (geological) and secondary sources. Furthermore, we must ensure that used materials and products find their way into new product lifecycles in an energetically and economically meaningful way to ensure a greener future.

Essential in finding the solutions to many of the challenges related to the energy transition involves understanding the formation and occurrence of its natural resources (i.e. geoscience). This presentation will focus on the energy transition, the strategies for achieving it and how geoscience can help deliver it, specifically in the context of metals and minerals.

# Crystal Structure, the foundation for apatite's many and varied uses

Rakovan, J.

New Mexico Bureau of Geology and Mineral Resources, New Mexico Institute of Mining and Technology, 801 Leroy Place, Socorro, NM 87801 USA. John.Rakovan@NMT.edu

---

The ability of the apatite crystal structure to accommodate such a wide diversity of elemental substitutions is based in the variety of crystallographic sites of different size and coordination, as well as its flexibility in site modification in response to specific substitutions (Fig.). In the $P6_3/m$ space group, the three distinct cation sites M1 (coordination number, CN,= 9-fold), M2 (CN= 7) and T (CN=4) can accommodate almost half of the periodic table of elements [1]. Simple substitutions of similarly charged ions, e.g. $Sr^{2+} \leftrightarrow Ca^{2+}$ result in varying degrees of solid solution depending on their relative sizes. Coupled substitutions are common and allow for incorporation of heterovalent ions. Common examples include $Na^{1+} + REE^{3+} \leftrightarrow 2Ca^{2+}$, and $Si^{4+} + REE^{3+} \leftrightarrow P^{5+} + Ca^{2+}$ [2]. The three oxygen sites show essentially no substitution, as is common among anion sites in crystal structures. However, the column anion site(s) allow for complete substitutional solid solutions among F, OH and Cl, with other substitutions, e.g. O and $CO_3$ occurring to a much lesser extent. One of the important accommodation mechanisms for the column anion substitutions is the variability of the site position, 0 0 z, along the column [001]. Recent studies [3] have shown that column anion sites shift in their positions, creating new sites, to accommodate variable amounts of F, OH and Cl relative to their positions in end member compositions. These shifts allow for complete series among these anions and for the structure to retain its putative space group symmetry. Other crystallographic sites can shift in their position to accommodate the steric constraints of certain substitutions. For example, displacement of the M2 site, to form an M2' site that enables reasonable column anion bond distances with Ca2 atoms in ternary apatites.

At the crystal surface the coordination of bulk crystallographic sites is incomplete (especially during dynamic periods of crystal growth and dissolution) or is modified by surface complexing species, which are dependent on the nature of the environment around a crystal. One of the fundamental crystal chemical rules that has emerged in the last half century of mineral/crystal surface studies is that a bulk crystallographic site will have distinctly different representations on symmetrically non-equivalent surfaces [4]. Differences among surface sites can lead to differential reactivity. During crystal growth such surface specific reactivity can lead to differential sorption and eventual incorporation of substituent elements. Depending on the distribution of different surface sites, differential incorporation will lead to compositional zoning within a crystal, I.e. sectoral zoning and intrasectoral zoning. If different surface sites are adjacent to one another on a unit cell scale, differential incorporation will lead to ordering and dissymmetrization.

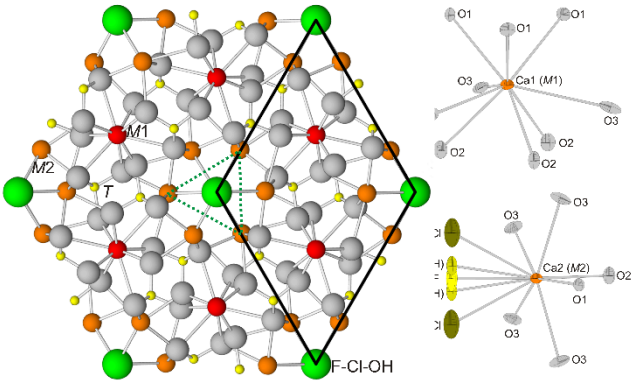


Fig. (001) projection of the apatite structure and perspective views of the two Ca sites, M1 and M2. Modified from [5]

*References:*

[1] Hughes J M and Rakovan J (2002) Rev. Min. Geochem. 48:1-12

[2] Pan Y and Fleet M E (2002) Rev. Min. Geochem. 48:13-50

[3] Hughes J M et al. (2018) Amer. Min. 103:1981-1987

[4] Rakovan J (2002) Rev. Min. Geochem. 48:51-86

[5] Hughes J M and Rakovan J (2010) Elements 11:165-170.

## Contaminant metal desorption induced by apatite additions to a contaminated sediment

Kaplan, D.I.[1] and Knox, A.S.[2]

[1]Savannah River Ecology Laboratory, University of Georgia, Aiken, South Carolina USA Daniel.Kaplan@uga.edu

[2]Savannah River National Laboratory Aiken, South Carolina USA

---

Apatite, a calcium phosphate mineral, has been successfully used as a soil amendment at numerous sites to immobilize metals. Such sites commonly contain multiple contaminants; the impact of apatite on these contaminants is expected to vary greatly. The objective of this study was to determine the influence of apatite on the tendency for contaminant metals to be mobilized or immobilized in sediments. Laboratory batch experiments were conducted under oxidized (several weekly wet/dry cycles) and reduced (water-saturated) conditions with a sediment collected from a wetland contaminated with numerous metals and radionuclides. Apatite additions resulted in the significant ($p \leq 0.05$) reduction of porewater cadmium (Cd), cobalt (Co), mercury (Hg), lead (Pb), and uranium (U) concentrations. However, apatite additions also resulted in the enhanced desorption of arsenic (As), selenium (Se), and thorium (Th). Increases in porewater As and Se concentrations were detected and attributed to phosphate competitive exchange and not to the release of these contaminants directly from the apatite, which contained 29 mg/kg As and 0.2 mg/kg Se. Apatite additions also increased porewater Th and organic carbon (C) concentrations under oxidized (Eh = 497 mV) but not reduced (Eh = 65 mV) conditions. In the oxidized system, the leachate from the apatite treatment had a brown coloration and contained 226 mg/L organic C, as compared to 141 mg/L in the unamended samples. The desorbed organic C likely contained significant quantities of Th. This conclusion was supported by (i) the observation that porewater Th partitioned to hydrophobic resins, (ii) thermodynamic calculations which predicted that essentially all porewater Th existed as organic matter complexes, and (iii) there were significant correlations ($r = 0.91$, $n = 8$, $p \leq 0.01$) between porewater organic C and Th concentrations. Sediment additions of zero-valent iron particles along with the apatite eliminated the enhanced desorption of As, Se, and Th observed when only apatite was added. This study underscores the importance of monitoring the influence of sediment amendments on nontarget contaminants and provides examples of how the sediment additions of apatite can effectively immobilize some contaminants while enhancing the mobility of others.

# Facts and myths about the environmental role of hydroxylpyromorphite $Pb_5(PO_4)_3OH$

Manecki, M.

[1] AGH University of Kraków; al. Mickiewicza 30, 30-150 Kraków, Poland; gpmmanec@cyf-kr.edu.pl

In the world of apatite, hydroxylapatite $Ca_5(PO_4)_3OH$ (Hap) occupies a special place. It is not only an important biomineral for vertebrates, but also a technologically significant synthetic phase. Therefore, its properties and synthesis methods have been studied in depth for years by scientists of various disciplines. Fluorapatite $Ca_5(PO_4)_3F$ and chlorapatite $Ca_5(PO_4)_3Cl$ also occur in nature, but they hardly crystallize from aqueous solutions under environmental conditions and are known rather as accessory minerals in rocks, mainly magmatic and metamorphic. In the world of apatites, there is also a relatively numerous subgroup of lead apatite $Pb_5(AO_4)_3X$, e.g., pyromorphite $Pb_5(PO_4)_3Cl$ (Pym), mimetite $Pb_5(AsO_4)_3Cl$ or vanadinite $Pb_5(VO_4)_3Cl$ and their varieties. Lead apatites crystallize relatively easily from aqueous solutions making some of them of environmental importance. There is a soil remediation method based on *in situ* Pb immobilization by inducing Pym precipitation with phosphate fertilizers (see for example [1] and the literature cited therein). It is also easy to precipitate other varieties of lead apatites from aqueous solutions, including those not found in nature (e.g., with substitutions in the halides position: fluor-, chlor-, brom- or hydroxyl- lead apatites).

Hydroxylpyromorphite $Pb_5(PO_4)_3OH$ (Hpm) is an extremely rare mineral in nature. In the environment on the Earth's surface, it has practically no chance to form. Due to the ubiquitous presence of chloride ions in almost all atmospheric, surface, industrial, or waste waters, the competition for crystallization from solutions will always be won by the chloride variety of lead apatite - Pym. This is due to both the greater thermodynamic stability of Pym (expressed in terms of the lower Gibbs free energy of the precipitation reaction $\Delta G_r$) and its lower solubility constant $K_{sp}$. The $\Delta G_r$ for the dissolution reaction $Pb_{10}(PO_4)_3X = 5Pb^{2+} + 3PO_4^{3-} + X^-$ (where X stands for $Cl^-$ or $OH^-$) equals to 1016 kJ/mol for Pym and 1005 kJ/mol for Hpm while the $K_{sp}$ equals to $10^{-89}$ for Pym and $10^{-88}$ for Hpm [2].

Environmental potential of Pym was noted thermodynamically in the 1970s by J.O. Nriagu (see for example [3]) and applications were developed in the 1990s [4]. This resulted in intensive research on lead apatites in the environment over the past 30 years. From the very beginning, however, researchers were burdened by a subconscious false analogy with calcium apatite. The environmental role of Hpm rather than Pym is often emphasized (see for example [5]). In many cases, the presence of Hpm in environmental samples has even been reported, although by principle its presence there is excluded. This is partly due to the high similarity of morphology and XRD patterns, as well as the limitations of the methods used producing inconclusive results at very low content levels. Nevertheless, with inconclusive results, researchers often point to Hpm rather than Pym. This should be avoided. Certainly, if lead apatite precipitates from environmental solutions it is $Pb_5(PO_4)_3Cl$ pyromorphite rather than $Pb_5(PO_4)_3OH$ hydroxylpyromorphite. At the availability of $Pb^{2+}$, $PO_4^{3-}$, $Cl^-$ and $OH^-$, Pym crystallizes preferably over a wide range of pH, temperatures, and concentrations. Therefore, the term "environmental role of Hpm" should be avoided, because Hpm does not play such a role.

*References:*

[1] Manecki M (2020) Lead in water and soil: speciation, toxicity, and treatment technologies. Wiley
[2] Puzio B (2023) Doctoral diss. AGH University of Kraków, Poland
[3] Nriagu J O (1974) Geochim Cosmochim Acta 38: 887–898
[4] Ma Q Y et al. (1993) Environ Sci Tech 27: 1803–1810
[5] Zhou Y et al. (2021) Environ Sci: Proc Impacts 23: 170-178

# Thermodynamic sublattice model for the solid-solution aqueous-solution equilibria in the apatite system $(Ca,Sr)_5[(P,V)O_4]_3(OH,F)$

Kersten, M.[1], Kulik, D.A.[2]

[1]Geosciences Institute, Johannes Gutenberg-University, Mainz 55099, Germany

[2]Waste Management Laboratory, Paul-Scherrer-Institute, Villigen 5232, Switzerland

---

To understand elevated vanadate concentrations in contaminated soils and aquifers and toxic effects of the oxyanion on the human skeletal system, solubility products of the solid solutions between phosphate and vanadate phases in the triple co-substituted apatite supergroup system $(Ca,Sr)_5(PO_4,VO_4)_3(OH,F)$ were investigated. Binary apatite solid solutions of different compositions between the eight endmembers were synthesized hydrothermally at 200°C and characterized using Rietveld and chemical analysis. The lattice parameters increased linearly with increasing V and Sr content. All the binary sub-systems followed Vegard's law and mixed ideally in the solid-solution phase. The dissolution of the phases was studied at 25°C in a series of aqueous batch equilibrium experiments. The concentrations of solutes indicated congruent dissolution with stoichiometric release of cations and anions. The solubility of the solid solutions increased with increasing mole fraction of vanadate or strontium, with orders of magnitude higher solubilities of the respective hydroxyl- or fluorapatite endmembers. The thermodynamic constants for the endmembers thus derived were justified by theoretical evaluation based on the Simple Salt Approximation model. A theoretical interpretation of the data was further performed, for the first time, based on a sublattice solid-solution aqueous-solution equilibrium thermodynamic model developed for cement phases [1] and applied for the first time on an apatite supergroup. Lippmann phase diagrams were plotted for any of those subsystems using the GEM-Selektor code [2]. This allows the prediction of solubilities in any of the possible solid solution subsystems, which can be easily extended by including other endmembers in the apatite supergroup. The experimental and model results demonstrated that even a trace of Ca or phosphate substitution in the vanadate or Sr apatite endmembers reduces the solubility of the resulting solid solution, which has important environmental implications.

References:

[1] Kulik DA et al. (2022) Cement Concr Res 151:106585

[2] https://gems.web.psi.ch/

## Exploring iodine-containing apatite: synthesis, characterization, and environmental implications

Puzio, B.

[1]Department of Mineralogy, Petrography and Geochemistry; AGH University of Kraków; al. Mickiewicza 30, 30-059 Kraków, Poland; bpuzio@agh.edu.pl

---

Iodine apatite syntheses of different varieties are a promising avenue explored for the development of new materials with applications in nuclear waste management and environmental remediation of radioactive $^{129}I$. Recently, theoretical calculations have proposed hypothetical chemical compositions of apatite-like materials containing Ca, Sr, Ba, Pb, P, As, and V, that are suitable for iodine incorporation, are thermodynamically stable and theoretically feasible for synthesis [1][2][3]. In this study, the predictions were experimentally verified.

In the syntheses carried out from aqueous solutions, stoichiometric amounts of divalent nitrate solutions of Ca, Sr, Ba and Pb were dropwise mixed with a mixture of phosphate, arsenate or vanadate solution containing sodium iodide, maintaining the pH in the range of 3.5-12 depending on the specific apatite. In the cases of the formation of iodine apatites by this method (e.g., $Cd_5(AsO_4)_3I$, $Ca_5(PO_4)_3(I,OH)$, $Pb_5(VO_4)_3I$), the effect of dropping in was immediate precipitate formation. The obtained materials were characterized by X-ray diffraction, scanning electron microscopy, energy dispersive X-ray spectroscopy, Fourier transform infrared spectroscopy, Raman spectroscopy and X-ray fluorescence. The characterization results confirmed the formation of crystalline material with iodine incorporated into the crystal lattice of phases with a hexagonal apatite structure and desirable properties. However, the conditions for obtaining the proposed compounds are extremely different. For example, $Pb_5(AsO_4)_3I$, $Pb_5(VO_4)_3I$ and $Ca_5(PO_4)_3(I,OH)$ precipitate from aqueous solution, where $Ba_5(AsO_4)_3I$ does not. $Ba_5(AsO_4)_3I$ can be synthesized under hydrothermal conditions, and others by solid state synthesis at higher temperatures. These approaches were also tested in this study. In no case was it possible to obtain pure iodine apatite. Secondary substitutions in the halide position also included an OH group and a $CO_3^{2-}$ carbonate ion, which slightly reduces the atomic content of iodine per formula unit. This limitation does not hamper the possibility of using this material in nuclear waste management. The form in which iodine is incorporated into the structure ($I^-$ or $IO^{3-}$) of phases with an apatite structure but extremely different chemical composition is still under discussion and requires further research.

This research was funded by AGH University of Kraków project No 16.16.140.315.

*References:*

[1] Wang J (2015) Front Earth Sci 3:20
[2] Hartnett T et al. (2019) MRS Communications 9:882-890
[3] Puzio B and Manecki M (2022) Contrib Mineral Petr 177:103

## Sequestration of arsenic from aqueous solutions by lead apatites precipitation strategy

Stępień, E. and Manecki, M.

[1] AGH University of Kraków, Department of Mineralogy, Petrography and Geochemistry, Kraków, Poland (estepien@agh.edu.pl)

---

Arsenic contamination of water has become a problem in many areas in recent decades. The toxicity of arsenic and its impact on human health drives intense research on its removal. This project implies that efficient sequestration of As from aqueous solutions can be performed by inducing the precipitation of lead apatite, mimetite $Pb_5(AsO_4)_3Cl$. This process can be initiated, e.g. by reacting an As-contaminated solution with cerussite $PbCO_3$ or anglesite $PbSO_4$ in the presence of Cl ions. Test experiments were carried out using synthetic and natural cerussite and anglesite reacted with $AsO_4^{3-}$ solutions (5 or 50 mg As/L) in the presence of $Cl^-$ ions in the pH range 2-8. Furthermore, the method was tested on natural water contaminated with As (0.7 mg As/L; pH=8.8; Poisonous River, Złoty Stok, Poland).

Both the reaction with cerussite and anglesite with As-containing solutions leads to a rapid and significant reduction in As concentration. In all cases, in the pH range of 4-8, the reaction product is crystalline mimetite. At pH = 2, a mixture of schultenite ($PbHAsO_4$) and mimetite is formed. Both homogeneous and heterogeneous precipitation of lead arsenates, which usually occur as incrustations on the surface of primary phases, was observed. For an initial concentration of 50 mg As/L, the As level is reduced by half within 24 hours, and as the reaction proceeds, the arsenic concentration decreases further, dropping by 84.4% for $PbSO_4$ and by 94.5% for $PbCO_3$. Repeating the experiments with cerussite in the presence of other cations (Mn, Fe, Ni, Cu, Zn, Cd, Al) or anions ($CO_3^{2-}$, $SO_4^{3-}$, $PO_4^{3-}$, $F^-$) showed that their presence has no significant effect on the progress and efficiency of the process. Only Al may slightly reduce the effectiveness. In the presence of phosphate anions, the reaction product is a solid solution of the pyromorphite $Pb_5(PO_4)_3Cl$ and mimetite $Pb_5(AsO_4)_3Cl$. Reaction with solutions with an initial concentration of 5 mg As/L resulted in a 98.2% reduction in As content. The same observations were noted for experiments conducted with natural water contaminated with As.

Scanning electron microscopy observations of natural crystals reacted with a solution containing $AsO_4^{3-}$ have shown that the process of replacing cerussite and anglesite by mimetite follows a similar pattern. Pb ions released by dissolution of the primary mineral react with As and Cl ions from the solution to form mimetite. This process is controlled by the course of dissolution of the primary phase and diffusion of ions in solution, and its nature is a product of pH conditions and the initial concentration of As. At pH 4-8, disordered aggregates of automorphic mimetite crystals in the form of a porous crust crystallize in the immediate vicinity but separated from the dissolved surface. In contrast, schultenite precipitating at pH=2 crystallizes on the surface penetrating into the dissolving mineral. The exchange features indicate an interface-coupled dissolution-precipitation mechanism of the reaction.

The results of the experiments highlight the role of secondary lead minerals, e.g. lead carbonate, lead sulphate and lead arsenate, as phases controlling toxic metals concentrations in a polluted environment. Induced precipitation of lead apatite generates a highly stable, crystalline product. The reaction can potentially be used for the sequestration of As from aqueous solutions.

## REE recovery from apatite-rich rock containing accessory monazite

Staszel, K.[1], Manecki, M.[1], Majka, J.[1,2]

[1]AGH University of Kraków; al. Mickiewicza 30, 30-059 Kraków, Poland; kstaszel@agh.edu.pl
[2]Department of Earth Sciences, Uppsala University, Villavägen 16, SE-752 36 Uppsala, Sweden

---

Green transformation, in fields of energetics and high-tech industries, creates a demand for new sources of Rare Earth Elements (REE), with inexpensive and efficient methods of their extraction. Recently, mineral sources that before were not economically feasible for extraction are viewed as a source of critical elements, including REE. Currently proposed methods of REE extraction from this kind of material are either technologically advanced or give low extraction rates [1].

This research focuses on improving the method of REE extraction previously proposed by Sordyl et al. [2]. Described method consists of acid leaching followed by precipitation of lead-phosphate apatite – pyromorphite (Pym) $Pb_5(PO_4)_3Cl$ and concluded with separation of Pb from REE (formation of REE-oxalates). In this study, alkaline leaching was proposed as an additional step after acid leaching to address REE carriers associated with apatite, such as monazite $(Ce,La,Th)PO_4$. In the following step, REE-pregnant acid is neutralized by REE-containing base to pH 3.5 and the REE-bearing pyromorphite is precipitated. Thanks to REE's compatibility with Pym [3], the amount of Pb used for precipitation could be minimized. The effects of temperature, leaching time and reagent concentration were investigated.

The solutions were analyzed by inductively coupled plasma atomic emission spectroscopy, while powder X-ray diffraction was used to identify the mineral composition of the sediments, scanning electron microscopy to examine the morphology of the final sediment, and energy dispersive X-ray spectroscopy to analyze the elemental composition of the solids.

Extraction from the carbonate-phosphate Alum Shale occurring at the Caledonian front in Fetsjön (Västerbotten, Sweden) was used in model experiments. Most of the initial REE content was released in acid leaching step due to reaction with carbonates and calcium apatites. Reaction of sodium hydroxide with remaining mineral phases (including monazite) resulted in release of additional amounts of REE to alkaline solution. After neutralization, the precipitation step resulted in removal of REE from the solution in the form of REE-rich pyromorphite concentrate. The effect of presence of other elements leached into the solutions was examined.

This research was funded by Polish National Science Centre grant no. 2021/43/O/ST10/01282.

*References:*

[1] Kumari A et al. (2015) Minerals Engineering 79: 102-115, http://dx.doi.org/10.1016/j.mineng.2015.05.003
[2] Sordyl J et al. (2023) SEG 2023 Conference: Resourcing the Green Transition.
[3] Staszel K and Manecki M (2024) EGU 2024, abstract 8290, https://doi.org/10.5194/egusphere-egu24-8290

# Effects of Phosphorus Concentration on Apatite Trace Element Partitioning and the Formation of Immiscible Phosphorus Rich Melts in the Lower Crust

Manselle, P.A.[1], Foley, S.[1] and Shcheka, S.S.[1]

[1] School of Natural Sciences, Macquarie University, North Ryde, New South Wales, Australia

---

Apatite is a common accessory phase in igneous, sedimentary, and metamorphic systems. Experimental studies show that apatite tends to have higher partition coefficients than most major rock forming minerals, which has led to an increased interest in apatite as an indicator of petrogenetic processes [1,2,3]. However, it is difficult to form large apatites in experiments for apatite-silicate melt partitioning while approximating natural amounts of phosphorus in starting materials. In order to ensure the formation of apatites large enough to analyze, many experimental studies have added large amounts of phosphorus in starting materials, commonly exceeding those which would be realistic for a natural melt. While this is common for many experimental studies, phosphorus has been shown to strongly influence the structure of silicate melts, including increasing the affinity for rare earth elements in phosphorus-rich basic melts [4], increasing silica activity [4, 5], and decreasing the $Fe^{3+}/Fe^{2+}$ ratio of a melt [6]. These alterations to the structure of the melts could strongly influence factors like trace element partitioning between minerals and silicate melts by stabilizing trivalent elements such as the rare earth elements in the melt [7]. The stabilisation of phases such as pigeonite, plagioclase, and even quartz can alter the composition of residual melts, making targeting silica rich melt compositions such as dacites or rhyolites difficult. Our study investigates the complex effects that phosphorus has on silicate melts, and whether the addition of phosphorus affects the trace element partition coefficients of apatite significantly. Comparison of apatite $D^{Min/Melt}$ values from our andesitic to basaltic andesitic experiments show that there is a decrease in apatite $D^{Min/Melt}$ values for trivalent ions with increasing $P_2O_5$ in the melt. However, differences between andesite and basaltic andesite experiments indicate that $P_2O_5$ is not the only influence on $D^{Min/Melt}$ values for apatite.

In addition to its effects on the structure of silicate melts, phosphorus has also been shown to encourage the formation of immiscible, phosphorus+iron-rich melts [8]. These immiscible melts have important implications for the formation of Kiruna-type and Nelsonite deposits, which are rich in iron oxides and apatite [8]. However, many of these experiments use extremely high amounts of iron or phosphorus in their starting materials, which may not be realistic for natural magma compositions [8, 9]. Experiments using a natural basaltic andesite powder show that it is possible to form Fe and $P_2O_5$ rich immiscible melts due to the fractionation of feldspar and pigeonite increasing the $P_2O_5$ content of melts. Our experiments at 1GPa and 1000°C indicate that the processes that enrich melts in $P_2O_5$ and iron may take place under lower crustal conditions.

*References:*

[1] Ji D and Dyget N (2023) GCA 369: 141-159
[2] Prowatke S and Klemme S (2006) GCA 70: 4513-4527
[3] Watson E and Green T (1981) EPSL 56: 405-421
[4] Mysen B et al. (1981) Am Min 66: 106-117
[5] Toplis et al. (1994) GCA 58: 797-810
[6] Borisov et al. (2013) Cont Min Pet 166: 1577-1591
[7] Ryerson F and Hess P (1978) GCA 42: 921-932
[8] Hou T et al. (2018) Nat Comm 9: 1415
[9] Lledo H et al. (2020) Cont Min Pet 175: 111

## In-situ laser ablation Lu-Hf apatite geochronology: applications to date mafic intrusions and detrital apatite

Kharkongor, M.B.[1], Glorie, S.[1,4], Mulder, J.[1], Dare, S.[2], Abersteiner, A.[1], Kirkland, C.[3], Bedoya, A.[1,4]

[1] Department of Earth Sciences, The University of Adelaide, SA 5005, Australia.

Email: melissa.kharkongor@adelaide.edu.au

[2] Department of Applied Sciences, University of Quebec at Chicoutimi, G7H 2B1, Canada

[3]Timescales of Mineral Systems Group, School of Earth and Planetary Sciences, Curtin University, WA 6102, Australia

[4]Mineral Exploration Cooperative Research Centre, School of Earth & Environmental Sciences, University of Adelaide, Adelaide, Australia

---

Dating mafic rocks is often challenging since zircons do not readily crystallize in low $SiO_2$ rocks and other minerals that can occur in mafic rocks, such as zirconolite or baddeleyite, are often in very low abundance or too small to date. However, the recent development of laser ablation Lu-Hf dating, using reaction-cell mass-spectrometry [1], can now be applied to rapidly obtain primary crystallization ages for apatite [2], including from mafic rocks [3].

In this study, we examine the U-Pb and Lu-Hf systematics in apatite-rich samples from mafic-ultramafic layered intrusions such as the Bushveld complex in South Africa. We observe that smaller apatite grains exhibit U-Pb resetting by volume diffusion, resulting in a younger age 1994 ± 27 compared to the coarser apatite grains. Conversely, the Lu-Hf system remained undisturbed and accurately records the 2055 ± 22 crystallization age of the intrusion.

In addition, we applied the laser ablation Lu-Hf method to detrital apatite from the Pilbara Craton, Australia, which yielded U-Pb dates of ~2.8-2.9 Ga. In contrast, the Lu-Hf dates for the same grains are much older, with modes at 2.9 Ga, 3.2 Ga, 3.5 Ga and at 3.7 Ga. Eoarchean zircon grains are only rarely observed in the Pilbara Craton, indicating the apatites were derived from a predominant lithology that lacked zircon but grew apatite. The apatite grains have a TTG affinity based on their trace element composition.

Both studies demonstrate the power of the novel laser ablation apatite Lu-Hf method to obtain precise and accurate dates in (1) rocks where zircons are absent, (2) where the U-Pb system is affected by Pb- diffusion, and (3) in detritus with implications for early Earth evolution.

[1] Simpson et al. (2021) Chemical Geology 577: 120299
[2] Glorie et al. (2024) The Geological Society of London 0305-8719
[3] Kharkongor et al. (2023) Chemical Geology 636: 121630

## Insights into the tectonometamorphic evolution of the Norwegian Caledonides and Fennoscandia from apatite petrochronology

Piraquive, A.[1], Machado, J.P., Huyskens, M., Redfield, T.F., Schönenberger, J., Jakob, J., Knies, J.

[1]Geological Survey of Norway, Trondheim, Norway *alejandro.piraquive@ngu.no*

---

Recent advances in microanalytical techniques have enabled the simultaneous application of laser ablation apatite U-Pb dating (AUPb) and trace element geochemistry, delivering comprehensive geochemical and isotopic information. This study presents new AUPb ages and trace element data from various regions of Norway, recording the diverse tectonometamorphic histories within these domains. Our results demonstrate widespread apatite recrystallization at ca. 450-395 Ma within the Western Gneiss Region and the Caledonian Nappes. Conversely, comparatively undeformed Baltican basement locally exposed in tectonic windows closer to the Caledonian frontal thrust yield AUPb ages spanning from 2.6 Ga (Alta Kvænangen Window, northern Norway) to ca. 0.7 Ga (Tømmerås Antiform, mid-Norway), and ca. 1.6 Ga (Atnasjøen Window, southern Norway). Similarly, the Fennoscandian Shield east of the Caledonian frontal thrust yields AUPb ages ranging from 2.2 to 1.6 Ga. Apatite geochemistry showcases varying enrichments in LREE, indicating diverse magmatic and metamorphic affinities. While apatites from the Western Gneiss Region, Baltican basement window exposures, and the Fennoscandian Shield suggest I-type magmatic, high-grade metamorphic, and Archean-TTG affinities, those from the Caledonian Nappes reflect S-type peraluminous compositions and metamorphic recrystallization at low-to-medium grades.

Our findings show that the Baltican basement exposed in tectonic windows in the hinterland of the orogen and the Caledonian nappes experienced a significant thermal overprint. Meanwhile, the basement that is locally exposed in tectonic windows closer to the Caledonian frontal thrust and outside of the confines of the Caledonian orogen remained largely unaffected by apatite recrystallization. Therefore, pre-Caledonian ages in Baltican tectonic windows suggest that metamorphic temperatures did not exceed the AUPb closure temperature of ca. 400-500°C in this structural position.

These distinct AUPb ages underscore the significance of the thermal overprint during the Scandian orogeny and provide insights into the variations of the thicknesses of the orogenic wedge across the different parts of the orogen, even where the nappes are not preserved today. Moreover, contrasting AUPb ages and geochemical data with existing $^{40}Ar/^{39}Ar$ and zircon U-Pb ages will be paramount in unraveling the complex thermal histories across the Norwegian Caledonides and Fennoscandia.

# Pb mobility in Apatite: Exploring chemical influences and its potential for nano-scale petrochronology

Ullah, M.[1-2]*, Klötzli, U.[1], Černok, A.[3], Khubab, M.[4] and Goudarzi, M.[1]

[1] Department of Lithospheric Research, University of Vienna, Vienna, Austria

[2] Department of Geology, Khushal Khan Khattak University, Karak, Pakistan

[3] Department of Mathematics, Informatics and Geoscience, University of Trieste, Italy

[4]Department of Geology, University of Vienna, Vienna, Austria

**Presenting Author:**
*Matee Ullah, Department of Lithospheric Research, University of Vienna, Vienna, Austria.
Email: mateeu89@univie.ac.at

---

Advancing into the age of geologically motivated nano and atomic scale experiments, it is obvious to explore the effectiveness of the desired analysis at these scales. One such effort is exploring the diffusion patterns of lead (Pb) within phosphate minerals like apatite which is essential for advancing our comprehension of (U–Th)/Pb geochronology at different scales. However, unravelling the intricate interplay of various factors influencing Pb diffusion remains an ongoing challenge. Apatite minerals, integral to the (U–Th)/Pb isotope decay system, exhibit closure temperatures in this system ranging from 375°C to 600°C, presenting a unique opportunity to probe mid-temperature thermochronological and petrochronological problems, such as reconstructing past thermal events within Earth's and other planets crusts. The mechanisms governing Pb diffusion in apatite, whether driven by thermally activated volume or anisotropic diffusion or influenced by chemical substitutions and growth processes, is still puzzling. The structural flexibility of apatite, characterized by extensive compositional variability and solid solutions resulting from partial or complete substitutions at cationic and anionic sites, requires a comprehensive investigation into how these factors contribute to Pb diffusivity and (U–Th)/Pb geochronometry at micro- and nano-scales. This study aims a novel, multi-scale investigation into the influences of chemical composition, anisotropy, and growth structure on Pb diffusion in apatite and its implication for nano-scale petrochronology. It uses computational methodologies such as density functional theory and transition state theory at the atomic level, integrated with atomic probe tomography at the nano-scale level, and kinetic monte carlo simulations at the macroscopic scale in order to get an insight into the previously less explored Pb diffusion behaviour in apatite and its potential for nano-geochronology. The outcomes suggest the complete anisotropic nature of Pb diffusion along the preferred z-axis or [001] direction, with notable variations observed in pure Fluorine-apatite as compared to pristine Chlorine-substituted apatite. The interplay between anisotropy and chemical substitutions dictates Pb diffusivity, with potential enhancements or diminution depending upon the specific site and type of substitution. In instances of blocking effect, Pb diffusion navigates alternative pathways, hinting at a tendency towards isotropic diffusion. Notably, our investigation extends beyond conventional boundaries, with a focus on elucidating the intricate interrelationships between chemical substitutions and Pb diffusion behaviour in apatites. By comparing/combining our modelled apatites' closure temperatures (Tc), as a function of effective grain sizes with experimentally derived Tc values under defined conditions, we shed light on the pivotal role of chemical substitutions in influencing the effective closure temperatures at atomic and nano scales. This underscores the paramount importance of apatite's chemistry in determining the permissibility of Pb diffusion pathways within apatites and its applicability for nano-geochronology therefore helps in elevating our understanding of their geological and planetary significance.

**Keywords:** U-Th/Pb dating, petrochronology, nano-geochronology, atomic prob tomography, computational modelling.

# Bat guano-derived hydroxylapatite: an overlooked testimony of past biological activity and a sink of metals in cave environments

Galliano, Y.[1], Bellatreccia, F.[2], Bruxelles, L.[3], De Waele, J.[4], and Carbone, C.[1]

[1]DISTAV, University of Genoa, C.so Europa 26, 16132 Genoa, Italy, yuri.galliano@edu.unige.it

[2]Department of Science, Roma Tre University, Largo S. Leonardo Murialdo 1, 00146 Rome, Italy

[3]TRACES Lab, CNRS, Université Toulouse Jean Jaurès, Allée Antonio Machado 5, 31058 Toulouse, France

[4]BIGEA, University of Bologna, Via Zamboni 67, 40127 Bologna, Italy

---

The members of the apatite supergroup bear great importance for the investigation of a variety of geological processes; among them, hydroxylapatite (HAp) also stands out for its involvement in biological systems. A seldomly studied mode of occurrence of HAp concerns its development as an authigenic phase in cave environments, where it develops from the interaction between acidic phosphatic solutions resulting from the degradation of bat guano and the Ca-carbonates which constitute speleothems and limestone bedrocks [1]. Whereas guano deposits disappear due to organic-matter degradation, bio-derived HAp is preserved as evidence of past biological activity and carries important information on past environmental conditions through its mineral chemistry.

We have collected and characterized guano-derived HAp crusts and speleothems occurring on the walls and ceilings of 10 caves – 5 in Italy, 4 in France and 1 in the Philippines. We considered both (i) sites with current bat roosts and (ii) sites where past bat colonization can only be assumed due to the presence of phosphate mineralization and biocorrosion features [2]. A multi-method approach was adopted to investigate the mineralogical and geochemical features of the samples, including optical microscopy, XRPD, SEM-EDS, EPMA-WDS, Raman and FTIR spectroscopy, XRF and ICP-MS.

All the studied samples are nanocrystalline aggregates of carbonate- and Zn-bearing HAp. The calculation of coherent scattering domains through Rietveld refinement of XRPD data yielded mean crystallite sizes of 15 – 80 nm. Absorption bands at 876 $cm^{-1}$, 1419 $cm^{-1}$ and 1454 $cm^{-1}$ in FTIR spectra confirm the presence of $CO_3^{2-}$ ions in the structure of HAp, according to the B-type substitution mechanism [3]. Chemical data are indicative of the incorporation of Zn, with concentrations reaching up to 2.4 wt% and a mean content of 0.77 wt% (from 170 point analyses). Interestingly, SEM imaging revealed evidence of alveolar and globular textures attributable to the presence of bacterial colonies that might be coeval with the emplacement of the mineralization.

Further investigations will be aimed (i) at understanding whether the mineralization pathway is indeed influenced by the presence of phosphate-metabolizing microorganisms, (ii) at probing the local coordination chemistry of Zn ions in guano-derived HAp using X-ray absorption spectroscopy experiments at the Zn K-edge (an application for beamtime at the European Synchrotron Radiation Facility is currently under review), and (iii) at revealing whether specific changes in the local structure and coordination chemistry that characterize HAp speleothems during growth are inherently linked to past environmental change.

*References:*

[1] Audra P et al (2019) Int Journ of Speleol 48:75–105
[2] Hughes A C et al (2023) Ecol Indicat 155:111051
[3] Fleet M E (2009) Biomat 30(8):1473-1481

## Oxygen isotope study of fluorapatite in conodonts – insights from chemical analyses

Wudarska, A.[1,2], Wiedenbeck, M.[2], Männik, P.[3], Lepland, A.[3,4], Hints, O.[3], Wilke, F.D.H.[2], Emsbo, P.[5], Couffignal, F.[2] and Scicchitano, M.R.[2]

[1]Institute of Geological Sciences, Polish Academy of Sciences, Twarda 51/55, 00-818 Warsaw, Poland, ndgiera@cyf-kr.edu.pl
[2]GFZ German Research Centre for Geosciences, Telegrafenberg, 14473 Potsdam, Germany
[3]Department of Geology, Tallinn University of Technology, Ehitajate tee 5, 19086 Tallinn, Estonia
[4]Geological Survey of Norway, Leiv Eirikssons vei 39, 7491 Trondheim, Norway
[5]U.S. Geological Survey, Geology, Geochemistry, and Geophysics Science Center, Denver, CO 80225, USA

---

Oxygen isotope compositions ($^{18}O/^{16}O$; $\delta^{18}O$) of mm-size conodont elements have been widely used to reconstruct the temperature of ancient oceans. These tooth-like structures of probably early vertebrates are composed mainly of calcium phosphate with a general chemical formula commonly described as $Ca_5Na_{0.14}(PO_4)_{3.01}(CO_3)_{0.16}F_{0.73}(H_2O)_{0.85}$ [1] and contain minor albeit various amounts of organic matter. Recent studies have shown, however, that conodonts consist of fluorapatite characterized by more complicated crystal chemistry with clear differences in crystallinity and numerous additional cationic and anionic substitutions associated with different morphologic components of individual conodonts.

Oxygen isotope research of these microfossils has traditionally relied on gas source isotope ratio mass spectrometry, which usually involves combining several dozen conodont elements to obtain a single measurement of phosphate-bonded oxygen. This poses difficulties in studies of conodont-poor stratigraphic intervals and evaluating taxon-specific $\delta^{18}O$ variability. To overcome these challenges, *in situ* secondary ion mass spectrometry (SIMS) can be used to conduct analyses which require only picogram sampling masses. However, SIMS measurements cannot discriminate between the various oxygen carriers in the mineral and hence SIMS inherently pools the isotope compositions of various components: $(PO_4)^{3-}$, $(CO_3)^{2-}$, $(SO_4)^{2-}$, $(OH)^-$ etc. Consequently, reliable SIMS paleotemperature estimates require assessment of matrix effects related to different oxygen components of conodont apatite. It is thus essential to evaluate obtained $\delta^{18}O$ values in the context of the chemical compositions and morphologic variations in studied microfossils.

Here we present conodont data on two different taxa, *Amorphognathus* and *Pterospathodus*, which were extracted from Ordovician and Silurian strata in Estonia. We collected oxygen isotope data using a CAMECA 1280-HR large geometry SIMS instrument and we also conducted chemical analyses with an electron probe microanalyzer (EPMA). While quantitative measurements revealed large variations within individual conodonts in terms of both $\delta^{18}O$ values and mass fractions of some of the chemical components, no clear correlation could be found between SIMS and spot EPMA data. It was only through chemical mapping that a broader perspective emerged, revealing distinct patterns in the distribution of chemical elements across various conodont tissues known as hyaline crown, albid crown, and basal body. However, interpretation of the obtained data proves to be challenging due to the diverse surface properties of polished conodonts, which greatly affects *in situ* SIMS measurements.

*References:*

[1] Pietzner et al. (1968) Palaeontogr Abt A 128:115–152

*This research was partially funded by National Science Centre, Poland, grant no. 2023/49/B/ST10/03922.*

## Geochemistry and U-Pb isotopic characteristics of apatite from the Loch Roag xenolith suite

Badenszki, E.[1], Buczko, D.[2], Matusiak-Małek, M.[2], Upton B.G.J[3]. and Daly, J.S.[1,4]

[1] UCD School of Earth Sciences and iCRAG, University College Dublin, Ireland

[2] Institute of Geological Sciences, University of Wrocław, Poland

[3] School of Geosciences, University of Edinburgh, Scotland, UK

[4] Corresponding author and presenter

---

This study of the classic Loch Roag deep crustal and mantle xenolith localities explores the feasibility of establishing age constraints on events affecting the lower crust/upper mantle through *in situ* U-Pb apatite dating. Loch Roag stands out as one of the most extensively researched deep crustal and mantle xenolith localities in NW Europe.

The Loch Roag xenoliths and xenocrysts are hosted in a 45 Ma lamprophyre (monchiquite) dyke [1] that cuts Neoarchaean orthogneisses of the Lewisian Complex in NW Scotland. Although located in the Hebridean terrane, conventionally outside the Caledonian orogenic belt, a Rb-Sr isotopic investigation [2] suggested that chemical heterogeneities within a dioritic crustal xenolith equilibrated at c. 420 Ma similar to the protolith ages of lower crustal xenoliths from the Midland Valley [3].

To investigate the cryptic Devonian event at Loch Roag, we measured U-Pb isotopic, trace, and REE data by laser ablation ICPMS in apatite from eight thin-section samples, comprising one clinopyroxene and two K-feldspar megacrysts, two clinopyroxenites and three granulites (meta-diorites). All xenoliths and xenocrysts displayed similar chondrite-normalized trace element and REE patterns, yet distinct lithologies exhibited varying degrees of negative Sr anomalies – strongly for apatite in the granulites, minor in the megacrysts, and negligible to absent in the clinopyroxenites. On the Sr/Y vs ΣLREE biplot [4], apatite from feldspar megacrysts, clinopyroxenite xenoliths, and the clinopyroxene megacryst clustered tightly within the field of ultramafic rocks, whereas apatite from the granulites displayed greater dispersion, with two samples predominantly falling within the mafic I-type granitoids and mafic igneous fields, and the third granulite plotting in the alkali-rich igneous rocks field.

U-Pb results varied across xenoliths and xenocrysts with differing mineralogy and levels of alteration, apparently by the host magma. Notably, apatites hosted in K-feldspar megacrysts failed to yield meaningful data due to complete isotopic system compromise. Conversely, two highly altered diorites and two clinopyroxenites exhibited lower intercept ages of approximately 45 m.y., aligning with the age of the host magma. Most apatite grains from the least altered granulite yielded an older age of 164 ± 49 Ma and two groups of three apatite grains from the same sample, all hosted in clinopyroxene or Fe-Ti oxide exhibited even older (imprecise) ages. Apatites hosted in the clinopyroxene megacryst also yielded an older age of 101 ± 43 Ma, suggesting greater retentivity of Pb when apatite occurs as inclusions within clinopyroxene.

[1] Faithfull J.W. et al. (2012) J. Geol. Soc., London 169: 115-118
[2] Lee, D-C. et al. (1993) Geochim. Cosmochim. Acta 57: 219-230.
[3] Badenszki, E. et al. (2019) J. Petrology 60: 1543-1574
[4] O'Sullivan G. et al. (2019) Earth Sci. Rev. 201: 103044

## Potential of mineralogical characterization for improvement of calcium phosphate cements and their hydration

Goetz-Neunhoeffer, F.[1] and Hurle, K.[1]

[1]Friedrich-Alexander-Universität Erlangen-Nürnberg, GeoZentrum Nordbayern, Mineralogy, Schlossgarten 5a, 91054 Erlangen, Germany; Email: friedlinde.goetz@fau.de (corresponding author)

---

The inorganic fraction of bone is constituted by the biologically formed mineral apatite, the so called calcium-deficient hydroxyapatite containing carbonate and other minor elements [1]. Calcium phosphate cements (CPCs) are well established for clinical application as bone substitutes. They are composed of reactive calcium phosphates like tricalcium phosphate (whitlockite / β-TCP or a-TCP), which dissolve upon mixing with water or aqueous solutions. This results in precipitation of hydrate phases, either brushite, monetite or hydroxyapatite depending on conditions.

For successful clinical application, several properties of the cement paste and hardened cement need to be carefully adjusted. A variety of inorganic and organic additives (e.g. citric or phytic acid) can be used to improve properties like cohesion or injectability. Mineralogical characterization of the changes by additives on dissolution-precipitation reactions can be easily performed by quantitative X-ray diffraction (XRD) and heat-flow analysis [2, 3, 4].

Rietveld refinement of XRD data is a very powerful tool for investigation of solid solutions in ionic-doped calcium phosphates and to follow the kinetics of time-dependent formation of hydroxyapatite or brushite. Crystallographic data like lattice parameters provide information about the possible incorporation of biologically active ions into the crystal structure of either starting components or hydrate phases, which is important to assess the biological availability of the ion within the body. Additional information about amorphous fraction can be obtained by subsequent application of an external standard (G-factor). G-factor method allows amorphous content quantification, either of the anhydrous powder or in the hydrated pastes. Since biological and mechanical performance of the hardened cement depend on its quantitative phase composition as well as the crystallinity of the hydrate phases, quantitative XRD analysis with Rietveld refinement provides valuable information for assessment of bone cements.

The combination of mineralogical methods is highly valuable to obtain full characterization of the setting process and to analyse and understand the effect of different additives on it. Analyses result in essential data and support conclusions for the understanding and consequent improvement of CPCs.

*References:*

[1] H.A. Lowenstam, S. Weiner, On biomineralization, Oxford University Press on Demand 1989.
[2] K. Hurle, J. Weichhold, M. Brueckner, U. Gbureck, T. Brueckner, F. Goetz-Neunhoeffer, Acta Biomaterialia 2018, 80, 378–389.
[3] J. Weichhold, U. Gbureck, F. Goetz-Neunhoeffer, K. Hurle, Materials 2019, 12(13), 2098.
[4] K. Hurle, F.R. Maia, V.P. Ribeiro, S. Pina, J.M. Oliveira, F. Goetz-Neunhoeffer, R.L. Reis, Bioactive Materials 2022, 16, 403–417.

## Apatite as a provenance indicator for I-, S- and A-type granites and mafic intrusions

Kieffer, M.A.[1], Dare, S.A.S.[2] and Gendron, M.[3]

[1]Department of Applied Sciences, University of Quebec in Chicoutimi (UQAC), 555 Boulevard de l'Université, Chicoutimi, G7H 2B1, QC, Canada; marie.kieffer1@uqac.ca

[2]Department of Applied Sciences, University of Quebec in Chicoutimi (UQAC), 555 Boulevard de l'Université, Chicoutimi, G7H 2B1, QC, Canada; Canada Research Chair in Geochemistry Applied to Ore Deposits.

[3]Explo-logik Inc., Quebec, Canada

---

Apatite chemical composition is commonly used to trace its geological environment of formation. Detrital apatite is hence increasingly used as an indicator mineral for mineral exploration [1; 2] and provenance studies in secondary environments [3], such as in areas covered by glacial sediments. To date, most studies focus on the identification of apatite from different ore deposit types [e.g., 1, 2, 4] and the fertility of the host intrusion [e.g., 5]. However, apatite associated with mineralisation represents only a small fraction of detrital apatite relative to apatite from 'background' rocks. Thus, identifying the nature of the host intrusion (e.g., felsic or mafic) should be performed prior to identify a deposit type, as it helps to focus exploration and evaluate the prospectivity of a larger area. For example, different types of ore deposits and metals (e.g., Cu, Mo, W, Sn) are typically related to felsic intrusions, depending on the type of granite (I, S or A). On the other hand, mafic intrusions may be host to Fe-Ti-V-P (oxide-apatite) and/or Ni-Cu-Cr-platinum group elements (sulfide) mineralisation.

This study is the first to build a world-scale database of trace elements in apatite from I-, S- and A-type granites. It includes new analyses performed by laser ablation inductively coupled mass-spectrometer at the University of Quebec in Chicoutimi (LabMaTer; n = 273) and analyses compiled from the literature (n = 2146). A petrogenetic approach allowed to propose a new classification scheme to identify apatite of the different granite types from those of mafic rocks and carbonatites. The classification is performed in a sequence of four steps: (1) Sr/Y ratio and light rare earth elements (REE) isolate apatite from felsic and mafic intrusions from those of other intrusions, using the diagram of O'Sullivan et al. [3]; (2) apatite from mafic intrusions is excluded from apatite from felsic intrusions using REE+Y, Sr/Y and Eu/Eu*, or As, $(Gd/Yb)_N$ and Pb+Th+U if required; (3) apatite from post-Archean and Archean felsic intrusions are identified using log(La/Yb)N vs YbN diagram of Antoine et al. [6]; finally, (4), the origin of apatite from post-Archean felsic intrusions can be classified as I-, S- and A-type using Mn, V and $(La/Nd)_N$. This new, robust workflow, proposes to enlarge the footprint of apatite as an indicator mineral by including information about the host intrusion. It strengthens the use of apatite as an indicator mineral and its application will contribute to mineral exploration and provenance studies in secondary environments.

*References:*

[1] Mao M et al. (2016) Econ Geol 111: 1187-1222
[2] Zhou T et al. (2023) Minerals 13 : 491
[3] O'Sullivan G et al. (2020) Earth Sci Rev 201 : 103044
[4] Tan H et al. (2023) Ore Geol Rev 153: 105269
[5] Li C-Y et al. (2017) Lithos 272-273 : 291-300
[6] Antoine C et al. (2020) Geochem Geophys Geosyst 21 : e2020GC008923

## Controlled calcium phosphate precipitation via vapor diffusion sitting drop methodology in bacterial cellulose template

Navarro-Zabarburú, I.[1*], Zavaleta, A.I,[1], Calderón-Toledo, S.[1] and Alvarez-Lloret, P.[2]

[1]Laboratory of Molecular Biology, Faculty of Pharmacy and Biochemistry, Universidad Nacional Mayor de San Marcos, Lima, Peru. Email: isabel.navarro@unmsm.edu.pe

[2]Deparment of Geology, University of Oviedo, Oviedo, Spain

---

Bacterial cellulose (CB) is a widely used biopolymer in producing biocomposites due to its high purity, biocompatibility, and non-toxic nature [1]. This study explores the use of CB as an organic template for the controlled precipitation of calcium phosphate (CaP) to develop a hybrid CaP-CB material [2]. The CB was synthesized from *Komagataeibacter sp.* SU12, utilizing a medium obtained from fruit juice waste (*Mangifera indica*) [1]. Controlled crystallization assays were conducted via vapor diffusion sitting drop methodology ("crystallization mushrooms"), placing 40 ml microdroplets (mixing $Ca(CH_3COO)_2$ 50 mM and $(NH_4)_2HPO_4$ 30 mM solutions) in the CB surface, and pH control through $NH_4HCO_3$ 40 mM solution decomposition in the reservoir chamber. The experiments were performed for different reaction times (i.e., 1, 3, 5, 7, and 15 days) at room temperature (≈ 25 °C). The CaP-CB materials were characterized by complementary analytical techniques: SEM, XRD, TG-DSC, Raman, and ATR-FTIR [4]. The formation of CaP nanocrystals on the surface of CB nanofibers was observed forming flower-like aggregates. The crystalline phase was identified as apatite crystals ($CaPO_4$), presenting phosphate groups ($v_1$-$v_3$ $PO_4$ absorption modes) with different levels of crystallinity. Additionally, characteristic absorption bands (IR spectra: O-H, C-H, and C-O-C bond stretching) were also identified for the CB template. In addition, it was also determined that increased experimental time promotes CaP-CB mineral precipitation. This research confirms the effectiveness of CaP nanocrystal production on the surface of CB nanofibers, opening up exciting opportunities for future investigation in tissue regeneration and advanced materials engineering [2,4].

*References:*

[1] Calderón-Toledo et al (2022) J. Chem. Technol. Biotechnol. 97:1482 - 1493
[2] Torres M et al. (2021) Polymer Reviews 61:736 - 764
[3] Torres A et al. (2023) Biomaterials Advances 154: 213605
[4] Khan S et al. (2022) Int. J. Biol. Macromol 209: 9 - 30

## Raman spectroscopic analysis of the As-bearing apatite supergroup minerals from pyrometamorphic xenoliths of the Upper Chegem Caldera, Russia

Środek, D.[1], Dulski, M.[2], and Balin, K.[3]

[1]University of Silesia, Faculty of Natural Sciences, Institute of Earth Science, Będzińska 60, Sosnowiec, Poland, dorota.srodek@us.edu.pl

[2]University of Silesia, Institute of Materials Engineering, Silesian Center for Education and Interdisciplinary Research, 75 Pułku Piechoty 1A, 41-500 Chorzów, Poland

[3]A. Chełkowski Institute of Physics, University of Silesia, 75 Pułku Piechoty 1A, 41-500 Chorzów, Poland

---

Calcium-arsenate members of the apatite supergroup - svabite, $Ca_5(AsO_4)_3F$, johnbaumite, $Ca_5(AsO_4)_3(OH)$, and As-bearing hydroxylellestadite, $Ca_5(SiO_4)_{1.5}(SO_4)_{1.5}(OH)$ has revealed in a calcium-silicate xenolith from ignimbrite of the Upper Chegem Caldera (Kabardino-Balkaria, Russia). We have observed gradual substitutions at the tetrahedral (*T*) site of the apatite structure, which has provide a unique opportunity to study the correlation of the variations in the $(SiO_4)^{4-}/(SO_4)^{2-}$ to $(AsO_4)^{3-}$ ratio and Raman spectra.

Variations in the Raman spectrum associated with *T* site occupancy were observed in the range 300-1200 $cm^{-1}$. Bands corresponding to symmetric stretching ($v_1$) vibrations were noted at ca. 1006 $cm^{-1}$ for $(SO_4)^{2-}$ groups, 856-860 $cm^{-1}$ for $(SiO_4)^{4-}$ groups, and 961 $cm^{-1}$ for $(PO_4)^{3-}$ groups. In the Raman spectrum of samples containing arsenic in the structure, overlap of the $v_1\,(AsO_4)^{3-}$ and $v_1\,(SiO_4)^{4-}$ bands is about 860 $cm^{-1}$, as well as the asymmetric stretching vibrations of the $v_3\,(AsO_4)^{3-}$ groups and the $v_1\,(PO_4)^{3-}$ vibrations. A broad, low-intense band with a maximum around 1141 $cm^{-1}$ was attributed to overlapping bands related to $v_3\,(SiO_4)^{4-}$, $(SO_4)^{2-}$, and $(PO_4)^{3-}$ groups. The bands corresponding to $v_4$ vibrations are at 630 $cm^{-1}$ $(SO_4)^{2-}$, 538 $cm^{-1}$ $(SiO_4)^{4-}$, and 581 $cm^{-1}$ $(PO_4)^{3-}$. The band at 467 $cm^{-1}$ is most likely related to $v_2\,(SO_4)^{2-}$, while 426 $cm^{-1}$ corresponds to $v_4\,(AsO_4)^{3-}$. Bands associated with $v_2$ vibrations are observed at 368 $cm^{-1}$ for $(AsO_4)^{3-}$ and ca. 325 $cm^{-1}$ for $(SiO_4)^{4-}$. Our studies have shown that even a slight change in the occupation at the tetrahedral site in this mineral series has a notable effect on the Raman spectra. The most noticeable change is associated with a decrease in the intensity of the bands associated with the vibrations of the $SO_4$ groups, which coincides with an increase arsenic in mineral composition. We do not observe a similar effect for the 860 $cm^{-1}$ band. One possible explanations is that in hydroxylellestadite this band has a high intensity because the T site is mainly occupied by Si and S. With an increasing of the As content in the composition of the studied mineral series, we observe a broadening of the 860 $cm^{-1}$ band and presence of the shoulder indicate the being there of multiple overlapping bands. Due to the overlap of the $v_1\,(SiO_4)^{4-}$ and $v_1\,(AsO_4)^{3-}$ bands and formation of a broad complex band at 860 $cm^{-1}$, we do not observe a reduction of the intensity of this band, while the Si content decreases.

## Exotic radio-minerals in the geological disposal of radioactive waste

Corkhill, C.L.[1], Mottram, L. M.[2], Friskney A. A.[2], Harding L.[3], Kvashnina K.,[4,5] Bazarkina E. F.[4,5] and Hyatt N.C.[1]

[1]School of Earth Science, The University of Bristol, Bristol, BS8 1RJ, UK c.corkhill@bristol.ac.uk

[2]Department of Materials Science and Engineering, The University of Sheffield, Sheffield, S1 3JD, UK

[3]School of Physics, The University of Bristol, Bristol, BS8 1TL

[4] Helmholtz-Zentrum Dresden-Rossendorf (HZDR), Institute of Resource Ecology, PO Box 510119, 01314, Dresden, Germany

[5]The Rossendorf Beamline at ESRF – The European Synchrotron, CS40220, 38043 Grenoble Cedex 9, France

---

Naturally-occurring radioactive accessory minerals, containing a significant proportion of U and Th, are of interest in the development of safe disposal strategies for actinide-containing radioactive wastes generated through civil nuclear energy and nuclear military operations. Two key examples of these wastes are U-containing spent nuclear fuel and inventories of separated $PuO_2$ derived from spent nuclear fuel reprocessing, both of which require safe immobilisation over timescales of many hundreds of thousands of years. The eventual disposal solution for such actinide-bearing radioactive wastes is in a geological disposal facility, up to 1 km below the surface of the Earth. In this environment, the eventual release of U or Pu to the geosphere and biosphere will be controlled by the dissolution of waste by groundwater. To mitigate against this, and to build a robust post-closure safety case for disposal to the satisfaction of the environmental safety regulators, it is necessary to develop innovative, durable materials for actinide immobilisation.

A suite of naturally occurring “exotic radiominerals” have been identified as being excellent templates for actinide immobilisation materials, having retained most of their U/Th inventories for up to 1 billion years, despite undergoing hydrothermal alteration and becoming metamict as a result of self-alpha radiation damage. Studying naturally-occurring specimens of these minerals, including titanate pyrochlore [$(Ca,U)Ti_2O_7$], zirconolite [$(Ca,U)ZrTi_2O_7$] and, to a lesser extent, brannerite [$UTi_2O_6$] and thorutite [$ThTi_2O_6$], can give insight to the long-term behaviour of actinide-containing radioactive waste materials in geological disposal environments.

While these minerals have attracted attention from researchers for a number of decades, advances in analysis techniques have enabled new insights into the speciation of U in these minerals. In particular, a combination of X-ray spectroscopic techniques, including High Energy Resolution Fluorescence Detected X-ray Absorption Near Edge Spectroscopy (HERFD XANES) at the U $M_4$-edge, in both bulk and macro-focus mode, and micro-focused Extended X-ray Absorption Fine Structure (μ-EXAFS) at the U $L_3$- and U $L_1$-edges have been used to evidence novel U speciation and local coordination in these exotic radio-minerals. These results lay the foundations for the development of an entirely new range of materials for actinide immobilisation, with particular relevance to the UK’s 140 tonne inventory of civil separated plutonium.

## Titanite as a petrogenetic indicator of the magmatic and post-magmatic evolution – Closepet Batholith (Dharwar craton, southern India)

Gmochowska, W.[1], Słaby, E.[2], Gumsley, A.[3], Anczkiewicz, R.[3], Kozub-Budzyń, G.A.[4] and Bhattacharya, S.[5]

[1]Institute of Geological Sciences, PAS, Research Centre in Wrocław, ul. Podwale 75 (Poland); e-mail: wiktoria.gmochowska@twarda.pan.pl

[2]Institute of Geological Sciences, PAS, Research Centre in Warsaw, ul. Twarda 51/55 (Poland)

[3]Institute of Geological Sciences, PAS, Research Centre in Kraków, ul. Senacka 1 (Poland)

[4]AGH University of Science and Technology, Faculty of Geology, Geophysics and Environmental Protection, al. A. Mickiewicza 30, Kraków (Poland)

[5]Dept. of Earth and Environmental Sciences, IISER Mohali, India

---

Accessory minerals are used to describe the path of igneous, metamorphic, and hydrothermal changes. The best for this purpose are minerals with a complex composition, where a complex scheme of substitutions of trace elements is observed. Here titanite is used to decipher magmatic and post-magmatic events in the Neoarchaean Closepet Batholith, in which hydrothermal processes were previously documented [1].

An integrated textural, geochemical and geochronological studies of titanite were applied. The differences reveal five generations of titanite: (1) magmatic titanite; (2) hydrothermally altered titanite with zoned to patchy textures and secondary fractures and veinlets; (3) homogeneous titanite, interstitial to other accessory minerals; (4) titanite overgrowth on Fe-Ti oxides; (5) titanite inclusions within biotite. The results indicate a decrease in the content of trace elements with different magnitudes in all generations compared to igneous titanites (1). Generations 1, 3, and 4 are interpreted to be of igneous origin and multi-stage formation in a given environment. In contrast, generations 2 and 5 are connected with post-magmatic stages, i.e., hydrothermal fluids percolated within the Closepet Batholith.

The LA-ICP-MS U-Pb ages confirm that magmatic titanite (1) are of igneous origin. The ages are within the analytical error of previous studies [1-2], pointing to a Neoarchaean age. The magmatic ages are likely related to the large-scale processes of the Dharwar Craton assembly. The crystallization of Closepet Batholith is linked with the last thermal event, which is considered as the final stage of cratonization [3]. In contrast, the hydrothermally altered titanites (2) indicate previously documented metasomatic processes [1] that occurred in the Paleoproterozoic.

Textural and geochemical variations of titanite together with geochronological results track the evolution of the Closepet Granitoid from magmatic to post-magmatic stages and fluid-rock interaction event, indicating multistage processes.

The study funded by the National Science Centre (NCN Project UMO - 2018/31/B/ST10/01060).

*References:*

[1] Słaby E et al. (2021) Lithos 106039: 386-387
[2] Jayananda M et al (2000) Precambrian Res. 99: 225-254
[3] Jayananda M et al (2020) GR 78: 228-260

## Super- and Subsolidus Processes in the Rolvsnes Granodiorite, W Norway, Recorded by Titanite

Drivenes, K.[1], Buisman, I.[2], Coint, N.[1], Huyskens, M[1], Knies, J[1], Larsen, R.B.[3], and Sørensen, B.E.[3]

1Geological Survey of Norway, Leiv Eriksons vei 39, 7491 Trondheim, Norway. Kristian.drivenes@ngu.no

2Department of Earth Sciences, University of Cambridge, Cambridge, United Kingdom

3 Department of Geoscience and Petroleum, Norwegian University of Science and Technology, Trondheim, Norway

---

Titanite has a range of uses as a geological tracer mineral. It can incorporate significant amounts of Nb, Y, and REE into the crystal structure, has a (near-)magmatic closure temperature of the U-Pb isotopic system, a defined relationship with Zr content and temperature, and distinct alteration products, making it a potential geochronothermometer, in addition to an indicator of melt fractionation, metamorphic recrystallization, and fluid infiltration. In the Rolvsnes Granodiorite and associated granites at Bømlo Island, Western Norway, titanite is observed as euhedral crystals in the matrix and K-feldspar phenocrysts, as inclusions in epidote, and overgrowths of Fe-Ti-oxides. Titanite U-Pb ages of the three main rock types (granodiorite, porphyritic and equigranular granites) varying from 463 to 466 Ma conform with the reported zircon ages of the granodiorite from 463-467 Ma [1]. Zr-in-titanite thermometry [2] using the calculated pressure from Al-in-hornblende of 400 Ma, gives temperatures from 710 to 740° C, similar to the Zr saturation temperatures [3] of ~720-740° C from the same samples calculated using the same pressure and $X_{H2O}$ = 0.05.

Titanite found as inclusions in epidote is likely crystallized due to Ti excess during replacement of amphibole or biotite by epidote. The inclusions are characterized by low Mn and Nb, <0.05 and <0.015 wt% oxides, respectively, compared to typical levels of a few thousands ppm in primary titanite in the granitoids. The heavy rare earth (HREE) pattern is consistent in all rock types with a gentle negative slope. The light rare earth patterns are more erratic, but generally have a positive slope from La to Pr, possibly due to co-crystallization with allanite. The trace element composition of titanite included in growth zones in K-Feldspar phenocrysts are distinctly different from the matrix titanite. The inclusions are chemically more similar to titanite found in the granodiorite, and the matrix titanite plot among granite titanite in various discrimination plots, indicating a two-stage crystallization process. The Nb/Ta ratio plotted against the total HREE provides a fractionation trend. Titanite in a titanite-chlorite-epidote-ilmenite cluster in a granite sample is strongly zoned and host up to 5 wt% $Nb_2O_5$ and up to 1 wt% $Y_2O_3$. The relationship between the cluster and the granite is unclear, but it may be an altered mafic xenolith.

In all samples with observable carbonate veins, titanite is altered to rutile and quartz +/- calcite, and in samples exposed to significant low temperature alteration, smectite is the main alteration product, in addition to $TiO_2$ mineral(s) and quartz. This shows that titanite not only records the high temperature crystallization, but is also useful to identify low temperature fluid influx.

*References:*

[1] Scheiber T et al (2016 Terra Nova 28: 374-382
[2] Hayden LA et al (2008) Contrib Min Pet 155: 529-540
[3] Crisp LJ and Berry AJ (2022)n saturation in silicate melts. Contrib Min Pet 155

# Two types of titanites in the Precambrian granitoids of southern Lithuania, East European Craton

Demina, O.[1], Šiliauskas, L. [2] and Skridlaitė, G.[3], Næraa, T.[4]

[1]Nature Research Centre, Institute of Geology and Geography, Akademijos 2, LT-08412 Vilnius, Lithuania, olga.demina@gamtc.lt

[2] Nature Research Centre, Institute of Geology and Geography, Akademijos 2, LT-08412 Vilnius, Lithuania, laurynas.siliauskas@gamtc.lt

[3] Nature Research Centre, Institute of Geology and Geography, Akademijos 2, LT-08412 Vilnius, Lithuania and Institute of Geosciences, Vilnius University, M.K. Ciurlionio 21/27, LT-03101 Vilnius, Lithuania, grazina.skridlaite@gamtc.lt

[4] Lund University, Department of Geology, Sölvegatan 12, 221 00 Lund, Sweden

tomas.naeraa@geol.lu.se

---

The Kabeliai granite intrusion features the southernmost part of Lithuania. It belongs to the Marcinkonys complex in the Precambrian crystalline basement of Lithuania hidden by sedimentary cover [1]. The Kabeliai intrusion consists of K-Feldspar granites, biotite and muscovite bearing plagiogranites, diorites and granodiorites, alteration zones and quartz veins. The rocks contain a variety of accessory minerals including titanite which is mostly concentrated in plagioclase-dominated zones proximal to contacts with diorites and granodiorites.

A biotite bearing, altered plagiogranite from the Marcinkonys-7 drill core (M7) containing spots and clusters of titanite grains was investigated by polarizing and scanning electron microscopy (Quanta 250 with EDS) for mineral composition. The titanites were dated by means of LA-ICPMS at the Lund university, Sweden.

The studied samples come from a equigranular medium to coarse grained, leucocratic, mostly biotite-bearing granite. The granite is composed of quartz (~15-25%), plagioclase (up to 70% of oligoclase, $An_{10}$-$An_{26}$ with more than 5% of albite), biotite (5-15%, #Mg=31-43, Ti=1.7-2.9 wt.%), rare potassium feldspar (~1-3%) and muscovite. Accessory minerals are represented by titanite (up to 2-5%), zircon, apatite, rutile, magnetite, chalcopyrite, pyrite, magnetite, and bornite. Titanite is more abundant and forms clusters in the altered parts of the granite where biotite is replaced with chlorite and plagioclase is predominantly albite.

Two types of titanites can be distinguished. Euhedral, up to 4.5 mm large titanite crystals are only slightly altered, while smaller (0.3-0.8 mm), irregularly shaped titanite grains are corroded (embayed) and intergrown with rutile, magnetite and, in places, calcite. Some of the small titanite grains are enriched in Rare Earth elements (REE), i.e. they may contain up to 1 wt.% of Nd, Ce and La. Some of the calcite inclusions are also enriched in the REE.

Large, euhedral, compositionally zoned titanite crystals of the first group yielded an age of 1519 ± 5 Ma (MSWD = 6.3). This age may be considered as the intrusion emplacement age as is confirmed by euhedral shape and compositional growth zoning of the dated titanite crystals.

The smaller, irregularly shaped titanite grains adjoining the biotite replacements by chlorite or forming clusters of titanite, rutile and magnetite intergrowths have recorded an age of 1479 ± 15 Ma (MSWD=0.33). Likely, it dates the later hydrothermal reworking.

The first age of 1519 ± 5 Ma is within error with the earlier obtained (1505 ±11 Ma) crystallization age of the Kabeliai granite [1]. The second age of 1479 ± 15 Ma is consistent with the age of molybdenite mineralization in the Kabeliai granites (1486 ±5 Ma) obtained by the Re-Os method [2].

*References:*

[1] Sundblad K. et al. (1994) Mineralogy and Petrology 50:43-57

[2] Stein H. J. et al. (1998) Mineralium Deposita 33: 329±345

## Bahalda Pluton of Singhbhum Craton (eastern India) - Archean crust undisturbed for three billion years

Gumsley, A.[1], Słaby, E.[1], Dey, S.[2], Chew, D.[3], Gmochowska, W.[1], Wudarska, A.[1], Gumsley, A.P.[4], Szopa, K.[4] , Krzykawski, T.[4], Marciniak-Maliszewska, B.[5], Drakou, F.[3]

1Institute of Geological Sciences PAS, Poland, anna.salacinska@twarda.pan.pl

2Department of Earth Sciences, Indian Institute of Science Education and Research, Mohanpur, India

3Department of Geology, School of Natural Sciences, Trinity College Dublin, Ireland

4Institute of Earth Sciences, Faculty of Natural Sciences, University of Silesia in Katowice, Poland

5Faculty of Geology, University of Warsaw, Poland

---

The Bahalda Pluton is an I-type granodiorite belonging to the Singhbhum Suite (Singhbhum Craton, eastern India). The Singhbhum Suite is highly unusual among Eo- and Paleoarchean rocks because large parts of the Singhbhum Craton escaped post-magmatic deformation and metamorphism. Here, we present petrological, geochemical and geochronological results from the Bahalda Pluton, with particular focus on its accessory minerals. Accessory zircon, titanite, and apatite, when studied together, serve as a powerful tool for exploring magmatic and post-magmatic processes.

The Bahalda granodiorite was emplaced at ca. 3.35 Ga (U-Pb zircon and titanite dating) and affected by low-grade metamorphic or hydrothermal events between ca. 3.27–3.05 Ga (U-Pb apatite dating). Both titanite and fluorapatite are enriched in LREE compared to HREE. The fluorapatite has complex zonation, indicating that primary igneous fluorapatite has been recrystallized with the removal of REE and overgrown by REE-depleted rims. The fluorapatite trace element systematics indicate that the fluorapatite cores are of mafic I-type granitoid affinity, with rims of low- and medium-grade metamorphic/metasomatic origin. While no textural evidence of titanite alteration was detected, some domains have minor REE depletion compared to crystal interiors. The titanite and fluorapatite display similar trends in LREE vs Sr/Y space due to metamorphic/hydrothermal alteration. The Archean magmatic and post-magmatic evolution of the Bahalda Pluton, which did not exceed greenschist facies metamorphic conditions for 3 Gyr, invites comparison with other stabilized cratons from the Mesoarchean.

This research was funded by the IGS PAS statutory grant SANUK.

## Modern-style cold subduction in the Proterozoic: Insights from detrital rutile analysis

Lueder, M.[1], Hermann, J.[1], Pereira, I.[2], Tamblyn, R.[1] and Rubatto, D.[1,3]

[1]University of Bern, Institute for Geological Science, Baltzerstrasse 1+3, 3012 Bern, Switzerland

[2] Universidade de Coimbra, Centro de Geociências, Departamento de Ciências da Terra, Coimbra, Portugal

[3] Institute of Earth Sciences, University of Lausanne, Géopolis, Quartier Mouline, 1015 Lausanne, Switzerland

---

Earlier Precambrian, clastic sedimentary rocks may contain minerals from eroded high-pressure, low-temperature metamorphic rocks indicative of subduction, for which there is limited other unequivocal evidence in the geological record. In order to use detrital minerals as subduction tracers, peak metamorphic pressure and temperature, time of metamorphism, and source lithology (P-T-t-X) need to be estimated from single detrital grains. Rutile is a very abundant accessory mineral in the subducted oceanic crust, is stable during sedimentary processes, and is widely used as a petrogenetic indicator mineral (T-t-X), making it a prime candidate to trace subduction processes through time.

We have developed a new approach to discriminate rutile formed at cold subduction conditions from other settings, by combining in situ polarised Fourier Transform Infrared Spectroscopy (FTIR) and Laser Ablation Inductively Coupled Plasma Mass Spectrometry (LA-ICP-MS). The highest $H_2O$ contents (~500–2000 µg/g) are observed in mafic low-T eclogite-facies rutile, suggesting that H-in-rutile is a viable pressure indicator. Combined with Zr in rutile thermometry, we can use $H_2O$/Zr ratios (>4 for low-T eclogite) as a proxy for geothermal gradients (P/T) enabling tracing low T/P conditions. Source lithologies can be differentiated using Nb, W, and Sn contents, which are typically low in rutile from mafic protoliths. Because the $H_2O$ and trace element composition of rutile are preserved during sedimentation, it is possible to use detrital rutile as tracer of subduction of oceanic crust over time.

To test this novel approach, we analysed detrital rutile from the Torridon Group, Hebrides, NW Scotland, with detrital ages ranging between 1.0–1.9 Ga [1]. Some of the analysed grains show high $H_2O$/Zr ratios (~5) with low Nb+W+Sn contents (<1000 µg/g), typical of mafic low-T eclogite rutile. This indicates that low-T eclogites were exhumed, exposed and eroded in the catchment of the sedimentary basin, suggesting that modern-style cold subduction was active during the Mesoproterozoic. This combined approach can be applied to other sedimentary basins worldwide to trace modern-style cold subduction through Earth's history.

*References:*

[1] Pereira I et al. (2020) Earth Planet. Sci. Lett. 537, 116193

## Crystal mush formed and remobilized within 1 Ma: insights from glomerocryst-loaded silicic laccoliths

Pietranik, A.[1], Słodczyk, E.[1], Pańczyk, M.[2], Schaltegger, U.[3], Senger, M.[4]

[1]University of Wrocław, Institute of Geological Sciences, Pl. M. Borna 9, 50-204 Wrocław, Poland

[2]SwitzerlandPolish Geological Institute-NRI, Rakowiecka 4, 00-975, Warsaw, Poland

[3]Earth and Environmental Sciences, University of Geneva, Rue de Maraîchers 13, 1205 Geneva

[4]Arizona LaserChron Center, University of Arizona, Tucson, AZ 85721-0077, USA

---

The link between plutonic and volcanic silicic rocks resolves around the question if granites are frozen magma, or cumulate remnants after rhyolitic magma removal. The evidence is ambiguous, on one hand composition of plutonic and volcanic rocks seems similar and does not support the cumulate-magma relationship. On the other hand, primitive remnants of crystal mushes, termed glomerocrysts, are commonly entrained in evolved rhyolitic magmas. Such glomerocrysts are interpreted as early crystallized crystal cargos destroyed and incorporated by ascending more evolved magma. The cumulate nature of glomerocrysts is consistent with the presence of accessory minerals (zircon, apatite), which is taken as evidence of interstitial melt crystallization. Glomerocrysts in shallow level laccoliths or volcanic rocks may be pictured as a record of plutonic sources, however, they are not observed in the plutons themselves. It leaves us with a notion that perhaps the good records of the magmatic stage of crystallization are preserved within quickly cooled volcanic rocks.

In this study, we analysed two laccoliths from the Halle Volcanic Complex representing voluminous, post-orogenic magma formation loosely correlated with the Skagerrak-Centered Large Igneous Province magmatic activity. Both laccoliths contained numerous glomerocrysts distributed along depths of more than 500 meters. The main characteristic of the studied samples from both laccoliths was the occurrence of accessory phases, including zircon, apatite, rutile and monazite, almost entirely concentrated within glomerocrysts. Some grains were found in the matrix, but often very close to a glomerocryst suggesting that the majority of zircon and other accessories crystallized within such early crystallized portion of magma. Maps and traverses of Hf content [ppm] in zircon can be related to the degree of magmatic fractionation; they revealed complex patterns in zircon from one laccolith (Landsberg), while zircon from the Petersberg laccolith is unzoned but show very different Hf contents from one grain to the other. The CA-ID-TIMS ages of zircon were measured for ten grains with known Hf [ppm] and ranged from 298.96 to 299.58 Ma with a single grain yielding age 302.55 Ma. The older grain was the only one containing high-Hf [ppm] core, whereas the ca. 299 Ma zircon population had diverse Hf contents within the general trend of increasing Hf [ppm] towards the rim. These ages agree with the whole dataset of CA-ID-TIMS zircon ages (n=35) with the range of 293.30-302.55 Ma.

We conclude that the zircon population was dominated by grains crystallized in the mush/cumulate and it might be better recorded in the studied laccolith than in erupted rhyolites because the record was not interrupted by the eruption. However, despite the crystallization in mush and complex zoning patterns most of the zircon crystallized and were remobilized within 1 Ma.. Prolonged crystallization is only suggested for a grain that contained a core representing a more evolved stage and can be interpreted as an antecrystic or even xenocrystic component e.g. incorporated from wall-rocks. Altogether, a short crystallization and remobilization of crystal mush is suggested.

Acknowledgments: This project is supported by the Polish National Science Centre (Narodowe Centrum Nauki) grant no. UMO-2017/25/B/ST10/00180.

## New features on the use of apatite as a petrogenetic indicator in mafic layered intrusions

Kieffer, M.A.[1], Dare, S.A.S.[2], Namur, O.[3] and Mansur E.T.[4]

[1]Department of Applied Sciences, University of Quebec in Chicoutimi (UQAC), 555 Boulevard de l'Université, Chicoutimi, G7H 2B1, QC, Canada; marie.kieffer1@uqac.ca

[2]Department of Applied Sciences, University of Quebec in Chicoutimi (UQAC), 555 Boulevard de l'Université, Chicoutimi, G7H 2B1, QC, Canada; Canada Research Chair in Geochemistry Applied to Ore Deposits.

[3]Department of Earth and Environmental Sciences, KU Leuven, 3000 Leuven, Belgium

[4]Geological Survey of Norway, PO Box 6315 Torgarden, Trondheim, 7491, Norway

---

Mafic layered intrusions represent natural laboratories to investigate petrogenetic processes using the variations of trace element content in apatite. Several studies have shown that the chemistry of apatite is reliable to trace magmatic processes, such as fractional crystallisation [e.g., 1; 2] and new magma injections [3] using rare earth elements (REE), Y, the Eu anomaly and Sr. However, apatite can incorporate a wide variety of trace elements [4], that can now be readily determined by laser ablation inductively coupled plasma mass spectrometry (LA-ICP-MS). In this project, we show that additional trace elements can trace a wider range of petrogenetic processes in layered intrusions. Our dataset comprises LA-ICP-MS analyses (determined in this study and compiled from the literature) and in-situ LA-multicollector-ICP-MS analyses of Sr isotopes of cumulus apatite (this study) from well documented mafic layered intrusions (Sept-Iles, Skaergaard, Bushveld, Panzhihua, Hongge and Taihe), as well as the Sudbury Igneous Complex. These mafic intrusions record a wide variety of differentiation processes, including magma replenishment, and variable degrees of crustal contamination.

The global process of fractional crystallisation is marked by an enrichment in REE, Th, U, K and Pb, and depletion in Sr, Ba, V and Mg. As expected, we confirm that an increasingly negative Eu anomaly and decreasing Sr/Y ratio in apatite is indicative of fractional crystallisation of plagioclase. Magma mixing causes a reversal to more primitive composition, with high Sr, V, Mg and Sr/Y, and lower REE+Y, As and Na concentrations in apatite. Contamination with continental crust is expressed as high $(La/Nd)_N$, Th, U, Pb, and As, correlated with high $(^{87}Sr/^{86}Sr)_{initial}$ in apatite. Lastly, melting of a mantle source deep enough to retain Yb in garnet might be expressed as elevated $(Gd/Yb)_N$ ratio in apatite. Although all this information is usually provided by whole rock or isotope analyses, or by the mineral assemblage (i.e., plagioclase), being able to identify petrogenetic processes through apatite alone is critical in cases where the silicates are altered or lacking (e.g., massive oxide-apatite mineralisation).

*References:*

[1] Tollari N et al. (2008) Chem Geo 252: 180-190
[2] Pedersen J M et al. (2021) Contrib Mineral Petrol 176: 102
[3] Xing C-M et al. (2014) Lithos 204: 188-202
[4] Pan Y and Fleet M E (2002) Rev Mineral Geochem 48: 13-49

## Lu-Hf, Sm-Nd and U-Pb isotopic decoupling in phosphates from the Central African Copperbelt

Vincent, V.I.[1,2*], Torremans, K.[1,2], Chew, D.M.[3], Subarkah, D.[4], Fisher, C.M.[5], Gilbert, S.[6], Farkas, J.[4], Drakou, F.[3], Doran, A.L.[1,2], Collins, A.S.[4], Stacey, J.[7], and Hitzman, M.[1,2]

1. Faculty of Earth Sciences, University College Dublin, Belfield, Dublin, Ireland (victor.vincent@ucdconnect.ie)
2. SFI Irish Centre of Research in Applied Geosciences, University College Dublin, Dublin, Ireland
3. Department of Geology, School of Natural Sciences, Trinity College Dublin, Dublin 2, Ireland
4. Department of Earth Sciences, University of Adelaide, Adelaide, SA 5005, Australia
5. Department of Earth Sciences, University of Western Australia M0009, Stirling, Perth, Australia
6. Adelaide Microscopy, University of Adelaide, Adelaide, SA 5005, Australia
7. Tangila Exploration Limited, Lusaka, Zambia

---

Recent advances in collision cell (MS/MS) and multi-collector (MC) laser ablation ICP-MS technology allow for the application of multiple (e.g., U-Pb, Sm-Nd and Lu-Hf) geochronometers in direct in-situ dating of authigenic minerals. The application of these geochronometers in sedimentary basins allow for precise constrains on the timing of diagenesis, mineralization and isotopic overprinting. One such basin is the Central African Copperbelt (CACB) of Zambia and Democratic Republic of the Congo (DRC), characterised by a long-lived complex fluid flow and alteration history driven by hypersaline brines [>30wt% Ca-K-Na(Cl)] [1]. Here, we present novel in-situ triple (LA-Q-ICP-MS U-Pb, LA-MC-ICP-MS Sm-Nd and LA-MS/MS-ICP-MS Lu-Hf) dating of apatite and double (LA-Q-ICP-MS U-Pb and LA-MC-ICP-MS Sm-Nd) dating of monazite from the Lubambe, Konkola and Mingomba (formerly known as the Lubambe Extension) Cu-Co deposits. Our study tests the robustness of geochronometers in hypersaline mineralized systems and constrain primary crystallization ages for phosphates in the CACB.

Single-spot Lu-Hf ages from host rock matrix- and vein-hosted apatite return a wide array of detrital (~2500 to 1000 Ma; similar to detrital zircon U-Pb data) and authigenic ages (~870 to 600 Ma). Post-depositional Lu-Hf ages in the clastics at the base of the sequence and in the ore-bearing intervals are interpreted as recording a mix of (a) 'primary' phosphate precipitation during diagenesis, (b) phosphate precipitation concomitant with early sulphide mineralization, and (c) phosphate (re)-crystallization during later fluid-induced alteration likely related to the injections of mafic sills, halokenesis and Cryogenian deglaciation. Sm-Nd dating of apatite and monazite records broad re-equilibration of the Sm-Nd isotope systematics in phosphates during basin inversion and the regional Lufilian orogeny [2]. Similarly, U-Pb dating of apatite and monazite yield ages between 550-470 Ma overlapping with the peak of the Lufilian orogeny (~530 Ma) and post-orogenic uplift [2]. Our data demonstrate significant decoupling between the Lu-Hf, Sm-Nd and U-Pb geochronometers likely related to their different 'closure temperatures' and higher susceptibility of U-Pb and Sm-Nd geochronometers to isotopic homogenization during metasomatic events [3, 4]. The robustness of the Lu-Hf geochronometer is likely related to the relative immobility of HREE during metasomatic overprinting and high thermal closure temperatures of ~660° - 730°C [5]. Overall, our data highlights the power of the novel laser ablation Lu-Hf and Sm-Nd methods to constrain primary phosphate crystallization age(s) and subsequent metasomatic/metamorphic overprinting in complexly altered sedimentary rocks. Our data also highlights the need for caution in using U-Pb ages from phosphates to constrain the timing of primary sulfide mineralization in the CACB.

References:

[1] Hitzman., (2010) *Economic Geology 105:627-639*
[2] *Selley et al., (2018) Economic Geology Special Publication 21*
[3] *Chew et al., (2021) Minerals 11.10: 1095*
[4] Janots et al., (2018) *Chemical Geology* 484: 120-135
[5] Glorie et al., (2023) *Geological Society, London, Special Publication* 53

## The geochemical signature and trace-element remobilisation in the Prakovce-Zimná Voda REE-U-Au quartz-vein hydrothermal mineralisation developed in exocontact of rare metal granites, Western Carpathians, Slovakia

Ondrejka, M.[1], Uher, P.[1], Ferenc, Š.[2], Majzlan, J.[3], Bačík, P.[1,4], Molnárová, A.[4] and Števko, M.[4]

[1]Department of Mineralogy, Petrology and Economic Geology, Faculty of Natural Sciences, Comenius University, Mlynská dolina, Ilkovičova 6, 842 15, Bratislava, Slovakia, martin.ondrejka@uniba.sk

[2]Department of Geography and Geology, Faculty of Natural Sciences, Matej Bel University, Tajovského 40, 97401 Banská Bystrica, Slovakia

[3]Institute of Geosciences, Friedrich-Schiller University, Burgweg 11, 07749 Jena, Germany

[4]Earth Science Institute, Slovak Academy of Sciences, Dúbravská cesta 9, 840 05, Bratislava, Slovakia

---

A hydrothermal quartz vein with REE-U-Au mineralization in the Zimná Voda (Gemeric Unit, Western Carpathians, Slovakia) is associated with contact metamorphism between Permian granites and host phyllites and metaquartzites. It contains unique REE minerals of the monazite (Mnz) and xenotime (Xtm) groups. Mnz-(Ce), Mnz-(Nd), Mnz-(Sm), and Mnz-(Gd), along with Xtm-(Y) to Xtm-(Gd) and Gd-rich hingganite-(Y) show heterogeneous compositions and reflect a strong fractionation trend towards the enrichment of middle REE (MREE: Sm to Dy), particularly Gd (≤23.4 wt.% $Gd_2O_3$, 0.31 apfu Gd in Mnz and ≤29.3 wt.% $Gd_2O_3$, 0.38 apfu Gd in Xtm) [1, 2]. This exotic REE signature and precipitation of Gd-bearing minerals is a product of selective complexing and enrichment in MREE in low-*T* hydrothermal fluids by alteration of primary uraninite, brannerite, and fluorapatite on a micro-scale. This process is responsible for the strong enrichment of the MREE, especially Gd in the later minerals. The substantial incorporation of Gd into both REE-selective Mnz and Xtm structures that are accompanied by light REE (LREE) vs. heavy REE (HREE) segregation indicates the possibility of differently sized $REE^{3+}$ miscibility in $REEPO_4$ solid solutions, as well as the stabilization of the Gd-rich orthophosphate structure by substitution of the remaining A-site cations with smaller HREE+Y in the Xtm-type, and/ or larger LREE in the Mnz-type structure [1]. The existence of Xtm-Gd and Mnz-Gd is the first naturally occurring dimorphism among REE phosphates.

Beside primary hydrothermal minerals, this site hosts also assemblages of supergene minerals. Uranyl arsenates-phosphates of the autunite group together with scorodite and Sb–Bi-rich philipsbornite–segnitite-series minerals formed by oxidising fluids during decomposition and leaching of hypogene uraninite, brannerite and base-metal sulfides and sulfosalts. A progressive neutralization due to the gradual consumption of sulfides resulted in the formation of late phosphuranylite, pharmacosiderite and arseniosiderite. Goethite and other Fe oxides represent the latest hydrous ferric mineral phases and were formed after most of the As was already fixed in Fe arsenates. Antimony and Bi were taken up only into philipsbornite–segnitite and suggest unusual conditions during this process. X-ray absorption spectroscopy indicates that Sb in the philipsbornite–segnitite is fully oxidised (0.1–0.4 apfu $Sb^{5+}$, octahedral coordination on the G site). Pentavalent Sb together with the presence of ferric oxides and arsenates and uranyl minerals suggest oxidative conditions during weathering [3].

Supported by the Slovak Research and Development Agency under the contract APVV-22-0092 and VEGA 1/0563/22.

*References:*

[1] Ondrejka M et al. (2023) Am Min 108:754-768
[2] Ondrejka M et al. (2023) Min Mag 87:568-574
[3] Ondrejka M et al. (2023) Min Mag 87:849-865

# REE mineral assemblage in *REE*-fluorite masses from Kråkmo pegmatite, Tysfjord-Hamarøy area, Norway

Škoda, R.[1]

[1]Department of Geological Sciences, Masaryk University, Kotlářská 2, 611 37, Brno, Czech Republic / rskoda@sci.muni.cz

---

Masses of *REE*-fluorite (0.X to >X wt% of $REE_2O_3$) are occasionally present in NYF pegmatites, similarly to pegmatites of the Tysfjord-Hamarøy area, Norway. They are associated with the Tysfjord granites (1810-1660 Ma), and two pegmatite populations in this region were distinguished: 1) large pegmatites which were intensively deformed during Caledonian orogenesis, and 2) undeformed, amazonite-bearing rather smaller bodies [1,2].

The Kråkmo pegmatite, known as a type locality of fluorbritholite-(Ce) [3] belongs to the deformed pegmatites and forms vertical lens-shaped elongated body circa 15xX00 m long, and it is opened by an abandoned oblong pit. The pegmatite shows distinct deformation, however the characteristic textural-paragenetical units are evident. The *REE*-rich fluorite masses occur in central part of pegmatite and forms intensively sheared, flattened, and folded small (cm to dm in size) lenses located between quartz and fine- to coarse-grained albite unit, locally with biotite flakes. Fluorite is highly enriched in Y (5.1-8.7 wt%) and Σ*ln* (1.0-3.7 wt%). The fluorite masses are rimmed by a thin layer of Ca, Y enriched allanite-(Ce) with elevated $ThO_2$ (<0.5 wt%). On the other hand, actinide free allanite-(Ce), with low $Y_2O_3$ and elevated $Na_2O$ (<0.3 wt.%) locally propagates as schlieren into the central parts of the nodule along healed fractures. Gadolinite-(Y), thalénite-(Y), fergusonite-(Y) and Y-enriched uraninite (up to 21 wt% $Y_2O_3$) commonly associates in moderate to minor quantities. A spectrum of accessories disseminated in the fluorite includes common bastnäsite-(Ce) to bastnäsite -(Nd) and fluorbritholite-(Ce) and more seldom keiviite-(Y), yttrialite-(Y), thalénite-(Y), hundholmenite-(Y) like phase, rowlandite-(Y) to magnesiorowlandite-(Y), törnebohmite-(Ce), alnaperbøeite-(Ce)-perbøeite-(Ce) series, iimoriite-(Y), cayalsite-(Y), xenotime-(Y) etc. Minerals commonly show oscillatory zoning in BSE reflecting strong *REE* fractionation during the crystal growth. Peripheral allanite is more enriched in Ca and actinides than in the internal parts of *REE*-fluorite masses. Excluding uraninite and peripheral allanite, all mentioned minerals are well crystalline due to the very low actinide content. The textural relations and electron-microprobe dating of Y-rich uraninite indicates the *REE* minerals in *REE*-fluorite crystallized or recrystallized during the late Caledonian deformation. Various REE-secondary minerals were formed by subsequent processes.

[1] Müller, A et al. (2022) International Journal of Earth Sciences, 111, 987-1007.
[2] Müller, A et al. (2017) Geological Guides 6, 1-122
[3] Pekov IV, et al. (2011) Neues Jahrbuch fur Mineralogie, Abhandlungen, 191-197.

# Nb-Ta minerals in granitic pegmatites: tracers of magmatic to hydrothermal evolution (Western Carpathians, Slovakia)

Uher, P.[1], Ondrejka, M.[1], Bačík, P.[1], Broska, I.[2], Števko, M.[2,3], Georgiev, S.[4] and Kurylo, S.[5]

[1]Department of Mineralogy, Petrology and Economic Geology, Faculty of Natural Sciences, Comenius University, Ilkovičova 6, 842 15 Bratislava, Slovakia; pavel.uher@uniba.sk

[2]Earth Science Institute, Slovak Academy of Sciences, Dúbravská cesta 9, 840 00 Bratislava, Slovakia
[3]Department of Mineralogy and Petrology, National Museum, Cirkusová 1740, 193 00 Praha 9 – Horní Počernice, Czech Republic
[4]Geological Institute, Department of Geochemistry and Petrology, Bulgarian Academy of Sciences, Acad. G. Bonchev Street, Building 24, 1113 Sofia, Bulgaria
[5]Earth Science Institute, Slovak Academy of Sciences, Ďumbierska 1, 974 01 Banská Bystrica, Slovakia

---

The Nb-Ta oxide minerals represent widespread accessory phases of highly evolved, rare-element leucogranites and granitic pegmatites. Their internal textures, variations of chemical composition (major and trace elements), alteration products and geochronological age determinations are useful tools for understanding of magmatic and subsequent subsolidus (hydrothermal to metamorphic) processes and evolution of parental rocks. The LCT family, beryl-columbite subtype granitic pegmatites of Variscan basement of the Western Carpathians (Slovakia) are suitable examples of such study.

Investigated West-Carpathian beryl-columbite pegmatites are genetically related to parental orogen-related, S- to I-type Carboniferous granodiorites to granites of the Tatric Superunit. The pegmatites in granitic suites with I-type affinity (Ďumbier-Prašivá massif) contain primary magmatic Ti-enriched assemblage of Nb-Ta minerals: Fe-Nb-dominant ixiolite, columbite-(Fe), columbite-(Mn) to tantalite-(Mn), and exsolutions of Nb-Ta-rich Fe-dominant armalcolite and ilmenite in Nb-Ta-rich rutile. Conversely, the pegmatites in granites with S-type tendency (Bratislava, Bojná, Suchý and Žiar massifs) comprise primary magmatic, usually Ti-poor Nb-Ta minerals with dominant columbite-(Fe) to tantalite-(Fe), rarely columbite-(Mn) and Nb-Ta rutile, in more evolved pegmatites also with tantalite-(Mn), tapiolite-(Fe) and ferrowodginite. In-situ, LA-ICP-MS U-Pb dating of columbite-tantalite shows age interval of 360 ± 5.0 to 352 ± 8.5 Ma, coeval with determined solidification ages of the parental Variscan granitic rocks.

Post-magmatic (subsolidus) evolution stage of the Tatric West-Carpathian pegmatites is connected with their post-Variscan to Alpine hydrothermal alteration and/or low-temperature metamorphic overprint. Primary magmatic minerals were partly replaced by Ca-rich aqueous and F-bearing fluids to secondary assemblage of fersmite, members of pyrochlore supergroup (mainly fluorcalciomicrolite to hydroxycalciomicrolite, less frequently pyrochlore and roméite group phases), rarely stibiotantalite and Nb-Ta-rich titanite.

Consequently, the Nb-Ta oxide minerals represent excellent indicators of complex evolution of highly fractionated granitic pegmatites, from their magmatic solidification from residual, highly evolved magma to later subsolidus stages, including hydrothermal to metamorphic overprint during subsequent tectonic processes.

Supported by the Slovak Research and Development Agency under the contract APVV-22-0092.

# Fluorine and bismuth-bearing accessory minerals indicate magma evolution in rare element pegmatites in Embu County, Kenya

Muriungi, N.[1], Büttner, S.H.[1], Glodny, J.[2], Harder, S.[2]

[1]Department of Geology, Rhodes University, South Africa; n.kendi@outlook.com

[2]GFZ German Research Centre for Geosciences, Potsdam, Germany

---

Complex pegmatites were emplaced along a 3 x 15 km N-S trending corridor into Pan-African medium-to high-grade metamorphic rocks of Embu County, approximately 200 km NNE of Nairobi. Their ages, determined by Rb-Sr mineral isochron geochronology, range from 521-604 Ma [1]. Artisanal mining for aquamarine is well established, but recently, the extraction of coltan minerals has increased the economic significance of these pegmatites.

Here, we present SEM-EDS data for major element compositions of key minerals in the granitic pegmatites K3 and K11. These pegmatites are 2.6 km apart and formed during the same orogenic phase. Their Rb-Sr mineral isochrons indicate they are the same age (K3: 576.3 ± 6.9 Ma; K11: 576.1 ± 4.8 Ma).

The main rock-forming phases in these pegmatites are K-felspar, quartz, muscovite and biotite. Both pegmatites show beryl (aquamarine), but K3 and K11 contain different assemblages of accessory phases. K3 dominantly contains Nb-rich rare metal minerals, including columbite (~60 wt% $Nb_2O_5$ and 10% $Ta_2O_5$) and ilmenorutile ($(Ti,Nb)O_2$), containing ~26 wt% $Nb_2O_5$. K11's chemistry is more complex, showing in addition to Nb significant Ta, Y, REE, Th, U, as well as Bi and F. K11 tantalite contains ~60 wt% $Ta_2O_5$ and ~25% $Nb_2O_5$. Euxenite-(Y) with 18 wt% $Ta_2O_5$ and 17 wt% $Nb_2O_5$, also contains 18 wt% $Y_2O_3$, 7 wt% $ThO_2$ and 5 wt% $UO_2$. Bismutotantalite ($Bi(Ta,Nb)O_4$) contains ~65 wt% $Ta_2O_5$, 4 wt% $Nb_2O_5$, 11 wt% $Bi_2O_3$ and 3 wt% F. Other fluorine-bearing accessory minerals in K11 are topaz, fluorite and apatite. In addition, K11 contains accessory monazite, xenotime, thorite ($(Th,U)SiO_4$), amazonite, gahnite and bismite ($Bi_2O_3$).

The different rare metal and accessory mineral assemblages suggest that K3 and K11, despite their proximity to each other and their similar ages of emplacement, do not represent the same pegmatitic melts or the same stage of melt evolution. F and Bi typically partition into late-pegmatitic fluids, suggesting that K11 formed from a more evolved melt than K3. Fluorine mobilises U and Th [2], and the extraction of F into minerals such as topaz or fluorite may have triggered the precipitation of U and Th and other rare metals in phases such as euxenite-Y, monazite and thorite. The presence of Bi minerals also indicates a high stage of melt evolution. Bismuth is incompatible in granitic systems and mineralises in late fluids [3]. By contrast, K3 may represent a similar but less evolved pegmatitic melt in which rare elements did not reach the concentration that allowed the formation of a large variety of rare metal phases, as seen in K11.

*References:*

[1] Muriungi et al. (2024) IMSG 12 conference abstract
[2] Keppler and Wyllie (1990) Nature 348:531-533
[3] Deady et al. (2022) Ore Geology Reviews 143: 104722

## Mineralogy and petrography of Fe-Mn phosphates from the Varuträsk pegmatite, Sweden

Depret, M.[1], Hatert, F.[1], Bomal, F.[1], Langhof, J.[2] and Holtstam D.[2]

[1]Laboratory of Mineralogy B18, University of Liège, B-4000 Liège, Belgium (martin.depret@uliege.be)

[2]Department of Geosciences, Swedish Museum of Natural History, Box 50007, SE–104 05 Stockholm, Sweden

---

Iron-manganese phosphates are common accessory minerals that occur in rare-element pegmatites belonging to the LCT (Lithium-Caesium-Tantalum) petrogenetic family [1]. The Varuträsk pegmatite (Sweden) is a well-zoned and extremely differentiated pegmatite of the petalite subtype [1]. Due to the historical importance of that pegmatite, in which early phosphate transformation sequences were determined [2-3], phosphate samples stored in the Swedish Museum for Natural History, as well as new samples collected on the field, have been re-investigated.

Triphylite is the main primary Fe-Mn phosphate in Varuträsk. Chemical compositions obtained from electron-microprobe analyses show that triphylite contains significant amount of manganese, varying from 0.35 to 0.45 atoms per formula unit (Fe/(Fe + Mn) ≈ 0.56), while the magnesium content is generally very low. Triphylite is then frequently replaced by *ferrisicklerite* and heterosite during high-temperature hydrothermal alteration processes. During this replacement, the Fe/Mn ratio of primary triphylite is generally preserved. However, some *ferrisicklerite-sicklerite* show higher manganese contents reaching 0.72 atoms per formula unit, suggesting that lithiophilite also occurs as a primary phase in Varuträsk.

Some rims of montebrasite are observed around *ferrisicklerite* grains at the interface with muscovite. Alluaudite-group minerals are frequently formed by alteration of triphylite during Na-metasomatism. In Varuträsk, secondary alluaudite-type phosphates have been observed in various assemblages and under a wide range of compositions: assemblage (I) is composed of green to yellow varulite; assemblage (II) contain green hagendorfite forming unusual graphic textures with silicates (albite, quartz and tourmaline); assemblage (III) shows dark green alluaudite *sensu stricto* replacing primary triphylite ; assemblage (IV) is formed by yellow to orange fractures filled by alluaudite *sensu stricto* and cross-cutting *ferrisicklerite*.

Apatite is frequently found as a secondary phase. Some well-zoned fractures show a significant decrease of the fluorine content from the border to the core, highlighting changes in fluid composition during pegmatite evolution. Hydroxylation processes took place during the low-temperature hydrothermal transformations, and *ferrisicklerite* is then principally replaced by jahnsite-group minerals. Finally, during meteoric alteration, triphylite is locally replaced by vivianite, sometimes associated with colourless fairfieldite. LA-ICP-MS analyses were carried out on primary and secondary phosphates in order to determine the crystal-chemical and geochemical constraints governing trace-element distribution.

*References:*

[1] Černý P and Ercit T S (2005) Can Mineral 43: 2005-2026
[2] Quensel P (1937) GFF 59: 77-96
[3] Mason B (1941) GFF 63: 117-174

# Precipitation of Aluminum phosphate sulphates minerals: an experimental challenge for an environmental question.

Galán-Abellán, A.B.[1], Fernández-Barrenechea, J.[2] and Mateo-Martí, E.[3]

[1] Dpto. Geology and Geochemistry. Sciences Faculty. Universidad Autónoma de Madrid. C/ Francisco Tomás y Valiente 7, 28049 Madrid (Spain). ana.galan@uam.es

[2]Dpto. Mineralogía y Petrología. Facultad de CC Geológicas. C/ José Antonio Nováis 12, 28040 Madrid (Spain).

[3] Centro de Astrobiologia (CAB), CSIC-INTA, Dirección Postal (Carretera de Ajalvir km4, 28850 Torrejón de Ardoz, Madrid (Spain).

---

Aluminum phosphate sulphates (APS) are minerals belonging to the alunite-jarosite structural group with a general formula $AB_3(XO_4)_2(OH)_6$, where: A is a monovalent, divalent or trivalent cation (Na, K, Ca, Pb, Ba, Sr, and REE), B is occupied by divalent or trivalent cations (Al, Fe, Cu, Zn) and X is occupied by sulphur, phosphorus and occasionally arsenic [1]. The combination of these elements gives rise to a great variability of phases, related to a wide diversity of environments [2], which are still not well studied from a physicochemical point of view. Besides, there are few previous works describing the laboratory precipitation of APS [3,4,5].

Some of these minerals have been described and characterized as accessory minerals in continental siliciclastic rocks of Triassic age, which represent less than 0,1% of total weight [6,7,8,9]. These studies have revealed the presence of Ca-Sr rich APS, related to the dissolution of pre-existing detrital phosphates together with the influence of volcanic and/or marine aerosols. In addition, the abundance of these minerals coincides with an absence of organic matter or signs of biological activity in the in the siltstones and sandstones of early Triassic age, after the largest biotic extinction in Earth's history.

Thus, the interest of APS minerals lies in their complex composition and their formation conditions generally unfavourable for the development of life. Both P and S are fundamental elements for life, so their availability is key to possible prebiotic reactions. In this study, different experiments have been carried out trying to reproduce these Ca-Sr rich APS in the laboratory and so better understand their formation conditions and their relation to habitability conditions.

To reproduce the APS compositions two different experiments have been carried out: precipitation from solutions at low temperatures (40°C- 80°C) and acid pH and precipitation from precursor minerals attacked by acids. The preliminary results obtained by mixing dissolutions are fibrous crystals of calcium sulphate and rhombic crystals of strontium sulphate. The compositions change with variation of pH and temperature. As the dissolution is further acidified with hydrochloric acid, the precipitation of calcium sulphate is inhibited and that of strontium is favoured, while the increase in temperature seems to favour the incorporation into the mineral structure of other elements such as aluminium and phosphorus. The acid attack of precursor minerals indicate that the samples attacked with hydrochloric and nitric acid give rise to well-formed strontium sulphate crystals, while those attacked with hydrochloric and sulfuric acid give rise to less crystalline but more complex morphologies incorporating cations such as aluminium, lanthanum and cerium.

These results, although preliminary, are promising since they seem to point to precipitation conditions in an acid medium (pH 1-2) and at moderate temperatures, although always in the range of diagenetic conditions, which would coincide with the observations made in sandstones of early Triassic rocks.

Reproducing in the laboratory the precipitation of such complex compositions is an experimental challenge. However, a better characterization of these minerals and their physicochemical parameters may be key to better understand the sulphur and phosphorus cycles under acidic conditions, as well as their relationship with the habitability of the environments in which they occur. These environments are currently of great interest due to acidification as a consequence of climate change (ancient or actual), or even as analogues of the surface of Mars.

*References:*

[1] Jambor JL (1999). The Canadian Mineralogist 37: 1323–1341; [2] Dill HG (2001) Earth-Science Reviews 53: 35-93
[3] Ignatova L et al. (1965) Geochemistry international USSR 2: 1021- 1030; [4] Schwab RG et al. (1990) Neues Jahrbuch für Mineralogie Monatshefte 6: 241-254. [5] Schwab RG et al. (2004) Neues Jahrbuch für Mineralogie-Monatshefte 385-409
[6] Galán-Abellán AB et al. (2013a) Sedimentary Geology 289: 169-181
[7] Galán-Abellán AB et al. (2023b) Journal of Sedimentary Research 83, 406–426
[8] Borruel-Abadía V et al. (2016) Chemical Geology 429: 10–20
[9] Borruel-Abadía V et al. (2019) Chemical Geology 515: 77–86

## Titanite breakdown to rutile during the albitization of a granitoid: Natural observations and experimental results

Gumsley, A.[1], Harlov, D.[2], Juroszek, R.[3], Marciniak-Maliszewska, B.[4], Jokubauskas, P.[4] and Gerdjikov, I.[5]

[1]Institute of Geological Sciences Polish Academy of Science, Kraków, Poland, anna.salacinska@twarda.pan.pl

[2]Deutsches GeoForschungsZentrum, Potsdam, Germany

[3]Institute of Earth Sciences, Faculty of Natural Sciences, University of Silesia in Katowice, Sosnowiec, Poland

[4]Faculty of Geology, University of Warsaw, Warsaw, Poland

[5]Faculty of Geology and Geography, Sofia University "St. Kliment Ohridski", Sofia, Bulgaria

---

Petrologic and mineralogic studies of the Sakar Batholith (Strandja Zone, SE Bulgaria/NW Turkey) revealed that rutile-rich aggregates were formed during albitization at a temperature of ~600°C and 200 – 300 MPa [1]. This observation has been tested experimentally.

Four experiments involving fluid-aided alteration of titanite in a granitic system were conducted using cold-seal autoclaves on a hydrothermal line at 280 MPa and 600 °C. A series of four alkali-bearing fluids of $NaCl+H_2O$, $NaF+H_2O$, $Na_2Si_2O_5+H_2O$ and 2M NaOH were used. The starting material included crystals of titanite (Ttn) and fluorapatite (Fap) together with a mixture of plagioclase (Pl), K-feldspar (Kfs), quartz (Qz) and biotite (Bt).

Two experiments involving (1) $NaCl+H_2O$ and (2) $NaF+H_2O$ resulted in rutile (Rt) formation. Mineral assemblage formed in experiment (1) with $NaCl+H_2O$ consisted of Rt, monazite, and Ti-Th-U-oxides whereas the (2) $NaF+H_2O$ caused the formation of aggregates of Rt, Flr (fluorite), Lrz (lorenzenite) and glass.

The comparison between natural observation and experimental results support the premise that a $NaCl+H_2O$ fluid was responsible for the albitization of the Sakar Batholith.

This study presents that metamorphic/hydrothermal rutile in the granitic system can form at mid to upper crustal pressures in the presence of alkali-bearing fluids, specifically NaCl-bearing fluids. An important implication from these experiments is that rutile alone is not an indicator of high-pressure conditions, that is the formation of rutile from titanite is more a function of the chemistry of fluid rather than the P-T conditions (e.g [2]).

*References:*

[1] Gumsley A et al. (2023) Lithos 448-449, 107186,
[2] Angiboust and Harlov (2017) Am Mineral 102, 1696-1708.

# Accessory zircon as an petrogenetic indicator in granitoid rocks of the Vepor pluton (Fabova hoľa, Western Carpathians, Slovakia)

Molnárová A.[1], Ondrejka M.[2], Putiš M.[2], Nemec O.[2,]

[1]Earth Science Institute, Slovak Academy of SciencesDúbravská cesta 9, 840 05 Bratislava, Slovakia - alexandra.molnarova@savba.sk
[2]Department of Mineralogy, Petrology and Economic Geology, Faculty of Natural Sciences, Comenius University, Mlynská dolina, Ilkovičova 6, 842 15, Bratislava, Slovakia

---

The Fabova hoľa Massif and its surroundings belong to the Veporic Unit (Inner Western Carpathians, Slovakia). The structure of this part of the Veporic Unit consists of medium- to high-grade metamorphic rocks intruded by Variscan granitoids covered by Permian-Triassic sedimentary rocks. The basement and cover rocks underwent Alpine (Cretaceous) tectono-metamorphic overprinting in higher greenschist facies medium pressure conditions [1, 2].
The hypidiomorphic Variscan granitoid rocks of the Fabova hoľa Massif are represented by medium- to coarse-grained biotite (meta)granodiorites to (meta)tonalites of the Sihla type, and biotite (meta)granites to (meta)granodiorites of the Vepor and Ipeľ types. The Alpine metamorphic-mylonitic texture is grano-lepidoblastic to lepidoblastic with blastomylonitic foliation. The zircons (Zr) from all Variscan granite types are prismatic euhedral to subhedral, mostly in the size of 50-300 µm. Zircons from all analyzed samples contain dominantly light pink and transparent crystals and show crustal morphological type S, while morphological type L typical for very evolved granites was also determined. The most representative morphological subtypes acc. [3] for the Sihla granitoid type are $S_7$ in granodiorite and $S_{17}$ in tonalite and for the Vepor type are $S_8$ in granite and $S_7$ in granodiorite. Ipeľ type is distinctly more evolved phase with dominant type $L_2$ (granites). The saturation thermometry of Zr indicates a crystallization temperature in the range of 680-780 ˚C. A systematic decrease of temperature with increasing $SiO_2$ content reflects the fracrionation torwards more evolved peraluminou hybrid S/I-type varieties. Metamict light brown Zr are rarely present as well. Internal structures in zircons commonly contain zoned cores surrounded by rims showing magmatic oscillatory zoning. Individual zones reflect differences in distribution of trace elements during crystallisation of zircons. For the less fractionated Sihla type, the Zr/Hf ratio is highermost, 32-63 in the Vepor and Ipeľ granite types the Hf/Zr ratio is range of 18-64. The Th/U ratio in zircons from the Vepor and Ipeľ type granitoids vary between 0.006-1.020. The ages obtained for the granitoids of the Ipeľ type are 345 ± 2.9 Ma and 359 ± 1.5 Ma and the Vepor type shows age of 357 ± 1.3 Ma.
All of the above preliminary results suggest I-type affinity of the less differentiated Sihla type and hybrid S/I-type affinity of the granitoids of the Vepor and Ipeľ types. The Visean age of the Ipeľ type pointed out it is late and more evolved intrusive part in the Vepor pluton than more widespread Vepor type. The formation of studied Tournaisian and Visean granitoids may be related to Variscan (post)-collisional extension and are consistent with an anatectic event triggered by asthenospheric upwelling and heat input from the mantle after slab break-off in the Western Carpathians (e.g. [4]). Mapping of Ipeľ type is planned to provide.

Supported by the Slovak Research and Development Agency under the contracts *APVV-19-0065 and APVV-22-0092.*

*References:*
[1] Putiš M (1994) Mitt Osterr Geol Ges 86:83-99
[2] Plašienka D et al. (1997) Mineralia Slovaca 1-24
[3] Pupin J P (1980) Contrib Mineral Petrol 73:207-220
[4] Broska I et al. (2022) Lithos 412-413

## Garnet and vesuvianite – geochronological tools for U-Pb dating of skarns deposits

Stifeeva, M.V.[1], Salnikova, E.B.[1] and Kotov A.B.[1]

[1]Institute of Precambrian Geology and Geochronology RAS, Stifeeva.maria@yandex.ru

---

In present time non-traditional mineral-geochronometers as a garnet and vesuvianite are widely used for U-Pb studies of skarn rocks. Both minerals have a high potential as a geochronological tool because of relatively high U content and low level of common Pb. Unlike Ca-Fe garnet which is well-known source of information about the age of Fe- and polymetallic ore deposits, vesuvianite is still not sufficiently studied. Its partly related to the problem is high common lead contents or inherited radiogenic Pb in some vesuvianite samples which is a significant source of age uncertainties. U-Pb ID-TIMS studies allow to reveal multiple sources of nonradiogenic Pb and use the different methods for common Pb correction for these minerals. U-Pb study of both garnet and vesuvianite in different skarn deposits provides important constraints on its isotope system behavior and on the timing of skarn formation and staged associated with episodic fluid pulse.

The study was supported by grant No. 23-77-01051- from the Russian Science Foundation.

# Geological-paleooceanographic models of early Oligocene (Maikop) sedimentation in the Crimean-Caucasian segment of the Paratethys

Kokhan, O.M.[1], Hnidets V. P.[2]. Hryhorchuk K.H.[3], Rever A.O.[4]

[1, 2, 3, 4]Institute of Geology and Geochemistry of Combustible Minerals of the NAS of Ukraine, 3-a Naukova St., Lviv 79060, Ukraine, kohanom8@gmail.com

---

The Lower Maikop sedimentary complex was formed in a basin located on the northern (Crimean-Caucasian) periphery of the Paratethys.

At the turn of the Eocene and Oligocene, significant climatic, structural changes and hydrodynamic rearrangements occurred, and the Maikop megacycle of the Paleogene began [1]. The conditions of Maikop sedimentation within the Crimean-Caucasian segment of the Paratethys were determined by regional paleoceanographic features. The upward movements of the end of the Late Eocene caused by collisional processes in the Alpine belt led to an increase in land areas and the formation of a contrasting erosion-tectonic relief [1]. Marine conditions were preserved only in the Western and Eastern Black Sea depressions, Tuapse and Sorokin troughs [1], where mesopelagic probably existed. Epipelagic conditions were formed within the Black Sea-Crimean and Azov-Black Sea areas. The latter were separated from the mesopelagic zone by the Dobrudzhsko-Crimean-Caucasian ridge of submarine-surface uplands and the connection between them was through two straits: Pra-Kalamitska and Pra-Kerchenska located in the area of the Dobrudzhskaya and Crimean and Crimean and Caucasian uplifts, respectively.

The geological-paleogeographical model made it possible to recreate a complete picture of the sedimentation conditions of Early Oligocene deposits ithin the Crimean-Caucasian segment of the Paratethys, to localise the main sources of debris wear and to characterise the features of its supply and redistribution in the sedimentary basin.

The leading role in the supply of terrigenous material to the Azov-Black Sea and Black Sea-Crimean basins was played by different feeding provinces. In the first case, it was the Euro-Asian landmass drained by two large alluvial systems (the Pra-Don and Pra-Volga rivers); in the second case, it was the Moldovan one, from which the clastic material was supplied by three small rivers. These basins also differed in the nature of sedimentary material redistribution, which was primarily due to their different morphology [1]. The latter was more differentiated in the Azov-Black Sea basin (a number of local depressions and submarine-surface uplifts), which led to the widespread development of specific accumulative formations associated with interbasin channels.

References:
[1] Hnidets V. et al. (2023) Lithogenesis of maykop deposits of the Black Sea megadepression. Lviv. S. 1 – 192. electronic edition: ISBN 978-617-14-0159-4

# Accessory minerals as fingerprints of complex processes in volcanogenic massive sulphide systems

Volkmann, R.[1], Van Schijndel, V.[1], Codeço, M.S.[1,2], Relvas, J.M.R.S.[3] and Gleeson, S.A.[1,4]

[1]German Research Centre for Geosciences GFZ, Potsdam, Germany. e-mail: rebeccav@gfz-potsdam.de

[2]University of Arizona, Lowell Institute for Mineral Resources, Tucson, Arizona, USA

[3] University of Lisbon, Department of Geology, Lisboa, Portugal

[4] Freie Universität Berlin, Institute for Geological Sciences, Berlin, Germany

---

Volcanogenic massive sulphide (VMS) deposits contain exploitable metal contents of high economic importance and are actively mined globally. One of the most famous VMS metallogenic provinces is the Iberian Pyrite Belt (IPB), comprising multiple Cu-Zn-Pb (±Sn) deposits found in Portugal and Spain. These deposits are associated with submarine volcanism and the mobilization of metals by hydrothermal activity [1] and are hosted by Upper Devonian-Carboniferous felsic volcanic rocks, volcaniclastics, and black shales. The host units have undergone low-temperature oceanic metasomatism, alteration by the VMS hydrothermal systems, and prehnite-pumpellyite to greenschist facies metamorphism during the Variscan orogeny [2, 3]. The latter poses challenges for regional exploration with geochemical methods.

The Neves Corvo ore deposit is a unique locality in the IPB and is a major producer of Cu, Zn, and Pb. Previous studies by Relvas [4] and Relvas et al. [5] characterized the Corvo orebody as well as the footwall metavolcanic and metasedimentary rocks. They identified three main different types of mineralization: 1. stringer (or stockwork)-bearing and massive cassiterite mineralization, 2. Stringer (or stockwork) and massive sulphide mineralization, and 3. remobilized sulphide (Rubané) mineralization. Although extensive research has been conducted on ore mineralogy, ore-forming processes, and hydrothermal alteration, there is a knowledge gap regarding the superimposed complexity of metamorphic history on the surrounding host rocks. One possibility to understand the relationship between hydrothermal ore-forming processes and metamorphic alteration is to investigate accessory phases found in both mineralized and footwall rocks. Accessory phases such as phosphates, zircons, and $TiO_2$-polymorphs are common in other localities of the IPB (e.g., Codeço et al. [6]). In the Neves Corvo orebody, several accessory phosphate phases such as apatite, florencite, monazite, and xenotime were identified. Apatite was found to be a primary phase that underwent metasomatism through hydrothermal and/or metamorphic alteration [7].

Phosphate and other accessory phases can preserve distinct trace elemental and rare earth elemental (REE) patterns indicative of hydrothermal and metamorphic processes [8]. This study will focus on the phosphates and other accessory phases of the Neves Corvo footwall rocks and orebody. Microscopic textural evidence will be used to determine the paragenetic relationships of accessory phases, host rocks, and orebodies. With the help of geochemical analyses (electron microprobe analysis, X-ray fluorescence, laser ablation–inductively coupled plasma–mass spectrometry), the distinct REE patterns of the accessory minerals will be evaluated. Furthermore, O-isotopic analyses and U-Pb dating by secondary ion mass spectrometry will provide information on the fluid source and the ages of the phases.

The ultimate goal is to distinguish between hydrothermal and metamorphic processes by identifying geochemical fingerprints in the accessory phases of the Neves Corvo deposit. These characteristic fingerprints will be compared to the geochemical patterns of accessory phases in other VMS deposits and districts. If distinct trends in several deposits can be found, accessory phases will provide a new tool to unravel the complex histories of VMS ore deposits affected by metamorphism.

*References:*

[1] Galley A et al. (2007) in Goodfellow WD, ed., Geol Ass Can 5:141-161
[2] Inverno C et al. (2015) in Weihed P, ed., Min Res Rev 191-208
[3] Silva JB et al. (1990) in Dallmeyer R and Martinez Garcia E, eds., IGCP-Project 233, 416 p
[4] Relvas JMRS (2000) Unpub. PhD Thesis, Univ. Lisbon, 319 p
[5] Relvas JMRS et al. (2006) Econ Geol 101:753–790
[6] Codeço MS et al. (2018) Ore Geol Rev 98:80-108
[7] Codeço MS et al. under review, American Mineralogist
[8] Volante S et al. (2024) in van Schijndel V et al., eds., Geol Soc Lon 537

# Apatite texture characteristics in the Per Geijer Iron Oxide-Apatite-REE deposit, Sweden

Zanderink, B.B.G.[1], Krolop, P.[2], Miles A-J.[3] and Seifert T.[1]

[1]TU Bergakademie Freiberg, Freiberg, Germany, bas.zanderink@mineral.tu-freiberg.de

[2]Luossavaara Kiirunavaara AB, Kiruna, Sweden

[3]CSIRO Mineral Resources, Perth, Australia

---

The Per Geijer iron oxide-apatite (IOA)-REE deposit near Kiruna, northern Sweden, comprises a major exploration target for the Swedish mining company LKAB. Besides iron oxides in the form of magnetite and hematite, the Per Geijer deposit has an estimated 734 Mt resource grading 2.3% and 0.18% apatite-hosted phosphorous (P) and Total Rare Earth Oxides (TREO), respectively [1]. This makes the Per Geijer deposit the largest known resource of rare earth elements (REEs) in Europe. The elevated apatite content (up to 27 wt.% modally *in-situ*) and related REEs distinguishes the Per Geijer deposit from the rest of the IOA deposits in northern Sweden and most other IOA deposits worldwide. The demand for mineral fertiliser in conjunction with the global transition to renewable energy puts the Per Geijer deposit in a special position for future supply of these critical elements to the European economy. Both are included in the list of Critical Raw Materials [2]. This, in turn, has led to increased efforts at LKAB to diversify the product portfolio towards P and REEs as potential by-products of current (ReeMAP) and future iron ore mining.

Since 2018, the Per Geijer deposit is subject to intensified investigation by LKAB. Few descriptions of apatite and its characteristics in the Per Geijer deposit have been described [3,4], but more detailed information on its affiliation and general nature is needed to further develop the deposit into a mine. Currently, a detailed characterization of apatite is conducted both from a geological and a process mineralogical perspective to support internal investigations. The first step of this characterization process is the identification and classification of different apatite types based on textural variability and modes of occurrence throughout the Per Geijer deposit. Multi-scale petrographic observations from drill core to scanning electron microscopy are the framework for this categorisation. Discrimination between different textures is primarily based on the apatite grain characteristics (e.g. size, shape, fractures, and relative mineral and fluid/melt inclusion content), its association with other minerals and differing apatite-wall rock interactions.

At least six preliminary types of apatite have been identified so far from five drill cores which intersect the various types of mineralization. The identified apatite types show spatial relations to iron oxide mineralization, but to varying degrees, and do corroborate previous findings [3,4]. Furthermore, relations with other (minor) minerals and to wall rocks can be described as highly variable and complex. This highlights the importance of understanding the variability of apatite and REE, and how each type links to the wider processes that formed the Per Geijer deposit, to focus future exploration efforts. The apatite texture classification will be further utilised for conducting subsequent (micro-) analytical work on apatite mineral chemistry, fluid- and melt inclusion studies and isotopic systematics. These constraints will provide new insights in the formation of apatite in the Per Geijer deposit in corroboration with the genesis of the entire IOA system. Furthermore, the apatite texture classification will support the development of process mineralogical vectors for better understanding apatite amenability to the potential future beneficiation process.

*References:*

[1] LKAB (June 2023). Per Geijer summary, technical public report.
[2] Grohol, M., & Veeh, C. (2023). Critical Raw Materials for EU. Publications Office of the EU.
[3] Lindbom, M. (2016). MSc Thesis, Lulea University of Technology, Sweden.
[4] Krolop, P (2022). PhD Thesis, TU Bergakademie Freiberg, Germany.

# Fluorine-enriched skarn association: an evidence for fluid/rock interaction during pegmatite emplacement

Vassileva, R.D.[1], Georgieva, S.[1], Grozdev, V.[1], Cempírek, J.[2] and Škoda R.[2]

[1]Geological Institute, Bulgarian Academy of Sciences; rosivas@geology.bas.bg .

[2] Department of Earth Sciences, Masaryk University, Czech Republic

---

Numerous pegmatite bodies are intruded into the gneiss-marble-amphibolite metamorphic frame of the Rila-West Rhodope Batholith in southwest Bulgaria. In the western and central parts of the Rhodope Massif, the contacts between the pegmatites and host carbonate rocks are mostly sharp and do not record any visible metasomatic and fluid-involved interactions. However, in a locality southward of Velingrad town, skarn mineralization occurs along the pegmatite/marble contact, forming polymineral lenses and pockets of garnet, diopside, vesuvianite, wollastonite, scapolite and minor quantities of apatite, titanite, fluorite.

A complex approach involving SEM, EPMA and LA-ICP-MS revealed that the pegmatite in the studied outcrop is composed mainly by K-feldspar and albite with accessories of zircon, apatite, monazite, allanite and rare thorianite. On places nodule-like aggregates of decomposed monazite-(Ce) altered by fine-grained Th-bearing apatite are overgrown by inhomogeneous allanite-(Ce)/epidote rims. Characteristic hematite/epidote lamellae are formed by later hydrothermal alteration processes. Macroscopically, the skarns are dominated by cm-sized vesuvianite crystals and garnet masses with additional diopside, scapolite and wollastonite. BSE-observation revealed abundant apatite and titanite crystals, and fluorite/carbonate aggregates as well. Compositionally, vesuvianite is characterised by chemical inhomogeneity owing to substitutions in the *Y*-sites (Al vs. Fe, Mg, Ti). Certain amounts (in wt.%) of Na (0.15 $Na_2O$), Ti (up to 2.04 $TiO_2$), Mn (0.2 MnO), Zn (up to 0.14 ZnO), Ni (up to 0.06 NiO), and traces (in ppm) of Li (75-184), Be (65-158), V (78-207), Cr (27-139), Co (20), Ga (40), Sr (46-266), Y (23-105), Bi (68-131), Th (U (up to 139), ΣREE (reaches 1385) are detected. The measured B-content is below detection limit. Zonal grossular crystals show Al vs $Fe^{3+}$ variation and are characterised by average incorporation of Ti (0.7 $TiO_2$), Mg (0.1 MgO), Mn (0.6 MnO), P (up to 0.03 $P_2O_3$, wt. %) and traces of Li (90-120), Zn (158-201), Ga (40), Ge (30), Y (140-524), Zr (~30), HREE with predominance of Gd (16-27) and Dy (33-93, ppm). The sub- to euchedral crystals of diopside always show Mg-enriched cores (0.9-1.8 FeO; 15-17 MgO, wt. %) and rims with increased Fe (8-12 FeO; 10-13 MgO, wt. %). Diopside is characterised with trace amounts (in ppm) of Li (14-24), Sc (36-103), V (up to 350), Cr (41-146), Co (up to 73), Ni (to 170) and Zn (280-1513). Various compositions of the marialite-meionite series (0-9.56 $Na_2O$; 3.01-10.43 CaO, wt. %) reveal ppm contents of Ga (40), Rb (20), Sr (372-538). A distinct chemical feature of the studied mineralization is the fluorine-enrichment. The F-content in vesuvianite ranges 2.10-2.58 wt.%, while in associated titanite it reaches 4.55 2.74 wt.% and apatite shows full F-occupancy. Most grossular compositions are characterised by the constant F-incorporation of ~0.7, although sometimes amounts of 2.5-2.7 wt.% F are detected. Na-poor scapolite tends to incorporate more F (up to 0.13 wt. %). The only F-free mineral in the association is wollastonite. Based on the mineral and chemical composition the studied skarn association is formed in volatile-rich environment connected with the NYF-pegmatite emplacement.

*Acknowledgements*. The study is financially supported by the ERA-MIN3 PEGMAT project – grant KP-06-DO02/2 by the Bulgarian National Science Fund.

# Trace-element signatures of rare-metal accessory mineralization in Smilovene area pegmatites, Sredna Gora Mountain, Bulgaria

Georgieva S.[1], Vassileva R.D.[1], Grozdev V.[1], Cempírek J.[2], Škoda R.[2] and Stefanova E.[1]

[1] Geological Institute, Bulgarian Academy of Sciences, Acad. G. Bonchev Str, Bl. 24,
1113 Sofia, Bulgaria; sylvina@geology.bas.bg

[2] Department of Geological Sciences, Masaryk University, 611 37 Brno, Czech Republic

---

The development of high technology alongside with the growing need of critical raw materials increases the focus on detailed investigations of pegmatites as one of the essential sources of crucial elements like Li, Be, Cs, Nb, Ta, REE+Y etc. The complex geological processes on the territory of Bulgaria have resulted in the formation of numerous granite pegmatites with diverse morphology, structure, as well as mineralogical and geochemical characteristics in various geological settings, mostly concentrated in the southern regions of the country. The essential part of these pegmatites occurs in two main tectonic units: Srednogorie Zone (related predominantly to the Variscan magmatism) and Rhodope Massif (linked to the Alpine evolution on the territory).

The studied Smilovene pegmatites crop out in the Central Sredna Gora Mt. in the vicinity of the towns Koprivshtitsa and Strelcha. The irregular-shaped bodies are hosted in granites of Variscan age and are characterised as LCT pegmatites with a complex asymmetric zoning with rare-metal accessory mineralization. These pegmatite bodies consist of coarse-grained albite, oligoclase, microcline, quartz, muscovite, common accessories such as cm-sized beryl and garnet, fluorapatite, zircon, columbite, and minor samarskite-(Y), monazite-(Ce), magnetite, gahnite [1]. Late hydrothermal products as chlorite, prehnite, titanite and bertrandite were found. Using electron microprobe (EMP, Masaryk University, Brno) and laser ablation inductively coupled plasma mass spectrometry (LA-ICP-MS, Geological Institute, Bulgarian Academy of Sciences) the Smilovene beryls are characterized by low contents (in wt%) of FeO (≤0.69), $Na_2O$ (0.51), MgO (0.30), ZnO (0.07), $V_2O_3$ (0.06), CaO and F (0.04), and in ppm: Cs (≤581), Li (522), Ga (38), and Rb (23). The chemical composition of garnets reveals spessartine (54.9–52.0 mol.%), almandine (44.3–38.4), with minor pyrope (2.84–0.92), andradite (0.77–0.21), and grossular (0.84–0.17) component. Lower contents (in wt%) of $Y_2O_3$ (≤0.08), $TiO_2$ (0.09), ZnO (0.05) and $P_2O_5$ (0.2), and in ppm: $REE_2O_3$ (≤215), Li (122), Ge (64), Ga (39), Zr (34), Sc (16); and traces of Nb, Sn, Hf, Ta and U were found. Characteristic features of garnets (observed in scanning electron microscope, SEM) are oval or euhedral inclusions of apatite, monazite-(Ce), zircon, magnetite, gahnite, ilmenite, uraninite, and µm-sized Nb-bearing phases. SEM images in cm-sized zircon revealed a lot of anhedral uraninite and cheralite (≤5 µm) inclusions. The chemistry of zircon displays significant $HfO_2$ (≤9.2 wt%), and minor $UO_2$ (1.67), $REE_2O_3$ (0.76), and $ThO_2$ (0.13), and in ppm: Y (≤3091), Sc (273), Ta (207), Zn (164), Nb (147), Be (88), Li (59), V (56), and Rb (48). Fluorapatite shows almost full F-occupancy. Minor amounts of Cl (≤0.04), MnO (0.91), $Y_2O_3$ (0.08), $Ce_2O_3$ (0.05), $Gd_2O_3$ (0.07), and $La_2O_3$ (0.02) were found. The composition of monazite-(Ce) indicates dominant $Ce_2O_3$ (≤38.80 wt%), with common $La_2O_3$ (16.40), $ThO_2$ (11.37), and $Gd_2O_3$ (3.31).

In the past, Smilovene pegmatites were utilized for ceramic industry. Nowadays, considering the rising demand for critical raw materials, and given the presence of interesting Ta, Nb, REE+Y mineral association within their volumes, a detailed study of the pegmatites from this area as a potential concentrator of strategic elements is scheduled to continue.

Funding by ERA-MIN3 PEGMAT project KP-06-DO02/2 of the Bulgarian National Science Fund is acknowledged.

*References:*

[1] Ivanov IM (1991) Sofia BAS 204 pp. (in Bulgarian with English abstract)

# Monazite-(Ce) as a product of experimentally induced hydrothermal transformation of chevkinite-(Ce)

Urbanik , K. M.[1], Bagiński, B.[1] , Macdonald, R.[1], Harlov, D. E.[2]

[1]Department of Geochemistry, Mineralogy and Petrology, Faculty of Geology, University of Warsaw, Żwirki I Wigury 93, 02-089 – Warszawa (Poland), e-mail: k.urbanik2@student.uw.edu.pl

[2]Section 3-3, GeoForschungsZentrum, Telegrafenberg, 14473 – Potsdam (Germany)

---

Chevkinite group minerals (CGM), Ti-REE (rare earth element) silicates, occur in diverse parageneses, including igneous formations such as mafic gabbros to peralkaline granites, fenites, ore deposits, granulite facies gneisses, metacarbonates, and even inclusions within diamond structures[1]. Recent scientific research has placed significant emphasis on unraveling the behaviour of REE during hydrothermal alteration of alkaline rocks. A deeper understanding of these phenomena holds profound significance for elucidating the mechanisms underlying rock formation and the genesis of certain ore deposits, particularly those containing REEs.

Chevkinite-(Ce) was chosen as the subject of experiments. These experiments were conducted using a standard cold-sealed autoclave within a high-pressure hydrothermal setup, employing mineral assemblages typical of alkaline rocks and hydrothermal fluids with various compositions. Temperatures ranged from 500 to 600°C, while pressures varied from 200 to 400 MPa. The duration of the experiments spanned from 21 to 63 days. The outcomes of these experiments yielded a diverse array of mineral phases. The primary phases containing REEs synthesized were britholite-(Ce), fluorbritholite-(Ce), monazite-(Ce), and minerals of the epidote supergroup. Additionally, other mineral phases with significant light rare earth element (LREE) content, such as gagarinite-(Ce) and titanite, were also synthesized

Generally, the experimental results align well with the parageneses observed in natural settings, but with an overrepresentation of monazite-(Ce). The crystallization of monazite-(Ce) as a product of chevkinite-(Ce) is rare, and has been recognized in only a few locations, for example in the Sayan Foothills, Russia [2]

Based on the experimental findings, it is evident that the occurrence of monazite-(Ce) correlates with the presence of phosphorus-containing substrates, exemplified by Fluorapatite and $Ca_3(PO_4)_2$. Nevertheless, formation of monazite-(Ce) as an alteration produce of CGM is uncommon, presumably a result of the scarcity of P in the CGM or the metasomatising fluid.

Acknowledgements
Study was financed from the National Science Centre, Poland; grant no. 2017/26/M/ST10/00407

*References:*

[1] Macdonald R. and Belkin H.E. (2002) *Mineralogical Magazine*, *66*(6), 1075-1098.
[2] Savel'eva V.B. and Karmanov N.S. (2008). *Geology of Ore Deposits*, *50*, 681-696.

## Hexavalent Cr removal by carbonates and iron oxyhydroxides minerals in the presence the absence of organic chelating agents

Maftei, A.M.[1], Lupu, A.[1], Bulai, G., Rateau, R[2]. Rodriguez Blanco, J.D.[2] and Brinza L.[1]

[1]Department of Exact Sciences and Natural Sciences, Institute of Interdisciplinary Research, „Alexandru Ioan Cuza" University of Iași, 11, Carol I Bvd, 700506, Iași, Romania, loredana.brinza@uaic.ro

[2]The University of Dublin, Trinity College of Dublin, School of Natural Sciences, College Green, Dublin 2, Ireland

---

During minerals formation via amorphous and metastable nanoprecursors various elements are been scavenged via coprecipitation. Elements that impose risk to the environments such as toxic and heavy metals are taken up within final transformation polymorphs. Current research investigates the ability of amorphous and crystalline calcium carbonated (CC) and iron oxyhydroxides (IOH) to sequester Cr(VI) via coprecipitation from environments with acidic to basic pH (i.e., IOH from acidic to neutral and CC from neutral to basic). Guided by nature, the effect of organic compounds to minerals formation was considered. Quantitative approaches of Cr uptake via coprecipitation were addressed experimentally, and laboratory based *vs.* computational geochemical modelling approaches were considered to examine the effect of two organic chelating agents (ethylenediaminetetraacetic acid (EDTA) and ethylenediamine-N, N'-disuccinic acid (EDDS)) on Cr uptake. Morphology, structural, surface and mineralogical properties of the final coprecipitated minerals by microscopic, spectroscopic and diffraction techniques were assessed. The results showed that Cr is significantly sequestered via coprecipitation by iron oxyhydroxides (up to 80.5 mg/g) and not by carbonates (up to 1.7mg/g). However, the presence of Cr in a carbonate forming environment, rich in EDDS led to considerable change to crystalline polymorph morphology, despite the fact that it is not sequestered within their structure. The presence of organic chelating agents within coprecipitated minerals as proved by spectroscopic results, led to smaller particles of carbonates minerals with multifaced surfaces that improved surface area for further adsorption of other elements. Geochemical modelling offered information about Cr speciation within minerals and nano minerals structure and indicate that no Cr self-precipitated occurs within Cr concentration rage used, suggesting that all Cr species are sequestered within iron oxyhydroxides nanoparticles. This research brings insights to uptake processes that control Cr (bio)availability and mobility affecting its elemental cycling, including its way in trophic chain.

## Nanorocks in zircon from metamorphic rocks: a new frontier in the investigation of melt evolution

Tedeschi, M.[1], Ferrero, S.[2], Wunder, B.[3], Hermann, J.[4], Borghini, A.[5], Pettke, T.[4], Lanari, P.[4], Paiva-Silva, P.[1], Rubatto, D.[4], Van Schijndel, V.[3], Tollan, P.[6] and O'Brien, P.J.[7]

[1]CPMTC-IGC-Programa de Pós-graduação em Geologia, Universidade Federal de Minas Gerais, Belo Horizonte, Brazil; mtedeschi@ufmg.br

[2]Dipartimento di Scienze Chimiche e Geologiche, Università di Cagliari, Monserrato, Italy

[3]GFZ German Research Centre for Geosciences, Telegrafenberg, 14473, Potsdam, Germany

[4]Institut für Geologie, Universität Bern, 3012 Bern, Switzerland

[5]Faculty of Geology, Geophysics and Environmental Protection, AGH University of Kraków, Kraków, Poland

[6]Eidgenössische Technische Hochschule, ETH, Zürich, Switzerland

[7]Institut für Geowissenschaften, Universität Potsdam, Potsdam, Germany

---

Partial melting and melt evolution and migration play an important role in the differentiation of continental crust. These processes affect metal transport and concentration, volatile cycling, and the mechanical properties of the crust. The study of nanorocks, i.e. crystallised melt inclusions [1], has emerged in recent decades as a key approach in the investigation of melt evolution, as these inclusions are considered to retain pristine melt information [2]. While, most research has been carried out on nanorocks in garnet, melt inclusions in zircon are of growing interest because (i) none of the nanorock-forming major elements except $SiO_2$ are present in the host, (ii) zircon is formed by different (re)crystallization processes, and could therefore potentially record different stages of a metamorphic evolution, and (iii) the possibility of obtaining spatially resolved ages of the host.

Garnet-free granulites from the Guaxupé nappe (Brazil) record a complex history from protolith crystallization at ca. 2.55 Ga to ultra-high temperature (UHT) metamorphism at ca. 650-590 Ma [3]. The zircon crystals contain crystallized melt inclusions ranging in size from 1 µm to 15 µm distributed in cores and rims. MicroRaman spectroscopy combined with field emission gun electron probe microanalysis revealed that these inclusions consist of variable combinations of cristobalite/quartz, kokchetavite, kumdykolite, "phase 430", carbonate and, biotite and/or white mica. The re-homogenized nanorocks have a metaluminous to peraluminous composition, varying from granodioritic to granitic. These results were compared with the composition of stromatic granulite from quantitative micromaps and bulk rock of outcropping segregated leucosomes. Trace element (TE) data show an enrichment of Rb, Cs, Ba and LREE in the nanorocks relative to the leucosomes. The lower concentration of CaO, MgO, $P_2O_5$ and $TiO_2$ and the TE signature suggest that the nanorocks represent melts formed at lower temperatures than those formed during UHT conditions recorded in the leucosomes. Thus, the nanorocks may have been trapped in zircon during prograde metamorphism. This hypothesis is consistent with the CL images and the U-Pb (LA-ICP-MS) data, which show that the nanorocks are hosted in zircon domains recording discordant dates in line with partial resetting of Archean ages, rather than being formed during UHT metamorphism in the Neoproterozoic. The homogeneous composition of the inclusions and their location in cores and rims, disfavour the interpretation that the nanorocks record igneous crystallization.

*References:*

[1] Bartoli & Cesare (2020) Rendiconti dei lincei 31:249-257
[2] Cesare B et al. (2015) Lithos 239: 186-216
[3] Tedeschi et al. (2018) Precambrian Research 316: 103-126

# Multi-method geochronology (Lu–Hf, Rb–Sr and U–Pb) to unravel the evolution of complex metamorphic terranes

Bedoya, A.[1,2], Glorie, S.[1,2], Hand, M.[1,2], Kirkland, C.L.[3], Kelsey, D.E.[4], He, X.F.[5,1] and Kharkongor, M.B.[1]

[1]Department of Earth Sciences, School of Physical Sciences, The University of Adelaide, SA 5005, Australia. Corresponding author email: alejandra.bedoyamejia@adelaide.edu.au

[2]Mineral Exploration Cooperative Research Centre, School of Earth & Environmental Sciences, University of Adelaide, Adelaide, Australia.

[3]Timescales of Mineral Systems Group, School of Earth and Planetary Sciences, Curtin University, WA 6102, Australia.

[4]Geological Survey of Western Australia, WA 6004, Australia.

[5] School of Geosciences and Surveying Engineering, China University of Mining and Technology, Beijing 100083, China.

---

The thermal evolution of metamorphic belts is often studied by phase equilibria P–T–t modelling, accompanied by petrochronology. However, thermal histories can be complex and multiple overprinting events make establishing unique relationships between dates, rates, and P–T events challenging.

The Rudall Province (RP) is a Palaeo- to Mesoproterozoic metamorphic belt on the eastern edge of the West Australian Craton (WAC) [1,2]. Positioned on the edge of the ancient Pilbara craton the RP represents a key area for understanding the Proterozoic assembly and subsequent tectonic history of Western Australia. Several studies have provided constraints on the Palaeoproterozoic to early Mesoproterozoic amalgamation history; however, much of the subsequent thermal history is yet to be linked to age constraints. Here, we utilised geochronometers with different closure temperatures to establish a more comprehensive thermal history of the region via a range of dating methods. We present new *in situ* garnet and apatite Lu–Hf, muscovite Rb–Sr, and apatite, titanite and rutile U–Pb dates for 23 samples in the RP. Garnet and apatite Lu–Hf dates range between c. 1.76 and 1.26 Ga. Titanite U–Pb dates range between c. 1.36 and 1.33 Ga, apatite and rutile U–Pb dates range between c. 1.36 and 1.26 Ga and muscovite Rb–Sr dates range between c. 1.23 and 1.16 Ga. The different growth and closure temperature behaviour of these thermochronometers track a sequence of events during the metamorphic evolution of the terrane.

Our data indicate that the Palaeoproterozoic crust of the RP has undergone at least two episodes of reworking: (1) at c. 1.40 to 1.26 Ga, represented by the metamafic lithologies mainly in the SE of the RP, consistent with the timing of the Parnngurr Orogeny [3], and (2) at c. 1.32 to 1.22 Ga, represented by the schist lithologies and preserved in the NW. Additionally, an older event of c. 1.76 Ga was identified by the garnet Lu–Hf system suggesting metamorphism at the eastern margin of the WAC occurred prior to the WAC–North Australian Craton amalgamation. P–T modelling will be presented that is temporally constrained by isotopic datasets.

*References:*

[1] Bagas L (2004) Precambrian Res 128:475-496
[2] Lu Y et al. (2022) Geology 50:1202-1207
[3] Gardiner NJ et al. (2018) Precambrian Res 313:31-50

## Raman spectroscopy as a tool to measure stress-induced deformation in garnet

Gilio*, M.[1,2], Toffol, G.[3], Pennacchioni, G.[3], Campomenosi, N.[4], Mihailova, B.[1] and Alvaro M.[2]

[1]Mineralogisch-Petrographisches Institut, Universität Hamburg, Hamburg (DE)

[2]Department of Earth and Environmental Sciences, University of Pavia, Pavia (I)

[3]Department of Geosciences, University of Padova, Padova (I)

[4]Department of Earth, Environmental, and Life Sciences, University of Genova, Genova (I)

---

Most of the energy released during an earthquake is consumed within the fault zone by friction, fracturing and crystal straining, with a secondary portion radiated as seismic waves. The propagation of the earthquake rupture induces intense plastic deformation within the fault zone, measurable via High-Resolution Electron Backscatter Diffraction (HR-EBSD), which reveals a progressive increase in dislocation density within wall-rock minerals at decreasing distance from the fault slip zone [1].

The Raman spectrum of garnet is generated by three symmetrically different types of modes: non-degenerate A, doubly degenerate E and triply degenerate T modes. The intensity of the corresponding Raman peaks depends on the scattering geometry, i.e. on the crystal orientation with respect to the direction of propagation the incident light and scattering light as well as on the polarization of the incident and scattered light. The cubic Raman-active $A_{1g}$ modes of garnet, occurring near 350, 556, and 914 $cm^{-1}$ for almandine-rich garnets [2], exclusively contribute to parallel-polarized spectra (HH), regardless of the crystal orientation. Conversely, E and T modes may contribute to both parallel-polarized and cross-polarized light (VH), depending on crystal orientation relative to the scattering geometry. Ideally, the depolarization ratio ($I_{VH}/I_{HH}$) of the $A_{1g}$ modes of garnet should be zero. However, due to experimental imperfections, there may be a $A_g$-signal leakage in the VH spectra and by measuring the $I_{VH}/I_{HH}$ value from pristine garnet one can define the instrumental “zero”. Nevertheless, the ratio should remain negligibly small in the absence of structural deformation. This approach has been successfully applied to quantify the reduction of garnet symmetry due to small elastic strains near pressurized inclusions [3].

Here we demonstrate that the same strategy can be used to track the occurrence of plastic deformation in garnet. We measured the depolarization ratio of fractured garnets at progressive distances from a pseudotachylyte vein from the hanging wall of the Woodroffe Thrust (Musgrave Ranges, central Australia), at locations previously examined using HR-EBSD by Toffol [1]. Regions exhibiting high dislocation density in the HR-EBSD maps generally corresponded to a strong deviation from cubic symmetry in garnet as indicated by $(I_{VH}/I_{HH})_{915}$ that significantly exceeds the instrumental “zero”. Moreover, the peak positions of all modes remained constant, indicating the absence of substantial elastic strains in the crystal and consequently, no significant elastic stresses acting on the mineral grain [4]. Although HR-EBSD generally exhibits better spatial resolution than confocal Raman spectroscopy, our work shows that Raman spectroscopy can be used as a complementary method for rapidly and accurately assessing stress-induced plastic deformation in garnet.

*References:*

[1] Toffol G et al. (2024) Sci Adv 10(9)
[2] Kolesov BA and Geiger CA (1998) Phys Chem Miner 25(2): 142-151
[3] Campomenosi N et al. (2020) Contrib Mineral Petr 175:1-16
[4] Angel RJ et al. (2019) Z Krist -Cryst Mater 234(2):129-140

# Applying U-Pb calcite direct dating by LA-ICP-MS mapping to investigate shallow crustal deformation histories in Ireland

V. Monchal[1], K.Drost[1] and D.Chew[1]

[1]TCD Department of Geology, Trinity College Dublin, Dublin 2.

---

The near ubiquitous presence of carbonate in supracrustal rocks and the intimate association carbonate fracture fills with deformed carbonate successions has long made carbonate a desirable mineral phase for geochronology studies [1]. However direct dating of carbonates by the U-Pb method faces major challenges, such as unfavourable μ ($^{238}U/^{204}Pb$) ratios due to low U and/or high initial Pb along with potential later resetting by fluid ingress or neocrystalisation. This project employs a Laser Ablation - Inductively Coupled Plasma - Mass Spectrometry (LA-ICP-MS) mapping approach [2] to U-Pb in-situ geochronology with simultaneous acquisition of trace elemental data. The resultant 2D isotopic and elemental maps may be complemented by spatially-registered optical petrography, electron backscatter diffraction (EBSD) or scanning electron microscope (SEM) imagery. The method presented herein can potentially overcome some of the challenges inherent to U-Pb carbonate geochronology detailed above. For example when applied to calcite veins, the approach allow the isolation of small-scale growth zones with favourable μ ratios and with homogeneous chemical compositions that are likely age homogenous.

We have applied U-Pb calcite dating to structures in three regions in Ireland that are all assumed to Variscan in age, despite being north of the putative Variscan "front". All structures have associated vein sets are are developed in Lower Carboniferous limestones; the distance north of the Variscan front is also indicated: 1) chevron folds in the Carboniferous Dublin Basin (200 km), 2) the Kilfenora anticline in Co. Kerry (15 km) and 3) gentle monoclines in the Burren region, Co. Clare (110 km). In the Dublin Basin, Variscan ages are only partly preserved due to subsequent Cenozoic opening of the U-Pb system. The majority of veins (including bedding-parallel veins with slickenfibres indicative of flexural slip and N-S contraction) yield late Eocene ages, with evidence for protracted flexural slip for at least c. 4 My during late Eocene times that we interpret as related to far-field Alpine/Pyrenean tectonism [3]. At localities Fenit and the Burren in southwestern Ireland, Variscan ages are better preserved. Unequivocal evidence of Paleocene N-S contraction was provided by bedding-parallel slickenfibre veins indicative of flexural slip on the limb of the Kilfenora anticline at Fenit, which we attribute to Pyrenean shortening. A N-S trending, vertical vein set yielding Miocene ages is found at several localities in Fenit and the Burren indicative of either N-S shortening or E-W extension; the former is favoured and attributed to Miocene Alpine far-field stresses. Surprisingly, a regional trend of tectonic quiescence from the Early Permian to Early Cretaceous is revealed by the entire Irish sample set (including additional dated veins from central Ireland), with no veins growth or reactivation detected during this extended time period. Given the paucity of post-Variscan markers (e.g., dikes or sills, Mesozoic–Cenozoic cover sequences) in Ireland, calcite U-Pb geochronology represents the only feasible approach to reconstruct the post-Variscan deformation history of the Irish landmass.

*References:*

[1] Jahn and Cuvellier, 1994, Chemical Geology
[2] Drost et al., 2018, $G^3$
[3] Monchal et al., 2023, Geology

# Decoupled behaviour of $^{40}Ar$ and $^{87}Sr/^{86}Sr$ during deformation of metamorphic white mica in a high-pressure marble

Barnes, C.J.[1], Zack, T.[2,3], Bukała, M.[4], Dubosq, R.[5], Camacho, A.[6], Gerdes, A.[7], and Rösel, D.[2]

[1]Institute of Geological Sciences, Polish Academy of Sciences, Kraków, Poland (cjbarnes063@gmail.com)

[2]Department of Earth Sciences, University of Gothenburg, Gothenburg, Sweden

[3]Department of Earth Sciences, University of Adelaide, Adelaide, Australia

[4]Instituto Andaluz de Ciencias de la Tierra (IACT), CSIC and Universidad de Granada, Armilla, Spain

[5]Max-Planck-Institüt für Eisenforschung GmbH, Düsseldorf, Germany

[6]Department of Earth Sciences, University of Manitoba, Winnipeg, Canada

[7]Frankfurt Isotope and Element Research Center, Goethe-Universität Frankfurt, Frankfurt am Main, Germany

---

A micaceous marble was obtained from the Middle Allochthon, northern Scandinavian Caledonides, that records eclogite-facies metamorphism (2.4-2.6 GPa/590-660°C) at c. 486-481 Ma. Subsequent deformation at lower amphibolite/greenschist facies conditions occurred during emplacement of the overlying Upper Allochthon at c. 435-420 Ma. The fabric in the marble is related to the latter event, and is defined by shape-preferred orientations of white mica and calcite. It also contains minor quartz and titanite, as well as plagioclase porphyroblasts that include non-oriented white mica. The physical and chemical properties of all three mica types were characterized by: 1) transmitted light microscopy, 2) electron channelling contrast imaging, 3) electron backscatter diffraction analysis, 4) conventional back-scattered electron imaging, 5) quantification of major/trace element chemistry, and 6) boron stable isotope analysis. The collective results demonstrate that the matrix white mica were deformed during foliation development but remained chemically closed, preserving the eclogite-facies composition with no differences compared to undeformed white mica inclusions in plagioclase. Furthermore, individual white mica matrix grains exhibit widespread cleavage-parallel lenticular microfractures and sporadic micro-undulations of the crystal lattice intermediate to the microfractures. The boundaries of the micro-undulations are cleavage-normal, defined by low-angle misorientations, and terminate against the microfractures. The commonality of the microfractures throughout the white mica suggests an origin intrinsic to the white mica properties. Chemical analysis of the mica revealed that 83-96 % of the interlayer cation site is occupied by K, 3-9 % by Na, 0-3 % by Ca, and 0-13 % of sites are vacant. Thus, the microfractures are postulated to manifest variable interlayer cohesion resulting from chemical heterogeneity of the interlayer cation site. The spatial relationship of the lattice micro-undulations with the microfractures suggests that the latter act as slip plane to nucleate crystal lattice strain. Results of *in situ* white mica $^{40}Ar/^{39}Ar$ geochronology provided a dispersion of dates from 486 ± 4 Ma to 428 ± 4 Ma with finer grains producing younger dates, indicating $^{40}Ar$ loss from white mica due to deformation. In contrast, all *in situ* Rb/Sr dates reproduce the timing of eclogite-facies metamorphism, providing a weighted average of 485 ± 3 Ma, showing that Sr was immobile during deformation. Therefore, the defect networks of microfractures and lattice micro-undulation boundaries are interpreted as diffusion pathways that promoted $^{40}Ar$ loss during deformation, in contrast to Sr that remained immobile in the lattice structure.

Research funded by NCN grant no. UMO-2021/40/C/ST10/00264 (C.J. Barnes), supported by “Juan de la Cierva” Fellowship JFJC2021-047505-I by MCIN/AEI/10.13039/501100011033 and CSIC (M. Bukała)

## Coupling apatite and zircon petrochronology to reveal (U)HP to retrograde metamorphic evolutions of eclogites from the Scandinavian Caledonides

Jaranowski, M.[1*], Budzyń, B.[1], Barnes, C.[1], Majka, J.[2,3], Sláma, J.[4], Kozub-Budzyń G.A.[3], Roddatis, V.[5], Wirth, R.[5], Schreiber, A.[5], and Kośmińska K.[3]

[1] Polish Academy of Sciences, Institute of Geological Sciences, Kraków, Poland; *e-mail: ndjarano@cyf-kr.edu.pl

[2] Uppsala University, Department of Earth Sciences, Uppsala, Sweden

[3] AGH University of Krakow, Faculty of Geology, Geophysics and Environmental Protection, Kraków, Poland

[4] The Czech Academy of Sciences, Institute of Geology, Prague, Czech Republic

[5] GeoForschungsZentrum Potsdam (GFZ), Section 3.5 Interface Geochemistry, Potsdam, Germany

---

Five eclogite samples from three separate locations within the Scandinavian Caledonides were selected: two from the Lofoten Archipelago (Lofoten-Vesterålen complex - LVC), two from Northern Jämtland (Lower Seve Nappe - LSN) and one sample from the Nordøyane Archipelago (Blåhø Nappe). In order to resolve the metamorphic evolution of the eclogite samples, coupled petrochronological research of zircon and apatite was conducted using laser ablation – inductively coupled plasma mass spectrometry, electron probe microanalysis, transmission electron microscopy , and whole rock analysis.

Rare earth element composition and internal zonation of zircon grains revealed by cathodoluminescence imaging distinguished between metamorphic and inherited domains in the grains where they occurred. U-Pb dating of inherited zircon domains provided information about the protolith rocks of LVC and LSN eclogite samples. Metamorphic zircon domains from the collective eclogites date different events along the pressure-temperature pathways for the different regions. Zircon geochronology resolves the timing of prograde metamorphism in eclogites from the LVC at 427.8 ± 5.7 Ma, and in one eclogite from the LSN at 467.2 ± 5.9 Ma. A zircon age representing retrograde metamorphism at 444.5 ± 5.5 Ma is yielded by the second eclogite from the LSN. In contrast, protracted high-grade metamorphic event(s) from ca. 430 to 395 Ma are recorded in the Blåhø Nappe eclogite.

Geochemical and geochronological analyses of apatite grains constrained the timing of the late metamorphic stages or cooling during exhumation. In three out of five eclogite samples, apatite characteristics indicate that metasomatic alteration occurred. For the LVC eclogites, apatite U-Pb dates of ca. 354–322 Ma represent retrogressive metamorphism and fluid-induced alteration during exhumation. The dates of 436 ± 18 Ma and 415 ± 25 Ma, yielded by apatite from the two LSN eclogites respectively, potentially correspond to separate exhumation stages, with apatite in one of the samples bearing characteristics of a fluid alteration. The 390 ± 12 Ma date of apatite from the Blåhø Nappe eclogite resolves cooling of the eclogite after periodic or prolonged (U)HP-HT metamorphism with unique apatite geochemical characteristics suggesting that apatite growth occurred during the prograde stage of metamorphism, supported by the presence of apatite nanoinclusions in zircon.

In summary, this work demonstrates the high potential for applying coupled petrochronology of zircon and apatite from eclogites in order to reconstruct the metamorphic histories of (U)HP terranes.

Acknowledgements: This work has received funding from the IGS PAS Research Funds “Petrochron”and the European Union’s Horizon 2020 research and innovation programme under grant agreement No 101005611 for Transnational Access conducted at Helmholtz-Zentrum Potsdam Deutsches GeoforschungsZentrum (GFZ)

## How is a polyepisodic magmatic and metamorphic history recorded in zircon (Aar and Gotthard units, central Alpine basement)

Schaltegger, U.[1], Noroña, E.[1], Ulyanov A.[2], Berger, A.[3], Abrecht, J.[4], Spikings R.[1] and Wiederkehr, M.[5]

[1]Earth Sciences, University of Geneva, rue des Maraîchers 13, Geneva, Switzerland; urs.schaltegger@unige.ch

[2]Institute of Earth Sciences, University of Lausanne, Géopolis, Lausanne

[3]Institute of Geology, University of Bern, Baltzerstrasse 1-3, Bern, Switzerland

[4]Dahlienweg 5, Jegenstorf, Switzerland

[5]Swiss Geological Survey, Federal Office of Topography, Swisstopo, Wabern, Switzerland

---

The Alpine basement records a ca. 600 Ma-long evolution in various geodynamic settings. The Aar massif (AM) and the Gotthard nappe (GN), appear as tectonic windows beneath the Alpine nappe pile and were not or only marginally deformed during nappe thrusting. They present the most complete and undisturbed record of the pre-Alpine tectonic, metamorphic and magmatic history in the Central Alps (Switzerland). In this contribution we report new laser ablation (LA) ICPMS U-Pb age determinations and interpret them in terms of growth textures observed by cathodoluminescence (CL) imaging. Samples are spread along a 35 km-long transect from northern AM to southern GN perpendicular to the dominant Alpine and Variscan NE-SW strike. We will concentrate on the importance and extent of Ordovician (ca. 480-445 Ma) and Variscan (ca. 350-295 Ma) episodes, and how they are recorded by the mineral zircon and by its U-Pb isotopic system. We dated high melt-fraction migmatites, ranging from layered and diatectic gneisses to granitoids.

All studied lithologies are invariably dominated by Ordovician-age zircon, occurring as (i) thick oscillatory-zoned (OZ) thick rims overgrowing ubiquitous Neoproterozoic (~600-800 Ma) cores; (ii) as entire OZ and sector-zoned (SZ) grains of magmatic appearance, or as (iii) OZ and SZ cores overgrown by thin, partly OZ and low-CL rims of younger age. Mean weighted $^{206}Pb/^{238}U$ ages from marginal OZ zones of several samples from both AM and GN cluster very reproducibly between 447 and 455 (± ~2-3 Ma internal error). This result points to a common UHT event preserved in the AM and GN basement producing diatectic migmatites and granitoids. We infer that our dating results and the rock textures point to melting of N. Gondwana active margin sequences at high temperatures in Ordovician times [1], which however preserved the Neoproterozoic inherited cores derived from detrital sediment infill in possibly Cambrian forearc sedimentary basins.

During the Variscan orogeny, multiple pulses of voluminous magmatism intruded between 350 and 295 Ma into these units in both AM and GN [2], pre- and postdating the peak of Variscan metamorphism. One of the main outcomes of this study is the astonishingly subordinate impact of the Variscan cycle, which occurs in all studied lithologies but is reflected by thin zircon overgrowths only. Variscan U-rich thin rims epitactically overgrew Ordovician and Neoproterozoic cores and can be dated successfully using a 12 µm spot size laser beam. Partial lead loss due to decay-damage yields scattering ages between ~450 and 320 and below 300 Ma, as well as cores being younger than rims in some cases. This partial lead loss may occur during both Variscan and Alpine overprints.

*References:*

[1] Zurbriggen (2015) Intern J Earth Sci 104: 335-350
[2] Ruiz M et al. (2022) Swiss J Geosci 115:20

## Dating metamorphism and metasomatism in the mantle

Kotková, J.[1,2], Čopjaková, R.[2], Millonig, L.J.[3], Marschall, H.[3], Gerdes, A.[3], Kutzschbach, M.[4]

[1]Czech Geological Survey, Klárov 3, Prague 1, Czech Republic, jana.kotkova@geology.cz

[2]Department of Geological Sciences, Masaryk University, Kotlářská 2, 61137 Brno, Czech Republic

[3] FIERCE, Goethe University Frankfurt, 60438 Frankfurt am Main, Germany

[4]TU Berlin, Institut für Angewandte Geowissenschaften, Ernst-Reuter-Platz 1, 10587 Berlin, Germany

---

Orogenic garnet peridotites in convergent orogens encapsulate multiple processes linked to deep subduction and crust-mantle interaction. However, dating these processes is challenged by temperatures that exceed those of the common geothermometers. Incorporation of U, Th and REE in garnet along with the advancement of in-situ analytical techniques enables garnet chronology. At the same time, REE distribution between garnet and other mantle phases allows petrological constraining of multiple mantle processes.

We used trace element data for garnet and clinopyroxene to assist in the interpretation of in-situ LA-ICPMS garnet U-Pb dating of garnet peridotites and garnet pyroxenite from the Saxothuringian domain of the Bohemian Massif, European Variscan Belt. The dating yielded three distinct ages of approximately 390, 360 and 340 Ma. The oldest age for a large U-poor garnet (≤0.01 µg/g U) with preserved Lu zoning is interpreted as garnet growth during prograde metamorphism. The date of approximately 360 Ma is recorded by inclusion-free garnet cores with low homogeneous concentrations of U (≤0.1 µg/g), Th and LREE, crystalized at ≥1000 °C/4.4–5.7 GPa [1]. Coeval early metasomatism due to infiltration of carbonated silicate melt is documented by the similar age of garnet pyroxenite, crystallized in the melt channel. Finally, the second metasomatic event at approximately 340 Ma is recorded by newly grown garnet rims enriched in U (≤2.7 µg/g), Th and LREE. The presence of numerous multiphase solid inclusions (MSI) [2] and slightly lower calculated pressure for this rim domain [1] suggest carbonated peridotite melting at initial decompression. Trace element concentrations on profiles through garnet along with distribution maps of U, Th and Ce were acquired to elucidate garnet evolution and to confirm different garnet generations. The distribution maps clearly show U-Th-poor cores, cut, rehealed and overgrown by the newly formed U-Th rich metasomatic garnet. No inclusions of U- or Th-bearing phases were found.

The finding of distinct ages of approximately 360 and 340 Ma within a single thin-section and even within distinct domains of individual garnet precludes resetting of the older U-Pb ages. This provides evidence for the very high temperature of age retention of the U-Pb isotope system in garnet, extending the earlier minimum estimates for the closure temperature of this geochronometer to more than 1000 °C. The age of approximately 390 Ma ads to yet rare Lu-Hf (Grt-Cpx-WR) ages for less metasomatized garnet peridotites of the Kutná Hora Crystalline Complex and German Erzgebirge, providing evidence for Devonian mantle subduction in the early stages of Variscan orogeny in the Bohemian Massif [3]. We conclude that Lu-Hf method can be successfully used for unravelling early high-temperature events in peridotites with low-U garnets and lacking younger metasomatism-related phases (clinopyroxene). By contrast, U-Pb garnet dating represents an excellent technique for deciphering multiple events in strongly metasomatized peridotites with garnet enriched in uranium.

*References:*

[1] Haifler J et al. (2024) Contrib Mineral Petrol 179: 31

[2] Kotková et al. (2021) Lithos 398-399: 106309

[3] Ackerman et al. (2020) J Petrol 61: 1-31

## Stabilization hiatus of the North China Craton revealed by microsampling garnet geochronology on single xenoliths

Du, K.Y., Cheng, H. and Yang, R.Y.

State Key Laboratory of Marine Geology, Tongji University, Shanghai 200092, China.
chenghao@tongji.edu.cn (Cheng, H.)

---

Xenoliths, sourced from the lower cratonic crust and transported to the Earth's surface within volcanic rocks, offer unique insights into the formation and destruction of cratons. Age determinations play a crucial role in constructing the thermal history of cratons. However, the accuracy of dating is challenged by the xenoliths' prolonged exposure to high temperatures and their intricate thermal histories. Specifically, the effects of protracted lower crust residency and entrainment heating on the Sm–Nd and Lu–Hf systematics are yet to be explored. Six xenoliths hosted in the Mesozoic dioritic porphyry from the eastern margin of the North China Craton were sampled from centre to edge using micro-drilling/sawing techniques. These xenoliths exhibit a granoblastic texture, with minerals that are mostly unzoned. Thermobarometric calculations suggest granulite-facies metamorphism equilibration at temperatures of ~750 °C and pressures of 1.2–2.0 GPa. Consistent Lu–Hf ages and U–Pb ages of *ca*. 1.7 Ga, obtained from garnet and zircon in chemical equilibrium, are attributed to granulite-facies metamorphism. The Lu–Hf and Sm–Nd dates are indistinguishable across all concentric zones within each xenolith, while Sm–Nd dates are consistent ~1.0 Ga older than the corresponding Lu–Hf ages. This discrepancy suggests a complex history for this section of the lower cratonic crust, marked by a high-grade metamorphic event around 1.7 Ga, followed by prolonged cooling. A significant heating event during the Tonian, likely due to regional mantle plume activity, is inferred to have partially or completely reset the Sm–Nd isochrons, thereby decoupling the Sm–Nd system from the Lu–Hf and signifying a stabilization hiatus of the North China Craton. The Mesozoic entrainment heating event appears to have had minimal influence on the Lu–Hf and Sm–Nd systematics. Our data highlight the potential of coupled microsampling Lu–Hf and Sm–Nd chronology on individual xenoliths to reveal tectonic episodes within the lower crust that might be undetected by accessory mineral U–Pb geochronology.

## Petrochronology reveals extremely slow cooling of granulites in the Dniester–Bouh Domain, Ukrainian Shield

Shumlyanskyy, L.[1,2], Wilde, S.A.[2], Johnson, T.[2], Alfing J.[2], Jourdan, F.[2], Lisna, I.M.[3], Stepanyuk, L.M.[3]

[1] Institute of Geological Sciences, Polish Academy of Sciences, Kraków, Poland, lshumlyanskyy@yahoo.com

[2] School of Earth and Planetary Sciences, Curtin University, Perth, Australia

[3] M.P. Semenenko Institute of Geochemistry, Mineralogy and Ore Formation, Kyiv, Ukraine

---

The Dniester-Bouh Domain of the Ukrainian Shield comprises at least three tonalite-trondhjemite-granodiorite associations, various mafic and ultramafic igneous rocks, and supracrustal rocks, all metamorphosed in granulite facies. The oldest enderbites preserve magmatic ages reaching 3.8 Ga. The second event occurred between ca. 3.0 and 2.7 Ga and resulted in the formation of igneous charnockites and metasomatic rocks. It was possibly accompanied by high-grade metamorphism. The final igneous and metamorphic event, recognized in zircon and monazite dates, took place in response to granulite facies metamorphism at ca. 2.0-1.9 Ga [1, 2].

A petrochronological study permits a more refined understanding of the history of the rocks. Garnet Lu-Hf and apatite Sm-Nd ages in the studied rocks fall in the range between ca. 2000 and 1800 Ma. Amphiboles yielded consistent $^{40}Ar/^{39}Ar$ ages of ca. 1682 and 1670 Ma. U-Pb ages for rutile range from ca. 1495 to 1475 Ma, with apatite U-Pb ages at around 1400 Ma.

The PT parameters of granulite facies metamorphism at ca. 2000 Ma were estimated at 825–720 ℃ and 7.5–6.2 kb [3]. Our data indicate that at ca. 1800 Ma the temperature declined to ~650 ℃, then to ~530 ℃ at 1680 Ma, and finally to 450–400 ℃ at ca. 1500–1400 Ma. Hence, assuming an average geothermal gradient of 30 ℃/km, the entire area experienced slow exhumation from ca. 25 km to ca. 10 km over 500–600 Myr, corresponding to a cooling rate of around 1 ℃/Myr.

The reason for slow exhumation remains unclear. According to recent continental reconstructions [4, 5], the Dniester–Bouh Domain of the Ukrainian Shield was attached to West Africa and located in the internal part of the Nuna supercontinent. No tectono-magmatic events that might cause slow exhumation of the lower crust are currently known from this area in the Paleo- to Mesoproterozoic.

This research is part of project No. 2021/43/P/ST10/02283 co-funded by the National Science Centre and the European Union Framework Programme for Research and Innovation Horizon 2020 under the Marie Skłodowska-Curie grant agreement No. 945339.

*References:*

[1] Claesson S et al (2016) Precam Res 273:1-11
[2] Shumlyanskyy L et al. (2021) Precam Res 352:106001
[3] Stepanyuk LM et al. (2020) Mineral J (Ukraine) 42(3):50-68 (In Ukrainian)
[4] Johansson Å et al. (2022) Precam Res 371:106463
[5] Shumlyanskyy L et al. (2021) Precam Res 358:106185

## Shear zone petrochronology

Villa, I.M.[1]

[1]IfG, Universität Bern, 3012 Bern, Switzerland; CUDAM, Università di Milano Bicocca, 20126 Milano, Italy

Dating deformation requires a work-intensive characterization of textures and petrogenesis of the studied rocks. The key to dating deformation and producing correct, regional-scale (up to 100s of km) tectonic models is the assumption that minerals consist of atoms, whose transport is only firmly constrained by nm-scale analyses. The implications of the atomistic physics are not always realized, or intentionally neglected for convenience or ease of modelling.

Geochronology is pursued by communities that use different approaches and workflows, often do not communicate, and sometimes have incompatible agendas. Hygrochronology dates the retrograde metasomatic/metamorphic reactions caused by aqueous fluid circulation events. It is based on microtextural and microchemical observations. Thermochronology models time-temperature histories by assuming that the only process occurring in minerals is Fick's Law diffusion; therefore minerals must be homogeneous and inert, in order for their ages to be uniquely modelled by a "closure temperature Tc". Diffusion by definition produces a bell-shaped concentration profile, which however is almost never observed [1]. The burden of proving the existence of a true diffusion profile lies on the proponents of the improbable assertion that volume diffusion was the one and only mechanism controlling the isotope record of a mineral chronometer. And still it took forty years for the realization that Fickian diffusion of radiogenic Pb* [2] is negligible [3] to sink in. For petrochronometers such as micas in shear zones [4-6], the observations of N different ages for the N compositionally different mica generations requires that at most one is a "cooling age", and N-1 are formation ages. More often, all N are formation ages, due to the observed coincidence of mica ages with monazite U-Pb, garnet Lu-Hf , and muscovite Rb-Sr ages [7-9]. In contrast, patchy intra-grain isotope concentration profiles denounce aqueous retrogression, whose rate is many orders of magnitude faster than diffusion [5], reassigning alleged "thermochronometers" to hygrochronology. Petrochronology is based on the observation that the mobility of structure-forming major cations is higher than that of radiogenic Pb, Ar, Nd, Hf and Sr. This guarantees that the age information corresponds to the P-T-A-X information based on major elements. The presence of petrographic relicts always coincides with isotopic inheritance. Whenever one mineral generation grows at T<Tc, its apparent age dates its formation.

The observations at the nm-scale [10-12] illuminate atomic-scale processes, e.g. open-system transport of soluble ions along self-sealing networks of nanopores. They confirm that Fickian diffusion always occurs, but also that its rate is very very slow. This ensures that very few minerals behave as bona fide thermochronometers, whereas most are petrochronometers. Thus, the work-intensive combination of microtextural and microchemical variations in shear zone micas and feldspars with $^{40}Ar/^{39}Ar$ systematics provides uniquely reliable petrochronological constraints.

*References:*

[1] Wasserburg GJ and Steiger RH (1967) IAEA-SM--87/14, ISSN 0074-1884, 331-347 – [2] Tilton G (1960) J Geophys Res 65, 2933-2945 – [3] Cherniak DJ and Watson EB (2000) Chem Geol 172, 5-24 – [4] Montemagni C and Villa IM (2021) J Geol Soc178, jgs2020-235 – [5] Bosse V and Villa IM (2019) Gondwana Res 71, 76-90 – [6] Villa IM (2022) J Geol Soc 179, jgs2021-098 – [7] Tartèse R et al (2011) Terra Nova 23, 390-398 – [8] Villa IM et al (2014) J Petrol 55, 803-830 – [9] Villa IM et al (2023) J Metam Geol 41, 401-423 – [10] Valley JW et al (2014) Nature Geosci 7, 219-223 – [11] Plümper O et al (2017) Nature Geosci 10, 685-691 – [12] Turuani MJ et al (2023) Contrib Mineral Petrol 178, 31

## Ultrafast geological processes on the grain scale

Angel, R.J.[1], Campomensoi, N.[2], Gilio, M.[3], Morana, M.[4] and Alvaro M.[3]

[1]Institute of Geosciences & Georesources, CNR, Via Giovanni Gradenigo, 6, 35131 Padova, Italy, ross.angel@igg.cnr.it

[2] Dept. of Earth, Environmental and Life Sciences, University of Genova, Corso Europa 26, 16132 Genova, Italy.

[3]Dept. of Earth and Environmental Sciences, University of Pavia, Via Ferrata 1, 27100 Pavia, Italy.

[4]Department of Earth Sciences, University of Florence, Via G. La Pira 4, 50121 Florence, Italy

---

Determining the timescales of processes such as diffusion or cation exchange on the appropriate length scales is necessary for interpreting the measurements of compositional gradients, isotopes, or cation order in terms of geological processes on geological timescales. Plastic deformation offers the same challenges and many unknowns but is crucially important for interpreting the remnant pressures of inclusions.

Inclusion piezobarometry in which the pressure of inclusions (Pinc) is interpreted as entrapment conditions normally relies on the assumption of perfect elastic behaviour of the host-inclusion system. Both synthesis experiments and independent petrological determinations of entrapment conditions have validated this method for quartz in garnet (QuiG). However, while zircon in garnet (ZinG) inclusions return the correct entrapment conditions for low-P high-T terranes [1] they indicate incorrect entrapment pressures for metamorphic terranes in which garnet grew at much higher pressures, but lower temperatures [2]. This cannot be explained simply by the temperature dependence of plastic deformation.

In-situ laboratory measurements [3] now reveal that zircon inclusions in garnet immediately relax by plastic deformation of the garnet once they have passed into a tensile regime at high temperatures but develop positive pressures again on subsequent cooling. This shows that the rate of local plastic deformation of garnet depends not only on temperature but differs by orders of magnitude between tensile and compressive stress states. Resetting of natural ZinGs therefore depends on the PT path followed by the rock after entrapment; ZinGs that have followed a clockwise exhumation path that takes them into the under-pressure regime of the inclusion are rapidly reset, and the Pinc measured in the lab represents the turning point at low-pressure on the exhumation path at which cooling becomes dominant over decompression.

Different inclusion systems behave differently. Heating of QuiG does not lead to resetting because the inclusions are in the compressive regime, but neither does the room-T compression of QuiG into the tensile regime [4,5]. The contrast in behaviour between different host-inclusion systems can therefore be exploited to reveal the stress dependence of plastic deformation in garnets and be used to determine different points on the prograde and retrograde paths of the rocks in which they are found.

*References:*

[1] Gilio M et al. (2022) J Met Geol 40:229-242
[2] Campomenosi et al (2021) Contribs Min Pet 176:36
[3] Campomenosi et al (2023) Geology 51:23-27
[4] Morana et al (2023) Phys Chem Min 50:21
[5] Campomenosi et al (2023) Contribs Min Pet 178:44

## Potentiality of titanite petrochronological tool in the metacarbonate system

Bonazzi, M.[1], Simonetti, M.[2], Maino, M.[3] and Langone, A.[3]

[1]Institute of Geosciences and Earth Resources of Pavia (IGG-CNR), Via Ferrata 7, Pavia 27100, mattia.bonazzi@crystal.unipv.it

[2]Geological Survey of Italy, ISPRA, Roma, Italy

[3]Department of Earth and Environmental Sciences, University of Pavia

---

Metacarbonates lithologies are poorly studied for obtaining information about the timing of metamorphic reactions or deformation events since they usually do not contain commonly used geochronometers (e.g. zircon, monazite). On the contrary, titanite ($CaTiSiO_5$) commonly occurs as an accessory mineral in metacarbonates of middle to high metamorphic grade. This mineral phase contains several important geochemical elements, such as REE, Pb, U, Zr working as potential petrological and geochronological tool [1]. Despite of this, the potentiality of titanite as a petrochronological tool in the metacarbonate systems is poorly known.

In this study, we conducted a complete petrographical, textural and geochemical characterization of metacarbonate rocks occurring at different levels of the Variscan continental crustal section exposed along the Valle Strona di Omegna, Ivrea-Verbano Zone. The crustal section consists of metapelites/metapsammites and metabasites, with numerous lenses of metacarbonate rocks. The metamorphic grade of the crust section increases progressively in P-T conditions, from amphibolite to granulite facies, with increasing crustal paleo-depth. Metacarbonates range in composition from impure marble to calc-silicates, showing several textures from granoblastic to porphyroblastic. Clinopyroxene, amphibole appear from amphibolite facies whereas scapolite, garnet and olivine became stable from granulite facies conditions. Titanite is almost ubiquitous across the amphibolite-granulite facies rocks except for the olivine-rich marble recording the highest metamorphic grade. We determined major and trace elements and U–Pb data in the titanite crystals. Trace elements and U–Pb are acquired simultaneously from the same spot.

Titanite chemistry displays interesting correlations with mineral assemblages, metamorphic grade and U–Pb data. Zr remains constant in the titanite from the same sample. By adopting the Zr-in-titanite thermometer [2], temperature varies in the range of 650-900 °C, coherently with temperature conditions obtained for the surrounding metapelites/metabasites during regional metamorphism at Upper Carboniferous – Lower Permian interval [3]. Geochronological analyses have been restricted to some samples characterized by titanite with a U content higher than 100 ppm. Preliminary results from porphyroclastic samples suggest a good correlation of U–Pb data and Y. In this samples, the titanite with similar Y and U contents defines a good alignment of the U–Pb data in the Tera-Waserburg diagram with a lower intercept pointing to 242 Ma. This age corresponds to the end of the long-lasting HT regional metamorphism [4,5]. These preliminary results suggest a decoupling between titanite petrogenesis, based on microstructures, trace element composition and timing.

*References:*

[1] Kohn M J (2017) Rev Mineral Geochem 83:419-441
[2] Hayden L A et al. (2008) Contrib Mineral Petrol 155:529-540
[3] Redler C et al. (2012) J Metamorph Geol 30:235-254
[4] Kunz et al. (2018) Contrib Mineral Petrol 173:1-21
[5] Williams et al. (2022) Contrib Mineral Petrol 40:1015-1042

## Coupled petrochronology on monazite and titanite to unravel the evolution of shear zones from mid- to low continental crust (Ivrea-Verbano Zone; Italy)

Corvò, S.[1,2*], Maino M.[1,2], Bonazzi, M.[1,2], Simonetti M.[3], Montemagni C.[4], Zanchetta S.[4], Piazolo S.[5], Langone A.[1,2]

[1]Department of Earth and Environmental Sciences, University of Pavia, Pavia, Italy; stefania.corvo@unipv.it

[2] Institute of Geosciences and Earth Resources of Pavia, C.N.R., Pavia, Italy

[3] Geological Survey of Italy, ISPRA, Roma, Italy

[4] Dipartimento di Scienze dell'Ambiente e della Terra, Università degli Studi di Milano – Bicocca, Milano, Italy;

[5] School of Earth and Environment, University of Leeds, Leeds, United Kingdom

---

Dating the time of shear zone activity remains challenging. Here we present the results of several studies from different mid/low-crustal shear zones exposed in the Ivrea-Verbano Zone (Southern Alps, Italy): the Anzola shear zone (ASZ), the Forno-Rosarolo shear zone (FRSZ) and the Premosello shear zone (PSZ) [1, 2, 3]. Although the activity of these structures has been associated with the Mesozoic rifting phase [4], the age of their activities is poorly constrained. In particular, we report an attempt to date the deformation by combining monazite and titanite U-(Th-)Pb data.

Studied shear zones display a sub-vertical attitude and a thickness between 100 and 500m. While the ASZ and the FRSZ formed at the amphibolite- to granulite-facies transition, the PSZ occurs within rocks that experienced high-T granulite-facies. (Ultra)-mylonites developed in a lithologically complex made of paragneisses, mafic rocks and minor calc-silicates. Paragneisses consist of Grt, Kfs, Plg, Bt and Sill; mafic rocks contain Cpx, Amph, Plg, Opx, and Grt whereas calc-silicates are made of calcite-rich and calcite-poor layers plus Amph, Px, Plg/Kfs and Grt. For in-situ U-(Th-)Pb dating purposes, we selected monazite from FRSZ and PSZ paragneisses and titanite grains from FRSZ and ASZ mafic rocks and calcsilicates [5, 6]. Monazite from (ultra)-mylonitic paragneisses occurs in different microstructural positions (either included in porphyroclasts or along the mylonitic foliation) and commonly presents complex Th and Y chemical zoning. Titanite from mylonitic mafic rocks and calc-silicates are common along the foliation. Two types of titanite textures were identified: i) strongly zoned grains with LREE depleted rims/tips and ii) homogeneous grains. Both types show evidence for intracrystalline deformation (e.g., deformation twins and systematic crystal lattice bending).

U-(Th-)Pb dating across monazite and titanite revealed a contrasting behaviour of the two geochronometers. The Y-poor monazite domains give mostly Early Permian-Triassic ages, while the Y-rich domains provided late Triassic-Early Jurassic dates likely associated with fluid-assisted syn-deformational recrystallization. On the other hand, the titanite domains characterized by deformational features provide a lower intercept age at the Jurassic age. According to chemistry and isotopic data, while monazite experienced intense reactivity during Triassic ages, titanite was almost unreactive during these time lapse developing only locally rims or external domains at Jurassic time suggesting the involvement of fluids-induced deformation.

This contrasting behaviour could be interpreted as the result of different response to changing P-T-composition and fluid availability conditions during the same deformation history. However, the combination of petrochronological and microstructural results and the contrasting behaviour of the two independent geochronometers lets to constrain a long-lasting deformation of the shear zones throughout the Triassic until Jurassic time. In particular, during this time interval, the activity of shear zones in the Ivrea-Verbano Zone was, within error, simultaneously at different crustal levels.

*References:*

[1] Rutter EH et al. (1993) J Struct Geol 15:647-662; [2] Simonetti M et al. (2021) Ofioliti 46(2):147-161 ; [3] Corvò S et al. (2023) Earth Planet Sci Lett 620(C):118349; [4] Petri B et al. (2019) Earth Planet Sci Lett 512:147-162; [5] Corvò S et al. (2022) Lithos 106745; [6] Simonetti M et al. (2023) J Struct Geol 104896

## The stiffening of the elastic tensor of quartz and its effect on strain-stress relationship. Implications for elastic geobarometry

Gilio*, M.[1], Angel, R.J.[2] and Alvaro, M.[3]

[1]Mineralogisch-Petrographisches Institut, Universität Hamburg, Hamburg (DE)

[2]Department of Earth and Environmental Sciences, University of Pavia, Pavia (I)

[3]IGG-CNR, Padova (I)

---

Elastic geothermobarometry, a method in metamorphic petrology for retrieving the pressure and temperature conditions of inclusion entrapment, has undergone significant development since its theoretical origins described by Rosenfeld and Chase [1], with widespread applications in mantle and metamorphic petrology ([2] and references therein). Consider a scenario with a softer inclusion inside a stiffer host (e.g., quartz in garnet). During entrapment, both the inclusion and host are in elastic equilibrium with the external pressure. Decompression and cooling lead to strain and pressurization of the inclusion, measurable directly through X-Ray diffraction or indirectly through Raman Spectroscopy.

Two primary methods are commonly employed to calculate inclusion pressures. The first method assumes hydrostatic stress, converting volume strain into pressure using the equation of state. However, recent studies indicate that quartz inclusions are seldom under hydrostatic stress, and strong differential strains can lead to significant errors [3]. The second method utilizes the elastic tensor ($C_{ij}$) for the inclusion to convert strain into stress: $\sigma_i = C_{ij}\varepsilon_j$. A phase subjected to a certain pressure normally becomes stiffer ($\frac{\partial C_{ij}}{\partial P} > 0$). In elastic geothermobarometry the inclusion pressures are low and so this stiffening is generally assumed to be negligible. Inclusion stress is therefore calculated with the elastic tensor values measured at room pressure and ambient temperature.

We will discuss the validity of assuming $\frac{\partial C_{ij}}{\partial P} = 0$ in quartz and other minerals commonly used in geothermobarometry (zircon and olivine) and we will describe a method to account for $C_{ij}$ stiffening when calculating inclusion pressures to show the implications in elastic geobarometry.

*References:*

[1] Rosenfeld JL and Chase AB (1961) Am J Sci 259:519-541
[2] Kohn MJ et al. (2023) Annu Rev Earth Pl Sc 51:331-366
[3] Gilio M et al. (2021) Am Mineral 106:1530-1533

# Hybrid veins and heterogeneous deformation in the Saih Hatat window, Oman belt: a possible record of fossil episodic tremors and slow slip events

Petroccia, A.[1], Giuntoli, F.[1], Callegari, I.[2], Viola, G.[1]

[1]Dipartimento di Scienze Biologiche, Geologiche ed Ambientali-BiGeA, Università degli Studi di Bologna, Via Zamboni 67, 40126 Bologna, Italy

[2]Department of Applied Geosciences - German University of Technology in Oman - P.O. Box 1816, PC 130, Muscat, Sultanate of Oman

---

Relics of deep episodic tremor and slow slip events (ETS) can only be investigated in deeply exhumed fossil subduction zones and may be used as an analogue of modern settings (e.g., [1,2]). Thus, a promising approach is to look for heterogeneous continuous and discontinuous deformation associated with high pore-fluid pressure fluctuations, in both exhumed oceanic and continental shear zones (e.g.,[3,4]).

We studied the so-called "upper plate–lower plate discontinuity", also called the Hulw Shear Zone (HSZ), in the Saih Hatat window in the NE of Oman. This shear zone separates two blueschist facies units named Mayh (at the top) and Hulw (at the bottom) with no significant differences in pressure and temperature [5]. Field observations reveal that the Hulw Unit is mainly composed of weak metapelite, affected by a pervasive mylonitic foliation, enclosing dolomite lenses, which are intensely fractured with a chaotic texture. Similarly, the Mayh Unit is made of foliated and banded marbles that embed boundinated and brecciated layers and lenses of dolostone. The HSZ plane is parallel to the high-pressure mylonitic foliation measured in the overall area. In both units, the strain increases towards the core of the HSZ, corresponding to 60-100 cm thick high-strain zones. Progressively moving toward the core of the HSZ, the deformation changes from asymmetrical folds to S-C' fabric and finally to S-C and minor C' fabric with a top-to-the-N/NE sense of shear. Dilational tension gashes occur mainly in the stronger lithotypes, oriented at a high angle to the foliation, whereas dilational shear veins are more common in weaker rocks and are subparallel to the mylonitic foliation. Shear veins are composed of iso-oriented stretched quartz and ankerite fibres (with minor calcite and white mica), are characterized by crack-and-seal textures and define a stretching direction coherent with that observed in both units.

The HSZ displays evidence of heterogeneous deformation developed at minimum high-pressure greenschist-facies condition, driven by different rock types response to stress, and by repeated alternation of localised brittle failure and more diffuse ductile deformation. Concluding, these structures can potentially be ascribed to fossil deep ETS in the deeply subducted Oman continental crust.

*References:*

[1] Kirkpatrick JD et al. (2021) Nat Rev Earth Environ 2:285-301.
[2] Behr WM and Bürgmann R (2021) Philos. Trans. R. Soc. A Math. Phys. Eng. Sci. 379.
[3] Fagereng A et al. (2011) Tectonophysics 510
[4] Giuntoli F and Viola G (2022) Sci Rep 12
[5] Agard P et al. (2010) Tectonics 29

Giutoli acknowledges financial support under the National Recovery and Resilience Plan (NRRP), Grant Assignment Decree No MUR 2022X88W2Y_002 by the Italian Ministry of Ministry of University and Research (MUR).

# Typical spinifex structures of Archean komatiite metabasalts of the Sur greenstone structure, Middle Dnieper, Ukrainian shield

M. Reshetnyk[1,2], V.Sukach[1], D.Starokadomsky[1,3]

[1]M.P. Semenenko Institute of Geochemistry, Mineralogy and Ore Formation, National Academy of Sciences of Ukraine (NASU), Kyiv

[2]National Museum of Natural History, NASU

[3] Chuiko Institute of Surface Chemistry, NASU

---

The subject of the performed research is the komatiite basalts of the Surska Greenrocks Structure, which belong to the Alferiv stratigraphic level (the Sursko-Mykhailiv section in the central part of Greenrocks Structure). It was established that metacomatiites are represented by carbonate-amphibole-talc and carbonate-chlorite-talc rocks. Metadolerites, chlorite-quartz-carbonate shale and talc-carbonate-chlorite microshale are the underlying sedimentsThe 2 komatiite flows can be distinguished - at the interval of 61.7-88 m, and at the interval of 93-103 m. Microscopy observes needle-like skeletal crystals (pseudomorphosis of serpentine, actinolite and tremolite on olivine), they are grouped into packets, the gaps between which filled with devitrified glass or serpentine. Less-often, small (up to 0.8 mm) radially-radiating and rosette-shaped clusters of acicular relict olivine exudates, replaced by actinolite or tremolite, are noted.

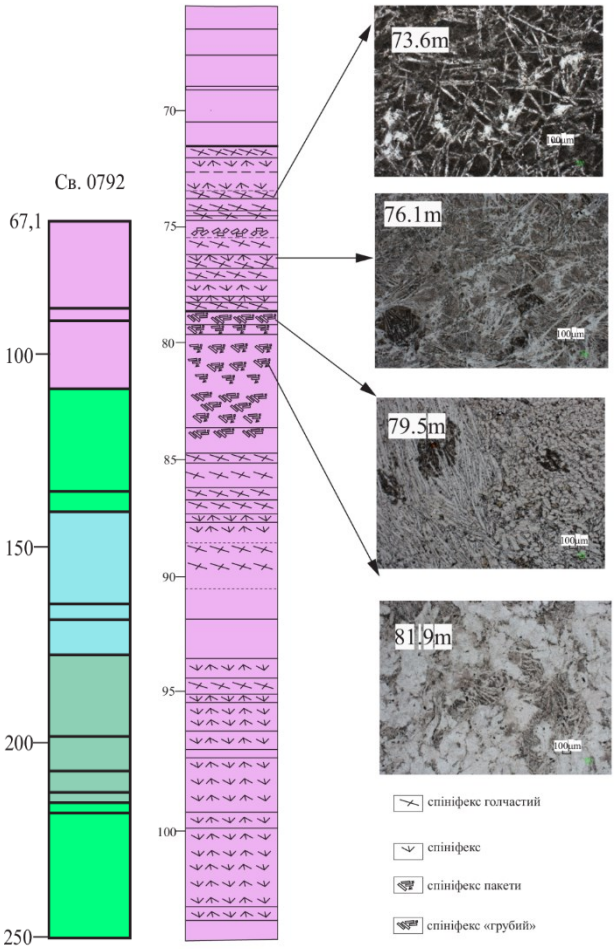


***Fig. 2**. Column with two lava flows fixed in St. 0792 and spinifex types.*

## Early Paleozoic Andean-type evolution recorded in the Dunhuang block (NW China): insights from petro-structural, geochronological and metamorphic *P–T* constraints

Soldner, J.[1], Jiang, Y.D.[2,3], Štípská, P.[5], Schulmann, K.[4], Yuan, C.[2,3], and Anczkiewicz, R.[1]

[1] Institute of Geological Sciences, Polish Academy of Sciences, Senacka 1, 31-002 Kraków, Poland (j.soldner@ingpan.krakow.pl)

[2] State Key Laboratory of Isotope Geochemistry, Guangzhou Institute of Geochemistry, Chinese Academy of Sciences, Guangzhou 510640, China

[3] CAS Center for Excellence in Deep Earth Science, Guangzhou 510640, China

[4] Institut Terre et Environnement de Strasbourg, UMR 7063 Université de Strasbourg—CNRS, 1 Rue Blessig, 67084 Strasbourg, Cedex, France

[5] Centre of Lithospheric Research, Czech Geological Survey; Klárov 3,118 21 Praha 1, Czech Republic

---

The Dunhuang block connecting the Central Asian Orogenic Belt to the Proto-Tethyan orogenic system was affected by multiple Paleozoic crustal reworking events. However, relationships between metamorphic ages, *P–T* evolutions and deformational history characterizing these events remain ambiguous. In order to address this issue, *P–T–t–D* paths of paragneisses from the basement of the southern Dunhuang block were investigated. Inclusions in garnet and kyanite are considered as vestiges of M1 metamorphism corresponding to the initiation of the prograde evolution. The earliest continuous metamorphic fabric is an originally steep N-S striking foliation S2. This fabric was further reworked by vertical folds F3 associated with development of a ubiquitous steep E-W striking axial planar foliation S3. The foliation S2 is mainly associated with the Grt–St–Ky–Sil–Bt–Ms–Pl–Qz–Rt and Grt–Ky–Sil–Bt–Kfs–Pl–Qz–Rt assemblages, whereas the S3 foliation is associated with the Grt–Sil–Bt–Ms–Pl–Qz–Kfs–Ilm assemblage. Early prograde (M1) to peak (M2a) metamorphic stages are constrained from 4.0–6.5 kbar and 540–560°C to 9–10 kbar and ~650–675°C. Subsequent decompression is initially accompanied by heating (M2b) up to 6–6.5 kbar and ~730°C, followed by cooling (M3) through 4–6.5 kbar and 550–650°C. In-situ U–Pb dating of monazite combined with monazite trace-element compositions suggest that prograde evolution (M1) most likely started at ca. 406 Ma, peak-P conditions (M2a) were reached at 400–394 Ma, decompressional heating (M2b) took place at 393–391 Ma, and cooling (M3) during exhumation probably occurred at 380 Ma. The prograde metamorphism probably reflects burial during underthrusting of neighbouring continental basement below the Dunhuang block. This event culminated in pure shear thickening (D2a) of the whole supra-subduction margin followed by minor heating and exhumation (D2b). The D3-M3 event is interpreted as reflecting exhumation during orthogonal shortening of the system. Combined with the available regional data, this study reveals the existence of a complex tectono-metamorphic evolution for the Dunhuang block characterized by (i) the thickening of a previously thinned arc–back-arc crust recorded at 420–410 Ma in the pro-wedge side of the active margin, followed by (ii) the 410–390 Ma thickening in the retro-wedge side. Such a tectonic evolution resembles Andean-type migration of crustal thickening from the convergent front to hinterlands. The D3-M3 event potentially responsible for the juxtaposition of rocks from different geological occurrences and depths is seemingly independent from this Andean-type orogenic cycle.

## Multi-method approach for deciphering the growth mechanisms of non-typical textures in Archaean garnet

van Schijndel, V.[1], Cutts, K.[2], Stevens, G.[3], Hoffmann, E.[4], Ohl, M.[5], Ji, Y,[5], Plümper, O.[5]

[1]GFZ German Research Centre for Geosciences, 14473 Potsdam, Germany

[2]Geological Survey of Finland, P.O. Box 96, FI-02151 Espoo, Finland

[3]Centre for Crustal Petrology, Department of Earth Sciences, Stellenbosch University, Private Bag X1, Matieland 7602, South Africa

[4]Institut für Geologische Wissenschaften, Freie Universität Berlin, Malteserstrasse 74-100, 12249 Berlin, Germany

[5]Department of Earth Sciences, Utrecht University, Budapestlaan 4, 3584CD Utrecht, The Netherlands

*E-mail: valby@gfz-potsdam.de

---

The Dwalile Supracrustal Suite of the Ancient Gneiss Complex (Eswatini) represents one of the oldest greenstone belts in the world with a crustal evolution history from Palaeo- to Mesoarchaean times. The main metapelitic rock type is dominated by garnet and staurolite porphyroblasts in a layered matrix of biotite, muscovite, quartz and retrograde sericite. Minor components are andalusite, chlorite and chloritoid with accessory ilmenite and monazite. This mineral assemblage indicates peak metamorphic conditions at a maximum pressure of 4 kbar and a temperature between 510-540 °C. The age for the amphibolite facies metamorphism is recorded by monazite at ca. 3.15 Ga.

Pressure, temperature, bulk composition and fluid-rock interaction are important factors for controlling garnet growth. The garnet-staurolite bearing metapelites have similar mineralogy and bulk rock compositions, with high Al, Fe and low Ca, Na. The rocks mainly differ in their garnet and staurolite modes and their unusual garnet microstructures. In some samples the almandine garnets are distributed as thin boudinaged layers consisting of elongated ribbons, with local resorption textures and peninsular features surrounded by coarse recrystallised quartz. The euhedral garnet cores are only visible in compositional maps, which show a typical bell-shaped growth zoning ($X_{alm}$ = 0.70-0.81, $X_{prp}$ = 0.06-00.12, $X_{grs}$ = 0.05-0.01, $X_{sps}$ = 0.19-0.07).

EBSD maps of the crystallographic orientations of the garnet were created for four samples with different garnet textures. Two samples were also imaged using high-resolution X-ray tomography for the purpose of visualising the relationship of the garnet porphyroblasts and the matrix in 3D.

The next step is to investigate other possible factors controlling the garnet growth such as the fluid-rock interaction processes. An indication of fluids interacting with the surrounding rocks during metamorphism is the presence of a small lens of mica schist located nearby the garnet-staurolite rocks. This schist has an assemblage of primarily muscovite, quartz, coarse andalusite with minor chloritoid and accessory rutile, ilmenite, tourmaline and monazite. The monazite in this sample is the same age as the monazite in the garnet bearing samples. Trace element abundances of the different generations of garnet will be measured by LA-ICP-MS in order to distinguish between a hydrogenous (sea water) or hydrothermal input during garnet growth.

## Residual stress mapping in diopside as tool to reconstruct seismogenic faulting in the lower crust

Van Schrojenstein Lantman, H.W.[1*] and Menegon, L.[1]

[1] The Njord Centre, Department of Geosciences, University of Oslo, Norway (* h.w.van.s.lantman@mn.uio.no)

---

Exhumed rocks can be under residual stress from a variety of sources, for example induced by defects such as dislocations or from mineral host-inclusion systems with contrasting properties. The measurement of such stresses has proven useful for the reconstruction of conditions and mechanisms of mineral growth and deformation. In this contribution, we use the mapping of stress variations via high-angular resolution electron backscatter diffraction (HR-EBSD) to reconstruct the residual stress in the wall rock of a fault zone and elucidate the deformation processes that led to this residual stress preservation.

Pseudotachylytes (frictional melts formed during seismic slip) in the metamorphosed anorthosites of the Lofoten archipelago preserve a record of seismic rupture in the dry lower crust at 650–750 °C, 0.8 GPa. GPa-level transient stresses are suggested from microstructural evidence, however such high stresses have not been quantified. Spatial datasets of residual stresses that are retained in the crystal lattice of diopside are obtained on a sub-micron scale via HR-EBSD. We combine this method with microstructural analysis on a sample from the Nusfjord locality to reconstruct the spatial heterogeneities and link them to the seismic cycle.

Diopside contains micro- to nanoscale deformation twins within 3 mm from the fault and in clasts in the pseudotachylyte. Within clasts, strong undulations of the diopside lattice are observed, indicating low-T plasticity at high stress. Residual stresses obtained via HR-EBSD vary between ~450 and ~200 MPa and are only elevated within 200 µm of the pseudotachylyte. The highest residual stresses are found in grains exhibiting lattice distortion resulting from dislocation glide. Although at the hundreds of MPa level, these stresses are lower than estimated stress drops for the locality and stresses expected during rupture propagation (both >1 GPa).

To test whether thermal shock from the frictional heating stage had an impact on the deformation and residual stress, we calculated the thermal gradient in the wall rock at the moment peak temperature was achieved, for various combinations of stress drop and diopside orientation. The results indicate that thermal pressure is only relevant within 10 µm of the pseudotachylyte margin, and hence do not correlate with our HR-EBSD results.

We conclude that residual stresses in diopside record the progressive build-up of stress during preseismic loading, confirmed by microfaults crosscutting structures that are linked to the stress build-up. Additionally, the stress build-up in diopside may have partially dissipated by the formation of twins.

## Partial melting in the continental crust: thermal & chemical consequences of melting reactions and melt–rock interaction

Schorn, S.[1,2]

[1]Department of Earth Sciences, University of Graz, Universitätsplatz 2, 8010 Graz, Austria

[2]Institute of Geosciences, Johannes Gutenberg University, J. Becher Weg 21, D 55128 Mainz, Germany

---

Partial melting is a complex process influencing the chemical, thermal and mechanical properties of the crust in a variety of geodynamic settings. From a thermal perspective, the production of partial melts requires significant amounts of heat, thereby dominating the thermal properties of the rocks involved in anatexis. In fertile lithologies such as metapelites and hydrated metabasites, melting is a continuous but episodic process where the bulk of melt production is focussed around specific temperatures where low-variance breakdown reactions occur. These reactions involve the consumption of hydrous minerals in favour of silicic melt in equilibrium with a less hydrated assemblage and occur over narrow temperature intervals. As the reactions advance, heat is predominantly consumed to drive mineral breakdown and melting, causing a quasi-isothermal state. For isobaric heating of metapelite at around 22 km depth, akin to low-pressure–high-temperature granulite terranes, the reactions involved in mica breakdown alone produce about a fourth of the total melt and consume approximately one eighth of the enthalpy required to heat the rock from 600°C to ultrahigh-temperature conditions, while occupying <10°C of the entire heating path [1]. By contrast, dry bulk continental crust and preconditioned polymetamorphic granulites produce negligible volumes of melt and experience linear heating paths. Lithology can therefore exert a control on the attainable metamorphic temperature. Given the same heat budget, fertile rocks reach markedly lower temperatures compared to more refractory compositions. While dry rocks are inherently more refractory, they represent strong sinks of fluid and fluid-mobile elements. Using bimineralic eclogite hosted in orthogneiss from the northern Sulu belt (China), thermodynamic modelling suggests that gradients in the chemical potentials of $H_2O$ and $K_2O$ as proxy for large-ion lithophile elements (LILE) drive material transport from the host gneiss towards the eclogite, where it favours partial melting and enrichment in LILE in small leucosome pockets within the eclogite [2]. Similarly, fluid-fluxed melting of eclogite during exhumation at the eclogite type-locality (Austria) leads to the formation of hydrous, subaluminous melts. The injection and crystallization of these melts within nearby pristine eclogite causes the hydration and retrogression of the surrounding rocks as fluids exsolve from the solidifying melts [3]. Using these and other examples, it is shown how the prograde melting, melt–rock interaction and the retrograde crystallization of partial melts can exert a first-order control on the thermal and chemical evolution of the continental crust.

*References:*

[1] Schorn et al. (2018) Geology 46.7:643-646
[2] Wang et al. (2024) EPSL (in review)
[3] Schorn et al. (2021) Lithos 390-391:106118

## A reappraisal of granite emplacement mechanisms, temperatures and time-scales using thermal aureoles: A case study at Ballachulish and Strontian (UK)

Sudholz, Z.J.[1], Copley, A.[1] and Weller O.M.[1]

[1]Department of Earth Sciences, University of Cambridge

---

The temperature, ascent and emplacement of granitic magmas plays a crucial role in the chemical differentiation of continental crust, and transport of heat and volatiles through the lithosphere [1-3]. These processes influence the rheology and deformation of continental crust, the formation of critical metal deposits, and long-term stability and evolution of the Earth's lithosphere. However, despite their widespread occurrence and importance, the temperatures of granitic magmas and their ascent and emplacement mechanisms remains enigmatic and subject to ongoing research [1]. Constraining these properties of granite magmas is hampered by the large temporal and spatial scale over which granites crystalize, therefore preventing the confident application and interpretation of magmatic geothermobarometers and most geochronometers. In this study we attempt to better constrain the temperatures, timescales, and emplacement mechanisms for two late Caledonian granite intrusions at Strontian and Ballachulish (northwest Scotland) using an inter-disciplinary method based on geothermometry and thermal diffusion modelling applied to metamorphosed pelites in the contact aureole. The temperatures of contact metamorphism have been calculated using conventional Ti-in-biotite and Ti-in-quartz geothermometry, and phase equilibria modelling [4-5]. The results from geothermobarometric analysis are integrated with models of thermal diffusion using finite differences method to produce site-specific temperature versus distance profiles for each intrusion and their thermal aureole [1]. Our integrated results provide insights into the plausibility of different granite emplacement mechanisms, namely, granite diapirism and dyke-sill accretion. We also obtain new insights into the thermal evolution of granitic magmas, including the temperature and timescale of emplacement. Future work will focus on exploring the temperatures, emplacements and time-scales of global compilations of granitic magmas using thermal aureoles at different crustal levels, tectonic settings and back-ground temperatures, and integrating these new results with thermal-mechanical models of crustal deformation.

References:

[1] Copley A et al. (2023) Sc. Rep. 13.1:13730.
[2] Brown M (2013) GSA Bull. 125(7–8):1079–1113.
[3] Moyen JA (2020) Geol. Soc. Lond. Spl. Publ. 491:77–100.
[4] Henry DJ et al. (2005) Am. Miner. 90(2–3): 316–328 (2005).
[5] Wark DA and Watson EB (2006) Contrib. Mineral. Petrol. 152.6: 743-754

## The evolution of the lower continental crust constrained through high-precision HFSE systematics

Emo, R.B.[1*], Münker, C.[1] Pakulla, J.J.[1], Downes, H.[2], Murphy D.T.[3]

[1] Institut für Geologie und Mineralogie, Universität zu Köln, Cologne, Germany (*remo@uni-koeln.de)

[2] School of Natural Sciences, Birkbeck College, University of London, London, UK

[3] School of Earth and Atmospheric Sciences, Queensland University of Technology, Brisbane, Australia

---

The lower continental crust (LCC) is a significant geochemical reservoir for understanding the evolution of the crust-mantle system. For instance, the LCC has been suggested to play a key role in the distribution of the high field strength elements (HFSE) in the continental crust. Specifically, the lower Nb/Ta value in the upper continental crust (ca. 12) relative to the mantle (ca. 14-15) is suggested to be complemented by higher Nb/Ta in the LCC [e.g., 1]. Several common LCC minerals, including amphibole, rutile and Fe-Ti oxides, could be significant in controlling Nb/Ta and HFSE distributions. However, the LCC composition is poorly constrained due to its inaccessibility and the low abundance of several highly incompatible elements, including the HFSE Ta and W, in depleted LCC. Therefore, more high-quality HFSE data are needed to better constrain the HFSE composition of the LCC.

In this study, lower crustal xenoliths from several localities (Eifel, Germany; Kola Peninsula, Russia; central and northern Queensland, Australia) are investigated using a combined phase equilibrium and geochemical approach. Xenoliths were analysed for their HFSE concentrations using high-precision isotope dilution multi-collector inductively coupled plasma mass spectrometry (ID-MC-ICP-MS). Other trace elements were analysed by quadrupole ICP-MS. The rutile-rich Kola granulite xenoliths have superchondritic Nb/Ta and high W/Th. Several Queensland xenoliths also have high Nb/Ta and W/Th, albeit at lower absolute concentrations. The lithologically diverse Eifel xenoliths have highly variable HFSE concentrations. Yet, many have mantle-like Nb/Ta and W/Th, indicating a significant role for mafic-ultramafic underplating in this region, where Nb/Ta fractionation is negligible.

These geochemical results are combined with phase equilibrium modelling in the NCKMASHTO system using recent thermodynamic models [2] to better constrain which mineral phases are controlling the HFSE budget in the deep crust and complementary upper crustal melts. Melting of different crustal protoliths at lower crustal conditions is modelled in THERMOCALC. The trace element compositions of these melts are also modelled using partition coefficients of the residual phases. The combined modelling highlights the importance of residual Ti-bearing phases (rutile and ilmenite) and amphibole in controlling the behaviour of the HFSE during crustal melting. Melting reactions involving the consumption of amphibole can lead to the formation of peritectic ilmenite in thin crustal settings such as central Queensland, and rutile in thicker crust such as in the Kola Peninsula and parts of northern Queensland. These residual phases would then sequester the majority of the HFSE budget in the LCC, leading to relative HFSE depletions in the complementary escaping melts.

*References:*

[1] Tang M et al. (2019) Nat Commun 10: 235

[2] Holland et al. (2018) J Petrol 59: 881-900

## Bimodal Miocene volcanism in the Hegau region (SW Germany) by differentiation of primitive melilititic to nephelinitic magmas towards evolved nosean phonolites

Binder, T.[1], Marks, M.A.W.[1], Friedrichsen, B.-E.[1], Walter, B.F.[2], Wenzel, T.[1] and Markl, G.[1]

[1]Department of Geosciences, Eberhard Karls Universität Tübingen, Schnarrenbergstraße 94–96, 72076 Tübingen, Germany. E-mail address: thomas.binder@uni-tuebingen.de

[2]Chair of Geochemistry & Economic Geology and Laboratory of Environmental and Raw Materials Analyses (LERA), Karlsruhe Institute of Technology, Adenauerring 20b, 76131 Karlsruhe, Germany

---

Alkaline volcanism of the Hegau region (SW Germany) in the southernmost part of the Central European Volcanic Province (CEVP) is characterized by strong compositional bimodality. Two contrasting $SiO_2$-undersaturated rock suites comprise primitive olivine melilitites to melilite-bearing olivine nephelinites (12–9 Ma) and evolved nosean phonolites (14–11 Ma). The primitive suite is characterized by high MgO, CaO, $Fe_2O_3$, $TiO_2$, Ni, V, F, moderate alkalis, $Al_2O_3$, $P_2O_5$, Ba, Nb, Zr, and low $SiO_2$, Rb, Pb, and U concentrations. The corresponding rocks contain olivine ($Fo_{79-92}$), diopsidic clinopyroxene, melilite, perovskite, Cr-bearing oxyspinel, F- and Ba-rich phlogopite/kinoshitalite, and fluorapatite. In contrast, the evolved rocks reveal high alkali, $Al_2O_3$, $SiO_2$, Rb, Nb, Zr, U, Pb, S, and low MgO, CaO, $Fe_2O_3$, $TiO_2$, $P_2O_5$, Ba, Ni, and V concentrations. Their crystal load comprises abundant Ba-bearing alkali feldspar and nosean-haüyne-sodalite$_{ss}$ macrocrysts, aegirine-augite, as well as accessory apatite, titanite, zircon, and pyrochlore. The melilititic–nephelinitic rocks formed by low degrees of partial melting of a carbonated amphibole ± phlogopite-bearing garnet wehrlite in the uppermost asthenosphere or the thermal boundary layer. They are widespread in the southern CEVP but their close spatial and temporal association with evolved nosean phonolites is a unique feature.

Coarse-grained (nepheline) syenitic cumulates, present as enclaves in both rock suites, as well as the geochemistry of the phonolites, including strongly negative P and Ti anomalies and a trough of MREE in primitive mantle-normalized trace element patterns, indicate fractionation of clinopyroxene, mica, alkali feldspar, nepheline, apatite, and titanite. Thermodynamic modelling using MELTS supports that the nosean phonolites can be approximated by removal of 11–19% oxyspinel, 4–10% olivine, 42–57% clinopyroxene <3% mica, <9% feldspathoids, <8% feldspar from melilititic–nephelinitic parental melts at upper crustal pressures (c. 200 MPa), leaving 12–35 mass% of the initial melt. The modelling further indicates crystallization of the (nepheline) syenite cumulates between 1050 and 800 °C and ascent and eruption of the phonolite residues at no less than 900 °C with complete solidification of the observed assemblage at >750 °C and without the necessity for crustal assimilation. The wide range in composition of the nosean phonolites can be reproduced by relatively small compositional differences of the primitive parental melts and by variable degrees of fractionation. We suggest that the temporal progression from evolved rocks that experienced prolonged differentiation in the upper crust towards near-primary, fast ascending primitive melts was caused by stress field changes from an extensional to a more compressive regime. After a regional phase of erosion due to pronounced uplift, a period of crustal shortening during progressive graben formation caused intensification of uplift and disruption of the upper crust by emergence of local and/or (re)activation of deep-seated fault systems, coinciding with the younger volcanic phase that produced the primitive melts. The magma ascent increasingly became structurally controlled, supported by brittle deformation, and thus accelerated.

## Nephelinites from the Northern Tanzania Divergence Zone

Schmitt, F. H.[1], Marks, M. A. W.[1] and Markl, G.[1]

[1]Universität Tübingen, Fachbereich Geowissenschaften, GUZ, Schnarrenbergstrasse 94-96, D-72076 Tübingen, Germany. f.schmitt@uni-tuebingen.de

---

Nephelinites are alkaline, $SiO_2$-undersaturated rocks, generated by low-degree partial melting of the metasomatized mantle. In the East African Rift System (EARS), these melts are produced by a thermal mantle anomaly, which is also involved in the rifting process. Rift-related volcanic activity in our study area – the Northern Tanzanian Divergence Zone (NTDZ) – started ~6 Myr ago [1] comprising basalts, basanites, trachytes, phonolites, nephelinites, and carbonatites. They are divided into two age groups, with an older phase (~6-1.2 Ma) mostly encompassing basaltic-trachytic volcanos and a younger phase (<1.2 Ma), which produced mainly nephelinitic–phonolitic ±carbonatitic rocks.

The major nephelinitic–phonolitic volcanoes in the region are Burko, Essimingor, Kerimasi, Meru, Mosonik, Oldoinyo Lengai, Sadiman, and Shombole [2]. They are variably evolved, ranging from $X_{Mg}$ of ~0.25-0.70 [3] and typically evolve to peralkaline ((Na + K)/Al >1) compositions with decreasing $X_{Mg}$ and increasing $SiO_2$ contents. Relatively primitive nephelinites ($X_{Mg}$ >0.6) typically contain nepheline, diopside, Fe-Ti oxides, perovskite ± olivine ± melilite ± biotite or amphibole. In contrast, more evolved nephelinites display a mineral assemblage of nepheline, aegirine-augite, titanite ± garnet ± feldspar, in few cases together with wollastonite and combeite. Associated plutonic, mostly ijolitic inclusions contain similar mineral assemblages, mainly with slightly lower $X_{Mg}$ compared to their volcanic equivalents. However, cumulate rocks like pyroxenites and glimmerites exist as well as evolved lithologies including syenites and foid syenites [2].

The mineralogical and textural variations within at first sight similar nephelinites hint to heterogenous mantle sources, different degrees of partial melting, variable storage conditions of the evolving melt, different crystallization conditions, or combinations thereof, causing different crystallization paths. Yet, there is no clear distinction between nephelinites associated with carbonatites such as Oldoinyo Lengai, Kerimasi, and Shombole (which were formed prior to or during their carbonatitic phase) and nephelinites from non-carbonatite volcanoes like Burko and Sadiman.

We present a detailed petrological study focusing on mineralogy, mineral chemical and textural data of nephelinites and their plutonic inclusions from the major nephelinitic volcanoes in the area and compare them. We further use geothermobarometry and thermodynamic modelling to constrain and compare their crystallization and storage conditions in terms of temperature (T), pressure (P), oxygen fugacity ($fO_2$), and silica activity ($aSiO_2$). We will quantify different phase relationships and deduce fractionation trajectories to understand the observed variation between the investigated volcanoes. This will shed light on the genesis of these enigmatic rocks and contribute to understand rift-related volcanism.

*References:*

[1] S Mana et al. (2015) J. Geol. Soc. 172 (3): 368–389
[2] JB Dawson (2008) Geol. Soc. Lond., ISBN 1862392676
[3] HB Mattsson et al. (2013) Lithos 179: 175–192

# Petrogenesis of mid-Neoproterozoic, ferroan to magnesian charnockites from the Madurai block, India: Constraints from U-Pb geochronology, geochemistry, and geochemical modelling

Ashish Kumar Tiwari, Tapabrato Sarkar*

Indian Institute of Science Education and Research Kolkata, India

tapabrato@iiserkol.ac.in

---

Charnockites constitute a dominant proportion of the mid-Neoproterozoic rock ensemble in the Madurai block of the granulite terrane of south India. The compositional diversity observed in the charnockites has led to diverse hypotheses regarding their origin, spanning from the fractional crystallization of basaltic precursors in an arc environment with crustal input to crustal melting in an early-stage rift setting. Herein, we present a comprehensive analysis of zircon U-Pb ages and major and trace element chemistry of the charnockites from the Madurai block and integrate petrological and geochemical modelling to explore their origin and primary factors affecting their compositional diversity.

The zircon U-Pb geochronology yield weighted mean $^{206}Pb/^{238}U$ ages of ca. 820–790 Ma from the oscillatory zoned zircon cores, dating the age of magmatic crystallization. The zircon rims yield weighted mean ages of ca. 630 Ma and ca. 550–530 Ma, dating the ages of metamorphic overprinting. Geochemically, the charnockites display a broad range of compositions and are categorized into dominantly felsic and ferroan (group A) charnockites and dominantly intermediate and magnesian (group B) charnockites. The molar Fe+Mg content (maficity) effectively distinguishes the two groups, with group A charnockites having lower maficity compared to group B charnockites. Both groups are metaluminous to slightly peraluminous, with group A charnockites being relatively richer in potassium compared to group B charnockites. The overall chemistry resembles amphibole calc-alkaline granites (ACG). As for trace elements, both charnockite groups are rich in Ba and Sr, show negative Nb (Ta), Ti, P and a positive Ba anomaly on a primitive mantle-normalized trace element plot. On the chondrite normalized REE plot both the groups exhibit an enriched LREE with a flat HREE pattern and variable negative to slight positive Eu anomaly.

The scarcity of voluminous mafic-intermediate microgranular enclaves within the charnockites and absence of contemporaneous mafic intrusions suggest that these charnockites are unlikely derived from admixed mantle-derived mafic melts. Instead, they may have been generated by partial melting of the lower crust within the plagioclase stability zones. However, the compositions of group B charnockites, enriched in Ca, Mg, and Ti compared to experimental amphibolite melts, suggest the likely entrainment of phases containing these elements into the melt. Consequently, phase equilibria modelling was conducted using the R-crust program, considering two distinct melting scenarios common in granite petrogenesis: melt segregation from the system (purely melt loss events) and peritectic assemblage entrainment in the magma. We used the average lower crust composition as the starting material and performed calculations along multiple isobaric heating paths (IBH: @5, @7, @9, and @11 Kbar) within a temperature range of 600 to 1050 °C. Trace element partitioning was done using appropriate partition coefficients of the elements, melt composition, and residual mineralogy. The first melts generated by partial melting of the lower crust are ferroan and potassic and have trace element signatures similar to group A charnockites, while variable peritectic assemblage entrainment during melt extraction leads to the formation of melts resembling the intermediate and magnesian group B charnockites. Our findings suggest that the mid-Neoproterozoic granitoids likely formed through crustal anatexis of a mafic lower crust, possibly during the early stages of rifting associated with the breakup of Rodinia. This interpretation is supported by the observation of contemporaneous alkaline magmatism in the Madurai Block.

## High- to Ultrahigh-Temperature Evolution and partial melting of the Central Adirondack Highlands Gneiss Complex (New York State, US)

Ferrero, S.[1], Nicoli, G.[2], Darling, R.[3], Yakymchuk, C.[4], Wannhoff, I.[5], and Gresky, K.[2]

[1]Università degli Studi di Cagliari, 09042 Monserrato, Italy (silvio.ferrero@unica.it)

[2]University of Potsdam, 14476 Potsdam, Germany

[3]SUNY Cortland, NY 13045, United States of America

[4]University of Waterloo, Waterloo, ON N2L 3G1, Canada

[5]Freie Universität Berlin, 12249 Berlin, Germany

---

The Adirondack Highlands Gneiss Complex, New York State, USA, is one of the most renown natural laboratories to understand high-grade metamorphic processes and Mesoproterozoic crustal evolution. Despite more than 150 years of petrological studies, the Adirondack Highlands still has the potential for new discoveries; recent evidence of previously unreported ultrahigh temperature (UHT) metamorphism [1;2]and partial melting [3] have been found to be associated with megacrystic garnet growth.

Here we present the results of a detailed petrological study of mafic rock samples from four open pit mine sites in the vicinity of Gore Mountain in the south-central Adirondack Highlands: the Barton, the Ruby Mountain, the Hooper and the Old Hooper. With the notable exception of the garnet amphibolites of Barton Mine – world renowned for its garnet megacrysts occurrence, petrological data (including mineral chemistry) acquired with modern techniques on these quarries are scarce. To our knowledge, they are either completely absent, or are found in master's theses and doctoral dissertations difficult to access in the larger petrological community. With this work we attempt to fill this gap in knowledge by combining field and petrological observations, major elements mineral analyses, thermodynamic modeling and titanium-in-quartz geothermometry.

Three out of four localities share similar peak temperatures in the UHT field and slightly variable peak pressures. Ti-in-quartz thermometry and phase equilibrium modeling on Ruby Mountain Mine suggest a clock-wise path with prograde metamorphism from 650 °C and 10 kbar to the metamorphic peak at 950–1000 °C and ~12k bar, followed by near isothermal decompression to ~10 kbar and cooling/decompression to ~800 °C and 9 kbar. A similar post-peak evolution is also found in the Barton Mine metagabbro, albeit at slightly lower P. UHT metamorphism locally involved melt production, as testified by the presence of (former) silicate melt in three out of four investigated locations, i.e., namely leucosome bodies visible at the outcrop scale at Hooper and Ruby Mountain Mines, and nanogranitoids at Hooper Mine and in the garnet megacrysts of Barton Mine.

With this new knowledge we provide novel pressure–temperature (P-T) constraints on these different locations to better clarify the evolution of the late- Mesoproterozoic to early-Neoproterozoic Grenvillian Orogeny, and in turn improve our worldwide understanding the processes involving the continental crust during the enigmatic Boring Billion period (1.8–0.8 Ga) of Earth's history.

*References:*

[1] Shinevar et al. (2021) J Petrol 1-28
[2] Metzger et al. (2021) Geosphere 18: 261–297
[3] Ferrero et al. (2021) Earth Planet Sci Lett 569: 117058

# Early Paleoproterozoic high-K granites of the Bastar craton formed by reworking of TTGs: Insights from phase equilibria and trace element modeling

J. Padmaja[1]*, Tapabrato Sarkar[1], Somnath Dasgupta[1, 2]

[1]Department of Earth Sciences, Indian Institute of Science Education and Research Kolkata, Mohanpur-741246, India.

[2]Geological Studies Unit, Indian Statistical Institute, 203, B.T. Road, Kolkata-700108

---

The Neoarchean era is marked by significant thickening of the continental lithosphere, which coupled with the secular cooling of the mantle, led to the onset of mobile-lid plate tectonics. In the Archean cratons, this era is marked by transition from tonalite-trondhjemite-granodiorite (TTG) magmatism to high-K calc-alkaline magmatism. Insights on the genesis of this Neoarchean high-K calc-alkaline granites can contribute to a deeper understanding of the geodynamic evolution of early earth. The Bastar craton, situated in central India, documents a widespread high-K calc-alkaline granite magmatism at 2.50-2.45 Ga, namely, Dongargarh, Malanjkhand and Kanker granites, that has intruded the Paleoarchean TTG gneisses. This study focuses on the petrogenesis of the high-K Kanker granites through phase equilibria and trace element modelling to decode the processes of crustal growth and reworking during that era.

The Hbl-Bt bearing Kanker granites were emplaced during latest Neoarchean to earliest Paleoproterozoic (2.50-2.45 Ga), but show a protolith age of ~3.2 Ga. They exhibit a broad range of $SiO_2$ (61-74 wt.%) content, high $FeO_T/(FeO_T+MgO)$ ratios ranging from 0.6 to 0.9, and a calc-alkaline composition that is slightly peraluminous to metaluminous. The compositions of both major and trace elements in these granites exhibit characteristics of A-type, syn- to post-collisional granite magmatism, along with strong enrichment in incompatible elements and depletions in elements such as Eu, Nb, Ta, Sr and Ti. Available experimental and numerical studies on the Archean cratons worldwide suggest that ferroan A-type magma can be generated by, (1) fractional crystallization of an alkali basalt, (2) partial melting of the older TTG crust and (3) mixing of partial melts of older TTG crust with high-K metasomatized mantle melts. However, a concrete model for the generation of the Kanker granite is lacking.

We started with an average composition of the Paleoarchean TTGs reported from the Bastar craton. Using the program Rcrust, we simulated the partial melting of the TTG with nominal free water at varying depths (7 - 11 kbar), from the solidus temperature to around ~1000°C along an isobaric heating path, under open system conditions. Additionally, we also modelled varying degrees (0 – 30%) of peritectic assemblage entrainment into the partial melts. By considering the major element composition of the different generations of melts, residual mineralogy, and mineral-melt partition coefficients, the trace element compositions of the modeled melts are reconstructed. The model melts are ferroan, high-K calc-alkaline in nature with major and trace element compositions closely resembling those of the Kanker granites. Such enriched, ferroan granite magmatism typically occurs in an extensional setting, during the stabilization phase of continental lithosphere in a post-collisional environment. Our findings suggest that the ferroan, high-K calc-alkaline Kanker granites of the Bastar craton have originated through the reworking of older TTG crust, without the involvement of the mantle derived melts, in a post-collisional extensional setting. This model can be extended to other similar granites in Bastar as well as in other Archean cratons around the world.

## Mantle lithology of Cenozoic continental basalts in Central Asia: Constraints from olivine chemistry and whole-rock Mo-B isotopes

Zhang, Y.Y.[1], Sun, M.[2] and Yuan C.[3]

1 – Key Laboratory of Ocean and Marginal Sea Geology, South China Sea Institute of Oceanology, Chinese Academy of Sciences, 510301, Guangzhou, China, zhangyunying@scsio.ac.cn

2 – Department of Earth Sciences, The University of Hong Kong, Pokfulam Road, Hong Kong, China

3 – State Key Laboratory of Isotope Geochemistry, Guangzhou Institute of Geochemistry, Chinese Academy of Sciences, 510640, Guangzhou, China

---

Cenozoic continental alkaline basalts with oceanic island basalt (OIB)-like trace element features are diffusely distributed in central Asia. The geodynamic settings and ultimate magma origin of these basalts remain mysterious, which are largely due to the short of knowledge on their source lithology. Phenocrystic olivine is always the first silicate phase crystallizing from primary basaltic melts and could faithfully record information about the magma source. Besides, molybdenum and boron isotope systematics, in the past two decades, have proven to be of great value in tracking recycled oceanic crust in the mantle source of within-plate basalts. Voluminous basalts with ages from 30 Ma to 5 ka and volume up to 2900 $km^3$ erupted in Central Asia (e.g., Hangai dome and Mongol–Chinese Altai region). Representative basalts from the Central Hangai and Chinese Altai were collected for geochemical investigation to constrain their mantle lithology and related geodynamic mechanism. The phenocrystic olivines are featured by lower Ca, Mn, Mn/Zn and Mn/Fe but higher Ni than their counterparts in the peridotitic melts, indicating a pyroxenite-rich mantle source. Moreover, the light B and variable Mo isotopic compositions of the Chinese Altai basalts indicate that recycled, dehydrated oceanic crust was likely involved in the mantle source [1], since subduction dehydration preferentially releases heavy $^{11}B$ and $^{98}Mo$ to the fluid phase and residual oceanic crust will be gradually depleted in B, Mo, $^{11}B$ and $^{98}Mo$ with ongoing subduction. It is proposed that the secondary pyroxenite was formed by reaction of recycled oceanic crust with its ambient peridotite, based on their light B and Mo isotopic compositions, negative correlations between B isotopes and B contents, and between oxygen fugacity and olivine Mn/Zn [2]. The far-field effect of India–Eurasia convergence possibly tapped the upper asthenospheric mantle, subsequent melting of which gave rise to the dispersive Cenozoic volcanoes.

*References:*

[1] Zhang Y.Y. et al. (2021) Am Mineral 106: 251–264
[2] Zhang Y.Y. et al. (2019) Contrib Miner Petrol 174: 83

# The electrical conductivity in riebeckite, $Na_2Fe^{2+}_3Fe^{3+}_2Si_8O_{22}(OH)_2$, and geophysical implication

Bernardini, S.[1,2], Della Ventura, G.[1,3], and Mihailova, B.[2]

[1]Department of Sciences, University of Roma Tre, Rome, Italy, giancarlo.dellaventura@uniroma3.it

[2]Fachbereich Erdsystemwissenschaften, Universität Hamburg, Grindelallee 48, D-20146 Hamburg, Germany

[3]LNF-INFN, Frascati (Rome), Italy

---

In this presentation we will focus on the high-T behavior of riebeckite, a sodic amphibole with ideal composition Na2(Fe2+3Fe3+2)Si8O22(OH2) considered as a proxy for Fe-rich hydrous silicates in subduction zones. At high-temperature, ferrous iron in riebeckite oxidizes to ferric iron via the Fe2+ + OH- = Fe3+ + O2- reaction and without any structural breakdown. Fe oxidation couples with the delocalization of an electron and dissociation of the bonded OH- anion to O2- and H+; in the presence of external oxygen, the latter may migrate out of the structure, combine with surface O2- and be released as H2O in the system. Under these conditions, the amphibole transforms into an oxo-phase thus remaining stable to very high-T. Under low fO2 conditions, no Fe oxidation occurs, and the amphibole stability is reduced by ~100 °C. Although relatively simple, the oxidation reaction has been shown by Della Ventura et al. [1,2] to be a complex and dynamical process, being reversible in a T range that depends on the amphibole composition [3-6]. Due to the above processes, riebeckite (as well all other Fe-rich hydroxy-silicates) may develop both electron and ionic conductivity.

Geophysical measurements show the occurrence of anomalous high-conductivity layers (HCL) in subduction zones at different depths, and these are typically associated with low-velocity layers where most of seismicity is generated [7,8]. The explanation of HCL has been attributed to several different causes, including partial melting of crustal rocks, the presence of high-conductive fluids or minerals (graphite, metal oxides/sulfides) or thermal processes on Fe-bearing phases. Our research shows that one main explanation of these anomalies can be related to thermal enhancement of the electrical conduction via small-polaron hopping in Fe-bearing hydrous silicates. The thermal ranges of activation of the whole process can be elegantly followed via polarized Raman scattering, a technique widely accessible in Earth Science Laboratories that is both sensitive to phonon and electron states. This result represents an important aspect of our work, emphasizing to the Scientific Community the importance of Raman scattering in characterizing complex processes in a (relatively) straightforward way, thus opening the road to systematic experiments focused on the physical properties of common rock-forming minerals of geophysical interest.

References cited

[1] Della Ventura G et al. (2018) Am. Mineral. 103: 1103-1111
[2] Della Ventura G et al. (2023) Am. Mineral. 108: 59-69
[3] Mihailova B et al. (2021) Communication Mat.: doi.org/10.1038/s43246-021-00161-y
[4] Mihailova B et al. (2022) Con. Matter 7: 68, doi.org/10.3390/condmat7040068
[5] Bernardini S et al. (2023) Geochemistry: doi.org/10.1016/j.chemer.2022.125942
[6] Bernardini S et al. (in press) Am. Mineral: doi.org/10.2138/am-2023-9138
[7] Kasaya T (2005) Earth Planets Space 57: 209–213.
[8] Peacock SM and Wang K (1996) Science 286: 937–939

## Developing new web based software for analysing and interpreting spectroscopy in Earth and Environmental Sciences

Byrne, J.M.

[1]School of Earth Sciences, University of Bristol, james.byrne@bristol.ac.uk

---

The continuing and growing relevance of earth and environmental sciences is resulting in an explosion of experimental data. Analysis of this data seeks to address specific environmental questions, such as how soil bacteria are connected to the release of greenhouse gases, or how changes in geochemistry influences the release of pollutants into drinking water. Accumulation of this information raises challenging questions about how to efficiently store, analyse, and share the data especially in the era of open science. Spectroscopy data is often analysed manually, with domain expertise used to interpret and eventually publish results. This approach works for specialists or experienced researchers; however, it creates an invisible barrier to new adopters or more general users such as those working in multidisciplinary contexts. To overcome this barrier and advocate for an open culture in data analysis, this project is focusing on implementing machine learning to provide semi- and fully automated fitting routines for spectroscopic data, especially focusing on those data which are relevant to environmental sciences.
This presentation focuses on the development of a web application (written in Python/Streamlit) designed to read, fit, and interpret spectroscopy data. This cutting-edge project is aiming to deliver a framework to accelerate the analysis and interpretation of data via a combination of supervised and unsupervised machine learning methods. This will make data analysis tools available to researchers across the world. We are currently working on three key aspects: (a) automated data interpretation tools to assist with analysis; (b) validation of the concept through analysis of complex environmental samples as part of a case study; (c) simplification of learning approaches used for spectral analysis to encourage more widespread uptake of different techniques. The project has initially focussed on just a few techniques, including Moessbauer spectroscopy and X-ray diffraction, but is planned to be expanded into a range of analytical methods. The resulting platform will thus cater to a range of research fields, including (bio)geochemistry, geophysics, paleomagnetism, geomicrobiology, and astrobiology amongst countless others. This presentation will discuss the development of this project as well as ongoing challenges and new opportunities.

## From rocks to wastes: Tracing the fate of chromium in nickel mining areas

Delina, R.E.G.[1,2*], Perez, J.P.H.[1], Prieur, D.[3,4], Scheinost, A.C.[3,4], Bazarkina, E.F.[3,4], Kvashnina K.O.[3,4], Benning L.G.[1,2]

[1]GFZ German Research Centre for Geosciences, Telegrafenberg, 14473 Potsdam, Germany

[2]Department of Earth Sciences, Freie Universität Berlin, 12249 Berlin, Germany

*rgdelina@gfz-potsdam.de

[3]The Rossendorf Beamline at ESRF, The European Synchrotron, CS 40220, 38043 Grenoble Cedex 9, France

[4]Institute of Resource Ecology, Helmholtz-Zentrum Dresden-Rossendorf, Bautzner Landstraβe 400, 01328 Dresden, Germany

---

Weathering of ultramafic rocks to form iron (Fe) (oxyhydr)oxide-rich laterites often result in the enrichment of critical (e.g., nickel (Ni), cobalt (Co), rare earth elements) and potentially toxic metals (e.g., chromium (Cr)) in laterite deposits [1]. Today, laterites are extensively mined as they remain one of the world's major sources of Ni as well as Co [2]. During ore processing to extract these valuable metals, non-targeted metals like Cr are also affected, yet little is known about its fate. This is particularly relevant because there are still huge uncertainties about the speciation of Cr in the laterite host phases or during processing, to make a proper assessment of its potential release into surrounding environments. Combining mineralogical and geochemical characterization (e.g., XRD, S/TEM) with synchrotron-based X-ray absorption spectroscopy (XAS), we traced the fate of Cr from weathered ultramafic rocks to the resulting laterite deposits and all the way to the ore processing wastes. Based on quantitative analysis of Cr, Mn, and Fe K-edge XAS spectra, we could document how weathering repartitions Cr from the primary chromite and silicate hosts to Fe (oxyhydr)oxides (e.g., goethite, hematite). Concomitant with the formation of Fe (oxyhydr)oxides, weathering enriches Mn oxides (e.g., asbolane), oxidizing ≤14% of the total Cr to its toxic form, Cr(VI). During ore processing, it is Fe (oxyhydr)oxides that mainly control the environmental mobility of Cr. Overall, our results provide new insights on Cr cycling in laterite mining areas, contributing to improved strategies for environmental management and remediation efforts.

*References:*

[1] Delina et al. (2020) Chem Geol 558:119863
[2] USGS (2024) MCS 2024:63-125

## Tc and Pu retention by magnetite – Combining experimental and theoretical techniques

Katheras, A.S.[1], Zimmermann, T.[2], Karalis, K.[1], Krack, M.[3], Scheinost, A.C.[2,4] and Churakov, S.V.[1,5]

[1]Institute of Geological Sciences, University of Bern, CH-3012 Bern, Switzerland; E-mail of presenting author: anita.katheras@unibe.ch.

[2]Institute of Resource Ecology, Helmholtz-Zentrum Dresden-Rossendorf (HZDR), DE-01328 Dresden-Rossendorf, Germany.

[3]Laboratory for Materials Simulations (LMS), Paul Scherrer Institute (PSI), CH-5232 Villigen PSI, Switzerland.

[4]The Rossendorf Beamline (BM20), European Synchrotron Radiation Lab, FR-38043 Grenoble, France.

[5]Laboratory for Waste Management (LES), Paul Scherrer Institute (PSI), CH-5232 Villigen PSI, Switzerland.

---

In many European countries (e.g., France, Switzerland), thick steel casks are foreseen for the containment of high-level radioactive waste in deep geological repositories. In contact with pore-water, steel corrodes forming mixed iron oxides, mainly magnetite ($Fe_3O_4$). After tens of thousands of years, the casks may breach allowing for leaching of the radionuclides (e.g., Tc and Pu) into pore-water. The radionuclides can be retarded by corrosion products either by adsorption or via structural incorporation [1,2]. The molecular scale mechanisms of these phenomena are investigated by ab initio simulations and X-ray absorption spectroscopy (XAS).

The dominant low-index surfaces of magnetite particles and their termination at the relevant conditions were identified based on density functional theory (DFT), using the open-source CP2K code [3]. The DFT+U method was employed for the strongly correlated 3d- and 5f- electrons of Fe and Pu, respectively. After benchmarking the model setup, the surface energies of the (111) facet with different surface terminations and water coverage were analysed as a function of redox conditions and pH. The Eh and pH predominance diagram was used to predict the most stable mineral surfaces under real repository conditions [4]. Further, the stability of nanocrystals with approximately 2 nm size were evaluated. Subsequently, ab initio molecular dynamics (MD) were applied to simulate sorption structures of radionuclides on the expected magnetite (111) surfaces based on experimental findings [2,5].

Complementary, wet-chemical batch sorption experiments of magnetite nanocrystals in the presence of Tc or Pu were conducted. The resulting complexes represent the expected incorporation and sorption structures [1,2,5] and were analysed by the XAS techniques (EXAFS, XANES) available at the European Synchrotron Radiation Facility [6].

Finally, the synergy of the experimental and theoretical studies contributes to the understanding of the retention mechanism of radionuclides in deep geological repositories.

*References:*

[1] Kirsch R et al. (2011) Environ Sci Technol 45: 7267-7274
[2] Yalçintaş E et al. (2016) Dalton Trans 45: 17874-17885
[3] Kühne T D et al. (2020) J Chem Phys 152: 194103
[4] Katheras A S et al. (2024) Environ Sci Technol 58: 935-946
[5] Dumas T et al. (2019) ACS Earth Space Chem 3: 2197-2206
[6] Scheinost A S et al. (2021) J Synchrotron Rad 28: 333-349

# Raman spectroscopy to study mineral host-inclusion systems: when experiments meet *ab initio* simulations

Murri, M.[1], Prencipe, M.[2], Mihailova, B.[3], Angel, R.J.[4] and Alvaro M. [1]

[1]Department of Earth and Environmental Sciences, University of Pavia, Italy (mara.murri@unipv.it)

[2]Earth Science Department, University of Torino, Italy

[3]Department of Earth System Sciences, Universität Hamburg, Germany

[4]Istituto di Geoscienze e Georisorse, CNR, Padova, Italy

---

Raman spectroscopy is a powerful tool and when it is applied to mineral host-inclusion systems it can provide fundamental insights about their journey from depth in the Earth to the surface. These studies have crucial implications for plate tectonic mechanisms [1].
However, state-of-the-art Raman spectroscopy experiments do not provide us access to all of the possible modifications and structural changes experienced by minerals during subduction or exhumation. Contrasts in the thermoelastic properties of minerals, non-hydrostatic stress and strain regimes: these are just a few aspects that come into play when dealing with natural samples and that need to be considered. On the other hand, computer simulations have been recently revealing a huge potential in solving problems raised by the experimental world and can provide complementary information that is otherwise inaccessible [2].

We have explored the use of Density Functional Theory simulations to reproduce as closely as possible the conditions that minerals attain in metamorphic processes, and we combined these results with experimental data. We have applied this approach to different combinations of symmetries and properties of host-inclusion systems in metamorphic rocks [3,4,5]. Our work shows that this combined use can provide reliable and accurate results suggesting that the best method to study mineral host-inclusion systems by means of Raman spectroscopy lies exactly halfway between the experiments and the computational calculations.

*References:*

[1] Alvaro M et al. (2020) Geology 48: 24-28
[2] Prencipe M (2019) Rendiconti Lincei 30: 239-259
[3] Murri M et al. (2022) Lithos 422, 106716
[4] Musiyachenko K A et al. (2021) Am Mineral 106: 1586-1595
[5] Stangarone C et al. (2019) Eur J Mineral 31: 685-694

# Identification of ferrous hydroxychlorides in rocks and inclusions - hibbingite ($\gamma$-$Fe_2(OH)_3Cl$) *versus* parahibbingite ($\beta$-$Fe_2(OH)_3Cl$)

Koděra, P.[1], Majzlan, J.[2], Pollok K.[2], Kiefer, S.[2], Šimko, F.[3], Scholtzová, E.[3], Luptáková, J.[4] and Cawthorn, G.[5]

[1]Dep. of Mineralogy, Petrology and Econ Geol, Comenius University, Bratislava, Slovakia, kodera1@uniba.sk

[2]Institut für Geowissenschaften, Mineralogie, Friedrich-Schiller-Universität Jena, Germany

[3]Institute of Inorganic Chemistry, Slovak Academy of Sciences, Bratislava, Slovakia

[4]Earth Science Institute, Slovak Academy of Sciences, Bratislava, Slovakia

[5]School of Geosciences, University of the Witwatersrand, Johannesburg, South Africa

---

Ferrous hydroxychlorides are mineral species with extreme sensitivity to oxidation and hydration in contact with air, consequently they are rarely recognised in geological materials. Only the orthorhombic mineral hibbingite was previously known as the $\gamma Fe_2(OH)_3Cl$, associated with altered mafic intrusive rocks [1]. The β-polymorph was recognised just in archaeological and corrosion sciences as the product of iron corrosion. This polymorph of $Fe_2(OH)_3Cl$ was now found in pyroxenite from the Karee platinum mine in the Bushveld Complex, South Africa and described as a new mineral parahibbingite [2]. Both minerals were distinguished by a combination of Raman spectroscopy and FIB-SEM-TEM-EDX and FIB-TEM-SAED analytical techniques. Raman spectra of parahibbingite have two strong vibration bands at ~3550 and 3560 $cm^{-1}$, accompanied by much weaker bands at ~124 and 160 $cm^{-1}$ while hibbingite has a sharp strong band at 3450 $cm^{-1}$ and two moderate bands at 199 and 385 $cm^{-1}$. Thus, Raman spectroscopy provides a fast and reproducible tool for their quick and non-destructive recognition.

Parahibbingite is trigonal (space group $R\bar{3}m$, a=6.94(5) Å; c=14.5(2) Å), with an empirical formula $(Fe^{2+}_{1.98}Mn^{2+}_{0.01}Ca_{0.01})(OH)_{3.08}Cl_{0.92}$. In pyroxenite from the Bushveld Complex, it occurs as fine-grained reaction rims on the contact of orthopyroxene phenocrysts and talc, inside a drill core. Therefore, the origin of this mineral most likely results from late hydrothermal alteration of pyroxenite.

Applying Raman spectroscopy, hibbingite was found as an abundant daughter mineral hosted by brine fluid inclusions and salt-melt inclusions in hydrothermal quartz associated with granitic systems, especially related to Au-, Cu-Au- and Sn-porphyry and Fe-skarn deposits. Based on microthermometry data, it crystallizes upon cooling from ~460 to <150°C under reducing conditions [3]. Hibbingite from salt-melt inclusions in the Au-porphyry deposit Biely Vrch (Slovakia) has lattice parameters a=6.30 Å, b=7.12 Å, c=9.89 Å, obtained by TEM-SAED. In salt melt inclusions, hibbingite is the only phase that carries hydrogen (as a hydroxyl group) in otherwise $H_2O$-free salt-melt inclusions.

Both hydroxychloride minerals are geochemically important as they could be regarded as reservoirs for Cl and $H_2O$ in large volumes of hydrothermally altered ultramafic rocks, that are able to transport volatiles into shallow levels of subduction zones. Furthermore, their later dissolution can cause remobilization, transport, and deposition of sulfidic ores in saline fluids. Their detection in natural outcrops and samples, however, is difficult, because of their sensitivity to air (typically they convert rapidly to akaganéite [$Fe^{3+}$(O,OH,Cl)]) and thus, their presence can be easily overlooked.

Acknowledgements: This work was supported by the grants VEGA-1/0313/20 and APVV-22-0134.

*References:*

[1] Saini-Eidukat, B. (1994) Am Min 79:555-561

[2] Koděra P. et al. (2022) Am Min 107:826-841

[3] Zubkova et al. (2012) Z Kristallogr - Cryst Mat 234: 379–382.

## Spectroscopic and minero-petrological investigation of boninites from Cyprus as potential analogues of Mercury lavas

Landi, A.I.[1,4], Carli, C.[2], Capaccioni, F.[2], Maturilli, A.[3], Helbert, J.[3], Alemanno, G.[3] and Pratesi, G.[4]

[1]annairene.landi@unitn.it, Università degli Studi di Trento, Via Sommarive, 14, 38123 Trento, Italy

[2] INAF-IAPS Via del Fosso del Cavaliere, 100, Tor Vergata 00133 Roma, Italy

[3] German Aerospace Center (DLR), Rutherfordstraße 2, 12489 Berlin, Germany

[4]Dipartimento di Scienze della Terra, Università degli Studi di Firenze, Via G. La Pira, 4, 50121 Firenze, Italy

---

Despite the clearly different formation conditions regarding oxygen fugacity, water contribution and iron abundance in the source region, terrestrial boninites and komatiites are considered promising analogues for Mercury's lavas based on MESSENGER Mission data [1]. This study aims to compare terrestrial boninites with Mercury lavas, considering spectroscopic, petrological, and mineralogical characteristics. We are investigating samples coming from three distinct locations (labeled PAR, ARA, ATH) within the Troodos massif, Cyprus island. We selected representative samples for each locality and performed X-ray Fluorescence (XRF), scanning electron microscopy (SEM), electron microprobe (EPMA) analysis and reflectance spectroscopy in the spectral ranges covered by the VIHI imaging spectrometer (0.4-2.0 µm) [2] and the MERTIS spectrometer (7-14 µm) [3] onboard the ESA's BepiColombo mission. XRF bulk composition analysis gave average values (wt%) of major elements ($SiO_2$ 53.2, $Al_2O_3$ 12.2; FeO 7.9; MgO 12.55; CaO 8.5) that are in good agreement with the average compositions of Mercury's geochemical terranes [1,4]. $SiO_2$ and $Al_2O_3$ contents fall right in the ranges of Mercury's terranes; MgO content in our samples is slightly lower and CaO higher; the only major difference is the higher FeO content, as expected. The spectroscopic and compositional differences observed between the samples, reflect their different mineralogy. Samples PAR show vitrophyric texture with olivine (Fo89) and clinopyroxene (En48Wo38Fs14) phenocrysts in glassy groundmass. Plagioclase crystals are not detected. Minor weathering is visible with the presence of sporadic calcite grains. Samples ARA are composed of clinopyroxene (En47Wo30Fs13) in albitic groundmass (Ab98An2). Weathering is clearly visible with the presence of clinochlore replacing olivine. ATH sample is holocrystalline and composed by euhedral clino- (En48Wo42Fs10) and ortho-pyroxene (En82Wo4Fs14) crystals surrounded by plagioclases (from Ab97An3 to Ab7An93). Olivine is not observed and some portions are composed only of clay minerals. VNIR spectra show an absorption band at ~1 µm which is associated with olivine and pyroxene. Some samples show also clear absorption features at ~1.4 µm, ~1.9 µm and 2.3 µm due to terrestrial hydrated alteration phases. Taking into account the differences intrinsic in the acquisition methods and in the objects under analysis [e.g. 5], we tried a preliminary comparison between laboratory reflectance spectra of boninite samples and MASCS/MESSENGER Mercury data [6]. This comparison will be implemented with ongoing measurements including VNIR reflectance analysis with different acquisition angles and on smaller grain sizes and TIR emittance spectroscopy investigation. These new data, in combination with minero-petrologic characterization, could also facilitate future comparisons with mineralogical data expected from SIMBIO-SYS/VIHI and MERTIS spectrometers.

*References:*

[1] Vander Kaaden K E et al. (2017) Icarus 285: 155-168
[2] Cremonese G et al. (2020) Space Sci Rev 216
[3] Hiesinger H et al. (2020) Space Sci Rev 216
[4] Mari N et al. (2023) Planet Space Sci 236
[5] Barraud O et al. (2020) J Geophys Res Planets 125
[6] Galiano A et al. (2022) Icarus 388

## Impact of crystal-to-glass ratio and acquisition geometry on the reflectance spectra of synthetic Nakhlitic rocks

Pisello, A.[1], Fastelli, M.[1], Baroni, M.[1], Schmitt, B.[2], Beck, P.[2], Zucchini, A.[1], Petrelli, M.[1], Comodi, P.[1] and Perugini, D[1].

[1] Department of Physics and Geology, University of Perugia, I-06100 Perugia, Italy
maximiliano.fastelli@unipg.it

[2] Univ. Grenoble Alpes, CNRS, IPAG, 38000 Grenoble, France

---

Silicates dominate volcanic terrains across the Solar System's terrestrial planets. Earth's volcanic landscapes consist of lava flows and pyroclasts with a predominantly glassy texture. Understanding how the glass/crystal ratio influences the spectral response of volcanic rocks is crucial for interpretation of planetary remote sensing data from Mars and other rocky bodies [1]. In the Petro Vulcanology Research Group (PVRG) laboratory, mafic volcanic materials were synthesized to mimic the composition of Nakhlite meteorites. A homogeneous silicate glass (Nglass) was created and then used to produce three samples by melting at 1500°C and gradually cooling to subliquidus temperatures of ~1200°C (N12), ~1100°C (N11), and ~1000°C (N10). Analysis revealed varying degrees of crystallinity, with N11 and N10 exhibiting similar mineralogical compositions, while N12 showed intermediate crystal content. X-Ray Powder diffraction (XRPD) coupled with Rietveld method for quantitative phase analysis, X-ray fluorescence (XRF) and scanning electron microscope (SEM) analyses were performed to assess the type, degree of crystallinity and glass content. Reflectance spectra were collected at room temperature in the 1-4.2 µm range considering a set of 3 incidence (i = 0°; 30°; 60°) and emergence angles between -70° and 70° using the custom-made bidirectional reflectance spectro-gonio radiometer SHINE (SpectropHotometer with variable INcidence and Emergence) at the Cold Surface Spectroscopy (CSS) facility laboratory at the Institut de Planétologie et d'Astrophysique (IPAG) (project number 21-EPN-FT1-025 Europlanet 2024). The spectral features of the single mineral phases are barely distinguishable for N10 and N11, due to the presence of magnetite that probably flattened the spectra, whereas the spectral signature of Fe in augite is distinguishable for N12 located at ~0.9 and ~1.15 µm. Spectral shifts from positive slopes for glasses to flat-negative slopes for crystalline materials were observed in the Visible and Near-Infrared range as crystallinity increased. When changing observation geometry, the reflectance values and spectral slope show important variations while the band positions remain unchanged. We observe important dependence of band and slope at both low phase angle (< 30°) and high phase angle (> 100°). Principal component analysis (PCA) identified four distinct clusters corresponding to the four samples, particularly for glass-bearing materials. These findings offer additional insights into the spectral characteristics of synthesized rock samples, particularly those containing glass materials. Such information is valuable for accurately modelling the spectral signatures observed from rocky bodies within the Solar system. Part of this work was supported by the Ministero dell'Istruzione dell'Università e della Ricerca (MUR) through the program "Dipartimenti di Eccellenza 2018-2022" (Grant SUPER-C).

*References:*

[1] Pisello A et al. (2022) Icarus, 388: 115222

# Investigating Uranium in Mineral Systems using $M_{4,5}$-edge X-ray Adsorption Spectroscopy

Shaw, S[1], Waters, C[1], Neill, TS[1], Morris, K[1], Baker, ML[2], Mosselmans, FW[3], Igatyev, K[3]

[1] Research Centre for Radwaste Disposal and Williamson Research Centre, Department of Earth & Environmental Sciences, The University of Manchester, Oxford Road, Manchester, M13 9PL, UK

[2] Department of Chemistry, The University of Manchester, Manchester, M13 9PL, UK

[3] Diamond Light Source, Harwell Science and Innovation Campus, Chilton, Didcot, OX11 0DE, UK

---

The transport and fate of uranium (U) in environmental and engineered systems is controlled by a range of biogeochemical processes. This includes contaminated land and radioactive waste geodisposal environments. In these systems a range of U mineral phases can be stabilised as a function of geochemical (e.g. pH and redox conditions) and physical (e.g. temperature) conditions. In addition, U can be stabilised via substitution into a range of environmentally relevant mineral phases, including iron (oxyhydr)oxides (e.g. goethite, FeOOH)[1]. The speciation of U with the environment, including its oxidation state, is key to controlling its mobility and fate. In particular, U(VI) and U(IV) are the most prevalent oxidation states of U under environmental conditions. U(VI) tends to be highly soluble, and therefore potentially mobile, whereas U(IV) has very low solubility often forming solid mineral phases (e.g. uraninite, $UO_2$) in environmental and geological systems. However, recent studies have shown that U(V) can also form during environmental processes e.g. via stabilisation during mineral incorporation[1] or bioreduction processes[2]. In addition, complexing ligands (e.g. $CO_3^{2-}$ and $PO_4^{3-}$) can also influence U solubility, mobility, and mineral phase formation. Investigating the speciation of U within mineral phases, including quantifying U oxidation state (i.e. U(VI), U(V) and (IV)) and local bonding environment, is challenging using more conventional techniques. In this study we have developed the application of High Energy Resolution Fluorescence Detected X-ray Adsorption Near Edge Structure (HERFD-XANES) spectroscopy at the U $M_{4,5}$ edges to probe the electronic structure of U in mineral phases in environmentally relevant systems, with the aim of exploring how changes in oxidation state and ligands complexation impacts on electronic structure of U, and in turn how HERFD-XANES may be applied to understand and predict the mobility and fate of U in the environment.[1, 2]

We have analysed a broad suite of U-based mineral phases, and U associated with iron oxide minerals (e.g. magnetite, $Fe_3O_4$) using U $M_{4,5}$ edge HERFD-XANES and Resonant Inelastic X-ray Scattering (RIXS) to identify changes in U electronic structure and thus specific sensitivities of these techniques to U environmental speciation. Results from this study, and other recent studies[1-4], show that HERFD-XANES is an essential tool for assessing the oxidation state of U, due to the significant increase in resolution resulting from smaller core-hole lifetime broadening effects of HERFD-XANES measurements at U M-edges. This highlights the potential for these techniques to enhance quantification in U(VI), U(V) and U(IV) oxidation state analysis. In addition, analysis of the HERFD-XANES spectra show significant sensitivity the local coordination environment and ligand present within the uranium mineral phase. Overall, the results highlight the potential for U $M_{4,5}$ edge HERFD-XANES and RIXS to provide a unique insight into U biogeochemical processes within engineered and natural environments.

*References:*

[1] Roberts HE et al. (2017) Env Sci Tech Lett 4:421-426
[2] Vettese GF et al. (2020) Env Sci Tech 54:2268-2276
[3] Kvashnina KO et al. (2022) Chem Comm 58:327-342
[4] Vitova T et al. (2017) Nat Comm 8:16053

## Cation order in omphacitic clinopyroxenes: implications for Raman elastic geothermobarometry

Baratelli, L.[1], Cámara, F.[1], Mihailova, B.[2] Murri, M.[3] and Alvaro M.[3]

[1]Department of Earth Sciences, University of Milan. lisa.baratelli@unimi.it

[2]Department of Earth Sciences, University of Hamburg.

[3]Department of Earth and Environmental Sciences, University of Pavia.

---

Omphacite is a common mineral found in many geological settings, thus its widespread occurrence makes it a valuable candidate for Raman elastic geothermobarometry. This approach uses the deformation recorded by mineral inclusions to determine the pressure and temperature conditions under which they were entrapped [1]. Raman scattering, highly sensitive to structural deformations, provides crucial insights into crystal structure variations that occur due to heating or compression. While many host-inclusion systems have been studied, clinopyroxene inclusions remain relatively unexplored. Therefore, accurate calibration of Raman-peak positions against hydrostatic pressure is essential for applying Raman elastic geobarometry to omphacites in different mineral hosts.

Natural omphacite crystals exhibit cationic ordering associated with crystallization temperature, which affects their elastic properties. To investigate these aspects, *in situ* high-pressure Raman spectroscopy measurements were performed on natural ordered and experimentally disordered omphacites from Münchberg Massif (Germany). By examining omphacite crystals with varying degrees of order achieved through isothermal annealing experiments, it was observed that increasing cationic disorder leads to peak broadening, while pressure variations influence Raman peak positions. However, the peak position is also affected by the chemical composition. Therefore, $Fe^{3+}$-rich crystals from Lugros and Camarate (SE Spain), and Voltri massif eclogites (Italy), already characterized by single crystal X-ray diffraction [2], along with synthetic Fe-free omphacites [3], were analyzed, as an initial step towards the chemical calibration of omphacites using Raman spectroscopy.

By considering the influence of chemical composition and cationic ordering, we have expanded our understanding of the elastic behavior of omphacite obtained through Raman spectroscopy and its potential use for geobarometric calculations, important for determining the pressure and temperature conditions involved in geological processes where omphacite growths.

*References:*

[1] Angel R J et al. (2019) Z Kristallogr Cryst Mater 234(2):129-140
[2] Cámara F (1995) PhD thesis, University of Granada, 504 pp.
[3] Pandolfo F et al. (2015) Phys Chem Minerals 42:1-14

## Ultra-Thin Sections - Illuminating the Spectra of Highly Opaque Minerals

Funaro, E.J.[1], Palfey, W.R.[1], Park, A.[2], Schlom, D.G.[2], and Rossman G.R.[1]

[1]Division of Geological and Planetary Sciences, California Institute of Technology, Pasadena, CA, efunaro@caltech.edu

[2]Department of Materials Sciences and Engineering, Cornell University, Ithaca, New York 14853,

---

It is no surprise that transmission spectroscopy has been very rarely applied to opaque minerals. By definition, opacity is the lack of light passage. Hence, collecting the information gathered by optical and Near IR wavelengths passing through a highly opaque mineral sample is rather counterintuitive. However, the insitu opaqueness of many minerals abundant in the deep earth that are known to be opaque at ambient temperatures have lately put into question. As major photon absorbing mechanisms such as Inter-Valance Charge Transfer (IVCT) and magnetic enhanced d-d transitions have both been suspected to decrease dramatically in high temperatures such as those found at depth [1,2] affecting the deep earth thermodynamic regime. In our work, we demonstrate how ultra-thin samples (0.15 nm - 2 µm) provide a window to the optical absorbance features in highly opaque samples. Here we present the first-ever collected absorbance spectra of magnetite (150 nm thick), ilmenite (~1 µm), and hematite (~1 µm) at temperatures ranging from ambient to 1100 ℃. We used synthetic and natural samples and achieved the minute thicknesses required for transparency using two different methods. Thin film specimens (<500 nm) were synthesized through Molecular-Beam Epitaxy (MBE) at the Schlom Lab at Cornell. Natural samples were manually thinned to 200 µm and further thinned to single digit µm thickness using a Dimpler TEM sample prepping apparatus.

Initial ambient temperature results agree with proposed mechanisms for the opacity of the measured phases, near-IR centered wide Inter-Valance Charge Transfer (IVCT) peak for the magnetite (~1250) and the ilmenite (~1300 nm in agreement with previous work [3]), and magnetically enhanced d-d transition bands for the hematite [4]. Despite their thinness, both synthetic and natural samples proved to be stable enough for the investigation of the temperature dependence of both mechanisms up to 700 ℃ and 1100 ℃ respectively. IVCT absorption bands have been previously shown to decrease at high temperatures in phases possessing diluted (non-stoichiometric) IVCT sites. Our results show for the first time that the intensity IVCT absorption bands fall dramatically upon heating in stoichiometric IVCT minerals. In hematite, the magnetically enhanced spin-forbidden absorption has been investigated beyond the curie temperature of hematite (>680 ℃) and has shown a decrease in D-D transition absorption suggesting a breakdown in magnetic enhancement. We believe that ultra-thin sections are a yet to be widely utilized very attainable tool that holds the power to elucidate the darkest of minerals and shed light on their electronic outlay, their trace components, and their crystallographic defects, in a quantitative and orientation specific manner.

*References:*

[1] Taran M N and Langer K (1998) N. Jb. Miner. Abh. 172:325-346
[2] Evans H V and Rossman G R (2018) Am Min (accepted)
[3] Taran M N (2019) Phys. Chem. Miner. 46: 839-843
[4] Rossman G R (1996) Geol. Soc. Spec. Publ. 5:23-27

# Raman Spectroscopy as an important tool for the study of lunar, Martian and other meteorites and for the collection of new Raman databases for future space missions

Kaliwoda, M[1], Zuncke, J.[1,2] Drozdovsky I [2]

[1]Mineralogical State Collection Munich, Bavarian National History Museums (snsb), Germany and kaliwoda@snsb.de

[2]European Astronaut Centre (EAC) - European Space Agency (Linder Höhe, D-51147 Cologne, Germany

---

At the Mineralogical State Collection Munich (MSM), Raman spectroscopy plays a key role in characterizing meteorites, particularly those from extra-terrestrial bodies. Our focus extends to lunar, Martian, and Vesta meteorite samples, aiming to unravel their mineral composition, high-pressure phases, potential glass components, and inclusions. By leveraging Raman spectroscopy, we delve into the geological history and thermal evolution of these bodies, drawing parallels to Earth's formation and early history. We are also expanding our existing Raman database with more and more new data on meteorite materials which plays another key role in future extra-terrestrial missions and training of astronauts.

For instance, our research examines into meteorites like NWA11266, classified as lunar feldspar breccia, discovered in 2017. Through Raman spectroscopy analysis, we identified main minerals such as mafic olivines, pyroxenes, anorthitic feldspar, graphite, and minor metallic components, alongside accessory phases like apatite and zircon. The advantage is that we can also carry out these investigations on non-embedded material and thus simulate the same conditions that exist in the rover missions. We also have a heating/cooling table that operates in a temperature range from -160 to 600 C, which means that we can also modify the samples subsequently if required.

Such investigations shed light on the geochemical structure and history of the Moon, aiding in understanding its geological processes, including volcanic activity, impact events, and differentiation. Moreover, our studies extend beyond lunar meteorites to encompass other extra-terrestrial bodies, including Mars, Vesta, pallasites, and various chondrites. Through comparative analysis with Earth's interior rocks like mantle xenoliths and ophiolitic mantle rocks, we aim to glean insights into planetary formation processes and compositional diversity.

In summary, our interdisciplinary approach, combining Raman spectroscopy with electron microprobe and SEM analyses, contributes to a deeper understanding of extra-terrestrial bodies, composition, evolution, and geological processes. These findings not only advance scientific knowledge but also inform future space missions and the application of spectroscopic methods in space exploration [1].

*References:*

[1] Drozdovsky I et al (2020) Journal D i Brief, S2352-3409(20), 30879-9, https://doi.org/10.1016/j.dib.2020.105985

## Basaltic glasses in the lower mantle: trace elements as markers of local structure changes

Kovalskii, G.[1], Rosa, A.D.[2], Mathon, O.[2], Morgenroth, W.[1], Morard, G.[3], Pennacchioni, L.[1], Wilke, M.[1]

[1] Institut für Geowissenschaften, Universität Potsdam, 14476 Potsdam, Potsdam, Germany

[2]European Synchrotron Radiation Facility, ESRF, Grenoble France

[3]Insitut de Minéralogie, de Physique, des Matériaux, et de Cosmochinie, IMPMC, Paris, 75005, France

---

Silicate melts play a key role in regulating global changes in both heat and material over geological timescale. They are highly important for understanding and modelling of chemical differentiation, the cooling history of the planet, petrogenesis, and ore genesis processes. Precisely defining the conditions under which silicate melts form with depth can help in understanding processes in the lower mantle, where direct access is currently unavailable. Specific crystallochemical criteria for accurate determination of PT parameters and depth of silicate melts formation can also be revealed [1].

The experiment was conducted to study the local structure of minor cations in silicate glasses and melts under extreme conditions of the lower mantle This experiment represented the first one that used the newly installed laser-heating setup that is dedicated to EXAFS and XANES at extreme conditions at ID24 (ESRF). A diamond anvil cell (DAC) with a culet of 150 microns was used as a pressure increasing technique. Compression series spectra in fluorescence mode were collected for Y in a simplified synthetic Ab-Di glass [2] up to 117 GPa (about 2500 km).
In the initial analysis of XANES spectra at different pressures for Y, a shift of the first EXAFS peak (17080 eV) to higher energies with increasing pressure is observed, indicating a decrease in the Y-O distance. The largest shift is observed for pressure changes between 1.7 and 16 GPa, 16 and 45 GPa and between 75 and 100 GPa. Further analyses were performed by fits of the EXAFS, resulting in Y-O distances that show a smooth decrease with increasing pressure from 2.417 Å at 1.7 GPa to 2.233 Å 117.5 GPa. In general, the largest changes in R (Y-O) correspond to pressure changes from 16 to 45 GPa, as well as from 75 to 100 GPa, which probably supports the assumption of structure changes based on the initial XANES analysis and pre-edge region at same pressure ranges. Starting from a pressure of 45 GPa, an increase in intensity is observed in the pre-edge region, which may indicate a change in the local structure around the absorbing atom towards non-centrosymmtrice symmetry. Thus, a pressure-induced densification mechanism associated with a decrease in the Y-O distance and an increase in the coordination number is observed. These structural changes likely impact melt viscosity, diffusivity of these melt components, and chemical separation.
In addition to cold-compression runs, first attempts of in-situ high pressure-temperature XANES/EXAFS at the Sr K-edge using laser-heating were performed. Successful runs at 2, 5 and 9 GPa provide insight to structural differences for Sr between the glass and the melt at 3500 K.

*References:*

[1] Elkins-Tanton LT (2012). Magma Oceans in the Inner Solar System. AREPS. 40(1):113-139
[2] Krstulović M et al. (2021), Chemical Geology 560, 119980, https://doi.org/10.1016/j.chemgeo.2020.119980

## Hydrothermal reduction of hematite to magnetite by molecular hydrogen

Ostertag-Henning, C.[1] and Plümper, O.[2]

[1]Federal Institute for Geosciences and Natural Resources, Hannover, Germany; christian.ostertag-henning@bgr.de

[2]Department of Earth Sciences, Utrecht University, Utrecht, Netherlands

---

The reduction of iron oxides, particularly hematite ($Fe_2O_3$), is crucial in steel production [1] and has been extensively studied in the gas phase at high temperatures and near atmospheric pressure, with a growing focus on using molecular hydrogen ($H_2$) to minimize $CO_2$ emissions. Unlike these gas-phase reactions, the processes involved in the transformation of hematite to magnetite in liquid water remains unclear, with various theories proposed. Many researchers [e.g. 2] favour the reduction of surficial ferric iron in the crystal lattice during oxidation of dissolved $H_2$ adsorbed onto the surface, and subsequent migration of either ferrous iron into the lattice or oxygen out of the lattice - for production of water as oxidation product of $H_2$ during the processes However, Otake et al. [3] and others [4] suggest a non-redox process driven by hematite's interaction with dissolved iron, where hematite transforms to magnetite through a dissolution and reprecipitation-driven replacement mechanism.

For research in the context of subsurface hydrogen storage in the project BiMiAb_H2 we investigated the reactions of molecular hydrogen with hematite in the aqueous system near in situ conditions, i.e., at temperatures of 80-120°C and a pressure of 120 bar in high pressure reactors for up to four weeks. We used sealed gold capsules with natural hematite, water ($H_2O$) and $H_2$ as starting material and quantified the conversion of $H_2$ to $H_2O$ as well as the reduction of hematite to magnetite by X-ray diffraction and Raman spectroscopic analyses. In addition, we employed isotope tracer techniques to assess the contribution of oxygen from the hematite to the water by using mass spectrometry and Raman microscopy. The rate of $H_2$ oxidation could not be described by a simple first-order reaction. The Raman spectroscopic analysesrevealed different patterns of magnetite formed on either near edges or crystallographic planes of reacted hematite grains. Consequently, we used X-ray microscopy and TEM analyses on FIB sections to investigate the reaction progress within the grain at various locations.

Depth transects on high-energy steps on the hematite grain reveal the reaction beginning at these steps, leading to the formation of magnetite that shows a multi-domain structure with increased depth, featuring numerous small pores and distinct subgrain boundary domains aligned with crystallographic orientations. In contrast, magnetite forming on the flat surfaces of hematite starts from a single point and expands uniformly along specific crystallographic paths. By examining the unique features at different structural locations on a single grain and by using Raman spectroscopy to analyze isotope label incorporation, we can explore various theories on how hematite is replaced by magnetite in water. This includes considering whether the process is a solid-state reaction or driven by dissolution-reprecipitation, potentially involving tiny clusters of amorphous iron oxide [5].

*References:*

[1] Abd Elhamid et al. (1996) J Solid State Chem 123:249-254
[2] Hallström et al. (11) Acta Mater 59: 53-60
[3] Otake et al. (2007) EPSL 257: 60-70
[4] Yin et al. (2022) EPSL 577: 117282
[5] Sun et al. (2007) Angew. Chem. 56: 4042-4046

## Elasticity of dolomite-ankerite solid solutions

Pennacchioni, L.[1,2,3], Speziale, S.[2] and Winkler, B.[3]

[1]Insitut für Geowissenschaften, Universität Potsdam, Potsdam, Germany, lea.pennacchioni@uni-potsdam.de

[2]Deutsches GoeForschungZentrum, GFZ, Potsdam, Germany

[3]Institut für Geowissenschaften, Goethe Universität, Frankfurt am Main, Germany

---

Dolomite, $CaMg(CO_3)_2$ (space group *R-3*), is one of the main carbonates in the Earth's crust and can be found in nature as a solid solution with isostructural ankerite, $Ca(Mg_{1-x}Fe_x)(CO_3)_2$ ($0 \leq x \leq 0.7$) [1]. X-ray diffraction studies (XRD) performed on dolomite and dolomite-ankerite solid solutions, revealed that Fe/Mg substitution produces moderate changes in the compressibility. However, no studies have been performed on the single crystal elastic anisotropy of ankerite to date, and the currently available elastic tensors in literature are limited to pure dolomite [2,3].

We measured the Brillouin scattering at ambient conditions of well characterized (by electron microprobe analysis and XRD), natural $CaFe_xMg_{1-x}(CO_3)_2$ crystals with x=0.05, 0.4, 0.63, covering almost the entire compositional range of natural dolomite-ankerite solid solutions, and determined the effect of Fe/Mg substitution on the elastic tensor of these solid solutions. Our results show that the presence of Fe leads to a decrease in the $C_{11}$, $C_{44}$ and $C_{66}$ coefficients (~14%, 13% and ~30% respectively) and an increase in the $C_{12}$ and $C_{13}$ coefficients (~20% and 8% respectively). $C_{33}$, $C_{14}$ and $C_{15}$ coefficients are less sensitive to compositional changes. The change in elasticity due to the substitution of Mg by Fe has little effect on the bulk modulus *K* of dolomite-ankerite, while high Fe contents cause a drastic decrease of the shear modulus *G* (23%). A similar result was observed for single carbonates by Sanchez-Valle et al. [4], who measured the Brillouin scattering of $MgCO_3$-$FeCO_3$ solid solutions.

*References:*

[1] Reeder R. J., Dollase W. A. (1989): Structural variation in the dolomite and ankerite solid-solution series; an X-ray Mössbauer, and TEM study. American Mineralogist, 74(9-10):1159-1167

[2] Humbert P., Plique F., (1972): Proprietés élastique de carbonates rhomboédriques monocristallins: calcite, magnésite, dolomie, Comptes Rendus de l'Académie des Sciences de Paris, 275, 391-394

[3] Chen P., Ling-Yun C., Huang P., Yang Y., Liu L., (2006): Elasticity of magnesite and dolomite from a genetic algorithm for inverting Brillouin spectroscopy measurements. Physiscs of Earth and Planetary interiors, 155(1-2):73-86

[4] Sanchez-Valle C., Ghosh S., Rosa A.D., (2011) Sound velocities of ferromagnesian carbonates and the seismic detection of carbonates in eclogites and the mantle, Geophysical Research letters, 38

## Spectroscopic feature on gem quality topaz from different localities after E-beam treatment

Tempesta, G.[1], Elettivo G.S. [1] Vadrucci M.[2,3] and Agrosì G.[1]

[1] Dipartimento di Scienza della Terra e Geoambientali, Bari (Ba), Italy / gioacchino.tempesta@uniba.it
[2] Italian Space Agency, Science and Research Directorate, Rome (RM), Italy
[3] ENEA, Development of Particle Accelerators and Medical Applications, Via E. Fermi, 45, Frascati, Italy

---

In the gemmological field the colour adds to the gem a great value in the market so the treatment to improve it has become frequently performed [1]. The e-beam irradiation is one of the possible treatments that enhance and induce the colour in minerals. Topaz is one of the most famous gemstones commonly undergoing to irradiation treatment, even if the causes of colour variation need to be fully known. To deeply investigate the processes of colour variation during the treatment we study, before and after e-beam irradiation, ten samples coming from: Brazil, Madagascar, Mozambique and Tanzania. Seven topaz samples are colourless, two are light blue and one is red orange.

All samples were sliced parallel to (001) this allowed to have more than one replica for each sample to treat and to analyse. Mineralogical and chemical characterization was performed by Scanning Electron Microscopy coupled with Energy Dispersive Spectroscopy (SEM-EDS), Ultraviolet, Visible and Infrared spectroscopy (UV-VIS-NIR) and Laser Induced Breakdown spectroscopy (LIBS).
SEM-EDS analysis performed before irradiation show that samples are similar respect to major and minor elements content and that belong to Type II (OH-poor) with OH content about 13 wt%. The OH content was calculated measuring the F content and tacking into account the OH/F substitution in the structure. The optical properties were investigated with UV-VIS-NIR spectroscopy to determine the absorption variations in a wide spectrum range (200-1100nm) before and after treatments. The e-beam irradiation treatment was performed using the REX machine [2] based on a 5 MeV linear accelerator, at ENEA Frascati research centre, employing fluences accordingly with Maneewong et al. [3] with a low dose $10^7$ Gy and then with a high dose 3.6 *$10^7$ Gy. All irradiated topazes at a low dose, accordingly with Krambrock et al. [4], changed colour becoming light brown uniformly or zoned someone dark brown. The annealing to eliminate the brown colour has been performed with a muffle furnace under ambient pressure conditions. At the end of the heat treatment all the samples were bleached. Only Tanzanian sample revealed a slight absorption in the visible spectrum around 600 nm, showing a very slight blue colour. All the samples treated with a high dose (3.6 *$10^7$ Gy) became blue or light blue only two show the brown tone also after the annealing by the heat treatment.
The results are very promising because the UV-VIS-NIR spectroscopy allow to identify the e-beam treatment due to a change in the absorption in UV range.

*References:*

[1] Nassau, Kurt., (1985) Gems & Gemology vol. 21, 1.
[2] Vadrucci, M., et al., (2019) NIM-A, 930, 126-131.
[3] Maneewong, A., et al., (2019) Journal of Physics: Conf. Series. Vol. 1285. N. 1. IOP Publishing.
[4] Krambrock, K., et al., (2007) Physics and Chemistry of Minerals, 34:437-444.

## The interdependence of structure and redox properties of clay minerals

Neumann, A.[1,2]

[1]PSI Paul Scherrer Institut, 5232 Villigen, Switzerland; anke.neumann-jenal@psi.ch.

[2]Newcastle University, Newcastle upon Tyne, UK

---

Clay minerals, or phyllosilicates, occur widespread in a variety of natural environments and usually are formed as a product of weathering. Depending on the location and pathway of formation, clay minerals may contain different amounts of redox-active elements such as iron (Fe), ranging from trace levels up to 25 wt%. Isomorphic substitution of Fe into the clay mineral structure can occur in both octahedral and tetrahedral sheets and with both ferrous (Fe(II)) and ferric (Fe(III)) iron. Redox reactions of this clay mineral-bound Fe significantly contribute to the biogeochemical cycling and environmental fate of contaminants, elements and nutrients, and the redox properties of clay minerals have been utilised and engineered to treat (waste)water or to serve as catalyst in industry. This talk will summarize own work and that of others on how clay mineral structure determines the resulting clay mineral redox reactivity, and how, in turn, the electron transfer reactions to and from clay mineral Fe affect the clay mineral structure. The aim of this presentation is to provide an overview of the mechanistic understanding and quantitative description of clay mineral iron redox reactions. An outlook on current and emerging questions concerning the interdependence of structure and redox properties of clay minerals will conclude this keynote presentation.

## Isotopic fractionation during Sr adsorption on clay minerals: comparison between theoretical calculations and macroscopic experimental data

Blanchard, M.[1], Ferrage E.[2], Dazas, B.[2], Tertre, E.[2], Isnard, E.[3] and Savoye, S.[3]

[1]GET, CNRS, Université Toulouse 3, France, marc.blanchard@get.omp.eu

[2]IC2MP, CNRS, Université de Poitiers, France

[3]Université Paris-Saclay, CEA, SPC, Gif-sur Yvette, France

---

Chemical and transport properties of materials rich in clay minerals have been widely studied in the context of the disposal of waste materials and sequestration of energy resources. More generally, cation exchange capacity of clay minerals is an important aspect controlling inorganic element cycling in superficial environments, such as soils. One of the processes occurring at the fluid/mineral interface is isotopic fractionation. However, little is known about the mechanisms of isotopic fractionation that can occur during Sr(II) and Ca(II) adsorption onto clay minerals.

This study then aims to assess the possible isotopic fractionation between different isotopes of Sr and Ca when they compensate the permanent charge of clay minerals. To this end, we compare theoretical calculations of $^{88/86}$Sr fractionation with macroscopic experimental data devoted to the study of Sr(II) for Ca(II) exchange; both obtained by considering cation adsorption on the basal surfaces of a highly charged dioctahedral model clay (i.e., vermiculite). Methodologically, the theoretical modelling combines Grand-Canonical Monte Carlo simulations, with classical and ab initio molecular dynamics simulations. The interlayer water content and the equilibrium state of water and strontium are first determined, before calculating the isotopic properties associated with each of the identified adsorption sites.

Theoretical calculations show that the adsorption of Sr in the hexagonal cavity of the clay layer increases the Sr-O bond lengths, and leads to an isotopic fractionation of about -0.15 ‰ in favour of the lighter Sr isotope ($^{86}$Sr) compared to the heavier one ($^{88}$Sr). These results are in good agreement with macroscopic experimental data showing a preferential adsorption of $^{86}$Sr over $^{88}$Sr isotopes during ion-exchange with Ca(II) (i.e., -1.2 ‰). Consequently, isotopic fractionation of divalent cations during their adsorption onto charged phyllosilicate could be non-negligible, and need to be considered within the continental Ca and Sr biogeochemical cycles, as well as in transport properties of radionuclides in the context of nuclear waste storages.

# Insights from single-crystal X-ray diffuse scattering on disorder in framework and layered minerals

Lepore, G.O.[1], Schmidt, E.M.[2], Morana, M.[1], Minelli, A.[3] and Margheri, S.[1]

[1]Earth Science Department, University of Florence, Italy. giovanniorazio.lepore@unifi.it

[2]Faculty of Geosciences and MAPEX Centre for Materials and Processes, University of Bremen, Germany

[3]Arianna Minelli, Oak Ridge National Laboratory, TN, U.S.A

---

Mineral crystal structures are routinely determined to characterize a particular species and its crystal-chemistry, helping to understand details such as genetic environment and correlations between structure and physical properties. Typically, the focus of our characterization lies in describing the average structure, which may overlook local deviations from the long-range order. Valuable information regarding structural disorder is found in the diffuse scattering (DS) pattern. Recent technological and methodological advancements have renewed interest in DS studies. However, possibly due to the intrinsic complexity of their structure, minerals have rarely been the subject of DS investigations.

This study focuses on several mineral groups, known for their structural complexity, having potentially different sources of DS. These phases include pyrochlore, hollandite and members of the layered lead oxychloride (LLO) group. Pyrochlores [1] and hollandites [2] are recognized for hosting disorder, primarily related to the positioning of tunnel cations. LLO minerals [3] comprise a variety of structures with disorder in the stacking sequence and/or within the layers. In order to get information on the causes and nature of disorder in these phases we performed single-crystal X-ray data collection at ID28 beamline at the European Synchrotron Radiation Facility (ESRF), using the continuous rotation method and a Pilatus 1M detector.

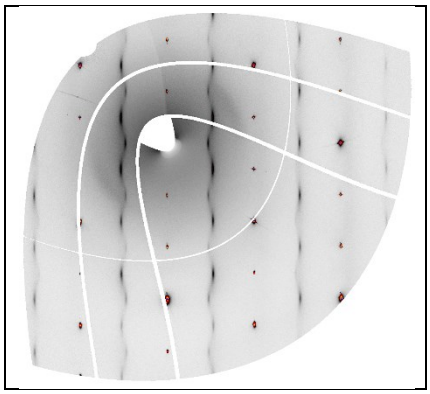

*Figure 1. (0kl) reconstruction of a mannardite crystal*

Preliminary analyses indicate that DS offers valuable insights in such intricate cases. For instance, synthetic Na-bearing elsmoreite displays diffuse features primarily linked to the rotation of octahedra with consequent distortion of the channels. On the other hand, the DS pattern of hollandites (Figure 1) is dominated by the short-range ordering of cations along the tunnels but also provides information on the structural response of the framework to these local features. In the case of LLO minerals [e.g. 3], diffuse features reveal significant differences in the origin of disorder, with janchevite primarily affected by stacking faults, whereas DS in thorikosite and schwartzembergite suggests partial ordering perpendicular to the stacking direction. Further analyses, including 3D-ΔPDF maps and modelling of DS, are underway to enhance our understanding on the origins of disorder in the studied phases.

*References:*

[1] Subramanian et al. (1983) Prog. Solid St. Chem. 15: 55-143

[2] Biagioni et al. (2013) Eur. J. Mineral. 25, 85-90.

[3] Chukanov et al. (2019) Eur. J. Mineral. 31: 619-628

# Exploring pyrochlores: incorporation of Tl and Pb in synthetic microlite and elsmoreite

Margheri, S.[1], Morana, M.[1], Taddei, A.[1], Checchia, S[2]., Goudjil, M.[1], Bindi, L.[1], d'Acapito, F[3]. and Lepore, G.O.[1]

[1] Dipartimento di Scienze della Terra, Università di Firenze, Italy. Email: simone.margheri@unifi.it

[2] European Synchrotron Radiation Facility, Grenoble, France.

[3] CNR-Istituto Officina dei Materiali (IOM)-OGG, Grenoble, France.

---

Dispersion of heavy metals in aqueous matrices is a major hazard for human health and a severe issue for natural environment. The toxicity associated with heavy metals makes it critical to develop effective strategies for remediating contaminated waters. The general formula for pyrochlores is $A_2B_2O_6Y$, where B is usually a high-field strength element like $Ta^{5+}$, $Nb^{5+}$, $W^{6+}$ or $Ti^{4+}$, while A and Y are mono- or divalent cations like $K^+$, $Na^+$, $Ca^+$, or small molecules like $OH^-$ or $H_2O$. Their crystal structure consists of a $BO_6$ octahedra framework defining an interweaving of channels, where the A and Y sites are hosted. Chanell ions are highly mobile and can be easily exchanged. Pyrochlores have thus been exploited in a variety of contexts, from ionic conductors [e.g., 1] to radioactive elements storage [e.g., 2] and battery research [e.g., 3]. Recently, Taddei et al. [4] showed that single crystals of hydropyrochlore can incorporate considerable amounts of Tl in the structure when immersed in a Tl-rich solution.

Microlite (Ta at the B site) and elsmoreite (W at the B site) powders and elsmoreite single crystals were synthesized via hydrothermal route and used in imbibition experiments in concentrated solutions of Tl and Pb. The crystal structure of the treated powders of microlite was investigated by means of synchrotron X-ray powder diffraction. Results of the Rietveld refinements indicate that Tl and Pb incorporation leads to variations of the unit cell size (+0.12% for Tl-treated microlite and -0.75% for Pb-treated microlite) and to an increase of the electron density at the A site (14 $e^-$ for untreated sample; 51 $e^-$ and 36 $e^-$ for the Tl- and Pb-treated sample, respectively). This is in good agreement with the hypothesis of a $Tl^+$ for $K^+$ and $Pb^{2+}$ for $K^+$ substitution mainly occurring at the A site. Indeed, the incorporation of the larger $Tl^+$ results in an increase of the unit cell parameters, while the smaller $Pb^{2+}$ has the opposite effect. On the other hand, the refinements of single crystal X-ray diffraction data of elsmoreite treated samples show a different structural response. Tl incorporation leads to a decrease in the unit cell parameter (-0.10%) while Pb uptake only moderately affects this parameter (-0.05%). The electron density in A remains constant (ca. 5-6 $e^-$) while it increases in Y (6 $e^-$ for untreated sample; 30 $e^-$ and 12 $e^-$ for the Tl- and Pb-treated sample, respectively). Variations in the features of the X-ray absorption spectroscopy data, collected for the treated powders of both phases, also support the hypothesis of different incorporation mechanisms occurring in the two pyrochlores. Tl and Pb spectra show distinct features even when hosted within the same structure, suggesting the presence of a slightly different incorporation mechanism for the two elements, not evident when studying the average structure alone. The presence of a clear second shell signal in the EXAFS spectra of all the investigated samples confirms that the Tl and Pb uptake mainly occurs within the crystal structure.
Imbibition experiments using diluted Tl- and Pb-solutions aimed at investigating the sorption capacity of these compounds in solutions with concentrations closer to those found in industrial wastewaters are currently in progress.

*References:*

[1] Anokhina I.A. et al (2021) Ceram Int 47: 1949-1961.
[2] McMaster S.A. et al. (2018) J Hazard Mater 360:2 57-269.
[3] Anantharaman A.P. and Dasari H.P. (2021) Ceram Int 47: 4367-4388.
[4] Taddei A. et al. (2024) Am Min., DOI: 10.2138/am-2023-9289.

## Temperature dependence of elastic properties and damage of natural and man-made silica materials during heating and cooling - From quartz sandstones to silica refractories

Pabst, W., Gregorová, E. and Kotrbová L.

Department of Glass and Ceramics, University of Chemistry and Technology, Prague (UCT Prague), Technická 5, 166 28 Prague 6, Czech Republic

---

The elastic properties of silica-based materials are remarkable, because of the low or even negative Poisson ratio of silica polymorphs [1]. Cristobalite is auxetic at room temperature [2], and quartz is auxetic in the temperature range from approximately 420°C to temperatures around the low-to-high-quartz transition (573°C) [1], leading to the auxetic or "anepirretic" [3] behaviour of quartz sandstone, which is retained during repeated heating-cooling cycles with a maximum temperature of 800°C [4].

Even more interesting is the behaviour of silica refractories [5]. Using high-temperature impulse excitation (ASTM 1876-01), it has been shown that the temperature dependence of Young's modulus exhibits anomalies related to the phase transitions of tridymite and cristobalite, hysteresis between heating and cooling (due to microcrack closure and re-opening), and irreversible damage accumulation when the maximum temperature of the heating-cooling cycle is 800 or 1000°C [6], whereas the hysteresis loops are reversible for a maximum temperature of 1200°C [7].

This contribution (project GA22-22562S, Czech Science Foundation) compares the temperature dependence of Young's modulus for three different sandstones cycled to 800 and 1200°C. In all cases thermal cycling causes irreversible damage, accompanied for maximum temperatures of 1200°C by large hysteresis loops. Thermal cycling of silica refractories, performed with maximum temperatures of 900, 1100, 1300 and 1500°C, shows that thermal cycling to temperatures below 1200°C leads to damage accumulation.

*References:*

[1] Pabst W and Gregorová E (2013) Ceram Silik 57:167-184
[2] Yeganeh-Haeri A et al. (1992) Science 257:650-652
[3] Dagdelen J et al. (2017) Nat Comm 8-323:1-7
[4] Kotrbová L et al. (2024) Int J Rock Mech Mining Sci (under review)
[5] Pabst W et al. (2016) J Eur Ceram Soc 36:209-220
[6] Gregorová E et al. (2015) Ceram Int 41:1129-1138
[7] Pabst W et al. (2014) Ceram Int 40:4207-4211

## Thermoelastic properties of paracelsian-related danburite and hurlbutite

Münchhalfen, M.[1] and Schreuer, J.[1]

[1] Institut für Geologie, Mineralogie und Geophysik, Ruhr-Universität Bochum, Universitätsstrasse 150, 44801 Bochum, Germany, marie.muenchhalfen@rub.de.

---

The three-dimensional frameworks of corner-linked tetrahedra of orthorhombic Danburite ($CaB_2Si_2O_8$) and monoclinic hurlbutite ($CaBe_2P_2O_8$) are topologically similar to that of monoclinic paracelsian ($BaAl_2Si_2O_8$). Paracelsian and hurlbutite posses a regular alternation of Al and Si or Be and P on the tetrahedral sites, while danburite contains alternating $Si_2O_7$ and $B_2O_7$ groups.

The elastic behavior provides insight into the a crystal's bonding system and its structural stability. While elastic properties at ambient temperatures have already been reported for danburite [1,2], little is known about the physical properties of hurlbutite other than the refractive indices [3]. Therefore, complete sets of single-crystal elastic stiffness coefficients of danburite and hurlbutite were determined using resonant ultrasound spectroscopy between 100 K and the decomposition temperature or melting temperature of 1223 K and 1673 K, respectively. The thermal expansion behavior was studied in the same temperature range employing high-resolution dilatometry.
The bulk modulus for danburite is slightly larger compared to the one for hurlbutite, with values of 110.7(6) GPa and 91.7(1) GPa, respectively. Both minerals posses a similar elastic anisotropy, with the longitudinal effect of elastic stiffness being nearly isotropic perpendicular to the *a*-axis, while its minimum is orientated parallel *a*. For both danburite and hurlbutite, the anisotropy of thermal expansion α is characterized by $\alpha_{11}>\alpha_{33}>\alpha_{22}$. Very little change in anisotropy of physical properties was discernible in dependence of temperature with no anomalies being observed in the investigated temperature range.

*References:*

[1] Aleksandrov K and Prodaivoda G (1993) Crystallogr. Rep. 38: 698–709
[2] Özkan H and Cartz L (1986) HTHP 18: 675–678
[3] Mrose M (1952) Am. Min. 37: 931–940

## Structure-properties relationships of flexible framework materials

Ross, N.L.[1,2]

[1]Departments of Geosciences, Virginia Tech, Blacksburg, VA 24061, USA. (nross@vt.edu)

[2]Department of Materials Science and Engineering, Virginia Tech, Blacksburg, VA 24061, USA.

---

Framework minerals and related materials display a complex set of behaviours traceable to the flexibility of the framework that results in a number of phenomena that include extensive polymorphism, negative volumes of fusion, very low to negative thermal expansion, pressure induced amorphization, and polyamorphism. Taken together, this combination of behaviour defines the "flexibility syndrome" of framework materials. The flexible nature of the framework in these materials is exploited in a wide range of technological applications.

In this presentation the factors that influence the flexibility syndrome in tetrahedral frameworks (zeolites and ZIFs), tetrahedral-octahedral frameworks (2-3-4 and 3-3-3 garnets) and octahedral frameworks (oxide and halide perovskites) are addressed. Results from crystallographic studies combined with spectroscopic studies (Raman, Inelastic Neutron Scattering), carried out at variable pressures and temperatures, are presented. The atomic-scale factors that control the flexibility of the framework are discussed and how they, in turn, influence the structure-property relationships of these important earth and technological materials.

## Zeolite for an effective solar protection: understanding the stability unravelling the structure

Arletti, R.[1], Fantini, R.[1], Fischer, M.[2], Brauer, J.[2], Cavalli, R.[3], Argenziano, M.[3] Mino, L.[4]

[1]Department of Chemical and Geological Sciences, University of Modena and Reggio Emilia, Modena, Italy rossella.arletti@unimore.it

[2]Crystallography & Geomaterials Research, Faculty of Geosciences, and Bremen Center for Computational Materials Science, and MAPEX Center for Materials and Processes, University of Bremen, Bremen, Germany

[3] Dipartimento di Scienza e Tecnologia del Farmaco - Università degli Studi di Torino, Torino, Italy.

[4]Department of Chemistry and NIS Centre, University of Torino, Torino, Italy

---

Exposure to both UVA and UVB radiation from the sun stands as the primary cause of skin cancers. Sunscreen products have become ubiquitous in personal-care products, packaging, plastics, dyes, and many other sectors. Ideal UV filters should be photostable and dissipate the absorbed energy efficiently. However, most organic UV filters are photolabile upon protracted UV exposure, leading to the formation of photoproducts of unknown toxicity for human health and environment. The chemical environment surrounding UV filters may strongly affect their behaviour: the interaction with other components of sunscreen formulations may enhance their degradation. Therefore, much effort has been invested in developing more effective and safe sunscreens.

Our team recently focused on the preparation and characterization of hybrid UVfs obtained by the encapsulation of organic UV filters into various zeolites differing for topology [1,2]. The most efficient zeolites for the encapsulation of organic UV filters, in term of stability and efficiency in radiation filtration, resulted to be potassium LTL and sodium FAU zeolites. This work reports the results of combined crystallographic investigation carried out exploiting X-ray powder diffraction, Fourier-transform infrared spectroscopy, and density functional theory (DFT).
Regarding LTL/OMC ZEOfilter, IR data indicate a perturbation of the ν(C=O) mode of the OMC carbonyl group and this was confirmed by structural refinement, highlighting that the reason of stability was the bond between molecules and the extraframework K.
The combination of IR and DFT was crucial to identify all the complex host-guest interactions occurring inside the FAU/OMC hybrid and to unveil that, although slightly thermodynamically unfavored, OMC is dominantly present in the trans form inside the NaX framework. Even for this hybrid, the interaction molecule-cations is the key feature for its stability and efficacy.

In addition, in this work, we report further proof indicating that the use of this encapsulate filter could potentially substitute for conventional UVfs. In fact, the hybrids were successfully incorporated into oil-in-water emulsions and permeation tests displayed a very low UV filter permeation through no UV filter accumulation in dermis layer, moreover the photostability of the hybrid-based emulsions resulted to be higher with compared with that of bare filter emulsions

*References:*

[1] Fantini et al. (2021) Materials 328 (2021) 11147
[2] Confalonieri et . (2022) Microporous and Mesoporous Materials, 344, Article number 112212

## Secondary and authigenic phase formation in the 50-year-old tuff from Surtsey (Iceland)

Montesano, G.[1*], Rispoli, C.[1], Petrosino, P.[1] and Cappelletti, P.[1]

[1]Department of Earth, Environmental and Resource Sciences, University of Naples Federico II (Italy)

*presenting author

---

Subaerial and submarine lapilli tuff samples retrieved from a 152 and 192 m-deep vertical boreholes (SE-02a and SE-02b) and a 283 m-deep inclined borehole (SE-03) drilled in 2017 in the frame of the SUSTAIN drilling project on the island of Surtsey (SW Iceland), which is one of the Earth's best-monitored volcanic sites, were characterized throughout petrographic studies, X-ray powder diffraction analysis and systematic SEM-EDS imaging and chemical analyses. The island of Surtsey formed over a near continuous 3.5-year effusive and explosive basaltic eruptions from 1963 to 1967 [1,2] and was affected by authigenic alteration and secondary minerals precipitation since its formation. Surtsey volcaniclastic deposits consists in armoured lapilli tuffs in which authigenic phases, either amorphous or crystalline, from a fresh basaltic precursor glass (i.e., sideromelane; [3]). Sideromelane experienced alteration to palagonite, a metastable alteration product [4,5] which consist in a variety of amorphous/slightly-to-highly crystallized mineral products, the latter exhibiting characteristics of smectites [5]. Secondary minerals are instead considered to precipitate from interstitial fluids in pores or vesicles and consist mainly of calcium-aluminium silicate hydrate (zeolites, tobermorite and xonotlite), together with minor carbonates and sulphates.
The alteration path along the analysed subaerial and submarine sequences was identified through the integrated results, trying to develop a minerogenetic model to explain their genesis, providing a reference framework for assessing the mineralogical evolution in other Surtseyan-type volcanoes.

*References:*

[1] Jakobsson SP and Moore JG (1982) Surtsey Research 9:76-93
[2 Jakobsson SP and Moore JG (1986) Geol Soc Am Bull 97:648-659
[3] Peacock MA and Fuller RE (1928) Am Min 13:360-383
[4] Prause S et al (2020) J Volcanol Geotherm Res 392:106754
[5] Montesano G et al (2023) Sci Rep 13:22855

## Pressure-driven crystal structure and fluids interaction in erionite-group zeolites

Battiston, T.[1], Lotti, P.[1], Comboni, D.[1,2], Gatta G.D.[1]

[1]Earth Sciences Dept., Univesity of Milan, Italy; paolo.lotti@unimi.it

[2]European Synchrotron Radiation Facility, Grenoble, France

---

The infiltration of molecules (or solvated ions) into the nano-cavities of microporous materials opens new routes for enhancing mass transfer from fluids to molecules incorporated in the structure. Thoroughly exploring this phenomenon, in both synthetic and natural zeolites, could expand their industrial applications, such as the development of new functional materials and enhancement of catalytic performance [1,2]. From a geological standpoint, understanding this phenomenon can unveil the role played by zeolites as fluid carriers during the early stages of subduction of oceanic sediments and altered basalts.

In this research, we examined the interaction between crystals and fluids, driven by pressure, in three distinct natural zeolites belonging to the ABC-6 group: erionite (ERI framework type, 6-membered ring sequence: AABAAC), offretite (OFF, with AAB seq.), and bellbergite (EAB, with AABCCB seq.). The objectives of the experiments were: 1) to understand the potential role of erionite as a fluid carrier during subduction, given its presence, as a secondary mineral, in altered oceanic basalts [3]; and 2) to compare the mechanisms employed by structurally similar frameworks (characterized by the presence of 6-membered rings) in accommodating bulk compression and adsorbing new molecules.

The investigation made use of in situ high-pressure synchrotron X-ray diffraction experiments on natural single crystals of erionite, offretite, and bellbergite, employing both potentially penetrating fluids (methanol:ethanol:water 16:3:1 mixture, ethanol:water 1:1 mixture, methanol, $H_2O$, liquid Ne) and non-penetrating *P*-transmitting fluids (silicone oil and daphne oil 7575). The use of the latters aimed to establish a benchmark for evaluating crystal-fluid interaction, as the adsorption of new molecules decreases bulk compressibility due to the "pillar" role played by guest species within the structural voids [1].

The results revealed that erionite exhibits the highest magnitude of adsorption among the three zeolites. Additionally, the occurrence and magnitude of the phenomena were found to be governed by the $H_2O$ content of the hydrous *P*-transmitting fluids. Offretite framework allowed Ne atoms to penetrate into the 12mRs channel in response to applied pressure, exhibiting weak Van der Waals interactions with the extra-framework population.

On the other hand, natural bellbergite proved to be nearly inaccessible to guest molecules from *P*-transmitting fluids, emphasizing the pivotal role played by "secondary structural factors", such as the extra-framework content of the sample, on these phenomena.

*References:*

[1] Gatta GD et al. (2018) Phys Chem Miner 45:115-138
[2] Comboni D et al. (2020) Catal Today 345:88-96
[3] Vitali F et al. (1995) Clays Clay Miner 43: 92-104

# Adsorption of chlorinated ethenes in hydrophobic zeolites studied by molecular simulations

Fischer, M.[1,2]

[1]Crystallography & Geomaterials Research, Faculty of Geosciences, University of Bremen, 28359 Bremen, Germany, email: michael.fischer@uni-bremen.de

[2]Bremen Center for Computational Materials Science and MAPEX Center for Materials and Processes, University of Bremen, 28359 Bremen, Germany

---

Chlorinated ethenes are important environmental contaminants, both with regard to air pollution [1] and water pollution [2]. A recent example receiving considerable news coverage is the spillage of the carcinogenic vinyl chloride (chloroethene) caused by a freight train derailment in East Palestine, Ohio, US, in February 2023.[3] Synthetic high-silica zeolites have been proposed as materials for the removal and destruction of chlorinated ethenes, and prior experimental work has investigated adsorption from the gas phase (example: tri- and tetrachloroethene in zeolite Y [4]) and removal from aqueous solution, sometimes followed by catalytic decomposition (example: vinyl chloride in Fe-loaded MFI-type zeolite [5]). So far, however, only a few zeolites have been considered, and there are only limited insights into the impact of framework topology on the affinity towards different chlorinated ethenes.

This contribution reports the results of a molecular simulation study investigating the gas-phase adsorption of ethene and chlorinated ethenes $CH_xCl_{4-x}$ ($0 \le x \le 3$) in hydrophobic zeolites, considering 16 different topologies and assuming an all-silica composition of the frameworks. Grand-canonical Monte Carlo (GCMC) simulations were employed, using empirical force field parameters to represent interatomic interactions (PCFF force field with Si and O parameters proposed by Emami et al. [6]). To begin with, it was ensured that the chosen force field reproduces experimental heats of adsorption. Henry constant and adsorption isotherm simulations were then performed to assess the affinity in the limit of zero coverage and to predict achievable uptakes under relevant conditions. To evaluate the potential competitive adsorption of nitrogen from air, $CH_xCl_{4-x}/N_2$ mixture adsorption simulations in which the partial pressure of $N_2$ was set to atmospheric pressure were carried out.

Among the set of zeolites, EUO, MTW, and TON frameworks were found to exhibit high affinities towards several chlorinated ethenes and comparatively high uptakes at low partial pressures, indicating that these zeolites should be particularly well suited for the removal of chlorinated ethenes from air. A closer look at low-energy configurations obtained from the simulations showed that the undulating nature of the channels in these zeolites is pivotal to reach high affinities, for example, towards tri- and tetrachloroethylene. Furthermore, it was noted that TON exhibits a high selectivity for *trans*-1,2-$C_2H_2Cl_2$ over other dichloroethene isomers, which might render it suitable for the separation of isomer mixtures. Although no direct conclusions can be drawn with regard to adsorption from water, it can be anticipated that the trends among different zeolite frameworks observed for gas phase adsorption should remain the same, provided that their hydrophobicity is also similar.

Funding by the Deutsche Forschungsgemeinschaft (project no. 455871835) is gratefully acknowledged.

*References:*

[1] Robichaud A (2020) J Air Waste Manag Assoc 70:341-378
[2] Stroo H F et al. (2012) Environ Sci Technol 46:6438-6447
[3] Oladeji O et al. (2023) Environ Sci Technol Lett 10: 680-685
[4] Chihara K et al. (2004) Stud Surf Sci Catal 154:1849-1857
[5] Georgi A et al. (2023) Chem Ing Tech 95:1999-2007
[6] Emami F S et al (2014) Chem Mater 26:2647-2658

# Atomistic modelling of the Tschermak and di-trioctahedral substitutions in chlorite

Françoise, M.[1], Dubacq, B.[1], Bourdelle, F.[2], Verlaguet A.[1]

[1]Institut des Sciences de la Terre de Paris (ISTeP), Sorbonne Université, Paris, France
mateo.francoise@sorbonne-universite.fr

[2]Géosciences et Environnement Cergy (GEC), CY Cergy Paris Université, Neuville-sur-Oise, France

---

Chlorite, a ubiquitous mineral in metamorphic rocks, is a useful record of petrological processes and pressure-temperature conditions. Unfortunately, the crystal chemistry of chlorite is complex and analytical and experimental difficulties have hampered thermodynamic modelling. Three substitutions prevail in the FMASH ($FeO$-$MgO$-$Al_2O_3$-$SiO_2$-$H_2O$) chemical system: the homovalent Fe-Mg ($^{VI}Fe^{2+} \rightleftharpoons {}^{VI}Mg^{2+}$), the Tschermak ($^{VI}[Mg^{2+}, Fe^{2+}] + {}^{IV}Si^{4+} \rightleftharpoons {}^{VI}Al^{3+} + {}^{IV}Al^{3+}$) and the di-trioctahedral ($3^{VI}[Mg^{2+}, Fe^{2+}] \rightleftharpoons 2^{VI}[Fe^{3+}, Al^{3+}] + {}^{VI}\square$) substitution. The first two are well characterised whilst the latter is more contentious. There are three opposed approaches for modelling this substitution: i) the solid solution is negligible and not taken into account (e.g., [1]), ii) the solid solution contains a large, asymmetrical solvus decreasing with temperature (e.g., [2]), or iii) the solid solution is complete at low temperature (<100°C) and shows a solvus expanding with increasing temperature (e.g., [3]). Such first-order differences ask for clarification to strengthen the use of chlorite as a geothermobarometer. This study aims at bringing independent constraints to reconcile petrographic observations and thermodynamic modelling. To do so, Monte-Carlo simulations of cation ordering and Gibbs free energy of mixing along the Tschermak and di-trioctahedral binaries are carried out with the *Js*' method [6]. Semi-empirical modelling with GULP (General Utility Lattice Program, [4], [5]) is used to calibrate exchange energies into simple models to reduce computing times to the extreme and allow evaluation of millions of configurations into compositional-fixed structures. Monte-Carlo simulations are carried out on chlorite structures containing tens of thousands of atoms, allowing to study ordering processes over short and long ranges. These simulations predict high short-range ordering over the entire temperature range of the lithosphere and shed light on the solvus between sudoite (di-trioctahedral chlorite) and clinochlore (tri-trioctahedral chlorite), and its temperature evolution. The simulations also provide constraints over tetrahedral ordering with changing tetrahedral composition (*i.e.* along the Tschermak substitution). In parallel, detailed measurements of the crystal chemistry of chlorite (including iron speciation [7] and light element contents [8]) on natural samples of blueschist- and eclogites-facies metapelites are conducted to assess the relevance of these substitutions.

*References:*

[1] White R W et al. (2014) J. Metamorph. Geol., 32, 261-286, DOI: 10.1111/j.1525-1314.2007.00711.x
[2] Vidal O et al. (2006) J. Metamorph. Geol., 24, 669-683, DOI: 10.1111/j.1525-1314.2006.00661.x
[3] Bourdelle F and Cathelineau M (2015) Eur. J. Mineral., 27, 617-626, DOI: 10.1127/ejm/2015/0027-2467
[4] Gale J D and Rohl A L (2003) Mol. Simul., 29:291–341, DOI: 10.1080/0892702031000104887
[5] Cope E R and Dove M T (2007) J. Appl. Crystallogr., 40:589–594, DOI: 10.1107/S0021889807016032
[6] Dove M T (2001) Eur. Mineral. Un. (EMU) Notes in Mineralogy, 3, p. 225–250, ISBN: 963 463 1347
[7] Masci L et al. (2019) Am. Mineral., 104, 403-417, DOI: 10.2138/am-2019-6766
[8] Dubacq B et al. (2023) Eur. J. Mineral., 35, 831-844, DOI: 10.5194/ejm-35-831-2023

## A multi-method, *in situ* temperature-dependent investigation of the taranakite-francoanellite phase transition

Galliano, Y.[1], Bellatreccia, F.[2], Campomenosi N.[1] and Carbone, C.[1]

[1]DISTAV, University of Genoa, C.so Europa 26, 16132 Genoa, Italy.

[2]Department of Science, Roma Tre University, Largo S. Leonardo Murialdo 1, 00146 Rome, Italy

---

Taranakite ($K_3Al_5(PO_3OH)_6(PO_4)_2 \cdot 18H_2O$, *trigonal*, $R\bar{3}c$) is a phosphate with a layered structure, composed of six $K_3Al_5(PO_3OH)_6(PO_4)_2 \cdot 12H_2O$ units separated from each other by water interlayers [1]. In natural environments, it occurs as microcrystalline powdery aggregates which form after the interaction of bat or bird guano with clay minerals, and as an important reaction product between soil minerals and phosphate-rich fertilizers [2]. As a highly ordered aluminophosphate forming readily at ambient conditions, its study poses particular interest for uses in the development of microporous $AlPO_4$ molecular sieves [3]. In fact, Schwieger and coworkers [4] report $NH_4$-taranakite as a precursor in the formation of $AlPO_4$-15 synthesized by precipitation at T=70°C. Moreover, taranakite is often found in association to the members of the leucophosphite group, which are natural analogues of $AlPO_4$-15.

In this study we explore the dehydration mechanisms that lead taranakite to transform into francoanellite ($K_3Al_5(PO_3OH)_6(PO_4)_2 \cdot 12H_2O$, *trigonal*, $R\bar{3}c$) by completely loosing interlayer water molecules. The studied sample is natural taranakite from the Pollera Cave (Liguria, Italy), where the phase forms from the interaction between a fossil guano deposit and alluvial clays in damp conditions. The sample has been characterized by XRPD, SEM-EDS, FTIR and Raman spectroscopy. Furthermore, we conducted a multi-method temperature dependent study including TG-DTA and *in situ* HT(High Temperature)-XRPD, HT-µRaman and HT-FTIR spectroscopy in the temperature range 25-225°C, to gain a comprehensive understanding of the kinetics that steer this dehydration reaction.

We show that the heating process determines (i) the onset of the transition from taranakite to francoanellite at T≈85±5°C and (ii) the progressive amorphization of the material starting at 135±5°C.

A thorough characterization of natural aluminophosphates and precise constrains of their stability fields are of major concern for the successful development of new techniques to tailor open-framework compounds. Moreover, the genetic mechanisms that result in the rare registered occurrences of francoanellite in nature are still unclear; comprehensively constraining its formation from the partial dehydration of taranakite could make it a viable marker of past environmental conditions in cave environments.

*References:*

[1] Dick S et al (1998) Inorg Chim Acta 269(1):47-57.
[2] Liu C et al (2002) Soil Sci Soc of Amer Journ 66(1):109-116.
[3] Wei L et al (2009) Journ of cryst growth 311(13):3359-3363.
[4] Schwieger W et al (1998) Zeitschr für Anorg und allgem Chem 624(10):1712-1717.

## Evolution of Young's modulus and changes in phase composition of kaolins and $CaO\text{-}Al_2O_3\text{-}SiO_2$ ceramics during heating and sintering

Gregorová, E., Pabst, W. and Šimonová P.

Department of Glass and Ceramics, University of Chemistry and Technology, Prague (UCT Prague), Technická 5, 166 28 Prague 6, Czech Republic

---

Clay minerals, e.g. kaolinite, are the basic components of raw materials for kaolin-based ceramics, including those based on the CAS system, i.e. $CaO\text{-}Al_2O_3\text{-}SiO_2$. Since the phase composition determines the properties of these ceramics, monitoring the phase composition as a function of the firing temperature is of great interest. The impulse excitation technique (IET) according to ASTM 1876-01 [1] is an ideal tool for this purpose because it allows monitoring of changes in Young's modulus from the unsintered (e.g. as-pressed) powder compact to the final ceramic body.

This contribution (part of the project GA22-22562S), correlates the evolution of Young's modulus, as measured via the IET, with the concomitant changes in the phase composition, as determined via X-ray diffraction (XRD) of powders using the Rietveld method, with glass phase estimates using the internal standard method and alternative approaches, including two new approaches combining XRD with helium pycnometry and X-ray fluorescence analysis [2].

In particular, two types of Czech kaolins are compared by IET measurements of as-pressed powder compacts from room temperature to 1200 °C. During heating the processes of drying, dehydroxylation, spinel phase formation, mullitization, silica release and glass melting are clearly discernible. During cooling Young's modulus increases, exhibiting a flat maximum around 800 °C and a steep decrease below 200 °C. Based on these two kaolin types, CAS ceramics are prepared by adding 20 % of calcite. After cooling, Young's modulus is nicely predicted by a benchmark relation for partially sintered ceramics with concave pores [3].

*References:*

[1] ASTM 1876-01 Standard test method for dynamic Young's modulus, shear modulus, and Poisson's ratio by impulse excitation of vibration. ASTM, West Conshohocken 2001.
[2] Gregorová E et al. (2024) J Eur Ceram Soc (under review)
[3] Pabst W and Uhlířová T (2021) J Eur Ceram Soc 41:7967-7975

## Single crystals at high-pressures and high-temperatures: constraining planetary interiors

Boffa Ballaran, T.[1], Criniti, G.[1,2], Kurnosov, A.[1] and Glazyrin, K.[3]

[1]Bayerisches Geoinstitut, University of Bayreuth, Bayreuth, Germany. tiziana.boffa-ballaran@uni-bayreuth.de

[2]Earth and Planets Laboratory, Carnegie Institution for Science, Washington, DC, USA

[3]Deutsches Elektronen-Synchrotron DESY, Notkestr. 85, 22603 Hamburg, Germany

---

The close relationship between the structure of a material and its physical properties resulted in X-ray diffraction to become one of the most used technique in mineral physics. In this context, single crystals, when available, have been usually preferred to powdered samples because they allow mapping the three-dimensional reciprocal lattice and therefore are better suited to constrain small structural changes associated with variations in composition, pressure or temperature. To date, however, single-crystal X-ray diffraction data at simultaneously high-pressure and high-temperature are scarce, due to the intrinsic challenges associated with such technique which require a stable and homogenous heating of the whole crystal for a time significantly longer than that needed for collecting data from powdered samples at the same conditions. Recent advances at synchrotron facilities have permitted to overcome some of these challenges, allowing to collect high-quality data for single-crystal structural refinements. As an example, data collected for Al-bearing bridgmanite samples up to 35 GPa and 1000 K in the diamond anvil cell (DAC) to constrain the effect of Al substitution on the behaviour of one of the most abundant minerals of the Earth's lower mantle will be shown. The subtle distortions associated with the substitution of Al into the $MgSiO_3$ structure have been in this way accurately determined and their evolution as a function of pressure and temperature as well as their influence on the bulk modulus of this material carefully characterised.

Single-crystal measurements are also preferred in elasticity studies because they allow to determine the full elastic tensor of a material instead of only its aggregate properties, as it is the case of polycrystalline samples. Single crystals, however, require the sampling of different crystallographic directions even for cubic phases; this proves to be particularly challenging at high pressure and high temperature since the samples need to be measured at the same conditions in different orientations. A promising but challenging approach to this problem is to combine Brillouin scattering and $CO_2$ laser heating in the DAC to probe transparent samples at conditions of deep planetary interiors. A novel technology, mainly developed for medical surgery, has been used in the present study to heat single -crystals of Fe-rich ringwoodite at temperatures up to 1900 K in order to constrain their elastic tensor at the conditions of the martian mantle. This will allow to model the wave velocity structure of the Mars interior which has become available thanks to the seismometer on the NASA InSight lander.

## Phase evolution and thermal behavior of hydrous Fe sulfate minerals: coquimbite $AlFe_3(SO_4)_6(H_2O)_{18}$, römerite $Fe^{2+}Fe^{3+}{}_2(SO_4)_4(H_2O)_{14}$ and aluminocopiapite $Al^{3+}{}_{2/3}Fe^{3+}{}_4(SO_4)_6(OH)_2(H_2O)_{20}$

Abdulina, V.[1], Borisov, A.[2], Siidra, O.[1], Holzheid, A.[2]

[1]Department of Crystallography, St Petersburg University, St Petersburg, Russia

[2]Institute of Geosciences, Christian-Albrecht University of Kiel, Kiel, Germany

---

Hydrous iron sulfates are of importance upon acid mine drainage [1] as well as upon the formation of oxidation zones of ore deposits. A number of these minerals has also been detected on the surface of Mars under extraterrestrial conditions [2]. Nonetheless, certain issues related to their properties and phase evolution of hydrous iron sulfate minerals remain unresolved and are still under debate. Thermal behavior of several hydrous iron sulfates was studied in previous contributions mainly by spectroscopic methods. Hereby, we examine their thermal behavior by *in situ* high-accuracy single-crystal and powder X-ray diffraction and simultaneously acquiring data upon heating. We report a comprehensive study of the thermal properties and phase transformations of coquimbite $AlFe_3(SO_4)_6(H_2O)_{18}$, römerite $Fe^{2+}Fe^{3+}{}_2(SO_4)_4(H_2O)_{14}$ and aluminocopiapite $Al_{2/3}Fe^{3+}{}_4(SO_4)_6(OH)_2(H_2O)_{20}$ (all collected at the Alcaparossa mine, Chile) over a temperature and reduced pressure relevant to the Martian surface conditions. Using temperature-dependent single-crystal X-ray diffraction, the transformations of crystal structures and, in particular, hydrogen bonding systems as a key factor in the structural organization of hydrated sulfates have been studied. Based on powder diffraction data in the temperature range from -170 °C to ~700 °C, we show the stability limits of these minerals as well as their decomposition products – other sulfates and oxides of Fe and Al. For each mineral the tendencies of thermal expansion are characterized. These studies are complemented by a complex thermal analysis, which was used to evaluate the transformation energy release during the decomposition of each mineral. The combination of the obtained results makes a new contribution to the understanding of the behavior of iron-bearing hydrated sulfates in different thermodynamic environments.

*References:*

[1] Akcil A and Koldas S (2006) J Clean Prod 14: 1139e1145

[2] Farrand W H (2014) Icarus 241: 346-357

## Is newer always better? Not for quartz!

Angel, R.J.[1], Casati, N.P.M.[2], Morana, M.[3], Nestola, F.[4] and Alvaro M.[5]

[1]Institute of Geosciences & Georesources, CNR, Via Giovanni Gradenigo, 6, 35131 Padova, Italy, ross.angel@igg.cnr.it

[2]Paul Scherrer Institut, Forschungsstrasse 111, 5232 Villigen, Switzerland

[3]Department of Earth Sciences, University of Florence, Via G. La Pira 4, 50121 Florence, Italy

[4]Department of Geosciences, University of Padova, Via Giovanni Gradenigo, 6, 35131 Padova, Italy

[5]Department of Earth and Environmental Sciences, University of Pavia, Via Ferrata 1, 27100 Pavia, Italy

---

Given the enormous progress in the precision of measurement techniques used to characterise minerals, and advances in radiation sources that allow smaller and smaller sample volumes to be characterised, it is rather surprising that the two most recent determinations of the thermal expansion of alpha-quartz by in-situ diffraction [1,2] show substantial disagreement of more than 20K for the same volume between 400 and 600 K. Which of the modern datasets is correct is very important because the interpretation of the pressures of quartz inclusions trapped inside other minerals critically depends on the correct description of their PVT behaviour.

The more recent dataset [2] clearly displays better internal consistency than [1]. But dilatometry data of a century ago [3,4] including one using thermometers directly calibrated against national reference standards agrees with the data of [1], as do several other independent measurements below room temperature. We have confirmed this conclusion with new powder diffraction data from beamline X04SA at the Swiss Light Source. Further analysis suggests that the deviation of dataset [2] is due to at least two causes: one is a difference in the *c*-cell parameter and the second is a temperature calibration issue. This re-examination shows that attention to calibration remains essential to exploit the capabilities of modern instrumentation.

*References:*

[1] Carpenter MA et al. (1998) Am Min 83: 2-22
[2] Antao SM (2016) Acta Cryst B 72: 249-262
[3] Randall HM (1905) Phys Rev 20: 10-37
[4] Buffington RM and Latimer WM (1926) J Amer Chem Soc 48: 2305-2319

## Sound velocity of metals at megabar pressures, and implications for the Earth's Inner Core

Ohtani, E.[1], Ikuta, D.[2], Fukui, H.[3,4], Ishikawa, D.[3,4], Sakamaki, T.[1] and Baron, A.Q.R.[3,4]

[1]Department of Earth Science, Tohoku University, eohtani@tohoku.ac.jp

[2]Institute for Planetary Materials, Okayama University

[3]Japan Synchrotron Radiation Research Institute

[4]Materials Dynamics Laboratory, RIKEN SPring-8 Center

---

We developed techniques to measure the sound velocity at high pressure by using Inelastic X-ray scattering (IXS). We performed sound velocity measurements in diamond anvil cell with an improved anvil design (a stepped bevel DAC) under extreme pressures of the inner core boundary (ICB) at the RIKEN beamline BL43LXU of SPring-8. We doubled the static pressure conditions for IXS and successfully measured the sound velocity of metallic iron under a pressure equivalent to ICB (~330 GPa) [1]. The present results reveal that the $v_p$ and $v_s$ of the Preliminary reference Earth model (PREM) inner core are 4(±2)% and 36(±17)% slower than those of the pure iron, respectively at the centre of the core [1] when we use the conventional pressure scale [2].

Establishing pressure scale has been a subject of intensive research but still involves significant extrapolation and approximations, especially at the inner core pressures. We developed a primary pressure scale extending to the multi-megabar pressures of the core by measuring $v_P$, $v_S$, and density of rhenium with using IXS and XRD. Our new pressure scale agrees with previous primary scales at lower pressures and also shock compression experiments but is significantly different from previous secondary pressure scales at Earth's core pressures. Our new pressure scale suggests the density deficit of the inner core is doubling the light-element content [3].

*Reference:*

[1] Ikuta D, Ohtani E, Fukui H, Sakai T, Ishikawa D, Baron AQR (2022) Nature Comm. 13:7211
[2] Dewaele A. et al. (2006) Phys. Rev. Lett. 97, 215504
[3] Ikuta D, Ohtani E, Fukui H, Sakamaki T, Heid R, Ishikawa D, Baron AQR (2023) Science Advances 9, eadh8706

## Quantitative mineralogical analysis of drill cuttings by calibrated SEM-EDS mapping and lithofacies classification

Fialips, C.I.[1], Olivier, M.[1], Turpain, M.[1], edelabat Lartigau, M.[1], Mouret, N.[1], Bacque, M.[1], Martinez, L.[1] and Teinturier, S.[1]

[1]TotalEnergies, CSTJF, Avenue Larribau, 64018 Pau Cedex, FRANCE, Claire.Fialips@Totalenergies.com

---

In the context of oil and gas exploration/production or carbon capture and storage (CCS), well logs are often the only continuous acquisitions across the targeted reservoir rocks and caprock intervals. Accurate interpretation and calibration of well logs are essential for evaluating effective porosity and fluids saturation throughout the logged formation. The most important uncertainties are often related to the clay content and clay typology, but difficulties also arise from complex mineral mixtures without a well differentiated lithology. Accurate mineralogical analyses are therefore essential for calibrating logs interpretations quantitatively. Precise quantification of clay content and evaluation of clay swelling properties are also crucial for the prediction of geomechanical response to drilling operations and the suitable design of drilling mud fluids.

Ideally, mineralogical analyses should be performed on core samples selected considering the geological context and covering all sedimentological lithofacies. However, in most drilled wells, no or only short sections are cored nowadays to save cost. Consequently, mineralogical analyses and petrographic observations are increasingly conducted on drill cuttings. Drill cuttings are however generally contaminated with drilling mud additives, such as barite, BARACARB (calcite), bentonite (montmorillonite-rich clay material), Lost Circulation Material (LCM), etc. These contaminations are often impossible to remove through washing and do affect the relevance of quantitative mineralogical analyses performed on crushed samples through conventional techniques. To provide accurate mineralogical data for quantitative log interpretations and for insuring the most reliable level of information on both clay content and typology for drilling (well stability or clay-mud compatibility issues) or CCS applications, we have developed an in-house methodology of drill cuttings analysis based on calibrated SEM-EDS mapping and lithofacies classification.

Our in-house workflow is based on the mineralogical mapping of polished-sections or resin-impregnated cuttings using Scanning Electron Microscopy equipped with Energy Dispersive X-Ray Spectroscopy (SEM-EDS). SEM-EDS elemental maps are post-treated using a dedicated software allowing the deconvolution of each EDS spectrum using up to three mineral spectra. Raw SEM-EDS mineralogical data are not directly equivalent to volume% due to various petrophysical and analytical issues. They are therefore systematically calibrated with a limited number of quantitative mineralogical analyses performed on crushed samples using our reference quantitative mineralogy method, integrating X-Ray Diffraction (XRD) and X-Ray Fluorescence (XRF) analyses with a series of other measurements. Our in-house method of cuttings mineralogical classification is then applied to identify the main lithological classes (lithofacies) and pollutions (fall-out material, mud additives, cement casing fragments, etc.), evaluate their relative proportions in each sample, and determine the evolution of the calibrated mineralogical composition of each class with depth. Corrected mineralogical compositions are hereby produced allowing reliable calibration of well log interpretations and prediction of geomechanical properties and fluid-rock interactions.

Results of various case studies will be presented to illustrate the great benefits of this advanced workflow of quantitative mineralogical analysis of drill cuttings.

## High-pressure elastic behaviour and structural re-arrangement in monazite-type minerals

Lotti, P.[1], Pagliaro, F.[1], Comboni, D.[1,2], Battiston, T.[1] and Gatta, G.D.[1]

[1]Earth Sciences Department, University of Milan, Italy - paolo.lotti@unimi.it

[2]European Synchrotron Radiation Facility, Grenoble, France

---

$ATO_4$ compounds crystallize with different structural topologies (e.g. zircon, monazite, scheelite, barite) as a function of the crystal radii of the *A* and *T* cations as well as of temperature and pressure. Monazite-type compounds include, among the others, phosphates, arsenates, chromates and the most common mineral is the LREE-bearing monazite-(Ce), ideally $CePO_4$. These compounds share a monoclinic $P2_1/n$ structure with *T* cations in tetrahedral coordination and *A* cations showing a nine-fold coordination with the surrounding oxygens. In Earth Sciences, monazite, that is a common accessory mineral in different kinds of rocks, is of interest for petrological and geochronological implications. In materials science, monazite-type compounds find several technological applications, including phosphors, lasers, ionic conductors, and radioactive waste management [1]. Such a multidisciplinary interest has led to extensive studies on the behaviour of these isostructural compounds at non-ambient conditions [2], resulting in a deep characterization of the elastic and structural response to compressional, thermal and chemical stimuli. However, the adoption of up-to-date synchrotron facilities and crystallographic methods can still disclose undiscovered features of such a behaviour. In this contribution we present the compressional and combined high-*P* and high-*T* behaviour of natural monazite-(Ce) and gasparite-(Ce) (ideally $CeAsO_4$, [3]). In situ isothermal high-*P* single-crystal experiments have been performed at the beamlines ID15B of ESRF (Grenoble, France) and P02.2 of Petra-III (Hamburg, Germany). Combined H*P*H*T* in situ single-crystal experiments on monazite-(Ce) have been performed at the P02.2 beamline of Petra-III making use of the available graphite resistive heated DAC [4]. The analysis of the unit-cell evolution with pressure of both the minerals allowed to describe a slight change in the elastic behaviour at around 15-18 GPa, magnified by the compressional trend of the monoclinic $\beta$ angle. The refined structural models allowed to track for both monazite-(Ce) and gasparite-(Ce) the *P*-driven approach towards the REE site of a tenth oxygen atom, which enters the coordination sphere of the *A* (REE) cation at a pressure corresponding to the change in the elastic behaviour. Independently from the different crystal chemistry, both the monazite-type minerals showed *P*-induced structural re-arrangements with an increase in the coordination number of the REE site from 9 to 10, occurring before the known phase transition to a post-barite type polymorph [2].

*References:*

[1] Clavier L et al. (2011) J Eur Ceram Soc 31: 941.
[2] Errandonea D (2017) Phys Status Solidi B 254: 1700016
[3] Pagliaro et al. (2022) Mineral Mag 86: 150-167
[4] Hwang et al. (2023) Rev Sci Instrum 94: 083903

## Accurate structure geometry of *P*2/*n* omphacite at variable pressures

Baratelli, L.[1], Merlini, M.[1], Nestola, F.[2], Joseph, B.[3] and Cámara, F.[1]

[1]Department of Earth Sciences, University of Milan. lisa.baratelli@unimi.it

[2]Department of Geosciences, University of Padua.

[3]Elettra Sincrotrone, Trieste.

---

Our recent high-pressure (HP) Raman spectroscopy study of natural omphacite (space group *P*2/*n*, with composition close to $Jd_{45}Di_{55}$ from Münchberg Massif, Germany) up to 10 GPa revealed some interesting changes in elastic behavior. The pressure dependence of the wavenumber of few Raman peaks shows a discontinuity near 5 GPa, that can be related to the homogenization of the volume compressibility associated with chemical order at the six- and eight-coordinated sites in the structure. Available HP diffraction data of omphacites [1-3] is not sufficient to make a one-to-one comparison with the pressure dependence of the structure and our HP Raman results. Considering this we have recently done a HP single-crystal diffraction study of the same sample at the Xpress beamline of the Elettra Synchrotron, Trieste. The crystal, previously cut in two different perpendicular directions with a focused ion beam, was loaded to the diamond anvil cell (DAC) to maximize the available reciprocal space information during our HP investigation. This permitted us to overcome the limitations in accessible reciprocal space in usual HP studies and enabled us to obtain a structure refinement with anisotropic atomic displacement parameters (adp's). In particular, the data was sufficient to refine adp's of all the atoms in the structure of omphacite while changing pressure, and to obtain accurate structural variations in terms of deformation of bonds and coordination polyhedra.

The description of the elastic and structural behavior of omphacite crystals during compression will further help to understand the genetic processes of omphacite-rich rocks, such as eclogites.

*References:*

[1] McCormick et al. (1989) Am Mineral 74:1287-1292
[2] Pandolfo et al. (2012) Am Mineral 97:407-414
[3] Zang et al. (2016) Phys Chem Miner 43:707-715

## The phase transitions of $CaSiO_3$ perovskite at extreme conditions

Thomson, A.R.[1,2], Crichton, W.A.[2], Huang, R.[1], Rosenthal, A.[2], and Brodholt, J.P.[1]

[1]Department of Earth Sciences, University College London, UK

[2]The European Synchrotron (ESRF), Grenoble,

---

Calcium silicate perovskite (CaPv) is the third most abundant mineral in Earth's lower mantle. After entering phase assemblages at ~ 19-21 GPa [1] it constitutes ~ 5 to ~ 30 wt.% of ultramafic to mafic lower mantle assemblages respectively [2]. Additionally, it is commonly observed as mineral inclusions trapped within diamonds that are believed to have been exhumed from the transition zone and/or lower mantle, e.g. [3]. The crystal structure, phase transitions, elastic properties, and equation of state of $CaSiO_3$ perovskite are all, therefore, of great significance for the interpretation of seismological data. Recent studies of CaPv's elasticity [4, 5] demonstrated that its seismic velocities were significantly slower than previous theoretical estimates such that, if present, it will be geophysically observable. Additionally, it was also observed that CaPv undergoes multiple elastically anomalous phase transitions as a function of increasing temperature (*T*) at mantle pressures (*P*) [4]. However, estimates of the *PT* slope of CaPv's phase transitions are extremely variable [6], preventing their inclusion in geophysical models of the deep mantle.

We have performed high pressure experiments in the large volume press at beamline ID06-LVP of the ESRF. The experimental design was optimised to study the phase transitions occurring in CaPv, which involve extremely subtle variations in peak width and/or the appearance of new (but very weak) superlattice peaks, at pressure conditions of 10-30 GPa. Low density amorphous gaskets were combined with B-doped polycrystalline diamond furnaces and MgO components to provide low and continuous background, with few Bragg reflections from the sample environment to complicate interpretation. Additionally, the sample detector distance and 2-theta diffraction range were set to achieve the highest angle dispersive diffraction resolution possible. In combination this setup facilitated the unequivocal detection of superlattice peak appearances as well as the evolution of CaPv Bragg peaks during heating/cooling ramps as pressure was increased. Combined these observations are diagnostic of the crystallographic structure for CaPv. Results allow extrapolation of the *PT* conditions of CaPv's phase transitions, permitting improved interpretation of seismic observations from the lower mantle.

*References:*

[1] Holland et al. (2013), JPet, 54(9), 1901-1920
[2] Kesson et al. (1998), Nature, 393, 252-255
[3] Nestola et al. (2018), Nature, 555, 237-241
[4] Thomson et al. (2019), Nature, 572, 643-647
[5] Greaux et al. (2019), Nature, 565, 218-221
[6] Hirose et al. (2017) Science, 358, 734-738

# Hazard and risk sensing in dating by optimized isotopic diversity and quantifications

Akai R.[1]

[1] Post-Research student of Universityof Tsukuba ( r1.akai@gmail.com )

---

The dating in geology was established by comparing fossils in the sequence geologic formation, and an absolute value by counts carefully to be converted by radioisotope approach with error. The radioisotope dating originates from Rutherford's identification of alpha particles and related amounts of their chemical transformation[1]. An ideal isotopic reverser provides a half-life for the radiative equilibrium or some isotopic steady states. The mass generation lost from the reserve formulates a reaction coefficient of radioisotope and temporal research in statistics as the isotopic earth reserve. At the same time, those isotopic reactions can be truncated linearly by max-min reaction rate. These linear bands ideally connect with twice analogue meters like a body weight scale. This link will count their loss by a range in an error propagation of a dating. In the end, a half-life constant is stoichiometry in a reaction and a systematic analogue count standard. Those equilibrium systems having a half-life might concern sluggish reactions or pollution in open systems or subsystems. It excites us to notify unspecified factors of a relatively simple range by the ideal comparison. These mentions come from the mathematical theorem in a simple truncation of isotope range for an isotopic reaction with a validated geochemical standard(e.g. three isotopes in oxygen) and the limited volume[2]. By calculating an upper/lower isotope of a single phase, linear programming takes significant simplification with some hypothetical interpretations in engineering in contrast to the diverse earth science. Three isotope/isotopologue applications have only been allowed by limited bulk composition and a standard isotope rate. So, some interested daughter/stable isotope or isotopologue can be recognized as a radiative equilibrium in some chains, and analysis of trustable values and statical interpretations are appropriate in thermodynamics. Its significant contributions might be systematic changes in absolute/relative dating or environmental indexes. Such comfortable modelling in comparing provides controlling twice data (weighted Age), a statical view for the primitive (an upper limit) and an essential weak in scale (an error in a system) or a numeric span for some geologically radical/sluggish events. Those diversities of isotopes in the geological events link with any isotope unit.

Ideal interpretations or similar constraints optimize the approaches by removing risky elements in thinking the own scientific best. This future will leave or lead to systematic easy wonders on your experiences or will carry irregular equipping special terms, and/or blind or hide our learning objective in their social steps. Such optimization in finding an object seems a disadvantage and doubtful bridge for the grad technological view. It will be similar to beauty diet, peace and scientific tag, and makes us yearn for the lack of modern ethical history or information literacy in computing. Such a sensitive dating view will avoid expensive calculations in precise or violent hazards in controlling moralism, manner, escape, etc. This dual care in processing resembles the engineering or scientific philosophy. And, it activates the trivial examinations or too much excitation in a fated criticism of understanding duality in linear algebra. A safe way is a limit to usage for safe universal isotopes with general terms for obstructs in addiction or evasion from numeric modelling. So, the best optimization research brings a high level of sincerity and mentions the several challenges in mathematics and physics. Generally, economic improvement helps to further dating opportunities in any region where people try. The above-simplified dating opens modern theory, the memorized discretized geological events or their diversity in radical/sluggish systems by essential sensing.

*References:*

[1] Allègre C.J. (2008) Isotope Geology, Cambridge University Press, p512
[2] Akai R(2023) Goldschmidt conference poster

## First-principles investigations of antigorite polysomatism under pressure

Tsuchiya, J.[1], Mizoguchi, T.[1], Inoue, S[1]. and Thompson E.C.[2]

[1]Geodynamics Research Center, Ehime University, 2-5 Bunkyo-cho, Matsuyama, Ehime 790-8577, JAPAN, junt@ehime-u.ac.jp

[2]Department of Earth and Environmental Systems, The University of South, Sewanee, TN 37383, USA

---

Antigorite is the high-temperature member of the serpentine group minerals and is broadly considered a primary carrier of water in the subducting oceanic lithosphere. It has a wavy crystal structure along its *a*-axis and several polysomes with different m-values (m = 13-24) have been identified in nature. The m-value is defined as the number of tetrahedra in one wavelength and is controlled by the misfit between the octahedral and tetrahedral layers. The degree of misfit primarily depends on the volumes of the $MgO_6$ octehedra and $SiO_4$ tetrahedra within the layers, which vary as a function of pressure and temperature. However, it is not well understood which m-values of antigorite are stable at different pressure and temperature conditions. To investigate the pressure dependence of the stability of different m-values in antigorite, we performed first-principles calculations for several polysomes (m = 14-19) at high pressure from 0 to 14 GPa and compared their enthalpies at static 0 K. We found that although the energy differences between polysomes are small, polysomes with larger m-values are more stable at ambient pressure, while polysomes with smaller m-values are more stable at elevated pressures. This suggests that the structure of antigorite in the oceanic lithosphere subducting into the deep Earth may gradually evolve into a different polysome structure than the antigorite samples observed at ambient or near-surface pressure conditions. These changes in the m-values are accompanied by a minor dehydration reaction. By modulating the available amount of free water in the system, antigorite polysomatism may influence the distribution of intermediate-depth seismicity, such as the observance of double seismic zones.

## HP-HT behaviour of Jamesonite: A combined Single-Crystal Synchrotron X-ray Diffraction and Raman spectroscopy study

Comodi P.[1], Fastelli M.[1], Pennacchioni L.[2], Balic-Zunic T.[3], Hanfland M.[4], Zucchini A.[1]

[1]Department of Physics and Geology, University of Perugia, Perugia, Italy paola.comodi@unipg.it
[2]Institut f. Geowissenschaften, Universität Potsdam, Karl-Liebknecht-Str. 24, Hs. 27 14476 Potsdam-Golm
[3]Department of Geosciences and Natural Resource Management, University of Copenhagen, Copenhagen, Denmark
[4]European Synchrotron Radiation Facility, Grenoble, France

---

Jamesonite ($FePb_4Sb_6S_{14}$) belongs to the group of rod-based sulfosalt structures made of infinite $(Pb_6Sb_6S_{14})\infty$ rods extending along *a*, connected by the chain of Iron (Fe) coordination octahedra into layers parallel to (010). It has remarkably interesting electric and magnetic properties because it is an intrinsic semiconductor with an optical band gap equal to 0.48 eV and it has unusual magnetic anisotropy with the susceptibility parallel to the *a* axis, superior to the susceptibility perpendicular to that axis.

The high-pressure behavior of jamesonite (*a* =4.08(3) Å, *b* =19.08(3) Å, *c* =15.67(3) Å, β = 91.89◦, space group $P2_1/c$) has been investigated using *in situ* high pressure synchrotron X-ray single-crystal diffraction up to ~17 GPa with a diamond anvil cell under hydrostatic conditions. Results of the volume isothermal equation of state (EoS), determined by fitting the pressure-volume (*P-V)* data with a third-order Birch–Murnaghan (BM) EoS, are $V_0$= 1207.1(4) $Å^3$, $K_0$= 36(1) GPa and K' = 5.7(7). At high pressure, jamesonite undergoes a phase transition to an orthorhombic structure with a *Pmcb* space group (β-jamesonite) [1]. The compressibility β-jamesonite up to 16.6 GPa, determined fitting the data with a second-order BM-EoS, gives $V_0$= 1027(2) $Å^3$, $K_0$= 74(2) GPa.

The comparison of the structural refinements at different pressures indicates that Fe, Pb and Sb do not change their coordination number over the whole investigated *P* range, respectively, 6 for Fe, 7 and 8 for Pb and 5 + 2 for Sb. However, a significant change occurs in the orientation of Sb lone electron pairs upon the phase transition following the change in symmetry. Furthermore, a discontinuity in the Fe chain evolution at the transition pressure is observed.

Raman spectroscopy collected at different pressures between 0.0001 and 11.5 GPa shows the evolution of main bands assigned to the stretching and bending modes of $Sb\text{-}S_3$ groups.

It was observed that blue shifts affect the main stretching and bending of symmetric and asymmetric bands. Following Hook's law, where the increase of wavenumber (namely the blue shift) may is correlated to the reduction of the bond distances with *P*, the comparison between single crystal X-ray diffraction and Raman spectra allows to determine the relationship between Sb-S distances evolution and the band shifts. A discontinuity in the Raman spectra around 9 PGa with the disappearance of the 236 $cm^{-1}$ band could be related to the phase transition described with X-ray data.

The effect of the temperature on the structural evolution and the phase transition was investigated, by collected data along isotherm at 426 and 523 K. The results will be illustrated.

*References:*

[1] Comodi P. et al. (2023) *Crystals*, 13.8: 1258

## Cation disorder and Fe-content in ankerite: their effect on its mineral physics

Zucchini, A.[1], Boffa Ballaran, T.[2], Masotta, M.[3], Pennacchioni, L.[4], McCammon, C.[2], Fastelli, M.[1], Comboni, D.[5], Hanfland, M.[6], Frondini, F.[1], Comodi, P.[1]

[1] Department of Physics and Geology, University of Perugia, Piazza Università, 06100 Perugia, Italy. *azzurra.zucchini@unipg.it

[2] Bayerisches Geoinstitut, University of Bayreuth, D-95440 Bayreuth, Germany.

[3] Department of Earth Sciences, University of Pisa, Via S. Maria 53, 56126 Pisa, Italy.

[4] Institut f. Geowissenschaften, Universität Potsdam, Karl-Liebknecht-Str. 24, Hs. 27 14476 Potsdam-Golm

[5] Department of Earth Sciences "Ardito Desio", University of Milan, Via Mangiagalli 34, 20133 Milano, Italy.

[6] European Synchrotron Radiation Facility, 71 avenue des Martyrs, 38000 Grenoble, France.

---

Fe-bearing carbonates have attracted the interest of the scientific community given their importance in understanding the Fe-enrichment in the inner Earth. The present work focuses on the H*P* behaviour of ankerite, [$Ca(Mg_{1-x}Fe_x)(CO_3)_2$ ($0 \le x \le 0.7$), *R*-3 space group]. Data from synchrotron single crystal X-ray diffraction (SC-XRD) at H*P* show that ordered ankerite undergoes phase transition to ankerite-II (*P*-1 space group) in the *P* range 12.15 – 13.54 GPa at room *T* (RT), whereas, in disordered ankerite, no phase transition is observed up to the highest investigated *P* (~30 GPa), resembling the behaviour of the isomorphous dolomite [1][2]. Disordered ankerite is more compressible [$K_{0V}$=99(1) GPa - *K*'=2.7(1)] than the ordered one [$K_{0V}$=95(1) GPa - *K*'=3.8(3)], with compressibility that increases as *P* increases; whereas, the compressibility of high-pressure polymorph decreases to $K_V$=110(11) GPa and *K*'=7(3) at the transition pressure. In all the three crystal structures, the *a* parameter has the lowest compressibility and it even expands in ankerite-II, being strictly related to the observed increase in γ angle with *P*, that is a consequence of the shear of cation layers in the (0 1 -1) plane. The results obtained from the present work show the strong influence of cation ordering on the stability and compressibility of the ankerite structure, with important consequences on its elastic behaviour, that might help in partially explaining the observed seismic anisotropic anomalies in the mantle wedge [3] as well as contributing in the carbonate's detection in the inner Earth [4].
Given the similarity of ankerite with dolomite, further studies at H*P* up to ~50 GPa by Raman spectroscopy are in progress in order to follow, in both ordered and disordered ankerites, the soft phonon mode responsible for the dolomite to dolomite-II transition [3] and understand its contribution on the missing phase transition in disordered ankerite and dolomite. The analysed *P* conditions will also give the chance to reach *P* conditions typical of the Fe spin crossover in carbonates, *i.e.*, ~43 GPa (RT) [5][6], being another important factor that is supposed to stabilize the Fe-carbonate's structures.
The project was partially founded by "DFG core facility for high pressure research" (2018) and "SIMP Research Grant in Crystal - chemistry, in memory of Prof. Fiorenzo Mazzi" (2022).

*References:*
[1] Zucchini A et al. (2014) Phys Chem Miner 41(10):783-793
[2] Zucchini A et al. (2017) Eur J Mineral 29:227-238
[3] Liu X and Zhao D (2017) Geophys J Int 210:1410-1431
[4] Chariton S et al (2020) Am Miner 105(3):325-332,
[5] Cerantola V et al. (2017) Nat Commun 8:15960
[6] Liu J et al. (2014) Am Mineral 99:84-93

## Mesothelioma and asbestos-induced carcinogenesis

Felley-Bosco, E.

Department of Biomedical Sciences, University of Lausanne, Switzerland

---

Mesothelioma is an aggressive, short-survival neoplasm that originates from the pleura, peritoneum and pericardium. Exposure to asbestos fibers increases the risk of developing mesothelioma and a causal link between asbestos exposure and mesothelioma development has been documented in experimental studies. Asbestos fibers are naturally occurring silicates that have been extensively used in the past, including in house construction but, because of their toxicity, their use has been banned in sixty-nine countries. Despite this, more than two million metric tons of asbestos are still consumed annually. Asbestos-related disease incidence is still increasing in several countries, including those countries that banned the use of asbestos more than thirty years ago. We review recent knowledge obtained in experimental models about the mechanisms leading to tumor development following asbestos exposure, including genetic and epigenetic changes. The landscape of alterations observed experimentally in tumor samples is consistent with alterations observed in clinical tumor samples; therefore, studies performed on early/pre-cancer stages should help inform secondary prevention, which remains crucial in the absence of an efficient primary prevention. Knowledge gathered on asbestos should also help address future challenges, especially in view of the increased production of new materials that may behave similarly to asbestos fibers.

## Slag dust from Kabwe (Zambia) - one of the most polluted places on Earth: mineralogy and contaminant bioaccessibility

Ettler, V.[1], Mihaljevic, M.[1], Drahota, P.[1], Kribek B.[2] and Nyambe, I.[3]

[1]Institute of Geochemistry, Mineralogy and Mineral Resources, Faculty of Science, Charles University, Albertov 6, 128 00 Prague 2, Czech Republic (ettler@natur.cuni.cz)

[2]Czech Geological Survey, Geologicka 6, 152 00 Prague 5, Czech Republic

[3]Department of Geology, University of Zambia, School of Mines, P. O. Box 32379, Lusaka, Zambia

---

The former Pb-Zn mining town of Kabwe in central Zambia is ranked amongst the worst polluted areas in both Africa and the world. The fine dust particles from the Imperial Smelting Furnace (ISF) slags and Waelz slags deposited in Kabwe represent a health risk for the local population.

We combined a detailed multi-method mineralogical investigation with oral bioaccessibility testing in simulated gastric fluid (SGF; 0.4 M glycine, pH 1.5, L/S ratio of 100, 1 hour, 37 °C) to evaluate the risk related to incidental dust ingestion. The slag dust fractions contain up to 2610 mg/kg V, 6.3 wt.% Pb, and 19 wt.% Zn [1]. The metals are mainly bound in a slag glass and secondary phases, which formed during the slag weathering or were windblown from nearby tailing stockpiles (carbonates, Fe and Mn oxides, phosphates, vanadates). No specific Cd-bearing phases were found, but As mostly substitutes for V in the structure of metal vanadates or is bound in secondary Fe oxyhydroxides [1]. The bioaccessible fractions (BAFs) are rather high for all the main contaminants, with the BAF values generally higher for the ISF slags than for the Waelz slags: Pb (24-96%), V (21-100%), Cd (42-82%), Zn (54-81%) and As (4-57%) [1].

The results clearly indicate the potential risks related to the incidental slag dust ingestion. Even when a conservative value of the dust daily intake (100 mg/day) is considered [2], the daily contaminant intake significantly exceeds the tolerable daily intake limits, especially for Pb>>V>Zn. At higher ingestion rates, minor contaminants (As, Cd) also become a health risk, especially for children. The slag heaps in Kabwe should be fenced to prevent local people entering and should be covered to limit the dust dispersion [1,2].

This study was supported by the Czech Science Foundation (23-05051S and 22-27939S) and OP JAC project CZ.02.01.01/00/22_008/0004605.

*References:*

[1] Ettler V et al. (2020) Chemosphere 260: 127642.
[2] Ettler V. and Kierczak J. (2021) Chapter 6, In Piatak N.M. and Ettler V. (eds) Metallurcial Slags: Environmental Geochemistry and Resource Potential, Royal Society of Chemistry, Cambridge, UK.

## Health effects of cristobalite dusts: comparison of their physico-chemical and mineralogical features in different occupational settings

Di Benedetto F., Belluso E., Capella S., Ardit M., Baroni T. and Capacci F.

[1]Dip. Fisica e Scienze della Terra, Università di Ferrara; francesco.dibenedetto@unife.it

[2]Dip. Scienze della Terra e Centro Interdip. Studio degli Amianti e di altri Particolati Nocivi "Giovanni Scansetti", Università di Torino

[3]Dip. Geoscienze, Università di Padova

[4]Dip. Scienze della Terra, Università di Firenze

[5]Formerly at Health Agency of Florence

---

Long-term investigation of the health effects of exposure to respirable crystalline silica dust has led a huge improvement in knowledge of the specific features that may determine these effects as a variable entity. The molecular and mechanistic foundations of respirable crystalline silica toxicity have been explored both under controlled laboratory conditions and directly in occupational settings, allowing close comparisons between model and real-world exposure conditions.

Because of its abundance and ubiquitous use, quartz would be expected to play a major role in the toxicity issue. However, a number of recent cases of occupational exposure to silica dust have the second most abundant polymorph, cristobalite, in common. All of these cases have occurred in occupational settings not previously claimed as critical for silica risk and in countries where industrial hygiene practices have reduced workers' occupational exposure of  to low levels.

In the present contribution, we aim to closely compare the cristobalite-bearing materials coming from three of these recent cases through a thorough multi-method mineralogical and chemical investigation. The materials are the artificial stone, the gold microcasting, and the dental alginate preparation. The specific aim of this study is to compare the results of experimental studies carried out in different contexts where cristobalite is used as a raw material or as a byproduct in industrial production processes. The techniques used are XRD, SEM, TEM, and spectroscopic EPR investigations. The results derived from this comparison have been interpreted in the light of a detailed consideration of the peculiarities of each production line, especially with respect to the steps where a significant dust generation is observed. This comparison suggests that each occupational context is characterised by its own specificity, with the low crystallinity of cristobalite being the only parameter common to all settings. Accordingly, one could infer that the toxicological effects of cristobalite should be sought in the organisation of the surface structural terminations (i.e. the nearly free silanols that act as toxicological primer for quartz), in close relation with the diffuse structural defects observed in all industrially produced/modified cristobalite materials.

## Simulations of temperature-driven release of arsenic from minerals and phases related to wildfires

Tuhý, M.[1,3], Ettler, V.[1], Rohovec, J.[2], Matoušková, Š.[2], Drahota, P.[1]

[1]Institute of Geochemistry, Mineralogy and Mineral Resources, Faculty of Science, Charles University, Czech Republic (marek.tuhy@natur.cuni.cz)

[2]Institute of Geology, Academy of Sciences of the Czech Republic

[3]Bushfire Behavior and Suppression, CSIRO Environment, Black Mountain, ACT Canberra, Australia

---

Increasing frequency and intensity of wildfires in the last decades may also cause their occurrence in environments polluted by mining and ore processing. In these areas, metal(loids) can be thermally remobilized from minerals and phases into the atmosphere and/or the surrounding environment. Previous research has shown that the thermally induced release of an element depends on many factors, but mostly on the temperature reached and the solid-phase speciation of the element. We studied the temperature-dependent release of arsenic (As) from samples representative for natural and contaminated environments: conichalcite [$CaCu(AsO_4)(OH)$], mimetite [$Pb_5(AsO_4)_3Cl$], scorodite [$FeAsO_4{\cdot}2H_2O$], orpiment [$As_2S_3$], realgar [$As_4S_4$], enargite ($Cu_3AsS_4$), synthetic analogues of minerals with adsorbed As: goethite [$FeO(OH)$], ferrihydrite [$Fe_{10}O_{14}(OH)_2$]; cacodylic acid [$(CH_3)_2AsO_2H$] and arsenic-rich mushroom as an analogue of organoarsenic compounds. The homogenized samples were continuously heated in a resistance furnace in the temperature range of 25-800 °C. The released elements were transported from the furnace in a continuous argon flow directly to ICP-OES, allowing their continuous detection. The interpretation of released As was combined thermogravimetry, XRD, and FEG-SEM/EDS analyses.

The results show that organic As-bearing materials exhibited the peak of As release at the lowest temperatures of 275 °C (As-rich fungi) and 350 °C (cacodylic acid), followed by arsenolite ($As_2O_3$) with the maximum As emission at ~400 °C. Realgar ($As_4S_4$) and orpiment ($As_2S_3$) exhibited the maximum As release at 425–450 °C, while enargite ($Cu_3AsS_4$) and arsenopyrite (FeAsS) released As at much higher temperatures at ~625 and >725 °C, respectively. Similarly, As-bearing Fe oxyhydroxides emitted As at temperatures exceeding 650 °C. The temperature-dependent As emission from arsenates was rather variable and peaked around 700 °C for conichalcite, $CaCu(AsO_4)(OH)$, and scorodite, $FeAsO_4{\cdot}2H_2O$, while for mimetite, $Pb_5(AsO_4)_3Cl$, increases towards the upper limit of the temperature range. These experimental results can be used as a reference dataset for deciphering the sources of As emissions from the burned contaminated materials (biomass, topsoils) in wildfire-affected areas.

This study received funding from the Czech Science Foundation (GAČR project no. 23-06344O).

## Effects of Simulated Lung Fluids (SLFs) on zeolite fibres through real-time SC-XRD investigations

Giordani, M.[1], Cametti, G.[2] and Mattioli, M.[1]

[1]Department of Pure and Applied Sciences, University of Urbino Carlo Bo, Urbino, Italy
matteo.giordani@uniurb.it.

[2]Institute of Geological Sciences, University of Bern, Baltzerstrasse 1+3, 3012, Bern, Switzerland

---

Zeolite minerals are widely distributed in different geological environments, and due to their unique structural properties are currently used in a multitude of processes. Among natural zeolites, the fibrous variety of erionite has been classified as carcinogenic to humans, if inhaled and, in the last decades, its interaction with biological tissues has been widely investigated. Similarly, other fibrous zeolites have been object of growing concern and minerals like mordenite, offretite, ferrierite, mesolite, etc., are currently under study by the scientific community. In particular, any change/transformation at the lung cell/mineral interface could represent the focal point for triggering the cascade processes that lead to the development of lung diseases, such as malignant mesothelioma.

For this reason, in the present study we investigated the chemical and structural modifications of three natural fibrous zeolites in contact with simulated lung fluid (SLF). Chemical and crystal-structural analyses were conducted on erionite $[Ca_{3.39}K_{2.05}Mg_{0.31}Na_{0.08}](Al_{9.48}Si_{26.47}O_{72})\cdot 28.1H_2O]$, offretite $[K_{1.1}Mg_{0.98}Ca_{0.95}Na_{0.01}](Al_5Si_{13.01}O_{36})\cdot 15.37H_2O]$, and mordenite $[Na_{3.35}Ca_{2.04}K_{0.13}Mg_{0.01}](Al_{7.86}Si_{40.21}O_{96})\cdot 25.23H_2O]$ at selected times of interaction (once a week, up to 5 weeks) in SLF. The measurements were performed by single crystal X-Ray Diffraction (SC-XRD) for structural determination and by Scanning Electron Microscopy with Energy Dispersive X-ray spectroscopy (SEM-EDX) for the chemical composition. Overall, the structural and chemical analyses consistently point to an exchange-process between the Na-ions in the solution and the extra-framework cations (mainly Ca) in the zeolites. Less obvious are the changes observed in offretite, which behaves differently from erionite and mordenite. Structural refinements clearly indicated that Na is replacing Ca atoms located at the centre of the 12-membered ring channels. However, the trend as a function of time is not clear, and there seem to be other mechanisms, probably occurring at the surface, involved in the exchange process.

These variations may represent a fundamental process in lung disease development, and this simulation, conducted in a simplified system, represents a further step towards a direct and in real-time knowledge of the processes that can develop following inhalation of hazardous fibrous zeolites.

## Geological occurrence, morphological characterisation, and toxicological evaluation of erionite in New Zealand

Patel, J.P.[1]*, Brook, M.S.[1], Scarfi, S.[2], Mirata, S.[2], Almonti, V.[2], Hamilton, A.[1], Kah, M.[1] and Gualtieri[3,] A.F.

[1]School of Environment, University of Auckland, Private Bag 92019, Auckland 1010, New Zealand (*janki.patel@auckland.ac.nz*)

[2]Department of Earth, Environmental and Life Sciences, University of Genova, Genoa, 16132, Italy

[3] Department of Chemical and Geological Sciences, University of Modena and Reggio Emilia, Via G. Campi 103, 41125, Modena, Italy

---

Volcanic activity in New Zealand has given rise to a wide variety of minerals, one such group of minerals are zeolites, which primarily form though diagenesis or hydrothermal alteration of volcanic rocks such as basalts and tuffs. While there are over 40 naturally occurring zeolites worldwide, erionite in particular is prominent zeolite due to its association with malignant mesothelioma (MM) – a disease commonly linked to asbestos exposure. In the 1970s a MM epidemic was discovered in the Cappadocia region of Turkey, where erionite was found in the tuff bearing rocks used to build house and pave their roads. International Agency for Research on Cancer (IARC) has designated erionite as a Group 1 carcinogen due to its hazardous potential when disturbed or inhaled. However, undisturbed erionite is not considered a risk. In New Zealand erionite has been found in numerous locations throughout the North and South islands, with some particularly exceptional localities at Mount Somers in the Canterbury region of the South Island where woolly erionite was found within vesicles of rhyolitic rock and acicular bundles of erionite found disseminated through a thin layer of tuff at Timber Bay in Kaipara. Various analytical techniques are being utilised to detect and characterise erionite including; Scanning Electron Microscopy, X-Ray Powder Diffraction with the Rietveld method, Transmission Electron Microscopy, Electron Microprobe Analysis and micro-Raman spectroscopy. *In-vitro* toxicity tests have also been conducted on two of the erionite samples (Mount Somers and Kaipara) with results indicating that NZ erionite signifies an acute toxic potential especially in relation to non-carcinogenic fibres such as wollastonite. Indeed, over a 7-day period Gawler Downs erionite led to 90% cell death and Kaipara led to 80% cell death of THP-1 macrophages during a cytotoxicity test assessed by the MTT assay. Due to the potential adverse health effects linked to erionite exposure, this research aims to develop an understanding of erionite occurrence in New Zealand, to mitigate any potential environmental hazards.

# Surveying airborne fibrous zeolite deposition on leaf surfaces around sedimentary and volcanic zeolitic outcrops in New Zealand

Fan, W [1]., Dirks, N, K [2]., Hamilton, A [1]., Patel, P. J [1]. and Salmond, A. J [1].

1. School of Environment, Faculty of Science, University of Auckland, Auckland, New Zealand (wendy.fan@auckland.ac.nz)

2. Department of Civil and Environment Engineering, Faculty of Engineering, University of Auckland, Auckland, New Zealand.

---

Naturally occurring fibrous zeolites (such as erionite), are recognized as known or potential carcinogens to human respiratory system (1,2). These minerals are predominantly found in altered volcanic ash layers (in sedimentary rocks), with smaller quantities occurring in vesicles within volcanic rocks (volcanic) (3,4). These fibrous zeolites pose a health risk when they become airborne, either by natural forces (weathering, wind transportation) or through human disturbances (5). A notable gap exists in our understanding of the characteristics and the atmospheric dispersion dynamics of these fibrous minerals related to their occurrence in geological deposits source (outcrops).

This study investigated settled dust on leaf surfaces before and after direct disturbance (e.g., collecting geological samples and vehicle movements) near 11 fibrous zeolite (e.g. erionite, mordenite) outcrops across three regions in New Zealand (Rotorua, Gawler Downs, and Auckland). SEM-EDS analysis was employed to identify fibrous zeolites and their morphology in both airborne and rock samples, while TEM-SAED was utilized to differentiate between different types of zeolite fibres.

The airborne fibrous zeolites were observed to be significantly smaller in size compared to fibres found in geological samples collected from the outcrops. Additionally, the deposition of fibrous zeolites was found to be higher in sedimentary outcrops with a greater concentration of these minerals. Notably, the presence of fibrous particles on plant surfaces was only detected after disturbance near volcanic outcrops.

*References:*

*1.* Carbone M et al. (2007) Nat Rev Cancer. 2007 Feb;7(2):147–54.
2. IARC. (1997). Vol. 68. World Health Organization; 1997.
3. Mumpton F and Ormsby W.C (1976) In: Natural zeolites. Pergamon press. p. 119.
4. Van Gosen B. S et al. (2013) Environ Geochem Health. 35(4):419–30.
5. Gualtieri A. F (2023). Journal of Hazardous Materials. 442:130077.

# A Mobile Sampling Method for Monitoring Vehicle-Induced Dispersion of Elongate Mineral Particles from Unsealed Gravel Roads

Chen, S.[1], Dirks, K.[2], Costello, S.[3], Chen, G.[4], Salmond, J.[5]

[1]Faculty of Engineering, University of Auckland, sche660@aucklanduni.ac.nz

[2]Faculty of Engineering, University of Auckland.

[3]Faculty of Engineering, University of Auckland.

[4]Centre for Public Health Research, Massey University.

[5]Faculty of Science, University of Auckland.

---

Recent research has identified elongate mineral particles (EMPs), particularly zeolites such as mordenite and erionite, in bedrocks in various locations in New Zealand [1]. Resuspension of these particles as road dust from passing vehicle poses exposure risks to local residents, especially in areas where these minerals are found along unsealed gravel roads, used in roading materials or transported in open truck from mines and quarries in New Zealand [2] [3]. However, the level of risk to human health as a result of exposure remains unclear as limited studies have investigated the dispersion patterns of traffic-induced dispersion of airborne EMPs, especially those of erionite fibres needed to estimate “risk zones” with respect to human exposure. To address this gap, this research describes an on-road sampling method using air filters with pumps, placed at different locations behind a moving vehicle and trailer. The campaign was conducted on two unsealed gravel roads and one sealed road in a region known to have large zeolite deposits close to an active and disused zeolite quarry, where mordenite has been found.

Filters were analysed using Scanning Electron Microscope (SEM) for both visual morphology and Energy Dispersive X-ray Spectroscopy (EDS) for identifying zeolite species. On the bases of analysis, mineral fibres are discernible on the filters from all of the collection points and from both sealed and unsealed gravel roads. Notable differences in EMPs concentrations were observed at different heights behind the vehicle. This allows for further research to investigate the correlation between the height of dispersion and the horizontal dispersion of EMPs, and the influence of various environmental determinants such as precipitation and wind conditions on EMP dispersion and hence identify the extent of “risk zones” with respect to human exposure. This result demonstrate that the methodology is useful as a screening method for identifying the presence of EMPs in the air and, hence, quantifying the potential health risks.

*References:*

[1] Patel J P and Brook M S (2021) “Erionite asbestiform fibres and health risk in Aotearoa/New Zealand: A research note.” *New Zealand Geographer*, vol. 77, no. 2, pp. 123-129. DOI: 10.1111/nzg.12291

[2] Brook M S et al. (2020) “Erionite in Auckland bedrock and malignant mesothelioma: an emerging public and occupational health hazard?” *New Zealand Medical Journal*, vol. 133, no. 1518, pp. 73-78.

[3] Bluett J et al. (2017). “Impacts of exposure to dust from unsealed roads” NZ Transport Agency. Wellington, New Zealand. Rep. RR 590, 2017. Accessed: March 20, 2024. [Online] Available: https://www.nzta.govt.nz/resources/research/reports/590/

## Correlating dissolution kinetics, surface alterations, and chemical reactivity: new insights into the mechanisms of mineral fibre toxicity

Di Carlo, M.C.[1], Ballirano, P.[1], Bloise, A.[2], Campopiano, A.[3], Fantauzzi, M.[4], Montereali, M.R.[5], Nardi, E.[6], Petriglieri, J.R.[7,8], Rossi, A.[4], Tomatis, M.[7,9], Turci, F.[7,10] and Pacella, A.[1]

[1]Department of Earth Sciences, Sapienza University of Rome, mariacristina.dicarlo@uniroma1.it

[2]Department of Biology, Ecology and Earth Sciences, University of Calabria

[3]Department of Medicine, Epidemiology, Occupational and Environmental Hygiene, National Institute for Insurance against Accidents at Work, INAIL, Roma

[4]Department of Chemical and Geological Sciences, INSTM Research Unit, University of Cagliari

[5]Italian National Agency for New Technologies, ENEA, Casaccia Research Centre

[6]Institute for Environmental Protection and Research, ISPRA, Roma

[7]"G. Scansetti" Interdepartmental Centre for Studies on Asbestos and Other Toxic Particulates, University of Torino

[8]Department of Earth Sciences, University of Torino

[9]Department of Veterinary Sciences, University of Torino

[10]Department of Chemistry, University of Torino

---

Inhalation of respirable-sized asbestos and asbestiform mineral fibres has been associated with the development of several lung diseases, including pleural diseases [1]. Nevertheless, the understanding of the precise mechanisms driving the toxicity of mineral fibres remains incomplete.

In this study, we aimed at providing further insights by i) modelling the kinetics of fibre dissolution in an artificial lysosomal fluid (ALF) that mimics the intracellular regions of phagocytic cells [2], and by ii) investigating possible fibre surface modification, following dissolution, and modulation in its chemical reactivity (as planned in the BRIC 2022 project; CUP: B87G23000090005).

To comprehensively assess the possible different behaviour of mineral fibres, we studied UICC chrysotile, UICC crocidolite, fibrous tremolite (Basilicata, Italy) and two samples of fibrous antigorite (Calabria and Liguria, Italy). The samples were incubated in ALF at pH 4.5, up to 28 days at T = 37±1 °C. The leached cations were quantified by inductively coupled plasma optical emission spectrometry (ICP-OES). Chemical reactivity was evaluated following the generation of •OH radicals, an extremely reactive species, able to damage DNA, proteins, and lipids *in vivo*. Pristine and incubated fibres were tested up to 15 days using the spin trapping technique associated with electron paramagnetic resonance (EPR) spectroscopy. Due to the primary role of Fe in •OH radical generation [3], the chemical speciation of surface Fe was determined by X-ray photoelectron spectroscopy (XPS) on both pristine and incubated samples.

The calculated dissolution rates, normalized to the specific surface area, revealed that the samples exhibit different biodurability (tremolite > crocidolite > antigorite > chrysotile). After dissolution the fibres undergo changes in surface composition, with alteration in surface Fe speciation, and reactivity.
Our results suggest that different fibre dissolution rates may drive different surface chemical modifications, which in turn modulate •OH radical generation.

*References:*

[1] Mossman B T and Gee J B L (1989) N Engl J Med 320(26):1721-1730
[2] Marques M R C et al. (2011) Dissolution Technol 18:15-28

# Transforming waste into resource: Synthesis of tobermorite from crystalline silica

Bernini, M., Galamini, G., Fantini, R., Malferrari, D. and Gualtieri, A.F.

Department of Chemical and Geological Sciences, The University of Modena and Reggio Emilia, Modena, Italy. Via G. Campi 103, Modena, I-41125, Italy. alessandro.gualtieri@unimore.it

---

Prolonged exposure to fine particles of crystalline silica dust can pose serious health risks as it can lead to a range of respiratory problems, including silicosis, lung cancer, and other lung diseases. Furthermore, exposure to crystalline silica has been linked to other health issues such as chronic obstructive pulmonary disease (COPD), tuberculosis, and autoimmune disorders. To mitigate the risks associated with crystalline silica exposure, regulatory agencies have established permissible exposure limits and employers are required to implement measures to control silica dust exposure.

Crystalline silica powders may be naturally contained in raw materials or they may be released from the processing of a variety of types of geomaterials. In the latter case a waste is generated for which it would be desirable to find a form of reuse. The synthesis of microporous materials such as tobermorite to be used for adsorption of metals or other molecules could represent a possible solution. Tobermorite identifies a group of natural hydrated calcium silicate minerals with a strong resemblance to 2:1 swelling layer silicates, including variability of basal spacing with $H_2O$ content, specific surface area, polytypism and cation exchange capacity (CEC). The latter property characterizes substituted-tobermorites, geomaterials that can be synthesized with modest energy consumption [e.g., 1-3].

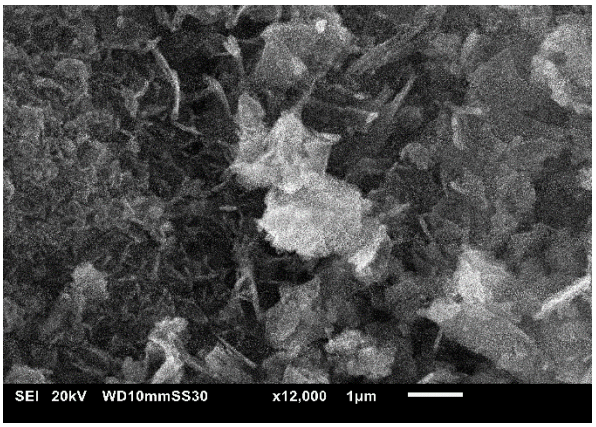


SEM images of lamellar of tobermorite crystals

Through this research, we evaluated the possibility of synthetize a tobermorite-rich material using both crystalline silica from quarry processing and an End-of-Waste obtained from cement asbestos thermal inertization. For each gram of tobermorite, obtained in 24 hours by operating at 120°C, about 250 mg of crystalline silica is inert. The synthesized tobermorite was then used to adsorb volatile organic molecules (e.g., limonene, linalool, ethylfuran, etc.) and the release kinetics were also evaluated.

The goal was to obtain a material with slow release of the specific target molecules and thus enable their reduction with savings in economic and environmental terms.

*References:*

[1] Coleman N.J. et al (2009) Int J Miner Process 93(1): 73-78
[2] Guo X and Li D (2019) J Wuhan Univ Technol Mater Sci Ed 34(6): 1345-1349
[3] Malferrari et al (2022) ACS Omega 7: 1694−1702

*This research is under **PRIN2022** "SEEDS - Sediments Eco-recycling Exploitation, Development and Sustainability" – Project Code 2022BCL34N.*

## Understanding Asbestos in Calabria: Assessing Mineralogy and Geochemistry with Insights into Groundwater Quality and Secondary Airborne Exposure Risks

Bloise, A.[1], Fuoco, I.[1], Vespasiano, G.[1], Pacella, A.[2], Villella, S.[1], Piersante, C.[1], Malvasi, G.[3], Campopiano, A.[4], Ballirano, P.[2], Bruno, M.R.[5], Bruni, B. M.[6], Sinopoli, F.[5], Di Carlo, M.C.[2] and Apollaro, C.[1]

[1]Department of Biology, Ecology and Earth Sciences, University of Calabria, Italy, andrea.bloise@unical.it

[2]Department of Earth Sciences, Sapienza University of Rome, Italy

[3]Radioactivity and Asbestos Office ARPA Basilicata, Potenza, Italy

[4]National Institute for Insurance against Accidents at Work, INAIL, Roma, Italy

[5]National Institute for Insurance against Accidents at Work (INAIL), Lamezia Terme, Italy

[6]National Health Institute (ISS), Department of Environment and Health, Rome, Italy

---

Asbestos is a group of six minerals that belong to the class of silicates and have a fibrous appearance. These minerals are categorized into two groups: amphiboles (tremolite, actinolite, anthophyllite, crocidolite and amosite) and serpentine (chrysotile) which naturally occur in ophiolite rocks worldwide. Asbestos, known for its carcinogenic properties [1], has historically been predominantly assessed in air, neglecting its possible presence in water resources. Recently, growing attention is being paid on asbestos fibers into groundwater, recognizing this environmental matrix as unconventional source of exposure to asbestos fibers. Use of polluted waters for household, agricultural and industrial purposes poses a risk of fiber migration from water to air into domestic, public and working spaces. Studies indicate that polluted waters can lead to airborne fiber concentrations surpassing legal limits through evaporation or mobilization processes [2]. Indeed, water acts as a carrier for fibers, facilitating their transport and accumulation in distant areas. Thus, hydrodispersed asbestos represents an emerging pollutant, as its presence hasn't been systematically assessed. Furthermore, the risk of ingesting asbestos fibers via drinking water has been hardly discussed and conclusive evidence is still lacking. This study investigates asbestos pollution in groundwater in ophiolite area of Calabria Region (Southern Italy) (as planned in the frame of the BRIC 2022 project; CUP: B87G23000090005). In surrounding Mount Reventino area, 22 water samples (springs and riverine waters) were collected and in detail characterized. From a mineralogical point of view, tremolite represents the most abundant asbestos phase, followed by chrysotile, actinolite and anthophyllite. Performed analyses also revealed the presence of non-asbestos minerals such as Mg-hornblende, gedrite, edenite and rutile. Geochemical characterization pointed out that collected samples belong mainly to Ca-$HCO_3$ and Mg-$HCO_3$ hydrogeochemical facies with concentration of heavy metals ranging from 0.23-17.13 ppb, 4.72-49.12 ppb, 1.12-30.36 ppb, 5.37-30.24 ppb for Cr, Fe, Ni and Zn, respectively. Analyses revealed ubiquitous asbestos fibers presence, with concentrations up to 350000 fibers/Liter. Morpho-dimensional analysis showed variability in fiber dimensions, with a significant portion falling within the WHO criteria for respirable fibers [3]. The maximum value was recognized in Mg-$HCO_3$ riverine water sample. These results point out the issue related to fibers transport and accumulation in distant areas from source. For these reasons a distribution maps of fiber levels were also elaborated. These findings underscore the need to consider groundwater as a potential pathway for asbestos contamination and highlights the importance of comprehensive assessment and further research to mitigate health risks associated with asbestos exposure through water sources.

*References:*

[1] IARC-International Agency for Research on Cancer, 2012.
[2] Avataneo C et al. (2022). Journal of Hazardous Materials 424: 127528.
[3] World Health Organization - WHO (1986). Asbestos and other natural mineral fibres.

## Geo-inspired nanotubes for Alzheimer's Disease treatment by low dose radiotherapy: preliminary results

D'Alessio, D.[1], Secchi, V.[2], Campione, M.[1], Malaspina, N.[1] and Monguzzi, A.[2]

[1]Department of Earth and Environmental Sciences, University of Milano-Bicocca, Piazza della Scienza 4, 20126 Milan, Italy Corresponding email: daniela.dalessio@unimib.it

[2]Department of Materials Science, University of Milano-Bicocca, Via R. Cozzi 55, 20125 Milan, Italy

---

The neurodegenerative Alzheimer's Disease (AD) affects memory and behaviour, and causes dementia. Presently, no cure is available for AD, and only experimental therapies on monoclonal antibodies to target and remove the harmful substances from the brain have been approved by Food and Drug Administration (FDA). However, the controversy over their efficacy highlights the need for better therapeutic treatments.

We employed hydrated magnesium silicate [$Mg_3(Si_2O_5)(OH)_4$] nanotubes (NTs) as nanoscintillators, in their highly biocompatible stoichiometric form, synthesized under hydrothermal conditions. The outer surface of NTs is brucitic, and in aqueous environment is modified by concentrating $Mg^{2+}$ ions towards the surface, giving rise to a positive Z-potential. This allows to bind to the surface the Chlorin e6 (Ce6) as negatively charged singlet oxygen (SO) photosensitizer (PS) and the cyclic D,L-α-peptides (CP-2) for selective Aβ-targeting. Size and composition of NTs were adequately tuned to maximize the interaction with ionizing radiation, SO production, Aβ aggregation inhibition efficacy, and therapeutic effect [1,2]. Synthesized NTs, before and after functionalization with Ce6 and CP-2, were characterized with a multi-analytical approach.

Soluble Aβ oligomers are identified as neurotoxic species in AD. Therefore, their targeting has emerged as promising approach for AD-specific drugs to prevent cognitive decline. Here we present a strategy to inhibit the formation of Aβ oligomers by selectively oxidizing specific amino acids in Aβ sequence, preventing its aggregation. Targeted oxidation is achieved using a biocompatible and blood-brain barrier-permeable nanomaterial of dense scintillating geo-inspired NTs, functionalized by optically active conjugated PS, generating SO upon low doses of X-ray irradiation.

*References:*

[1] Secchi V. et al. (2023) ACS Appl. Mater. Interfaces 15: 24693-24700
[2] Secchi V. et al. (2022) Int. J. Mol. Sci. 23: 8736

## Arsenic bioaccessibility in environmentally significant arsenic mineral(oid)s

Drahota, P.[1], Ettler, V.[1] and Košek, F.[1]

[1]Institute of Geochemistry, Mineralogy and Mineral Resources, Faculty of Science, Charles University, Albertov 6, 128 00 Prague, Czech Republic; petr.drahota@natur.cuni.cz

---

The stability of arsenic minerals in biofluids is important for understanding the potential health risks associated with exposure to arsenic in various environmental settings. Arsenic, a naturally occurring element, exists in different mineral forms (nearly 800 mineral(oid)s) [1], but only a limited number of them have been consistently identified in mine wastes and soils [2]. This study explores the As bioaccessibility in these environmentally significant phases, referring to the proportion of arsenic released and available for absorption in the human body during ingestion and inhalation. The studied phases included 16 supergene arsenate mineral(oid)s, including synthetic analogues of adamite (Zn), annabergite (Ni), arseniosiderite (Ca-Fe), erythrite (Co), mimetite (Pb), olivenite (Cu), pharmacosiderite (Fe), schultenite (Pb), scorodite (Fe) and yukonite (Ca-Fe). Additionally, the study includes natural samples of X-ray amorphous ferric arsenate (Fe), arsenolite, bukovskýite (Fe), kaňkite (Fe), pharmacolite (Ca), and picropharmacolite (Ca-Mg). Arsenic bioaccessibility was determined using USEPA SW-846 Test Method 1340 [3], which has already undergone inter- and intra-lab validation to predict relative bioavailability (RBA) of As in soil and for which in vitro bioaccessibility data for As are strongly correlated with mice and swine RBA [4, 5].

Arsenic bioaccessibility ranged from 0.1% to 100% of the total As. The highest As bioaccessibility was associated with Ca, Co, Cu, Ni, and Zn arsenates. Other arsenic phases exhibited an intermediate bioaccessibility (1% to 50%; reactive Fe arsenates, As oxide, Pb arsenate) or low bioaccessibility (<1 %; pharmacosiderite and scorodite). This study is crucial first step in assessing the behaviour of these mineral(oid)s in heterogenous and complex environmental media, such as soil and mine waste.

This study was supported by the Czech Science Foundation (GACR 22-27939S).

*References:*

[1] IMA (2024) http://cnmnc.units.it
[2] Drahota P and Filippi M (2009) Environ Int 35:1243-1255
[3] USEPA (2017) https://clu-in.org/download/contaminantfocus/arsenic/arsenic-SOP-OLEM-9200.2-164.pdf
[4] Bradham et al. (2015) Environ Sci Technol 49:6312-6318
[5] Juhasz et al. (2014) Environ Sci Technol 48:12962-12969

## Study of the mineral fibres associated to the clay from Gomsiqe-Puka (Albania)

Gualtieri, A.F.[1] and Mugnaioli, E.[2,3]

[1]Department of Chemical and Geological Sciences, University of Modena and Reggio Emilia, Modena, Italy – alessandro.gualtieri@unimore.it

[2]Earth Sciences Department, University of Pisa, Pisa, Italy

[3]CISUP, University of Pisa, Pisa, Italy

---

The family of asbestos minerals includes chrysotile (serpentine asbestos) and five amphiboles species (asbestos actinolite, amosite, asbestos anthophyllite, crocidolite and asbestos tremolite) [1]. These six minerals are classified by the International Agency for Research on Cancer (IARC) as *Group 1* carcinogens. Mineral fibres, including asbestos, can sporadically contaminate natural raw materials used in the global market of traditional ceramics. In the past, contamination of asbestos tremolite was discovered at a feldspar mine in Orani, Sardinia [2] used for 40 years for the production of stoneware tiles.

Here, we present the case of a plastic clay raw material from the mine of Gomsiqe-Puka (Albania) which contains mineral fibres and compare it to the case of Orani.

Overall, the X-ray powder diffraction analyses carried out on the sample revealed a major smectite phase, illite and talc. The presence of minor fibrous tremolite and diopside was discovered by transmission electron microscopy, micro-Raman, and electron Probe microanalysis. Three fibrous species were observed and classified: an Al-rich tremolite, tremolite and diopside. The crystal-chemical and morphological nature of these fibres is discussed.

*References:*

[1] Gualtieri, A. F. et al. (2022) Human health hazards associated with asbestos in building materials. Ecological and health effects of building materials, Springer, 297-325.

[2] Gualtieri, A. F. et al. (2018) Journal of Hazardous Materials 350:76-87.

## A new approach to quantitatively assess the asbestos-like morphology of mineral fibres

Petriglieri, J.R.[1-2-7], Barale, L.[2-7], De Giuli, C[3-7], Tomatis, M.[4-7], Belluso, E.[1-7], Campopiano, A.[5], Piana, F.[2-7], Pacella, A.[6] and Turci, F.[3-7]

[1]Department of Earth Sciences, University of Torino, Italy, jasminerita.petriglieri@unito.it

[2]CNR-IGG, Italy

[3]Department of Chemistry, University of Torino, Italy

[4]Department of Veterinary Sciences, University of Torino, Italy

[5]Department of Medicine, Epidemiology, Occupational and Environmental Hygiene, INAIL, Italy

[6]Department of Earth Sciences, Sapienza University of Rome, Italy

[7]"G. Scansetti" Interdepartmental Centre for Studies on Asbestos and Other Toxic Particulates, University of Torino, Italy

---

The evaluation of hazard posed by potentially hazardous elongated mineral particles (EMPs) requires the assessment of the toxicological profile of each EMPs, encompassing the estimation of its fibrous morphology. Indeed, the correlation between the carcinogenic potency of asbestos and its fibrous habit is widely recognized, an elongated morphology is not an indication of toxicity per se. Asbestos and asbestos-like minerals are characterized by crystalline planes that easily split along the growth axis, resulting in long and thin fibres, even after strong mechanical stress. A quantitative parameter to describe the asbestos-like morphology of a suspected mineral fibre is therefore pivotal. This work introduces the "fibrosity parameter" to quantitatively express the fibrous asbestos-like morphology of mineral fibres. A protocol was designed to verify whether a mineral that is suspected to have asbestos-like properties preserved its fibrous behaviour after standardized mechanical stress, such as milling. Morphology and morphometry were estimated by light microscopy coupled with automated image analysis (FPIA) and Scanning Electron Microscopy (SEM). The fibrosity parameter was evaluated on a set of antigorite and tremolite samples showing a fibrous to lamellar habit at the macroscopic scale. Data on investigated minerals were compared with data obtained with asbestos (UICC crocidolite and long amosite), non asbestos-like fibres (MMVF), and a lamellar mineral phase (talc). A quantitative assessment of the asbestos-like morphology of the samples was proposed. Fibrous antigorite preserved its fibrous morphology, indicating that this antigorite fractures easily along the growth axis and exhibits an asbestos-like morphology. Standardized grinding generated from 65% to 80% of EMPs (% of particles with Length/Width >3 of the total particles; NIOSH, 2011) most of which have the dimensions of respirable fibres (L>5 µm, W<3 µm, L/W>3; WHO, 1997). Fibrous antigorite is in the class range of fibrosity of asbestos (% EMPs 83% and 82%, for UICC crocidolite and amosite respectively). Most fibrous tremolite samples preserved their fibrous morphology (% EMPs in the range 69-80%), exhibiting a trend similar to fibrous antigorite. One fibrous tremolite sample lost the fibrous morphology, indicating that non-asbestos tremolite does not fracture preferentially along the crystal growth direction. % of EMPs generated decreased from 42% to 13%, increasing the grinding time. This tremolite sample is in the class of fibrosity of non asbestos-like fibres (% EMPs 28-55% for MMVF). As expected, lamellar antigorite and lamellar tremolite preserved their lamellar habit. The % EMPs generated after grinding (% EMPs 35% and 30%, respectively) are in the range of non asbestos-like fibres and lamellar minerals (% EMPs 13% and 28%, for talc and MMVF).

Application of the fibrosity parameter to suspected asbestos-like minerals will be promising for quantifying the asbestos-like morphology of natural mineral fibres from the perspective of their toxicological profiling.

## Tracing Fluids in the Early Solar System Using Carbonates

King, A. J.[1], Schofield, P. F.[1] and Russell, S.S.[1]

[1]Natural History Museum, Cromwell Road, London (a.king@nhm.ac.uk)

---

Asteroids are the leftover building blocks of the Solar System, providing a ~4.6-billion-year-old record of the processes and events that formed the planets. Dark, carbon-rich asteroids that accreted near or beyond the orbit of Jupiter are thought to contain water and organic matter and likely played a key role in the origin of hydrogen and prebiotic molecules on Earth [e.g., 1]. The geological history of carbon-rich asteroids can be revealed through a combination of remote observations and laboratory analysis of returned samples and meteorites, with carbonate minerals particularly sensitive tracers of fluid compositions and the timescales of fluid-rock reactions in the early Solar System.

Carbonate minerals have been detected on the surface of several carbon-rich asteroids and also the dwarf planet 1 Ceres, where spectacular bright deposits of natrite ($Na_2CO_3$) are consistent with the upwelling of brines [2]. NASA's OSIRIS-REx mission discovered bright, metre-long veins of carbonate on the surface of the near-Earth carbon-rich asteroid (101955) Bennu that possibly formed in a large, open hydrothermal system [3]. This hypothesis is now being tested by analysis of carbonate minerals in pristine samples of Bennu recently returned to Earth by the OSIRIS-REx spacecraft [e.g., 4], alongside particles collected by JAXA's Hayabusa2 mission from asteroid (162173) Ryugu [e.g., 5].

However, much of what we know about conditions within carbon-rich asteroids comes from analysis of aqueously altered, phyllosilicate-rich carbonaceous chondrites. These meteorites typically contain up to ~5 vol.% carbonate including calcite ($CaCO_3$; plus its polymorph aragonite), dolomite ($CaMg(CO_3)_2$), breunnerite ($(Mg,Fe)CO_3$), and siderite ($FeCO_3$). Petrographic observations indicate that the carbonates precipitated directly from extraterrestrial fluids into void spaces or by replacing other phases, with some of the grains even recording the aftermath of impacts between asteroids [e.g., 6]. Oxygen isotopic compositions and trace element concentrations are consistent with multiple generations of carbonate formation at temperatures of < ~200°C, relatively high water/rock ratios, and neutral to alkaline pH [e.g., 7]. Carbon isotopes suggest that organic matter and/or $CO_2$-rich ices were the main source of carbon [e.g., 8].

The carbonate minerals in returned asteroid samples and meteorites can also be used to constrain the timing of hydrothermal activity within carbon-rich asteroids through the short-lived (~3.7 Ma) $^{53}Mn$-$^{53}Cr$ radiochronometer. Mn-Cr dating of asteroidal carbonate minerals remains challenging, in part due to a lack of suitable standards, but measured ages hint at precipitation within the first ~2 to 8 million years after the formation of the Solar System [e.g., 9]. This demonstrates that fluids were crucial in shaping the evolution of planetary bodies from the earliest days of the Solar System.

*References:*

[1] King, Daly et al. (2022) Sci Adv 8:eabq3925
[2] Carrozzo et al. (2018) Sci Adv 4:e1701645
[3] Kaplan et al. (2020) Science 370:eabc3557
[4] Connolly Jr. et al. (2024) LPSC #1281.
[5] Nakamura et al. (2023) Science 379:787
[6] Lee et al. (2014) GCA 144:126
[7] Vacher et al. (2019) ApJL 882:L20
[8] Fujiya et al. (2019) Nat. Astro. 3:910
[9] Bischoff et al. (2021) GCA 293:142

# Carbonation hardening of cements produced from recycled concrete fines

Neubauer, J., Villmow, S. and Mielkau, A.

FAU Erlangen-Nürnberg, GeoZentrum Nordbayern, Mineralogy, Erlangen, Germany

Email: juergen.neubauer@fau.de (corresponding author)

---

Up to date there is no commercial use for the fines from recycled concrete. These fines contain most of the hardened cement paste and they can be used as basis for a new cement binder. During clinkering of this new binder much limestone and fuel can be saved compared to OPC (Ordinary Portland Cement) production. The remaining low **$CO_2$** emission from clinkering process of the new binder can be **captured** and used later during carbonation hardening.

These new binders display a much lower $CaO/SiO_2$ ratio and are not suitable for pure hydration hardening. In the presence of $CO_2$, such new binders exhibit fast reaction and high compressive strength development. **Captured $CO_2$** from clinkering process can be **stored** in the product during hardening. This concept allows for manufacturing of concrete products with a very low overall $CO_2$ footprint.

We followed an upscaled production process of the new clinkers and determined the mineralogical phase composition of the cements. As the raw materials for clinkering contain considerable amounts of magnesium and are low in calcium, the phase assemblage differs strongly from OPC composition. Dicalciumsilicates ($Ca_2SiO_4$) and Ca-Al,Mg-silicates (e.g. bredigite, åkermanite, gehlenite) are now main phases. The carbonation behaviour of the phases present in the new clinkers was followed by wet carbonation in a lab reactor. Reaction turnover of more than 80% of the clinker phases within 20 minutes could be achieved. Carbonation-hydration-products are mainly $CaCO_3$ (ACC, calcite, aragonite, vaterite) and silicon-aluminum-gels, delivering high mechanical strength of concrete products.

*References:*

[1] Rocha, J. H. A., & Toledo Filho, R. D. (2023). The utilization of recycled concrete powder as supplementary cementitious material in cement-based materials: A systematic literature review. Journal of Building Engineering, 107319.

[2] Zajac, M., Skocek, J., Skibsted, J., & Haha, M. B. (2021). $CO_2$ mineralization of demolished concrete wastes into a supplementary cementitious material–a new CCU approach for the cement industry. RILEM Technical Letters, 6, 53-60.

[3] Zajac, M., Skocek, J., Gołek, Ł., & Deja, J. (2023). Supplementary cementitious materials based on recycled concrete paste. Journal of Cleaner Production, 387, 135743.

[4] Oliveira, D. R. B., Leite, G., Possan, E., & Marques Filho, J. (2023). Concrete powder waste as a substitution for Portland cement for environment-friendly cement production. *Construction and Building Materials*, *397*, 132382.

[5] Chen, X., Li, Y., Bai, H., & Ma, L. (2021). Utilization of recycled concrete powder in cement composite: Strength, microstructure and hydration characteristics. Journal of Renewable Materials, 9(12), 2189-2208.

[6] Wang, S., Gao, F., Li, B., Liu, Y., Deng, T., Zhang, Y., & Chen, W. (2024). Clinkerization of carbonatable belite–melilite clinker using solid waste at low temperature. Construction and Building Materials, 418, 135357.

[7] Zajac, M., Skibsted, J., Skocek, J., Durdzinski, P., Bullerjahn, F., & Haha, M. B. (2020). Phase assemblage and microstructure of cement paste subjected to enforced, wet carbonation. Cement and Concrete Research, 130, 105990.

[8] Villmow, S., Mielkau, A., Goetz-Neunhoeffer, F., & Neubauer, J. (2023). Wet carbonation of $C_3A$ and pre-hydrated $C_3A$. *Cement and Concrete Research*, *173*, 107259.

## Utilising mining waste materials for carbon sequestration: A novel laboratory method assessing enhanced weathering potential in an arctic climate

Mouchos, E.[1*], Pearce, S.[2], Shiimi, R.[1], Savage, W.[1], Buckley, L.[2], Lim, C.[3], Brussee, O.[4] and Ronne, E.[4]

[1]Mine Environment Management, Cardiff, CF11 9BE, UK. *emouchos@memconsultants.co.uk

[2]Mine Environment Management, Denbigh, LL16 3AD, UK.

[3]KU Leuven, Bruges, 8200, Belgium.

[4]Boliden, Stockholm, 101 20, Sweden.

---

Implementation of the EU Green Deal and attainment of net-zero greenhouse gas emissions, requires policies supporting transition from traditional to clean energy sources, which will increase demand on mining key resources, that will likely increase $CO_2$ emissions and waste production. Many previous studies have assessed the potential utilisation of mafic/ultramafic mine waste for $CO_2$ capture (carbonation) via natural or enhanced weathering (EW). EW is the process of utilising fine grained rock material favouring carbon capture, to accelerate carbon biogeochemical cycling by removing higher amounts of $CO_2$ from the atmosphere than are produced in the process. In theory, this is considered a well-defined carbon dioxide removal (CDR) method, but in practice it is still not used on large scale/long period trials, and hence no widely accepted monitoring, reporting & verification (MRV) standards exist to date. More precisely, there are significant gaps in understanding physicochemical controls for carbonation, such as mineral chemistry, particle size, $CO_2$ supply, temperature, soil porosity, porewater pH, saturation and salinity. To consider EW as a viable CDR method, strong evidence is needed that the material sequesters more $CO_2$ than it emits under given conditions. Our research focuses on determining the net $CO_2$ flux from the EW of Ca- and Mg-rich mine wastes, considering physicochemical controls for carbonation, under various conditions (e.g. arctic climate). A series of novel laboratory experiments were set up, which indicated the potential for this material to sequester $CO_2$, and allowed development of the method to measure the process. $CO_2$ capture was particularly efficient for tailings, producing higher carbonation rates due to smaller grain size/larger surface area compared to waste rock. These findings will now be tested at field sites in Northern Europe, using a new CDR MRV methodology determining the net $CO_2$ flux generated from mine wastes, under the EU/UKRI-funded C-SINK project.

## Crystallisation of Carbonates to Make Anthropogenic 'Rocks'

MacDonald, J.M.[1]

[1]School of Geographical and Earth Sciences, University of Glasgow, Glasgow, G128QQ, UK; john.macdonald.3@glasgow.ac.uk

---

Anthropogenic processes and products can result in the formation of 'rocks'. By-products from industrial processes, such as slags from iron and steel making, are deposited as piles of loose material but can become lithified at geologically rapid timescales. The mechanism of this lithification is crystallisation of carbonate minerals.

Using case study sites from Scotland and England, we document the lithification of legacy slag deposits through cementation with calcite via drawdown of atmospheric $CO_2$. We present field, X-Ray Diffraction and carbon isotope data to fingerprint calcite as the cementing phase, formed from atmospheric $CO_2$ and Ca leached from the slag [1]. Microstructural analysis via scanning electron microscope shows this Ca leaching from slag particles.

Anthropogenically-derived carbonate rocks can also take the form of tufas [2]. We present field and isotope data from anthropogenic tufas from case study sites in Scotland and England, where tufa carbonate deposits have formed through mineralisation of atmospheric $CO_2$ reacted with Ca derived from anthropogenic by-products.

Overall, formation of anthropogenic 'rocks' through crystallisation of carbonates (either as the main constituent or as a secondary cement) has the potential to be a significant marker of the 'Anthropocene'. The carbonate crystallisation process in this context also has implications for atmospheric $CO_2$ removals and ground stabilisation.

*References:*

[1] MacDonald J et al. (2023) Dep Rec 9:810-819
[2] Mayes W et al. (2018) Env Sci & Tech 52:7892-7900

## Uncovering the Mineralogy and Metal Concentrations in Metal Processing Wastes: A data-driven microstructural approach

Hilderman, R. X.[1], Einsel, J.F.[1], and MacDonald, J.M.[1]

[1] University of Glasgow, University Avenue, Glasgow, G12 8QQ 2797467h@student.gla.ac.uk

---

Industrial waste presents the opportunity for Critical Raw Material (CRM) recovery [1]. Using the scanning electron microscope and an X-ray energy dispersive spectrometer (SEM-EDS), companion metals found in the ores of target metals can be identified and extracted from legacy slag [2]. However, traditional quantification software packages requiring labelled references for characterisation combined with limited documentation of these anthropogenically derived rocks present the opportunity for significantly misfitting the data. In this study, large and highly-dimensional EDS datasets of a legacy iron and steel slag deposit were quantified using a machine learning approach leveraging non-negative matrix factorisation (NMF) and Hierarchical Density-Based Spatial Clustering of Applications with Noise (HDBSCAN) to identify the mineral phases and trace metals. By revealing the variable mineralogy and metal content between the five stratigraphic horizons of the deposit, we demonstrate the semi-automated approach is a turnkey operation for processing numerous large datasets. Applying the approach to specific phases (iterative phase classification (IPC)) drove the analysis that confirmed and revealed both the microstructures and trace Ba, Fe, and Mn from the model outliers and more statistically representative phases.

This work shows that legacy iron and steel slag deposits can be sources of CRM. The iterative approach utilising unsupervised learning provides a tool for locating hidden and non-statistically significant regions, enhancing microstructural analysis. This new approach for finding trace metal content in industrial waste can be applied to document the evolution of metallurgical processing methods, which can inform environmentally sensitive CRM recovery.

*References:*

[1] Habib, A., H. N., & Iqbal, M. Zeitschrift Für Physikalische Chemie *234*(2) (2020).
[2] Nassar, N.T. et al. E.M. Science advances *1*(3), p.e1400180 (2015).

# Accelerated Carbonation from Aqueous Ca/Mg Hydroxide Systems to Hazardous Waste Incinerator Residues

Wehrung, Q.[1], Pastero, L.[1], Bernasconi. D.[1], Cotellucci, A.[1], Bruno, M.[1], Destefanis, E.[1], Caviglia, C.[1], Cavagna, S.[1], Pavese, A.[1].

[1]Earth Sciences Department of Turin, Italy. Corresponding author: quentin.wehrung@unito.it

---

This Ph.D. research offers a self-consistent experimental dataset (500+ lab-scale tests) for comparing the most highly reactive aqueous carbonation systems, spanning from pure Ca/Mg hydroxides ($Ca(OH)_2$/$Mg(OH)_2$) to hazardous incinerator residues, including intermediate systems with varying impurity levels. Multiple collections of fresh Bottom Ash (BA), Fly Ash (FA), and Air Pollution Control residues (APCr) samples from incinerators were undertaken to assess temporal and spatial variability in residue composition. Investigated parameters include temperature, reagents concentration, $CO_2$ flow rate, reactor design and wastewater reuse conditions.

An innovative methodology involved the systematic use of high-precision gas flow sensors (GFS) to generate $CO_2$ absorption rate vs. time patterns ($(t)$). These graphs not only allowed for the assessment of system performance but also facilitated investigations into carbonation mechanisms. Solid-liquid phases characterization was conducted using XRPD with Rietveld refinement, SEM-EDS, ICP-MS, XRF and BET analysis. EN 12457-2 leaching tests were performed on both raw and carbonated waste residues. Computational models were developed using phreeqc to interpret $(t)$ patterns and analyse the pH dependence of heavy metal leaching.

Relevant findings include: 1) High liquid-to-solid (L/S) ratio carbonation misconceptions persist, while our study demonstrates that proper $CO_2$ diffusion through static mixers leads to fast $Ca(OH)_2$/$Mg(OH)_2$ carbonation, achieving $CO_2$ absorption rates ($(t)$) nearing 100% even at L/S > 50. 2). The optimal $(t)$ efficiency within the $Ca(OH)_2$ system is achieved at the average NaCl seawater concentration, 3.5 wt.%, with higher concentrations exceeding ≈10 wt.% NaCl hindering $(t)$. 3) $Na_2SO_4$ enhances $(t)$ the most among tested salts (NaCl, KCl, $K_2SO_4$, $Na_2SO_4$), with a substantial 75% increase at 55 g/kgw [$Na_2SO_4$]. 4) Among the tested residues, fly ash exhibits the highest $CO_2$ uptake capacity at ≈150 $gCO_2$/kg, behaving kinetically akin to an ionically enhanced $Ca(OH)_2$ system, achieving near 100% $(t)$ once again. Calibration between $(t)$ and pH enables continuous in-situ pH monitoring via GFS, minimizing heavy metal leaching.

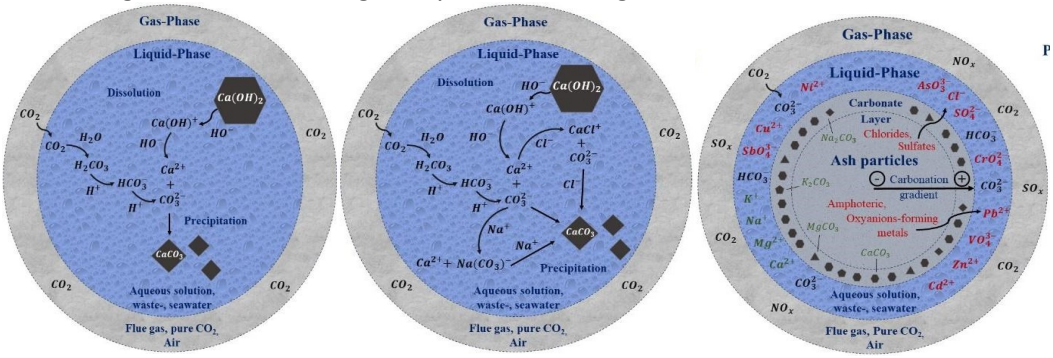


Progressive complexity in $Ca(OH)_2$ aqueous carbonation mechanisms

## On the growth of ikaite ($CaCO_3x6H_2O$) in the presence of phosphate

Strohm, S.B.[1]; Saldi, G.D.[2,3]; Mavromatis, V.[2,4]; Schmahl, W.W.[1]; Jordan, G.[1]

[1] Department für Geo- und Umweltwissenschaften, Ludwig-Maximilians-Universität München, Theresienstr. 41, 80333 München, samuel.strohm@lrz.uni-muenchen.de

[2] Géosciences Environnement Toulouse (GET), CNRS-UPS-OMP UMR5563, 14 Avenue Edouard Belin, 31400 Toulouse

[3] Dipartimento di Fisica e Geologia, Università di Perugia, Via Pascoli 35, 06123 Perugia

[4] Institut für Geologie, Universität Bern, Baltzerstraße 1+3, 3012 Bern

---

The metastable formation of ikaite was observed in manifold settings of near-freezing environments on Earth ($T$ < 7 °C). Particularly, its appearance in sea ice indicated a more widespread appearance than previously assumed implying a significant contribution to the polar carbon cycle [1].

Formation of ikaite requires distinct physicochemical conditions that favour its nucleation over anhydrous $CaCO_3$-minerals. In this context, the presence of calcite inhibitors, such as phosphate ions, was suggested promoting the precipitation of ikaite. Although in sea water phosphate is a minor constituent, it might support the crystallization of ikaite [2]. Nevertheless, the role of phosphate remained ambiguous and interactions of phosphate and ikaite are barely understood as the fundamental growth kinetics of ikaite has not yet been studied as extensively as that of anhydrous $CaCO_3$-polymorphs.

Using cryo-mixed-flow-reactor experiments, we investigated the growth kinetics of ikaite in phosphate-containing solutions at 1 ±1 °C. Our experiments revealed a reaction order $n = 0.8 \pm 0.3$ for ikaite growth ($1.5 \leq \Omega_{ikaite} \leq 4.9$), which implies a mechanism controlled by transport or adsorption. This reaction order, therefore, supports the suggestion of a growth mechanism via the attachment of hydrous $CaCO_3^0$ complexes without extensive dehydration of aqueous species [3]. Furthermore, the growth of ikaite proceeded without any detectable depletion of aqueous phosphate in the supersaturated growth solution which reflects a negligible uptake by ikaite. This finding agrees with the proposed growth mechanism which does not allow considerable substitution of carbonate by phosphate [4].

*References:*

[1] Jones et al. (2023) Limnology & Oceanography 68:208–231
[2] Bischoff et al. (1993) Journal of Geology 101:21–33
[3] Strohm et al. (2022) Chemical Geology 611:121089
[4] Strohm et al. (2023) Aquatic Geochemistry 29:219-233

## Transformation of ikaite into less hydrated $CaCO_3$ minerals – from *in-situ* observations of tufa columns, Ikka Fjord and IceLab-RAMAN experiments

Stockmann, G.J.[1,2], Peternell, M.[2], Konrad-Schmolke, M., and Rasmussen M.B.[3]

[1]Jarvik Geoconsulting AB, Gothenburg, Sweden, gabrielle@jarvik.dk;

[2]Department of Earth Sciences, University of Gothenburg, Sweden

[3]Department of Geosciences and Natural Resource Management, University of Copenhagen, Denmark

---

Recent years' research on the tufa columns in Ikka Fjord, SW Greenland have shown a change in mineralogy from almost pure ikaite ($CaCO_3 \bullet 6H_2O$) into less hydrated calcium carbonate minerals of monohydrocalcite (MHC), aragonite, and calcite [1]. These dehydration reactions are interpreted as a response to an increase in seawater temperature supported by *in-situ* observations of summer 2019 of temperatures ranging from 6 – 9 °C in the submarine column area. An upper stability threshold of 6 °C was previously suggested for the ikaite columns based on past *in-situ* temperature recordings from Ikka Fjord. In recent laboratory experiments, small pieces of ikaite columns were heated incrementally while submerged in natural seawater from Arsuk Fjord, SW Greenland. They were mounted in a special-designed thermal cooling stage at the University of Gothenburg that allows for contemporaneous Raman analysis. The aim of the experiments was to discern the role of fluids for the transformation of ikaite with respect to temperature and alteration mineralogy. In one series of experiments, a sample of pure ikaite was submerged in seawater throughout the experiment conducted at 2.5 – 23.0 ± 0.1 °C for 2.5 months. This caused a mineral transformation into MHC initially at 10 – 11 °C. With increasing temperature, ikaite disappeared completely by altering into MHC. A further transformation of MHC into aragonite and minor calcite occurred at 22.0 °C. In a second series of experiment, the ikaite column sample was dried out at 6 °C, which caused a complete and instant alteration into aragonite. For comparison, a piece of ikaite column was taken straight from the freezer and left to dry at a laboratory temperature of ~22 °C for four days. The alteration product was pure calcite. Hence, we conclude that fluids and incremental heating are paramount for a prolonged stability of ikaite and has consequential effect on its mineral alteration assemblage. These results allow us to predict the fate of the tufa columns of Ikka Fjord exposed to increased warming of the Arctic region.

*References:*

[1] Stockmann GJ et al. (2022) Min 12, https://doi.org/10.3390/min12111430

## The Key Role of Sulfate in the Conversion of Aragonite into Calcite

Forjanes, P.[1], Astilleros, J.M.[2,3] and Fernández-Díaz L.[2,3]

[1] German Research Centre for Geosciences (GFZ), 14473, Potsdam, Germany

[2] Departamento de Mineralogía y Petrología. Universidad Complutense de Madrid, 28040, Madrid, Spain

[3] Instituto de Geociencias (CSIC, UCM), 28040, Madrid, Spain

---

Aragonite, a metastable form of calcium carbonate ($CaCO_3$), is widespread on Earth's surface. Thermodynamics dictate that under surface-like conditions, aragonite should convert to the more stable form of calcium carbonate, which is calcite, in a transformation which can occur rapidly through a coupled dissolution-crystallization mechanism [1,2]. Nevertheless, the geological record contains a plethora of aragonite relics, both biogenic and abiogenic, where this conversion has not taken place. Traditionally, it has been widely accepted that the chemical elements that favour the metastable precipitation of aragonite, primarily magnesium, may also hinder its subsequent conversion to calcite. However, in recent years, there has been an increasing focus on the role of other chemical elements, particularly anionic groups, in the formation and preservation of calcium carbonate polymorphs [3].

This study evaluates the influence that dissolved sulfate in solution has on the preservation of abiogenic aragonite single crystals. To do so, aragonite fragments were exposed to sulfate-rich solutions (ranging from 0 to 30 mM $SO_4^{2-}$) at 220°C for increasing durations. The findings of this work demonstrate that sulfate plays a key role in preserving aragonite fragments. Aragonite crystals interacting with sulfate-free solutions or solutions with sulfate concentrations below 0.1 mM were extensively replaced by calcite aggregates, linked to the formation of fracture networks. In contrast, aragonite crystals exposed to sulfate-rich solutions ($[SO_4^{2-}]_{aq}$ > 0.1 mM) remained virtually indistinguishable from the pristine crystals. These results underscore the significance of sulfate, the second most abundant anion in seawater, in preserving aragonite. Further research should explore the synergistic effects of magnesium, sulfate, and other chemical elements in this preservation.

*References:*

[1] Carlson, W. D (1983). Rev. Min. 11, 191-225.
[2] Perdikouri C et al. (2011). Geochim. Cosmochim. Acta. 75, 6211-6224.
[3] Fernández-Díaz L et al. (2010). Geochim. Cosmochim. Acta. 74, 6064-6076.

# Pseudomorphism and Porosity Formation during the Conversion of Gypsum Single Crystals into Strontianite via intermediate Celestine

Forjanes, P.[1], and Benning, L.G.[1,2]

[1] German Research Centre for Geosciences (GFZ), 14473, Potsdam, Germany

[2] Department of Earth Sciences, Freie Universität Berlin, 12249 Berlin, Germany

---

Pseudomorphism is a commonly observed feature of fluid-driven mineral replacement reactions when these two processes occur simultaneously and in close proximity [1]. Pseudomorphs constitute valuable geological proxies, as their internal microstructures offer insights into the original mineral structure and composition and they can also provide information about the nature of the fluid which triggered the transformation. In recent years, a significant progress has been made in understanding the physico-chemical conditions leading to the formation of pseudomorphs, particularly in the case of sparingly soluble salts like carbonates and sulphates. However, certain aspects remain unexplored, such as the behaviour of pseudomorphs when exposed to new fluids that may trigger additional replacement phenomena.

To delve into this issue, we have evaluated the conversion of gypsum ($CaSO_4 \cdot 2H_2O$) single crystals into celestine ($SrSO_4$) by following the interaction of gypsum with Sr-rich solutions. Once the 1st pseudomorphic reaction was completed, we explored the transformation of the so formed celestine pseudomorphs into strontianite ($SrCO_3$) after exposing the pseudomorphs to carbonate-rich fluids. The first transformation (gypsum-celestine) yielded pseudomorphs with a high amount of porosity that exhibited features typical of an interface coupled dissolution-precipitation mechanism [2]. During the 2$^{nd}$ transformation (celestine-strontianite), the shape of the gypsum precursor was again preserved, but a new generation of microporosity developed. The end product, strontianite pseudomorphs after gypsum, thus hosted two generations of pores, each corresponding to a replacement reaction, while the original shape remained. These findings highlight how the internal microstructures of pseudomorphs reflect their replacement history, underscoring their utility as geological proxies.

*References:*

[1] Putnis A (2009). Rev. Min. 70, 87-124

[2] Forjanes P et al. (2020) Minerals. 189

# $CO_2$-hardening of slag-based bricks – a novel approach of direct carbon usage

L. Gronen[1], E. Schieferstein[2], M. Prokein[2], D. Hoffmanns[2], V. Feldrappe[1] and T. Fusswinkel[3]

[1]FEhS Institute of Building Material e.V., Germany, l.gronen@fehs.de

[2]Fraunhofer Institute for Environmental, Safety and Energy Technology UMSICHT, Germany

[3]RWTH-Aachen University, Institute of Applied Mineralogy and Economic Geology, Germany

---

In general, when producing masonry stones, quicklime is used as a binder, which is activated through hydrothermal curing. Commonly, in sand-lime brick recipes the added quicklime acts as binder activated by hydrothermal hardening methods. The treatment triggers the hydration of the quicklime and the formation of CSH phases at the interfaces of quartz aggregate resulting in the desired development of compressive strength. However, the use of quicklime comes along with high amount of $CO_2$ emissions impairing the environmental impact of construction projects.

This study presents an alternative hardening method which is based on the carbonisation of ground Ca-Si rich slags from iron and steel making industry. Therefore, masonry bricks were prepared by mechanical pressing using common aggregate and fine ground slag as potential binder. The hardening was conducted under $CO_2$ atmosphere at pressures up to 1.5 MPa, at 50° C for 6 h in autoclaves. Carbon dioxide uptake to the brick matrix was proven gravimetrically and by monitoring the autoclave $CO_2$ partial pressure dropping periodically during the experiment. In this way, this presents a savings potential in the range of 315–337 kg $CO_2$,eq/$m^3$ over conventional sand-lime bricks.

The experiments have shown that with, decreasing particle size, the compressive strength of the produced bricks is increased. The finer the grinding of the slag, the more particle interfaces are present where carbonation can occur. The formation of micro carbonate at the edges of the Ca-silicates could be one possible mechanism for the increased hardness or increased $CO_2$ uptake.

However, the milling effort is the biggest limiting factor, as the exponentially increasing energy requirement for finer milling counteracts the $CO_2$ savings from the use of e.g. waste $CO_2$ from industrial processes for the alternative hardening process presented. Therefore, an optimum between the particle size and the hardness to be obtained must be determined.

The produced bricks have a satisfying compressive strength between 24 and 49 MPa matching international regulations for building materials. By XRD the formation of carbonates such as calcite and vaterite were detected on the expend of slag´s Ca-silicates and gaseous $CO_2$ in the hardened brick matrix. However, no optical evidence for the carbonate formation was observed on thin section scale.
For the future, elucidating the hardening mechanism is of particular interest to produce bricks with optimal strength and minimal energy consumption respectively $CO_2$ emissions.

## Heterogeneous lithification across a legacy coastal slag bank: the creation of new sedimentary rock from anthropogenic material

Hilderman, R. X.[1], MacDonald, J.M.[1], Griffin, S.[1], Slaymark, C.[1], Einsel, J.F.[1], and Monaghan, A.[1]

[1] University of Glasgow, University Avenue, Glasgow, G12 8QQ 2797467h@student.gla.ac.uk

---

Lithification of artificial ground comprising by-products of legacy iron and steel workings presents a range of opportunities including atmospheric carbon dioxide ($CO_2$) storage. The natural environmental processes altering these waste sites can also pose challenges such as ecotoxic metal leaching, so it is important to characterise these largely undocumented anthropogenically derived rocks. This study documents the lithification mechanisms and mineralogic and geochemical features across a legacy coastal iron and steel slag deposit (Warton, England).

X-Ray Diffraction (XRD) and energy dispersive X-ray spectroscopy (EDS) analysis of the slag and thermogravimetric analysis (TGA) of the cream-coloured material covering the deposit shows lithification on the top surface and seaward side above the mean high-water mark (MHWM) is the result of carbonate mineralisation. This is driven by water and leached calcium from weathering slag minerals (i.e., gehlenite, åkermanite, pseudowollastonite) reacting with ingassed and hydroxylated atmospheric $CO_2$, forming calcite with slightly to strongly depleted $\delta^{13}C$ values (-6.4 ‰ to -22.7 ‰) following partial dissolved inorganic carbonate (DIC) equilibration. Calcium-silicate-hydrate (CSH) precipitation was responsible for lithifying the deposit where more frequent and abundant seawater washed over, preventing subsequent slag mineral dissolution and carbonate precipitation. This work shows that legacy iron and steel slag deposits are prone to lithification, particularly in coastal settings. As such, lithification can draw down atmospheric $CO_2$ and the CSH precipitation could help to slow the release of toxic metals, enhancing the possibility of repurposing.

## The effect of organic chelating agents on the kinetic of amorphous calcium carbonates formation and transformation: a facile in situ and real-time monitoring and off-line particles characterization

Ignat, M.[1], Rodriguez Blanco, J.D.[2] and Brinza, L.[3]

[1]Department of Chemistry, „Alexandru Ioan Cuza" University of Iași, 11, Carol I Bvd, 700506, Iași, Romania, maria.ignat@uaic.ro,

[2]Department of Geology, School of Natural Sciences, Trinity College Dublin, College Green, Dublin 2, Ireland

[3]CERNESIM, Department of Exact Sciences and Natural Sciences, Institute of Institute of Interdisciplinary Research „Alexandru Ioan Cuza" University of Iasi, 11, Carol I Bvd, 700506, Iași, Romania, loredana.brinza@uaic.ro

---

Following a nature hypothesis that organic compounds may play an important role in minerals formation and morphology, such as corals, shells, pearls, earthworms biomineralized calcium carbonate granules, etc, current research aims to investigate the effect of organic chelation agents on formation, morphology and surface properties of amorphous calcium carbonate and their final transformation to carbonates polymorph minerals. A very simple and handy UV-VIS method was used to monitor in situ and in real time the kinetic of amorphous calcium carbonate nucleation and growth in the presence and the absence of two environmentally friendly organic chelating agents, like EDTA and EDDS at various concentrations. Experimental kinetic data were modelled by JMAK model. Quenching nanoparticles synthesis reaction at very early times of formation (within a minute) and measuring particles by spectroscopic (ie. SAXS) and microscopic (SEM) techniques allowed an detailed investigation of initial stages of synthesis. Final carbonates polymorphs were characterized by diffraction, microscopic, BET and spectroscopic techniques. The results suggested that the addition of EDTA and EDDS did affect the morphology of the final carbonate products, surface properties and mineralogy. In addition, only the addition of EDDS (the cis isomer of EDTA) led to a 25% delay in crystal transformation, preserving the amorphous phase within the system for longer time. These outputs may have significant implications in pollutants uptake processes that can take place in natural environments (hot springs, soil porewater, sediments, caves) and environmental / industrial applications (waste water treatment plants).

A contribution by Prof. I.R. Olariu to this work is acknowledged.

## Immobilisation of chromium in magnesium carbonate minerals

Lacinska, A.M.[1], Bateman, K.[1], Chenery, S.[1], Kemp, S.J.[1], Liddy, T.[2], Rushton, J.C.[1], Saha, D.[3] and Schroeder, S.L.M.[3,4]

[1]British Geological Survey, Natural Environment Research Council, Environmental Science Centre, Keyworth, Nottingham NG12 5GG, UK

[2]The University of Nottingham, University Park Nottingham NG7 2RD, UK

[3]The University of Leeds, School of Chemical and Process Engineering, Leeds LS2 9JT, UK

[4]Diamond Light Source Ltd, Harwell Science and Innovation Campus, Oxfordshire OX11 0DE, UK

---

Hexavalent chromium ($Cr^{6+}$) is a toxic carcinogenic pollutant that might be released by the mining and processing of ultramafic rocks and nickel laterites, and which requires permanent removal from the contaminated biosphere. Ultramafic material can also serve as a feedstock for the sequestration of $CO_2$ resulting from the growth of new minerals, raising the intriguing proposition of integrated sequestration of both pollutants, $CO_2$ and chromium, into magnesium carbonates. Such a synergistic process downstream of ore recovery and mineral processing could be an elegant proposition for more sustainable utilisation and management of the Earth's resources. We will present the results of experimental and microanalytical study on the uptake of chromium in carbonate phases. The results suggest that neither nesquehonite nor hydromagnesite have the structural capacity to incorporate $Cr^{6+}$ or $Cr^{3+}$ significantly at room temperature. We therefore propose that further research into this technology should focus on laboratory assessments of other phases, such as layered double hydroxides, that have a natural structural capacity to uptake both chromium and $CO_2$.

# Alteration of siderite ($FeCO_3$) in the presence of multi-component rare earth element (REE) aqueous solution at hydrothermal conditions (50-205 °C)

Maddin, M.[1], Rateau, R.[2] , Szucs, A.M.[3] , Terribili, L.[4] , and Rodriguez-Blanco, J.D.[5]

[1]Department of Geology, School of Natural Sciences, Trinity College Dublin, Dublin 2. maddinm@tcd.ie

[2-5]Department of Geology, School of Natural Sciences, Trinity College Dublin, Dublin 2, Ireland

---

Iron oxides, such as hematite ($\alpha$-$Fe_2O_3$) and magnetite ($Fe_3O_4$), are among the most abundant minerals in the Earth's crust [1]. They are of interest due to their capacity to accommodate a broad range of elements, in particular the lanthanide group elements [2]. Concomitantly, REE-rich hematite carbonatites are found in various carbonatite complexes worldwide [3]. As REE are essential in many green technologies they play a critical role in a more sustainable future. However, there is a substantial risk to their supply as the availability of rare earth deposits with mineable concentrations are limited [4]. A better understanding of the interaction between iron oxides and REE would contribute to new and alternative future targets for recovery, improved recovery strategies and separation techniques.

In our study, we investigated the interaction between multi-component rare earth element (REE) aqueous solutions and siderite ($FeCO_3$) grains was studied at hydrothermal conditions (50-205 °C). The effect of ionic radii of five rare earths (La, Ce, Pr, Nd and Dy) on solid formation were analysed using two types of solution: equal concentrations and concentrations normalized to Post Archean Australian Shale Standard (PAAS). At 50 °C, the siderite grains are completely covered by a thin layer of goethite, promoting a state of partial equilibrium, thereby inhibiting the formation of any rare earth minerals. At 165 and 205 °C, alteration of siderite to hematite occurs rapidly, <24 hours, with full decomposition of siderite after 1 week. Small amounts of kozoite and bastnasite (<6 % in equal concentration, and <15% in PAAS solution) were recorded in the early stages of the experiment, however, these were quickly replaced by the rare earth oxide cerianite ($CeO_2$). The effect of initial concentration of the rare earths in solution can also be seen in the rate and volume of cerianite formation, with more cerianite forming in the PAAS solutions than the equal concentrations and in less time.

*References:*

[1] Cornell RM and Schwertmann U (1996) Weinheim and New York: VCH, 573
[2] Cook NJ, Cioban CL, Ehrig K, Slattery AD and Gilbert SE (2022) Front. Earth Sci. 10:967189
[3] Anderson T (1987) Applied Geochemistry 0883-2927
[4] Jordens A, Cheng YP and Waters KE (2013) Minerals Engineering, 41, 97-114

## Key insights into CDR standards requirements supporting MRV methods

Savage, W.[1], Mouchos, E.[1*], Shiimi, R.[1], Pearce, S.[2], Buckley, L.[2], Štyriaková, D.[3], Šuba, J.[3], Kraljić, D.[3], Prekopova, M.[3], Pike, D.[4] and Kurt, Z.[5]

[1]Mine Environment Management, Cardiff, CF11 9BE, UK (*emouchos@memconsultants.co.uk)

[2]Mine Environment Management, Denbigh, LL16 3AD, UK

[3]Ekolive, Košice, SK-040 13, Slovakia

[4]Biosteam, Burträsk, 93793, Sweden

[5]Middle East Technical University, Ankara, 06800, Türkiye

---

As a result of anthropogenic climate change there is a call to implement a rapid transition to Net-Zero greenhouse gas (GHG) emissions. However, reducing emissions is not going to be sufficient for climate stabilisation, and there is a need to remove $CO_2$ from the atmosphere through carbon dioxide removal (CDR). CDR will require more rigorous Monitoring, Reporting and Verification (MRV) because of the complexity of some of the processes and the requirement for $CO_2$ to be stored long-term. With a range of different novel approaches to CDR being developed there are difficulties in ensuring that the quality of each approach is regulated, as well as scalable to make meaningful impacts on climate change. The majority of standards and technology-specific methodologies available for CDR currently lack the scope required to become a governing standard. It is evident, from the formation of alliances and certified methodologies, such as the Enhanced Weathering Alliance and European Biochar Certification, that progress in developing CDR approaches requires collaboration from industry. Yet, as more companies develop new standards there is a risk of making meaningful comparisons of CDR approaches more complex, because of inconsistent MRV methodologies.

Current approaches for CDR can be engineered or nature-based. In both cases monitoring of large temporal and spatial zones is required, and permanence is an important consideration, thus models must be deployed to quantify the evolution of captured $CO_2$. To verify such models, accurate sampling and testing methodologies are critical. At a practical level, engineering specifications are needed to assure quality. If these specifications are not built on proper standards (e.g. CEN and ISO) problems will arise in defining the requirements of the process between customers, producers, and regulators. C-SINK, an EU/UKRI-funded project, aims to deliver a package to support the large-scale deployment of CDR, including pre-standards for a range of different land application technologies, such as enhanced weathering, biochar, artificial soils, and biological $CO_2$ fixation. These technologies introduce key challenges, such as the sources of variance, that must be considered to determine CDR efficiency, ensuring also a robust method for high precision carbon credit calculation. Therefore, field trials will be carried out across Europe to evaluate pre-standards through *in situ* MRV testing as part of the C-SINK project.

## Calcimetry as a reliable method for monitoring soil inorganic carbon stocks: a parametric assessment of its reliability and interferences

Silva, J.M.P.[1,2], Khalidy, R.[1] and Santos, R.M.[1]

[1]School of Engineering, University of Guelph, Guelph, Ontario, Canada; santosr@uoguelph.ca
[2]LSQM – Laboratory of Chemical Synthesis of Materials, Department of Materials Engineering, Federal University of Rio Grande do Norte – UFRN, Natal, Rio Grande do Norte, Brazil

---

The reliable measurement of the inorganic carbon content of soils and its changes resulting from land management practices and amendments is crucial for precisely quantifying carbon stocks as part of monitoring, reporting and verification (MRV) schemes. While various methods are available for evaluating carbonate content in soils, the most direct approach is calcimetry, which involves the dissolution of solid-phase carbonates and the evolution of gas-phase $CO_2$ through acid-initiated reactions. Despite being a well-established method, uncertainties about how reliable calcimetry is for measuring small changes in soil inorganic carbon (SIC) or how its measurement may be affected by potentially interfering reactions, sample size, and solid–liquid contact call for a dedicated investigation of these effects. Previous studies [1,2] have suggested the following potential limitations of calcimetry: (i) possible gas leakage; (ii) possible evolution of other gases ($SO_2$, $H_2S$) resulting from side reactions of certain soil components; (iii) a relatively high lower limit of detection, suggested to be ≥0.5 wt% IC (4.17 wt% calcium carbonate equivalent (CCE)); and (iv) a loss of reliability when SOC >16 wt%.

The present study demonstrates the reliability of the calcimetry method and its limitations through a parametric analysis that investigated the effect of the solid-to-liquid ratio, the presence of unweathered silicate phases, and the presence of copious amounts of organic matter. In contrast to previous studies that compared calcimetry to other methods or that used a variety of soils, the present study applied the principles of parametric investigation and standard additions to provide clearer interpretations. For this purpose, five sets of experiments were carried out to investigate the influences of the sample size (and consequently the solid-to-liquid ratio), the SIC content (through the addition of precipitated calcium carbonate (PCC)), the copresence of fresh (i.e., unweathered) silicate minerals (wollastonite skarn and olivine), and the level of coexisting SOC (through the addition of peat moss). In this study, it was decided to use soil from a deeper horizon as the baseline of the experimental soil with naturally low SOC and naturally elevated SIC, as these deeper layers of soil are likely to be the longer-term storage sinks of pedogenic carbonates formed as a result of ERW (compared to topsoil) [3,4]. A challenge here is that naturally elevated levels can make it harder to monitor gradual changes, so precision and accuracy are important even at elevated SIC levels.

In terms of accuracy, the study revealed that the lowest measurable CCE value was 0.22 g/kg (or 0.002 wt% IC), and the replication of the measurements yielded a linear correlation of sample size with the CCE value, with a coefficient of determination ($R^2$) of 0.9999 and a ρ value of 0.045. Moreover, the calcimetry method reliably measured the CCE for carbonate contents up to at least 2.6 times greater than the original carbonate content of the C horizon soil, indicating that increasing carbonate content due to long-term ERW could be monitored quantitatively. The results point to the reliable performance of calcimetry within the range of soil conditions that can be expected to be encountered during MRV activities involving enhanced rock weathering (ERW) and other best management practices (BMPs) that aim to boost global soil carbon stocks as a climate change mitigation strategy.

*References:*

[1] Rodriguez JB et al. (2016) Soil Sci Soc Am J 80: 1107-1113
[2] Shamrikova E et al. (2023) Catena 228: 107151
[3] Khalidy R et al. (2021) J Visualized Exp 172: e61996
[4] Khalidy R et al. (2023) Catena 233: 107524

## Transient epitaxial overgrowths in the $CaCO_3$-$REECO_3OH$ system formed during pseudomorphic mineral replacement processes

Szucs, A.M.[1], and Rodriguez-Blanco, J.D.[1]

[11]Department of Geology, School of Natural Sciences, Trinity College Dublin. Dublin 2, Ireland.

---

Rare earth elements (REEs) are essential components of many green energy technologies and electronic devices, thus, to cover the future REEs need, it is critical to understand the interaction of REE elements with common carbonate minerals in natural deposits. This study explores the surface precipitation of oriented REE carbonates during the interaction of individual and multiple REE bearing (La, Ce, Pr, Nd, Dy) aqueous solutions with calcite and aragonite ($CaCO_3$) at low hydrothermal conditions (25-220 °C) [1,2]. This mineral-fluid interaction was translated into a temperature-dependent solvent-mediated surface precipitation and subsequent pseudomorphic mineral replacement of the $CaCO_3$ seeds by newly formed REE carbonates. The complex replacement sequence included the crystallisation of metastable kozoite (orthorhombic $REECO_3OH$), which took place via the formation of individual spindle-shaped crystals following a transient non-random orientation on the surface of the host grains, gradually covering their full surfaces.

An explanation of the epitaxial overgrowth's configuration and the atomic arrangement of the structures of the $CaCO_3$ polymorphs and REE-kozoite will be discussed. These replacement processes are relevant for the understanding of mineralization reactions occurring in REE-bearing carbonatite deposits and demonstrate that these elements can be rapidly immobilized as REE hydroxycarbonates, even at low hydrothermal conditions.

*References:*

[1] Szucs AM et al. (2021) Cryst. Growth Des., 21:512–527.
[2] Szucs AM et al. (2022) Global Challenges, 2200085.

## Novel kinetic and mechanistic findings into the fluorite-fluocerite-bastnasite transformation reaction

Terribili, L.[1] and Rodriguez-Blanco, J.D.[1]

[1]Department of Geology, School of Natural Sciences, Trinity College Dublin. Email:terribil@tcd.ie.

---

Fluocerite is a rare earth element (REE) fluoride mineral with chemical formula (REE)$F_3$. It is found in nature as an accessory mineral in magmatic-hydrothermal REE ore deposits, including alkaline complexes and carbonatites [1]. There, is usually associated, amongst the others, with with REE fluorocarbonates (i.e. bastnasite, parisite, synchysite), REE-bearing fluorite, cerianite, monazite and xenotime [2]. Due to its relatively rarity in nature, fluocerite kinetics and mechanisms of crystallisation, its role in REE fractionation and as phase for the evolution of magmatic-hydrothermal REE have not been yet studied in detail [1]. Recently instead, the study of fluocerite is gaining importance as it was suggested to be a precursor phase of bastnasite and cerianite [1, 3-5]. Bastnasite is one of the main minerals used for the extraction of REE, indispensable in modern world due to their wide range of hi-tech industry and in clean energy applications [6]. Understanding the mechanisms of fluocerite crystallization and its role in the genesis of REE fluorocarbonates could significantly enhance our comprehension of the evolution of REE deposits.
The present study has two main objectives: 1) To study the kinetics and mechanisms of the fluocerite formation at temperatures ranging from ambient to low hydrothermal; 2) To demonstrate experimentally that fluocerite reacting with a $CO_3$-rich solution can transform into REE fluorocarbonates or cerianite under hydrothermal conditions. In order to achieve the first objective, fluocerite was synthesized by reacting pure fluorite ($CaF_2$) powder with different REE-bearing solutions. To reach the second goal, synthetic fluocerite was then reacted with $Na_2CO_3$ solutions at hydrothermal conditions up to 200 °C. Samples of solids were taken at specific time intervals to follow the ongoing of the crystallisation reactions. The nature of crystallising solids, their quantification and growth morphology were determined with a combination of powder X-ray diffraction (XRD) and scanning electron microscopy with energy dispersive microscopy (SEM-EDS). Our results showed that the fluocerite crystallisation rate decreases proportionally with the REE atomic number whereas increases with increasing T. The activation energy of crystallisation is similar irrespective of the REE used in the synthesis (~75 KJ/mol) while the activation energy of nucleation increases with the REE atomic number (80 - 96 KJ/mol). All fluocerites reacted with the $CO_3$-bearing solutions transformed into bastnasite at all temperature, also forming cerianite and kozoite respectively in the Ce and Nd bearing experiments.

*References:*

[1] Strzelecky A et al. (2022) Nature Geoscience 15:327-333
[2] Lahti S and Jones P (1988) Bull Geol Soc Finland 60:45-53
[3] Zhang W et al. (2023) Contrib Mineral Petrol 178:34
[4] Holstam D and Andersson U (2007) Canad Min 45:1073-1114
[5] Beukes G J et al. (1991) S Afr J Geol 94(4):313-320
[6] Balaram V (2019) Geosc Front 10:1285-1303

## Crystallisation of $CaCO_3$ polymorphs in the presence of microplastic glitter particles

Zubovic, K.P.[1], Horvath, A.[1], Brien, M.D.[1], Rateau, R[1], Guyett, P[1]., and Rodriguez-Blanco, J.D.[1]

[1]Department of Geology, School of Natural Sciences, Trinity College Dublin. Dublin 2, Ireland.

---

Biomineralization, the biological process of inorganic mineral deposition by organisms, primarily involves the production of Ca-Mg carbonate minerals [1]. This study investigates the interaction of solid pollutants, specifically microplastics (<500 µm), during the formation process of carbonate minerals. Focusing on polyethylene terephthalate (PET) glitter, a widely produced primary microplastic [1], we explore its underrepresented role in microplastic pollution, noting its hazardous chemical leachates and unique physical structure.

We synthesised Ca-Mg carbonate minerals in the presence of six PET glitter colour variants at different temperatures (21-60 °C), varying levels of supersaturation and Mg/Ca ratios, emulating seawater. Using scanning electron microscopy (SEM) with energy dispersive spectroscopy (EDS), Fourier transform infrared spectroscopy (FTIR), and powder X-Ray diffraction (XRD), we identified glitter characteristics (rough textures, uneven edges, structural deformities) that enhance $CaCO_3$ nucleation. Our findings reveal a preferential attachment of calcite, aragonite, vaterite and monohydrocalcite to glitter surfaces, with aragonite and vaterite forming weaker associations concentrated around surface imperfections. Glitter demonstrated a tendency for moderate degradation under ambient conditions, as evidenced by surface cracking and the peeling of external layers, a process accelerated by calcite growth. This growth was able to alter the glitter's plastic structure significantly, promoting the formation of fractures and the release of nanoplastic particles.

Our study suggests the possibility of biogenic $CaCO_3$ to encase and degrade PET glitter in marine environments, thereby impacting biomineralisation processes, highlighting the potential complex interactions between micro- and nanoplastics and calcifying organisms.

*References:*

[1] Addadi L, Raz S and Weiner S (2003). Adv. Mater, 15:959-970.
[2] Tagg A S and do Sul J A I (2019) Mar. Pollut. Bull., 146: 50-53.

## Carbon Capture and Mineral Storage: Italy as natural laboratory for its application

Boschi, C.[1,2] Baneschi I. [1], Castellari, I.[2], Dini, A. [1], Ganci F.[2], Marieni C.[3], Sigfússon B.[3], Snaebjornsdottir S.3, Trumpy E. 1, and Rielli A.1

[1] Institute of Geosciences and Earth Resources, CNR, Italy

2 Department of Earth Sciences, University of Pisa, Italy

3 Carbfix, Iceland

---

Carbon Capture and Mineral Storage (CCMS) is a key technology for the energy transition. The process takes its idea from the natural carbonation reaction of silicate rocks, one of the major geological sinks for $CO_2$. $CO_2$-rich fluids have the potential to dissolve silicate minerals, olivine, serpentine, and oxides, such as brucite, and precipitate carbonate minerals. The resulting mineralogical trapping of $CO_2$ into the crystallographic structure of calcite, magnesite or other carbonate minerals is permanent and arguably the safest way to remove $CO_2$ from the atmosphere. Thanks to its geological diversity Italy offers the opportunity to study natural carbonation systems from mafic to ultramafic rocks and under a variety of P-T conditions.

In the Ligurian Ophiolite of Tuscany, serpentinised peridotites host magnesite deposits formed from their interaction with $CO_2$-rich fluids under epithermal conditions, sequestering millions of tons of $CO_2$ in lodes and stockworks [1,2]. Instead at ambient conditions brucite-rich serpentinised dunites continuously absorb atmospheric $CO_2$, forming hydromagnesite coatings on rock surfaces [3]. This process is paralleled in serpentinite-hosted mine tunnels, where air-captured $CO_2$ forms hydromagnesite and kerolite through capillary seasonal carbonation [4]. Southern Sicily provide further insights on natural analogues for $CO_2$ storage in basalts, where $CO_2$ interacting with basaltic rocks has resulted in calcite formation within the rock porosity and fractures under various P-T conditions.

Through the study of these natural analogues, we aimed to identify the diverse physico-chemical conditions under which carbonation reactions can achieve high efficiency in a relatively short timeframe, with the goal of replicating these conditions on an industrial scale. In addition, our results suggest that the significance of carbonation in mafic and ultramafic rocks has been underestimated within the global carbon cycle. Updated estimates, grounded in our field evidences, reveal its fundamental role in regulating this cycle over geological time.

The strength of CCMS, and its flexibility of application, can be upscaled for the needed Energy Transition. Recently, the European Commission proposed the Net-Zero Industry Act, working towards achieving the 'Fit-for-55' benchmark to reduce EU carbon emissions by 55% by 2030 compared to 1990 levels. This ambitious target is intended to be achieved through a massive increase in low-carbon energy technologies together with the carbon capture and storage (CCS) technology, with an annual storage capacity of 50 million tonnes of $CO_2$ by 2030. CCMS is the safest and the most flexible option of the CCS technologies and a substantial increase of in its use and in its development is suitable in the near future.

*References:*

[1] Boschi C. et al. (2009) Chem Geol 265: 209–226
[2] Rielli A. et al. (2022), Ore geology review, 149,105022.
[3] Boschi C. et al. (2017) Lithos, 288–289: 264–281
[4] Boschi C. et al. (2020) Minerals, 10 (1).

# Geological storage of $CO_2$ in Anatolian ophiolites: Reaction experiments between fluids and ultramafic rock suites at 25-100℃ and 1-125 Bar

Ünal Ercan, H.[1], Gülmez, F.[2], Göçmengil, G.[3], Topkafa, M[1], Ündül, Ö[2], and Deveci, İ [1]

[1]Konya Technical University, Vocational School of Technical Sciences, Chemistry and Chemical Processing Technologies, Konya, Türkiye, hunalercan@ktun.edu.tr, Hatice Ünal Ercan.

[2]İstanbul Technical University, Department of Geological Engineering, İstanbul, Türkiye

[3]Department of History of Science, Faculty of Letters, Istanbul University, İstanbul, Türkiye

---

Anatolia, as a part of the Alpine-Himalayan orogenic belt, extensively preserved the remnants of the Tethys in the form of ophiolitic nappes and ophiolitic mélanges. Orhaneli Ophiolitic Complex in Northwest Anatolia is a Supra-Subduction-Zone type ophiolite that contains mantle-crust transition zone lithologies. It is dominated by dunite and harzburgite consisting of subordinate pyroxenite and gabbro. Various serpentinization, argillization, and carbonation processes have affected the ultramafic and mafic rocks, locally resulting in extensive alteration.

To reveal the carbon sequestration potential of Orhaneli Ophiolite, altered and fresh dunite, harzburgite, pyroxenite and serpentinite samples were systematically derived from the field. The rocks then underwent reaction experiments with carbonic acid in a batch reactor at 25°C, 50°C, and 100°C. Experiments are being carried out on two sets of samples for each rock type: blocks (1 cm3) and aggregates (between 0.3 to 0.1mm). The samples' pre- and post-experiment mineralogic, petrographic, micromorphological, and chemical features will investigate using XRD, FE-SEM, EDX, Micro-CT and ICP-OES instruments.

The preliminary evaluations of the ultramafic rock samples assessed the dissolution and precipitation mechanisms that occur in the mineral grains' reactive surface area and fracture/pore spaces due to the interaction between liquid and minerals, and their properties. Thus, the interaction of the fluid phase in the specimens with all surfaces and interfaces was discussed, and the transport of carbon dioxide in the fluid phase and primary data regarding the evaluation and determination of properties such as carbon dioxide retention were provided.

# A mineralogical and geochemical approach to evaluate the redox capacity of basaltic glass and crystals via experiments

Pierozzi, A. [1,2,*], Rateau, R.[1], Orlando, A.[3], Borrini, D. [4], Tassi, F.[4], Rodriguez Blanco, J.D. [1,2]

[1] Department of Geology, School of Natural Sciences, Trinity College Dublin, Ireland

[2] iCRAG, Department of Geology, School of Natural Sciences, Trinity College Dublin, Ireland

[3] CNR—Consiglio Nazionale delle Ricerche, Istituto di Geoscienze e Georisorse, 50121 Florence, Italy

[4] Dipartimento di Scienze della Terra – Università di Firenze, via G. La Pira, 4-50121 Florence, Italy

*corrisponding author, pierozza@tcd.ie

---

The levels of greenhouse gases, particularly $CO_2$, rise globally. To tackle this problem, scientists and engineers have been exploring carbon capture and storage (CCS) technology to reduce $CO_2$ concentrations in the atmosphere. Mineral carbonation is a promising CCS technique that involves $CO_2$ reacting with Ca-Mg-Fe bearing basaltic rocks to store it in the rocks as carbonate minerals. The CarbFix project in Iceland is an excellent demonstration of this approach. However, much remains to be discovered about the intricate physicochemical connections between water, dissolved ions, and crystal growth in complex multicomponent systems at the atomic and nanoscale. These factors are vital for the successful deployment of CCS in basaltic reservoirs.

This research explores the use of supercritical $CO_2$, which is achieved by exceeding the critical temperature and pressure of 30.97 °C and 73.773 bar, respectively. In this state, $CO_2$ exhibits the properties of both a gas and a liquid. The study presents the results of an experiment conducted on basaltic crystals and glasses under varying temperatures (between 100 and 200 ºC) and pressures (64 to 79 bar) to investigate the reaction between $CO_2$ (sc), water, crystals (mainly forsterite) and basaltic glass. The results highlight the partial dissolution of mineralogical phases and the formation of new alteration phases, in addition to the precipitation of carbonates containing Ca, Mg, and Fe. A comparison will be made between the obtained carbonation to the findings of Aaberg [1] study, in which synthetic forsterite was reacted with $CO_2$. Furthermore, the composition of the post-reaction gases will be analyzed to evaluate the redox conditions occurring in water-$CO_2$-basaltic glass and water-$CO_2$-basaltic crystal reactions.

*References:*

[1] Aaberg, I., (2013) University of Copenhagen

# The potential of Kenyan basalts for carbon sequestration via enhanced rock weathering and geological sequestration with *in-situ* mineralization

Santos, R.F.[1], Khalidy, R.[1], Basimalla, J.[2], Roobroeck, D.[3], Collinson, J.D.[4], Manga, M.[5], Marangu, M.[6]

[1] School of Engineering, University of Guelph, Guelph, Ontario, Canada; santosr@uoguelph.ca

[2] Department of Mining Engineering, Indian Institute of Technology Kharagpur, West Bengal, India

[3] International Institute of Tropical Agriculture, Nairobi, Kenya

[4] Retired Professor, Newcastle-under-Lyme, Staffordshire, United Kingdom

[5] Olsuswa Energy, Naibori, Kenya

[6] The Mutuma Marangu Sculpture and Art Collection, Nairobi, Kenya

---

Pathways to net-zero carbon emissions pledged under the Paris Agreement rely on both $CO_2$ reduction and removal. Under the best-case abatement scenario of anthropogenic emission, there is need for 10 Gt $CO_2$ or more to be removed from the atmosphere annually. Geological sequestration in solid carbonates and dissolved alkalinity has the potential to store gigatonnes of $CO_2$ per year globally, and thereby act as a 'climate stabilization wedge'. For this, suitable mineral resources must be identified for injecting $CO_2$ and *in-situ* mineralization as part of direct air capture (DAC) or carbon capture and sequestration (CCS), or for application on croplands as part of enhanced rock weathering (ERW). For DAC and CCS parameters linked to injectivity, composition and reactivity are critical[1], whereas for ERW the morphology is of less importance and it has the added benefit of improving soil and plant health and food security[2]. Kenya possesses vast basalt deposits that can support both strategies, but little is known about their suitability in terms of their chemical and mineral composition, reactivity, permeability and porosity[3].

Here, basalts from three distinct geological formations within the Kenya Rift System (Kissi metabasalt (Pre-Cambrian); Kajiado dyke (Pliocene); Barrier basalt (Recent)) were characterized and compared to basalts from Canada, Mongolia, and India. Through scanning electron microscopy rock samples were assessed for degree of amorphicity and macroporosity. Wavelength dispersive X-ray fluorescence was used to determine the elemental composition of the samples. X-ray diffractometry was used to identify major and minor crystalline mineral phases and quantify their proportions. Results were cross-referenced with basalt properties reported in both ERW and geological sequestration publications to delineate which Kenyan basalts may be more suitable for DACS/CCS or ERW. This collaboration has also aimed to translate and transfer the scientific knowledge to the wider public via a series of exhibitions, including the "ROOTS OF REMOVAL: KENYAN BASALT ROCK AND MINERAL SCULPTURE ART AND THE CARBON REMOVALS ODYSSEY" during the 2023 African Climate Summit.

*References:*

[1] Rasool MH and Ahmad M (2023) Minerals 13:1154
[2] Haque F et al. (2023) ACS Earth and Space Chemistry 7:1294-1305
[3] Okoko JB and Olaka LA (2021) Scientific African 13: e00924

## Boosting of the water-mediated mineral carbonation by microwave chemistry

D'Alessio, D.[1], Corti, M.[1], Campione, M.[1], Capitani, G.[1], Lucotti, A.[2], Yivlialin, R.[3], Tommasini, M.[2], Bussetti, G.[3] and Malaspina, N.[1]

[1]Department of Earth and Environmental Sciences, University of Milano-Bicocca, Piazza della Scienza 4, 20126 Milan, Italy Corresponding email: daniela.dalessio@unimib.it

[2]Department of Chemistry, Materials and Chemical Engineering, Politecnico di Milano, Piazza Leonardo da Vinci 32, 20133 Milan, Italy

[3]Department of Physics, Politecnico di Milano, Piazza Leonardo da Vinci 32, 20133 Milan, Italy

---

Carbon Capture Utilization and Storage (CCUS) is one of the main technologies in the Green Transition, aimed at a more sustainable and low-carbon industrial compartment. CCUS allows the use of captured $CO_2$ for the production of raw materials from wasted ones, in a perspective of Circular Economy. Mineral carbonation (MC) involves the chemical reaction in aqueous environment between $CO_2$ and magnesium and calcium rich minerals. During this reaction, $CO_2$ is converted into a stable and solid mineral form. Despite it might be thermodynamically spontaneous for magnesium and calcium rich minerals, MC reaction can be hindered by activation barriers.

Microwaves (MW) accelerate the heating process and improve its efficiency, thanks to their ability to directly couple with polar molecules, such as water, and electrolytes. The energy transfer might be highly localized and reactant-specific, promoting an accelerated reaction kinetics. For this reason, MW chemistry results often in substantially shorter reaction times compared to conventional heating methods.

We focussed on the effects of MW chemistry on the MC reaction of brucite [$Mg(OH)_2$], which is a model system of magnesium rich minerals, since it is made of only two components ($MgO + H_2O$) [1]. We explored various combinations of temperature and reaction time, and of specific chemical additives, to define the optimal conditions to obtain crystallization of magnesite [$Mg(CO_3)$] and magnesium hydroxide-carbonate hydrates (MHCH), such as nesquehonite [$Mg(HCO_3)(OH)\cdot 2H_2O$] and hydromagnesite [$Mg_5(CO_3)_4(OH)_2\cdot 4H_2O$], with the minimum energy expenditure.

The carbonation products were characterized by X-ray Powder Diffraction, Raman Spectroscopy and Scanning Electron Microscopy, to define their composition, crystallinity and morphology, and then evaluate the mass yield of the MC reaction as function of temperature. Nesquehonite, hydromagnesite and magnesite characterize the products of the brucite carbonation in experiments performed from room temperature to 220 °C, with $CO_2$ partial pressure as low as 6 bar in a 50% mixture with $N_2$, and without additives, and represent the dominant phases up to 55 °C, between 70 and 205 °C, and above 220 °C, respectively [1].

These results set the starting point to optimize the use of MW for accelerating the carbonation of brucite and promoting the crystallization of magnesite at a temperature lower than those previously reported.

*References:*

[1] Campione M. et al. (2024) J. CO2 Util. 80: 102700

## Investigation of early signs of mineral weathering through tea bag experiments

Khalidy, R.[1], Jariwala, H.[1], Chiang, Y.W.[1] and Santos, R.M.[1]

[1]School of Engineering, University of Guelph, Guelph, Ontario, Canada; rkhalidy@uoguelph.ca

---

Deemed as a promising carbon capture technique, enhanced rock weathering (ERW) accelerates weathering of calcium (Ca) and magnesium (Mg)-rich minerals followed by sequestration of atmospheric $CO_2$ in form of pedogenic carbonate in soil [1]. Many studies have been conducted to monitor the evolution of mineral weathering during ERW through measurement, reporting and verification (MRV) methods [2]. However, detecting weathering evidence over the short timescales (e.g., a few months to years) have proven challenging due to slow nature of weathering of minerals in soil [3]. Therefore, there is a need to develop methods capable of detecting early indications of mineral weathering in soil, which could aid in the large-scale deployment of ERW. Once minerals are spread onto soil, they are exposed to transport and mixing with soil particles [1]. To mitigate this, a teabag-based experiment was devised to minimize mixing of mineral and soil particles.

The present study involved detecting early signs of weathering in several fast-weathering Ca- and Mg-rich silicate minerals (basalt, kimberlite, olivine, and wollastonite) through a tea bag experiment utilizing different morphological and mineralogical analyses. The experimental setup was maintained for a duration of 32 weeks with replicates, and tea bag samples were collected at intervals of the first, second, fourth, eighth, sixteenth, and thirty-second weeks. Each tea bag, filled with 50 grams of mineral, was sealed, and buried under the soil inside a pot. All pots were watered regularly, and tea bag samples were collected by the end of the designated week. Subsequently, all the tea bag samples were dried and prepared for further analysis. The experimental analyses conducted on the tea bag samples included laser particle size distribution (PSD), X-ray diffraction (XRD), X-ray fluorescence (XRF), scanning electron microscopy (SEM), and Brunauer, Emmett, and Teller (BET) surface area analyses. PSD was used to assess the size of the mineral particles (e.g., to detect transportation of finer particles during the experiment); XRD was used to observe changes in the peaks of the minerals present; XRF facilitated the quantification of the elemental composition of the minerals and the determination of the effect of weathering on the mineral composition; SEM images provided insights into how weathering affected the surface morphology; and BET results provided information on minor changes in the surface area and pore size distribution of the mineral particles in the tea bag.

This study revealed that tea bag conditions help to predict early signs of mineral weathering. The SEM images revealed microbial degradation on the surface of the minerals, confirming that mineral weathering in the soil is not solely a chemical process but can also be influenced by microbial activity. The XRD results indicated changes in the peaks of minerals at the end of the experiment, providing strong evidence of mineral weathering. Our finding suggests that such investigations can be employed as part of MRV tool as the proof of carbon sequestration through ERW at the initial stages [4].

*References:*

[1] Khalidy R et al. (2023) Catena 233: 107524
[2] Abdalqadir M et al. (2024) Environ. Sci. Pollut. Res. Int. 31: 19047–19070
[3] Haque F et al. (2019) ACS Omega, 4: 1425–1433
[4] Santos R et al. (2023) Front. Earth Sci. 11: 1215930

# The fate of nickel during ex-situ mineral carbonation of serpentinized peridotites

Cieślik, B.[1], Kierczak, J.[1], Lacinska, M.A.[2], Bateman, K.[2], and Pietranik, A.[1]

[1]University of Wrocław, Institute of Geological Sciences, Pl. M. Borna 9, 50-204 Wrocław, Poland

[2]British Geological Survey, Natural Environment Research Council, Environmental Science Centre, Keyworth, Nottingham NG12 5GG, UK

---

Mineral carbonation of peridotites and serpentinites (ultramafic rocks) is considered one of the most promising carbon capture and storage (CCS) technologies to combat climate change. This method relies on the interaction between magnesium (Mg)-bearing silicates, commonly found in ultramafic rocks, and $CO_2$-rich aqueous solutions, resulting in the formation of Mg carbonates. While the significant Mg content is crucial for efficient $CO_2$ sequestration, the relatively high nickel (Ni) concentration in ultramafic rocks and its effect on the carbonation process remain poorly characterized. We demonstrate the fate of Ni during ex-situ mineral carbonation experiments conducted at different P-T-t parameters, utilising peridotites with varying degrees of serpentinization.

Ultramafic rocks, selected for carbonation experiments, exhibit consistent concentrations of $SiO_2$ and MgO, with values around 41 wt.% and 36 wt.%, respectively. The whole-rock Ni content ranges from 1.9 to 2.1 g/kg. The main Ni-bearing minerals are olivine, minerals from the serpentinite subgroup, and accessory Ni-Fe sulfides. Carbonation experiments were exploring a range of P-T-t parameters (20-150 bar, 50-185°C, 4-168 h). Pulverised and sieved ultramafic feedstock (<50 µm) was placed in stainless steel batch reactors and poured with ultrapure water with the fluid-rock ratio of 10:1.

Four types of post-carbonation solid products have been found so far, including magnesite, Ni-bearing carbonates, amorphous silica, and Ni-bearing silicate. Pure magnesite [$MgCO_3$] is abundant (up to 50 modal %) in almost every experimental run apart from the lowest P-T settings. Ni-bearing carbonates, representing the gaspéite-magnesite series [$Ni_{0.37\text{-}0.69}Mg_{0.31\text{-}0.63}CO_3$], have only been observed in material carbonated at 100 bar, 185°C, and for 96 hours. In the same sample, spherules of amorphous silica [$SiO_2$] with diameters of up to 12 µm have been observed. These spherules are partly or fully overgrown by the Ni-bearing silicate (probably smectite group), which displays a Ni concentration of ~28 wt.%. ICP-MS/OES analysis of the post-carbonation fluids revealed that as the P-T-t parameters increased, the Ni concentration in the fluid also increased, reaching 17.5 mg/kg after 96 hours at 185°C and 100 bar.

This study shows that Ni is partly redistributed during ex-situ mineral carbonation of serpentinized peridotites. The presence of Ni-rich carbonates and silicates in post-carbonation solid products suggests that under specific conditions newly formed phases may serve as a sink for this metal. In the following steps, we plan to investigate selective Ni uptake during carbonation, focusing on metal recovery and environmental risk assessment.

Acknowledgements: This project is supported by the NCN OPUS 2021/43/B/ST10/01594 grant, and the EU Horizon 2020 research and innovation programmes under grant agreement No 101005611 at the Helmholtz-Zentrum Potsdam (GFZ), as part of the PISA facility, and grant agreement No 871143 at the Hydrothermal Laboratory (HTL) facility from the ECCSEL partner British Geological Survey.

## Insights into incipient carbonation phases of synthetic Mg- and Ni-serpentine end members

Corti, M.[1], D'Alessio, D.[1], Campione, M.[1], Capitani, G.[1], Murri, M.[2] and Malaspina, N.[1]

[1] Department of Earth and Environmental Sciences, University of Milano-Bicocca, Piazza della Scienza 4, 20126 Milan, Italy. Corresponding e-mail (mattia.corti@unimib.it)
[2] Department of Earth and Environmental Sciences, University of Pavia, Via A. Ferrata 1, 27100 Pavia, Italy.

---

In the last decades, many studies have focussed on carbon capture utilization and storage (CCUS) as possible solution to reduce the increasing $CO_2$ concentration in the atmosphere. Among all, mineral carbonation (MC) has been recognised as the best possible route to achieve a long term carbon sequestration. In this respect, Mg-bearing minerals, in particular serpentine [$Mg_3Si_2O_5(OH)_4$], olivine [$Mg_2SiO_4$] and brucite [$Mg(OH)_2$] [1] were targeted as naturally occurring phases for CCUS by water-mediated MC.

The reaction consists in the combination of $Mg^{2+}$ cations and $HCO_3^-$ and $CO_3^{2-}$ anions in aqueous environment to form Mg-carbonates. Although spontaneous in nature, this reaction is hindered by activation barriers. This reduces its capability to permanently store carbon in silicate minerals, and consequently its exploitation in profitable applications.

To understand the MC early-stage mechanisms, model Mg- and Ni- serpentine end members nanocrystals were synthetized and characterized. The chosen crystal sizes allow the maximization of their reactivity through their surface-to-volume ratio. These nanophases were subjected to mild MC experiments with the aid of a microwave-driven apparatus, under controlled partial pressure of $CO_2$ as low as 6 bar, and temperatures of 100 and 200 °C.

The results of the characterization of the incipient carbonation products of synthetized serpentine, both as solid precipitate and solid residue in the dried supernatant liquid are presented. The role of morphology and structure of the synthetized phases on the progress of carbonation are discussed, both in terms of their dissolution propensity in acidic aqueous environment and the possible onset of self-passivating effects. This can be also environmentally relevant for the topic of MC, and consequently for the research on CCUS.

*References:*
[1] Campione M. et al. (2024) J. CO2 Util. 80: 102700

## Effect of carbon on thermoelastic properties of $(Fe, Mg)_2SiO_4$-olivine under upper mantle P-T conditions

Gholamimahmoodabadi, Z.[1]*, Rabindranath Mondal[1], Swastika Chatterjee[1]

[1]National Centre for High-Pressure Studies and Department of Earth Sciences, Indian Institute of Science Education and Research-Kolkata, Nadia-741246, West Bengal, India.

*zgm19rs077@iiserkol.ac.in

---

The mantle is known to be the Earth's largest carbon reservoir [1]. Observations on natural rocks indicate that at least some mantle carbon may be dissolved in the silicates at high pressure. However, the extent of dissolution is highly disputed. Olivine ($(Fe, Mg)_2SiO_4$), which is the most dominant mineral phase in the Earth's upper mantle may play a crucial role in the planet's carbon storage [2]. Hence, using a combination of first principles of density functional theory and quasi-harmonic approximation, we have determined the thermodynamic stability of C-doped olivine with varying Fe-concentration under upper mantle Pressure and Temperature (P-T) conditions. Our calculations indicate that C prefers to be doped at the Si tetrahedral site [3]. The C-doped tetrahedron is found to be smaller than its undoped counterpart, which is expected to influence the elastic properties of the mineral phase. Our calculations show that with the introduction of C in olivine there is an enhancement in the compressional and shear wave velocity of the sample. By plotting the shear wave velocities along an Indian continental geotherm for varying levels of carbon doping, we observe consistency between the reported percentage change in shear wave velocities associated with the Hales discontinuity and the range predicted in our simulations. These results suggest that carbon incorporation at silicon sites in appropriate proportions may be the cause behind the observed seismic anomaly, offering new insights into the underlying mechanisms of the Hales discontinuity and highlighting the importance of considering carbon's role in mantle dynamics and seismic behavior.

*References:*

[1] Sleep N H et al. (2001) Geophys 106:1373–1399
[2] Shcheka S S et al. (2006) Earth and Planetary Letters 245:730–742
[3] Ernst T et al. (1969) Fluid Incl. Res 69:16–17

# $CO_2$-negative Mg-binders based on olivine for carbon capture and storage

Neubauer, J.[1], Goetz-Neunhoeffer, F.[1] , Franke, S.[1] , Rafalski, F.[1] and Bellmann, F.[2]

[1]Friedrich-Alexander-Universität Erlangen-Nürnberg, GeoZentrum Nordbayern, Mineralogy, Schlossgarten 5a, 91054 Erlangen, Germany; Email: juergen.neubauer@fau.de (corresponding author)

[2]Bauhaus-Universität Weimar, Werkstoffe des Bauens, Coudraystr. 11a, 99423 Weimar, Germany

---

In-situ carbon capture and storage by mineralization (CCSM) in mafic and ultramafic rocks is studied since long as an opportunity for long-term $CO_2$ sequestration. According to measurement on compact sample cylinders (3 cm length, 2 cm diameter, 70°C, 100 bar) ≈30 kg $CO_2$ per ton of host rock can be captured by reaction to magnesite [1].

A new concept for the production of $CO_2$-negative building materials is based on olivine-containing raw material. Several stages are necessary to produce binders from olivine-containing rock, whereby first a fine grinding and then an activation process is required. In contrast to conventional cement production, however, there is no burning process with considerable $CO_2$ emissions from limestone and fossil fuel.

The hardening reaction is simplified below for the Mg end-member of olivine (forsterite, $Mg_2SiO_4$). When forsterite reacts with water, magnesium silicate hydrate (e.g. lizardite, antigorite) and magnesium hydroxide (brucite) are formed. This reaction of olivine with $H_2O$ at temperatures of 100-350°C is also known as serpentinization.

Gl. 1: $2\ Mg_2SiO_4 + 3\ H_2O \Rightarrow Mg_3Si_2O_5(OH)_4 + Mg(OH)_2$

As milled olivine rock flour has a considerably lower reactivity than conventional cement, additional activation steps must be used in order to achieve sufficient strength for practical building applications. By accelerating the hardening reaction via autoclave treatment, a strength of up to 20 MPa can be achieved after a few days.

Magnesium hydroxide can also fix $CO_2$ in the form of magnesium carbonate during the use of the concrete component or already during production.

Eq. 2: $Mg(OH)_2 + CO_2 \Rightarrow MgCO_3 + H_2O$

This reaction of brucite with $CO_2$ to form magnesite ($MgCO_3$) therefore enables the production of $CO_2$-negative binders based on olivine. In this way, around 100 kg of $CO_2$ per ton of Mg-binder can be permanently stored without even using the potential of the $Mg_3Si_2O_5(OH)_4$.

The role of reaction kinetics and the factors that control olivine $(Mg,Fe)_2SiO_4$ dissolution under hydrothermal conditions and their interaction with $CO_2$ was intensively studied [2, 3]). With regard to the kinetic principles of the reaction, data are available on the dissolution of olivine as a function of pH, temperature etc. under geological conditions. But optimum conditions for the binder application are necessary and are determined experimentally in our study with model systems based on forsterite and brucite.

*References:*

[1] Lacinska, A.M, et al. (2017) *Front. Earth Sci.* 5:37. doi: 10.3389/feart.2017.0003

[2] Giammar, D. et al. (2005). *Chem. Geol.* 217, 257–276. doi: 10.1016/j.chemgeo.2004.12.013

[3] Gislason, S. R., et al. (2016). *Int. J. Greenhouse Gas Control* 4, 537–545. doi: 10.1016/j.ijggc.2009.11.013

## Understanding and replicating natural basalt carbonation: the case study of Sverrejfellet Volcano (Svalbard, Norway)

Pierozzi, A.[1,2,*], Faulkner, N.[1,2], Rodriguez Blanco, J.D.[1,2]

[1] Department of Geology, School of Natural Sciences, Trinity College Dublin, Ireland

[2] iCRAG, Department of Geology, School of Natural Sciences, Trinity College Dublin, Ireland

*corresponding author, pierozza@tcd.ie

---

This study aims to investigate the formation of carbonate cement on a natural host rock and the evolution of carbonate cements during the carbonation of basaltic rocks from the Sverrefjellet volcano in Svalbard, Norway. The Sverrefjellet volcano erupted around 1 million years ago and comprises a cone of cinders, pillow lavas, and dikes. The eruption occurred in a subglacial context. After the volcanic eruption and interaction with fluids, some parts of the basalt underwent a process of carbonate cementation. These cementations have peculiar characteristics that have been discussed in the literature. Specifically, the carbonate cements are made of calcite-type carbonates that fall within the magnesite-calcite-siderite range of compositions. The cements went through different stages of carbonation which correspond to a crystal chemistry evolution from calcian proto-dolomite to Ca-poor magnesite and finally to a mixture of Fe-rich carbonates (siderite) and non-carbonate cements.

The objective of this study is to replicate the formation of carbonate cement in a laboratory by using basaltic samples from the same volcano. To achieve this, experiments will be conducted in a reactor with pure $CO_2$ ranging to low $CO_2$ pressure (1 atm) up to supercritical conditions. It is important to control the chemical and physical parameters during the experiment, including the temperature and composition of the water. We will then evaluate the differences between the natural sample and the experimental counterpart and analyze the mechanisms responsible for their specific mineralogical composition using a combination of spectroscopic, microscopic, and solid-state techniques.

# Assessing carbon dioxide storage potential in Swedish and Finnish mine waste

Rees, E.[1], Warlo, M.[1], Crafoord, E.[1]-and-Bark, G.[1]

[1]Department of Civil, Environmental and Natural Resources Engineering, Luleå University of Technology, Luleå, Sweden, emily.rees@ltu.se

---

To avoid the worst-case scenario consequences of anthropogenic global warming, the Intergovernmental Panel on Climate Change (IPCC) has reported that warming should be limited to 1.5–2 °C above pre-industrial temperatures. Last year global average surface temperatures showed an average increase between 1.34 and 1.54 °C [1] with a trajectory towards 3.2 °C by the end of the century [2]. Mitigation of this global warming requires global $CO_2$ emissions to reach net zero by 2050. To achieve this ambitious goal, phasing out fossil fuels and transitioning to renewable energy sources must be complemented by the implementation of large-scale carbon dioxide removal (CDR) initiatives. This demands a rapid upscaling of global carbon storage rates several hundred times, from the current 30 Mt $CO_2$ per year to 3–10 Gt $CO_2$ permanently injected into the bedrock per year by 2050 [3].

Mineral carbonation is a safe and effectively permanent storage method. Carbon sourced from the atmosphere or industrial point emission sources is integrated into stable mineral structures. Hydrated $CO_2$ reacts with divalent cations (mainly $Ca^{2+}$ and $Mg^{2+}$) to form carbonate minerals spontaneously. Ultramafic and mafic rocks are an ideal source of divalent cations. The reaction has slow kinetics, therefore, acceleration is required for this natural carbon sequestration method to significantly mitigate anthropogenic $CO_2$ emissions. Larger relative surface area of minerals increases their reactivity, and thus the sequestration potential, however, milling rocks to such fine powder is an energy intensive and costly process. Mine waste is a potentially viable source for divalent cations, as it is a vastly abundant source of pre-milled material with high sequestration potential. Ultramafic mine tailings have been shown to have beneficial sequestration potential [4] although, more widely available mafic tailings may also have significant potential to be used for sequestering carbon.

The TAILOR-MADE project investigates the sequestration potential of typical Swedish and Finnish mine tailings, by carbon capture and storage (CCS) and direct air capture (DAC), and seeks to enhance this potential with the use of enzymatic catalysation, Carbonic Anhydrase (CA). The carbonate mineralisation pathways, reaction kinetics, thermodynamics, elemental partitioning, and mineral habits etc. will be studied. CA has been shown to increase the rate of $CO_2$ hydration [5], a rate limiting step in the sequestration of $CO_2$ [6]. Novel experimental methods will be utilised to assess the sequestration of $CO_2$ under both natural and catalysed conditions. Tailings from three Swedish mines and one Finnish mine have been sampled based on their perceived potential for carbon sequestration. This project seeks to explore potential storage media for both in- and ex- situ sequestration to increase global carbon storage rate capacity.

*References:*

[1] Witze (2024) Nature 625, 637-639
[2] IPCC (2023) Synthesis Report, 184 pp
[3] Krevor (2023) Nat Rev Earth Environ 4, 102–118
[4] Lackner (1995) Energy 20: 1153-1170
[5] Meldrum & Roughton (1933) The Journal of physiology, 80(2), 113–142
[6] Wilson (2010) Environ. Sci. Technol. 44, 9522–9529

## Metal mobility during serpentinite carbonation: evaluating recovery potential and environmental impact

Rielli A.[1], Dini A.,[1] Baneschi I.,[1] Ricci L.[1], Brugger J.[2], Etschmann B.[2] and Chiara B.[1]

[1]Institute of Geosciences and Earth Resources, National Research Council of Italy, Via Moruzzi 1, 56124 Pisa, Italy

[2]School of Earth, Atmosphere and the Environment, Monash University, Melbourne, Victoria 3800, Australia

---

Mineral carbonation represents one of the most favourable $CO_2$ storage options, as it ensures the permanent trapping of $CO_2$ in stable carbonate minerals. Serpentinites are an ideal starting material because they are abundant on or near the Earth's surface and are rich in $Mg^{2+}$, which is required to form carbonates, primarily magnesite ($MgCO_3$) that traps $CO_2$ [1]. Serpentinites also contain significant amounts of transition metals including Ni, Co, V, Mn and Cr which can be mobilised during carbonation [2]. Since only trace amounts of these metals can be accommodated in magnesite, they must be redistributed or concentrated in different parts of the carbonation system. If these metals were to disperse into soils and superficial/ground-waters they could pose significant environmental, ecosystem, and human health risks. Serpentinites can be especially rich in Cr. $Cr^{3+}$ is the main oxidation state of Cr in serpentinite minerals, but it can be oxidised in aqueous fluids to $Cr^{6+}$ [3], which highly toxic to humans. Therefore, it is also essential to understand the speciation of Cr during mineral carbonation before its large-scale deployment.

The Ligurian ophiolites (Italy) host several magnesite deposits that formed when deep $CO_2$ was injected into serpentinite lenses through regional faults at 100-200° C and depths of 1-2 km [4, 5]. These deposits effectively resemble the *in-situ* storage of $CO_2$ by "natural pilot plants" active millions of years ago [4, 5], providing the opportunity to study the long-term metal mobility associated with serpentinite carbonation. We used synchrotron X-ray fluorescence microscopy to map metal distribution during carbonation and X-ray near edge structure spectroscopy (XANES) to assess the formation of $Cr^{6+}$. The environmental and ecosystemic impacts of carbonation were investigated in the framework of the PRIN 2022 PNRR STORECO2 project granted by the European Union—NextGeneration EU through the study of soil profiles, vegetation developed onto the magnesite deposit, and spring waters circulating through the carbonated area. Our findings offer a framework for assessing the potential of metal recovery and evaluating the impact of mineral carbonation.

*References:*

[1] Lackner et al. (1995) Energy 20: 1153-1170
[2] Hamilton et al. (2018) Int. J. Greenhouse Gas Control 71: 155-167
[3] Langone et al. (2013) Ofioliti 38: 41-57
[4] Rielli et al. (2022a) Ore Geol. Rev. 149: 105022
[5] Boschi et al. (2009) Chem. Geol. 265: 209-226

## Characterisation of PGEs in Minerals Using X-ray Absorption Spectroscopy

Filimonova, O.N.[1,2], Bikondoa, O.[1,3], Kutyrev, A.[4], Vymazalova, A.[5], Wermeille, D.[1,2]

[1] BM28 CRG c/o European Synchrotron Radiation Facility, Grenoble, France, email: olga.filimonova@esrf.fr;

[2] Department of Physics, University of Liverpool, Liverpool, UK;

[3] Department of Physics, University of Warwick, Warwick, UK;

[4] School of Earth and Ocean Sciences, Cardiff University, Cardiff, UK;

[5] Czech Geological Survey, Prague, Czech Republic.

---

In the sulphide ore deposits, platinum group elements (PGEs, Pd, Rh, Ru, Os, Ir) either (i) form discrete minerals – mostly compounds with other PGEs, base and nonferrous metals (Fe, Cu, Sn, Bi, Pb), and metalloids (As, Sb, Te, Se), or (ii) enrich base metal sulphide, oxide, arsenide etc. minerals, such as pyrrhotite $Fe_{1-x}S$, pentlandite $(Fe,Ni)_9S_8$, chalcopyrite $CuFeS_2$, pyrite $FeS_2$, magnetite $Fe_3O_4$ [1,2]. Despite the large accumulated knowledge on the content and distribution, the mechanism of PGEs incorporation into the sulphide matrixes is still ambiguous. The state of PGEs in the minerals (formal oxidation state and local atomic environment) can be reliably determined only by spectroscopic methods, e.g. X-ray absorption spectroscopy (XAS, e.g. [3]). In our talk, some advantages and challenges of using synchrotron methods for X-ray fluorescence mapping and XAS analysis of natural PGE-bearing minerals will be discussed. We will also report the recently obtained XAS data on the state of Pd in the matrixes of pyrite [4] and pyrrhotite, as well as Os in the matrix of pentlandite. Pd *K*-edge and Os $L_3$-edge spectra of the admixtures in the Fe/Ni sulphides were recorded at the XMaS/BM28 beamline of the European Synchrotron (ESRF). We used the XAS method to identify the states of the PGEs in synthetic and natural Fe/Ni sulphides including their formal charges, types of the neighbouring atoms at $R < 5$ Å, coordination numbers, and interatomic distances around the absorbing atoms.

*References:*

[1] Gunn G (2014) John Wiley & Sons 1-439
[2] Mansur E T (2021) Miner Deposita 56(1): 179-204
[3] Iglesias-Juez A et al. (2022) Can J Chem Eng 100 (1): 3-22
[4] Filimonova O et al. (2024) Sci Total Environ 170927: 2-12

## Platinum-group minerals from Norilsk – a tribute to S.F. Sluzhenikin

Vymazalová, A.[1*], Kozlov, V.V.[2], Laufek F.[1] , Antsiferova T.[2], Stanley C.[3],

[1]Czech Geological Survey, Geologická 6, Prague 5, Czech Republic, *anna.vymazalova@geology.cz

[2]IGEM RAS, Moscow, Russia

[3]Natural History Museum, London, United Kingdom

---

As of January 2024, there are 166 known platinum-group minerals (PGM) approved by IMA. Most PGM were described from localities in Russia (64) followed by Canada (17) and South Africa (17), and then by China (15) and USA (11). Almost half of PGM are known to occur in Norilsk-Talnakh ores. Furthermore, in total 23 PGM have a type locality in the Norilsk`s deposits. In terms of new PGM and variety of PGM, Norilsk`s deposits belong to the most unique localities in the world.

Majority of new PGM from Norilsk ores were described from early 60s until late 80s of the last century, predominantly by the group of A.D.Genkin. The next stage of discovery of new PGM from Norilsk`s ores, after a gap of more than 20 years, appeared with findings of S.F. Sluzhenikin (norilskite, kravtsovite, vymazalováite, thalhammerite and sluzhenikinite).

Norilsk`s ores, based on PGE-Cu-Ni content are divided on: massive, disseminated, brecciated, vein-disseminated in contact-metamorphic and metasomatic rocks and low-sulphide ores. PGM in **massive ores** are mainly represented by sperrylite, cooperite, rustenburgite, Fe–Pt alloys, atokite, stibiopalladinite, palladoarsenide, paolovite, $Pd_2X$ (X = Sn, Sb, As), sobolevskite and hollingworthite.

**Pegmatoidal schlieren** are represented by a diverse group of PGM. Most common are PdBi-PdTe-PdSb, $PtBi_2$-$PtTe_2$-$PtSb_2$ systems, Sb-bearing insizwaite, Bi,Te-bearing geversite, Pd-bearing maslovite. Paolovite, Sb-bearing paolovite, and sluzhenikinite are also common.

**The veinlet-disseminated ores** are characteristic by occurrence of sperrylite, Pd and Ni arsenides, stibioarsenides, arsenostannides, stibiostannides, in chalcopyrite–pyrrhotite ores. Kotulskite, moncheite, cooperite, braggite, vysotskite, sperrylite, Fe–Pt alloys, kharaelakhite, sobolevskite, stibiopalladinite, laflammeite, and vymazalovaite are common for chalcopyrite-enriched ores. Ores with millerite, bornite, and pyrite contain Pd–Ag minerals: sopcheite, stromeyerite, thalhammerite, kravtsovite.

**Pyrrhotite breccia-like ores** are characteristic by **c**ooperite, sperrylite, Fe–Pt alloys, atokite, Bi-tellurides, and stibiostannides. While **chalcopyrite breccia-like ores** are dominant by cooperite, braggite, Fe–Pt alloys, insizvaite, geversite, sperrylite, moncheite, stumpflite, sobolevskite, kotulskite, merenskyite, stannopalladinite, sudburyite, and rarely with vysotskite.

The most common PGM in **low-sulphide ores** are: Pt and Pd sulphides - cooperite, braggite, vysotskite, kharaelakhite; Fe–Pt alloys, tellurobismuthides (kotulskite, sobolevskite, moncheite, merenskyite), stibnides (mertieite, stibiopalladinite), stannides (paolovite, atokite, taimyrite, stanopaldinite), plummbides (zvyagintsevite), arsenides (sperrylite), palladoarsenides (isomertieite), minerals with composition $Pd_2A$, $Pd_3A$, $Pd_5A_2$, $(Pd,Ni)_2X$, $(Pd,Ni)_5X_2$, where X = Sn, Sb, As. Rare minerals are törnroosite, hollingworthite and Ir–Os alloys.

This contribution is a tribute to Sergey F. Sluzhenikin (†2024). He dedicated most of his professional career to the geology of Norilsk`s deposits. We had a priviledge to describe jointly five new platinum-group minerals that were discovered in his findings.

The support from the Grant Agency of the Czech Republic (project No. 22-26485S) is greatly acknowledged.

## Platinum-group minerals of the Freetown Intrusion, Sierra Leone

Bowles, J.F.W.[1] and Suárez, S.[2]

[1] School of Earth and Environmental Sciences, University of Manchester, Manchester, M13 9PL, UK. john.bowles@uclmail.net

[2] Department of Geology, University of the Basque Country (UPV/EHU), 48940 Leioa and Ikerbasque, 48009 Bilbao, Spain.

---

The outcrop of the Freetown Intrusion, Sierra Leone, West Africa is represented by the Freetown Peninsula. The age of this layered mafic intrusion is 196-201 Ma, coincident with formation of the Central Atlantic Magmatic Province. The Atlantic margin of the West African Craton saw episodes of closure of earlier oceans evidenced by klippen and thrust slices as well as a suture that marks the latest line of closure. This suture provided a conduit for magma ascent as an open system with layering of the intrusion created by repeated magma injection. The intrusion continues to the west beneath the ocean; geomagnetic reversals indicate that intrusion took place over >1 Ma [1, 2].

Platinum-group minerals (PGM) are known to be present in streams draining the western side of the Freetown Peninsula. There was extraction of alluvial PGM from 1928 [3]. The closed canopy tree cover, the extensive lateritization and slow economic development prevented the source rocks from being identified for many years. We have demonstrated the existence of four PGE-bearing horizons that define the primary occurrence of the PGM. They contain fine-grained (<7 µm) disseminated PGM. The upper horizon (Horizon B) typically reaches 0.33 ppb Pt, 0.009 ppb Pd. It is the best exposed horizon with a thickness of 12 m and it has been followed along strike for 5.2 km [4, 5]. Fresh rock from Horizon B has Pt/Pd ~30 and the PGM are mainly cooperite (PtS) and isoferroplatinum ($Pt_3Fe$). The cooperite is found associated with titaniferous magnetite enclosed in interstitial amphibole (cannilloite). Both cooperite and isoferroplatinum are also found enclosed in chalcopyrite. Tulameenite ($Pt_2CuFe$), laurite ($RuS_2$), bowieite ($Rh_2S_3$) and Pt-Ir-Rh-Cu-Fe sulphides are present in minor amounts. All are disseminated with no sulphide-rich layer; chromite has not been seen. Horizon C lies some 75 m stratigraphically below Horizon B and is notable for higher Pd contents (Pt/Pd ~0.2) and the presence of Pd-Cu alloys including $PdCu_3$ (possibly nielsenite) [5]. Within weathered rock cooperite and isoferroplatinum have been altered to form reaction rims of Pt-Fe alloy with corona, symplectic and flame-like textures that include fine-grained Pt-Fe alloy with either Pt-Fe oxides or a mixture of Pt-Fe alloy and Fe-oxides [6]. Assays of saprolite derived from barren rock show PGE contents that demonstrate down-slope movement of PGE in solution [6]. The alluvial PGM differ significantly from the PGM found in the rocks. The larger size (mm) is immediately obvious. In addition, there are crystals of laurite/erlichmanite ($RuS_2/OsO_2$) and hexagonal platelets of Os-Ir-alloy attached to irregular masses of Pt-Fe alloy as well as cubes of Pt-Fe alloy. There are compositional variations from $Pt_3Fe$ to PtFe and, with the addition of Cu, towards tulameenite [7, 8, 9]. Internal variation in composition is commonplace. What is the relationship between the primary PGM and the PGM found in the alluvium?

*References:*

[1] Wells M (1962) Overseas Geol Min Res Bull Suppl 4:1-115
[2] Bowles J et al. (2024) J African Earth Sci 211:105160
[3] Pollett J (1931) Eng Mining World 2:747-748
[4] Bowles J (2000) Min Dep 35:583-586
[5] Bowles J et al. (2013) Can Min 51:455-473
[6] Bowles J et al. (2017) Min Dep 52:1127-1144
[7] Bowles J (2000) Min Mag 47:465-471
[8] Bowles J (1981) Bull Min 104:478-483

## Platinum-group minerals and gold particles from the Elbe, Germany

Junge, M.[1,2], Goldmann, S.[3], Wotruba, H.[4]

[1]Mineralogical State Collection (SNSB-MSM), Germany, junge@snsb.de

[2]Department of Earth and Environmental Sciences, Ludwig Maximilian University of Munich, Germany

[3]Natural Resources, Federal Institute for Geosciences and Natural Resources (BGR), Germany

[4]Mineral Processing Unit (AMR), RWTH Aachen University, Germany

---

In heavy mineral concentrates of the Elbe, gold and platinum-group minerals (PGMs) are observed. Two fractions (> 63 and < 63 µm) of the concentrate are analyzed by reflected-light microscopy, scanning electron microscopy with automated mineralogy software and electron microprobe analysis (EPMA). Other heavy minerals are cassiterite, ferberite, monazite, uraninite, columbite–tantalite, magnetite, zircon and cinnabar. Scanning electron microscopy determined the modal abundance of PGMs, gold and the other heavy minerals. The PGMs are mainly Os–Ir–Ru–(Pt) alloys, Pt–Fe alloys, sperrylite and rustenburgite. Compositional variation of PGMs and gold was analyzed by EPMA. This showed that Pt–Fe alloys are (1) native platinum (> 80 atom %), (2) ferroan Pt (20 atom % to 50 atom % Fe), (3) isoferroplatinum (2.64 to 3.04 apfu of sum PGE, platinum-group element), (4) tetraferroplatinum group with Ni + Cu + Fe ≈ 50 atom %, and (5) γ(Pt,Fe) with sum PGE > 3.04 apfu. The Os–Ir–Ru–(Pt) alloys show large compositional variations. Platinum and Fe enrichment is typically observed for Ir-rich Os–Ir–Ru alloys. Gold particles often show compositional zoning of Ag-rich cores and Ag-poor rims due to selective leaching of Ag. Similarly, Hg-rich rims of gold particles are analyzed. These are interpreted as the results of in situ amalgamation due to mobilization of Hg from the associated cinnabar particles. The size and shape of the gold particles generally argue for short transportation distances. Similarly, almost euhedral sperrylite and Pt–Fe alloys suggest a source region close to the sampling site. However, roundish Os–Ir–Ru–(Pt) alloys presumably have experienced longer transportation in the river. Gabbroic dikes of the Lusatia block contain sperrylite and gold particles [1], which can be the source for these particles found in the concentrate. The composition of the Os–Ir–Ru–(Pt) alloys is similar to previous studies on the Vestřev placer in Czech Republic [2]. Both locations are within the drainage area of the Elbe and can therefore be the source of the PGM and gold particles in the concentrate.

*References:*

[1] Járóka T et al, (2021) Ore Geol Rev 133:104055
[2] Pašava et al (2015) Ore Geol Rev 68:117–126

# Chemistry in 3D: Deep Learning Fusion of X-ray Datasets for Characterisation of Platinum Group Element Enriched Chromitite

Divers, M.[1,2], Einsle, J.F.[1], Dobson, K.J.[2,3], O'Driscoll, B.[4], Butcher, A.R.[5], Jolis, E.M.[6]

2251460d@student.gla.ac.uk

[1]University of Glasgow, School of Geographical & Earth Sciences; [2]University of Strathclyde, Department of Civil & Environmental Engineering ([3]Department of Chemical & Process Engineering); [4]University of Ottawa, Department of Earth & Environmental Sciences; [5]Hafren Scientific, UK; [6]Geological Survey of Finland, Circular Economy Solutions Research Laboratory.

---

Mafic/ultramafic layered intrusions are studied for their insights into open-system magmatism and platinum group element (PGE) mineralisation [1]. Laterally continuous chromitite seams found at macro unit boundaries form the most PGE rich subregions of layered intrusions, referred to as reef-type deposits [1]. The Unit 7/8 boundary chromitite seam of the Eastern Layered Intrusion (ELI) (Rùm, NW Scotland) provides an opportunity to study reef-type deposits in a relatively young and undeformed intrusion [2]. Additionally, the ELI chromitite seams exhibit "cone-structures" (**fig. 1a**) originally interpreted to be akin to fluid escape structures [2, 3], making them important features in understanding magma mixing and PGE mineralisation. X-ray computed tomography (XCT) offers an effective method for imaging the cone structures in 3D (**fig. 1a**). However, XCT is unable to easily quantify mineralogy and chemistry in highly heterogeneous samples. As such, scanning micro-X-ray fluorescence (µXRF) was used to chemically analyse the 2D surfaces of our sample (**fig. 1b**), enabling assessment of mineralogy and chemistry to trace quantities. Often, correlation of 3D and 2D datasets is performed qualitatively; however, in this study we use a convolutional neural network (CNN) to fuse the two datasets together, bypassing challenges with segmenting XCT data and minimising bias. This methodology has previously been pilot tested with limited volumes of data with moderate success [4].

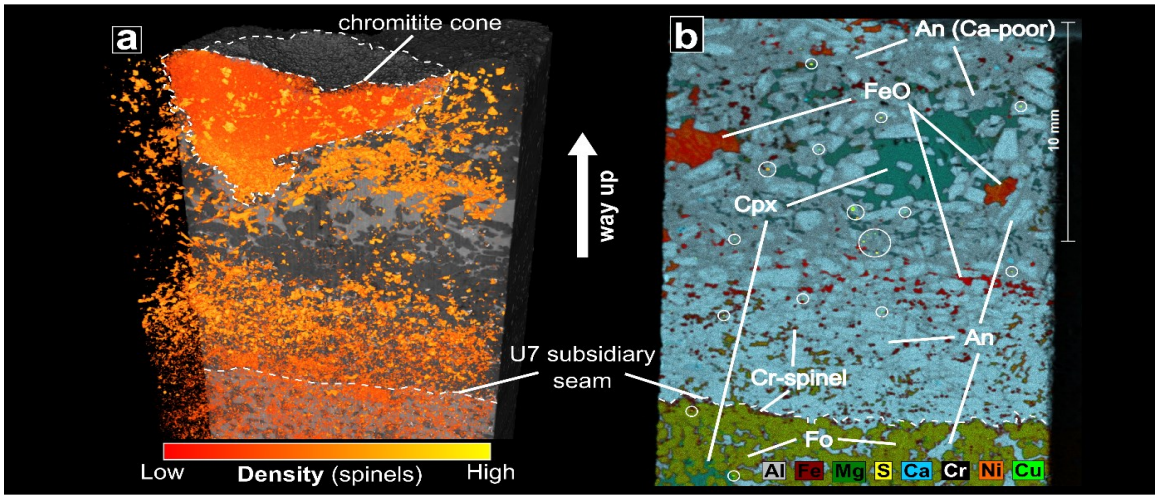


**Fig. 1** a) 50 keV monochromatic synchrotron XCT rendering. Sample is sliced with rendering of minerals Cr-spinel and denser. b) 50 kV µXRF image. Element maps overlain. Mineral abbreviations: An - anorthite, FeO - Fe-oxides/spinels, Cpx - clinopyroxene, Cr-spinel, Fo - forsterite. White circles indicate sulfide minerals (e.g. chalcopyrite, pyrrhotite, pentlandite).

We envisage this technique will allow greater understanding of chromitite cones than previously possible from standard petrographic studies. The results may allow us to predict the location of PGE minerals at a hand specimen scale to be further analysed using high resolution techniques.

*References:*

[1] Maier W. 2005. DOI: https://doi.org/10.1016/j.jafrearsci.2005.03.004; [2] O'Driscoll B. Emeleus C.H., Donaldson C.H., Daly, J.S. 2010. DOI: https://doi.org/10.1093/petrology/egq013; [3] Young I.M. 1984. DOI: https://doi.org/10.1180/minmag.1984.048.348.04; [4] Divers M., Einsle J.F., Dobson K.J. 2023. [Poster]. Available on request from leading author.

# The crystal structures of Pd-Ni arsenides: majakite (PdNiAs) and menshikovite ($Pd_3Ni_2As_3$)

Laufek, F.[1], Vymazalová, A.,[1] Chareev, D.A.[2], Grokhovskaya, T.L.[3], Kozlov, V.V.[3], Plášil, J.[4]

[1]Czech Geological Survey, Geologická 6, Prague 5, Czech Republic, frantisek.laufek@geology.cz

[2]Institute of Experimental Mineralogy, RAS, Chernogolovka, Moscow, Russia

[3]Institute of Geology of Ore Deposits, Petrology, Mineralogy and Geochemistry RAS, Moscow, Russia

[4]Institute of Physics ASCR, v.v.i., Na Slovance 2, 128 21 Prague 8, Czech Republic

---

Majakite, PdNiAs and menshikovite, $Pd_3Ni_2As_3$, were described as new minerals by Genkin [1] and Barkov [2], respectively. Majakite was found in intergrowths with other platinum minerals in chalcopyrite and thalnakhite ores of the Mayak mine (Talnakh deposit), menshikovite was discovered in mafic-ultramafic layered complexes Lukkulaisvaara and Chiney, Russia. A fragment of menshikovite extracted from a sample from Lukkulaisvaara intrusion, Russia, was used for a structure analysis of this mineral. As the natural majakite proved to be unsuitable for a structural analysis, crystal structure analysis was carried out on a synthetic phase PdNiAs.
The synthetic analogues of majakite and menshikovite were prepared using the Kullerud´s evacuated silica-glass tube method. Pure elements were used as starting materials for synthesis. The evacuated tube with charges were heated at 400 °C for several weeks. The experimental products were rapidly quenched in cold water.

The crystal structure of PdNiAs, a synthetic analogue of majakite, was solved from single-crystal X-ray diffraction data and refined to $R$ = 6.68 %. Synthetic PdNiAs shows *Pnma* symmetry and $a$ = 15.517, $b$ = 3.597 and $c$ = 6.017 Å unit cell. Its crystal structure contains a mackinawite-like blocks of edge sharing [$NiAs_4$] tetrahedra parallel to (001). Pd show unusual five-fold coordination resembling a tetragonal pyramid by As atoms. The coordination of Pd is further completed by close contacts with Ni and Pd atoms. Pd atoms are located in voids between blocks of [$NiAs_4$] tetrahedra. The structural identity between majakite and synthetic analogue PdNiAs was confirmed by comparison of powder X-ray diffraction patterns of majakite published by Genkin [2] and from our synthetic PdNiAs. Moreover, electron back-scattered diffraction (EBSD) patterns generated from our orthorhombic structure model fit very well to the measured patterns obtained from natural grains of majakite. Evstigneeva [3] determined a hexagonal structure for $Pd_{1.19}Ni_{0.81}As$ synthetic phase. It is very likely that the symmetry of phases within the $Pd_{1+x}Ni_{1-x}As$ composition depends on temperature and on Pd-Ni ratio.

Menshikovite crystal structure, $Pd_3Ni_2As_3$, was solved from single-crystal X-ray diffraction data and refined to $R$ = 10.30 %. The crystal structure was also refined from powder X-ray diffraction data using a synthetic analogue of menshikovite. Menshikovite crystalizes in *Cmcm* space group and shows and unit cell parameters $a$ = 15.728, $b$ = 6.000 and $c$ = 4.955 Å. Menshikovite crystal structure contains deformed [$NiAs_4$] tetrahedra. Each [$NiAs_4$] tetrahedra shares one edge with one adjacent tetrahedra along the **a**-axis and two opposing edges with adjacent tetrahedra along the **c**-axis forming chains of edge-shared [$NiAs_4$] tetrahedra running in 001 direction. Ni atoms have three close contacts with adjacent Ni atoms across the shared tetrahedral edges. Pd atoms show trigonal bipyramidal coordination by As atoms. The crystal structure of menshikovite also contains number of Ni-Ni and Pd-Ni close contacts.

*References:*

[1] Genkin et al (1976) Int Geol Rev 20:96-100
[2] Barkov et al. (2002) Can Mineral 40:679-692
[3] Evstigneeva et al. (2000) Mater Sci Forum 321-324: 700-704

# Experimental study of kotulskite solid solution

Kamenský, J.[1,2],Vymazalová, A.[1], Laufek, F.[1] and Tuhý M.[1,2]

[1]Czech Geological Survey, Prague, Czech Republic; jan.kamensky@geology.cz

[2]Institute of Geochemistry, Mineralogy and Mineral Resources, Faculty of Science, Charles University, Prague, Czech Republic

---

We have experimentally investigated the solubility of ternary elements in the synthetic analogue of kotulskite (PdTe) at 400 °C. Based on occurrences of kotulskite solid solutions at natural conditions we selected elements for experimental investigation. We performed the experimental runs in series of Pd–Te–X, with X = Ag, As, Bi, Cu, Sb, Sn, Se and Pb, at tie-line Pd50(Te50-X) with a compositional step from 5 to 10 at.%, up to the potential end member of solid solution.

For the purpose of this study silica-glass tube method was used. Experiments were performed in evacuated and sealed silica glass tubes in horizontal furnaces. Charges of about 300 mg were carefully weighed out from the native elements. The starting mixtures were first melted at 1000 °C, then, the run products were ground and reheated to 400 °C (for 3 to 4 months). Phases in the run products were characterized by X-ray powder diffraction and, in polished sections examined under reflected light and with electron-microprobe techniques (EPMA).

Our experimental results have shown the following maximum ranges of solid solutions: Kotulskite does not dissolve Ag at 400 °C. The maximum solubility of As in kotulskite is up to 3 at.%. Kotulskite dissolves up to 1 at.% Cu. Our investigations in the Pd-Sb-Te system confirmed the continuous solid solution (ss) between sudburyite (PdSb) and kotulskite (PdTe). This is in agreement with the experimental study of [1] at 400 °C, and also at 600 °C by [2]. It also supports the observation from natural occurrences showing the formation of kotulskite – sudburyite series. Kotulskite forms an extensive solid solution with Pb, dissolving up 30 at.% Pb [3]. Kotulskite dissolves up to 19 at.% Sn as suggested by [4]. It dissolves up to 10 at.% Se. The experimental series with Bi have shown that sobolevskite (PdBi) and kotulskite (PdTe) do not form a complete solid solution at 400 °C. The solution breaks with the composition of $Pd_{50}Bi_{40}Te_{10}$, indicating that kotulskite dissolves up to 40 at.% Bi and sobolevskite up to 2 at.% Te.

We have assessed the maximum solubility of selected elements in kotulskite. We also studied the dependance of unit-cell parameters on solubility and incorporation of ternary elements in the kotulskite structure.

Financial support through the Project No 22-26485S from the Grant Agency of the Czech Republic (GACR) is gratefully acknowledged.

*References:*

[1] El-Boragy M and Schubert K (1971) Int J Mater Res 62:314-323
[2] Kim W S and Chao G Y (1991) Can Mineral 29:401-409
[3] Vymazalová A and Drábek M (2011) Can Mineral 49:1679-1686
[4] Vymazalová A and Drábek M (2010) Can Mineral 48:1051-1058

## CARBONATITES: A Key Resource for REE

Giebel, R.J.[1]

[1]Technische Universität Berlin, Department of Applied Geochemistry, Ernst-Reuter-Platz 1, D-10587 Berlin, Germany, r.j.giebel@tu-berlin.de

---

Carbonatites are magmatic rocks (melts of mantle origin) with a carbonate content of at least 50 modal%. They are relatively rare rocks with around 609 occurrences worldwide [1]. Nevertheless, they are important economic targets that serve as a significant resource for numerous commodities, including a number of critical raw materials [2]. In contrast to other rock occurrences, where the occurrence/ mine-ratio is typically 1:1000, carbonatites feature an occurrence/mine-ratio of 1:10, with around 60 of the 609 carbonatite occurrences being mined or at least under exploration. In addition to carbonates, carbonatites are usually rich in apatite, which makes them an important target for phosphorus (e.g. Siilinjärvi, Finland and Kovdor, Russia). Fluorite and magnetite contents can also significantly exceed cut-off grades, occasionally resulting in world-class fluorite and iron deposits (e.g. Okorusu, Namibia and Palabora, South Africa). Further important, but smaller (or only rarely present) resources can be identified for Zr, Cu and vermiculite, for example. However, carbonatites are certainly best known for their high potential to exhibit elevated concentrations of Nb and REE (in particular LREE). The world´s largest Nb deposits (Morro dos Seis Lagos [not mined], Araxá and Catalão, all Brazil, and the Niobec Mine, Canada) are carbonatites. The world´s largest producer for REE (Bayan Obo, Maoniuping, Weishan, all China, and Mountain Pass, USA) are carbonatites as well. In particular, REE are omnipresent in most carbonatites, with some reaching economic concentrations, making carbonatites a preferred exploration target for REE projects. Most commonly, economic REE concentrations are found either in highly evolved dolomite or ankerite carbonatites or in hydrothermal overprinted portions where REEs are redistributed and accumulated by remobilization from the primary rock. Studies of mineralized and barren carbonatites show that the enrichment of REE depends on several factors that may favour/support or inhibit the accumulation of REE in a carbonatitic melt. Contamination of carbonatitic melt by silicate wall rock material can cause both, early consumption of REE by non-REE minerals (e.g., apatite; consequence: prevention of REE enrichment in more evolved melts, [3]) and late-stage mobilization of REE by supported ligand transportation at lower temperatures (e.g., $SO_4$-complexes that are most effective in Si-saturated hydrothermal fluids, [4]). However, not only the enrichment of REE in carbonatites plays a role in economic feasibility, but also the formation of certain processable REE minerals that must occur in dominant quantities (the formation of only one REE phase or as few different REE phases as possible is advantageous). This highlights that multiple parameters need to be considered to understand REE enrichment or depletion in carbonatites and their economic viability.

*References:*

[1] Humphreys-Williams ER and Zahirovic S (2021) Elements 17(5): 339-344
[2] Simandl GJ and Paradis S (2018) Appl Earth Sci 127(4): 123-152
[3] Giebel RJ et al. (2019) J Pet 60(6): 1163-1194
[4] Cui et al. (2020) Geology 48(2): 145-148

## Precious and base metal sources and enrichment processes in a proto-arc VMS system

Belgrano, T.M.[1,2] Milton, J.A.[2], Diamond, L.W.[3], Wolf, R.C.[3], Teagle, D.A.H[2]

[1]UCD School of Earth Sciences, University College Dublin, Ireland Email: thomas.belgrano@ucd.ie

[2] School of Ocean and Earth Science, National Oceanography Centre Southampton, University of Southampton, UK

[3]Institute of Geological Sciences, University of Bern, Switzerland

---

Intra-oceanic subduction initiation marks the transition between the mature divergent and convergent stages of the Wilson cycle, each with its distinct and relatively well understood metallogeny. The metallogenic systematics of the transition, however, are less clear, with uncertainties regarding controls on Au endowment in proto-arc volcanogenic massive sulfide (VMS) deposits and the potential for magmatic–hydrothermal ore formation. The lavas of the Samail ophiolite (Oman) formed during Tethyan subduction initiation and host VMS deposits with Au/Cu ratios that increase up through the volcanostratigraphy. Our new analyses of volcanic glasses reveal this increase is closely paralleled by Au/Cu ratios in the footwall lavas, implying a footwall source compositional control on proto-arc VMS Au endowment.

Supporting trace element analyses and magmatic modelling indicate that Au enrichment of the boninites was enabled by sulfide-undersaturated fractionation. This occurred due to remelting of mantle that had already lost most of its sulfide during production of MORB-like melts earlier in the subduction initiation sequence. The early melting left a refractory residue with high Au/S and high Au/Cu, which was completely extracted during the later remelting to produce boninites with similar characteristics. Despite $H_2O$ enrichment in the boninites, low S contents may have suppressed efficient magmatic–hydrothermal extraction and transport of Au and Cu, thereby limiting magmatic–hydrothermal input to the VMS deposits. Subduction maturation and the re-fertilization of the wedge with S and metals by mantle corner flow would then have been necessary to produce melts capable of forming magmatic–hydrothermal ore deposits. This stage that was not reached prior to detachment of the Samail lithosphere but was by many other well-endowed Tethyan and circum-Pacific arcs. The Samail ophiolite thus provides a record of subduction initiation metallogeny and elucidates the ‘starting gun’ for porphyry-type mineralization in nascent arcs.

## Prerequisites for large SMS deposits along slow-spread mid-ocean ridges: implications for the Polish contract area at the MAR (26–33°N)

Ciazela, J.[1], Kozłowska-Roman, A.[2], Tomczak, M.[2] Elsherif, E.[1], Wozniak, W.[1] and Wojtulek, P.[3]

[1] Institute of Geological Sciences, Polish Academy of Sciences, ul. Podwale 75, 50-449 Wrocław, Poland; e-mail: j.ciazela@twarda.pan.pl

[2] Polish Geological Institute – National Research Institute, ul. Rakowiecka 4, 00-975 Warsaw, Poland

[3] Institute of Geological Sciences, University of Wrocław, M. Borna 9, 50-204 Wrocław

---

Slow-spreading ridges host much larger seafloor massive sulfide (SMS) deposits than fast-spreading ridges. The highest-tonnage SMS deposits are hosted in plutonic rocks from oceanic core complexes (OCC), which expose the lower crust and mantle uplifted to the seafloor along detachment faults at slow-spreading ridges. All seven contractors of the International Seabed Authority for sulfide exploration, including Poland, operate on slow- to intermediate-spreading ridge segments with OCCs.

The slow-spread oceanic crust is thinner and often more heterogeneous than the fast-spread oceanic crust. The structural differences affect sulfide differentiation during magmatic processes and metal transport between the mantle and the ocean floor. In large gabbroic bodies of the Atlantis Bank OCC (57°E, Southwest Indian Ridge), sulfides differentiate mainly through fractional crystallization. Sulfides fractionate early and accumulate at the lower part of gabbroic bodies. In the Kane Megamullion OCC (23°N, Mid-Atlantic Ridge) with low magma supply, sulfides typically differentiate through melt-mantle reaction, which leads to high sulfide enrichment at the contacts of gabbro and peridotite, often shallow under the ocean floor. This enrichment in melt-mantle reaction might explain why most large SMSs occur along slow-spread oceanic lithosphere with relatively low magma supply.

In this study, to understand the migration of metals from the mantle to the seafloor and the formation of seafloor massive sulfide deposits along the slow-spreading ridges, we also incorporate data from the Oman Ophiolite and the Central Sudetic Ophiolite (CSO). CSO is a well-preserved slow-spreading ridge-related ophiolite with a lithosphere architecture similar to the Polish sulfide exploration area along the 26–33°N Mid-Atlantic Ridge (Elsherif et al., this issue; Woźniak et al., this issue). Therefore, our results will aid in searching for SMSs within the Polish contracted area, where a low magma supply shapes the lithosphere structure. The first Polish expedition in the Summer of 2022 performed acoustic imaging, including multi-beam bathymetry and backscatter supported with sub-bottom profiling to characterize three known OCCs (Atlantis Massif, the Southern OCC, Dante's Domes) and two new OCCs in the area. These sites' precise bathymetry (25 cm/pixel) and geophysical features have been investigated using Autonomous Underwater Vehicles since last year, and the first samples will be collected with remotely operated vehicles in 2025.

Funded by National Science Centre Poland (grant no 2021/43/B/ST10/03343).

# Ore resources on Mars: comparative study of 16 martian meteorites

Fitt, M.[1], Ciazela, J.[1], Mojzsis, S.[2], Lazarov, M.[3], Junge, M.[4], Kaliwooda, M.[4], Jokubauskas, P.[5], Szczęśniewicz, M.[6], Pańczyk, M.[7], and Lei, Ch.[8]

[1]Institute of Geological Sciences, Polish Academy of Sciences, Poland, e-mail: m.fitt@twarda.pan.pl

[2]Research Centre for Astronomy and Earth Sciences, HUN-REN, Hungary;

[3]Institute of Mineralogy, Leibniz Universität Hannover, Germany;

[4]Mineralogical State Collection, LMU Munich, Germany;

[5]Faculty of Geology, University of Warsaw, Poland;

[6]Faculty of Geoengineering, Mining and Geology, Wroclaw University of Science and Technology, Poland;

[7]PIG-PIB, Warsaw, Poland;

[8]School of Earth Sciences and Resources, China University of Geosciences (Beijing), China.

---

Understanding the geology and formation of ore deposits – new constraints on the enrichment processes of metals.

Until August 2023, ~350 meteorites on Earth were confirmed to be martian, compared to only 25 specimens in 2000 [1]. Their constantly growing number, along with the availability of remote sensing data, allows for extensive research to estimate Mars's ore potential. Herein, we report on investigating a set of 16 ore-bearing martian meteorites, covering all lithologies sampled so far, which we analysed using ore microscopy, electron microprobe, laser ablation, and secondary ion mass spectrometer. We determined major element and trace metal contents in various mineral phases to estimate the potential for Cu-Ni-PGE deposits on Mars. $^{34}S/^{32}S$ ratio in sulfides was measured to distinguish between the hydrothermal and mantle sources of sulfur.

Our samples include ten shergottites: four basaltic [46.3–75.6 vol.% clinopyroxene (Cpx), 19.3–44.4% maskelynite (Mask), 1.6–4.3% merrillite (Mer), 0.8–2.4% oxides (ox): titanomagnetite (Ti-Mag), and ilmenite (Ilm), 0.2–1.4% pyrrhotite (Pyh)], three olivine-phyric [45.7–70.1% Cpx, 10.9–38.1% olivine (Ol), 14.9–18.0% Mask, <1.1% Mer, 0.7–3.6%, ox (Ti-Mag, Ilm, Chr – chromite), 0.3–2.7% Pyh +Pentlandite (Pn) grains], three poikilitic [32.6–48.0% Ol, 38.0–48.4% Cpx, 9.6–13.2% Mask, 0.5–1.5% Mer, 3.0–3.3% Ox (Ti-Mag, Ilm, Chr), 0.9–1.1% Pyh with Pn exsolutions], three nakhlites [76.1–83.3 vol.% Cpx, 1.8–10.6% Ol, 7.1–17.8% mesostasis (Meso), 0.8–3.9% Ti-Mag, 0.2–0.4% Pyh], one chassignite [95.0 vol.% Ol, 1.2% Cpx, 0.7% plagioclase (Pl), 1.7% Meso, 1.3% Chr, <0.1% pyrite (Py)], two pieces of orthopyroxenite [95.4 vol.% orthopyroxene, 2.6% Mask, 0.3% Mer, 1.7% Chr, and <0.1% Py], and one regolith breccia comprised of various basaltic and impact melt glass clasts.

Nickel content in the olivine of terrestrial mantle peridotites is ~2500 ppm [2], but it does not exceed 1000 ppm in our samples. Such low values and the rarity of Ni-bearing minerals indicate the depletion of the martian mantle in nickel compared to the Earth's. The dominance of Fe sulfides (pyrrhotite) points towards high Fe enrichment of martian magma, while its $\delta^{34}S$ value −1.0 to +2.5, similar to MORB basalts [3], indicates their primarily magmatic origin. Apart from primary magmatic features, nakhlites, breccia, and orthopyroxenite show some degree of alteration due to the post-magmatic hydrothermal activity manifested by veins and secondary mineral assemblages such as hydrothermal pyrite in regolith breccia NWA 7034. In the near step, remote sensing data will help us to determine the spatial distribution of presumed ore deposits and provide new insights into ore-forming processes in the martian lithosphere.

National Science Centre Poland funded this research with grant no. 2020/37/B/ST10/1420.

*References:*

[1] International Society for Meteoritics and Planetary Science (2023) Meteoritical Bulletin Database, https://www.lpi.usra.edu/meteor/

[2] Herzberg et al. (2016) American Mineralogist 101: 1952-1966

[3] Greenwood et al. (1997) Gechim. Cosmochim. Acta 61: 4449-4453

# Mineral chemistry and texture of metasomatic mica in halos around the Leinster spodumene pegmatites, Ireland

Geiger, E.J.[1,2], Brodbeck, M.[2], Menuge J.F.[1,2] and Nazari-Dehkordi, T.[2]

[1]SFI Research Centre in Applied Geosciences (iCRAG), Ireland

[2]School of Earth Sciences, University College Dublin (UCD), Belfield, Dublin, Ireland

---

Lithium has been widely recognized by governments, economists and researchers as a strategic and critical metal, representing a central commodity for the clean energy transition [1,2]. Currently, most Li is mined from hard rock sources, the most important source being spodumene pegmatites [3]. The crystallisation of spodumene pegmatites is complex and involves exsolution of magmatic-hydrothermal fluid. The formation of exomorphic metasomatic halos in country rock around pegmatites is related to this process and typically involves loss of Li, Rb, Cs, Sn, Ta, B and other metals from the crystallising pegmatite. However, timing, frequency and fracture mechanisms of fluid expulsion remain poorly understood. In addition, the mineralogy, mineral chemistry and texture of halo lithologies have received little research attention and are therefore the focus of this presentation.

In South Leinster, Ireland, barren and spodumene pegmatites intrude the East Carlow Deformation Zone, a major ductile shear zone running along the eastern margin of the late Caledonian Leinster batholith. In the study area Moylisha, the majority of pegmatites intrude the porphyritic granite/ granodiorite of the Tullow Lowlands Pluton. Relatively narrow halos with pervasive metasomatism are developed at the contacts to spodumene pegmatites. They can extend up to 80 cm but are usually 10-20 cm thick. However, halo mineralization is also visible in mm-scale veinlets in samples from up to 8 m distance to the contact. The halo chemical signature in these occurrences is essentially restricted to lithium micas, which develop in the host granite at the expense of original mica and feldspar. Through a combined analytical approach of detailed optical petrography, quantitative analysis, and mapping by both scanning electron microscope (SEM) and laser ablation inductively coupled mass spectrometry (LA-ICP-MS) as well as spot analysis, we characterised the mineral chemistry and texture of proximal mica immediately adjacent to the granite contacts and in veinlet-hosted samples up to 8 m distal to the contact. Petrographic observations reveal a relative increase of the mica content in halo samples. The dominant phase is a pale brown ferroan muscovite, which with increased distance from the contact is accompanied by dark brown siderophyllite. Muscovite is seen to replace both dark mica and feldspar in the samples. Grains of white mica often contain small specks of residual dark mica, but otherwise appear homogeneous. Optically invisible complex zoning of both white and dark mica is visible in the LA-ICP-MS maps. The zoning pattern is most clearly defined for Cs, Rb, Ba and Sn, while Li is comparatively homogeneous. Concentric zoning is observed in white mica that are believed to be completely newly formed, with the highest concentrations located in the core region. Other grains exhibit more complex zoning, often with sharply defined core areas that seem to represent pristine compositions of the original micas. These observations appear to indicate a complex process where multiple pulses of fluid with different compositions were released into the country rock.

*References:*

[1] European Commission (2023) Publications Office of the European Union: 154p
[2] Bibienne et al. (2020) Elements 16: 265-270
[3] USGS (2024) Mineral Commodity Summaries: 110-111

## The Partitioning of Lithium between Granitic Minerals and Melts

Horányi, B.[1], Gaillard, F.[1], Gion A.M.[2], Gloaguen É.[3], Melleton J.[3], and Plunder A.[3]

[1]Institute des Sciences de la Terre d'Orléans, CNRS, BRGM, Univ. Orléans, UMR 7327, Orléans, France

[2]Department of Earth Sciences, University of Oxford

[3]BRGM, Orléans, France

---

Lithium is a high-demand, critical metal used in the production of modern-day technologies. Peraluminous granites and pegmatites are the source of approximately half of the world's Li supply [1]; therefore, it is important to constrain the genetic model of these bodies to aid with the exploration of new ore deposits. Lithium may become enriched in felsic melts during the partial melting of metasediments and subsequent fractional crystallization, which are processes that concentrate incompatible elements in the melt. The degree of Li enrichment during these processes can be estimated by considering mineral-melt partition coefficients ($D_{Li}^{Mineral-Melt}$); however, these are poorly constrained in felsic systems. In order to better constrain the behaviour of Li in felsic systems, crystallization experiments were performed on peraluminous rhyolites in an internally-heated pressure vessel at 600-675°C and 300 MPa. The high mobility of $Li^+$ and the lack of mineral zonation demonstrates that equilibrium was attained in the experiments. Mineral-melt partition coefficients of Li were determined for quartz, plagioclase, k-feldspar, biotite, and muscovite by laser ablation inductively coupled plasma mass spectrometry (LA-ICP-MS). Lithium is strongly incompatible in feldspars, moderately incompatible in quartz, and slightly incompatible in micas. Variations in partition coefficients are a complex function of mineral and melt composition. The partitioning of Li into quartz is controlled by the coupled substitution of $Li^+$ and $Al^{3+}$ with $Si^{4+}$. The concentration of Al in quartz is in turn a function of the aluminium saturation index (ASI), which is the molar ratio of aluminium to alkali metals and Ca in the melt ($Al_2O_3/(Li_2O+Na_2O+K_2O+CaO)$). Consequently, alkali-rich melts have a lower ASI, less Al in quartz, and hence a lower $D_{Li}^{Quartz-Melt}$. In the case of Li-rich melts, which are normally considered to be peraluminous, the effect of including Li in the calculation of ASI becomes pronounced above Li concentrations of ~3000 ppm, wherein the melt becomes metaluminous. The low ASI of Li-rich granites and pegmatites is consistent with the low $D_{Li}^{Quartz-Melt}$ in experiments on Li-rich felsic melts [2]. The effect of mineral composition on $D_{Li}^{Mineral-Melt}$ is also pronounced in the micas. Lithium is enriched in Fe and F-rich muscovite and Al and F-rich biotite, which is consistent with the substitution mechanism of Li in mica solid-solution series [3]. Contrary to quartz and the micas, the Li content of feldspars does not vary as a function of mineral composition. The evolution of $D_{Li}^{Mineral-Melt}$ as a function of mineral and melt composition can be used to determine the enrichment of Li in granites and pegmatites. The fractionation of pre-enriched melts (2000 ppm Li) by 65% crystallization can produce economic grade granite and pegmatite deposits with over 5000 ppm Li. The experimental and modelling results demonstrate that the genesis of Li-rich felsic melts is a multi-step process, involving the pre-enrichment of Li by the partial melting of Li-rich metasediments, followed by the moderate fractionation of these melts.

*References:*

[1] Benson T et al. (2017) Nature Communications 8:270
[2] Pichavant M (2022) Journal of Petrology 63:1-28
[3] Tischendorf G (2007) Mineralogical Magazine 71:285-320

## Examining the relationship between Organic matter-rich Cenomanian-Turonian limestones and base metals in the Kebbouch South Pb-Zn deposit (Diapirs zone, Northern Tunisia): insight from LA-ICP-MS trace element analysis

Jaballah, S.[1], Jemmali, N.[2, 3] , McClenaghan, S.[4] , Rddad, L.[5] and Henchiri M.[2]

[1]University of Tunis El Manar, Faculty of Sciences of Tunis, Laboratory of Geodynamic, Geonumeric and Geomaterials. sammoura.jaballah@gmail.com /corresponding author.

[2]University of Gafsa, Faculty of Sciences of Gafsa, Sidi Ahmed Zarrouk, 2112 Gafsa, Tunisia

[3]Laboratory of Useful Materials, National Institute of Research and Physico-Chemical Analysis, 2026 Technopole of Sidi Thabet, Tunisia

[4]Trinity College Dublin, Raw Materials Characterization Laboratory iCRAG, Department of Geology, College Green, Dublin 2, Ireland

[5]Earth and Planetary Division, Department of Physical Sciences, Kingsborough Community College of the City University of New York, 2001 Oriental Boulevard NY 11235-2398, Brooklyn, New York, USA

---

The Kebbouch South Pb-Zn ore deposit is situated in the Triassic Diapirs zone of the Tunisian Atlas. It comprises two primary ore types with differing mineral assemblages. Type 1 stratabound ores are hosted in the Triassic to Cretaceous transition breccia zone (caprock). These ores are characterized by mineralization comprising marcasite, pyrite, galena, sphalerite, and celestite. These are capped by organic matter-rich limestones of the Upper Cenomanian-Lower Turonian Bahloul Formation. Type 2 stratiform mineralization occurs within laminated black limestone of the Bahloul Formation which contains disseminated sphalerite and galena associated with diagenetic framboidal pyrite. Gangue minerals in this ore type comprise calcite, celestite, and quartz. Petrographic examination and microanalysis of the black laminated limestone reveals the presence framboidal pyrite and organic matter embedded within the carbonate matrix. Furthermore, LA-ICP-MS analysis of diagenetic framboidal pyrite and carbonate fractions reveal trace-element enrichments in Pb, Zn, As, Cd, Cr, Ni, and Co. Of particular significance are the notably high concentrations of Pb and Zn, reaching up to 10078 ppm and 19147 ppm, respectively in diagenetic pyrite, with similar concentrations reported in the carbonate matrix (Pb up to 2445 ppm, Zn up to 67475 ppm). Considering this metal endowment, we suggest that organic matter in the Bahloul Formation plays two roles both as metal supplier and a reservoir for ore deposition. Moreover, organic matter in this formation also serves as a reducing agent, resulting in dissolved Triassic sulfates to be reduced to hydrogen sulfide, likely via bacterial sulfate reduction. The juxtaposition of the organic matter-rich Bahloul Formation and salt-bearing Triassic diapirs create a favorable geochemical setting for the genesis of Pb-Zn ore in Kebbouch South. Organic matter-rich rocks have long been considered a potential source of Pb and Zn in the MVT ores of Tunisia, as observed in mining districts such as Bou Grine [1, 2], Slata and Guern Halfaya [3], and El Akhouat [4].

*References:*

[1] Montacer et al. (1988) Org Geochem 13: 423–431.
[2] Bechtel et al. (1998) Chem Geol 144: 1-21
[3] Rddad et al. (2019) Ore Geol Rev 113:103070
[4] Jemmali et al. (2022) Min Petrol 116:71-91

# The role of trisulfur radical ion in the transport of molybdenum by hydrothermal fluids

Kokh, M.A.[1,2], Wilke, M.[2], Klemme S.[1] and Pokrovski G.S.[3]

[1]University of Münster, Institut für Mineralogie, Corrensstraße 24, D-48149 Münster, Germany kokh@uni-potsdam.de

[2]Universität Potsdam, Institut für Geowissenschaften, Campus Golm, Haus 27, Karl-Liebknecht-Str. 24-25, D-14476 Potsdam, Germany

[3]Géosciences Environnement Toulouse, Université Toulouse III, GET-CNRS-OMP-UPS-IRD-CNES, 31400 Toulouse, France

---

Knowledge of the chemical speciation of molybdenum in hydrothermal-magmatic fluids is a key to understanding the formation of porphyry deposits, which are the primary economic source of molybdenum. Previous studies have invoked various Mo complexes such as (hydrogen)molybdate ions ($HMoO_4^-$, $MoO_4^{2-}$) and their ion pairs with alkalis (*e.g.*, $NaHMoO_4^0$, $KHMoO_4^0$) in S- and Cl-poor fluids, oxy-chloride species ($MoO_mCl_n^{(6-2m-n)-}$) in strongly acidic saline fluids, or thio-molybdate complexes (e.g., $MoS_4^{2-}$, $MoOS_2^0$) in reduced $H_2S$-bearing fluids and vapors [1-6]. However, these available data are unable to account for the massive transport of Mo in porphyry-related fluids revealed by natural fluid inclusion analyses demonstrating 100s ppm of Mo (*e.g.*, [7]). A potential missing ligand for Mo may be the trisulfur radical ion, $S_3^{\bullet-}$, which is predicted to be abundant in sulfate-sulfide $H_2S/SO_4^{2-}$ rich acidic-to-neutral porphyry-like fluids [8]. To explore the effect of $S_3^{\bullet-}$ on Mo transport, we performed in situ X-ray absorption spectroscopy measurements at the Mo K-edge (20.0 keV) in hydrothermal autoclaves available at BM30 beamline of the ESRF synchrotron and at P65 beamline of the DESY synchrotron [9-10], to study the molybdenite ($MoS_2$) solubility in model $S_3^{\bullet-}$-bearing aqueous solutions. We found that Mo can efficiently be transported by $S_3^{\bullet-}$-bearing fluids at concentrations of 1-10 ppm, whereas the available data on OH-Cl-S complexes predict much smaller Mo concentrations at our conditions (<0.01 ppm). The observed solubility increase can be quantitatively described by the following chemical reaction, with formation of a mixed sulfide-trisulfur complex: $MoS_2$ (s) + $H_2S$ (aq) + $S_3^{\bullet-}$ + 0.5 $O_2$ (aq) = $MoS_3(S_3)^-$ + $H_2O$ (liq), with an equilibrium constant value $\log_{10}K$ of 14.3 ± 0.3 at 300°C and 500 bar. Our experiments point to polysulfide ions as important carriers of Mo in hydrothermal fluids, disregarded so far, that would require future systematic studies over the range of temperature, pressure and fluid composition.

*References:*

[1] Minubayeva & Seward (2010) GCA 74: 4365–4374
[2] Borg et al. (2012) GCA 92: 292–307
[3] Kokh et al. (2016) GCA 187: 311–333
[4] Kokh et al. (2017) GCA 197: 433–466
[5] Dadze et al. (2018) J. Chem. Eng. Data 63: 1827-1832
[6] Liu et al. (2020) GCA 290: 162–179
[7] Kouzmanov & Pokrovski (2012) Soc. Econ. Geol. Spec. Pub. 16: 573–618
[8] Pokrovski and Dubessy (2015) Earth Planet. Sci. Lett. 411: 298–309
[9] Testemale et al. (2005) Rev. Sci. Instrum. 76: 043905
[10] Klemme et al. (2021) Rev. Sci. Instrum. 92: 063903, 1–6

Funding: Deutsche Forschungsgemeinschaft WI 2000/25-1, KL 1368/13-1, SCHM 2415/6-1, ESRF ES-1050, DESY I-20220251, Agence nationale de la recherche (France) ANR-16-CE31-0017.

## Critical raw materials contents in Fe-Mn crusts from Canary Island Seamount Province: controls of the mineralogy and environment

Marino, E.[1], González, F.J.[1], Medialdea, T.[1], Somoza, L.[1], Lobato, A.B.[1], Reyes, J.[1] and Bellido, E.[1]

[1] Geological Service of Spain (IGME-CSIC), Madrid, Spain, e.marino@igme.es

---

Ferromanganese crusts are found in all the oceans and seas of the world covering hard substrates on seamounts and banks at water depths ranging between 250 and up to 5000 m growing during several million years. Due to their slow growth rates and their mineral these mineralizations have been proved to be an important potential source of different critical and strategic elements especially cobalt, nickel, copper, vanadium, molybdenum, tellurium and Rare Earth Elements plus yttrium (REY).

The investigation on Fe-Mn crusts from Canary Islands Seamounts Province (CISP) allowed identify in which minerals the different elements are concentrated and how the environment could affect the concentration of some of them. Forty-two Fe-Mn crusts recovered on eight different seamounts have been studied in this area, allowing the acquisition of a very comprehensive knowledge of the different genetic processes and element concentration in the different minerals forming CISP ferromanganese deposits. High resolution mineralogical and geochemical analyses show that vernadite is the main mineral enriched in critical elements like manganese, cobalt, vanadium, molybdenum, tellurium and REY (respectively in average 18 wt. %, 4800, 1000, 450, 60 and 3000 µg/g), while manganese, nickel and copper are mostly enriched in buserite/asbolane (respectively in average 45, 5 and 2 wt. %) with less contents cobalt and REY.

The geochemical studies together with the location of the different samples evidence a correlation between the depth and the REY contents in vernadite rich samples. Shallowest Fe-Mn crusts, around 2000 m water depth, show the highest REY contents (up to 3800 µg/g) that slowly decrease to contents of 2600 µg/g at depths of 3100 m in samples faced to the north. On the other hand, samples recovered at higher water depths (4800 m) but faced to the south show REY contents of 3500 µg/g. This behaviour on REY contents in CISP Fe-Mn crusts depends on 1) the action of a thick oxygen minimum zone due to the high fertilization of the ocean that allow the concentration of dissolved REY that slowly enrich the shallowest samples, and 2) the presence of a bottom water mass enriched in REY that influence Fe-Mn crusts composition at higher depths.

## The Geyer SW tin skarn deposit, Erzgebirge, Germany: mineral chemistry records changing fluid/rock ratios and metal fluxes

Meyer, N.*[1], Burisch, M.[2,3], Gutzmer, J.[3] and Markl, G.[1]

[1]Eberhard Karls Universität Tübingen, Fachbereich Geowissenschaften, Petrologie und mineralische Rohstoffe; Nicolas.meyer@uni-tuebingen.de

[2]Mineral Systems Analysis Group, Department of Geology and Geological Engineering, Colorado School of Mines

[3]3Helmholtz-Zentrum Dresden-Rossendorf, Institute Freiberg for Resource Technology Germany

---

Textural, mineralogical, and geochemical characteristics of skarn systems worldwide have been extensively studied, but little attention has been paid to the minor and trace element chemistry of minerals in tin skarns. The Geyer SW tin skarn system, located in the central part of the Erzgebirge, Germany, comprises an early skarnoid stage (stage I, ~320 Ma) and a second, younger metasomatic stage (stage II, ~305 Ma). It is a typical example of a stratabound and laterally extensive system of skarn units. The present study provides detailed chemical data of skarn minerals of this deposit, giving important insight into the origin of polyphase Sn-skarn systems.

The anhydrous skarn stage I at Geyer SW is represented by skarnoids formed by contact metamorphism of marly, reactive lithologies under low fluid/rock ratios and with only low concentrations of Sn. The early assemblages of metasomatic stage II are marked by the presence of two generations of stanniferous garnet, clinopyroxene, members of the titanite-malayaite solid solution, vesuvianite and minor amphibole. Aluminous garnet, clinopyroxene, titanite and vesuvianite display characteristics of minerals forming under low fluid/rock ratios; they show elevated concentrations of HFSE and REE distributions governed by their individual partition coefficients. In contrast, high fluid/rock ratios lead to enhanced incorporation of W, In, and Sn in observed in metasomatic garnet, malayaite, and amphibole and the trace and REE element signatures appear to mimic the signature of the magmatic-hydrothermal fluid. Texturally and mineral chemically, two major fluid fluxes were identified in the anhydrous skarn stage II with an oscillation between rock and fluid buffering. During these changes, tin was remobilized from earlier Sn-rich silicates and re-precipitated as malayaite because of the limited capacity of grossular-rich garnet to incorporate Sn in their crystal lattice. The hydrous skarn stage II continues with the formation stanniferous epidote and amphibole originating from a magmatic-hydrothermal fluid in a clearly fluid-buffered environment. An increasing proportion of meteoric water and decreasing temperatures during the waning phase of stage II lead to the formation of cassiterite, low-Sn amphibole, chlorite, and sulphide minerals; very late-stage remobilization of tin lead to the replacement of cassiterite by stokesite. Minor and trace element compositions (including REE patterns) of cassiterite formed during stage II are very similar, even if host rock and gangue minerals vary, suggesting a fluid-dominated system and a similar precipitation mechanism.

Major and trace elements of major skarn forming minerals are, hence, powerful tools to understand the change between rock- and fluid-buffered conditions during formation of a tin skarn. They also record the influx, the distribution and the remobilization of tin in various solid phases which are governed by various episodes of magmatic and magmatic-meteoric fluids in tin skarn systems.

# Overprinting of primary magmatic signature by fluid-driven processes in a F-bearing system: The Mueilha granite (Central Eastern Desert, Egypt)

Michaud, J. A-S.[1], Holtz, F.[1], Kontak, D. J.[2], Goldmann, S.[3], Abu El-Rus, M.[4]

[1]Institute of Mineralogy, Leibniz University Hannover, Germany

[2]Laurentian University, Ontario, Canada

[3]BGR, Hannover, Germany

[4]Department of Geology, University of Assiut, Egypt

---

Fluids are major fractionation agents in granitic systems because they contribute to control the behaviour of rare elements during the magmatic-hydrothermal transition and their redistribution at a subsolidus stage. Magmatic fluids exsolution from a crystallizing magma and their circulation can trigger important textural and geochemical changes to the point that early magmatic features are entirely overprinted and compositions re-equilibrated. Then, reconstructing granite evolution become a difficult task. The Mueilha Nb-Ta-Sn-F granitic system is a good example to identify melt- and fluid-driven processes. Based on a detailed textural study coupled with geochemical data, a four stages model of evolution is proposed: (i) crystallization of anhydrous magmatic minerals at the level of magma emplacement, including oscillatory zoned albite Ia (Ab; Fig. 1); (ii) crystallization of interstial F-Li-rich mica and fluorite, Mn-columbite and cassiterite from the residual melt; (iii) magmatic-fluids exsolution and pervasive circulation triggering partial (i.e., obliteration $Ab_{Ia}$ of magmatic zoning; $Ab_{Ib}$; Fig. 1) to total replacement ($Ab_{I}$ to $Ab_{II}$ ± fluorite; Fig. 1) and progressive re-equilibration of magmatic plagioclases (Fig. 1). This stage is also marked by the formation of miaroles and the dissolution-recrystallization of Mn-columbite evolving toward Ta-rich compositions; (iv) pervasive circulation of fluids under a subsolidus stage, derived from the ongoing crystallization of deeper magmas, triggering dissolution of $Ab_{I-II}$ and crystallization of $Ab_{III}$ (Fig. 1) in the porosity, muscovitization of magmatic F-Li-mica, crystallization of Y-REE-bearing minerals derived from fluorite leaching and partial to total replacement of columbite by Fe-tantalite and microlite. The high F content in the system triggered autometasomatism and redistribution of rare elements within the intrusion preventing the formation of a large Nb-Ta-REE hydrothermal deposit in Mueilha.

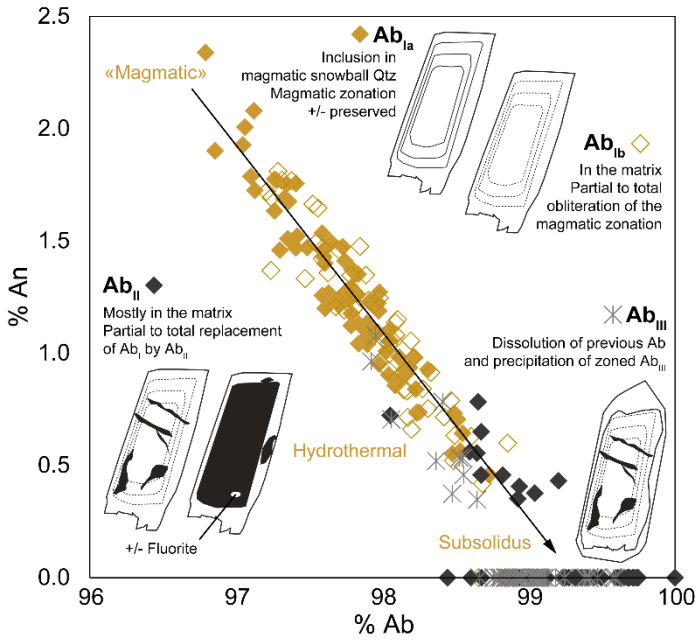


Fig. 1: Progressive textural and chemical evolution of plagioclases in the Mueilha granitic intrusion at the magmatic-hydrothermal transition and subsolidus. Note the stepwise re-equilibration of magmatic plagioclases toward 0 % anorthite (An; black arrow). “Magmatic” is in quotation mark because plagioclases compositions are already partially re-equilibrated. Ab: albite.

# Exploring Critical Element Enrichment Pathways in Black Shales: A Case Study of Türisalu Formation in Estonia

Ndiaye, M.[1], Kallaste, T.[1], Graul, S.[1] and Hints, R.[1]

[1] Department of Geology, Tallinn University of Technology, Tallinn, Estonia
mawo.ndiaye@taltech.ee

---

To address the growing demand for metals for green energy technologies, new unconventional ore deposits, including metalliferous black shales, abundant in elements such as V, Mo, and U, are becoming increasingly appealing. We investigated enrichment pathways of redox-sensitive metals in shallow water Tremadocian black shales (Türisalu Formation) from Estonia based on high-resolution geochemical and mineralogical studies [1]. X-ray fluorescence spectroscopy and organic element analysis (CHNS-O) were conducted on over 360 samples from two drill cores, using a 1 cm sample interval. The results reveal hyper-enrichment of V (up to 2300 ppm), Mo (up to 4500 ppm), and U (up to 500 ppm), but also mismatching enrichment patterns, indicating a complex redox environment and specific mechanisms of element enrichment. Our findings suggest that the specific surface area of clay particles acted as the primary limiting parameter for V hyper-enrichment and that V was delivered to the shallow sea bottom trough clay-organic nanocomposites [1], thus confirming the enrichment model recently suggested by Lu et al. [2].

Further experiments were conducted to separate organic matter and fine mineral fractions. The results demonstrate that the finest mineral fractions (<2µm) composed of illite and illite-smectite are the primary carriers of V, with concentrations reaching up to 4832 ppm. Separated organic rich fractions at the same time produced a value of an order of magnitude lower Mo/U>10 and Fe-Mn covariance with Mo in the hyper enriched basal part of the Türisalu Formation point to preferential sequestration of Mo, possibly via adsorption of Fe-Mn oxyhydroxide particles in the water column. Nevertheless, extremely high concentrations of Mo indicate that euxinic conditions prevailed at the sediment-water interface and further suggest a highly productive shallow sea setting for primary mud accumulation.

*References:*

[1] Ndiaye, M. et al. (2023) Chem Geol 624: 121583
[2] Lu, Z. et al. (2021) Chem Geol 567: 120100

## Lithostratigraphic controls on the mineralizing system at the Stonepark Zn-Pb deposit, SW Ireland

Rieger, P.[1], Hitzman, M.W.[1], Susin, V.[1], Holdstock, V.[2], Dunlevy, E.[3] and Melo, A.[1]

[1] SFI Centre for Research in Applied Geosciences (iCRAG), University College Dublin, Dublin, Ireland

[2] Group Eleven Mining & Exploration Ltd, Dublin, Ireland

[3] Terranta GmbH, Aachen, Germany

---

Base metal demand is projected to increase significantly to sustain the energy transition. Zinc is an essential element for building the infrastructure for renewable energy production. A large proportion of global Zn resources are hosted in sedimentary basins and to meet the future Zn demand current mineral system models need to be refined in order to aid exploration programs. The Lower Carboniferous basin in Ireland ( “Irish Orefield”) is one of the most prospective sedimentary basins for Zn-Pb mineralization. Irish-type Zn-Pb deposits are typically associated with normal faults and form stratabound bodies within fine-grained limestones. Pre- and syn-ore dissolution/brecciation of the host limestones (i.e., Waulsortian Limestone Fm) is a common feature in many Irish-type deposits. The Stonepark and neighbouring Pallas Green deposits share many characteristics with other Irish-type mineralization, but previous studies have noted two major differences: (1) the apparent absence of faults controlling the location of zones of mineralization and (2) the close spatial association of zones of mineralization and brecciation with igneous rocks (dykes, sills, diatremes). To better constrain the mineral system at Stonepark, we present a 3D model that integrates drill core logging, exploration drilling data, and regional seismic interpretation. There are considerable differences in Waulsortian limestone facies (mudmound micrites, mudmound-flank wackestones, off-mudmound argillaceous wackestones). Our 3D modelling suggests that this initial facies architecture of the Waulsortian limestones had a strong control on the spatial distribution of zones of alteration/mineralisation due to the lithological contrasts (e.g., permeability, reactivity) between the different facies. The 3D-distribution of Waulsortian limestone facies may also be a proxy for identifying initial, now blind or obscured, normal faults at the Stonepark deposit. This study highlights how comprehensive 3D geological modelling utilizing multiple data sets can be used to identify controls on the formation of Zn-Pb deposits in highly complex basin-hosted mineral systems.

## Critical-Ireland: Using Irish mafic intrusions as a natural laboratory to understand PGE mineralising processes

Stock, M.J.[1], Beckwith, J.[1], Geifman, E.[1], Morrison, A.[1], Bretagne, E.[1], Carter, E.[1,2], Cooper, M.[3], Holness, M.B.[4], Andersen, J.C. Ø.[5], Huber, C.[6] and Chew D.M.[1]

[1]Discipline of Geology, School of Natural Sciences, Trinity College Dublin, Ireland (STOCKM@tcd.ie)

[2]School of Geography, Geology and the Environment, Keele University, UK

[3]Geological Survey of Northern Ireland, British Geological Survey, UK

[4]Department of Earth Sciences, University of Cambridge, UK

[5]Camborne School of Mines, University of Exeter, UK

[6]Department of Earth, Environmental and Planetary Sciences, Brown University, USA

---

The European Commission has identified Platinum Group Elements (PGEs) as critical raw materials which are essential in modern green technologies but have a high risk to supply, urgently requiring innovative research to assist in locating new deposits. Palaeogene igneous centres in the north of Ireland have been identified as promising European PGE exploration targets [1] and provide a unique opportunity to understand mineralising processes due to excellent bedrock exposure and the availability of high-resolution Tellus geophysical data [2]. *Critical-Ireland* is an ongoing SFI-GSI co-funded project which (alongside associated research projects) is using these Irish centres as a natural laboratory to interrogate the first-order mechanisms of PGE deposit formation.

This presentation will give a summary of research progress to date, highlighting the link between discreet project components and demonstrating how the international research team are using Irish Palaeogene centres to target outstanding issues in our current understanding of PGE deposit formation. This includes briefly outlining work to characterise PGE enrichment in the Irish lithospheric mantle, constraining crustal processes through chemical characterisation of both intrusive and extrusive Palaeogene rocks, investigating how magma-country rock interactions impact oxygen fugacity/sulphide solubility in basaltic melts, and developing a global physical model of magma intrusion dynamics. Together, the new petrological, geochemical and physical insights from this project will improve our fundamental understanding of PGE deposit formation in both magma conduits and layered intrusions.

*References:*

[1] Andersen, J.C.Ø. et al. (2002). *The geology, geochemistry, mineralogy, and mineral beneficiation of platinum-group elements*, 54, 637-667.

[2] Anderson H., *et al*. (2016). Unearthed: impacts of the Tellus surveys of the north of Ireland, 14, 179-189.

## Revived interest in dismissed historical Cu-Fe-Zn deposits in the Northern Apennine ophiolites (Italy)

Tagliacollo, L.*, Bonadiman, C., Saccani, E., Bianchini, G., Brombin, V. and Tassinari, R.

Department of Physics and Earth Science, University of Ferrara (Italy)

*tgllsi@unife.it

---

The increasing need of Critical Raw Materials (CRMs) stable supply has led many European countries to focus their attention on the metal recovery from dismissed mines, mine wastes, and landfills in the circular economy spirit. Northern Italy is characterised by more than 100 abandoned mining sites. Among them, in the Emilia Romagna Region, the Boccasuolo Ophiolite is receiving interest because the numerous disseminated dismissed historical extractive sites of Volcanogenic Massive Sulphide (VMS) deposits with a Cyprus-type metallogenic signature (Cu-Fe-Zn) [1]. These deposits occur as pods within small bodies of ophiolitic basalts cropping out as olistoliths in the Northern Apennine External Ligurian units. These ophiolites represent remnants of the Jurassic Alpine Tethys, which formed in an ocean-continent transition zone [2]. They are indeed characterised by sequences of pillow lavas associated with serpentinite and gabbro breccias, radiolarian cherts, limestones, and abundant serpentinised subcontinental mantle peridotites. Basalts show OCTZ chemical features with transitional-MORB affinity and a garnet signature ($Dy_n/Yb_n$=1.2-1.4). Boccasuolo Ophiolite's VMS deposits were formed by circulation of metal-rich hydrothermal fluids which, mixed with heated seawater through a network of fissures, developed quartz-sulphide veins [3]. To better constrain the CRMs potential of these VMS deposits, we performed bulk rock geochemical analyses for major and trace elements, and S and C elemental content and relative stable isotopic ratio. Preliminary results reveal that basalts with mineralisation are enriched in Cu (200 times CC), Zn (118 times CC), and Ag (12 times CC) [4]. Such analyses are crucial to reconstruct the ore-formation processes and trace metal enrichment of the main rocks, which led to the formation of Cu-Fe-Zn-bearing sulphide deposits associated with basaltic rocks.

*References:*

[1] Garuti G. et al., (2011) Lithos 124 243-254 https://doi.org/10.1016/j.lithos.2010.11.006
[2] Kiss G. et al., (2023) Minerals 13 8 https://doi.org/10.3390/min13010008
[3] Saccani, E. (2015) Geosci. Frontiers https://doi.org/10.1016/j.gsf.2014.03.006
[4] Rudnick, R.L., Gao, S. (2014) Treatise on Geochemistry https://doi.org/10.1016/B978-0-08-095975-7.0.00301-6

## Constraining REE enrichment in alkaline-silicate magmatic systems using new thermodynamic models

Weller, O.M.[1], Holland, T.J.B.[1], Soderman, C.R.[1], Green, E.C.R.[2], Powell, R.[2], Beard, C.D.[1], & Riel, N.[3].

[1]Department of Earth Sciences, University of Cambridge, UK, ow212@cam.ac.uk

[2]School of Geography, Earth and Atmospheric Sciences, The University of Melbourne, Australia

[3]Dept. of Geosciences, Johannes Gutenberg University, Germany

---

Alkaline-silicate magmatic systems are geologically and economically important, for example as small fraction metasomatic melts and as hosts of rare earth element (REE) deposits. While phase equilibria modelling is an increasingly popular tool for the analysis and contextualisation of igneous systems, currently it is not possible to model most alkaline compositions. This limitation is due to the absence of an appropriate thermodynamic model for alkaline-silicate melts, as well as a dearth of models for their crystalline products.

Here we present a new thermodynamic model for alkaline-silicate melt (in the $Na_2O$–$CaO$–$K_2O$–$FeO$–$MgO$–$Al_2O_3$–$SiO_2$–$H_2O$–$TiO_2$–$O_2$–$Cr_2O_3$ model system), extended from [1], along with new models for nepheline, kalsilite, leucite and melilite. The new thermodynamic models are calibrated using experimental data on phase relations among minerals and melt, and the model performance is benchmarked via detailed comparison with independent experimental datasets, encompassing a range of pressure (0–22 kbar), temperature (680–1350 °C), oxygen fugacity ($\log fO_2 \otimes \mathrm{FMQ}$-3 to +1), total alkali (3–16 wt%) and silica (37–70 wt%) conditions. The calculated phase diagrams successfully reproduce experimental crystallisation sequences and phase compositions, indicating that the thermodynamic models are well calibrated across this spectrum of conditions.

We use our new models to show how evolved alkali-rich silicate magmas can be generated during fractional crystallisation of primitive mantle melts. We then apply our models to the crystallisation of these evolved alkaline-silicate bulk compositions (e.g., nepheline syenite, syenite), yielding solid assemblages consistent with those reported for natural systems in each case, including model analogues to common exsolution textures. Analysis of the liquid line of descent reveals that for silica-undersaturated compositions, the final fraction of melt and associated equilibrium mineralogy (e.g., pyroxene, feldspar) evolves to extremely alkali-rich compositions, consistent with alkali-rich 'autometasomatic' and 'fenitised' zones observed in and around some alkaline-silicate intrusions. We also investigate mechanisms for residual enrichment of REE in alkaline-silicate systems by integrating phase equilibrium and mineral-melt trace-element partitioning models. This approach has allowed us to explore the controls of bulk composition and crystallisation conditions on the generation of REE-rich melts, which likely represent precursors to magmatic ore deposits of the REE.

Overall the new models provide a novel tool to explore the role of variables such as pressure, fractional crystallisation and crustal assimilation in the petrogenesis of alkaline-silicate magmatic systems and their associated mineralisation.

*References:*

[1] Holland T et al. (2018) J of Pet 59: 881-900

# Tracing the fluid and metal sources of the polymetallic mineralization in the Cyclades, Greece, by a multi-isotope study of hydrothermal barite

Wind, S.C.[1,2], Schneider, D.A.[2], Hannington, M.D.[2], Fietzke, J.[3]

[1] Institute of Geosciences, Christian-Albrechts-University Kiel, 24118 Kiel, Germany (sandra.wind@ifg.uni-kiel.de)

[2] Department of Earth and Environmental Sciences, University of Ottawa, Ottawa K1N 6N5, Canada

[3] GEOMAR Helmholtz Centre for Ocean Research Kiel, 24148 Kiel, Germany

---

In the Cyclades continental back-arc, Greece, middle Miocene polymetallic mineralization formed by a mixture of fluid sources and interaction of the hydrothermal fluids with the basement rocks. These complexities are recorded in the isotopic and geochemical signature of ore associated barite.

We present a multiple isotope and geochemical approach to characterize the hydrothermal barite, including mineral separate analysis of $\delta^{34}S$ and $\delta^{18}O$ and sequential laser ablation multi-collector inductively coupled plasma mass spectrometry (LA-MC-ICP-MS) measurements of $^{87}Sr/^{86}Sr$ and $\delta^{34}S$ on the same ablation spot [1]. The advantage of spatially resolved LA-MC-ICP-MS analysis of $^{87}Sr/^{86}Sr$ and $\delta^{34}S$ in barite is highlighted by two case studies: (A) barite from carbonate-hosted vein and breccia Pb-Zn-Ag mineralization at Lavrion, Attica and (B) polymetallic vein-type mineralization on Mykonos Island.

Carbonate-hosted barite mineralization at Plaka, Lavrion, show strong zoning in $\delta^{34}S$, Sr concentration, and $^{87}Sr/^{86}Sr$ ratios in individual crystals. Low $\delta^{34}S$ (2.1-7.4‰) close to magmatic values occur in the core and high $\delta^{34}S$ values (~20‰) close to Miocene seawater sulfate towards the rim of barite. Barite with low $\delta^{34}S$ values but high $\delta^{18}O$ values, indicates that the magmatic fluids likely exchanged with the carbonate wall rocks, which is further supported by the elevated Ca concentrations in the barite core. The shift to high $\delta^{34}S$ values and intermediate $\delta^{18}O$ values is permissive of a seawater-dominated fluid. Strontium isotope ratios, similar to the values of Miocene intrusions, are interpreted to record dominantly magmatic hydrothermal fluids, where small variations are related to the interaction of the hydrothermal fluids with the wall rocks.

On Mykonos, vein-type mineralization consists of banded barite veins with polymetallic sulfides filling open spaces between barite crystals. High $\delta^{34}S$ values (25-37‰) and $\delta^{18}O$ values (4-12‰) of barite are consistent with a fractionated Miocene seawater-dominated fluid source and interaction of the hydrothermal fluid with the surrounding host rocks. On a crystal scale, a positive correlation between the $\delta^{34}S$ values and Sr content exist, while $^{87}Sr/^{86}Sr$ ratios remain constant, which likely reflects a temperature-controlled covariance. Local variations in Sr isotope ratios between the deposits in the east and central part of Mykonos suggest distinct sources of Sr, derived from leaching of different basement rock types. Regional differences in the metal sources for the mineralization on Mykonos were previously reported by Wind [2] based on the Pb isotope ratios and trace element concentrations of galena. This highlights the strength of in-situ multi-isotope studies of barite to trace the complex ore-forming processes (e.g., fluid mixing, leaching of basement lithologies) in continental back-arc settings.

*References:*

[1] Wind S et al. (2023) Econ Geol 118:1959-1994
[2] Wind S et al. (2020) Lithos 366-367:105559

# Ore Minerals and Metal Migration within the Oceanic Crust of the Central Sudetic Ophiolite, Poland

Elsherif E. A.[1], Ciążela J.[1], Wojtulek P.[2], Strauß, H.[3], Kuhn Th.[4], Pańczyk M.[5], Woźniak W.[1], Fitt M.[1], Stawikowski W.[6], Kukula A.[1], Łuszczek K.[7]

[1]Institute of Geological Sciences, Polish Academy of Sciences, Poland (eman-elsherif@twarda.pan.pl)

[2]Institute of Geological Sciences, University of Wroclaw, Poland

[3]Institut für Geologie und Paläontologie, University of Münster, Germany

[4]Bundesanstalt für Geowissenschaften und Rohstoffe, Germany

[5]Polish Geological Institute, National Research Institute, Poland

[6]Institute of Geology, Adam Mickiewicz University, Poznań, Poland

[7]Faculty of Geoengineering, Mining and Geology, Wroclaw University of Science and Technology, Poland

---

The study examines ore mineral, chalcophile metal, sulfur, and sulfur isotope variability within a slow-spreading ridge-related Central Sudetic Ophiolite (CSO) oceanic crust. We used a set of 142 samples representing all mafic and ultramafic lithologies from 24 outcrops in the largest Ślęża Massif (SM), smaller Nowa Ruda Massif (NRM), and Przecławice IG-2 borehole (605 m deep).

The microscopic examination revealed the dominance of magmatic sulfides of pyrrhotite, chalcopyrite, and pentlandite within the crustal rocks, particularly in dikes and ferrogabbro horizons. Hydrothermal sulfides in the crust are mainly pyrite, chalcopyrite, and sphalerite, with minor pyrrhotite. The crust's oxides are mostly ilmenite and titanomagnetite. A higher average loss-on-ignition value (2.40 wt.%) in gabbros confirms more substantial alteration compared to the dikes (0.81 wt.%) and the basalts (0.64 wt.%). The Mg# ranges within the SM crust vary from 34 to 74 for gabbros, 37 to 69 for dikes, and 47 to 53 for basalts. The BSE images revealed pyrite exsolutions within pyrrhotite grains, massive chalcopyrite crystals on the rims, and separate and intergrown grains of sphalerite up to 10 µm in size. Average major element contents in pyrrhotite ($Fe_{0.91}S$), chalcopyrite ($Cu_{0.97}Fe_{1.09}S_2$), pyrite ($Fe_{1.05}S_2$), sphalerite ($Zn_{0.94}Fe_{0.17}S$), and ilmenite ($Fe^{2+}_{0.92}$, $Mn_{0.07}$)($Fe^{3+}_{0.03}$, $Ti_{0.99}$)$O_3$) have been determined.

Whole-rock analyses show that dikes of the SM are more enriched in major (15.8 wt.% $Fe_2O_3$, 2.7 wt.% $TiO_2$, 0.31 wt.% MnO) and chalcophile metals (50 ppm Cu, 205 ppm Zn) compared to the gabbros (12.02 wt.% $Fe_2O_3$, 2.10 wt.% $TiO_2$, 0.19 wt.% MnO; 34 ppm Cu, 77 ppm Zn) and the basalts (13.41 wt.% $Fe_2O_3$, 2.36 wt.% $TiO_2$, 0.21 wt.% MnO; 21 ppm Cu, 94 ppm Zn). The total sulfur content, on average, is more enriched in the mafic dykes (0.19 wt.%) compared to the gabbros (0.03 wt.%) and basalts (0.002 wt.%) of the SM. The total sulfur content in the gabbros of the Przecławice IG-2 hole showed an average of 0.04 wt.%, with enrichments at depths of 356–357m and 550–551m. The troctolites and basalts of NRM have a decreased average of 0.01 wt.% sulfur content, likely due to depleted sulfur magma composition. $\delta^{34}S_{whole\text{-}rock}$ of the SM gabbro, Przecławice IG-2 borehole, and NRM samples reflect a mantle signature (+0.1 to +1.9%, −1.8 to +1.5%, −0.5 to 1.5%). Seven samples with hydrothermal signatures (+2.3 to +3.4%) were identified among the SM's dikes. $\delta^{34}S_{In\text{-}situ}$ of pyrrhotites (+1.2 to +10‰), chalcopyrites (+0.5 to +6.6‰) and pyrites (+3.1 to +4.8‰) translate to a bulk hydrothermal sulfide $\delta^{34}S_{in\text{-}situ}$ (+2.1 to +3.6‰) similar to $\delta^{34}S_{whole\text{-}rock}$ (+1.8 to +3‰) in the four respective samples. In summary, magmatic processes likely control the enrichment in sulfides and metals within the lower oceanic crust of the SM, while hydrothermal processes enrich the overlaying dike crustal layer as reflected in their $\delta^{34}S$ values.

# Mineral chemistry of hydrothermal biotite from Na-Ca-K-silicate alteration associated with the Elatsite porphyry copper deposit, Bulgaria

Georgieva, H.[1], Nedialkov, R.[2], Stefanova, E.[1] and Milenkov G.[1]

[1]Geological Institute, Bulgarian Academy of Sciences, 24 Acad. G. Bonchev, Sofia
ch_georgieva@geology.bas.bg.

[2] Sofia University, 15 Tsar Osvoboditel Blvd., Sofia

---

The Elatsite porphyry copper deposit is one of the biggest deposits in Bulgaria and Europe. It is part of the Apuseni-Banat-Timok-Srednogorie magmatic and metallogenic belt [1]. Hydrothermal alterations are described as K-silicate, K-silicate-sericitic, sericitic, propylitic and argilic [2,3,4,5], alongside Ca-K alteration [5], Na-Ca alteration and Na-Ca-K-silicate alteration [6]. Na-Ca-K-silicate alteration is examined in drill holes, occur in the porphyritic rocks from the deposit. This study present new information about the mineral chemistry of hydrothermal biotite.

The mineral assemblage of the Na-Ca-K-silicate alteration includes biotite, amphibole, plagioclase, K-feldspar, titanite, magnetite, rutile, apatite and single pyroxene. The hydrothermal biotite has pale brown color and occurs as pseudomorphs on primary minerals (rarely) and most commonly as disseminated within the ground mass or infilling veins. Typical for the biotite is the formation of aggregates with secondary amphibole. Secondary biotite has Mg* ratio (Mg/Mg+Fe) 0.53-0.68 and is described as biotite on the graphical constructions of Deer et al. [7].

Comparative analysis with hydrothermal biotite from K-silicate alteration and magmatic biotites from the Elatsite [8] reveals transitional Mg* ratio values, characterized by higher ratios for hydrothermal biotite from K-silicate alteration and lower in magmatic biotites. Additionally, lower concentrations of Cl and heightened levels of Fe and Ti are present for the biotite from Na-Ca-K-silicate alteration compared with the hydrothermal biotite from K-silicate alteration. A negative Mg-Cl correlation is present in hydrothermal biotite from Na-Ca-K-silicate alteration and in magmatic biotite, which probably corresponds to the Fe-F avoidance [9].

The transitional composition of biotite from Na-Ca-K-silicate alteration, exhibiting intermediate characteristics between magmatic biotites and hydrothermal biotites from K-silicate alteration, suggests a predominance of magmatic fluid during its formation. However, the presence of Ca minerals within the studied alteration hints at the involvement of external fluids in the alteration process.

*Acknowledgment:* This study is partly supported by the KP-06-N44/4 project, financed by the Bulgarian National Science Fund.

*References:*

[1] Popov P et al. (2002) Geol Balc 32, 2-4:145-163
[2] Kanazirski et al. (2002) Geol Balc 32: 77-80
[3] Strashimirov et al. (2002) Min Dep 37: 587-598
[4] Ivanov et al. (2014) In: Proceeding of XX CBGA Congress: 158–161
[5] Georgiev G (2019) Hydrothermal metasomatites in Elatsite porphyry copper deposit: 99
[6] Georgieva et al. (2019) In: Proceedings of Geologica Carpathica 70: 65–68.
[7] Deer et al. (1991) An introduction to the rock forming minerals: 528
[8] Georgieva H. and Nedialkov R. (2017) Bulg Geol Soc Geosci: 51-52
[9] Munoz J (1984) Rev in Miner 13: 469-493

## Mineralogical and chemical characterization of tungstenite

Goldmann, S.[1] (presenter), Wegorzewski, A.V.[1] and Fuchs, S.[1]

[1]Federal Institute for Geosciences and Natural Resources (BGR), Germany, simon.goldmann@bgr.de

Tungstenite ($WS_2$) is a rare mineral, and its occurrence is only reported from a few locations worldwide; for example, the Emma Pb-Ag mine as type locality [1], the dolomite marble of Crevola d'Ossola [2], and the volcanogenic massive sulphide (VMS)-type Kidd Creek deposit [3]. We present new chemical as well as mineralogical data for tungstenite and associated minerals from the skarn-hosted scheelite mine of Brejuí in the State of Rio Grande do Norte in northeastern Brazil. The first reported occurrence of tungstenite at this locality was in 1993 by Falster et al. [4].

Tungstenite and associated minerals were investigated using polarized light microscopy, electron probe microanalysis (EPMA), Raman spectroscopy as well as X-ray diffraction (XRD). Tungstenite occurs in association with vesuvianite, scapolite, calcite, and pyrite. In another assemblage, molybdenite is associated with quartz, calcite, diopside, grossular-andradite garnet, and scheelite; this assemblage is devoid of tungstenite. Both assemblages were sampled from two different mining levels and their spatial or paragenetic relationship is ambiguous. Due to very similar atomic radii of W and Mo, there is a complete solid solution series between tungstenite and molybdenite. Chemical composition of tungstenite by EPMA (n=51) shows in median 73.87 wt.% W and 25.52 wt.% S with Mo ranging from <0.03 to 0.82 wt.% Mo (median 0.11 wt.% Mo). Molybdenite is of almost ideal composition without any W (<0.02 wt.%) and occasionally Fe concentrations of up to 0.59 wt.%. Scheelite associated with molybdenite is chemically zoned with Mo concentrations ranging from 1.2 to 6.0 wt.% Mo and up to 0.6 wt.% Sr. In XRD, tungstenite and molybdenite show identical reflexes at ~6.14 Å (002), ~2.28 Å (103), ~2.04 Å (104) and ~1.825 Å (105). These reflexes are characteristic for the 2H-polytype with hexagonal symmetry (both minerals may also occur as trigonal 3R-polytype), but both minerals cannot be distinguished from each other because of identical unit cell parameters [2]. However, tungstenite and molybdenite can be differentiated by Raman spectroscopy as both minerals are characterized by two distinct main peaks in their spectra. For tungstenite, the first major peak can be recognized at 345 $cm^{-1}$ and the second peak at 410 $cm^{-1}$, whereas molybdenite displays two distinct peaks at 390 $cm^{-1}$ and 405 $cm^{-1}$ with a minor peak at 280 $cm^{-1}$.

Tungstenite is a very rare sulphide mineral in natural systems, probably because of its small stability field in the system of $fS_2$ and $fO_2$ [5,6], which is from the conditions for the major tungsten minerals scheelite and wolframite. Tungstenite commonly precipitates from W-bearing high-temperature hydrothermal fluids that are (moderately) reduced and rich in sulphur. These hydrothermal fluids probably also contain low amounts of Mo, but under these conditions the formation of molybdenite is likely restricted, and instead Mo is incorporated by substitution for W in tungstenite. In contrast, at more oxidizing conditions (higher $fO_2$) molybdenite together with Mo-bearing scheelite can be formed [6] instead of tungstenite. The lack of reduced $W^{4+}$ in molybdenite as well as higher Mo concentrations (as oxidized $Mo^{6+}$) in scheelite indicate formation in strongly oxidizing environment.

*References:*

[1] Wells RC and Butler BS (1917) J Washington Acad Sci 7: 596-599
[2] Graeser S (1964) Schweiz Miner Petrog 44: 121-128
[3] Hannington MD et al. (1999) Econ Geol Monog Series 10: 163-224.
[4] Falster AU et al. (1997) Mineral News 13: 6-8
[5] Hsu LC (1977) Econ Geol 72: 664-670
[6] Pašava J et al. (2015) J Geosci 60: 149-161

# Paragenetic sequence and mineral chemistry of the scheelite skarn deposit of Monleón (Salamanca, NW Spain)

Posado-De Castro, J.[1], Timón-Sánchez, S.M.[1], Fernández-Fernández, A.[2], Llorens-González, T.[1] Díez-Montes, A.[1], Sánchez-García, T.[3]

[1] IGME-CSIC, Plaza de la Constitución 1, 37001, Salamanca, Spain.

javierposado@usal.es

[2] Geology Dept., University of Salamanca. Pza. de Los Caídos, s/n, 37008, Salamanca, Spain.

[3] IGME-CSIC, Ríos Rosas, 23, 28003, Madrid, Spain.

---

Tungsten (W) is recognized as a strategic metal due to its high melting point and strength properties, and therefore is widely used in hard metals and steel alloys industries [1]. In order to ensure a stable W supply, there has been an increase in mining exploration to identify potential resources of this metal.

Within the Iberian Variscan Belt, W mineralization primarily occurs in the wolframite-scheelite-sulphide-quartz vein type, greisen type as well as skarn type. In the skarn-type mineralization, scheelite ($CaWO_4$) is the dominated economic mineral. One of the prominent examples in the Central Iberian Zone, include the Los Santos calcic scheelite skarn [2], and next to it, a small outcrop of mineralized limestones in the Monleón area. Due to the scarce surface development of this deposit, at this time, it does not appear to be of economic interest; however, its study is important to know the metallogenic potential of the carbonate series near the N edge of the western end of the Ávila batholith.

The Monleón skarn shows several chemical and mineralogical features common to many other W-bearing calcic mesozonal reduced skarns deposits. Early exoskarn consists of hedenbergite ($Hd_{82-83}$) and grossular ($Gr_{68-90}$). The mineral assemblage which formed during the cooling of the system is complex and is constituted by subcalcic garnet and other hydrated silicates, such as amphibole, vesuvianite, epidote group minerals, chlorite, white mica and zeolite. A fine-grained leucogranite is replaced by a calcic plagioclase, clinopyroxene and grossular ($Gr_{63-67}$) endoskarn.

Metallic mineralisation at the Monleón deposit mainly consists of scheelite. Based on textural and chemical data the scheelite can be classified into two types. Scheelite I (Sch I) occurs in small disseminated subrounded crystals (100-350 μm) and is intergrown with the pyroxene in the early skarn. Sch I shows substantial $MoO_3$ contents ranging between 0.24 wt.% and 1.62 wt.%. Scheelite II (Sch II) is anhedral to subhedral in shape, ≤2mm in size, and it's associated to the subcalcic garnet, filling fractures and intergranular spaces. The Sch II has lower contents of $MoO_3$ (0-0.21 wt.%) than Sch I. There are also sulphides, mainly pyrrhotite, chalcopyrite and sphalerite.

Acknowledgements: To the EIT RawMaterials RIS Intership Programme, to the Research Project "Geological and mineral mapping at 1:5.000 scale of the N edge of the Los Santos-Valdelacasa batholith" (LI99). Univ. of Salamanca-Daytal Resources Spain, S.L. and to the MINCE project, Study of critical and strategic raw materials for the ecological transition and the supply of the main industrial value chains in Spain, funded by the Subdirectorate General of Mines, MITERD (000X-730).

*References:*

[1] European Commission et al. (2023) https://data.europa.eu/doi/10.2873/725585

[2] Timón-Sánchez SM et al. (2009) Econ Geol 104: 961-995

# Tetrahedrite group minerals and their weathering products from Chamrousse, Belledonne Range, Western Alps, France

Skrzyńska, K.[1], Müller, H.[2]

[1]Faculty of Natural Sciences, University of Silesia in Katowice, Będzińska 60, Sosnowiec, Poland/ corresponding author: katarzyna.skrzynska@us.edu.pl

[2]European Synchrotron Radiation Facility, 71, avenue des Martyrs, CS 40220, 38043 Grenoble Cedex 9, France

---

The minerals of the tetrahedrite group are one of the most widespread and complex isotypic series among sulfides. Ores containing minerals of the tetrahedrite-tennantite series (fahlore) are industrially attractive due to their high copper content and significant substitution by silver. Unfortunately, these minerals are prone to weathering, implying the release of potentially toxic elements (PTE, such as As, Sb, Hg, Cd) into the environment [1]. Secondary phases are of considerable geochemical importance as they play a significant role in the immobilisation of pollutants and can serve as a temporary or final sink for PTE [2–3]. Recently, a progressive model of fahlore weathering process has been established [4]. It includes at least three stages of weathering differing in the degree of alteration, mobile elements and secondary mineral association. Here, we present new results on the fahlore mineralization and associated weathering products of the Chamrousse massif, France. The importance of this Variscan ophiolitic complex, located 30 km South of Grenoble, for regional geology and mineralogy,
is paramount. The only comprehensive mineralogical description of the massif was published over 70 years ago [5]. This prompted us to re-investigate the area in 2023. Mineralogical explorations have focused on the N-S-oriented fracture zone separating feldspathoid amphibolites (W) and ultrabasic rocks (E). The fahlore mineralization is associated with a hydrothermal quartz vein related directly to a tectonic fault. The use of reflected light microscopy, scanning electron microscopy with an energy-dispersive X-ray spectroscopy detector, electron microprobe analyser (EMPA), together with Raman and IR spectroscopy, enabled the accurate identification of both ore mineral phases and weathering products. EMPA analyses revealed the presence of tetrahedrite-(Zn) $(Cu_{5.92}Ag_{0.02})_{\sum 5.94}(Cu_{4.00}Zn_{1.55}Fe^{2+}_{0.33}Hg_{0.06})_{\sum 5.94}(Sb^{3+}_{3.92}As^{3+}_{0.08})_{\sum 4.00}S_{13.05}$, argentotetrahedrite-(Zn) $(Ag_{3.85}Cu_{2.15})_{\sum 6.00}(Cu_{4.17}Zn_{1.69}Fe^{2+}_{0.15}Hg_{0.03})_{\sum 6.04}(Sb^{3+}_{3.91}As^{3+}_{0.09})_{\sum 4.00}S_{12.89}$ and rozdestvenskayaite-(Zn) $Ag_{6.00}(Ag_{2.65}Cu_{1.73}Zn_{1.53}Hg_{0.11})_{\sum 6.01}(Sb^{3+}_{3.69}Fe^{2+}_{0.26}As^{3+}_{0.05})_{\sum 4.00}S_{12.65}$, all belonging to the tetrahedrite group. Interestingly, Chamrousse is the first French occurrence of the latter two minerals. Besides, native gold, cinnabar, acanthite and tenorite were found for the first time at this locality. Weathering products are represented by numerous phases, malachite and azurite being the most common.

In addition, unusual secondary minerals, such as Cu-bearing hydroxycalcioroméite $Ca_{0.78}\square_{0.76}Cu_{0.37}Zn_{0.06}Fe_{0.03}Pb_{<0.01}K_{<0.01})_{\sum 2.00}(Sb_{1.71}Si_{0.29})_{\sum 2.00}(O_{5.23}OH_{1.74})_{\sum 6.90}$ and the Sb-analogue of auriacusite $Fe^{3+}_{1.00}(Cu_{0.53}Fe_{0.30}Zn_{0.16}Ca_{0.01})_{\sum 1.00}(Sb^{5+}_{0.76}Si_{0.15}Fe^{3+}_{0.08}As^{5+}_{0.01})_{\sum 1.00}O_{5.00}$ were identified. Interestingly, a shattuckite-like phase $Cu_5(Si_2O_6)_2(OH)_2$ was found, which displays a distinctive Raman band at 674 $cm^{-1}$. The OH-stretching vibrations of the hydroxyl group and water appear at 3633 and 3482 $cm^{-1}$, respectively. This investigation revealed the occurrence of mineral species hitherto unknown at this locality and enabled the observation of progressive weathering of fahlores.

Acknowledgement: The investigations were supported by NCN of Poland, grant no. 2019/35/O/ST10/01015.

*References:*

[1] Barago N et al. (2023) Environ Sci Pollut Res 30:63754-63775
[2] Radkovaá A B et al. (2017) Am Min 102:1091-1100
[3] D'Orazio M et al. (2024) Ore Geology Reviews 164: 105847
[4] Keim M F et al. (2018) Chemical Geology 499: 1-25
[5] Den Tex E (1950) Leidse Geologische Mededelingen 15:1-204

## Major and trace element composition of tourmaline in the Kaustinen Li-pegmatites: implications for melt origin and evolution

Tvauri, A.V.[1], Kalliomäki, H.[1], Law, K.A.[1], Ranta, E.[1] and Rämö, O.T.[1]

[1]Department of Geosciences and Geography, University of Helsinki, Finland.

artur.tvauri@helsinki.fi

---

The albite-spodumene pegmatites of the Kaustinen Li-province host one of the most significant lithium resources in Europe. Economic potential and petrogenesis of the Kaustinen Li pegmatites have been studied previously [1][2], however the magmatic-hydrothermal processes behind the petrogenesis and lithium enrichment are not yet fully understood. Due to its wide P-T-X stability range, complex mineral chemical structure with an abundance of varying trace elements, and high resistance to alteration [3], tourmaline is an ideal proxy for the study of the Kaustinen Li province. In this study, the major (electron probe microanalysis) and trace element (laser ablation–inductively coupled plasma–mass spectrometry) compositions of tourmaline from six albite-spodumene pegmatites and the Kaustinen pegmatite granite are analysed in order to investigate: 1) the regional variations in tourmaline chemistry between the individual pegmatites and the assumed source pluton, and- 2) how this reflects the origin, evolution, and fractionation of the pegmatite forming melts.

Preliminary results show that most tourmalines belong to the alkali group, with Ca being very low in tourmalines within the pegmatites and varying in the tourmalinized wall rock, depending on the wall rock composition. Tourmaline species generally follow a trend of dravite – schorl – elbaite from the wall rock to the inner zones of the pegmatites, with the Rapasaaret pegmatite dike having the most Li-rich tourmaline compositions. Similarity in composition between the tourmalines in the contact and inner zones of the Rapasaaret and Heikinkangas dikes indicates simultaneous crystallization of tourmaline throughout the dike width. In the Matoneva dike, the composition of tourmaline in the inner zone is significantly more evolved than in the border zone, indicating stronger internal zonation and fractionation inwards from the walls than in Rapaasaaret and Heikinkangas. Zoned tourmalines in the contact and inner zone of the Heikinkangas dike show an increase in fluid-mobile elements (Li, Na, Zn, Ca, Mg) and a decrease in fluid immobile Zr from core to rim, which indicates that the rims crystallized from an exsolved aqueous fluid [4]. The upcoming trace element results will give further insight into the origin evolution of the pegmatite forming melts.

*References:*

[1] Ahtola T et al. (2015) Geological Survey of Finland, report of investigation 220:1-28

[2] Martikainen A (2012) Unpublished Master's thesis, University of Helsinki, p.77

[3] Van Hinsberg VJ et al. (2011) The Canadian Mineralogist 49:1-16

[4] Zajacz Z et al. (2008) Geochimica et Cosmochimica Acta 72:2169-2197

# High resolution mineralogy and petrography of Mn-oxyhydroxides from Caribbean Ni-Co laterite deposits

Villanova-de-Benavent, C.[1], Nieto, F.[2], Domènech, C.[1], Domínguez-Carretero, D.[1], Galí, S[1], and Proenza, J.A.[1]

[1]Departament de Mineralogia, Petrologia i Geologia Aplicada, Facultat de Ciències de la Terra, Universitat de Barcelona (UB), Martí i Franquès s/n, 08028 Barcelona, Spain

[2]Departamento de Mineralogía y Petrología, Facultad de Ciencias, Universidad de Granada, Av. Campus Fuentenueva s/n, 18002 Granada, Spain

---

Manganese oxyhydroxides are ubiquitous in Ni-Co laterite profiles worldwide [1,2,3,4], and they may occur in deposits of the oxide- [5], hydrous silicate- [4] and clay-types [6]. They have been typically classified as asbolane ($(Ni,Co)_xMn(O,OH)_4 \cdot nH_2O$; hexagonal) and lithiophorite ($(Al,Li)MnO_2(OH)_2$; trigonal) [1,4,5,6], although other species like romanèchite have been reported [3]. Mn oxyhydroxides are important ore minerals as they may contain significant amounts of Ni and Co, which are currently considered critical metals. Asbolane and lithiophorite, considered valid mineral species, occur as fine-grained, poorly crystalline, massive aggregates, with a similar layered structure [7]. In the case of asbolane, the structure is composed of alternating octahedra sheets occupied by $Mn^{4+}$, Ni and Co [8].

Previous results from the Loma de Hierro Ni-Co laterite deposit (Venezuela) revealed that Mn oxyhydroxides displayed a wide variety of textures, including colloform aggregates, sub-rounded, zoned grains, fibrous crystals, and tabular aggregates. According to Electron Microprobe (EMP) data, their compositions in terms of Mn, Al, Fe, Ni and Co are highly variable [4]. One sample was selected for this study, from which two lamellae were extracted by Focussed Ion Beam (FIB) at Laboratorio de Microscopías Avanzadas, Universidad de Zaragoza, Spain, to be examined under the Transmission Electron Microscope (TEM) at Centro de Instrumentación Científica, Universidad de Granada, Spain. The area of interest is a sub-rounded multi-phase Mn-oxyhydroxide grain, measuring approximately 100x50 µm, consisting of a homogeneous Mn-oxyhydroxide core and a complex rim. The composition of the core is 76-79 wt.% MnO and low NiO (< 0.3 wt.%), CoO (< 1.4 wt.%), $Fe_2O_3$ (0.5-1.8 wt.%), and $Al_2O_3$ (1.0-1.7 wt.%). The rim, with regular thickness, has lower MnO (29-55 wt.%), and is enriched in NiO (2.4-7.8 wt.%), CoO (2.0-6.1 wt.%) and $Al_2O_3$ (8.5-19 wt.%), with variable and low amounts of $Fe_2O_3$ (1.6-4.2 wt.%; EMP). Low magnification TEM images from the rim display elongated (~2x0.5 µm), zoned crystals enriched in Fe, Ni and Al, coexisting with long and thin (a few nm) platelets enriched in Co. The $d_{001}$ spacing of ~9 Å of asbolane was measured in the selected area electron diffraction (SAED) patterns. Textural and compositional complexity as seen under the TEM indicate that further examination is needed to constrain the crystallochemical nature of asbolane, and its relationship with lithiophorite.

*References:*

[1] Manceau A et al. (1987) Geochim Cosmochim Acta 51:105-113
[2] Dzemua GL et al. (2012) Min Dep 48:155-171
[3] Putzolu F et al. (2018) Ore Geol Rev 97:21-34
[4] Domènech C et al. (2023) Minerals 12:927
[5] Roqué-Rosell J et al. (2010) Chem Geol 275:9-18
[6] Tauler E et al. (2017) Min Dep 52:1011–1030
[7] Post JE (1999) Proc Natl Acad Sci USA 96:3447-3454
[8] Chukrov et al. (1982) Int Geol Rev 24:598-604

# Understanding the origine and formation process of goethite framboids in Cretaceous sedimentary rocks by nanoscale analysis

Ohfuji, H.[1], Konishi, S.[1] and Yamamoto, K.[2]

[1] Department of Earth Science, Graduate School of Science, Tohoku University, 6-3 Aramaki-Aza-Aoba, Aoba-Ku, Sendai 980-8578, JAPAN, ohfuji@tohoku.ac.jp

[2]Faculty of Science, Kagoshima University, 1-1-35 Korimoto, Kagoshima, 890-0065, JAPAN

---

Framboidal aggregates are the most common and unique texture in sedimentary pyrite [1]. Pyrite framboids occur widely in sediments of a wide range of geological ages from Archean to modern times, and in anoxic water columns in inner bays and lakes, and their size distribution has been used as a paleoindicator of the surrounding redox environment. On the other hand, framboidal aggregates composed of iron oxide/oxyhydroxide such as hematite and goethite, have also been reported [2-3], although they are relatively rare. Of particular interest is that such goethite framboids were found in clays in the Cretaceous/Tertiary (K/T) boundary layers [3], which are closely linked to the mass extinction of animal species including dinosaurs. The K/T boundary layers are also enriched in noble metals and other trace elements, suggesting that the pyrite oxidation may have also caused the redistribution of other chemical components [4], but the origin of goethite framboids has not been fully understood. In this study, to search for clues understand the origin and formation process of such “oxidized” framboids, micro- and nano-scale analyses were performed using SEM and TEM on goethite framboids in Cretaceous sandstones of the Lower Shimanto Formation distributed in western Kagoshima, Japan. Thin sections and polished resin mounts were prepared from blocks sampled from the outcrops and used as samples for SEM-EDS.

SEM observation showed that framboidal aggregate are distributed locally in the sandstone and often form clusters (polyframboids). Framboids are mostly surrounded by clay minerals (montmorillonite) produced by alteration, but no sulphur-containing minerals such as pyrite and sulphate minerals were observed. In the cross section of the framboidal aggregates, microcrystals are often infilled by secondary growth products composed mostly of goethite, and Si and Al were also detected from the interstitial area inside and between microcrystals by EDS analysis. To examine the microtexture of framboids in more detail, thin films were cut out using focused ion beam (FIB) and observed by TEM.

TEM observation revealed that microcrystals that constitute the framboids are not single crystals, but are filled by assemblages of nano-sized crystals with a concentric layer pattern, which consists of several alternating layers of goethite nanocrystals and a mixture of clay minerals and amorphous silica. The goethite nanocrystals grew inward from the microcrystal outline, indicating that they were formed by alternation (replacement) of pyrite microcrystals. We also observed overgrowth of goethite nanocrystals growing outward from the periphery of the microcrystals, which are considered to be the main components of the infillings observed on the cross-section in SEM. These observations suggest that the transformation from framboidal pyrite to goethite proceeds by 1) desulfurization induced by oxidizing fluid penetration, 2) formation of nanocrystals of goethite grown from the interface (outline) of the original microcrystals, and 3) subsequent precipitation of clay minerals from the fluid. Since pyrite framboids show a diagenetic origin, it is clear that their oxidation must have occurred at a later stage and cannot be used as a paleoindicator of the oxidation state of the marine environment.

*References:*

[1] Rickard, D. (2021) Framboids, Oxford Univ Press 334pp
[2] Lougheed, M.S. and Mancuso, J.J. (1973) Econ Geol 68:202-209
[3] Martinez-Ruiz, F. et al. (1995) Ancona 1995:117-119
[4] Sawlowicz, Z. (2000) Prace Mineralog PAN 88:1-80

## Nanoscale characterization of (Ca-REE) fluorcarbonates

Conconi, R.[1], Capitani, G.[1] Gentile, P.[1] and Fumagalli, P.[2]

[1] Department of Earth and Environmental Sciences, University of Milano-Bicocca, Piazza della Scienza 4, 20126, Milano, Italy r.conconi@campus.unimib.it

[2] Department of Earth Sciences "Ardito Desio", University of Milan, Via Botticelli 23, 20133, Milano, Italy

---

Bastnäsite and synchysite are the end-members of the homologous polysomatic series and primary ores for Rare Earth Elements (REE). Fundamental research on CaREE-fluorcarbonates holds significant potential to enhance prospecting methods, metallurgical processes, and recycling strategies. Moreover, differences in morphology, microstructure, and REE content among different CaREE-fluorcarbonates may provide clues about mineral crystallization pathways and REE partitioning in hydrothermal systems. In this context, we studied CaREE-fluorcarbonates found within the miarolitic cavities of a granophyre in the Western Southern Alps (Italy). We extended the investigation from the microscale to the atomic scale, employing scanning (SEM) and transmission electron microscopy (TEM), microanalysis and Raman spectroscopy. The observations revealed the presence of (i) synchysite-(Ce) forming hexagonal prisms and rosette-like aggregates, (ii) bastnäsite-(Ce) forming blocky aggregates and (iii) bastnäsite-(Nd) forming more complex micro and nanostructures. Moreover, at the TEM scale, bastnäsite-(Nd) exhibits a nanostructure consisting of an intergrowth of bastnäsite-(Nd) nanocrystals with hematite nanocrystals and phyllosilicates. At the end, a possible scenario about their formation has been proposed, suggesting that the different CaREE-fluorcarbonates followed a crystallization sequence as a function of temperature and fluid fractionation: first synchysite-(Ce) formed, followed by bastnäsite-(Ce) and finally bastnäsite-(Nd). The diverse morphologies, in this case, were induced not only by the dominant REE in the fluid, but also by varying temperatures and cooling rates.

Our study highlights that nature may efficiently separate REE one from the other, such as Y from La, Ce and Nd; Ce from Nd and La; and Th, a radioactive and toxic element, seems to enter the structure of CaREE-fluorcarbonates mineral during the final stages of crystallization.

## A FIB-HRTEM investigation of (Co-Ni-Cu)-rich Fe sulfides in basic rocks from the internal zones of the Betic Cordillera

Ferreira, A. R.[1], González-Jiménez, J.M.[1], Yesares, L.[2], Blanco-Quintero, I. F.[3], Piña, R.[2], Gervilla, F.[4]

[1]Instituto Andaluz de Ciencias de la Tierra (IACT). CSIC-Universidad de Granada, España. amirarosa.ferreira.g@csic.es.

[2]Dpto. de Mineralogía y Petrología, Universidad Complutense de Madrid, España.

[3]Dpto. de Ciencias de la Tierra y del Medio Ambiente, Universidad de Alicante, España.

[4]Dpto. de Mineralogía y Petrología, Facultad de Ciencias, Universidad de Granada, España.

---

Hypabyssal basic igneous rocks, displaying evidence of hydrothermal alteration associated with metamorphism in green-schist facies, crop out in the internal zones of the Betic Cordillera (SE Spain). Metamorphic-related hydrothermal fluids precipitated a suite of iron sulfides of the pyrite-group enriched in Co, Ni and Cu in equilibrium with secondary silicate, mainly epidote, albite and quartz. In order to evaluate the mineralogical sitting of these three critical metals, thin foils were cut using Focused Ion Beam (FIB-SEM) and later analyzed by High-Resolution Transmission Electron Microscopy (HRTEM) from three different areas in the zoned iron sulfides. We identified a first type of grains made up of cores of marcasite wrapped by Ni, Co and Cu-rich bands with d-spacings corresponding to carrollite. A second type of grains consists of euhedral Rim-1 and botryoidal Rim-2 of pyrite. Within Rim-1, pyrite exhibits enlarged d-spacings due to the incorporation of these metals, while within Rim-2, the d-spacings identified in one of the bands increase correspondingly to those of cattierite. Finally, a third type of grains consists of a core of marcasite, wrapped by a euhedral Rim-2 of pyrite and a botryoidal Rim-2 composed of an alternation of pyrite-marcasite. Both core and rims show intercalations with Ni, Co and Cu-rich bands. Additionally, the presence of chalcopyrite, violarite and carrollite nanoparticles (<100 nm) is evidenced in Rim-1, demonstrating that these metals are present both in solid solution and as nanoparticles. A genetic model is proposed for the formation of this metallic mineralization, which includes the action of hydrothermal fluids with intermittent pulses and variable composition.

## Nanomaterials as agents for critical metal transfer in magmatic and hydrothermal ore systems

González-Jiménez, J.M.[1], Schettino, E.[2], Cano, N.[3], González-Pérez, I.[4], Ferreira, A.[1], Yesares, L.[5], Marchesi, C.[4], Camprubí, A.[3], Thomas N. Kerestedjian[6], Gervilla, F.[4]

[1]Instituto Andaluz de Ciencias de la Tierra (IACT). CSIC-Universidad de Granada, España

[2] Department of Earth Sciences, ETH Zürich, Switzerland

[3]Instituto de Geologia, Universidad Nacional Autónoma de México, Mexico

[4]Dpto. de Mineralogía y Petrología, Universidad de Granada, España

[5]Dpto. de Mineralogía y Petrología, Universidad Complutense de Madrid, España

[6]Geological institute, Bulgarian Academy of Sciences, Bulgaria

---

The formation of an ore deposit requires an optimal combination of common geological factors, namely: (1) source fertility (defined as the source for the metals and their ligands); (2) geodynamic trigger; (3) pathway (favorable lithospheric structure allowing transport by focused fluids/melts flow); (4) transport medium (melts and/or aqueous fluids); (5) deposition (trap allowing the selective crystallization/precipitation in a confined area); and (6) preservation of the mineral system. A common thought is that metals are transported in the melt and/or aqueous fluid as dissolved ionic species. New mineralogical data question such canonical hypothesis. For instance, quartz in deep-seated hypogene bornite-magnetite mineralization from porphyry copper deposits in Bulgaria hosts micron-to-nano sized blebs of Pd-rich tellurides, which suggest that the mechanical trapping of nanomelts enriched these deposits in critical metals. Similarly, jigsaw quartz in bonanza ores from southern Mexico contains droplet-like nanoparticulate acanthite ($AgS_2$), pearceite-polybasite ($[Ag_9CuS_4][(Ag,Cu)_6(As,Sb)_2S_7]$), and electrum (Au-Ag) precipitated by boiling of moderate-salinity hydrothermal fluids. Moreover, nanoscale investigation of silicate glass and pyroxene xenocrysts from rapidly erupted (sub)-volcanic rocks related to epithermal ores from SE Spain also reveal nano-sized droplets of Au, digenite (CuS), and galena (PbS). Nano-textural relationships suggest metal transport by nanomelts originated by: (1) direct transference from the magma to the hydrothermal fluid during fluid unmixing, (2) immiscibility from hydrothermal fluids due to the breakdown of metal-bearing aqueous complexes, or (3) adsorption–reduction operating on mineral surfaces due to fluid-rock interaction.

## Dual mineralogical sitting of the critical metals Nb-Ta-Sn-W in rutile.

Bermejo-López, D.[1], González-Jiménez, J.M.[2], Ortega, L.[1], Castiñeiras, P.[1], Crespo, E.[1]

[1]Departamento de Mineralogía y Petrología, Universidad Complutense de Madrid, 28040, Madrid (Spain). dabermej@ucm.es
[2]Instituto Andaluz de Ciencias de la Tierra, CSIC-Universidad de Granada, 18100 Armilla, Granada (Spain)

---

The Morille-Martinamor (Salamanca, Spain) tin and tungsten (Sn-W) mineralizations are related to the exhumation of a late-Variscan gneiss within the framework of a core-complex dome. In this geological context, the Sn-W vein-type mineralization also concentrated the critical metals like niobium and tantalum (Nb-Ta) in both rutile and columbite. A singular feature of the ore-forming rutile ($TiO_2$= 87.5 to 96.4 wt.%) is its complex chemical zoning, defined by appreciable variations in the content of $SnO_2$ (1.3- 2.4 wt.%), $WO_3$ (0.2-5.0 wt.%), $Ta_2O_5$ (0.3-0.1 wt.%), $Nb_2O_5$ (0.3 to 1.2 wt.%) and FeO (0.2 to 1.6 wt%). A the micron scale observed by means of Field Emission Scanning Electron Microscopy (FESEM), zoning microstructure of rutile is defined by oscillatory zoning with patchily distribution of the aforementioned elements in core and rims. A combination of Focussed Ion Beam (FIB) and High Resolution Transmission Electron Microscopy (HRTEM) applied on two selected interfaces between the core and rim of a single rutile grain reveals two distinct concentration mechanisms of Nb-Ta-Sn-W mineral phases. The first type of mineralogical sitting prevailing in the core of the grain is a patchy solid solution where Nb-Ta-Sn-W are found as patchily (both heterogenouesly and homogeneously distributed) nano-domains or modulations of the rutile lattice with d-spacings typical of hubnerite (1.609 Å for (300), cassiterite (3.410 Å for (110)) and manganocolumbite (1.536 Å for (313)). The second style of mineralogical fixation of the critical metals Nb-Ta-Sn-W are discrete mineral nanoparticles (NPs). These NPs ranging in size from 300 nm to 10 nm are essentially of wolframite (e.g. Hubnerite: 1.741 Å (202)) and columbite-group minerals: e.g. Ferrocolumbite: 2.350 Å for (600)). The duality in the concentration mechanisms of the critical metals Nb-Ta-Sn-W in rutile may have potential applications in understanding the transport, mobilization, and deposition of these metals in hydrothermal fluids.

# Microstructures of the Platinum Group Mineral nuggets in the Finnish Lapland.

Soukka, T.[1,2], Tuisku, P.[2], Moilanen, M.[1,2], Jaskari, M.[1,3], and Ranta, J.-P.[2]

[1] Centre for Material Analysis, University of Oulu, Finland, tapio.soukka@oulu.fi

[2] Oulu Mining School, University of Oulu, Finland

[3] FMT-Research group, Kerttu Saalasti Institute, University of Oulu, Finland

---

Platinum group mineral (PGM) nuggets have been excavated from gold panning areas as a side product in Finnish Lapland. However, source of these nuggets and their genesis are still poorly understood. In this study, detailed mineralogical study was conducted to collected nuggets in order to reveal their mineral paragenesis and favourable source rocks. Most important PGM's are isoferroplatinum and sperrylite. The aim of this work was to analyse inclusions and surface from isoferroplatinum grains and use them as a proxy for their source. Additional aim for this study was methodological development of studying PGM's at micro- and nanoscale.

Samples were obtained from Lemmenjoki and Ivalojoki gold panning areas from local gold panners. Polished sections were prepared from the heavy mineral samples. A total of 50 platinum group mineral grains were examined FE-SEM. A total of 1000 inclusions were analysed. Electron backscatter diffraction technique combined with EDS (EBSD-EDS) was employed using JEOL JSM-7900F FESEM equipped with Oxford instruments Symmetry EBSD and Oxford EDS detector. Combined EBSD-EDS mapping was made from 10 nuggets. More detailed nanoscale and structure studies were carried out from one Pt-Cu nugget. Total of 4 FIB-lamellaes and one cube was prepared by FIB-SEM. Cube was studied by Bruker SC-XRD for reveal Pt-Cu mineral structure. FIB-lamellaes were studied with JEOL JEM-2200 FS EFTEM/STEM for nanoscale studies.

22 different PGM minerals and alloys were identified from the samples. The most common inclusions were Ru-Os disulphides laurite and erlichmanite, which form zonal inclusions within the isoferroplatinum. The next most common minerals were PGE-sulfarsenides with irarsite being the most common. Rhodarsenide and hollingworthite occur as a smaller inclusions in the rutenium alloys and irarsite. Ru-Os-Ir alloys occur as small inclusions in the grain interiors. From the thiospinel group, cuproiridsite-malanite occurs in grain boundaries and as inclusions. Pt-Pd-Au-Cu mixtures appeared as their own grains. Pt-Fe-Cu mixtures appeared as inclusions and at the margin of isoferroplatinum. Isoferroplatinum nuggets contained silicate inclusions. Most common these were quartz, plagioclase and kaolinite. Some multiphase silicate inclusions were present also.

EBSD map from the studied Pt-Cu minerals showed polycrystals and structure of that was studied from one of the crystals. Hongshite was concentrated more in grain boundaries of $Pt_2Cu$ mineral. EBSD mapping showed that most of isoferroplatinum nuggets are monocrystals while the Pt-Cu nuggets contain polycrystals.

We suggest that the Os-Ir-Ru alloys, laurite-erichmanite minerals were formed at high temperature magmatic systems. As the temperature decreased, crystallographically oriented cuproiridsite, kashinite exsolutions formed. In late-magmatic and hydrothermal event, PGE-sulfarsenides, atokite, cooperite and speryllite inclusions were developed. Nuggets were affected by later weathering processes, which formed secondary platinum, kaolinite and rutile in surfaces.

# Nanomineralogy of Fe-rich sphalerite from the Santa Lucía Zn-Pb deposit (nothwest Cuba)

Gervilla, F.[1,3], Pérez-Vizcaíno, P.[2], González-Jiménez, J.M.[3], González-Pérez, I.[1],

[1]Departamento de Mineralogía y Petrología, Universidad de Granada, 18002 Granada, Spain/ gervilla@ugr.es

[2]Center for Research in Sustainable Chemistry-CIQSO, CSIC-UHU, 21071 Huelva, Spain

[3]Instituto Andaluz de Ciencias de la Tierra, CSIC, 18100 Armilla, Granada, Spain.

---

Reactions of coupled dissolution-reprecipitation (CDR) are common in pyrite and sphalerite forming SEDEX-type deposits, suggesting superimposition of multiple hydrothermal pulses. These micro-textures characterize the ore assemblage of the Santa Lucía Zn-Pb deposit in northwestern Cuba, a distal-type SEDEX deposit hosted by black shales in the upper part of the siliciclastic San Cayetano Formation. The deposit is made up of several tabular to lenticular bodies 40m thick on average and up to 1500m of lateral extent. The explored bodies show bottom-to-top mineralogical and textural zoning consisting of fine grained, laminated pyrite (mainly framboidal)-sphalerite-galena ore with intergranular quartz, evolving upwards to coarser sulfides associated with increasing amounts of quart and barite. Whereas the sulfide assemblage does not change in the upper part of the orebodies, its texture becomes brecciated and massive upwards, and is partly replaced by quartz and barite.

Two distinct types of sphalerite were identified in the ore assemblage: an early, most abundant, Fe-rich sphalerite and a late one almost free of Fe. Early sphalerite shows anhedral to colloform habits and contains frequent micron-sized pyrite inclusions mainly concentrated in the cores of the crystals, disseminated, or arranged according to the growing crystal planes of the host. Pyrite inclusions consist of framboidal aggregates or irregular crystal with corroded grain boundaries denoting their residual nature after dissolution/precipitation reactions. The late, Fe-poor sphalerite lacks pyrite inclusions and forms on the external grain boundaries of the early one.

A combination of electron-probe microanalysis (EPMA) and High-Ressolution Transimission Electron microscopy (HRTEM) on selected Fe-rich sphalerite grains show that relatively high iron contents in this type of sphalerite is due to dissolution of pre-existing pyrite via the formation of an intermediate phase that can be ascribed to rudashevskyite [(Fe,Zn)S]. The formation of this mineral may record a transitional stage between the dissolution of pyrite and its complete absorption by growing sphalerite.

# Mineralogy of Sn, W, Sc and Ga in ores of Ozernovskoe epithermal Au-Te-Se deposit, Kamchatka, Russia

Kozlov, V.V.[1], Vymazalova, A.[2*], Skilskaya E.D.[1] and Kudaeva Sh.S.[1]

[1] Institute of Volcanology and Seismology, Far Eastern Branch of the Russian Academy of Sciences, Piipa Boulevard, 9, Petropavlovsk-Kamchatsky, 683006 Russia.

[2] Czech Geological Survey, Geologická 6, 152 00 Prague, Czech Republic, *anna.vymazalova@geology.cz

---

Ozernovskoe epithermal Au-Te-Se deposit is represented by linear stockworks and pipes of quartz hydrothermal breccias with high sulfidation (HS) and intermediate-sulfidation (IS) assemblages hosted within a Miocene basaltic palaeovolcano. Ore deposition is related to multiple repeated cycles of extensive boiling and hydrothermal brecciation. The remarkable feature of this deposit is a very high Se content in ores and abundance of mixed sulphide-selenide and telluride-selenide minerals.

An Oxford Instruments AZtecLive EDS-WDS-EBSD system fitted with UltimMax 100 EDS, Wave 500 WDS and Symmetry EBSD detectors installed on Tescan FEG SEM was used during this study.

A complex Sn-W-Mo-Sc-Ga-bearing Au-Te-Se mineralization has been studied in several samples from relative deep horizon of the deposit. Several stages and substages of mineral deposition have been recognised here: (1) acid sulphate alteration (quartz, kaolinite, aluminium-phosphate-sulphate (APS) minerals, pyrite, rutile, anatase) (2a) Au-Te ore deposition (quartz, Mn-bearing dolomite, native tellurium, sylvanite, kawazulite, Se- and Te-bearing tetrahedrite-group minerals, etc.); (2b) Au-Sn-W-Mo-Sc-Ga-bearing ore deposition (quartz, cassiterite, illite-aluminoseladonite series minerals, Se-bearing tennantite-tetrahedrite minerals, mawsonite, hemusite, sylvanite-kostovite series, stützite, etc.).

The most important Sn, W, Sc and Ga carrier is cassiterite in close paragenesis with much less common scheelite, Sn-W-bearing rutile, Sc-bearing zircon and pure $TiO_2$ (rutile and anatase) in quartz. We suppose that their deposition represents a flux of high-temperature magmatic fluid during main-stage Au-Te-Se ore deposition.

Cassiterite is replacing rutile and forms epitaxial layers on rutile microcrystals. It contains unusually high concentrations of minor elements as a result of complex heterovalent substitution (wt%): W (1.2 - 7.9), Ga (0.8 – 1.6); V (1.5 – 3.05); Ti (1.3- 3.14); Al (0.2 – 0.7); Cr (up to 0.3), and Sc (up to 0.27). Scheelite is very rare and it does not contain any trace elements detectable by EPMA.

An interesting suite of Sn, W, Sc and Ga – bearing sulphides, selenides, oxides and silicates was formed during lower temperature dissolution of earlier cassiterite, its replacement and a short-range redeposition (from micron to mm scale) of its dissolution products. As a result, the following minerals (+quartz) were deposited: Sn-, W-, Sc-bearing tivanite (wt%: Sn 2.9-9.4; W 2.4-6.0; Sc up to 0.68), Ga-V-bearing aluminoceladonite (wt%: Ga 8.6 – 10.1; V 6.0-6.6); thortveitite, kiddcreekite, Se-bearing mohite, Se-bearing stannite, Se-bearing kuramite, Se-bearing herzenbergite, Sn-bearing clausthalite, Sn-, Se-bearing tetrahedrite-(Mn) (up to 2.7wt% Sn), Ga-, Se- bearing tetrahedrite-(Mn) (up to 1.8wt% Ga).

Several new Sn minerals were also recognised in this assemblage: svetlanaite (Sn(Se,S)), okruginite ($Cu_2Sn(Se,S)_3$), unnamed $Ag_8Sn(Se,Te)_6$ (a selenium analogue of Te-rich canfieldite) and unnamed $Cu_6SnTe_2S_4$.

## The replacement of pyrrhotite into pyrite-marcasite seen at the nanoscale

Yesares, L.[1], González-Jiménez, J.M.[2], Blanco-Quintero, I.F.[3], Ferreira, A.R.[2], González-Pérez, I.[4], Gervilla, F.[4]

[1]Dpto. de Mineralogía y Petrología, Facultad de Ciencias Geológicas, Universidad Complutense de Madrid, C/ José Antonio Nováis, 2, 28040. Madrid (España)

[2] Instituto Andaluz de Ciencias de la Tierra (IACT). CSIC-Universidad de Granada, Avda. de las Palmeras, 4, 18100. Armilla, Granada (España).

[3]Dpto. de Ciencias de la Tierra y del Medio Ambiente, Facultad de Ciencias, Universidad de Alicante, Carretera San Vicente del Raspeig s/n, 03690. Alicante (España)

[4]Dpto. de Mineralogía y Petrología, Facultad de Ciencias, Universidad de Granada, Avda. Fuentenueva s/n, 18002. Granada (España)

---

Pyrrhotite is one of main the mineral species of sulfurous Fe ore in nature originated in a wide range of geological settings. However, this monosulfide is relatively sensible to thermal changes so that it may be replaced by Fe disulfide (pyrite and/or marcasite) under hydrothermal conditions, which has been extensively reported in many natural rocks in the literature and tested in experimental works. For example, [1] have experimentally shown that in hydrothermal conditions up to 220ºC, the pyrrhotite to Fe disulfide reaction proceeded by a dissolution-reprecipitation mechanism. It seems that pyrite directly replaces pyrrhotite, simultaneously, by overgrowth from solution. In contrast, marcasite form preferentially by precipitation mechanism. However, to date, to the best of our knowledge there is no nanoscale evaluation of this process in natural samples. In this study we aim to fill this gap of pyrrhotite decomposition in hydrothermal conditions. We targeted the dominance of crystal growth (pyrite) vs. nucleation (marcasite) as a precipitation mechanism in natural sulfides found in sub-volcanic basic rocks of the external zones of the Betic Cordillera in south Spain. These rocks underwent hydrothermal alteration related with metamorphism in the greenschist facies providing a unique natural window to compare them with those conditions already applied in laboratory experiments. A careful inspection of thin-foils sampled by means of Focussed Ion Beam (FIB) under High-Resolution Transmission Electron Microscopy (HRTEM) confirm that transformation of pyrrhotite into pyrite-marcasite intergrowth takes place through a two-stage process. The first one is a dissolution processes in which monoclinic pyrrhotite is almost completely replaced by pyrite concomitant with crystallization of quartz; it is recorded as nanodomains of pyrrhotite with measured d-spacings of 3.063 Å close to 3.069 Å of plane (028), within a pyrite matrix with measured d-spacings of 2.222 Å corresponding to 2.2113 Å of plane (112). The second stage, involved oxidation of pyrite into marcasite [measured d-spacing of 1.6648 akin to 1.6749 Å of plane (130)] along with the crystallization of Fe-oxides like goethite [identified by the measured d-spacing of 4.5873 corresponding to the cell parameter 4-5800 Å along the crystallographic axis {101}]. We also observed that the replacement of pyrrhotite by pyrite-marcasite takes place preferentially along pre-existing crystallographic discontinuity in pyrrhotite, although both pyrite and marcasite matrix are polycrystalline made up of randomly oriented nanoscrystals.

[1] Qian et al (2011) Am Mineral 96: 1878-1893

# Critical metals in laterites, bauxites and red muds: concentration and distribution

Laita, E.[1], Yuste, A.[2], and Bauluz, B.[2]

[1]Departamento de Geología, Universidad de Jaén, Campus Las Lagunillas sn, 23071 Jaén, Spain, elaita@ujaen.es

[2] IUCA, Universidad de Zaragoza, Pedro Cerbuna 12, 50009 Zaragoza, Spain.

---

Laterites and Bauxites are products of intense chemical weathering processes at Earth's surface. During these processes, immobile elements such as critical metals (REE, Sc, V, Co, Ga, Sr, Nb, Hf, Ta and W) may be concentrated. Bauxite residues (red muds) resulting from alumina extraction via the Bayer process, also offer a valuable source of REEs [1]. Recently, remarkable attention has been paid to these materials as potential source of the metals considered critical to industry.

In this study, we evaluate the concentration and distribution of critical elements in laterites and bauxites (Lower Cretaceous, NE Iberia) as well as red muds supply by several alumina companies. The laterites are mainly formed by kaolinite, illite, smectite, quartz, hematite, goethite and minor proportions of orthoclase, ilmenite, rutile, anatase and diaspore [2]. The bauxites are composed by boehmite, kaolinite, hematite, goethite, gibbsite, and minor proportions of rutile and anatase [3].

Inductively coupled plasma mass spectrometry (ICP-MS) analyses of 25 lateritic samples, 22 bauxites and 3 red muds were carried out to evaluate their critical metal concentrations. In relation with the red muds, several fractions (<0.15mm/53 µm, <53µm/20 µm and <20 µm) were also analysed by ICP-MS to determine in which fractions are the critical metals concentrated. In addition, 4 lateritic samples with high critical metal content were selected to identified by scanning transmission electron microscopy (STEM) which mineral phases host the critical metals.

The laterites are included in continental profiles, being the lower levels of the profiles more weathered that the upper levels [3]. The critical metal concentrations are higher in the lower levels (752.49 ppm) than in the upper levels (337.49 ppm) [4]. The bauxites and the red muds provided by the companies present contents of critical metals of 1020.67 ppm and 1956.77 ppm, respectively, showing that the critical metals are more concentrated in the red muds. The analyses also show that critical metals are more concentrated in the <20 µm fraction (2045 ppm) of the red muds, suggesting that the phases controlling critical metals distribution have very small sizes.

In the laterites and bauxites, some critical metals (from Sc to W) present a good positive correlation with $Al_2O_3$, $Fe_2O_3$ and $TiO_2$, suggesting that these elements are associated to clay minerals (kaolinite, smectite and/or illite), to Fe and Ti oxides (hematite, goethite, anatase or rutile) and to Al hydroxides (boehmite, gibbsite or diaspore). The REE have also good positive correlation with $Al_2O_3$, $TiO_2$ and Th in the laterites, but they just correlate with $Na_2O$ in the bauxites. This suggest that the REE in the bauxites are probably dispersed in different phases. In the red muds, most of the critical metals are associated to resistate minerals according to their good positive correlation with $SiO_2$, MgO, CaO and $K_2O$. TEM images combined with energy-dispersive X-ray spectroscopy (EDS) showed the presence of REE-phases (monazite, xenotime, zircon, lanthanum oxide, cerium oxide and gold) adsorbed on the surface of kaolinite, which appear as nanoparticles that form aggregates of up to 100 nm.

*References:*

[1] Gentzmann, M.C et al. (2021) Appl Geochemistry 126: 104898
[2] Laita E. et al (2020) Sediment Geol 403: 105673
[3] Laita E. et al (2021) Ceram Int 47(10) Part A: 14527-14539
[4] Laita E. et al (2024) Appl Clay Sci 249: 107264

# Maghemite, a new key player to consider in the study of Ni-Co laterite deposits

Domínguez-Carretero, D.[1], Proenza, J.A.[1], Villanova-de-Benavent, C.[1] and Galí, S.[1]

[1]Departament de Mineralogia, Petrologia i Geologia Aplicada, Facultat de Ciències de la Terra, Universitat de Barcelona (UB), Martí i Franquès s/n, 08028 Barcelona, Spain

---

In the lateritic world-class district of Moa Bay (Eastern Cuba), maghemite, identified by means of X-Ray Diffraction (XRD), micro-Raman spectroscopy and Transmission Electron Microscopy (TEM), is an abundant mineral phase in the oxide zone, like in other Ni-Co laterite deposits. Maghemite in Moa Bay has average modal proportions of 5 % and eventually reaching up to 20 %. The studied maghemite represents an important ore mineral for both Ni and Co, reaching NiO and CoO concentrations of 13.9 and 1.84 wt.%, respectively.

Despite its potential for hosting notable concentrations of Ni and Co, both catalogued as critical metals by several national and international agencies [1, 2, 3], maghemite, whose formula is $(Fe^{3+}_{0.67}\square_{0.33})Fe^{3+}_2O_4$ [4], has usually been ignored in the study of Ni-Co laterites due to the difficulty to differentiate maghemite from magnetite. Both minerals have euhedral octahedral morphologies, they are mainly composed of Fe, and conventional analytical techniques do not allow distinguishing between $Fe^{2+}$ and $Fe^{3+}$. The overlook of maghemite as an important Ni- and Co-bearing mineral phase in laterite deposits makes the subsequent metallurgical processes inefficient at extracting the totality of Ni and Co from the mined ores.

Maghemite formation is produced in tropical areas with abundant rainfall, like in Eastern Cuba, in which maghemite is an intermediate phase in the ferrihydrite to hematite reaction [5,6]. The kinetics of the first part of the reaction (ferrihydrite □ maghemite) is very fast, however, the second part of the reaction (maghemite □ hematite) may take millions of years to complete. Thus, abundant maghemite may remain stable in the lateritic profiles for a very long time.

The correct identification of maghemite in lateritic profiles is critical to improve the Ni and Co recovery rates in oxide-type laterite deposits worldwide. This would lead to an increase in the economic revenue of laterite mining operations, and a reduction to the mine waste.

*References:*

[1] European Commission (2023). Study on the Critical Raw Materials for the EU (Final Report): 1-158.
[2] USGS (2023). Mineral Commodity Summaries: 210 p.
[3] International Energy Agency (2021). The Role of Critical Minerals in Clean Energy Transitions: 1-43.
[4] Bosi F. et al. (2019). European Journal of Mineralogy: 183-192.
[5] Barrón V and Torrent J (2002). Geochimica et Cosmochimica Acta: 2801-2806.
[6] Torrent J et al. (2006). Geophysical Research Letters: L02401.

# REE potential in sedimentary apatite: Delve deeper with microanalytics

Graul, S.[1], Monchal, V.[2], Rateau, R.[2], Joosu, L.[3], Moilanen, M[4]., Ndiaye, M.[1], and Hints, R.[1]

[1] Department of Geology, Tallinn University of Technology, Tallinn, Estonia; sophie.graul@taltech.ee

[2] Disciplines of Geology, Trinity College Dublin, Dublin, Ireland

[3] Geological Survey of Estonia, Rakvere, Estonia

[4] Centre for Material Analysis, University of Oulu, Finland

---

The growing need for raw materials and the decreasing availability of resources have led to an emerging interest in non-conventional deposits. This explicitly affects rare earth elements (REEs), for which one of the most significant prospects is phosphorites [1]. These formations represent high-tonnage, low-grade ore with complex genesis, resulting from multiple marine and diagenetic formation processes, leading to high variabilities. Ordovician phosphorites in Estonia are among Europe's most extensive phosphate rock reserves. Ore bodies consist of apatite-mineralised brachiopod shells in sandstone, sometimes cemented by carbonates [2]. Investigations were conducted in the Toolse and Aseri deposits to assess the geochemical variabilities and REE resources with whole-rock high-resolution exploration and LA-ICP-MS in situ imaging technique.

Shelly apatites generally have homogenous REE+Y patterns, with little variability, except Ce and Y. The REE+Y contents indicate distinctive middle-REE (MREE) enriched trends along with Y enrichment, compared to the average shale. Maximum values are reached in the lower part of the ores, where ∑REE+Y concentrations are enriched up to 1300ppm and 60% of apatite [2]. LA-ICP-MS analyses were to decipher uptake stages based on the stepwise distribution of Sr and U [3]. The extent of diagenetic overprint and enrichment varies locally. In Toolse, shells display early diagenetic textures with preservation of the Sr- and U-poor first uptake signals. In Aseri, U-sorting reveals a second diagenetic alteration-driven uptake in which the edges of the shell present a ΣREE up to 7020ppm. The genesis of the apatite phases was then modelled. Combinations of factors such as the accumulation of P and nutrients, the desorption of Fe-Mn phases and redox fluctuations led to a general REE enrichment. Localised development of euxinic conditions and lithogenic input promoted a later alteration-driven enrichment. Despite differences in enrichment level, the two deposits' REE distribution patterns are similar. The main REEs are Ce (33%), Y (21%), La (12%), Nd (16%) and Dy (3%). To determine ore prospectivity, the mineralisation prospectivity outlook coefficient ($K_{outl}$) was calculated [3]. Based on this approach, both deposits fall in the range of 'promising for economic development' ($33\% \leq REE_{def} \leq 50$; $0.9 \leq K_{outl} \leq 3.1$). Therefore, the ratio of valuable REEs is relatively high, and these ores are potential REE sources with low toxic element contents and predictable contents.

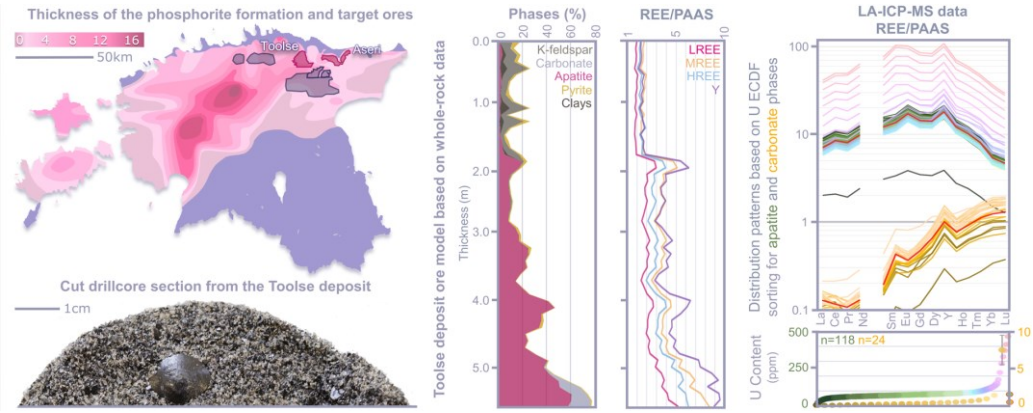


*References:*

[1] Emsbo (2014). Gondwana Research, 27:10008

[2] Graul (2023). Journal of Geochemical Exploration, 254: 107311.

[3] Graul and Monchal (2024). Under Publication.

# Graphitic sedimentary marbles and Sc-V-Y-REE bearing trace element minerals in carbonatite veins, The Aird, Scotland

Heptinstall, E.A[1], Parnell, J[1]., Schito, A[1]., Boyce, A.J[2]. Armstrong, J.G.T[1]., Muirhead[1]. and Still, J[1]

[1]School of Geosciences, University of Aberdeen, King's College, Aberdeen, AB24 3UE. Corresponding author, Eleanor Heptinstall, e.heptinstall.18@abdn.ac.uk

[2]Scottish Universities Environmental Research Centre (SUERC), East Kildbride, Glasgow, G75 0QF

---

The Aird is a geographical and distinctive geological region hosting marbles and intrusive pegmatite rocks in the Scottish Highlands. This work constrains previously underexplored carbonate-carbonatite geology of this distinct region that is adjacent to the Great Glen Fault, to discuss the paragenesis of graphitic-host rock and carbonatite-related fluids during the Caledonian Orogeny, and post-orogenic modification. Graphite occurs particularly in association with phlogopite mica, and also with other micas and Mg-chlorite. Although the graphite-phlogopite association is recorded widely elsewhere in mantle-derived rocks, our data suggests graphite at The Aird does not have a mantle origin. The carbon isotopic composition of the graphite ($\delta^{13}C$, 0.4 to -1.6 ‰) indicates graphitisation occurred from a $CO_2$-rich fluid associated with decarbonation or devolatilisation reactions of a carbonate-silicate protolith. Graphite-phlogopite bearing marbles in the Aird underwent extensive brecciation and haematite deposition that preceded carbon-rich, mantle-derived (carbonatite) fluids. Fenitized marbles contain calcite veins with mineral inclusions. The Sc-V-Y-rare earth element (REE)-bearing minerals include vanadate wakefieldite, sulphur-rich monazite, scandium-rich ilmenite and manganese oxides rich in barium and lead. Each of these phases is recorded in carbonatites elsewhere. An affinity with carbonatites is further suggested by the carbon isotope composition of the calcite veins, and anomalously high levels of manganese and strontium in the veins. Pyrite in veins within The Aird marble has a sulphur isotope composition depleted in $^{34}S$ (-15.5 to -16.6 ‰), suggesting a biogenic origin. Elsewhere in The Aird and in surrounding fenitized rocks $^{34}S$-enriched pyrite has sulphur isotope compositions between 7.7 to 6.1 ‰, outside the sulphur isotopic composition range of most carbonatite-hosted pyrite, suggesting pyrite veining was likely influenced by crustal fluid-rock interactions. The observations show that if the protolith has a carbonate-silicate composition, a graphite-phlogopite association can form without the need for mantle-derived fluids. These data also add weight to a model in which Scotland NW of the Great Glen Fault was affected by carbonatite-related fluids in the late-Caledonian Orogeny, that occurred following or transitional with hydraulic brecciation, haematite fluids, calcite veining and pyrite veining.

*References:*

[1] Heptinstall, E.A, Parnell, J., Schito, A., Boyce, A.J. Armstrong, J.G.T. and Muirhead. D., in Review. Graphitisation of Neoproterozoic sedimentary marbles in The Aird, Scottish Highlands. Scottish Journal of Geology, sjg2023-013.

[2] Heptinstall, E.A, Parnell, J., Boyce, A.J. and Still. J., 2023. Trace element minerals from carbonatite-related fluids, The Aird, Scotland. Scottish Journal of Geology, **59**, 1-2, sjg2021-015. https://doi.org/10.1144/sjg2021-015

# Genthelvite from Be-polymetallic ores of Perga deposit, NW Ukraine: Crystal chemistry, zonation and evolution during metasomatic events

Khomenko, V.[1], Kurzbach, M.[2], and Nissen, J.[2]

[1] Institute of Geochemistry, Mineralogy and Ore Formation, NAS of Ukraine, Kyiv, Ukraine; vladimir.khom@yahoo.com

[2] Institut für Angew. Geowissenschaften, Technische Universität, Berlin, Germany

[3]ZELMI, Technische Universität, Berlin, Germany

---

The Perga deposit (Ukraine) is the rare case of commercial concentration of beryllium in genthelvite (Ghv), $Be_3Zn_4(SiO_4)_3S$. It is located in the metasomatically altered “apogranitic” rocks of the Perga complex (1.80-1.70 billion years) in the NW part of the Ukrainian shield in the zone of Upper Proterozoic activation, controlled by an Intersection of several deep faults [1].

Ghv is widespread in various varieties of metasomatic rocks, but its content is highly variable. The richest ores were found in zones of albitization, where Ghv in forms of typical tetrahedral crystals or strongly resorbed grains, their aggregates or chains along borders of albite is closely associated with columbite, zircon, molybdenite, galena, fluorite, wolframite and sphalerite.

A systematic study of genthelvite from the Perga ores using EPMA, ICP-LA, XRD, µ-XRF, optical microscopy and Vis/IR spectroscopic methods reveals 3 main morphological types of Ghv, which also differ in composition: idiomorphic zoned small (0,0n-0,n mm) crystals; strongly resorbed slightly zoned grains or aggregates; and big (up to 4 cm) idiomorphic clearly zoned red crystals in silicification areas and in late quartz veins.

On the ternary diagram Ghv from Perga demonstrate large variability in composition with main vector close to Ghv – Danalite (Dan) series, typical of alkaline pegmatites [2]. Two main groups of Ghv composition with definite break between them can be definitely distinguished, one correspond to Ghv from alkaline metasomatites (3-15% of Dan component), another, with a larger admixture of the Dan component (up to 30%), – to Ghv from quartz veins. This difference can be caused by increase in oxygen activity in the fractured zones at the late low-temperature stages of the deposit formation. Mn component in all samples ranges from 0 to 10%. There is a weak general correlation between Fe та Mn.

The typical reddish-brown color of genthelvite is due to strong UV band, caused by charge transfer $O^{2-} \rightarrow Fe^{2+}$. The growth of $Mn^{2+}$ impurity and decrease of $Fe^{2+}$ increases the red-purple hues. A very strong complex band in the IR region 5500-2800 $cm^{-1}$ is attributed to the transition $^5E \rightarrow {}^5T_2$ in $^{IV}Fe^{2+}$ ions in the triangular pyramids $[Me^{2+}O_3S]$ of the genthelvite structure.

*References:* should be listed in a minimal way at the end, and in 10pt text:

[1] Metalidi SV and Nechaev SV (1983) Sushano-Perzhanskaya zone (geology, mineralogy, ores) 136 p

[2] Barton MD and Young S (2002) Rev Mineral Geochem 50:591-691

# Interactions of carbonatitic fluids with crustal wall rocks: A field-based study of Ondurakorume, NW Namibia

Ladisic, A.[1], Marks, M.A.W.[1], Walter, B.F.[1], Giebel, R.J.[2,3], Markl, G.[1]

[1]Tübingen University, Department of Geosciences, Schnarrenbergstr. 94-96, D-72076 Tübingen, Germany, andreja.ladisic@uni-tuebingen.de

[2]Technische Universität Berlin, Institute of Applied Geosciences, Ernst-Reuter-Platz 1, 10587 Berlin, Germany

[3]University of the Free State, Department of Geology, 250 Nelson-Mandela-Drive, Bloemfontein 9300, South Africa

---

In recent decades, there has been growing interest in carbonatites due to indications of their involvement in the deep Earth carbon cycle, as partial melting of carbonated peridotite or carbonated eclogite (e.g. carbon recycling in subduction setting) can play a significant role in the genesis of carbonatite melts. Additionally, carbonatites and associated alkaline silicate rocks have significant economic potential as they are often enriched in commodities, such as rare earth elements (REE) and high field strength elements (HFSE, e.g. Ti, Zr, Nb, U), as well as iron, copper, phosphorus, baryte, and fluorine.

This contribution focuses on the interaction between carbonatitic magmatism and wall-rocks at crustal levels. The pulsed release of alkali-rich fluids expelled by cooling and crystallization of the carbonatite intrusion causes a type of metasomatism called fenitization [1], whereas interaction between carbonatitic magma and wall-rocks produces the so-called antiskarn [2].

At the Ondurakorume carbonatite complex (OCC) in NW Namibia, calcite and dolomite carbonatites and related carbonatite dykes intrude associated syenites and nepheline syenites, and the Damaraland basement consisting of granites, marbles and other metasediments. The interaction between carbonatite and host rocks caused changes in mineralogy of country rocks on a micro scale, including alkali feldspar exsolution, changes in mineral chemistry of apatite and pyroxene, and formation of sodic pyroxene, sodic amphibole and REE-carbonates. The samples show two types of fenitization, as described in [1], as well as a combination of the two. The first type is pervasive, which produces patches rich in clinopyroxene, carbonate and apatite, and crystallizes additional finer-grained microcline along alkali feldspar grain boundaries. The second type of fenitization occurs when the fenitizing fluid invades the host rock as veins and veinlets, crystallizes fibrous and very fine-grained sodic clinopyroxene and sodic amphibole, often as intergrowths, as well as patches of albite. Clinopyroxene mineral chemistry reveals the evolution of clinopyroxenes from initial Na-rich clinopyroxene to almost aegirine end-member compositions in fenites. A certain preference in Ti and Zr distributions is observed, where clinopyroxenes from (nepheline) syenites are relatively more Zr-rich (from <0,01 to 0,03 a.p.f.u.), while clinopyroxenes from fenites are Ti-rich (up to 0,20 a.p.f.u.). Furthermore, cathodoluminescence has revealed five distinct generations of apatite crystallization across all lithologies. Mineral chemistry of apatite involves both britholite- and belovite-type substitutions. This information allows for a discussion on the evolution of minerals during carbonatite emplacement, and subsequent interactions with the wall rocks. It also raises questions about possible ways of distinguishing interactions of wall rocks with carbonatite melt from interactions with fenitizing fluid.

*References:*

[1] Elliott HAL et al. (2018) Ore Geol Rev 93: 38-59

[2] Anenburg M and Mavrogenes JA (2018) Am J Sci 318: 335-366

# Crystallochemical features of feldspars from Perga deposit (Ukraine)

Lunova, I.M.[1], Lunov, Ye.S.[1], Khomenko, V.M.[1] and Nissen, J.[2]

[1]Institute of Geochemistry, Mineralogy and Ore Formation, Kyiv, Ukraine

gerasimetsirina@gmail.com

[2]ZELMI TU Berlin, Germany

---

Perga beryllium deposit is located in the NW of the Ukrainian Shield (Zhytomyr region). It is situated within the Proterozoic Perga complex, which is connected with the intersection of several deep faults [1]. Geologically it is the part of the Sushchano-Perga zone (SPz). The SPz is composed of various rocks of different ages. Among them, the most widespread are quartzites, disthenic quartzites, greisens, syenites, alkaline syenites, alkaline metasomatites, granites, granite-porphyries, and subalkaline granites.

The main ore mineralization of the SPz, including unique beryllium (genthelvite type) deposit, is associated with Perga granites. The ore field is characterized by extensive development of alkaline metasomatites, represented by quartz-feldspar, albite-K-feldspar and biotite-K-feldspar rocks [2]. Since alkaline feldspars are the main forming minerals of ore-bearing rocks and ores, our goal is to investigate the evolution of their composition and structure in the processes of polymetasomatism, and the characteristic crystal chemical features of feldspars at different stages of ore formation.

The feldspars from a representative samples (17 specimens of metasomatites of various compositions, mostly from shaft No. 2) were investigated by means of EMPA, XRD, μ-XRF and optical microscopy. Most of the ore-bearing rocks contain two feldspars. K-feldspar, during the process of metasomatism, is replaced by albite with the formation of perthites and further progressive albitization. The content of $K_2O$ and CaO in albite varies from 0.02 to 3.8 % and from 0.001 to 0.006 %, respectively. The content of $Na_2O$ in orthoclase ranges from 0.02 to 1.3 %.

In feldspar-quartz metasomatites formed during albitization, the ZnO content in albite increases from 0.003 to 0.77 % near contacts or in inclusions within dissolved genthelvite crystals. The content of FeO in albite varies from 0,003 to 0,96 %, whereas in orthoclase − from 0.005 to 0.44 %. Bright blue amazonite with an elevated Pb content (0.03-0.08 % PbO) is characteristic of the late low-temperature stage of silicification.

Contrary to the previous works [2], our data revealed very insignificant amount of Rb in feldspars. Instead, increased concentrations of Rb were found in micas.

*References:*

[1] Bezpalko, N.A. (1970), Petrolohiya ta aktsesorni mineraly hranitiv ta metasomatytiv Pivnichnoyi Volyni, Nauk. dumka, Kyiv, 63 p. (in Russian)

[2] Metalidi, S.V. and Nechaev, S.V. (1983), Sushchano-Perzhanskaia zona (heolohiia, mineralohiia, rudonosnost), Nauk. dumka, Kyiv, UA, 136 p. (in Russian)

## The distribution of lithium pegmatites in Eastern Europe and Northern Asia

Naumenko, O. [1,2] and Dèzes, O.[2]

[1] Institute of Geological Sciences, NAS of Ukraine, 55-b O. Honchara str. Kyiv, 01601 od.naum@gmail.com

[2] BRGM, Direction des Laboratoires, Unité Isotopes, BP 6009, F-45060 Orléans cedex 2, France

---

Lithium is one of the most important strategic resources in the modern world. Lithium and its compounds are used in a variety of products, such as mobile phone batteries, laptops, electric vehicles, air conditioners and other electronic devices, as well as ceramics, lubricants and pharmaceuticals. Li plays a special role in the production of ceramics and glass. In the technological process, its oxide and aluminate are used to reduce the melting point. In addition, the presence of Li in the composition improves the resistance of ceramics and glass to thermal shock [1, 2].

Given the importance of this element in the modern technological process, it is necessary to account for all Li resources and develop an optimal international logistics system for its supply to the global market. Geological resources of Li include pegmatites and some volcanogenic clays [3]. Li is also extracted from continental brines [4] and Li-enriched water from oil fields, geothermal waters, mine waters, and concentrated seawater brines [5].

The United States Geological Survey has released a map of lithium deposits [6], but not all areas have been included. As part of the ANR TRANSFAIR project, we are compiling an inventory of lithium deposits genetically linked to pegmatites. In this presentation, we show the location, genetic type of deposits, percentage of Li, and known geological resources of Li for some deposits in - Ukraine, Kazakhstan, Tajikistan, Kyrgyzstan, Uzbekistan, Republic of Tyva, Azerbaijan, Armenia, and Georgia. Our work demonstrates that Li resources in the studied countries are distributed in such a way that their density potentially provides an opportunity to create a mining system that will not lead to the dominance of certain countries in monopoly ownership of the world market.

*References:*

[1] Bradley DC, McCauley AD, Stillings LM (2017) Mineral-Deposit Model for Lithium-Cesium-Tantalum Pegmatites. U.S. Geological Survey, Scientific Investigations Report 2010-5070-O, 48 pp
[2] Bibienne T, Magnan J-F, Rupp A, Laroche N (2020) From mine to mind and mobiles: society's increasing dependence on lithium. Elements 16: 265-270
[3] Bradley DC, Stillings LL, Jaskula BW, Munk L, McCauley AD (2017b) Lithium. In: Schulz KJ, DeYoung JH Jr, Seal RR II, Bradley DC (eds) Chapter K. Critical Mineral Resources of the United States-Economic and Environmental Geology and Prospects for Future Supply. U.S. Geological Survey, Professional Paper 1802-K, pp K1-K21
[4] Munk L and 5 coauthors (2016) Lithium brines: a global perspective. In: Verplanck PL, Mitzman MW (eds) Rare Earth and Critical Elements in Ore Deposits. Reviews in Economic Geology 18, Society of Economic Geologists, pp 339-365
[5] Bowell RJ (2019) Development of hard rock lithium deposits. In: Lithium Occurrence, Exploitation and Processing. Proceedings of the First South America Lithium Conference, Puno, Peru. Peruvian Institute of Mining Engineers, Lima. May 2019.
[6] U.S. Geological Survey (2019) Mineral Commodity Summaries 2019. U.S. Geological Survey, Reston, pp 98-99

# Kaolin diapirs of the Ukrainian shield – potential resource of titanium mineral deposits

Komliev O.O., [1], Remezova O.O.[2], Spytsia R.O. [3], Okholina T.V.[2], Vasylenko S.P.[2], Komlieva M.O.[1]

[1] Taras Shevchenko National University of Kyiv, Kyiv, Ukraine.

[2] Institute of Geological Sciences of the National Academy of Sciences of Ukraine, Kyiv, Ukraine; e-mail elena.titania2305@gmail.com

[3] Institute of Geography of the National Academy of Sciences of Ukraine, Kyiv, Ukraine

---

An important feature of the geological structure of the Ukrainian Shield (USh) is the developed kaolin weathering crust (KWC) formed in the Mesozoic-Cenozoic period. The KWC is an industrial object and the main source for various sedimentary minerals, including titanium and titanium-zirconium placers. The KWC is a physical body that can be tens of meters thick and occurs in fragments covering an area of thousands to tens of thousands of $km^2$. The KWC is developed on all elements of the ancient (buried) relief. In the valleys of modern rivers, the KWC is often eroded. The kaolin horizon is underlain by hydro-mica and micaceous horizons. The KWC is planar, and in fractured tectonic zones, a linear crust was formed, which in some places extends hundreds of meters deep and overlies the planar crust.

The KWC is a necessary stage for the formation of titanium (ilmenite) placer deposits in the USh. Thus, on the shield's plutons(Korosten and Korsun-Novomyrhorod), a thick weathering crust is formed on rocks of the crystalline basement. Titanium minerals are found in them mainly as accessory minerals. Ilmenite has the chemical composition of $TiO_2$ (52.7%) and $Fe_2O_3$ (47.3%). In the KWC, titanium minerals are released from igneous rocks, primary enrichment and formation of eluvial placers. FeO appears in the chemical composition of ilmenite. In the course of its subsequent erosion by exogenous processes and sedimentary differentiation, various genetic types of continental and coastal titanium and titanium-zirconium placers emerge.

The kaolin horizon, which is saturated with water, becomes plastic and can spread horizontally. However, in natural and artificial (quarry) excavations, in particular in the areas of ilmenite deposits development on the USh, vertical and inclined deformations of the kaolin horizon resembling diapirs and called kaolin diapirs (KD) were found. The apparent height of the KD in these sections reaches 10-12 m. However, the roots of the cut diapirs are observed at the bottom of the pits where mining is carried out. Such vertical deformations of the kaolin horizon could occur under the influence of external triggers, the main of which is certain structural and tectonic conditions. The KD are developed in the areas of tectonic faults, fractures, at the contact of small tectonic blocks, which are characterised by inversion movements, compression-stretching regime, and developed linear KWC. As a result, a peculiar geological and geomorphological paragenesis "KD-positive relief form (linearly elongated or circular ridge, hill)" occurs here. The alternation of compression and tension vectors creates conditions for extrusion (formation of a KD) and formation of a linear weathering crust. The nature of the geological structure of the areas of the KD development indicates two episodes of their formation - the Jurassic-Cretaceous boundary and the Oligocene-Miocene boundary. Above the KD, a change in the color of the moraine of the Dnipro glacier (from red to grey)is observed.

Within the northwestern part of the USh, due to the combination of their main factors (bedrock, KWC, tectonic regime, paleogeographic and paleogeomorphological conditions), significant placer fields and deposits of titanium (ilmenite) minerals were formed. The KD also contain the latter and, in our opinion, constitute a significant potential resource. A quick and effective method of prospecting for KD is a landscape and geomorphological analysis of the territory, which should be carried out using aerial survey data. Large-scale topographic maps and digital models of relief can also be used.

# Crustal wall-rock assimilation and metasomatism caused by carbonatites – key processes for HFSE enrichment?

Walter, B.F.[1], Marks, M.A.W.[1], Giebel, R.J.[2,3] and Markl G.[1]

[1] Tübingen University, Department of Geosciences, Schnarrenbergstr. 94-96, D-72076 Tübingen, Germany, b.walter@uni-tuebingen.de

[2]Technische Universität Berlin, Institute of Applied Geosciences, Ernst-Reuter-Platz 1, 10587 Berlin, Germany

[3]University of the Free State, Department of Geology, 250 Nelson-Mandela-Drive, Bloemfontein 9300, South Africa

---

Numerous carbonatites are hybrid rocks resulting from the interaction between carbonatitic melts and variable crustal host rocks during their ascent and emplacement in the crust. In the light of their re-evaluation as hybrid rocks, the origin and significance of abundant silicate minerals and partly related enrichments of rare earth (REE) and other high field-strength elements (HFSE, Ti, Zr, Nb, U) in carbonatites and associated silicate rocks need to be revisited. A major base for such metasomatic models are the very low solubilities for Si and Al in a carbonatite liquid under middle and upper crustal conditions [1]. Hence, abundant silicate minerals such as olivine, clinopyroxene, amphibole or mica may form within and around many carbonatites and represent key witnesses of interaction between carbonatites and their wall-rocks at various scales and can even reach economic grades and tonnages for mica (altered to vermiculite) like in Palabora or Siilinjärvi.

Beside processes leading to silicate mineral formation in the wall rocks, so called antiskarn processes can cause silicate mineral formation inside the carbonatite. During such silicate formation, $CO_2$ is released and can act as ligand for HFSE-REE [2] which can now be transported into the hybrid rocks outside the channel. The HFSE-REE behaviour during antiskarn formation is clearly to be distinguished from the process of liquid immiscibility which based on known partition coefficients [3] would enrich HFSE in carbonatitic liquid

Besides processes related to wall rock metasomatism during ascent, crustal contamination at emplacement level can be a first order process modifying a carbonatitic liquid supporting or suppressing enrichments of HFSE. In particular, Giebel [1] showed for the Kaiserstuhl carbonatite in Germany, that crustal contamination can have a significant influence on the REE-budget in a carbonatitic melt which is of fundamental and economic interest. Via coupled substitutions (triggered by shifts of the melt composition during contamination) in early magmatic minerals such as apatite and perovskite, REEs can be endowed or removed from the carbonatite melt [1,4].

Moreover, aureoles of hydrothermally altered host rocks (called fenites) occur around numerous carbonatite bodies and show a significant enrichment of Na-K silicates (orthoclase, albite, sodic pyroxene/amphibole) as well as halogens and sulfur. Fenite halos therefore record a significant loss of alkalis (Na, K) and HFSE-REE from the carbonatite liquid via aqueous-carbonic fluids of variable salinity (brine melt) and ligand contents (fluoride/sulfate/carbonate/chlorine). In particular beside $CO_2$, the sulfur content and the related sulfur-complexes in the brine [5] may be of outstanding importance as transport agent for HFSE-REE and their enrichment.

[1] Giebel J et al. (2019) J Petrol: 60(6), 1163-1194.
[2] Migdisov, A. et al. (2016) Chem Geol, 439:13-42.
[3] Veksler, I. V., et al. (1998) J Petrol, 39(11-12): 2095-2104.
[4] Gudelius G.et al. (2023) J Petrol. 64(6): egad036
[5] Walter B.F. et al. (2021) Earth-Science Reviews: 215, 103509.

## Germanium in sphalerite, but how and why? Atomistic simulations have an answer

Haghi, A. and Jahn, S.

Institute of Geology and Mineralogy, University of Cologne, Zülpicher Str. 49b, 50674 Köln, Germany, e-mail: ahaghi1@uni-koeln.de

---

Today, germanium is considered a rare but critical element due to its widespread use in semiconductor-based technologies such as fibre optic communications, infrared night vision, and in catalysis, e.g. for polymerization processes.
Geochemically, the crustal concentration of Ge is 1.7 ppm, which is similar to that of W, Mo, U and Sn. However, there is not a single deposit that can be considered a germanium mine. The reason behind this unusual behaviour is that germanium mimics Si in igneous, aqueous and crystalline environments and so Ge is almost uniformly distributed across the whole Earth's crust. Exceptions are zinc and coal mines where Ge is enriched up to 3000 ppm.
Alongside Ge-rich coal and recycling of used electronic devices, up to now, extraction of Ge as a by-product of sphalerite processing remains the main source of germanium. Various mechanisms have been suggested for the substitution of Ge within the structure of sphalerite, which is investigated here based on atomistic modelling. Different substitution mechanisms including the direct substitution of Ge(II) and Ge(IV) for Zn(II) and the coupled substitution of Ge(IV)+2(Cu(I)/Ag(I)) for 3 Zn(II) are examined by means of density-functional theory (DFT) calculations. Our simulations suggest that a coupled substitution of Zn by Ge alongside with Cu (+Fe) with a configuration similar to a briartite-like structure ($Cu_4(Fe,Zn)_2Ge_2S_8$) is the most probable substitution mechanism with lowest substitution energy.
So far, these findings suggest that Ge(IV) is energetically preferable for the substitution of Ge in sphalerite, if the co-incorporation of Cu(I) to balance the charge difference and of Fe(II) to reduce the strain energy are considered.

## Copper, Uranium and REE Mineralisation in an Exhumed Oil Reservoir, Southwest Orkney, Scotland

Heptinstall, E.A.[1], Parnell, J[1]., Armstrong, J.G.T[1]., Schito, A[1]. and Akinsanpe, T.O[1,2]

[1]School of Geosciences, University of Aberdeen, King's College, Aberdeen, AB24 3UE. Lead author, Eleanor Heptinstall, e.heptinstall.18@abdn.ac.uk

[2]Department of Geology, Obafemi Awolowo University, Ile-Ife, 220103, Nigeria

---

Copper, uranium, and rare earth element (REE) mineralisation occurs in hydrocarbon-bearing Devonian continental sandstones in southwest Orkney, Scotland. The aeolian Yesnaby Sandstone Formation and fluvial Harra Ebb Sandstone Formation were mineralised following oil emplacement. This study examines petrographic relationships at Yesnaby in the Devonian Orcadian Basin, and are assessed in terms of spatial relationships between mineralisation and hydrocarbons, the paragenetic relationships between mineralisation and hydrocarbons, and the timing of mineralisation and hydrocarbon emplacement within the burial/uplift history. The REE-bearing APS mineral florencite is particularly associated with bituminous nodules, many of which contain brannerite. Subsequently hydrothermal copper and other sulphides, and barite, further mineralised the oil reservoir at a temperature of ~ 190 ℃. Oil was mobilised through mineralised fractures at this stage. Biodegradation of the oil occurred later, following the Carboniferous-Permian uplift. The occurrence confirms that Cu-APS mineralisation is possible in relatively low-temperature regimes in sedimentary basins. The timing of mineralisation between the emplacement of bitumen and uplift suggests that the reducing environment conferred by the oil was the predominant factor that favoured Cu-U-REE ore mineral deposition.

*References:*

[1] Heptinstall, E.A, Parnell, J., Armstrong, J.G.T., Schito, A. and Akinsanpe, T.O. 2023. Copper, uranium and REE mineralisation in an exhumed oil-reservoir, southwest Orkney, Scotland. Geosciences, 13, 5, 151. https://doi.org/10.3390/geosciences13050151

# Rare Earth Element Distribution in Tošići-Dujići Bauxite Deposit: Insights from BCR Sequential Extraction

Topalović, E.[1], Čobić, A.[1], Fiket, Ž.[2] and Tomašić, N.[1]

[1]University of Zagreb, Faculty of Science, Department of Geology, Horvatovac 102B, 10000 Zagreb, Croatia (ena.topalovic@geol.pmf.unizg.hr)

[2]Ruđer Bošković Institute, Division for Marine and Environmental Research, Bijenička cesta 54, 10000 Zagreb

---

The Tošići-Dujići bauxite deposit is located in the Dalmatian inland near the village of Oklaj in Croatia and lies on Lower to Middle Eocene foraminiferal limestone in the high karst unit of the Dinarides [1]. Karst bauxites occurring in the Mediterranean region can contain a total of more than 1000 mg/kg of rare earth elements (REE), which can lead to the formation of authigenic REE minerals [2]. Previous studies of the Tošići-Dujići bauxite deposit showed the REE concentrations ranging from 959 to 3496 mg/kg in total, indicating the potential presence of REE minerals [3].

Overall six bauxite samples were collected for geochemical and mineralogical analyses. A standardized three-step Bureau Communautaire de Référence (BCR) sequential extraction procedure [4] was used to determine the concentrations of REE of each fraction. Additionally, X-ray powder diffraction (XRPD) was performed on the residual and heavy mineral fractions to establish the presence of REE minerals.

The results of the sequential extraction show that more than 62 % of the REE are present in the residual fraction. The oxidizable fraction (bound to organic matter, sulphur, sulphides) from step 3 exhibits the lowest REE concentrations and comprises only 1 to 4 % of the extracted REE in the relation to the REE of the whole-rock. The reducible fraction (bound to Mn and Fe oxides) from step 2 has significant REE extractions varying from 9 to 29 % relative to the whole-rock REE. Similarly, the exchangeable fraction (adsorbed on minerals, exchangeable ions in clays and carbonates) from step 1 also demonstrates higher REE extractions, ranging from 4 to 17 % relative to the total REE. The exchangeable fraction is characterised by a positive Ce anomaly ($Ce/Ce^* = 1.6 – 27.0$) and low La/Yb ratios from 0.001 to 0.073 indicating an enrichment of HREE. Likewise, the reducible fraction exhibits a positive Ce anomaly ($Ce/Ce^* = 2.4 – 85,1$) with the exception of two samples. Only one bauxite sample within this fraction is enriched in LREE (La/Yb = 16.6), the others are enriched in HREE. All samples in each fraction of the sequential extraction analysis show a negative Eu anomaly.

The findings indicate that a primary reservoir for REE in the Tošići-Dujići bauxites is the residual fraction. The XRPD analysis of the residual fraction identified gibbsite, böhmite, zircon, anatase, rutile and clay minerals, indicating the potential for REE to be present as impurities within these minerals. Minor REE may be associated with carbonates or Fe and Mn oxides, which are known for their ability to scavenge REE. A comparable mineral assemblage to residual fraction was observed in the heavy mineral fractions consisting of zircon, anatase, rutile, hematite, goethite and gibbsite. Although previous investigations of the Tošići-Dujići bauxite deposit revealed the presence of monazite-(Ce), xenotime-(Y) and florencite-(Ce) [3], our study did not find REE minerals in the heavy mineral fractions. Further analyses are necessary to accurately identify REE minerals within the Tošići-Dujići bauxite deposit, as these minerals may be present as accessory minerals requiring more sensitive techniques for detection.

*References:*

[1] Schmid et al. (2008) Swiss J Geosci 101:139-183
[2] Maksimović Z and Pantó G (1996) Chapman & Hall, UK:257-279
[3] Tomašić et al. (2021) Min 11:1260
[4] Rauret et al. (1999) J Environ Monit 1:57-61

## Preliminary Results of an Antimony Geochemical Study, Longford-Down terrane

Cooper, M.R.[1], Patton, M.A.G. [1], McNulty, K.[2], Murrells, A. [2] , Hollis, S.[3] and Torvela, T.[4]

[1]Geological Survey of Northern Ireland, 7th Floor, Adelaide House, 39-49 Adelaide Street, Belfast BT2 8FD, UK

[2]Conroy Gold and Natural Resources plc, 3300 Lake Drive, Citywest Business Campus, Dublin 24, D24 TD2, Ireland, UK

[3]Edinburgh School of Geosciences, Grant Institute, W Mains Rd, Edinburgh, EH9 3JW, UK

[4]School of Earth and Environment, University of Leeds, LS2 9JT, UK

---

Antimony (Sb) is listed as a critical raw material (CRM) in the UK and EU, due to its key role in the economy and the Green Energy Transition. Antimony is used in a wide variety of technologies, including semi-conductors, circuit boards, photovoltaic cells, and batteries. As of 2020, about half of the Sb mined in the world came from China, and much of the rest came from Russia and Tajikistan.

This study of stibnite bearing quartz veins and breccias, that cross-cut orogenic gold mineralization in the Longford-Down terrane, presents the initial findings of geochemical analysis of the mineralization and country rocks in the Clontibret-Clay Lake region. The mean Sb content of the stibnite veins and breccias analysed is around 10 %, compared to mean Sb for the surrounding country rock which is only 90 ppm. From the samples analysed, Sb content in mineralized veins and breccias is up to 36%. These high values are however restricted to narrow (~10cm) drill core intervals, whilst historic mining has proven grades of 14.5 % over 1.2 m. Tellus Project geochemical plots and GIS heat maps show very clearly the location of areas with anomalous Sb that will help guide future exploration and research.

Future research will involve a multi-scale study of outcrop to regional-scale geological, geochemical and geophysical datasets. Work is needed to look for inter-relationships between structural evolution, magmatism and fluid flow, on the Sb mineralisation. This work will inform the Department for the Economy (DfE) of potential opportunities for Sb and other CRMs in the region as it develops a policy position on mineral development.

# Typical features of the chemical composition of columbites from Perha metasomatites, North-West of Ukrainian Shield

Chernysh, D.S.[1], Khomenko, V.M.[1], and Nissen, J.[2]

[1]M.P. Semenenko Institute of Geochemistry, Mineralogy and Ore Formation, NAS of Ukraine, Kyiv, Ukraine; vladimir.khom@yahoo.com

[2]ZELMI, Technische Universität, Berlin, Germany

---

Among the tantal-niobates of the Perha deposit, hatchettolite, fergusonite, samarskite, marignacite, columbite, euxenite, and ilmenorutile were previously described [1, 2].

Columbite is the most widespread accessory ore mineral in the metasomatized A-type granites of the Perha deposit and can be used as a source of Nb in complex development of beryllium ores. We examined columbites in a series of metasomatite samples from the mine dumps of this deposit.

In the analyzed samples the mineral is present mainly in the form of remains of individual grains with corroded edges, sized up to 10×250 μm, sometimes up to 1.5 mm, also in the form of inclusions in zircon, and in intergrowths with cassiterite. Zoning is rarely preserved in columbite grains. The columbite paragenesis includes albite, zircon, cassiterite, quartz, genthelvite.

The chemical composition of columbites from different types of metasomatites was studied with electron microprobe analysis (EMPA). The generalized formula of columbite is $AB_2O_6$, where A is $Fe^{2+}$ or $Mn^{2+}$, and B is $Nb^{5+}$ or $Ta^{5+}$. The composition of Perha samples corresponds to columbite-(Fe). Its formula, based on the average content of elements: $(Mn_{0.16}Fe_{0.81})_{0,97}(Nb_{1,79}Ta_{0,04}Ti_{0,10}W_{0,07}Sn_{0,01})_2O_6$. The main and impurity elements varies in such intervals (wt%): $Nb_2O_5$ = 43.58-75.04; $Ta_2O_5$ = 1.47-4.06; FeO = 11.47-18.79; MnO = 1.87-5.80; $WO_3$ = 1.81-29.84; $TiO_2$ = 0-3.20; CaO = 0-0.41; $SiO_2$ = 0-0,07; MgO = 0-0,1.

The studied columbites are characterized by variations in the Mn/(Mn + Fe) and Ta/(Ta+ Nb) ratios in the ranges 0.09-0.29 and 0.005-0.03 respectively. Some samples are enriched with tungsten; they show a shortage of large-charge cations and a proportional increase in the sum of cations in site A. This can be explained by complex isomorphic substitution according to the following scheme: $W^{6+}+Fe^{3+}+OH \rightarrow 2Nb^{5+} + O$. Some of the W-enriched samples contain the highest Pb contents among the analyzed columbites, whereas in general, the Pb content is quite stable (0.32-0.47% of PbO).

Permanent low Ta (<0.06 at%) and poor Mn (<0.28 at%) contents allow us to suppose that the original metasomatized subalkaline A-granites belong to the Nb-Zr-Y type.

*References:*

[1] Buchinskaya KM, Nechaev SV (1994) Mineral Journ 1: 15-29 [in Russian]
[2] Metalidi SV, Nechaev SV (1983) Sushano-Perzhanskaya zona (geologiya, mineralogiya, rudonosnost) [in Russian]

## The potential of Mineralogy in Circular Economy

Pavese A.[1]

[1]Earth Sciences Department, University of Turin, Valperga Caluso Street 35, 10125-Turin (Italy) – alessandro.pavese@unito.it

---

Mineralogy has progressively developed an intrinsic multidisciplinary and transdisciplinary character, encompassing geology, crystallography, mathematics, physics, chemistry, material sciences and, nowadays, medical-social-economic issues, too [1]. Dating back to its origins, Mineralogy was designed to deal foremost with the solid phases that are the building units of the geological structures of our planet. Such a role went on widening upon time; a turning point was the recognition of minerals as active and interacting key-reactants in the complex natural reactions involving crystallization / dissolution / recrystallization at high-pressure and/or high-temperature, in a regime of ever changing open-systems that require extensions of the conventional thermodynamics for interpretation. This made Mineralogy put forth branches that involve, on the one hand, the use of advanced laboratory/large scale facilities for challenging experiments, new theoretical methodologies from chemical-physics (modelling), and, on the other hand, a wider frame of investigation, adding anthropic interaction and processes, to the natural ones. The modern Mineralogy has developed flexibility, knowledge and know-how to go further from its original purview and delve into the multi-faceted problems of “circular economy”, interweaving raw materials, secondary raw materials, traditional and novel manufacturing processes, and societal/environmental/economic/energetic issues, pointing to provide contributions to the overall target of “global sustainability”.

*References*

[1] Tribaudino M., Vollprecht D. and Pavese A. (2023) Minerals and Waste. Earth and Environmental Sciences Library. Springer

# Waelza slag as potential Fe source – a geometallurgical case study to convert waste to resource

Gronen L.[1], Gondorf C.[2], Gürsel, G.[3], Feldrappe V.[1] and Weitkämper, L. [3]

[1]FEhS Institute of Building Material e.V., Germany, l.gronen@fehs.de

[2]RWTH-Aachen University, Department for Industrial Furnaces and Heat Engineering, Germany

[3]RWTH-Aachen University, Unit of Mineral Processing, Germany

---

The Waelz process is the state-of-the-art application for Zn recycling from dust and sludge originating from steel mills in which Zn containing scrap is used as educt, extensively. Within a rotary kiln the mostly oxidised zinc phases of the dust are reduced by coke and Zn evaporates into the off-gas. In the countercurrent gas-phase in the kiln, the zinc is re-oxidized and extracted as crude Waelz-oxide. Due to reactions in the kiln, also amounts of the Fe-oxides from the dust being partially reduced to different Fe-phases and $Fe_{met}$. Together with the for metallurgical need added slagging agents, the Fe-phases form the Waelz slag of which app. $2x10^6$ t/a is produced worldwide [1]. Most slags are landfilled or being used as landfill construction material. Both leading to loss of significant amounts of valuable materials as Fe (> 30 wt. %), Cu, Cr and residual Zn.

One major issue hampering the direct use of the Waelz slag as Fe-source are trace metals, which potentially disturbing the pig iron quality and cannot be removed from pig iron nor from crude steel. Further, the use of Waelz slag as melting additive is limited due to the quantity of Ca-Si phases of the slags, which leads to issues during smelting due to increased energy consumption and intensive foaming.

Therefore, in this study we present the geometallurgical characterization and potential treatment and processing methods for improved utilization of Waelz slags as raw material substituting Fe-ores. Main emphasis of the investigations lies on the development of a mineral processing chain for the use of the mineral assemblage of the slag. Aside from Fe-oxid recovery, the identification and the possible recovery of Ca-Si phases is one major task to prevent “virtual $CO_2$”, from lime, being landfilled, too. Applications for the Ca-Si products being discussed as well as the possible applications of the Fe-oxides.

*Literature:*

[1] Gurdinsky P I et al. (2019) Inorg Mater 10:1220-1226

## Investigation of a Lithium-Ion-Battery Recycling Slag

Gantz, C.[1,2], Neumann, A.[1,2], Roggendorf, H.[1,3], and Stöber, S.[2]

[1]ITEL – Institute for Technologies and Economics of Lithium GmbH, Halle (Saale) 06108, Germany, cornelius.gantz@lithiuminstitut.de

[2]Institute of Geosciences and Geography, Martin-Luther-University Halle-Wittenberg, Halle (Saale) 06120, Germany

[3]Institute of Physics, Martin-Luther-University Halle-Wittenberg, Halle (Saale) 06120, Germany

---

The rising demand for lithium-ion batteries (LIB) and EU legislation require efficient recycling of all scarce metals in LIB [1,2]. Pyrometallurgical processes are already established for the recovery of most valuable metals from LIB with NMC cathodes as alloy or metal sulfide (e.g. Ni, Cu, Co); however, lithium dissolves into the slag and is currently lost for recycling [3]. The implementation of lithium recycling based on existing pyrometallurgical processes for Ni, Co, and Cu extraction could proof to be fast and resource efficient. Therefore, understanding the slags produced by pyrometallurgical recycling is essential for the development of a lithium recovery process.

Solid slag from an industrial LIB recycling process was sampled. The extractive pyrometallurgical recycling process produces one cone containing mainly metal sulfides with a slag cap on top (product cone) and two cones consisting mainly of slag (slag cone). One slag cone and the slag cap of the product cone, from the same recycling batch were sampled at selected positions. Bulk samples were analyzed by i.a. wavelength dispersive X-ray fluorescence (WDXRF), inductively coupled plasma optical emission spectroscopy (ICP-OES), and X-ray diffraction (XRD). Samples were also analyzed by laterally resolved methods including optical microscopy, micro-X-ray fluorescence (µXRF), and scanning electron microscopy (SEM) with energy dispersive X-ray spectroscopy (EDX).

The slag cone showed only little chemical zonation. The main constituents of the slag system are CaO, $SiO_2$, and $Al_2O_3$ with other major components being $Na_2O$, $Fe_2O_3$, MgO, $V_2O_5$, $Mn_2O_3$, and $Cr_2O_3$. The main phases were determined by qualitative XRD analysis and showed a mineralogical composition typical of non-ferrous slags (e.g. melilite, clinopyroxene, nepheline). Lithium formed β-eucryptite or a lithium metasilicate, the former being much more prominent. The slag cap had elevated levels of metal sulphides and contained variable, but generally reduced levels of Li, mineralogically bound in β-eucryptite. Eucryptite contains more lithium than the typical lithium ore spodumene, which may be advantageous in a recovery process.

Optical microscopy shows skeletal growth of the melilite and nepheline, indicating an insufficient element transport during the crystallization of the slag. SEM-EDX analysis allows for the indirect determination of lithium-containing phases using the differences in atomic contrast between, for example, eucryptite ($LiAlSiO_4$) and nepheline ($NaAlSiO_4$). The eucryptite crystals appear to be rather small, so thermal conditioning of the slag material is being tested. Further analysis of the thermally modified slag and additional methods like electron microprobe analysis (EMPA) and laser ablation inductively coupled plasma mass spectrometry (LA-ICP-MS) are planned.

*References:*

[1] Sommerville R et al. (2021) Resour Conserv Recycl 165:1-11
[2] 2020/0353/COD, Regulation (EU) (2023)
[3] Brückner L et al. (2020) Metals 10:1-29

# Material/Substance flow analysis of biomass ash in the United Kingdom

Dan Ting Chen[1], Julia A. Stegemann[2]

[1,2]Department of Civil, Environmental and Geomatic Engineering (CEGE), University College London (UCL), Chadwick Building, Gower Street, London WC1E 6BT, UK

[1]Email address: danting.chen.19@ucl.ac.uk

---

The combustion of solid biomass generates a substantial amount of biomass ash. Understanding of the availability of biomass ash is critical for developing its circularity, and has not been investigated in the United Kingdom. This study gathered and estimated the current production and management flows, and their chemical compositions, for ashes from the combustion of biomass feedstocks (i.e., woody biomass, agricultural biomass and biowaste such as meat and bone meal and poultry litter) in the UK. Substance Flow Analysis (SFA) was then performed to estimate the quantities of selected elements in the ashes, to better understand their suitability for recovery of critical raw materials (e.g., P). The results show that woody biomass is the dominant solid biomass in the UK, followed by biowaste and agricultural biomass, with generation of approximately 531 kt wood ash, 203 Kt biowaste ash and 94 kt agricultural ash in 2021. The majority of the bottom ash from single feedstocks was disposed of in landfill while the fly ash was primarily recovered, e.g., recovery of wood fly ash in manufacture of masonry blocks. A total of 170 kt Ca, 64 kt Si, 48 kt K, 27 kt P, 17 kt Mg, 14 kt Al, 9.1 kt Fe, 8.7 kt Na, 8.0 kt S, 6.8 kt Cl, 1.9 kt Mn and 1.0 kt Ti are found in the ashes generated in the UK. The ashes therefore have compositions that include useful elements and minerals for utilisation in construction materials, and also fertilizer. Some of these elements could extracted for recovery, e.g., biowaste ashes, as the feedstock with the highest P concentration, could provide 19.9 kt of P, and agricultural ashes, as the feedstock with the highest K concentration, could provide 13.7 kt of K. Biomass ashes also contain toxic elements, whose fate and management must be considered in any utilisation scenario, e.g., 332.5 kt Ba, 95.0 kt of As, 65.0 kt Cu, 29.5 kt Cr and 11.2 kt of Pb. As circularity of biomass ash is poor under current management practice, this study suggests opportunities for improving resource management.

## Why is Raman spectroscopy not used for characterizing MSWI Bottom Ash? – A comparative study of different analytical methods

Kremlicka, T.[1], Demschar, P.[1], Sedlazeck, K.P.[1]

[1]Chair of Waste Processing Technology and Waste Management, Montanuniversität Leoben, Franz Josef-Straße 18, 8700 Leoben, Austria – thomas.kremlicka@unileoben.ac.at

---

Incineration is a commonly used method to treat municipal solid waste (MSWI). Advantages of this method are sterilization and reduction of mass and volume by about 70% and 90% respectively [1]. One of the output streams of this process is MSWI bottom ash, a highly heterogeneous mixture of glass, various ceramics, iron- and non-ferrous metals and a mineral slag [2]. Common mineral phases found in the slag are quartz, calcite, melilites, feldspars and various iron oxides [3].

Using powder X-ray diffraction (XRD) no uncommon phases were found, hence literature was confirmed. Electron microprobe analysis (EMPA) was performed to investigate amorphous phases, metals and association of mineral phases. EMPA revealed some unexpected phases like ferrosilicone with varying mass fractions of Fe and Si. Investigations also discovered two different species of copper. Many phases with mineral-like chemical composition were found, but have not yet been investigated if they are present with an amorphous or crystalline structure.

Another potentially useful method to characterize MSWI bottom ash is Raman spectroscopy. Information on obtaining Raman spectra from MSWI bottom ash is very rare in the literature. Samouh et al. [4] were successful in characterizing fly ash using this technique. Therefore, we will attempt to use Raman spectroscopy to confirm the findings from XRD and EPMA and to evaluate if it can be a useful tool in the fields of waste management and waste mineralogy.

*References:*

[1] Eggenberger U (2004) Geo Soc London 236:411-422
[2] Wiles C.C. (1996) Haz Mat 47:325-344
[3] Eusden D.J. (1999) Appl Geochem 14:1073-1091
[4] Samouh H. (2023) Haz Mat 460:132462

# Reactivity of Municipal Solid Waste Fly Ash into Magnesium Phosphate Cement

Bernasconi, D.[1], Viani, A.[2], Zárybnická, L.[3], Das, G.[4], Bordignon, S.[5], Borfecchia, E.[5], Caviglia, C.[1], Destefanis, E.[1], Gobetto, R.[5] and Pavese, A.[1]

[1]Earth Sciences Department, University of Turin, Turin, 10125, Italy email: davide.bernasconi@unito.it

[2] Department of Chemical and Geological Sciences, University of Modena and Reggio Emilia, Modena, I-41125, Italy

[3] Institute of Theoretical and Applied Mechanics of the Czech Academy of Sciences, Centre Telč, Prosecká 809/76, Praha 9, 190 00, Czech Republic

[4] ELETTRA Sincrotrone Trieste S.C.p.A., Basovizza, Italy

[5] Chemistry Department, University of Turin, Turin, 10125, Italy

---

Municipal solid waste incineration fly ash (MSWI-FA) is one of the solid by-products of municipal solid incineration treatment, accounting for about 1–3%wt of the waste input mass. FA is collected in the plant purification system and bears important amount of heavy metals (up to 5-10%wt, in particular Zn, Pb, Cd) and salt (chloride and sulfate, up to 20-30%wt), therefore it is considered as hazardous waste [1]. For this reason, FA is often required to undergo stabilization/inertization treatment (one of the most common is acid and/or water washing), before being landfilled or used as secondary/supplementary raw material for cementitious systems [2,3]. Among these, magnesium potassium phosphate cements (MKPCs) are particularly interesting, as they have demonstrated very good stabilization/encapsulation properties for hazardous and radioactive wastes [4,5]. They represent an example of chemically-bonded ceramics, in which the hardening occurs at room temperature through the acid-base aqueous reaction between an alkaline magnesia source (MgO) and a phosphate source (potassium dihydrogen phosphate, $KH_2PO_4$), according to the following chemical equation [6]:

$MgO + KH_2PO_4 + 5H_2O \rightarrow MgKPO_4 \cdot 6H_2O$ (K-struvite).

Although MKPCs can display excellent properties, namely high early age and long-term strengths, resistance to sulphate attack, rapid setting, near-neutral pH and low shrinkage, the expensive cost of the starting materials, due to the high temperature calcination of MgO (at least 1500°C), have hampered their use [6]. The introduction of MSWI-FA would be economically beneficial both by reducing the amount of MgO needed and providing a destination for a waste residue which otherwise would require important management costs. On the other hand, a detailed understanding of MSWI-FA reactivity in the cement setting conditions is required to help designing the optimal formulations, both in terms of mechanical and stabilization properties.

In this work, the incorporation of water-washed MSWI-FA into MKPC is studied, paying major attention on how and in what extent MSWI-FA participates in the cement reaction. In particular, one formulation treats MSWI-FA as *fully inert*, replacing both magnesia and potassium dihydrogen phosphate, while in another one MSWI-FA is considered as *fully reactive*, thus replacing magnesia only. The obtained cement pastes are thoroughly characterized by employing X-ray diffraction, SEM-EDS and isocalorimetry techniques, in addition to compressive strength and setting time evaluation, in order to evaluate the impact of MSWI-FA on the cement setting. Moreover, the element selectivity provided by a combined spectroscopic approach ($^{27}Al$ and $^{29}Si$ solid-state nuclear magnetic resonance, Zn K-edge X-ray absorption spectroscopy) allowed to prove the partial dissolution of MSWI-FA minerals and their reaction with phosphate, thus demonstrating a chemical effect that improved the leaching performance.

*References:*

[1] Bernasconi D et al. (2022) Waste Manag 138: 318-327; [2] Caviglia C et al. (2022) Minerals 12: 742; [3] Weibel G et al. (2018) Waste Manag 76: 457-471; [4] Zhang Y et al. (2022) Environ Sci Tech 56: 9398-9407 [5] Pyo J-Y et al. (2021) Nucl. Eng. Int. 53:2261-2267; [6] Xu B et al. (2017) Cement Concrete Res 99: 86-94

# Sustainable binders for soil stabilisation of pavement roads based on recycling of wood biomass ash, municipal solid waste incineration ash and concrete demolition waste

Pandolfi Balbi E.[1], Comodi P. [1], Fastelli M. [1], Zucchini A.[1], Cambi C.[1], Corradini A.[4], Mantovani L.[5], Cerni G.[4], Bou Farhat H.[2], Snellings R.[2,3]

[1]Department of Physics and Geology, University of Perugia, Perugia, Italy, eliapando1@hotmail.com

[2]Department Earth and Environmental Sciences, KU Leuven, Belgium

[3]Department of Materials Engineering, KU Leuven, Belgium

[4]Department of Civil and Environmental Engineering, University of Perugia, Perugia, Italy

[5]Dipartimento di Scienze Chimiche, della Vita e della Sostenibilità Ambientale, University of Parma, Italy

---

Road subgrade layers have the important task of absorbing and redistributing external loads from the more superficial and bituminous layers of the pavement. Low load-bearing capacity and large volume variations in the subgrade can cause cracking and deformation of the road structure. During pavement construction, it is sometimes not possible to avoid soils with low bearing capacity which do not meet the conditions required by technical regulations. Nonetheless, quarry materials are becoming scarce, and they are not considered environmentally friendly since the expansion of quarries implies many environmental problems and quarries are often located far from construction sites, consequently increasing costs and environmental concerns. For these reasons, soils are often treated with cement able to improve their physical and mechanical characteristics while reacting with soil particles. However, the production of this kind of stabilising agent is very harmful to the environment as it generates large amounts of $CO_2$, which then has a negative impact on the Earth's climate processes. Therefore, to avoid this, the utilization of supplementary cementitious materials (SCMs) for the partial or total substitution of cement could represent a pragmatic solution to mitigate the $CO_2$ emissions of its production [1]. Thus, this work concerns a mineralogical study for the stabilisation of layers belonging to road pavements through partial replacement of Portland clinker (PC) by combinations of waste materials coming from Italy, including wood biomass ash (WBA) from an industrial thermal power plant located in Perugia (Umbria region), municipal solid waste incinerator bottom ash (MSWI) deriving from Parma (Emilia Romagna region) and concrete demolition waste (CDW) from buildings collapsed after Norcia's earthquake happened in 2016 (Umbria region). In this way, binders with a much lower $CO_2$ footprint and higher recycled content were formulated. In a first step, this study investigated the binding potential of the selected waste materials based on their physical, chemical, and mineralogical properties, as well as their reactivity towards lime using the SCMs reactivity testing (R3 test) [2]. In a second step, the partial substitution of PC by various combinations of waste SCMs was studied in terms of impact on the cement hydration kinetics and phase assemblage by using of x ray diffractions, thermogravimetric and calorimetric analyses. Results of R3 test show that WBA and MSWI in addition with portlandite, calcite and a potassium solution, present significant reactivity. However, the mineralogical and thermogravimetric results show that WBA, needs to presence of an aluminosilicate source to allow the growth of new cement hydration phases. Results about PC-SCMs blends demonstrate that WBA and MSWI have a considerable reactivity and formation of new minerals coming from cement's hydration such as portlandite, ettringite, hemicarbonate and monocarbonate. Finally, on the most promising mixes, proctor test and unconfined compressive strength (UCS) tests are underway to validate the binder formulation results.

*References:*

[1] Habert G. et al. (2020) Nat. Rev. Earth Environ. 1, 559-573

[2] Avet F. et al. (2016) Cem. Concr. Res. 85, 1-11

# Reactive binder components for building materials by thermochemical upcycling of mineral wastes and by-products

Steindl, F.[1,2], Grengg, C.[1], Rudic, O.[1,2], Radinger, S.[1], Hussein, A.[1], Weisser, K.[1,2], Krammer, A.[3], Doschek-Held, K.[3], Ratz, B.[4], Steiner, S.[2], Gatschlhofer, C.[3], and Mittermayr, F.[2,5]

[1] Institute of Applied Geosciences, Graz University of Technology, Rechbauerstraße 12, 8010 Graz, Austria

[2] Institute of Technology and Testing of Building Materials, Graz University of Technology, Inffeldgasse 24, 8010 Graz, Austria

[3] Chair of Thermal Process Technology, Montanuniversität Leoben, Franz Josef-Straße 18, 8700 Leoben, Austria

[4] Chair of Waste Processing Technology and Waste Management, Montanuniversität Leoben, Franz Josef-Straße 18, 8700 Leoben, Austria

[5] Institute for Material Technology, University of Innsbruck, Technikerstraße 13/V, 6020 Innsbruck, Austria

---

To reduce the high $CO_2$ emissions caused by the production of binders based on ordinary Portland cement (OPC) or alkali-activated materials (AAMs), supplementary cementitious materials (SCMs) like granulated blast-furnace slag (GBFS) are used to replace $CO_2$-intensive primary binder components. Due to dwindling supplies of these traditional SCMs, new and promising concepts utilise the vast available amounts of industrial mineral residues and by-products as reactive binder components in OPC or AAM systems. However, many of these materials exhibit unsuitable properties, such as a high content of harmful substances and/or low reactivity, hindering strength development and structural performance. This contribution covers the mineralogical and chemical characterisation of a large number of thermochemically treated wastes and by-products, such as metallurgical slags, mineral wool waste and incineration ashes. The thermochemical treatment above 1400°C, followed by rapid melt cooling, transformed the initial material into an amorphous, GBFS-like phase ("up-slag") while reclaiming other valuable material streams such as iron and/or phosphorus. Chemical and mineralogical analyses of the up-slags revealed that they consist mainly of CaO, $SiO_2$, $Al_2O_3$ and MgO with high amorphous contents and reduced amounts of unwanted elements such as Mn or Cr. The performance of these up-slags as binder components in OPC or AAM systems was determined by reactivity tests and fabrication of pastes and mortars, proving the reactivity in both cementitious systems. Especially in combination with other untreated wastes and by-products, the addition of up-slag led to significant improvements in both early and late strength of AAM pastes and mortars. The results reveal the mineralogical and chemical key characteristics of untreated wastes and by-products and their thermochemically upcycled counterparts, serving as benchmarks for the treatment and cooling process. In addition, the thermochemical treatment successfully produced GBFS-like up-slags to be used as alternative binder components, allowing significant performance improvements compared to the untreated initial materials. The approach presented enables the valorisation of previously unsuitable materials as reactive binder components, thus reducing waste arisings and alleviating bottlenecks in SCM availability for AAM or OPC binder systems on a path towards a more climate-friendly, energy-efficient circular economy for building materials.

**Acknowledgements**
This study was carried out within the Christian Doppler Laboratory for Waste-based geopolymer construction materials in the $CO_2$-neutral circular economy (GECCO$_2$) and the research projects "Upcyc-Slag-Binder" (Green Tech 100) and "Recover-Met-Binder" (Green Tech X). The financial support by the Austrian Federal Ministry of Labour and Economy, the Christian Doppler Research Association and the "Zukunftsfonds Steiermark" (future fonds Styria) is greatly acknowledged.

## Resource Optimization in Ceramics: Integrating MMVF Waste for Sustainable Glaze Innovations

Sisti, M.[1], Andreola, F.[2], Barbieri, L.[2], Guidetti, D.[1], Gualtieri, A.F.[1], Fantini, R.[1], Colombo, F.[1], Arletti, F.[1]

[1]Department of Chemical and Geological Sciences – University of Modena and Reggio Emilia, Via Campi 103, I-41125 Modena

[2]Department of Engineering "Enzo Ferrari" – University of Modena and Reggio Emilia, Via P. Vivarelli 10, I-41225 Modena

---

We have developed a ceramic glaze by utilizing the thermal inertization product of man-made vitreous fibres (MMVF) as a secondary raw material. In recent years, the ceramic sector has increasingly focused on resource optimization and waste recycling. In line with the principles of a circular economy, the production of ceramic tiles using "extramuros" waste, such as the product of thermal inertization of MMVF, has become a central theme. This waste material, characterized by being completely amorphous, serves as an ideal melting component in ceramic products. We have experimented with various formulations of ceramic glazes, incorporating between 40% and 50% of this glassy material. The most promising formulation involves 44% of waste, resulting in a lustrous, burgundy ceramic glaze. This outcome underscores the suitability of this waste material as a valuable secondary raw material for the manufacture of traditional ceramics.

## A circular approach in reusing sludges from water potabilization and urban wastewater treatment plants through alkaline activation

Clausi, M.[1], Cofano, V.[1], Medini, M.[1], Occhipinti, R.[2] and Pinto, D.[1]

[1]Earth and Geoenvironmental Sciences Department, University of Bari, Italy; marina.clausi@uniba.it

[2] Biological, Geological and Environmental Sciences Department, University of Catania

---

The decrease in the availability of drinking water due to global warming, as well as the exploitation of non-renewable resources and the accumulation of increasing amounts of wastes, represent nowadays critical issues alimenting researchers and governs debates and for which solutions or containments are being sought globally (i.e. Sustainable Development Goals promoted by United Nations or European environment policy). To this purpose, increasing attention is being reserved in the last times for promoting the circularity of materials and more sustainable processes. Geopolymeric technology represents, nowadays, a very promising vehicle to valorise several types of wastes, among which those deriving from water treatments [1].

Aiming to "close the loop," the present contribution deals with results concerning the potential reuse of two types of sludges from water treatment Apulian plants (Italy), i.e. water potabilization sludges (WPS) [2,3] and wastewater sludges (WWS) from a phytodepuration tank, as raw material for the preparation of geopolymer sorbents designed for water treatment. Geopolymers were prepared by blending in different proportions kaolinitic clay (MK) with the two types of sludges, and designed for maintaining constants the $SiO_2/Al_2O_3$, $SiO_2/NaO$, $H_2O/Na_2O$, $Al_2O_3/Na_2O$ molar ratios in different mixtures. Two sets of samples were thus prepared (the former with a variable amount of sodium silicate solution, the latter using a fix amount of alkaline activator blended with a further source of $SiO_2$) with the purpose to investigate the possibility to limit as much as possible the use of the alkaline activator.

The prepared samples were characterized by a multi-analytical approach using XRPD, FTIR, SEM-EDS techniques, to investigate compositions and microstructural features. Compressive strength tests showed variable values, reaching about 20 MPa. Preparations with variable amounts of sodium silicate solution showed generally better results in term of resistance. After 10 days of immersion in water, all samples maintained their physical integrity. The prepared samples were used for batch adsorption tests for the removal of ammonium ions from model solutions showing very promising results for their use in the treatment of contaminated waters.

*References:*

[1] Ahmad T et al (2016) J. Clean. Prod 124: 1-13
[2]Clausi M et al. (2023) Sustainability 15.24: 16623
[3] Clausi M and Pinto D (2023) Materials 16.5: 1998

## Recycling detoxified asbestos-cement in several industrial applications: Towards an end of the "asbestos problem"!

Capitani G.[1], Bernasconi A.[2], Bianchi A.[3], Bizjan B.[4], Conconi R.[1], Ferrario S.[3], Ferrini S.[8], Lavagna L.[5], Marian M.[6], Mauri M.[1], Dalpiaz M.[7], Pavese M.[5], Squitieri L.[1], Tarantino S.C.[6], Vergani F.[1], Viti C.[8]

[1]University of Milano-Bicocca (Italy), giancarlo.capitani@unimib.it; [2]University of Turin (Italy); [3]Graftonica SRL, Milano (Italy); [4]University of Ljubljana (Slovenia); [5]Polytehcnic University of Turin (Italy); [6]University of Pavia (Italy); [7]Rallk SRL, Milano (Italy); [8]University of Siena (Italy).

---

The "asbestos problem" arises from the fact that although asbestos was banned in most developed countries in the 1990s, significant amount of asbestos-containing materials remain in the built environment, posing a health hazard. A sustainable solution to this problem would be to apply a detoxification process followed by recycling the inert product as secondary raw materials (SRM) in the production of common goods, as recommended by the EU.

With the A-FIRE project (Asbestos Fast Inertization & Recycling), we thermally treated asbestos-cement (Eternit®-like) slates, commonly used for roofing, at 1100-1150 °C. This process transforms the asbestos mineral into non-toxic minerals, cement-like phases and glass [1,2]. The resulting product was used as SRM for the production of sanitary ware [3], as a filler in epoxy resin for flooring applications [4], in mortar for plaster applications [5], in rock-wool production [6], as partial substitution of cement, in biopolymers and geopolymers.

Recycling of detoxified asbestos cement (DAC) in sanitary ware is feasible up to 5 wt.%, provided that sulphates affecting adversely the workability of the slurry can be washed out and the whiteness of the fired vitreous china is not a mandatory requirement. In epoxy, DAC can be used as a filler up to 30 wt.%, replacing common inorganic filler such as barite and wollastonite, this reduces the cost of the composite and increases the durability of the flooring. It is possible to use up to 7 wt.% of recycled DAC as inert material in mortar for plaster application without altering the water demand and the workability of the mixture. Moreover, this process slightly increases the flexural and compressive strengths. Another possible application of recycled DAC is the production of rock-wool, where it can be mixed with diabase in a 70:30 weight ration. This results in fibres with morphology, composition, and biosolubility similar to commercial rock-wool. Tests are being conducted to use DAC as substitute of cement, as filler in thermoplastic biopolymers (polylactic acid) and as SRM in geopolymers. Preliminary results are very promising. Finally, Life Cycle and Cost Benefit Analyses suggest that asbestos inertization and recycling represents a sustainable alternative to deep landfilling [7].

*References:*

[1] Marian M et al. (2021) J Hazard Mater, https://doi.org/10.1016/j.jhazmat.2021.125419; [2] Vergani F et al. (2022) J Mater Cycles Waste, https://dx.doi.org/10.1007/s10163-021-01320-6; [3] Bernasconi A et al. (2022) Cer Int, https://doi.org/10.1016/j.ceramint.2022.09.147; [4] Campanale F et al. (2023) Polymers, https://doi.org/10.3390/polym15061410; [5] Capitani G et al. (2024) J Environ Manage, https://doi.org/10.1016/j.jenvman.2024.120507; [6] Capitani G et al. (2024) Constr Build Mater, submitted; [7] Ferrini S et al. (2024), J Environ Manage, submitted.

# Mineral wastes – key players to reach resource efficiency and $CO_2$ neutrality in construction industry

Grengg, C.[1], Rudic, O.[1,2], Steindl, F.[1,2], Raic, S.[1], Hussein, A.[1], Radinger, S.[1], Ratz, B.[3], Zögl, I.[1] and Mittermayr, F.[3]

[1] Institute of Applied Geosciences, Graz University of Technology, Rechbauerstraße 12, 8010 Graz, Austria

[2] Institute of Technology and Testing of Building Materials, Graz University of Technology, Inffeldgasse 24, 8010 Graz, Austria

[3] Chair of Waste Processing Technology and Waste Management, Montanuniversitaet Leoben, Franz Josef-Straße 18, 8700 Leoben, Austria

[4] Institute for Material Technology, University of Innsbruck, Technikerstraße 13/V, 6020 Innsbruck, Austria

---

The construction sector requires vast amounts of primary mineral resources and at the same time represents one of the most significant source of waste generation [1]. On top, recent data indicate that 9 % of all greenhouse gas emissions originate from the manufacturing of construction materials [2]. In the framework of these considerations, strategies to utilize mineral wastes and by-products to produce novel cement-based construction materials bear high potential to increase material circularity and to reduce the negative environmental impact of construction industry.
This contribution describes a comprehensive approach in which a novel generation of construction materials is envisioned, based on the alkali-activation technology and the utilization of mineral wastes and by-products, such as metallurgic slags, incineration ashes, mineral wools and construction and demolition wastes as major components. Thereby, the central challenge is to design the material mix design in a way to control the microstructural phase assemblage and corresponding physicochemical material properties in order to enable a tailored material manufacturing. To date, over 50 relevant waste streams were characterized in respect to their mineralogy, chemical composition and overall reactivity. First functionable construction materials have been developed exhibiting excellent workability, high strength development (up to 90 MPa after 28 days) and a waste content of up to 90 %. In a further step, the novel binder systems were combined with organic wastes, such as cooking oil and pyrolyzed wastes to modify physicochemical material properties and to enable $CO_2$ sequestration capacities. The oil addition led to the formation of water-insoluble metal-soap-phase precipitation in the pore spaces of the material, thereby strongly reducing the porosity and inner specific surface, with limited impact on the inorganic, framework-forming phase assemblage or on the solidification kinetics during alkali-activation. Described microstructural modifications had a strongly positive impact on well-known AAM weaknesses such as high drying shrinkage and low carbonation resistance and at the same time near carbon neutrality could be achieved. Comprehensive tests on relevant durability aspects, such as carbonation and acid resistance, leaching behaviour and shrinkage are ongoing with promising first results. Relevant findings will be presented at the conference.

*References:*

[1] European Environment Agency (2023): Waste generation in Europe. Available at https://www.eea.europa.eu/en/analysis/indicators/waste-generation-and-decoupling-in-europe, Accessed 21 February 2024.
[2] United Nations environment programme, 2022 Global status report for building and construction, 2022.

**Acknowledgements**
This study was carried out in the course of the Christian Doppler Laboratory for Waste-based geopolymer construction materials in the $CO_2$-neutral circular economy ($GECCO_2$). The financial support by the Austrian Federal Ministry of Labour and Economy and the Christian Doppler Research Association is greatly acknowledged.

## Nano- to microscale weathering of thallium in ore deposits

Đorđević, T.[1,2], Kolitsch, U.[3,2], Stöger-Pollach, M.[1], Schwarz, S.[1] and Majzlan, J.[4]

[1]E057-02 USTEM, Vienna University of Technology, Stadionallee 2, A-1020 Vienna, Austria

[2]Department of Mineralogy and Crystallography, University of Vienna, Josef-Holaubek-Platz 2, A-1090 Wien, Austria

[3]Mineralogisch-Petrographische Abteilung, Naturhistorisches Museum, Burgring 7, A-1010 Wien, Austria

[4]Institute of Geosciences, Department of Mineralogy, Friedrich-Schiller-Universität, Carl-Zeiss-Promenade 10, 07745 Jena, Germany

---

Some areas are affected by the natural weathering or the mining of thallium (Tl)-rich sulfide ores, such as the Sb-As-Tl-Au Allchar deposit in North Macedonia. There, Tl contents in sulfide-rich mining wastes reach up to 17 000 mg/kg [1] and Tl is mostly retained in secondary Tl-bearing minerals. The nature of these secondary minerals is expected to depend on the type of Tl-bearing sulfide from which they form, but also on the physicochemical conditions under which these primary minerals weather. Thus, different secondary minerals may result from the weathering of a primary mineral in a mine waste dump as compared to a nearby or remote Tl-bearing soil that received some waste input. In such a case, Tl may be retained by adsorption reactions onto phyllosilicates (mostly illite) and, under certain conditions, by adsorption of Tl(I) and Tl(III) onto manganese-oxides [2,3 and references therein]. Because Tl-bearing secondary phases are often minute in size, often not well-crystalline, and scarce, they are commonly overlooked. Yet, information on the types of Tl-bearing secondary minerals and their role in Tl attenuation is essential for the prevention, assessment, and effective remediation of Tl pollution.

Our research was focused on Tl-rich environmental samples from the Allchar deposit (e.g., supergene minerals, mining wastes, technosols). We employed transmission or scanning electron microscopy (TEM or SEM) complemented by electron probe microanalysis, X-ray diffraction and Raman spectroscopy. This work has shown that we can regularly find Tl-bearing minerals that are either known but have not previously been reported at the locality of interest, e.g. avicennite ($Tl_2O_3$) for Allchar or that represent new mineral species that show a wide range of crystallinity, such as novel Tl- and Tl-*Me*(II)-arsenates [*Me*(II) = Ca, Mn, Fe, Mg], Tl-Sb- and Tl-Mn-oxides. These minerals often show compositions that range from simple to complex, depending on the paragenesis of the source material and the weathering conditions.

Our findings highlight the ability of secondary oxide and oxysalt minerals to incorporate significant amounts of both Tl(I) and Tl(III), though some questions remain about their actual long-term suitability as sinks for thallium dispersed in polluted natural or industrial sites.

Financial support of the Austrian Science Fund (FWF) [P 36828-N] is gratefully acknowledged.

*References:*

[1] Đorđević et al. (2021) Appl Geochem 135: 105114-105130

[2] Voegelin et al. (2022) Environ Sci Processes Impacts 24: 1343-1359

[3] Wick et al. (2020): Geochim Cosmochim Acta 288: 83-100

# MinerAll - A new tool for characterizing the utilization potential of mine tailings

Kärenlampi, K.[1], Markkanen, M.[2], Jooshaki, M.[1], Salvador, D.[1], Rama, M.[2], Kauppila T.[3]

[1]Geological Survey of Finland, Tutkijankatu 1 83500 Outokumpu kimmo.karenlampi@gtk.fi

[2]Geological Survey of Finland, Vuorimiehentie 5 PL 96 02151 Espoo

[3]Geological Survey of Finland, Viestikatu 7A PL 1237 70211 Kuopio

---

The Geological Survey of Finland (GTK) is actively engaged in research projects focused on tailings management and re-mining, encompassing mineral reserve studies and beneficiation tests. These projects aim to minimize mining waste by extracting valuable resources from tailings and exploring innovative applications, thereby introducing new research challenges. At the beginning of 2023, GTK launched the MinerAll project, dedicated to advancing scanning electron microscopy-based automated mineralogy (SEM-AM) techniques for comprehensive tailings characterization. The outcome, a software tool named "MinerAll", is tailored for systematic particle-level analysis, offering insights into tailings beneficiation characteristics and potential utilization pathways. The initial version is set for completion by the end of 2024 and ongoing development is planned for subsequent years.

The MinerAll tool primarily serves process mineralogy researchers, working alongside beneficiation and mineral resource experts. It is used to conduct tailings analysis primarily through representative SEM-AM assessments, complemented by essential chemical and mineral analyses. SEM-AM data is integrated into the software via MS Access databases, compatible with various SEM-AM systems like MLA, AMICS, and INCA. Moreover, the software includes an extensive mineral database with information on beneficiation properties, application domains, and value assessments. Utilizing artificial intelligence tools for data search has significantly contributed to the construction of our database. Presently, it hosts more than 5800 mineral property entries alongside 1200 application entries. Developed in Python, the MinerAll tool features a user-friendly graphical interface and analytical algorithms to visualize characterization outcomes.

The primary outcome of the MinerAll analysis is a customized report, tailored to present tailings characterization data in a practical format for circular economy considerations. This report addresses key aspects, such as identifying valuable mineral concentrates, characterizing the occurrence of potential product minerals, quantifying the beneficiation properties, and assessing environmental and health risks. These outcomes serve as a roadmap for evaluation on the potential of tailings beneficiation, aiding the preliminary selection of optimal unit processes and technologies. This involves considering factors like size classification, need for comminution, selection of separation/concentration techniques, and conducting feasibility assessments.

GTK’s active engagement in tailings management and re-mining research demonstrates a strong commitment to minimizing mining waste while simultaneously exploring novel applications. As the MinerAll tool is developed, it is poised to become an essential asset for process mineralogy researchers. Its customized reports empower operators in the mineral circular economy, enabling informed decision-making and resource optimization.

## Exploring the use of magnetite to recover critical metals from waste

O'Neill, K.E.B.[1], Biswakarma, J.[1], Crane, R.[2] , and Byrne, J.M.[1]

[1]School of Earth Sciences. University of Bristol, Bristol, BS8 1TH. Katie.Oneill@bristol.ac.uk

[2] Camborne School of Mines, University of Exeter, Penryn, TR10 9EZ

---

The sustainable recovery of critical metals is a requirement in order to achieve net zero by 2050 with the demand for critical metals to increase by up to 90% [1]. To support this transition one novel avenue to ensure supply meets demand is to explore the critical metal rich wastes that have formed as a result of years of extracting from ore deposits. One approach is to explore the use of magnetic nanoparticles (MNPs) as an adsorbent for recovering critical metals like cobalt (Co), nickel (Ni) and zinc (Zn) from such wastes. Magnetite is a redox- active MNP with high surface area- to – volume ratios [2], can be easily produced and exhibits magnetic properties- allowing for its easy separation from solution. As a result magnetite is an ideal candidate for recovering critical metals.

In this research, magnetite MNPs were used to explore the recovery of Co, Ni and Zn from a mixed metal system. At circumneutral pH and anoxic conditions; varying concentrations of Co(II), Ni(II) and Zn(II) (10- 1000 ppm) were exposed to 5 g/L of magnetite in separate experiments. Samples were collected after 48 hours and metal concentrations were measured using ICP-OES to determine the dissolved and sorbed fractions. Mixed metal experiments were conducted whereby 20-800 ppm of Co(II), Ni(II) and Zn(II) in the same solution and conditions (pH 7, anoxic) were subjected to 5 g/L of magnetite. This was to establish whether there was any preferential adsorption between the metal ions. Samples were also left to equilibrate for 48 hours and metal concentrations were measured using ICP-OES.

Results showed that magnetite can successfully remove Zn(II), Co(II) and Ni(II) from solution. For Co(II) and Ni(II) adsorption decreased with increasing starting concentrations, however, for Zn(II) adsorption decreased up to 600 ppm and then increased dramatically at 800 ppm. The data were fitted with Freundlich and Langmuir isotherms, with Freundlich providing the most satisfactory fit for both Co(II) and Ni(II). However the linearised form of Freundlich best described the Zn(II) experiments. Results from the mixed metal experiments were best described by the Freundlich isotherm with preferential adsorption in the order of Zn > Ni > Co. TEM and XAS support these findings. Overall, this study has shown that 5 g/L of magnetite can be used to successfully recover Co, Ni and Zn individually and together from aqueous solutions.

*References:*

[1] IEA (2022), World Energy Outlook 2022, IEA, Paris https://www.iea.org/reports/world-energy-outlook-2022, Licence: CC BY 4.0 (report); CC BY NC SA 4.0 (Annex A)

[2] Usman, M., Byrne, J. M., Chaudhary, A., Orsetti, S., Hanna, K., Ruby, C., Kappler, A., & Haderlein, S. B. (2018). Magnetite and Green Rust: Synthesis, Properties, and Environmental Applications of Mixed-Valent Iron minerals. In *Chemical Reviews* (Vol. 118, Issue 7, pp. 3251–3304). American Chemical Society.

# The potential of recycling eggshell waste calcite for the sustainable capture of rare earth elements

Rateau R.[1], Maddin M.,[2] Szucs A.,[2] Terribili L.,[2] Drost K.,[3] Guyett.,[3] and Rodriguez-Blanco J.D.,[3]

[1]Discipline of Geology, School of Natural Sciences, Trinity College Dublin, rrateau@tcd.ie

[2] Discipline of Geology, School of Natural Sciences, Trinity College Dublin

[3] iCRAG, the Irish Research Centre in Applied Geosciences; Discipline of Geology, School of Natural Sciences, Trinity College Dublin

---

The production of rare earth elements (REE) for the green energy transition is damaging. In the context of the need for the development of a circular economy, we investigated the use of eggshell waste calcite as a sustainable alternative sorbent for the capture and separation of REE from aqueous solutions.

Calcite hen eggshell grains were reacted with multi-REE (La, Nd, Dy) solutions at 25 to 205 °C for up to three months. We observe diffusion of the REE inside the eggshell calcite, alongside pathways formed by the intracrystalline organic matrix and intra-palisade calcite crystal boundaries. At 90 °C, spherulites of kozoite, the orthorhombic polymorph of $REE(CO_3)(OH)$, precipitate on the surface of the dissolving calcite. At 165 and 205 °C, a two-fronts interface-coupled dissolution-precipitation occurs, resulting in the complete dissolution of calcite shell and its pseudomorphic replacement by polycrystalline kozoite. At 205 °C, kozoite is slowly replaced by the thermodynamically stabler form of the $REECO_3OH$ polymorphs, hydroxylbastnäsite.

Our results demonstrate two potential applications of eggshell waste for the uptake of rare earth elements in solution: 1) at lower temperatures, as a mixed organic-inorganic adsorbent and absorbent, albeit requiring long absorption times; and 2) at higher temperatures, as an efficient sacrificial template for the precipitation of rare earth hydroxycarbonates.

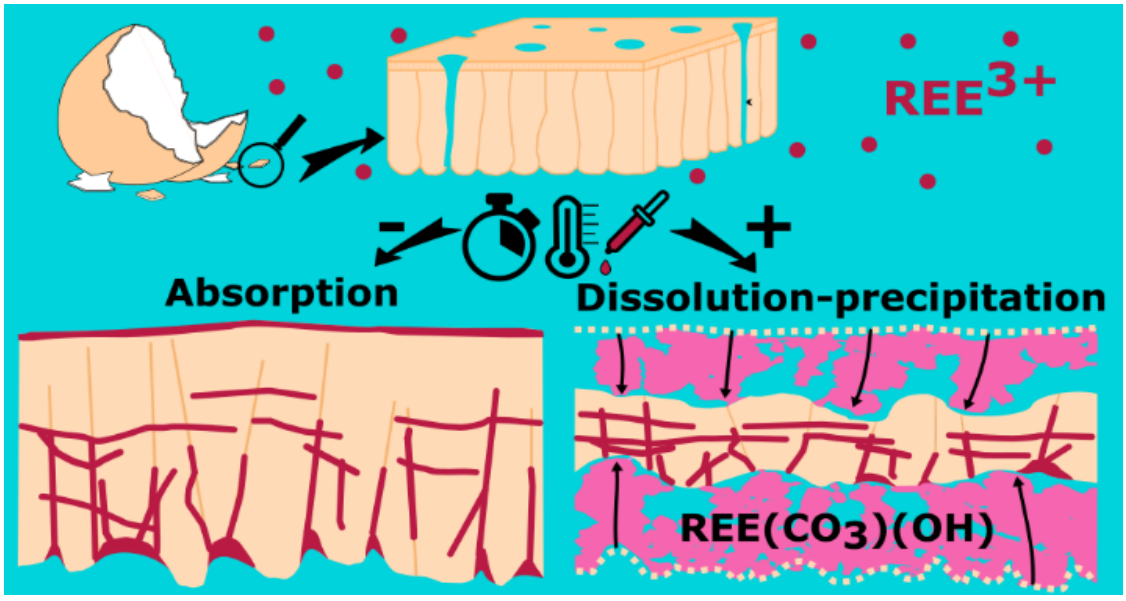


*Figure 1: Graphical abstract [1]*

*References:*

[1] Rateau R *et al.* (in review) ACS Omega

## A comparison between a flux and TEOS based synthesis of zircon-hafnon solid solutions

Neumann, A.[1,3], Kahlenberg, V.[2], Lerche, I.[1], Stöber, S.[1] and (†) Pöllmann, H.[1]

[1]Institute of Geosciences and Geography, Martin-Luther University Halle-Wittenberg, D-06120 Halle (Saale), Germany, E-mail: andreas.neumann@geo.uni-halle.de

[2]Institute of Mineralogy and Petrography, University of Innsbruck, Innrain 52, A-6020 Innsbruck, Austria

[3]ITEL - Institute for Technologies and Economics of Lithium, Leipziger Straße 70, D-06108, Halle (Saale), Germany

---

Zircon ceramics are potentially considered as host for long lived radionuclides due its irradiation resistance. The addition of hafnium which acts as neutron absorbing agent [1] could be beneficial for their long-term stability.

Two synthesis routes of the zircon-hafnon solid solutions series were carried out. The high temperature route uses the growth of single crystals via a $Li_2O$-$MoO_3$ flux, that has been cooled down slowly from 1400 °C within four weeks (cf. [2]) to approx. 900 °C. The reaction products were colourless and idiomorphic without by-products. The hydrothermal TEOS based route represents the low temperature method carried out at roughly 200 °C for approx. 7 days. The hydrothermal route yielded a white powder and SEM analysis thereof did not reveal any specific idiomorphic properties. However, the synthesis also featured some by-products beside the zircon-hafnon solid solutions. Thermogravimetric analysis coupled with differential scanning calorimetry, and mass spectroscopy indicated, that hydrothermal reaction products feature the presence of organic residues originating from the starting materials. However, a specific dependency on the hafnium content could not be observed due to the data scatter. IR analysis revealed the presence of Zr/Hf-oxides. The structural characterization by XRD ([3-5]) demonstrated that properties change constantly with the hafnium amount. Data of the end-members zircon and hafnon are consistent with published data [6-7]. This is also valid for the Raman data which are in good accordance with Grüneberger et al. [8]. However, gradual variations of some properties related to the composition of the solid solution series depend in part on the synthesis route, considering the c/a ratio and IR modes. Furthermore, analyses of the single crystals by Raman spectroscopy and µXRF suggested a non-equilibrated crystal growth based on the starting composition.

*References:*

[1] Meldrum A (1998) MRS Online Proceedings Library Archive 540: 754
[2] Cherniak D et al. (2004) American Mineralogist 89: 1533–1539
[3] Sheldrick G M (2008) Acta Crystallographica Section A 64: 112–122
[4] Rietveld H M (1967) Acta Crystallographica 22: 151–152
[5] Coelho A A (2018) Journal of Applied Crystallography 51: 210–218
[6] Kolesov B A et al. (2001) European Journal of Mineralogy 13: 939–948
[7] Speer J A and Cooper B J (1982) American Mineralogist 67: 804–808
[8] Grüneberger A et al. (2016) European Journal of Mineralogy 28: 721–733

## 13X Zeolite for Rare Earth Elements separation: evaluation of the selectivity and structural characterization

Colombo, F.[1], Fantini, R.[1], Di Renzo, F.[2], Confalonieri, G.[3], Sobczyk, M.[4], Malavasi, G.[1], Malferrari, D.[1], and Arletti R.[1]

[1]Dipartimento di Scienze Chimiche e Geologiche, Università degli Studi di Modena e Reggio Emilia, Modena, Italy rossella.arletti@unimore.it

[2]ICGM, University of Montpellier, CNRS, ENSCM, Place Eugène Bataillon, 34095 Montpellier, France

[3]Dipartimento di Scienze della Terra, Università degli Studi di Roma "La Sapienza" - Piazzale Aldo Moro 5, 00185 Roma

[4]AGH University of Science and Technology, Faculty of Geology, Geophysics and Environmental Protection, al. A. Mickiewicza 30, 30-059 Kraków, Poland

---

Domestic Material Consumption (DMC) quantifies the volume of materials required by an economy to fulfil both internal and external demands for goods and services. DMC surged by over 65% between 2000 and 2019, reaching 14.1 tonnes per capita in Europe by 2021 [1]. This surge, driven by factors such as population growth and industrialization, exerts immense pressure on natural resources and poses significant risks to human health, geopolitics, and the economy. A focused examination and the enhancement of recycling practices, particularly for materials now classified as critical raw materials, are needed. Rare Earth Elements (REEs) face scarcity due to extensive use, as they are fundamental for the development of new technologies, and geopolitical constraints. Among various waste sources rich in REEs, spent fluorescent lamps have garnered attention for recovery efforts. Various methodologies have been explored for REEs recovery, including selective precipitation, solvent extraction, liquid-liquid extraction, adsorption, and cation exchange. Zeolites, known for their ion-exchange properties, offer a promising way for REEs recovery but limited research has investigated their potential for REEs separation and recycling. In our study, $NH_4$-exchanged 13X zeolite's selectivity towards four REEs (*i.e.* Ce, La, Eu, and Y) with concentrations mimicking fluorescent lamp leachates [2] was evaluated. Both mono-elemental and bi-elemental (Ce+La and Eu+Y) exchanges were investigated, and different liquid/solid ratios were tested. SEM-EDS, EA and TG analysis were performed on the obtained powders, while ICP analysis were performed on the solutions. Results showed different exchange behaviours, with Ce and La exhibiting higher exchange ratio than Y, despite the higher initial concentration of the latter in the leachate, indicating potential selectivity. The study's findings hold promise for effective REE separation, contributing to sustainable resource management and mitigating the adverse impacts of escalating DMC on global sustainability. A structural investigation has also been carried out to further study the mechanism and the sites involved in the cation exchange exploiting both high resolution XRPD (patterns were collected at ID22 beamline @ESRF (Grenoble, France)) and X Ray absorption analyses (data were collected at ID08 beamline @ESRF). The results show that Ce and La exchange mechanisms are almost identical, while Eu and Y behave differently, confirming our hypothesis. The results obtained indicate zeolites as a viable option for REE separation from simple solutions.

*References:*

[1] United Nations (2022) - The Sustainable Development Goals Report 2022

[2] Eduafo P.M., Strauss M.L. & Mishra B. (2015) - Experimental investigation of recycling rare earth metals from waste fluorescent lamp phosphors. TMS Annual Meeting, 253-259, https://doi.org/10.1002/9781119093244.ch29

## Sustainable Solutions: Utilizing Extractive Waste in Ceramic Tile Production

Fantini, R.[1], Bernini, M.[1], Conte, S.[2], Zanelli, C.[2], Dondi, M.[2], Gualtieri, A.F.[1], and Arletti, R.[1]

[1]Department of Chemical and Geological Sciences, University of Modena and Reggio Emilia, Modena, Italy
Corresponding author: riccardo.fantini1@unimore.it

[2]Istituto di Scienza, Tecnologia e Sostenibilità per lo Sviluppo dei Materiali Ceramici (CNR- ISSMC), Ravenna, Italy

---

The recycling of extractive waste (EW) has the potential to convert landfills into valuable resources akin to "new mines," benefiting quarrying and recycling industries, as well as the environment and society. In this context, thorough characterization and laboratory analysis of the chosen EW are crucial, as the feasibility of recovery largely hinges on the waste's chemical composition, mineral makeup, and physical properties.

The focus of this study was on the extractive waste (EW) obtained from a company specializing in producing aggregates for construction purposes. These aggregates are primarily composed of organogenic limestone and calcarenites. The extraction process involves blasting the ore followed by transportation to two separate dressing plants for crushing, washing, and sieving. The EW originates from two water clarification systems that treat the effluents from the aggregate washing plant. These clarification systems collectively generate approximately 120 tons per day (15-20 thousand tons per year) of waste silts, which are categorized as non-hazardous special waste under Italian regulations. Typically, these silts are utilized for restoration activities within the quarry itself, or they are deposited in excavation voids or landfills for environmental restoration projects beyond the extraction site. Additionally, this waste was previously utilized in concrete production at a local cement plant until its closure in 2009.

In this project, four samples of waste silts (WS) were characterized from a chemical, mineralogical and rheological point of view, and added to different batches for porcelain stoneware tiles. Then the ceramic tile production was reproduced at the laboratory scale and the final ceramic products fully characterized.
This project is part of PNRR–M4C2INV1.5, NextGenerationEU-Avviso 3277/2021 -ECS_00000033-ECOSISTER-spk5.

# Preliminary results of the effect of nano Mg-Al layered double hydroxides (LDHs) on chemical and physical properties of cement paste

Fastelli, M.[1], Vivani, R.[2], Sassi, P.[2], Speranzini, E.[3], Schoubben, A.[4], Di Michele, A.[1], Zucchini, A.[1], Mortaro, F.[1], and Comodi, P[1].

[1]Department of Physics and Geology, University of Perugia, Perugia, Italy maximiliano.fastelli@unipg.it.

[2]Dipartmento di Chimica, Biologia e Biotecnologie, Università Degli Studi Di Perugia, Via Elce di sotto, 8, 06123 Perugia, Italy.

[3]Department of Civil and Environmental Engineering, University of Perugia, via Duranti 93, 06125 Perugia, Italy
[4]Department of Pharmaceutical Sciences, University of Perugia, Perugia, Italy.

---

The sustainability of cement production is of paramount importance for the construction industry, and a valuable way to improve it is the addition of appropriate additives and materials to the standard cement pastes. That is, the understanding of the physical and chemical mechanisms involved in blended cement hydration is fundamental [1]. Layered double hydroxides (LDHs) are promising additives given their ability to capture $CO_3^{-2}$ and improve the carbonation resistance of the cement as well as to remove the $CO_2$ and $Cl^-$ ions that affect the durability of the cement paste. They are classified as ionic solids with layered structure with general formula $[M_{1-x}^{+2} M_x^{+3} (OH_2)]^{x+}[a_{x/n}^{-n} * nH_2O]^{x-}$ and known as anionic clays with controllable supramolecular structure and unique physicochemical properties (e.g. anion exchange), which make them very interesting in the field of cementitious materials [2-3]. Nano Mg-Al-$NO_3$/$HCOO^-$ LDHs were synthesized by direct and ultrasonic precipitation methods The nanometric size and purity of the LDHs were verified by X-ray powder diffraction (XRPD), transmission electron microscopy (TEM), scanning electron microscope (SEM), dynamic light scattering (DLS) and Fourier-transform infrared spectroscopy (FTIR). The LDHs were mixed with Portland cement in different weight percentages (wt%), ranging from 1 to 10 wt%. First, the mixed dry cement powders were analysed using DLS, FTIR, XRPD and SEM to verify the actual homogenization of the powder that ensures the dispersion of the nano LDHs. The influence of LDHs on the hydration process of the cement paste as well as on the morphology and porosity of the hydrated samples is going to be studied after 1-, 7-, 14- and 28-days curing times, and analysed by XRPD, SEM, thermal (TGA/DTG) and spectroscopic analyses. This approach allows to discuss the chemical contribution of LDHs to the formation of hydrated calcium silicate hydrate (C-S-H) and hydrated calcium aluminate (Afm) phases together with the potential anion exchange process during hydration. Mechanical compression and flexural tests are also on the way in order to test the physical effect on the mixed cement paste.
The preliminary results here presented help understanding the actual contribution of the selected nanomaterials on the cement hydration process, also pointing out possible negative effects, and allow the fine tuning of the right procedure for integrating them into cement pastes. The use of aliquots of waste materials, e.g., construction and demolition wastes, as further additives will be also tested in order to obtain engineered cements with a low environmental impact while maintaining high physical-mechanical standards. This work has been funded by the European Union – NextGenerationEU under the Italian Ministry of University and Research (MUR) National Innovation Ecosystem grant ECS00000041 - VITALITY - CUP J97G22000170005

*References:*
[1] Wu Y et al, (2018) Appl. Clay Sci, 158, 123-131
[2] Yazdi A. M et al., (2023) Cem. Concr. Res. 163, 107037.
[3] Mishra G et al., (2018) Appl. Clay Sci. 153, 172-186.

# Quantitative mineralogy and potential recovery of metal(loid)s from copper metallurgical slag

Lichovník, M.[1], Ettler V.[1], Aiglsperger T.[2], Kříbek, B.[3] and Mapani, B.[4]

[1]Institute of Geochemistry, Mineralogy and Mineral Resources, Faculty of Science, Charles University, Albertov 6, 128 00 Prague 2, Czech Republic, email: martin.lichovnik@natur.cuni.cz

[2]Department of Civil Engineering and Natural Resources, Division of Geosciences and Environmental Engineering, Luleå University of Technology, SE 97187, Luleå, Sweden

[3]Czech Geological Survey, Geologická 6, 152 00, Prague 6, Czech Republic

[4]Department of Civil, Mining and Process Engineering, Faculty of Engineering and the Built Environment, Namibia University of Science and Technology, Private Bag 13388, Windhoek, Namibia

---

Wastes from ore mining and processing have been increasingly studied as secondary sources of technology-critical elements, such as Cu, Co, Ge, or Ni [1]. In this study, we examined copper smelter slags from Tsumeb, Namibia, combining the quantitative mineralogy analyses and tailored extraction tests to simulate the possible hydrometallurgical recovery of the elements of interest.

Samples of granulated Ausmelt slags were analysed by a combination of X-ray diffraction (XRD), scanning electron microscopy (SEM), electron probe microanalysis (EPMA), and automatic mineralogy (autoSEM). The extraction tests were performed using the original granulated material to evaluate the necessity of prior mechanical processing [2]. Extraction parameters were selected to simulate the settings of real hydrometallurgical plants [3]: $H_2SO_4$ (20, 50, and 100 g/L) as the extraction agent, liquid/solid (L/S) ratios of 5, 10, and 20 kg/L, ambient temperature and 1 h extraction time.

The slag material was rich in Fe (25%), Zn (4.8%), Pb (2.3%), Cu (0.67%), and As (0.44%) and consisted of glass fragments with inclusions of spinels, olivines, various sulfides (Cu-Fe, Pb, and Zn), Cu and Fe arsenides, and metals (Pb, Cu). The elements of interest (mainly Cu and Zn) were dominantly hosted in the glass phase. The extraction efficiencies increased with increasing acid concentrations and L/S ratios and reached 8–50% Cu, 10–56% Zn, and 13–97% As. These results served as a basis for further optimization of the extraction procedure and selective recovery of valuable metals via precipitation and solvent extraction.

This study was supported by the Czech Science Foundation (23-05051S) and OP JAC project CZ.02.01.01/00/22_008/0004605.

*References:*

[1] Dold B (2020) J Geochem Explor 219:106638
[2] Ettler V et al. (2022) J Clean Prod 379:134677
[3] Schlesinger M E et al. (2020) Extractive Metallurgy of Copper (5th ed), Elsevier

## Sustainable lime mortars by recycling waste animal fibres: a new use for pig and cow hairs.

Molina-Piernas, E. [1,2], Pacheco Orellana, M.J. [1], Domínguez-Bella, S. [1,2], Martínez-López, J. [1,2], Sánchez-Bellón, A. [1,2]

[1]Earth Science Department, University of Cadiz, Faculty of Science, Spain (**eduardo.molina@uca.es**)

[2]Unit of Geoarchaeology and Archaeometry Applied to Historic-Artistic and Monumental Heritage (UGEA-PHAM).

---

In many countries, construction, agriculture and livestock sectors produce and emit a large amount of waste and greenhouse gases, accelerating the climate change. For that, new trends and policies for waste management are required due to the high and constant demand for natural resources. The recent activities framed in the green economy are favouring the reuse and recycling of many waste products, in the so-called "Zero Waste" initiatives to reduce the carbon footprint, as well as to the reduction of associated energy expenditure. Among these waste products, those linked to animal by-products not intended for human consumption are usually incinerated for their elimination in Spain, contributing to the emission of $CO_2$. Consequently, new initiatives are required to promote the reuse of this waste, as for example, in the development of more sustainable construction products.

The main goal of this project is to obtain a more sustainable lime mortars by recycling waste animal fibres, in this case pig and cow hairs, and reducing $CO_2$ production by avoiding the incineration of animal by-products not usable in other sectors. To achieve this and establish optimal production and handling conditions, we are comparing samples with animal hairs and without (control samples) to evaluate the quality of the new products by the modification of their physical, mechanical, hydric and thermal properties, and the resistance to crystallization of salts. Three sets of samples with different fibre proportions (containing 10 g or 20 g of cow hair or pig hair per 2 kg), as well as a mixture of both types of fibres (5+5 g and 10+10 g per 2 kg) have been elaborated and tested. The results show that the adding pig hair makes it difficult to prepare mortars by the mixer due to their length and rigidity. On the contrary, cow hair accepts a greater amount but accumulations of hair can be generated, slightly reducing the mechanical resistance. Regardless of the amount and mix of hair, carbonation is completed, observing a good cohesion between the binder, the aggregate and, in some cases, the hairs become partially mineralized. This does not affect the hydric behaviour between samples with fibres but increases if it is compared to the control samples, but both the preparation of the mortar and the amount of hair decreases the UPV values. Salt damage in general is progressive due to sandblasting and peeling of the samples, except some samples which cracked into two halves due to the manufacturing process, not because of the amount of hair.

Acknowledgements: This study was financially supported by the Research Project TED2021-132417A-I00 funded by MCIN/AEI /10.13039/501100011033 and by the European Union NextGenerationEU/ PRTR.

## Forgotten wastes in coastal areas – tackling risks through mineralogy

Onnis, P.[1,2], Ramos, V.[2,*], Riley, A.L.[3], Gandy, C.[4], Jennings, E.[2], Nannoni, A.,[5] Rollinson, G.K.[2], Burke, I.[6], Byrne, P.A.[7], Crane, R.[2], Jarvis, A.[4], Mayes, W.M.[3], Hudson-Edwards, K.A.[2]

[1] Department of Chemical and Geological Sciences, University of Cagliari, Monserrato, Italy

2 Environment and Sustainability Institute and Camborne School of Mines, University of Exeter, Penryn Campus, UK v.i.monteiro-ramos@exeter.ac.uk

3 School of Environmental Sciences, University of Hull, Kingston upon Hull, UK

4 School of Engineering, Newcastle University, Newcastle Upon Tyne, UK

5 Department of Earth Science, Università di Firenze, 50120 Firenze, Italy

6 School of Earth and Environment, University of Leeds, Leeds, UK

7 School of Biological and Environmental Sciences, Liverpool John Moores University, Liverpool, UK

---

Legacy landfills are highly variable in their composition and can constitute a wide range of materials, including metal and coal mine wastes, metallurgical wastes and municipal solid waste. They can be enriched in ecotoxic metal(loid)s which can present a significant environmental hazard particular if they can be either mobilised as dust particles or undergo dissolution within environmental waters. Furthermore, about 10% of landfills in England and Wales are exposed to coastal erosion, flooding, and, therefore, to both chronic and sudden waste weathering and metal(loid) dispersion processes [1]. Understanding the potential metal(loid) release mechanisms is challenging due to the lack of geochemistry and mineralogy data known for such wastes. Metal(loid) concentrations and minerals were investigated in ~100 samples from six key UK legacy waste in coastal zone sites, spanning coal and metal wastes, ferrous and non-ferrous slags, municipal solid wastes (MSW), and bauxite residues. Estuarine sediments, receiving wastes from the upstream metal mining districts, showed As, Pb, Zn, and Cu median concentrations greater than environmental guidelines, with As minerals (namely arsenopyrite and scorodite) supporting the high As median concentration among all the wastes. Coal waste and ferrous slags posed a hazard for As and, occasionally, for Ni and V. Coal wastes hosted metal(loid)s such as As, Cu, and Zn in sulfide minerals, clay mixed pyrite mineral phases, and Fe-oxides. Nevertheless, ferrous slag had no clear metal(loid) hosting minerals. Non-ferrous slags had the greatest mineralogical and met(loid) trend variabilities. High Cr, Ni, Cu, Zn, As, Sb, Pb concentrations were associated with peramelaconite (Cu), cassiterite (Sn), cerussite (Pb), sulfides (Zn, As, and Cu), spinel (Cr), sulfates (Cu, Pb, Ni) and metal droplets (Pb, Zn, and Cu). MSW showed heterogeneity among sites and were generally enriched in Pb and Ni concentrations and metal(loid)-bearing Fe-oxides. Overall, legacy wastes in coastal areas pose hazards to the environment depending on waste type, site conditions, and metal-bearing mineral phases. Findings directly inform national schemes for site prioritisations and benefit the international community affected by the global challenge of coastal legacy wastes. The results of this study are also fundamental to understand the potential use of legacy waste as raw materials replacement, namely for the construction industry, among others, contributing to material circularity.

*References:*

[1] Riley A L et al. (2022). Front Env Sci 10:16 pp

# Wood biomass ash: a possible alternative to free lime and cement as stabilizing agent in clayey subgrade of road pavement

Pandolfi Balbi E.[1], Corradini A.[2*], Cambi C.[1], Fastelli M.[1], Cerni G.[2], Cotana F.[2], Zucchini A.[1], Comodi P.[1]

[1] Department of Physics and Geology, University of Perugia, Perugia, Italy, alessandro.corradini@unipg.it

[2] Department of Civil and Environmental Engineering, University of Perugia, Perugia, Italy

---

EU countries agreed upon increasing the use of renewable energy, which strongly stimulates usage of biofuels for reducing of $CO_2$ emissions. Following these goals, an increase in thermoelectric power plants powered by biomass is expected, which will cause an exponential increase in the amount of waste produced, thus making necessary their disposal. This work is aimed at researching and recycling of wood biomass ashes (WBA) coming from thermal power plants located in Umbria region (Italy), to be used as a stabiliser for a clayey soil belonging to the same area.

Based on the results of the ICL test, different samples were prepared adding to the clayey soil those amounts of lime and biomass ashes which determine a 12.4 pH value, respectively. Furthermore, densification properties of studied mixtures were investigated carrying out standard Proctor compaction tests. Data collected from these tests, performed on both the raw soil and the stabilized mixtures, made it possible to relate the Optimum Moisture Content (OMC) to the dry density (MDD) achieved in each mixture and to create mixes initially characterized by the same dry density and water content.

Such samples were then carried out mechanical tests such as UCT (unconfined compression test) and swelling tests to perform a comparative analysis among studied samples. Furthermore, these mechanical properties were studied at different curing time of the mixtures. The laboratory campaign aimed at investigating the mechanical performance of mixtures provided data through which a comparative analysis among studied samples was carried out. At the same time the chemical-mineralogical evolutions of the different mixtures were monitored using X-ray powder diffraction analysis (XRPD) combined with quantitative phase analyses (QPA) by use of Rietveld method, thermogravimetric analyses (TGA) and energy dispersive X-ray spectroscopy coupled with scanning electron microscopy (EDS-SEM).

The results of the initial lime consumption test (ICL) showed that WBA provides a sufficiently alkaline environment, therefore two mixtures were prepared by adding two different WBA to a clayey soil, which needs stabilization as it is not suitable for any purpose construction in its natural state. The addition of ash causes a reduction in both soil plasticity and maximum dry density, an increase in optimal moisture content and a shift towards coarser size of grain distribution. Furthermore, the addition of ash to clay soil provides a positive impact on bearing capacity and swelling, as well as both short-term and long-term compression parameters. The chemical-mineralogical characterization of the treated soil, together with TGA, show the formation of new cementitious phases (C-S-A-H phases) as the curing time increases. The results obtained indicate the possibility of reducing the use of traditional binders on road pavements (lime and cement) by incorporating WBA which are widespread and readily available in many geographical areas. This translates into a reduced environmental and economic impact as no extraction, processing or transport of raw materials is necessary.

# Mechanisms of metallurgical slag dissolution deciphered from contact and non-contact bioleaching experiments

Potysz, A.[1]

[1] University of Wroclaw, Faculty of Earth Sciences and Environmental Management, Institute of Geological Sciences, Pl. Maksa Borna 9, 50-204 Wrocław, Poland, anna.potysz@uwr.edu.pl

---

Metallurgical slags continue to be a key residual materials linked to the pyrometallurgical metal production. Metal demand in the modern world is expected to increase in magnitude and importance in the coming decades. Therefore, appropriate waste management options need to be put into practise [1]. It must be emphasized that metallurgical slags can serve as secondary metal resources if adequately processed. Thus, biohydrometallurgy applying microorganisms for metal recovery constitutes one of the priority chains in the future slag management. For this reason, the exploration of the interplay between individual factors affecting efficiency of leaching is a key to develop a well-established circular future of these materials [2].

Integrated experimental approach coupled to various analytical techniques has been designed to define optimal conditions for slag processing. Two different types of slags – crystalline and amorphous have been selected for this study. Incubation experiments were carried out with bacteria *Pseudomonas fluorescens.* This bacterial strain was chosen for experimental study because: (a) it was repeatedly identified in the environment, (b) it generates siderophores, and (c) it forms biofilm. To differentiate dissolution mechanisms contact and non-contact incubation experiments were carried out. Slags were separated from bacterial culture using a dialysis membrane characterized by the molecular cut of at 10000 Da. Non-contact experiment allowed passage of siderophore only and its interaction with slag material, whereas microbial attachment was prevented. Contact experiment allowed microbial contact with slag and formation of biofilm on its surface. Throughout the incubation experiments several parameters were monitored: bacterial growth, siderophore production, elements leaching rates and weathering features of individual slag components (phases).

This study highlights the role of siderophore producing bacteria as a key dissolution factor affecting the metal leaching kinetics. Siderophore was found to be a promising compound in metal recovery if operational parameters such as pulp density, fraction size and reactor configuration are properly combined.

*References:*

[1] Potysz A et al. (2018) J Environ Manage, 219: 138-152.
[2] Potysz A (2023) Chemosphere 311: 136964.

## Mineral characterization of the mining residues from the Golpejas mine (Spain): Implications for processing

San Cipriano-Mata, A.[1], Llorens-González, T.[2], Fernández-Fernández, A.[1], Timón-Sánchez, S.M.[2], Díez-Montes, A.[2], Sánchez-García, T.[3], López-Moro, F.J.[2], Menéndez-Aguado, J.M.[4] and Medina-Pierres, J.[4]

[1] Geology Dept., Faculty of Sciences, University of Salamanca. Pza. de Los Caídos, s/n, 37008, Salamanca, Spain. asancipriano@usal.es

[2] IGME-CSIC, Plaza de la Constitución 1, 37001, Salamanca, Spain.

[3] IGME-CSIC, Ríos Rosas, 23, 28003, Madrid, Spain.

[4] Polytechnic School of Mieres, University of Oviedo. C/Gonzalo Gutiérrez Quirós, s/n, 33600, Mieres, Spain.

---

The mining residues from the Sn-Ta-Nb Golpejas mine constitute a good example of potential recovery of critical raw materials in the framework of the circular economy. In this contribution, a characterization of the Sn-Ta-Nb minerals of these tailings has been carried out to determine their chemical composition, grain size and degree of liberation, which could be useful to design a suitable processing flowsheet.

A preliminary Sn-Ta-Nb preconcentrate, representative of the B1 tailings, was obtained by means of a shaking table and high-intensity magnetic separator. Mineralogical characterization was performed by powder X-ray diffraction, electron microprobe and mineral liberation analysis (MLA). As a result, Sn occurs only in cassiterite, whereas Ta and Nb are hosted by columbite-group minerals (CGM). Both cassiterite and CGM show medium grades of liberated grains (53 wt.%). Cassiterite mean grain size is 68 µm, and non-liberated grains are mainly associated with Fe oxi-hydroxides, muscovite, quartz and apatite. On the contrary, CGM grains have a slightly lower mean grain size (52 µm), and are mainly locked in quartz and muscovite. Cassiterite grains are relatively homogeneous, only few grains contain CGM inclusions, while CGM grains show complex internal zoning and are free of inclusions.

According to these findings, it can be concluded that low liberation of cassiterite and CGM could be responsible for the abundance of Sn-Ta-Nb oxides in the mining residues and therefore at least one grinding stage should be considered to achieve better liberation grades.

Acknowledgements: TED2021-130109A-I00, funded by MICIU/AEI/10.13039/501100011033/ and the “Unión Europea NextGenerationEU/PRTR”.

## Resource Optimization in Ceramics: Integrating MMVF Waste for Sustainable Glaze Innovations

Sisti, M.[1], Andreola, F.[2], Barbieri, L.[2], Guidetti, D.[1], Gualtieri, A.F.[1], Fantini, R.[1], Colombo, F.[1], Arletti, R.[1]

[1]Department of Chemical and Geological Sciences – University of Modena and Reggio Emilia, Via Campi 103, I-41125 Modena

[2]Department of Engineering "Enzo Ferrari" – University of Modena and Reggio Emilia, Via P. Vivarelli 10, I-41225 Modena

---

We have developed a ceramic glaze by utilizing the thermal inertization product of man-made vitreous fibres (MMVF) as a secondary raw material. In recent years, the ceramic sector has increasingly focused on resource optimization and waste recycling. In line with the principles of a circular economy, the production of ceramic tiles using "extramuros" waste, such as the product of thermal inertization of MMVF, has become a central theme. This waste material, characterized by being completely amorphous, serves as an ideal melting component in ceramic products. We have experimented with various formulations of ceramic glazes, incorporating between 40% and 50% of this glassy material. The most promising formulation involves 44% of waste, resulting in a lustrous, burgundy ceramic glaze. This outcome underscores the suitability of this waste material as a valuable secondary raw material for the manufacture of traditional ceramics.

## Bottom ashes from MSWI in/and ceramics: a higher value reuse of waste

Bernasconi, A.[1], Mantovani, L.[2] and Tribaudino, M.[1]

[1]Earth Sciences Department, University of Torino, mario.tribaudino@unito.it.

[2]Department of Chemistry, Life Sciences and Environmental Sustainability, University of Parma

---

In Europe about 30 Mtons of bottom ashes (BA) from incineration plants are produced every year. Not more than half is reused, most after quality-upgrade treatments as a substitute for natural aggregates in road building or other construction related activities [1]. Higher value applications are being sought, such as in the production of ceramic tiles, where careful processing and mixing are required to ensure compatibility with the ceramic matrix and to meet the necessary quality standards. However, research in this field is still in the preliminary stages [2]. The criticalities in the addition of BA in ceramics are: 1) the detrimental effect on the rheology of the paste from Cl and sulphates, 2) the behaviour under high temperature furnace heating, and the effect on technological properties 3) the release of potentially toxic elements in the manufactured product.

In this investigation, we explored the possible use of BA in sanitary ware ceramics. Sanitary ware is challenging due to strict technological and aesthetic constrains. A first part of the investigation was to heat the BA in runs between 200 and 1200°C, to determine their behaviour before addition in the sanitary-ware slip. Melting occurs at 1150°C, prompting their potential to enhance greification. Then, BA were added to a standard industrial (SI) paste, used in sanitary ware production. We observed that the use of BA negatively affects rheological properties, likely for the dissolved salts. An improvement was observed if the BA were therefore sieved, and the coarser fraction was used (> 8mm), after milling and repeated washing. Heating through a ceramic route produced the samples of interest. Each sample was analysed by XRD and XRF before and after each run; leaching tests were done, and ICP-MS were performed on the leachate.

Preliminary results show that: 1) addition of coarse and washed BA is not detrimental to rheological and technological properties of the paste and products; 2) despite the high-temperature firing process, all samples exhibit significant heterogeneity at the microscopic level; 3) heating of BA promotes the formation of wollastonite, melilite, pyroxene and feldspathoid, together with amorphous materials; 4) leaching test showed that increasing the heating temperature not all elements are efficiently immobilised. Elements such as Cr and V are strongly immobilized, Ti, Mn, Fe, Co, Zn and Pb increase their concentration in the leachate while for Ni, Cu, and Cd their behaviour is not clear.

The reuse of BA in sanitary ware ceramics is a strong opportunity in circular economy, but upgrade treatment are required, as simply heating BA does not guarantee the immobilization of potentially toxic elements.

*References:*

[1] Chen B et al. (2023) J Build Eng 71:106386
[2] Namkane K et al. (2016) Environ Earth Sci 75:1-11.

## Properties of low sulfur leached spodumene as supplementary cementitious material in ordinary portland cement

Woskowski, J. [1,2,*], Neumann, A. [1,2], Stöber, S. [1,2]

[1] Institute for Technologies and Economics of Lithium (ITEL), Leipziger Str. 70, 06108 Halle (Saale), Germany

[2] Mineralogy/Geochemistry, Martin Luther University Halle-Wittenberg,Von-Seckendorff-Platz 4, 06120 Halle (Saale), Germany

---

Large quantities of leached spodumene concentrate (LSC) are produced as a by-product when processing spodumene for lithium extraction. To avoid the deposition of the material, potential reuse of the material within the cement industry is investigated. XRD and XRF analyses show that the LSC consists predominantly of leached spodumene and thus of an $Al_2O_3$ and $SiO_2$ containing material. The pozzolanic composition of the material suggests a reusability of the material as supplementary cementitious material (SCM) within the cement industry. To test this approach, the hydration properties of LSC powders in combination with OPC cement are investigated. The chemical and mineralogical composition was determined using X-ray methods, followed by the assessment of the hydration behavior of LSC by puzzolanity testing and calorimeter of the heat flow. The test results indicate that a low-sulfur LSC (up to 1.8%) is highly reactive for mixtures of up to 20% and produces high mechanical strengths when combined with an OPC. The conversion rate from α to β spodumene is not significantly affected by variations in raw material sources or process-related fluctuations.

# Tailor Made High throughput Infrastructure for Synchrotron X-Ray Diffraction Measurement of Mineralogical Samples

Sin Ting Chang, C.[1], Jarkko Stenman[2], Nicola Casati[1,3], Christian Grünzweig[1] and Matthias Wagner[1]

[1]ANAXAM, Park Innovarre, Parkstrasse 1, CH-5234 Villigen, Switzerland

[2]STENMAN MINERALS Ab, Maununnevantie 1, FI-00430 Helsinki, Finland

[3] Paul Scherrer Institut, Forschungsstrasse 111, CH-5232 Villigen PSI, Switzerland

---

Obtaining information for the structures, phases and composition of the minerals is important to mineral exploration and mining operation. Resource model is then created using the information gathered through geostatistics. To create reliable resource model for resources estimation, the geological data gathered should be precise and statistically representable. In this work, we have built a high throughput infrastructure dedicated to robust tracking, feeding, exchanging, and sorting samples during synchrotron X-ray diffraction measurement for acquiring geological statistical data. The aim is to provide fully automated measurement and cost-effective solution for massive sample quantity, and to obtain high quality diffraction patterns in short acquisition time for later-on mineralogical quantitative phase analysis. From the phase information obtained, the chemical composition is also back calculated.

The high throughput infrastructure consists of the bunker, bowl feeder, the sample insertion unit with samples orientator, the camera, shaking unit, the carousel, and the software interface. The samples are crushed into powder and are filled and closed in a Data Matrix Coded (DMC) plastic container. Every sample has its own identical DMC code and is registered accordingly. Samples are fed into the bowl feeder and bunker, where the samples are aligned through guiding channels. The DMC code is read by the camera so that the next samples waiting for measurement is registered. The sample is then pushed into the measurement position, and it is shaken with a high-frequency to increase data statistics. After acquisition, the sample container is pushed to a carousel for batch sorting.

Thanks to the synchrotron X-ray source, fast acquisition can be made in 5s per sample maintaining high diffraction pattern quality. This is because of the high intensity and sensitivity of the synchrotron X-ray source, which we can obtain diffraction pattern with high signal to noise ratio, spatial resolution, and large angular range. With the above setup, we can automatically measure up to 10,000 samples per day with a single sample placement. The device has already been implemented at the Materials science (MS) beamline at the Swiss Light Source (SLS) and at ID31 at the European Synchrotron Radiation Facility (ESRF) and more than 25,000 samples were already measured and analysed.

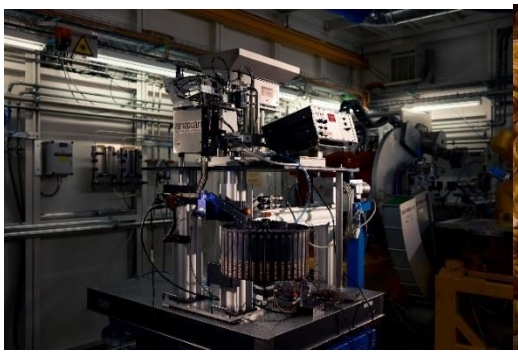

# Understanding the impact of platy morphology on the floatability of gangue minerals from X-ray diffraction patterns: A talc case study

Dodoo, D.[1,2*], Webster, N.A.S.[2,3], Forbes, L.[2,4], Usher, S.P.[1,2], Scales, P.J.[1,2], and Stickland, A.D.[1,2]

[1*] Department of Chemical Engineering, The University of Melbourne, Victoria 3010, Australia.

Email: ddodoo@student.unimelb.edu.au

[2] ARC Centre of Excellence on Eco-Efficient Beneficiation of Minerals, Australia

[3] CSIRO Mineral Resources, Victoria 3169, Australia

[4] Julius Kruttschnitt Mineral Research Centre, Sustainable Minerals Institute, The University of Queensland, Queensland, Australia

---

After years of continuous mining, high-grade copper ores are running out as copper demand increases, provoking the need to mine low-grade copper ores. However, low-grade copper ore deposits are often closely associated with hydrophobic gangue minerals like talc ($Mg_3Si_4O_{10}(OH)_2$), making selective recovery of the valuable minerals more difficult [1]. The experience of miners demonstrates that some talcs are more floatable than others, which causes issues for processing and requires methods that can easily and accurately be used to understand this difference in floatability across different mine sites.

This study used XRD to determine the morphologies of various talcs, which is a quick and easy way to understand how talcs float on mining sites. The orientation of the crystal plane obtained from XRD data of the talc peak intensity between positions 19 and 21° was used to quantify the morphological index (MI) [2] of the talcs, a measure of their aspect ratio. This was defined by considering how the plane (or indeed any parallel plane) intersects the main crystallographic axes of the solid using the monoclinic Miller indexing (hkl). There was a strong correlation found between the platy morphology quantification obtained from XRD and that from X-ray CT 3D analysis of talcs. For precise and accurate analyses, wet sample preparation methods were developed prior to the use of both X-ray and XRD techniques. The XRD results revealed that the particle morphology of talc ranged from platy to blocky, depending on its geological location. The floatability of the talcs varied based on their morphology index in a flotation test conducted on talc ground to a particle size of 106 to 53 µm. The talcs with the highest MI, regarded as highly platy, were more floatable than the other talcs, and the reverse was true for those with the lowest MI. This suggests that the floatability of various talcs is affected by their varying degrees of platiness. Hence, the XRD-determined morphological index of talc could be a straightforward tool for predicting their flotation in a real ore and determining the best course of action to maximise mineral recovery in a flotation system. Also, XRD gives the mineralogy of the sample directly, which simplifies the process of quantifying the platy morphology of the target mineral from a complex ore.

References:

[1] Zhao K, Gu G, Wang C, Rao X, Wang X, Xiong X. The effect of a new polysaccharide on the depression of talc and the flotation of a nickel-copper sulfide ore. Miner Eng. 2015;77.

[2] Holland HJ, Murtagh MJ. An XRD morphology index for talcs: The effect of particle size and morphology on the specific surface area. JCPDS-International Centre for Diffraction Data 2000, Advances in X-Ray Analysis 2000;42.

# Automated mineralogy as a part of complex analytical workflows

Dosbaba, M.[1]

[1]TESCAN GROUP, a.s., Libušina tř. 21, Kohoutovice, 635 00 Brno, marek.dosbaba@tescan.com

SEM-based automated mineralogy solutions such as TESCAN TIMA are very well-established in the field of mineral processing. It serves mainly as a tool for determining the degree of liberation and association of the phase of interest. These textural parameters directly impact the efficiency of ore concentration in the processing plants. Outside of the process mineralogy, however, the method of automated mineralogy is still very little known [1]. Besides basic outputs such as elemental maps, quantitative representation of individual minerals and their grain size distribution, it is also possible to obtain very valuable information on the association of individual phases, not only qualitatively but also quantitatively. Moreover, the grains of the minerals of interest can be directly sorted and filtered within the SW based on their association, chemistry, and morphology. Distribution of these properties can be visualized or delivered in tabular format. Exporting coordinates for use with other analytical methods is then just the next logical step leading to a huge saving of analytical time on instruments such as the electron microprobe or laser ablation (LA). Dedicated sample holders can be shared between automated mineralogy and LA system to ease the process. Simultaneously acquired correlative phase maps and cathodoluminescence images can enhance efficiency of LA analysis even further (see fig 1). More importantly the automatically acquired grain by grain elemental composition from automated mineralogy can be used for cross-calibration of the laser ablation data.

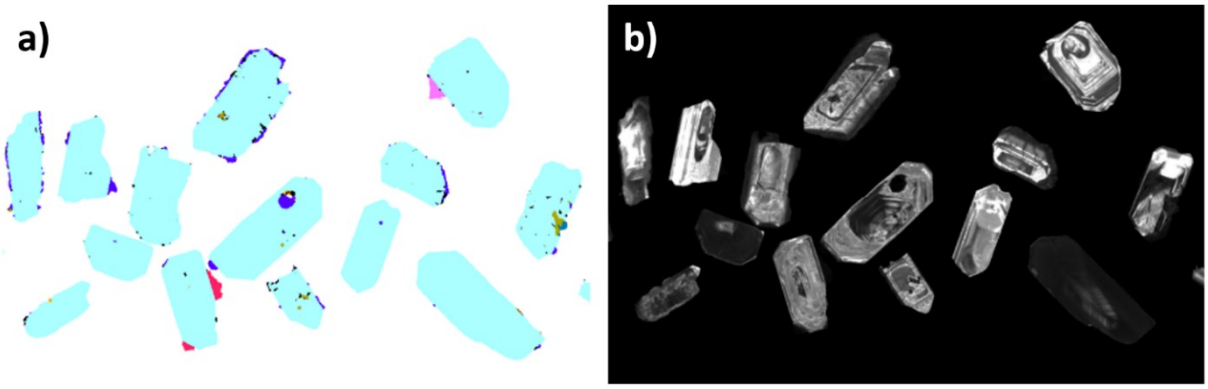


Fig. 1: a) phase map of zircon grains (light blue) and associated quartz (dark blue), orthoclase (red) and apatite (green) obtained by TESCAN TIMA simultaneously with panchromatic cathodoluminescence image (b).

*References:*

[1] Hrstka, T. et al. (2018): Automated mineralogy and petrology applications of TESCAN Integrated Mineral Analyzer (TIMA). Journal of Geosciences 63: 47–63.

# Analytical Advancements in Mining: High-Throughput Synchrotron Radiation X-Ray Powder Diffraction for Sustainable Efficiency

Stenman, J.[1,2], Kortelainen, L.[1,2], Sin Ting Chang, C.[3], Casati, N.[3,4], Grünzweig, C.[3] and Wagner, M.[3]

[1]Stenman Minerals Ab, Maununnevantie 1, FI-00430 Helsinki, Finland Jarkko.stenman@stenmanminerals.fi

[2] Aalto University, Department of Civil Engineering, Rakentajanaukio 4, 02150 Espoo, Finland

[3]ANAXAM, Park Innovarre, Parkstrasse 1, CH-5234 Villigen, Switzerland

[4] Paul Scherrer Institut, Forschungsstrasse 111, CH-5232 Villigen PSI, Switzerland

---

High-Throughput Synchrotron Radiation X-Ray Powder Diffraction (HT-SR-XRPD) is revolutionizing mineralogical analysis, providing a new level of precision and speed in identifying and quantifying mineral phases within geological samples. This method enhances the capability for rapid resource modelling, which has been previously time consuming due to the limitations of conventional analysis techniques.

HT-SR-XRPD employs high-intensity synchrotron radiation along with sample perturbation during the advanced high-resolution photon counting acquisition, seamlessly integrated with conventional Rietveld quantitative phase analysis. This combination enables exceptionally precise and accurate data acquisition and the precise differentiation of mineral species, even those with close structural similarities. It enhances the detection of accessory level minerals, often crucial for comprehensive mineralogical analyses. By enabling precise and rapid characterization of ore deposits, HT-SR-XRPD facilitates the development of optimized extraction processes that are both economically beneficial and environmentally responsible. The method's effectiveness has been demonstrated through successful implementation in customer cases involving tens of thousands of samples.
The integration of HT-SR-XRPD into routine mineralogical evaluations enables mining operations to swiftly adapt to evolving ore conditions, facilitating efficient extraction strategy planning. This adaptability is pivotal for optimizing resource utilization and mitigating environmental impact, in line with modern sustainability imperatives in resource management. Concurrently, in the academic domain, HT-SR-XRPD augments comprehension of intricate mineral systems and bolsters the formulation of sophisticated geological models. These models furnish essential insights into ore body genesis, thus informing more effective exploration and exploitation strategies. Adopting HT-SR-XRPD in mineralogical investigations promises to provide faster, more accurate assessments of mineral deposits in both academia and the mining industry.

## Improved XRD specimen preparation method for accurate morphological quantification of platy gangue minerals: A case study of talc

Dodoo, D.[1,2*], Webster, N.A.S.[2,3], Shu Huang[3], Owen, N.[3], Forbes, L.[2,4], Usher, S.P.[1,2] and Stickland, A.D.[1,2]

[1*] Department of Chemical Engineering, The University of Melbourne, Victoria 3010, Australia.

Email: ddodoo@student.unimelb.edu.au

[2] ARC Centre of Excellence on Eco-Efficient Beneficiation of Minerals, Australia

[3] CSIRO Mineral Resources, Victoria 3169, Australia

[4] Julius Kruttschnitt Mineral Research Centre, Sustainable Minerals Institute, The University of Queensland, Queensland, Australia

---

X-ray diffraction analysis (XRD) is becoming a popular method for quantifying the morphology of clays based on the ratio of their intensities. The preferred orientation challenges of clays make accurate morphological quantification extremely difficult; as a result, a random powder preparation method is necessary when quantifying clays with a platy morphology. This work details a simpler and more efficient method for accurate analysis of platy clays such as talc. It involves a filtration step that makes use of various solvents, as well as a droplet method where an appropriate quantity of drops is placed on a glass zero background mount and dried in a desiccator overnight. Filtration was performed using Milli-Q water, ethanol, surfactants, and synthetic polymeric solvents to identify the optimal solvent for platy talc particle dispersion on a 0.22-micron filter. The March-Dollase equation was used to calculate the degree of preferred orientation, *r*, by simulating in Topas version 7 (PA, USA) [1]. $P(\alpha, r) = (r^2 cos^2\alpha + r^{-1} sin^2\alpha)^{-\frac{3}{2}}$, where *r* stands for the degree of preferred orientation and α is the angle between the preferred orientation axis and the [hkl] direction for the Bragg peak that is being corrected, for talc, this was the (001) plane. It was observed that using polymeric solvents in a specific volume fraction allowed for more particle randomisation, whereas adding ethanol and surfactants increased the preferred orientation by dispersing the platelets. Overall, morphology quantification was accurate, reproducible, and correlated well with standard XRD sample preparation procedures across all approaches.

*Reference:*

[1] Dollase WA. Correction Of Intensities of Preferred Orientation In Powder Diffractometry: Application Of The March Model. J Appl Crystallogr. 1986;19(pt 4).

# Growth history of a multicoloured tourmaline crystal from the Mavuco gem deposit (Alto Ligoña pegmatite district, NE Mozambique)

Altieri, A.[1], Pezzotta, F.[2], Skogby, H.[3], Hålenius, U.[3] and Bosi, F.[1]

[1] Department of Earth Sciences, Sapienza University of Rome, Italy. alessandra.altieri@uniroma1.it

[2] MUM – Mineralogical Museum "Luigi Celleri", San Piero in Campo, Campo nell'Elba, Livorno, Italy

[3] Department of Geosciences, Swedish Museum of Natural History, Stockholm, Sweden

---

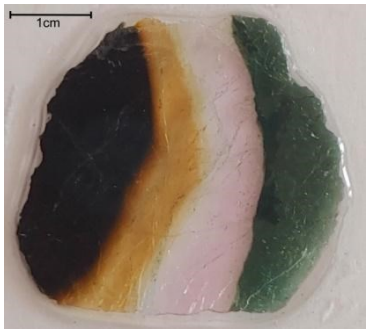


*Figure 1. Thin section of the sample analysed, characterised by a black core, an intermediate polychromatic zone, and a dark-green prismatic overgrowth.*

The Mavuco gem deposit is internationally known to be the source of a quantity of very valuable Cu-bearing gem tourmalines also known as "Paraiba" variety [1]. The mining area of Mavuco consists of a secondary deposit of over 12 $km^2$ in which tourmalines occur as fragments of sub-angular to sub-rounded shapes in a residual soil. A large fragment representing a core-to-rim section of a multicoloured crystal has been selected for the present study as it represents the variety of colours occurring in the deposit (Figure 1). To reconstruct the growth history of this sample, an in-depth analysis including electron microprobe and spectroscopic investigations has been conducted. Data revealed a wide variation in Fe-, Mn-, Ti- and Cu-concentrations and in their redox states throughout the crystal. The black core exhibits a significant enrichment in Fe and Mn (FeO > 5 wt% and MnO > 4 wt%, with Fe in the divalent state) as a result of the availability of such elements in the pegmatitic system during the early crystallisation of tourmaline. The yellow intermediate zone shows a decrease in Fe (FeO < 1 wt%) and a simultaneous increase in Mn (MnO up to 7 wt%). The yellow coloration is caused by $Mn^{2+}$-$Ti^{4+}$ intervalence charge transfer interactions and to a minor extent by $Mn^{2+}$ spin-forbidden transitions. The progressive decrease in Mn, coupled with the absence of Ti and the lack of Fe, allow $Cu^{2+}$ to act as the only chromophore in the pale blue-green zone. The dominant colour-causing agent of the following purplish zone is instead $Mn^{3+}$. The prismatic overgrowth, which has also been observed in many other samples of the residual deposit, is characterised by a sharp increase in Fe and Mn ascribable to a late-stage destabilisation of the pocket environment. A similar phenomenon has been described in the tourmaline crystals from Elba Island (Italy), which are often characterised by a sudden late-stage Fe and/or Mn enrichment resulting in a dark-coloured overgrowth, mostly evident at the termination of the crystals. In this context, a genetic model has been proposed in which a pocket rupture event led to mechanical brittle deformations of the enclosing pegmatite through the formation of late-stage fractures. The permeation of the highly reactive late-stage cavity fluids through the fractures, led to leaching and corrosion processes of the early-crystallised Fe- and Mn-rich cavity-lining minerals causing a sudden change in the chemical composition of the pocket environment [2]. A peculiar tourmaline crystal, recently discovered in a pegmatitic field close to the Alto Ligoña district, provided evidence that a scenario similar to Elba Island occurred for the Mavuco tourmalines. In fact, this sample is characterised by an extended Fe-rich black overgrowth covering all over the crystal from the analogous to the antilogous pole, including the prism faces. Structural and paragenetic information of the giant cavity in which this tourmaline crystal has been collected, indicated that an intense and widespread fracturing of the cavity occurred, which culminated with the subsequent collapse of the pocket roof. The intense collapse event was responsible for the release of large amounts of Fe in the system allowing the formation of overgrowths all over the crystal.

*References:*

[1] Laurs B M et al. (2008) Gems Gemol 44: 4-30

[2] Altieri A et al. (2023) Eur J Mineral 35: 755-771

## Detecting instability of opal: insights from infrared spectroscopy

Chauviré, B.[1], Mevellec, J.-Y.[2], Fereire, J.[3], Thomas, P.S.[4] and Fritsch E.[2]

[1] GeoGems, Guérande, France ; boris.chauvire@geogems.fr

[2] Nantes Université, CNRS, Institut des Matériaux de Nantes Jean Rouxel, IMN, F-44000 Nantes, France

[3] Centre de Recherche Gemmologique, Nantes, France

[4] School of Civil and Environmental Engineering, University of Technology, Sydney, NSW 2007, Australia

---

Opal is among gems offering a unique beauty, but their susceptibility to destabilize greatly affects their use in jewellery. Two distinct types of instability have been observed: (i) a loss of transparency ("whitening") and (ii) the development of fractures (Rondeau et al., 2011).

In addition to its silica framework, opal usually possesses a network of pores capable of containing water, either in the form of molecular water ($H_2O$) or as silanols (SiOH). Initial empirical studies highlight the loss of the water in pores as the main driving factor [1-2]. Whitening is thought to arise from the porosity that scatters light. Cracking in ambient conditions occurs when capillary pressure induces enough stress during the drying [3]. In both cases, the size of the pores containing the free water is a critical parameter.

Low-temperature infrared spectroscopy and differential scanning calorimetry (DSC) measurements have been successfully used to assess the pore size using the freezing temperature of water [4-5]. Measurements were performed using the IMN's characterisation platform, PLASSMAT, Nantes, France. Infrared spectroscopy is sensitive to the water content and its phase thus indicating when the freezing temperature is reached during low temperature experiments. The relation between the freezing temperature of water in pores and the pores size is well established (the smaller the pore is, the lower the freezing temperature is) [4-5].

To study the whitening, we analysed a set of hydrophane opal (defined as opal that becomes transparent when immersed in water, and returns back to opaque during drying) using low-temperature measurements before and after hydration (respectively opaque and transparent), combined with UV-Visible spectroscopy to monitor the loss of transparency. Most hydrophane opal samples do not contain water in pores when dry, but a significant amount when hydrated. By monitoring the changes in the hydration band at low temperature, we observed a sudden shift between -12 and -16°C in analysed samples in hydrated state, corresponding to pores of 2.5 to 3 nm, consistent with a light scattering. Comparing these data with scattering model, we may establish a way to predict the loss of transparency from the pore size.

*References:*

[1] Pearson G. (1985) Aust Gemmol 15:435-445
[2] Smith K. L. (1988) Gems Gemol 24:229-236
[3] Chauviré B. et al. (2023) Minerals 13:356
[4] Chauviré B. and Thomas P.S. (2020) J Therm Anal Calorim 140:2077-2085
[5] Thomas P.S. et al. (2020) Ceram Int 46:29443-29450

# Trace element composition as indicator of prehnite genesis in igneous rocks from Vis Island, Croatia

Topalović, E.[1], Čobić, A.[1], Paradžik, A.[1], Fiket, Ž.[2], Petrinec, Z.[1], Kniewald, G.[2†] and Bermanec, V.[3†]

[1]University of Zagreb, Faculty of Science, Department of Geology, Horvatovac 102B, 10000 Zagreb, Croatia andrea.cobic@geol.pmf.unizg.hr

[2]Ruđer Bošković Institute, Division for Marine and Environmental Research, Bijenička cesta 54, 10000 Zagreb

[3]Faculty of Metallurgy, University of Zagreb, Aleja Narodnih Heroja 3, 44000 Sisak, Croatia

---

Prehnite is a common mineral in the prehnite-pumpellyite facies of low-grade metamorphic rocks and basic igneous rocks related to hydrothermal alteration processes [1]. The ideal formula is $Ca_2Al(Si_3AlO_{10})(OH)_2$, with very scarce literature data on trace elements concentration [2].

The prehnite investigated in this study is hosted by hydrothermally altered andesites and basalts, collected on the southwest coast of Vis Island, near the township of Komiža. Trace element analyses (including rare earth elements – REE) in white, green, and yellow varieties of prehnite were studied by high-resolution ICP-MS in order to identify trace element composition as indicator of prehnite genesis.

Overall, four trace elements (Fe, Mn, Na and V) were present at concentrations above 100 ppm, while others were found at concentrations less than 100 ppm (Ba, Be, Cr, K, Mg, Ni, Sr, Ti, and Zn) or even under 1 ppm (Ag, Cd, Co, Cs, Mo, Rb, Sb, Tl and U). On average, the highest concentration of the majority of elements were observed in green prehnite, lower in yellow prehnite and the lowest in white prehnite. Exception to the latter were Ba, Cr, Mo, Na, Ni, and U in the yellow variety and Co, Cs, K, Mg, and Rb in the white prehnite, showing their highest average levels in said varieties. In all prehnite samples light rare earth elements were found to be more abundant with average ΣLREE/ΣHREE ratios of 4.3, 3.7 and 6.1, and with slightly negative to pronounced positive europium anomaly Eu/Eu* = 0.82, 1.56 and 2.45 for white, green and yellow prehnite samples, respectively.

Since the white variety is surrounded by the green and yellow varieties, is depleted in most trace elements and has a negative Eu anomaly due to little or no leaching, it can be considered the first one to crystallize. Due to the subsequent saturation of the hydrothermal fluids in the host rock, there is an increased dissolution of trace elements, i.e. elements such as Fe, Mn, Ti, and V are easily leached out of the andesite or basalt rock. Green prehnite probably crystallized during such high leaching rates, making it more abundant than yellow and white varieties and enriched in trace elements. The green colour may result from diagenetic substitution reactions with $Fe^{2+}$ and $Al^{3+}$. Yellow prehnite, the least common variety, represents the final stages of crystallization, with coloration probably caused by the oxidation of $Fe^{2+}$ to $Fe^{3+}$.

These results correspond to the proposed genetic model of prehnite formation, which implies its formation as a result of seawater circulation through hot basaltic rocks where Cr, Mn, Ti, and V indicate basaltic origin, while As, Li, Mo, Sr, and U indicate seawater influence during prehnite crystallization.

*References:*

[1] Deer et al. (1962) Longman, London, p. 333
[2] Elburg M A and Cairncross B (2022) S. Afr. J. Geol. 125: 113-122

# Baltic Amber Inclusions: a multi-analytical approach to their characterization

Costanzo A.[1] , Bojarski B. [2] ,Kosior M. [3], Klikowicz A. [3] Cipriani, M.[4]

[1] Earth and Ocean Sciences, School of Natural Sciences, University of Galway, Ireland
alessandra.costanzo@universityofgalway.ie

[2] Laboratory of Evolutionary Entomology and Museum of Amber Inclusions, Department of Invertebrate Zoology and Parasitology, University of Gdańsk, Poland

[3] Amber Experts, Gdańsk, Poland

[4]Department of Biology, Ecology and Earth Science, University of Calabria, Italy

---

Amber is a fossilized resin ancient trees, which underwent the process of fossilization in various epochs and depositional environments and which has been used for a long time as a source of paleobiologic information via the preservation of paleobiota. However, the resin does not just trap organisms, but amber can also preserve vapour phases of various composition. They may represent ancient air trapped at the time the original resin was exuded from its host tree but may also indicate modern air [1]. It was also suggested that the trapped air might be mixed with volatile components of the amber [2]. This study aims to investigate the nature of inclusions in Baltic amber Eocene in age and to determine their origin. The samples vary in size and have been all selected according to their inclusion's appearance. They consist of air bubbles, liquid, solid phases as well as spores. Previous studies demonstrate that resin and amber are not always closed systems. Fluids (e.g. sediment pore water, diagenetic fluid, groundwater) at different burial stages have chances to interact with amber throughout its geological history and affect the preservational quality and morphological fidelity of its organic inclusions. There are indeed numerous problems with the preservation of original compositions in the amber matrix and therefore experiments considering any man-made inclusions are also carried out.

References

[1] Berner R.A. and Landis G.P. (1987) *Am Jour of Sci*, **287**, 757-762.
[2] Roedder E. (1984) Rev in Min, 12, Min Soc of Am, 644 p.

# The southern Canadian Cordillera – a new gem district?

Groat, L.A.[1]

[1]Earth, Ocean & Atmospheric Sciences, University of British Columbia, Vancouver, BC, Canada V6T 1Z4, lee.groat@ubc.ca

In recent years there have been numerous discoveries of gem materials in the Omineca belt of the southern Canadian Cordillera. Most of these are associated with the Shuswap metamorphic complex, the largest metamorphic core complex (MCC) in North America, where high-grade crystalline rocks exhumed from mid-crustal levels in the Eocene are exposed over an area of >40,000 $km^2$. Within the Shuswap MCC is the Monashee Complex which is divided into a "basement assemblage" of gneisses and granite (and expressed as the Frenchman Cap dome to the north and the Thor-Odin dome to the south), and a "cover assemblage" of gneisses and other rocks.

Dzikowski et al. [1] described ruby and pink sapphire hosted in a marble layer within the Monashee Complex "cover assemblage" northwest of the Frenchman Cap dome. The gem corundum occurs in thin, folded and stretched layers with green muscovite + Ba-bearing K-feldspar + anorthite ± phlogopite ± Na-poor scapolite. Whole rock geochemistry data show that the silicate layers formed by mechanical mixing of carbonate with the host gneiss protolith. The silicate layers and the gneiss contain elevated contents of Cr and V due to the volcanoclastic component of their protolith. Petrography of the layers show that corundum formed from muscovite at the peak of metamorphism (~650–700 °C at 0.85–0.9 GPa).

Numerous sapphire occurrences have been reported from the Monashee Complex. Most recently Abdale et al. [2] described a sapphire occurrence in the south-eastern part of the Thor-Odin dome. The sapphire occurs in boudins or pod-like zones of restite within a garnet-bearing leucosome. Both zones are peraluminous and contain plagioclase, K-feldspar, biotite, and muscovite as the dominant mineral phases. Petrographic observations and thermodynamic models indicate that prograde dehydration melting was fueled by the breakdown of plagioclase followed by muscovite and that most of the corundum crystallized from the breakdown of muscovite at or near peak metamorphic conditions (~800 °C and 0.8–0.9 GPa).

Belley [3] described two new iolite (gem cordierite) occurrences in the southwestern part of the Thor-Odin dome where they are hosted in hydrothermally altered mafic volcanic rocks metamorphosed at upper amphibolite to granulite facies. Coarse-grained cordierite-rich rocks are widespread in the Thor-Odin dome, which indicates good potential for future iolite discoveries in the region.

Gem tourmaline (elbaite) and beryl (aquamarine) have been described from pegmatites on Boulder Mountain and Mount Begbie within the "cover assemblage". Approximately 170 km to the south star sapphire has been described from several localities associated with the Valhalla MCC.

It is obvious that conditions exist in southern British Columbia for several gem varieties and the prognosis for future discoveries is excellent. The placer potential in particular remains untested.

*References:*

[1] Dzikowski T et al. (2014) Lithos 198-199: 281-297
[2] Abdale A et al. (2023) Lithos 438-439: 106992
[3] Belley P (2023) Gems & Gemology 59: 340-355

## Why I study Diamonds

Harris, J.W.[1]

[1] School of Geographical and Earth Sciences, University of Glasgow, jeff.harris@glasgow.ac.uk

After an introduction about diamond occurrence within our Earth and the mineral inclusions found in diamond, this talk will focus on the results from two research programmes. The first will concern the diamond formation depths and the ranges in diamond ages, the second will propose a new origin for the very rare Matryoshka diamonds.
Within our Earth diamond principally occurs in two rock types called peridotite and eclogite with formation beneath cratonic areas at depths of 120 -150 km and temperatures of around $1150^0$ C. Other diamonds, however, form at greater depths and experimental petrology plays an important role in defining inclusion mineral boundaries and coexistences. For example, peridotitic olivine goes through two structural changes, one defining the transition zone, before eventually breaking down into ferropericlase and perovskite structured enstatite (bridgmanite) at the transition/lower mantle boundary, 660km below Earth's surface. Evidence of these transitions are recorded both in olivine inclusions in diamond and diamonds which have inclusions of lower mantle mineral assemblages. With depth, eclogitic clinopyroxene dissolves in garnet giving rise to the mineral majorite. This addition causes the Si/Al + Cr ratio in the original garnet to change and has been shown to be a geobarometer, indicating diamond formation down to at least 500km.
The main inclusions from both parageneses for diamond age dating are garnets, pyroxenes and sulphides, the assumption being that the inclusion is synchronous with diamond formation. For the silicates the radiogenic isotope Sm-Nd system is used and for sulphides Re-Os. The first analyses (Sm-Nd) were completed in 1984 and needed 200 garnet inclusions for an analysis. Nowadays a single inclusion can provide a meaningful result for both Sm-Nd and Re-Os.
Peridotitic (harzburgite) diamond range in age from 3.5 to 2.0 Ga, peridotitic (lherzolite) diamond range from 2.3 to 0.1 Ga and eclogitic diamonds are 2.9 to 0.6 Ga old. Depending on the location of the diamonds, ages are usually linked to tectonothermal events.

Thus, mineral inclusions provide unique and pristine information about inner Earth from depths of 120 to just over 800 km and over 3.5 to 0.1 billion years of Earth history. That is why I and many others study diamonds.

A Matryoshka diamond is one in which an inner diamond moves in a cavity within an encasing diamond. The current hypothesis for the origin of such diamonds involves the dissolution of a layer of impure diamond through access to that layer via dislocations or fractures in the outer diamond, events which happen whilst the diamond resides in its parent magma either kimberlite or lamproite. The discovery of an octahedral garnet layer inside a diamond from the Orapa diamond mine in Botswana casts serious doubt on the present hypothesis.

After firstly briefly outlining the unlikely current mechanisms for the origin of Matryoshka diamonds a new model will be proposed.

## Diffusivity of Al vacancies in corundum

Jollands, M.C.[1]

[1]Gemological Institute of America, 50 W. 47th St, New York, 10036 NY, USA

---

Heat treatments of corundum may involve diffusing in an external species (e.g. Ti, Be, Cr), or redistributing elements that are already present in the crystal, or its inclusions. In many cases, the diffusion mechanism will involve Al vacancies. However, a directly measured, unequivocal determination of the diffusivity of Al vacancies ($D_V$) is not present in the literature.

In this study, $D_V$ was determined by hydroxylating extremely pure synthetic corundum in a piston cylinder apparatus at 1GPa. In order to maintain charge-neutrality, hydrogen enters the crystal along with Al vacancies. Therefore the H, which can be easily detected using Fourier transform infrared (FTIR) spectroscopy, acts as a tracer for the vacancies. From profiles of H concentration versus distance, $D_V$ can be determined. Preliminary results suggest $\log_{10}(D_V[m^2s^{-1}])\approx-12$ at 1400°C. Comparison with literature data [1]shows that $D_V$ is around five orders of magnitude greater than $D_{Al}$.

The new $D_V$ allows other diffusivity data to be put into context, for example, $D_V$ is only 1-2 orders higher than $D_{Be}$, potentially implying that Be moves with its own vacancy. Additionally, the hydroxylation is associated with several bands in the FTIR spectra associated with OH stretching groups, notably one at 3420 $cm^{-1}$ which is often attributed to heat treatment.

*References:*

[1] Fielitz P et al (2020), Acta Mater 195: 416-424.

## Partially crystalline silica varieties in gemmology: The case study of the blue Andean opal

Monico, S.[1], Marinoni N.[1], Gatta G.D.[1], Adamo I.[2], Prosperi L.[2], Mácová P.[3] and Ševčík R.[3]

[1]Department of Earth Sciences "Ardito Desio", University of Milan, Via Botticelli 23, 20133 Milan, Italy; sara.monico1@unimi.it;

[2]Istituto Gemmologico Italiano (IGI), Piazza San Sepolcro 1, 20123 Milan, Italy;

[3]Institute of Theoretical and Applied Mechanics of the Czech Academy of Sciences, Centre Telč, Prosecká 809/76, 190 00 Praha 9, Czech Republic.

---

Opal is an amorphous or poorly crystalline hydrated form of silica (usually given as $SiO_2 \cdot nH_2O$) occurring in veins and nodules of various colours. The term *opal* defines several sub-categories of aggregates with varying structural orders, from a glass-like structure to packed silica nano-spheres or nanograins [1]. Opal's intrinsic and peculiar complexities enhance its desirable aesthetic aspect, appreciated in gemmology and jewellery. A well valued and popular opal variety is the blue Andean opal, from the Acari Mine (Arequipa Department, Peru). The distinctive blue hue of this variety is commonly ascribed to the presence of copper-rich mineral inclusions [2,3,4,5].

In this study, a multi-methodological approach has been used to investigate the features of the blue Andean opal. X-Ray diffraction methods have been used for the characterization of the mineralogical assemblage, along with the quantification of the amorphous fraction, showing the challenge in distinguishing among opal subcategories due to their blurred boundaries. Raman mapping highlighted different silica phases and the distribution of impurities within the matrix. The microstructure of the blue Andean opal resulted emblematic of the precipitation processes of the silica aggregate. The analysis of trace elements concentration provided information about the potential composition of the original fluids, from which the Andean opal precipitated. Notably, this research highlighted that the blue colouration of the Andean opal is ascribable to the presence of a mineralogical inclusion, but it is also influenced by the combined effect of factors closely dependent on the geological processes and environment of formation.

*References:*

[1] Gliozzo E (2019) The Contribution of Mineralogy to Cultural Heritage 20: 13-85
[2] Brajkovic A et al. (2007) Australian Gemmologist 23(1): 3-15
[3] Caucia F et al. (2015) Neues Jahrbuch für Mineralogie - Abhandlungen 192(1): 73-84
[4] Fritsch E et al (1999) Revue de Gemmologie 138/139: 34-40
[5] Gaillou E et al. (2008) Ore Geology Reviews 34(1-2): 113-126

# Crystallogenetic features of topaz and beryl from chamber pegmatites of Volyn (Ukrainian shield): elements of similarity and differences

Naumko, I.M.[1], Vovk, O.P.[2], Nedbailo D.R.[2]

[1]Institute of Geology and Geochemistry of Combustible Minerals of the NAS of Ukraine, 3-a Naukova St., Lviv 79060, Ukraine, naumko@ukr,net

[2]Lesya Ukrainka Volyn National University, 13 Voli Av., Lutsk 43025, Ukraine, geologygeochemistry@gmail.com

---

The topaz-morion chamber pegmatites of Volyn are spatially and genetically related to the rapakivi-like granites of the Korosten pluton in the northwestern part of the Ukrainian shield [1] and represent one of the primary sources of jewelry topaz, beryl, and morion in Ukraine.

According to crystal morphology, topaz and beryl from different mineral-structural zones of pegmatites exhibit marked differences. The topaz crystals from the chambers have the richest habit, with seventeen simple forms identified. Among them, the morphologically significant forms are prisms f {011}, y {021}, and d {101}, dipyramids o {111} and u {112}, and pinacoid c {001}. Only seven simple forms were found in other zones, with prism f {011} being the only morphologically significant form observed. Prism f {011} was the sole form observed in metasomatically altered rocks [2]. Beryl crystals from the leaching zones display the richest habit, while those from the chambers exhibit a less diverse morphology [3].

Based on the analysis of the crystal structure, it was determined that the most important simple forms in topaz should be f {011}, b {010}, M {110}, l {120}, d {101}, o {111}, c {001}, y {021}, for beryl - {0001}, {10$\underline{1}$0}, {11$\underline{2}$0}. Such faces should be observed on crystals under any conditions. Thus, all the simple forms mentioned above, except for b {010}, are clearly visible on topaz polyhedra from chambers [2]. For beryls, prisms and pinacoids are morphologically important regardless of the mineral-structural zone [3].

It was found that the crystal morphology of topaz polyhedra becomes poorer with a decrease in temperature; the same applies to beryl [3]. The main mass of topaz was formed during the 2nd acidic period of the post-inversion stage of the pegmatite process at a temperature slightly above 400°C through free crystallization in the chambers and, during metasomatism, in the leaching zones. In metasomatically altered rocks, topaz of the late generation crystallized from low-temperature solutions (180–200 °C) in the 3rd acidic period. The formation of beryl in the chambers occurred at a temperature of about 400 °C. In the leaching zones, the temperature of beryl crystallization was somewhat higher, and in the metasomatically altered rocks beneath the pegmatite body, it reached 500°C due to the influx of ascending high-temperature fluids. Beryl crystallized at a temperature close to that of topaz formation but at slightly different weakly alkaline pH values (7.5–8.5), whereas the pH value of inclusion solutions in topaz usually ranges from 4.3 to 5.6. The pressure at the same time did not exceed 30–40 MPa.

Therefore, clearly individualized crystallomorphologically and genetically, topaz and beryl are typomorphic minerals, reliable indicators of acidity-alkalinity of the fluid environment of mineralogenesis in chamber pegmatites. In view of this, the importance of crystal-morphological and genetic studies of this type of stone-colored raw material, which is important for Ukraine, is undeniable.

*References:*

[1] Lazarenko Ye et al. (1973) Mineralogy and genesis of chamber permatites of Volyn: 360

[2] Pavlyshyn V et al. (2017) Topaz in the subsoil of Ukraine and in the history of nations: 274

[3] Vovk O (2016) Crystal morphology of topaz and beryl of chamber pegmatites of the Korosten pluton (north-western part of the Ukrainian Shield): 25

# Crystal chemistry of tourmalines from Mozambican pegmatites

Bomal, F.[1], Hatert, F.[1], Philippo, S.[2] and Guennou, M.[3]

[1]Laboratory of Mineralogy, University of Liège B18, B-4000 Liège, Belgium (florent.bomal@student.uliege.be)

[2]Natural History Museum of Luxembourg, Münster street 25, L-2160 Luxembourg

[3] Materials Research and Technology Department, Luxembourg Institute of Science and Technology, rue du Brill 41, L-4422 Belvaux , Luxembourg

---

In the last few decades, Mozambique has become an important producer of high-quality tourmalines in the world. Most of these minerals formed within the granitic pegmatites of the Alto Ligonha region that is shared between the provinces of Zambezia and Nampula, in the northeastern part of the country. Minerals of the tourmaline supergroup are constituted by rhombohedral borosilicates with a R3*m* space group, and a general formula $XY_3Z_6[T_6O_{18}](BO_3)_3V_3W$ [1].

A set of tourmaline samples collected in September 2023 from various major deposits mainly located in the Alto Ligonha region has been analysed by electron-microprobe and LA-ICP-TOF-MS, in order to provide accurate data about the major and trace elements concentrations in each crystal. Compositions usually vary along the elbaite-schorl solid solution, with sometimes compositional zonings between both end-members. Several of these elbaites, showing a neon-blue colour similar to that observed in Paraiba tourmalines, are currently under investigation.

Elbaite-schorl samples from the Muhano and Naïpa deposits show similar trace element concentrations which implies that both deposits certainly formed under the same geological conditions. A more peculiar sample from the Mavuco pegmatite, located further to the North, turned out to be a liddicoatite. Compared to the Alto-Ligonha tourmalines, it showed a significant enrichment in Ca (2.21 wt% CaO), Pb (0.46 wt% PbO), Bi, Ga, and Sn. Values of 20 ppm Sr, 6 ppm Nb, 6 ppm In and 549 ppm Sb have also been measured, whereas rare-earth elements are reaching 177 ppm Sc, 103 ppm La, 289 ppm Ce, 28 ppm Pr, 56 ppm Nd, 4 ppm Sm, and 2 ppm Gd. This behaviour is similar, in a greater extent, to that of a Brazilian tourmaline from the Lavra do Urucum pegmatite, which also shows a compositional evolution towards the liddicoatite pole [2].

In order to refine their crystal structures, the tourmaline samples were investigated by single-crystal X-ray diffraction methods. Measured unit-cell parameters are consistent with elbaite-to-schorl compositions, and refined site populations have been calculated from the structural data and are similar to the assigned site populations given by the compositional analyses. Mean bond lengths determined through the refinement are also consistent with the calculated bond lengths, and bond-valence sums obtained for the different sites are close to the ideal theoretical values.

*References:*

[1] Hawthorne FC and Henry DJ (1999) Eur J Mineral 11(2): 201-215
[2] Bomal F (2021) Master thesis, University of Liège, 66 p.

# “Aquafire” beryl from Brazil: inclusions used as a tool to define a new variety of aquamarine

Costanzo, A.[1], Laurs, B.[2] Campos-Venuti, M.[3], Cipriani, M.[4]

[1]Geofluids Research Lab, Earth and Ocean Sciences, School of Natural Sciences, University of Galway, alessandra.costanzo@universityofgalway.ie

[2]The Gemmological Association of Great Britain, Encinitas, CA, USA

[3]Gems in Gems, Seville, Spain

[4]Department of Biology, Ecology and Earth Science, University of Calabria, Arcavacata di Rende, Italy

---

A new find of aquamarine from Minas Gerais, Brazil, displays abundant irregular and spotty orangey-yellow to yellowish-green or brownish-orange inclusions. About 200 kg of rough material was obtained by one of the authors (M.C.-V.), and so far ~5,000 carats have been faceted in sizes up to 23×13mm. The stones are cut to show their inclusion scenery, as well as iridescent colours displayed along fractures or on the surfaces of the inclusions. These beryls were named ‘Aquafire’ due to the combination of these characteristics, and preliminary characterisation of the inclusions has been carried out but the exact phases present have not been identified [1]. The orangey-yellow to yellowish-green inclusions ranged from a few millimetres to the width of the entire stone, and were sheet-shaped and typically oriented approximately perpendicular to the *c*-axis (i.e. parallel to the cleavage direction). They sometimes displayed a mosaic pattern with many six-sided reflective iridescent surfaces that were capable of producing a sunstone-like effect. Associated with the orangey-yellow to yellowish-green inclusions were small submillimetre-scale platy crystals with a hexagonal shape and a transparent dark green appearance. Fractures showing rainbow iridescence were locally present together with the orangey-yellow to yellowish-green inclusions. Fine acicular features with a brownish-orange appearance were oriented parallel to the *c*-axis and probably consisted of hollow tubes filled with epigenetic material. Data from optical and scanning electron microscopy, energy-dispersive and wavelength-dispersive X-ray spectroscopy (EDX and WDX), and Raman spectroscopy of the inclusions will be presented and compared to inclusions in other beryl samples from Brazil (i.e. ‘Leopard’ and ‘Sunstone’ aquamarines).

*References:*

[1] Costanzo A. et al. (2023). The Journal of Gemmology 38(7):646-648.

# Causes of colour changes in tourmalines from different pegmatite provinces after e-beam irradiation and thermal treatments

Rizzo, F.[1], Tempesta, G.[1], Bosi, F.[2], Vadrucci, M.[3,4], Skogby, H.[5] and Agrosì G.[1]

[1]Department of Earth and Geo-Environmental Sciences, University of Bari "Aldo Moro", 70125 Bari, Italy;

[2]Department of Earth Sciences, Sapienza University of Rome, Piazzale Aldo Moro 5, 00185 Rome, Italy;

[3] Italian Space Agency, Science and Research Directorate, Rome (RM), Italy;

[4] I ENEA, Development of Particle Accelerators and Medical Applications Laboratory, C.R. ENEA Frascati, RM, Italy;

[5] Department of Geosciences, Swedish Museum of Natural History, Box 50007, SE-10405 Stockholm, Sweden;

---

The tourmaline supergroup minerals are complex borosilicate belonging to the cyclosilicate class with the general formula: $XY_3Z_6(T_6O_{18})(BO_3)_3V_3W$, where the *Y* and *Z* sites can be occupied by several elements as well as the same element with different oxidation state: e.g. $Fe^{2+}$ and $Fe^{3+}$. This compositional variability allows tourmaline to display an extensive array of colours from colourless to pink, red, blue, green, and black.

To enhance their desirability in the gemstone market, treatments such as heating, or irradiation are often applied to refine their clarity and to intensify their colours. To deeply investigate the causes of colour change following electron beam irradiation and thermal treatment, we studied, before and after e-beam irradiation, five samples from pegmatites of Cruzeiro and Golconda (Brazil), Anjanabonoina (Madagascar), Nuristan, Kunar (Afghanistan) and Malkhan (Russia). Their different original colours varied from pink to blue and often they were zoned. The chemical compositions of tourmaline samples were studied using Scanning Electron Microscopy with Energy Dispersive Spectroscopy and Electron Probe Microanalysis, while concentrations of lighter elements were measured by Micro Laser-Induced Breakdown Spectroscopy. The samples were e-beam irradiated with doses equivalent to $5.1 \times 10^4$ Gray and heated with temperatures ranging from 450 to 600 °C. The samples were investigated by UV-Vis, and Optical Absorption Spectroscopy to analyse optical and structural properties. In particular, the causes of colour change were identified comparing UV-Vis and OAS spectra acquired before and after the treatments. We found that the different observed colours were due to the presence of multiple chromophores, such as Mn and Fe and negligible amounts of Ti and Cu and the colour changes occurred mainly when the oxidation states of Mn and Fe varied. Specifically, irradiation led to the oxidation of $Mn^{2+} \rightarrow Mn^{3+}$ and $Fe^{2+} \rightarrow Fe^{3+}$, resulting in darker colours. Subsequently, thermal treatments, carried out on irradiated samples, reduce $Mn^{3+} \rightarrow Mn^{2+}$ and $Fe^{3+} \rightarrow Fe^{2+}$, producing brightening and colourless hues.

# Bohemian garnet from the Dolní Olešnice deposit and its enigmatic source

Škoda, R.[1], Čopjaková, R.[1], Štefanová, M.[1], Millonig, L.J. [2], Kotková, J.[1,3], Gerdes, A.[2]

[1]Department of Geological Sciences, Masaryk University, Kotlářská 2, 611 37, Brno, Czech Republic / rskoda@sci.muni.cz

[2]Institut für Geowissenschaften & FIERCE, Goethe Universität, Frankfurt am Main, Germany

[3]Czech Geological Survey, Klárov 3, 118 21, Prague 1, Czech Republic

---

We studied pyrope concentrated and extracted in Quaternary placer deposit in Dolní Olešnice (north Bohemia), whose source rock is not known. We examined major and trace element composition of pyrope and its mineral inclusions and acquired in-situ LA-ICPMS garnet U-Pb data in order to constrain its provenance.

Pyrope shows uniform major element composition (Mg# ~80–84) with variable $Cr_2O_3$ contents decreasing from 3.1–6.0 (violet variety) to 1.1–2.3 (red variety) and to 0.4-0.9 wt. % $Cr_2O_3$ (orange variety). This suggests a composite mantle source comprising harzburgite, lherzolite and pyroxenite, respectively. Mantle Cr-rich spinel is absent in the heavy mineral concentrates. Multiphase solid inclusions (MSIs) of variable size (20-200 µm) and shape represent the only inclusions present in pyrope. Approximately 60% of pyrope contain common MSIs, dispersed randomly throughout the grain, preferentially concentrated in the rim domain, or along healed cracks. The MSIs show uniform mineral assemblages of amphibole, forsterite ($Fo_{95}$), magnesite, and spinel with minor phlogopite, rutile and sulphides. Rare earth element contents are very low in high-Cr harzburgitic garnets (∑REE 4-6 ppm) to low in Cr-poorer garnet sourced from lherzolites and pyroxenites (∑REE 8-15 ppm). MSI-rich garnet contains slightly higher REE, Zr and Hf concentrations. The LA-ICPMS garnet U-Pb data fall into two age groups: the older of c. 390 Ma is typical for MSI-free garnet, whereas the younger age of c. 370 Ma was confirmed exclusively in MSI-rich garnet domains.

In the Bohemian Massif, Lu-Hf and LA-ICPMS garnet U-Pb age data for peridotites cluster at c. 390 Ma, c. 360 – 370 Ma and c. 340 Ma [1-4 and references therein]. The age of c. 390 Ma, interpreted as dating Devonian mantle subduction, was retrieved in the Erzgebirge (Saxothuringian Unit) and the Kutná Hora Crystalline Complex [1, 2]. The silicate-carbonate MSIs in the studied garnets are similar to the MSIs in garnet peridotites of the German Erzgebirge and provide evidence for mantle metasomatism by carbonatitic fluids at 370 Ma. They are distinct from the MSIs in garnets from the Bohemian Saxothuringicum which show a significant crustal component in the metasomatic fluid and record c. 340 Ma metasomatic reworking [2]. The MSI assemblage in the Kutná Hora [1, 5] and Gföhl Unit, Moldanubian Zone [4] peridotites differ in the presence of rutile and ilmenite both in single inclusions and in MSIs, reflecting crystallization from trapped oxidic Ti-rich melts, exsolved from basaltic silicate melt that caused significant mantle refertilization [3]. To conclude, the studied pyrope crystals show a close affinity to the garnet peridotites of the German Erzgebirge (Saxothuringian Unit).

*References:*

[1] Ackermann L et al. (2020) J Petrol 61:8
[2] Kotková J et al. (2024) this volume
[3] Kubeš M et al. (2022) Lithos 422:106726
[4] Čopjaková R et al. (2024) this volume
[5] Vrána S (2008) J Geosci 53:17-30

## Light elements in gem quality topaz from different localities

Tempesta, G.[1], Elettivo, G.S. [1] and Agrosì, G.[1]

[1] Dipartimento di Scienza della Terra e Geoambientali, Bari (Ba), Italy / giovanna.agrosi@uniba.it

---

Topaz is a silicate mineral with formula $Al_2SiO_4(F,OH)_2$ that primarily consists of aluminum, silicon, and oxygen. The color of topaz (yellow, brown, blue, pink, red, and colorless) can be influenced by the presence of trace elements within its crystal structure. These trace elements can vary depending on the specific geological contest. Some samples containing relatively high concentrations of chromophorous elements, such as chromium (Cr), manganese (Mn), iron (Fe) and few traces of light element like lithium (Li) and boron (B). Li is not a common element in topaz, it may be sourced from lithium-bearing minerals or fluids that interact with the host rock during topaz formation. The Li presence in the mineral is usually in few ppm. The amount of Li in topaz can vary depending on the geological setting in which the mineral was formed [1]. While boron is less commonly found in topaz compared to other elements mentioned above. However, it can still influence the color of the gemstone, particularly in producing pink or reddish hues. Boron may be introduced to the topaz through interactions with boron-rich fluids or minerals in the surrounding geological environment. We analyzed by Laser Induced Breakdown Spectroscopy (LIBS) several samples colorless, very light blue and pink orange from different source (Brazil, Madagascar, Zambia, Nigeria and Tanzania), comparing the results with those from other localities (Pakistan and Siberia) [2, 3]. The analyses allow to find out the main emission lines of all the elements, except F and OH, also those in traces like Li and B not always found in other studies. This analytical approach could be useful in understanding the role of impurities in natural topaz relating them to their origin and their colors.

*References:*

[1] Agangi, A. et al., (2016) Min. Mag., August, vol. 80(5), pp. 881–899.
[2] M.Rossi , et al., (2014) Phys. Chem. Minerals, vol. 41, 127–140.
[3] Abbasi,S.A, et al., (2021) Minerals, 11, 367.

# Microdiamonds from the Zelenyi Yar Neogene placer (the Ukrainian Shield)

Vyshnevskyi O.A.[1], Kvasnytsya V.M.[1], Wirth R.[2], Schreiber A.[2] and Pavlyuk V.M.[1]

[1]M.P.Semenenko Institute of Geochemistry, Mineralogy and Ore Formation NAS of Ukraine, Kyiv, Ukraine, vyshnevskyy@i.ua

[2]Helmholtz Centre Potsdam, GFZ German Research Centre for Geosciences, Potsdam, Germany

The primary magmatic diamond-bearing rocks (e.g. kimberlite, lamproite, ultramafic lamprophyre) are widely distributed around the world. However, there are regions where only alluvial diamonds are known, but their primary sources have not been discovered. One of these is the Ukrainian Shield, where microdiamonds are widespread in Neogene placers, but their primary rocks are still unknown.

A collection of more than hundred microdiamonds (0.2-0.5 mm) from the Zelenyi Yar Neogene placer, in which their content in sands reaches 0.06 carats per 1 $m^3$ of ore concentrate, was studied. It was previously established [1] that most crystals are octahedra and cubes, others are cube-octahedra, transitional forms {111}+{110}, combinational crystals {111}+{110}+{100}; rhombic dodecahedrons are rare. Half of the examined crystals are nitrogen-free of type IIa. In others nitrogen content ranges from 57 to 612 ppm. They are of IaA (29%), IaAB (11%), Iab (5%) and Ib (5%) types. The $\delta^{13}C$ values of studied samples range from -26.74 to -3.55 ‰ VPDB. The content of helium isotopes measured in one sample is $73.42 \times 10^{-12}$ $cm^3/g$ of $^3He$ and $0.265 \times 10^{-6}$ $cm^3/g$ of $^4He$.

Using a FIB-SEM (Helios G4 Dual Beam) and analytical TEM (Tecnai F20 G2 X-Twin) the internal features of twelve microdiamonds from the Zelenyi Yar Neogene placer were investigated. Dislocations, carbon and nitrogen platelets, as well as mineral and fluid inclusions were detected in the studied samples. Based on the above characteristics, several types of diamond were distinguished: i) diamonds with only curved dislocations in the near-surface zone; ii) diamonds with only carbon platelets; iii) diamonds with dislocations and carbon platelets; iv) diamonds with dislocations and platelets of nitrogen; v) diamonds (mainly cube aggregates) with curved dislocations and multiphase nanoinclusions. By chemical composition and X-ray diffraction Ti-phlogopite, F-apatite, carbonates, K-Ti silicate (davanite?), K-Ti oxide (priderite?), sylvite were identified.

Multiphase nanoinclusions reproduce the composition of the liquid or melt from which this diamond originates. They indicate that the environment of crystallization of Zelenyi Yar microdiamonds contained carbonate, alkali, fluorine and chlorine. Judging by the composition of these multiphase assemblages, it can be assumed that the Zelenyi Yar diamonds grew from carbonatitic to low-silicon melts enriched in alkaline and volatile components. The presence of dislocations and platelets in the studied diamond samples is evidence of increased temperature influence on them, or their long-term residence in the mantle.

All the above features are characteristic to mantle type diamonds. Thus, it is possible to conclude about mantle origin of microdiamonds from the Zelenyi Yar placer. As for the nomenclature of their source rocks, the received data are insufficient, which requires their further examination on more representative material to get better statistics.

*The TEM data were carried out under Trans-National Access action under the support of EXCITE - EC- HORIZON 2020 - INFRAIA 2020 Integrating Activities for Starting Communities under grant agreement N.101005611.*

*References:*

[1] Kvasnytsya V.M. (2021) Mineralogical Journal (Ukraine) 43, No 2: 03-11

## Study of color mechanisms in natural and treated elbaite crystals

Luppi, R.[1], Pezzotta, F.[2], Skogby, H.[3], Hålenius, U.[3], Altieri, A.[1], Tempesta, G.[4], Vadrucci, M.[5,6], Sejkora, J.[7], and Bosi F.[1]

[1]Department of Earth Sciences, Sapienza University of Rome, P. Aldo Moro, 5, 00185 Rome, Italy; Riccardo.luppi@uniroma1.it.

[2]MUM – Mineralogical Museum Luigi Celleri, San Piero in Campo, Elba Island, Italy

[3]Department of Geosciences, Swedish Museum of Natural History, P.O. Box 50 007, 104 05 Stockholm, Sweden

[4]Dipartimento di Scienze della Terra e Geoambientali, Università degli Studi di Bari Aldo Moro, Bari, Italy

[5]APAM Laboratory, ENEA, Via E. Fermi, 45, 00044, Frascati, Italy

[6]Science and Research Direction, Italian Space Agency (ASI), 010133, Rome, Italy

[7]Department of Mineralogy and Petrology, National Museum, Cirkusová 1740, 193 00, Praha 9, Czech Republic

---

Tourmalines are borosilicate minerals that also represent a gem of great value due to their broad spectrum of colors. Specifically, the transition elements Ti, V, Cr, Mn, Fe and Cu act as important color-causing agents occupying the octahedrally coordinated sites, influencing color and color intensity [1]. However, defects due to impurities and distortion of polyhedra can also cause specific electronic transitions, which could influence the color appearance [2]. Understanding the mechanisms behind natural and treated coloration, especially the exact distinction between them, is an ongoing challenge in the tourmaline crystal chemistry and therefore demands further investigation.

In fact, the correct discrimination between "natural" red and "treated" red is currently not possible with gemological techniques alone. To address this issue, colorless tourmaline samples of achroitic variety from San Piero in Campo, Elba Island (Italy) and Stak Nala, Haramosh Mts., Gilgit-Baltistan (Pakistan) were chosen as case study. Two colorless crystals were exposed to electron irradiation and turned pink-red in color after treatment. More intense and evident color in the Italian sample compared to the Pakistan specimen. The color of the irradiated samples disappeared after the heat treatment at 500 °C for three hours. Untreated and treated samples were characterized using electron microprobe analysis, laser induced breakdown spectroscopy, single-crystal X-ray diffraction data, Fourier transform infrared and optical absorption spectroscopy. Results highlight that the studied samples can be classified as elbaite, but the Mn content in the Italian crystal (MnO = 0.47 wt%), is larger than the Mn content in the Pakistan crystal (MnO = 0.01 wt%). This different concentration of Mn in the samples appear to be responsible for the different intensity of red coloration at the end of the irradiation. The spectroscopic results show that the change in color from colorless to pinkish-red and vice versa can be attributed to the oxidation/reduction reactions of Mn ions, as confirmed in the literature [3,4]. However, the fate of the electron that is driven from the $Mn^{2+}$ has not yet been established. A topic that therefore requires more in-depth investigations. This research project will also be extended to rubellite tourmalines from Madagascar and Cu-bearing tourmalines of different colors from Mozambique, two of the rarest and most precious varieties of tourmalines.

*References:*

[1] Pezzotta F and Laurs B (2011) Elements 7: 333-338
[2] Li M et al. (2018) J Spectr 2018: 1-8
[3] Bosi F et al. (2021) Mineral Mag 85: 242–253
[4] Reinitz M and Rossman R (1988) Am Miner 73: 822-825

## Trading Egyptian blue – on material provenance and processing

Rodler-Rørbo, A.[1]

[1] Austrian Archaeological Institute, Austrian Academy of Sciences, Dominikanerbastei 16, AT-1010 Vienna (alexandra.rodler-rorbo@oeaw.ac.at)

---

People processed various materials to use them as colorants and ancient texts emphasize that material quality and provenance mattered. Yet, little is known about where these materials came from and where they were processed. Egyptian blue was produced from easily available resources (calcium-, silica- and copper compounds and a flux) in high-temperature workshops. It is considered among the most widely used ancient colorants between the Egyptian Bronze Age until Antiquity and it is evident that shared production workshops – perhaps even shared trade networks – with glass- and metal artifacts existed. However, currently only a few Egyptian blue production hubs are known, and provenance studies are scarce. The few studies that exist point at distant copper sources and encourage a first discussion of the organization of production and trade in (materials for making) Egyptian blue. Mineralogical-petrographic and geochemical analysis can help tracing raw material provenance and processing to reveal the role of pigments in connecting ancient societies and trade networks.

# Costa Rican gold and copper ore deposits and their potential significance for local pre-Columbian metal artwork production

Westner, K.J.[1], Klein S.[1,2], Gassmann, G.[3], Alvarado, G.E.[4], Schäfer, S.[5] and Welk, E.[5]

[1]Deutsches Bergbau-Museum Bochum, research department archaeometallurgy, Am Bergbaumuseum 31, 44791 Bochum, Germany. Katrin.Westner@bergbaumuseum.de

[2] Ruhr University Bochum, Institute for Archaeological Sciences, Am Bergbaumuseum 31, 44791 Bochum, Germany.

[3] Company ARGUs, Kastellweg 20, 71071 Tübingen, Germany.

[4]Centro de Investigaciones Ciencias Geológicas, Universidad de Costa Rica, San José, Costa Rica.

[5] University of Bamberg, Prehistoric Archaeology, Am Kranen 14, 96047 Bamberg, Germany.

---

Costa Rica boasts a wealth of pre-Columbian gold, copper and particularly *guanín* or *tumbaga* (an alloy consisting mainly of gold and copper) metal artwork suggesting that exploitation of its abundant ore deposits dates back before the Spanish conquest. Up to now, however, very little is known about pre-Columbian metal production in the country, or the origin of the gold and copper the objects were made of. In a transdisciplinary project, we aim to reconstruct the metallurgical process chain by combining (mining) archaeological research with geological surveys and mineralogical-geochemical analysis of local ores and metal artefacts [1].

In order to characterise local mineralisation types and collect analytical data of potential ores used as raw material sources, we representatively sampled gold and copper deposits throughout Costa Rica: a) Fossil placer gold from the Península de Osa, b) epithermal gold (-silver) ore from the Cordillera de Tilarán (including the Montes del Aguacate) and the Sarapiquí volcanic belt (Crucitas site), c) native copper from the Cordillera Central, and d) primary and secondary copper minerals from the Cordillera Central and the Cordillera Talamanca. Whenever possible, samples were collected from (weathered) outcrops of ore bodies and from streams cross-cutting mineralisation, or were derived from small-scale, near-surface mining operations in order to gain material comparable to what might have also been accessible to pre-Columbian people. Optical microscopy, scanning electron microscopy and X-ray powder diffraction were used to identify phase assemblages (and textures) of the samples. The bulk elemental composition and the Pb and Cu isotope signatures, respectively, were determined by inductively coupled plasma mass spectrometry. In our contribution, we will highlight differences between the gold and copper ore types and discuss their potential utilisation by pre-Columbian societies. By comparison with available data of metal artefacts from Costa Rica, we will aim at narrowing down their possible raw material sources and types, with implications for future studies dedicated to pre-Columbian metallurgy in Costa Rica within the larger context of Mesoamerican and Isthmo-Colombian metal artwork.

*References:*

[1] Gassmann G et al. (2023) Metalla 27: 149-166

## Improved classification of a large lithic find inventory using pXRF

Burri, T.[1], Eggenberger. U[2]and Widmer, A-B.[3]

[1]Naturhistorisches Museum Bern, Switzerland; thomas.burri@nmbe.ch

[2]Institute of Geological Sciences, University of Bern, Siwtzerland

[3]Boll, Switzerland

---

Neolithic assemblages obviously contain many lithic materials used for e.g. axes, grinding stones or net weights among many other possible uses. One of the basic needs for archaeologists is a correct petrographic classification of these artefacts. As this task needs a profound knowledge in petrography, geologist or archaeogeologist are invoked in the best case. But even when geologists work on the classification of such lithic artefacts, their results may differ. One point is the ambiguity of rock naming (e.g. greenschist, metabasalt, actinolite-chlorite-plagioclase-schist or just "greenstone" could be used for the same object [1]). But even worse, the determination of a lithic sample may simply be wrong – in most cases due to a simple rock property – the fine grain size. Indeed, many lithic artefacts that were used for demanding physical work (as e.g. axes) are made from very fine-grained material of high tenacity. Because archaeological objects are also objects of cultural heritage, they should remain intact and must not be treated as simple geologic objects. Thus, the classification of such artefacts is often based on macroscopic or "binocular" studies only. Especially with very fine-grained materials, such a task is very demanding and will most certainly lead to at least smaller inconsistencies.

The large excavation of a neolithic lakeside settlement at Cham, Canton of Zug, Switzerland, brought to light almost 17'000 lithic artefacts, 13'000 of which were cherts (Silex) [2]. Finally, 571 objects where selected for detailed studies and classification – mostly stone axes, hammer stones and lithic jewellery. Many of these artefacts consisted of fine grained, dense rocks. A classification without further analytical support would have been very challenging. We therefore used a portable Xray-Fluorescence Analyser (Niton XL3t GOLDD+) to receive additional chemical information on the samples in a non-destructive manner [3].

The use of a pXRF resulted in a larger (temporal) effort but also in a very robust classification. Because the samples were not allowed to be prepared for analysis, measurements were performed on unprepared surfaces, which of course lead to analysis results with larger errors. Nevertheless, the geochemical results were very helpful for classification, although not reliable enough for issues beyond that goal. But the use of pXRF in combination with simple optical methods severely improved our results and should be used more often for similar purposes [4].

In our talk we will present information on the general workflow of the project, and we will discuss pros and cons of pXRF assisted analyses for the classification of larger find inventories.

*References:*

[1] Santallier D. et al. (1998) Revue d'Archéométrie 22: 45-55
[2] De Capitani A (2023) Antiqua 57/1-4
[3] Burri T et al. (2019) Archäologisches Korrespondenzblatt 49: 479-506
[4] Burri T et al. (2023) in De Capitani A (2023) Antiqua 57/2: 176-215

## Stones and pigments made by Raimondo di Sangro: New findings in Eighteenth Century Naples

Tempesta G.[1], Monno A.[1], de Ceglia F.P.[2], Maraschi A.[2], Rigante E.C.L.[3] and Calvano C.D.[3,4]

[1]Interdepartmental Centre "Research Laboratory for the Diagnostics of Cultural Heritage", DiSTeGeo, University of Bari, via Orabona, 4, 70126, Bari, Italy / gioacchino.tempesta@uniba.it

[2]Interuniversity Research Center "Seminario di Storia della Scienza", Department dirium, University of Bari, via Orabona, 4, 70126, Bari, Italy

[3]Interdepartmental Centre "Research Laboratory for the Diagnostics of Cultural Heritage" and [4]SMART, Chemistry Department, University of Bari, via Orabona, 4, 70126, Bari, Italy

---

This multidisciplinary study led by Francesco Paolo de Ceglia within the project promoted by the Interuniversity Research Center "Seminario di Storia della Scienza" brings together approaches and methodologies from the history of science, mineralogy and chemistry, presenting innovative results obtained during two distinct surveys at the Museo Cappella Sansevero [1]. Raimondo di Sangro (1710–1771), Prince of Sansevero, is renowned for having made experiences on mineral palingenesis, among other things. This communication focuses on the techniques that Raimondo implemented to create stones and pigments used to adorn the family chapel. The analyses performed on-site on the cushion of St. Oderisius' statue, on St. Oderisius' Cardinal Hat and on the blue frame on the high altar, were executed by means of portable Raman spectroscopy, Ultraviolet, Visible, and Infrared spectroscopy (UV-VIS-NIR) and UV luminescence.

The cushion described as quartz amethyst in an old guide of the Chapel, appears to be an aggregate (like breccias) consisting of centimetre-sized clasts that shows a strong blue fluorescence. Raman analysis confirmed the assumptions made from observing the appearance and the fluorescence characteristics identifying the mineral as fluorite (CaF). As regards the traces of red pigment debris on the cardinal hat the VIS-NIR analyses show that Francesco Queirolo used cinnabar (also known as vermilion), a mercury sulphide (HgS) mineral to colour the white marble. Raman analyses confirmed the presence of cinnabar. Regarding the pigment within the blue frame, which imitates the lapis lazuli rock, analysis through the VIS-NIR spectrum has demonstrated its compatibility with ultramarine (lazurite), a mineral responsible for imparting the characteristic blue hue to lapis lazuli the natural rock. Further, detailed analyses on micro-fragments were performed in the laboratory by means by Optical Microscope (OM), Scanning Electron Microscopy coupled with Energy Dispersive Spectroscopy (SEM-EDS), Ultraviolet, Visible and Infrared spectroscopy (UV-VIS-NIR) coupled with OM and Matrix-Assisted Laser Desorption/Ionization - Mass Spectrometry (MALDI-MS) for organic matter. Our analyses confirm for the first time that the Prince of Sansevero was able to create artificial ultramarine 50 to 70 years before Guimet's ultramarine synthesis. The pictorial binder was a collagen-based one, which was widespread in Italy at least until the 16$^{th}$ century. The MALDI analyses show a 100% bovine collagen peptides identity and some trace collagen peptides from sheep and hen.

As of today, this seems to be the earliest ever recorded example of the production of this artificial pigment. Consequently, this study suggests that historical sources documenting di Sangro's experiences should be seriously reconsidered.

This work was supported by PRIN2022 cod. 2022CNNRWZ "REActive GEl for orgaNic bindERs recognition in Artworks" granted by MUR.

*References:*

[1] de Ceglia et al., (2024), Nuncius (published online ahead of print 2024)

# Material analysis of Egyptian and Egyptianising scarabs by XRF and Raman spectroscopy

Aspiotis, S.[1,2], Bonnerot, O.[1] and Mascia, L.[1]

[1]Cluster of Excellence "Understanding Written Artefacts", Universität Hamburg, email: stylianos.aspiotis@uni-hamburg.de

[2]Department of Earth System Sciences, Universität Hamburg

---

Scarabs are among the oldest rock-based amulets and seals of the ancient Egyptian world. Fashioned in great numbers since the Middle Kingdom (*c.* 1938-1630 BCE), scarabs soon crossed the borders of the Egyptian lands and began to be attested across the Mediterranean basin. The popularity of these artefacts led to the progressive instalment of centres of productions outside Egypt, which is reflected in the broad *repertoire* of motifs attested [1]. Besides the design of these objects, the engraved inscriptions and figural motifs created by scarabs' craftsmen, equally important information can be gained by studying their production process. Until now, the mineral phase characterization of scarabs kept in museum collections has mostly been based on naked eye observations, which are rather inconclusive or too general, especially since scarabs are mostly glazed. Since cultural-heritage objects cannot be sampled due to their uniqueness and historical value, non-destructive and non-invasive analytical techniques that are sensitive to both chemistry and structure are becoming increasingly popular in the scientific community. In general, X-ray diffraction, X-ray fluorescence (XRF) and Raman spectroscopy have been successfully used to determine the structure, elemental composition and firing conditions of glazed scarabs [2-4].
In this study, selected scarabs from the collection of the Museum für Kunst und Gewerbe Hamburg (MKG) were studied by XRF and Raman spectroscopy. We show that Raman spectroscopic analyses combined with XRF can (i) determine the major, minor, and trace element composition within each mineral phase comprising the scarabs, and (ii) separate the dominant glazing techniques and define the firing conditions of glazed steatite-based scarabs in particular**.**

*References:*

[1] Gorton A F (1996) Oxford University Press
[2] Colomban P and Paulsen O (2005) J Am Ceram Soc 88:390-395
[3] Costa M. et al. (2019) Microsc Microanal 25:214-220
[4] Xu S et al. (2024) J Archaeol Sci 163:105939

# Weathering of the tuffeau building materials under the microscope. Focus on gypsum

Naumenko-Dèzes, M.O.[1], Beck, K.[2], Wille, G.[1] and Kloppmann, W.[1]

[1]BRGM, Direction des Laboratoires, Unité Isotopes, BP 6009, F-45060 Orléans cedex 2, France. marie@geosphere.ch

[2]Univ. Orléans, Univ. Tours, INSA CVL, LaMé EA7494, 8 rue Léonard de Vinci, F-45072 Orléans

---

Detailed multi-method examination of stone weathering features play a pivotal role in safeguarding historical buildings. Many landmark buildings in France including the famous Loire castles are built with tuffeau, a fine-grained turonian limestone indigenous to the Loire Valley. This stone, comprising calcite, quartz, opal, micas, and clay minerals, is primarily characterised by its considerable porosity, ca. 45%, and modest durability [1]. It frequently shows several alteration features like granular disintegration, flaking, black crust, scaling and especially spalling [2].

Two samples of tuffeau weathered by black crust were taken from a house located on the Notre-Dame-de-Recouvrance street in the town centre of Orléans (France) during restauration work. These samples (length: 5 cm, width: 2 cm, height: 1 cm) were studied by energy-dispersive X-ray spectrometry (EDS), electron backscattered diffraction (EBSD) and micro-XRF mapping. Additionally, isotopic analyses of S and O were performed on the black crust.

The unaltered part of the sample consists of crystals of calcite, quartz, plagioclase, spherules of opal with occasional presence of larger (ca. 200 µm) mica flakes and (ca. 50 µm) ilmenite and monazite. When approaching the alteration zone on the surface, the plagioclase disappears while the amount of opal spherules increases. Calcite and opal spherules show curious patterns, one can often observe that calcite either was dissolving at the points of contact with opal or has grown later incorporating the spherules. This kind of mineral relationship is especially prevalent in the altered zone above 1.5 cm from the surface. This zone also appears to be more porous and opal spherules dominate near cracks. This is a zone of active dissolution and re-crystallization of the calcite under the influence of capillary water. An increasing amount of tiny gypsum grains appear when approaching the surface. The black crust is just a 0.5-1 mm surface zone. It consists of tiny (<2 µm) grains of gypsum and opal with single grains of barite and traces of Fe, Mg as well as Pb and P. The S and O isotopes indicate atmospheric pollution as main source of sulphates.

The location of gypsum is completely different between the black crust pattern and the spalling pattern in the tuffeau deterioration. Gypsum is more concentrated at the surface in the case of black crust or flaking, and it is more concentrated in 1 cm depth in the case of spalling. The recrystallization processes as well as crystallization of the gypsum in the first 1.5cm from the surface of the tuffeau might constitute an initial trigger of spalling. Indeed, spalling is the main pattern of degradation of tuffeau and the precise mechanisms of tuffeau alteration still need to be elucidated, which is the aim of the ongoing DETRESSE project funded by the Centre-Val de Loire region.

*References:*

[1] Beck K. and Al-Mukhtar M. (2010) In: Geological Society, London, Special Publications, 331, 103-111. [2] Janvier-Badosa S. et al. (2015) Environ Earth Sci 74, 2209-2221. [3] Kloppmann W. et al (2011) Sci Total Environ 409:1658–1669

## Thermal decomposition of dolomite: Raman spectroscopy as a thermometric tool for the analysis of carbonates in mortar binders

Zöllner, M.T.[1,2], Dariz, P.[3], Riedel, J.[1], and Schmid, T.[1,4]

[1] Division of Instrumental Analytics, Federal Institute for Materials Research and Testing (BAM), Richard-Willstätter-Str. 11, 12489 Berlin, Germany. E-mail: moritz.zoellner@bam.de

[2] Department of Chemistry, Humboldt-Universität zu Berlin, Brook-Taylor-Strasse 2, 12489 Berlin, Germany

[3] Conservation-Restoration, Bern University of the Arts, Bern University of Applied Sciences, Fellerstr. 11, 3027 Bern, Switzerland

[4] School of Analytical Sciences Adlershof (SALSA), Humboldt-Universität zu Berlin, Unter den Linden 6, 10099 Berlin, Germany

---

The reconstruction of the thermal history of minerals is an on-going challenge in the study of anthropogenic materials, *e.g.*, ceramics and mortar binders. For millennia carbonate rocks have been used as the starting material, though the exact manufacturing procedures are often unknown. Preparatory parameters such as firing temperature, heating and cooling rates, soaking time, and kiln atmosphere greatly influence the chemical and structural properties of the resulting products. Analysis of replicas produced under well-defined laboratory conditions help identify indicators for such process parameters and therefore provide valuable insights into historical production workflows. Raman micro-spectroscopy is a valuable method here because of its high sensitivity for crystal-chemical alterations coupled with a high spatial resolution. Previous studies on pyrogenic anhydrite were able to distinguish between gypsum materials that were heated at different temperatures between 400 – 900 °C [1, 2].

The poster presents the results of thermal experiments with natural dolomite powder between 500 – 900 °C, evaluating the thermal decomposition of dolomite and the consequent formation of calcium carbonate. Raman measurements were performed at room temperature on calcinated samples, as well as subsequently hydrated and re-carbonated samples. A peak-fitting routine using python scripts was employed to extract the peak positions and the full width at half maximum (FWHM) values of the $v_1$-, $v_4$- and *L*-bands of the carbonates. The results reveal the formation of Mg-calcite from dolomite at 700 – 750 °C and the formation of Mg-free calcite after calcination above 750 °C and subsequent hydration and re-carbonation. The findings from the thermal experiments are compared with Raman-microscopy mappings on medieval and reenacted mortars containing dolomite. Mg-calcite with comparable peak position and FWHM values have been successfully identified, proving Raman spectroscopy to be a suitable tool for elucidating the manufacturing procedures of anthropogenic materials.

*References:*

[1] Dariz P and Schmid T (2017) Mater. Charact. 129: 9-17

[2] Schmid T et al. (2019) J. Raman Spectrosc. 50: 1154-1168

## A new digital data infrastructure to make Pb isotope data fit for the future

Rose, T.[1], Greifelt, T.[1], Westner, K. J.[1], Hornschuch, A.[2], Hsu, Y.-K., Wiethoff, H.[3], Klein, S.[1,4,5]

[1]Forschungsbereich Archäometallurgie, Leibniz-Forschungsmuseum für Georessourcen/Deutsches Bergbau-Museum Bochum, Bochum, Germany

[2]Forschungsbereich Montanarchäologie, Leibniz-Forschungsmuseum für Georessourcen/Deutsches Bergbau-Museum Bochum, Bochum, Germany

[3]Rechenzentrum, Technische Hochschule Georg Agricola, Bochum, Germany

[4]Institut für Archäologische Wissenschaften, Ruhr-Universität Bochum, Bochum, Germany

[5]FIERCE, Frankfurt Isotope & Element Research Centre, Goethe Universität Frankfurt, Frankfurt am Main, Germany

---

In the archaeological sciences, lead isotopes became a standard method for reconstructing the raw material provenance of non-ferrous metals. The successful application of this method crucially depends on the availability of reference data from all potential ore deposits or artefacts whose raw material provenance can be reliably established through other methods. This in turn requires a digital data infrastructure, where lead isotope data can be stored together with metadata about their analytical, geoscientific, and archaeological background.

The first such database available in open access was OXALID [1] and many more followed since. They all have three major drawbacks: (1) They are published in static publication formats or are not maintained anymore. (2) They follow their own approach in describing and structuring the data, resulting in ambiguous information and making the combination of databases hard to impossible. (3) With each new published database, large parts of the data is republished because all databases use to a large extent the same data pool.

These drawbacks can be overcome with a central, community-driven digital data infrastructure, which ensures a standardised description of the data in compliance with the FAIR principles [2], open access to the data, tools to work with the data, and support in publishing new data. Here we will present a project that aims to become this infrastructure. Prototypes were developed as GlobaLID (Global Lead Isotope Database) since 2018 [3,4,5] and received overwhelmingly positive feedback from the community. Recently, acquired funding now allows the next step: Developing and implementing the full-fledged infrastructure close to the needs of the community.

This contribution will present the key features of the envisioned digital data infrastructure and the different ways for the community to get involved in its development and to actively shape the infrastructure. In addition, this contribution will present how we aim for meeting the specific needs of the geochemists and archaeologists alike and how we will build upon already existing infrastructures and initiatives to do so.

*References:*

[1] Stos-Gale Z and Gale N.H. (2009) Archaeol Anthropol Sci 1: 195–213. doi: 10.1007/s12520-009-0011-6
[2] Wilkinson et al. (2016) Scientific Data 3: 160018. doi:10.1038/sdata.2016.18
[3]Klein S et al. (2022) Archaeometry 64:935–950. doi:10.1111/arcm.12762
[4] Westner K et al. (2023) GFZ Data Services. doi:10.5880/fidgeo.2023.043
[5] GlobaLID Core Team (2021). https://globalid.dmt-lb.de/

# The study of alabaster art objects in the cultural heritage of Ukraine using isotopic analysis methods

Naumenko, U.[1,2], Dezes, M.[1], Borniak, U.[3], Lipinska, A.[4], Kloppmann, W.[1]

[1] BRGM, French Geological Survey, 45000 Orléans, France, w.kloppmann@brgm.fr

[2] Institute of Geological Sciences of the NAS of Ukraine, 01054 Kyiv, Ukraine, uznaum@gmail.com

[3] Ivan Franko National University, 79005 L'viv, Ukraine

[4] University of Cologne, 50923 Cologne, Germany, aleksandra.lipinska@uni-koeln.de

---

Recently, there has been a trend towards the increasing use of interdisciplinary tools in the study of cultural heritage and ancient artefacts. The use of modern analytical methods contributes to the creation of reference databases that will be available to address questions related to the sources of geomaterials used in European sculpture, their trade networks and the human actors involved in their use such as sculptors, commissioners, art and material traders.

Our study, conducted within the Materi-A-Net project co-funded by the FRAL program of French ANR and German DFG, examines the role of gypsum alabaster in the development of sculptural art in Ukraine. We have selected the period of the greatest flourishing of alabaster sculptural art, the Renaissance. This style was fostered by numerous Italian, Netherlandish and German artists working in the second half of the 16th - early 17th century in L'viv (modern Ukraine), at this time part of the Polish-Lithuanian Commonwealth [1]. Alabaster became then a chief material of a majority of tombs and altarpieces as well as architectural interior decorative sculpture in the western part of Ukraine.

Our research combines the methods of art history (stylistic and iconographic analysis of works of art and textual sources) [2], geology (localization of historical quarries), mineralogy and isotope geochemistry (determination of the origin of material samples) with the structuring of the research data set in a database [3, 4].

We analysed isotopes of Sr, S and O to identify the sources of material sampled for works of art and to determine the material from which the object was made. We have selected 21 samples from ancient quarries reputedly used by late medieval-early modern regional sculptors. According to the isotopic data, Ukrainian alabaster clearly differs from alabaster from other regions of Europe (Italy, France, Germany, Britain, and Poland) and has a very homogeneous overall signature. There is an overlap with Tuscan (Messinian) alabaster for S and Sr but distinction can be made by O isotopes. This gave us the opportunity to confirm Ukrainian origin for of 15 alabaster art objects sampled in Lviv, Berezan, Dobromyl (Ukraine) and Kraków, Tarnów (Poland).

These results not only contribute to our understanding of material provenance in Renaissance sculptural art but also serve as vital components in comprehensive examinations of cultural heritage sites. Because of the dissemination of Ukrainian alabaster it can be also instrumental in tracing a network of entanglement of Ukrainian culture with this of its European neighbours.

*References:*

[1] Lipińska A. (2014) Eastern outpost. The sculptors Herman Van Hutte and Hendrik Horst in Lviv ca 1560-1610, in: F. Scholten, J. Woodall, D. Meyers (Hg.), Netherlands Yearbook for History of Art 63: Art and Migration. Netherlandish Artists on the Move, 1400-1750, Leiden-Boston: Brill 2014, 136-179.
[2] Rajchel J. et al (2014) Geol.Quart 58 (3): 597–616
[3] Kloppmann W. et al (2014) Archaeometry 56: 203-219
[4] Kloppmann W. et al (2017) PNAS 114: 11856–11860

# Shipshape and Bristol fashion: Characterising the corrosion of the SS Great Britain

Rothwell, K. A.[1], Grahamslaw, N.[2], Grigg, A. R. C.[3] and Byrne, J. M.[1]

[1]School of Earth Sciences, Wills Memorial Building, Bristol, BS8 1RJ, United Kingdom, k.rothwell@bristol.ac.uk

[2]SS Great Britain Trust, Great Western Dockyard, Gas Ferry Road, Bristol, BS1 6TY, United Kingdom

[3]Soil Chemistry Group, Institute of Biogeochemistry and Pollutant Dynamics, ETH Zurich, CHN, Universitätstrasse 16, 8092 Zurich, Switzerland

---

Historic iron ships are extremely important for the cultural heritage of the UK, securing a tourist spend of £17 billion in 2018 (Historic England). For instance, the SS Great Britain, designed by Isambard Kingdom Brunel and the largest ship afloat on her launch in 1843, is the highest rated tourist attraction in Bristol, England (TripAdvisor) receiving over 200,000 visitors per year. Nevertheless, the vulnerability of marine iron archaeological objects to corrosion remains a huge and costly challenge for conservators, as the ingress of salt leads to increased corrosion rates driven by both microbial and chemical processes.

In order to fully understand the risks to iron heritage, and determine the most sustainable preservation methods, conservators must establish a baseline of the current state of corrosion. However, due to the irreplaceable nature of archaeological artefacts, corrosion baselines are often difficult to determine. Non-destructive, in-situ characterisation methods that cause minimal disturbance to the artefact are preferable yet few suitable techniques exist. Ex-situ techniques offer more options however are contingent upon access to representative samples that may have broken off from the archaeological object.

Here, we present a corrosion baseline survey of the wrought iron hull of the SS Great Britain. Using carefully selected samples that had previously fallen from the hull, we employ a suite of analytical techniques to comprehensively characterise the corrosion products including Mössbauer spectroscopy, optical microscopy, Scanning Electron Microscopy with elemental analysis (SEM-EDS), Raman spectroscopy and X-Ray Diffraction. Additionally, we introduce the use of portable X-Ray Fluorescence instruments to conduct in-situ elemental analysis of archaeological objects and discuss the potentials and limitations of this technique.

Our results show that the corrosion layer formed on the original wrought iron hull comprises not only the anticipated Fe (oxyhydr)oxides and chlorides, but also a significant portion of carbonate and Si- and Al- bearing minerals. Crucially, the presence of impermeable carbonate may inhibit corrosion by acting as a passivation layer that impedes moisture and $O_2$ from reaching the metallic iron below. We highlight the indispensable role of the mineralogist's unique skillset in addressing challenges faced across disciplines by corrosion scientists, heritage conservators, and archaeologists.

# Archaeometric study of the stone tesserae from the “A grandi fiori” mosaic in the archaeological site of Casignana (Reggio Calabria, Italy)

Barca, D.[1], Zicarelli, M.A.[1], La Russa, M.F.[1], Musella, M.[1], Randazzo, L.[2], Ricca M.[1], Rovella, N.[3]

[1]Department of Biology, Ecology and Earth Sciences, University of Calabria, Via P. Bucci, 87036 Rende, CS, Italy
donatella.barca@unical.it

[2]Department of Earth and Marine Sciences, University of Palermo, Via Archirafi 26, 90123, Palermo, Italy

[3]Institute on Membrane Technology, CNR-ITM, Via P. Bucci 17/C, 87036 Rende, CS, Italy

---

This study focused on the archaeometric investigation carried out on the stone tesserae constituting the “A grandi fiori” mosaic in the room “N” of the Residential area of the Roman Villa of Palazzi of Casignana which represents one of the most important Roman sites of Southern Italy thanks to the extension and refinement of its mosaics. The analysed mosaic is a bichrome tessellatum mosaic with white marble and green micritic tesserae dating back to the 3rd century AD, characterized by decorative motifs of bell-shaped flowers arranged within circles and enclosed within a border that extends along the perimeter.

The diagnostic analyses such as Polarized Optical Microscopy (POM), X-Ray Diffractometry (XRD) on powdered samples and Scanning Electron Microscope equipped with Energy Dispersive Spectrometer (SEM-EDS) are aimed to obtain information about the minero-petrographic features and chemical composition of both green micritic and white marble stones constituting the tesserae.

In addition, provenance study has been conducted on the white marble tesserae constituting the mosaic. It has been demonstrated that the employment of a single analysis is not efficient to solve provenance issues, on the contrary, a multi analytical approach is essential to establishing the marbles provenance [1,2]. For this reason, twenty-four white marble tesserae have been collected and investigated under complementary techniques. In particular, the results obtained from POM examinations on thin sections, XRD characterization, isotope ratio mass spectrometry (IRMS) of $^{13}C$ and $^{18}O$ and SEM-EDS analysis were combined. In more detail, the fabric type, shape of the boundaries (GBS) and the maximum grain size (MGS) of the calcite and/or dolomite grains were determined by POM. Furthermore, X-ray diffraction investigation allowed to identify the mineralogical phases, highlighting the presence of dolomite in some samples. In addition, oxygen and carbon stable isotope compositions ($\delta^{13}C$ and $\delta^{18}O$) were established through mass spectrometry. Finally, the SEM-EDS was performed to analyse the chemical composition and the presence of accessory minerals. The results from the different investigations were then compared with most recent uploaded databases for the main Mediterranean marbles used in antiquity in order to assess the most probable origin of the investigated marbles [1,2].

The preliminary results obtained showed a great variability and a significant heterogeneity among the marble tesserae, indicating the use of different lithotypes coming from diverse ancient Mediterranean quarries. This conclusion demonstrates and confirms the richness and the great archaeological importance of the Roman Villa.

*References:*

[1] Capedri S (2004) Archaeometry: 517-536
[2] Antonelli F, Lazzarini L (2015) Rend. Fis. Acc. Lincei: 399-413

## Characterization of chert by X-ray diffraction, infrared and Raman spectroscopy to identify Moganite.

De Uribe-Zorita, M.*[1], Álvarez-Lloret, P.[1], and Marcos, C[1].

[1]Department of Geology. University of Oviedo, 33007, Oviedo (Spain).
*Corresponding author: UO251780@uniovi.es

---

Samples of chert from outcrops of different geographic areas and different geological periods have been characterized with X-ray diffraction, Infrared and Raman spectroscopy techniques in order to detect and quantify unequivocally moganite. The content of moganite and the crystallite size of the quartz in the cherts would be indicative of its maturity and could potentially be used for dating chert-tools recovered from archaeological sites [1].

Chert is a siliceous rock, consisting mainly of phases such as quartz, chalcedony and moganite, with a micro- to cryptocrystalline texture. Chert is one of the most important lithic resources because of easily discovered in the quaternary sediments, its relative abundance in archaeological sites and due to their physical and mechanical properties. Chert has been utilized by people of upper Paleolithic, Mesolithic and Neolithic, besides many other rocks (quartz, quartzite, obsidian, basalt, rhyolite), and other materials such as wood, bone. Moganite, a metastable phase of silica, is found among the opaline phases (less mature) and quartz (more mature) in the diagenetic ageing sequence of siliceous rocks [2]. Depending on their content, the mineralogical maturation of the chert can be predicted, and thus mineralogical maturation of the chert [1].

Infrared spectroscopy of the investigated cherts showed absence of $H_2O$ vibration bands corroborating the absence of chalcedony. In addition, the typical band of the moganite (about 500 $cm^{-1}$) could not be resolved. However, with Raman spectroscopy, this band could be clearly detected in the samples in which the moganite had been identified with X-ray diffraction. With this last technique was also possible to observe variations in the moganite content within the same chert sample, because this phase presents textural variations, corroborating previous observations made previously by Rodgers and Cressey [2] on other types of chert.

This study corroborates that X-ray diffraction and Raman spectroscopy techniques are essential and complementary in the detection and quantification of moganite, a crucial phase in determining the mineralogical maturity of a chert.

*References:*
[1] Marcos C et al. (2021) Minerals 11:611
[2] Rodgers KA and Cressey G (2001) Mineral Mag 65:157-167

## Microbial reduction of metals: mechanisms, environmental implications, and biotechnological applications

Kimber, R.L.[1,2], Egan Morriss, C.[1], Byrd, N.[1], and Lloyd, J.R.[1]

[1]Department of Earth and Environmental Sciences, University of Manchester, UK, richard.kimber@manchester.ac.uk

[2]Department of Environmental Geosciences, University of Vienna, Austria

---

Microbial metal reduction is an important component in the biogeochemical redox cycling of metals, playing a key role in controlling metal speciation. Microbial reduction of metals can occur enzymatically, with some microbes able to utilize a range metals as terminal electron acceptors for growth, as well as through detoxification mechanisms to regulate metal homeostasis. Speciation changes following microbial metal reduction can result in the dissolution or precipitation of mineral phases, depending on the specific metal involved. These speciation changes help drive the biogeochemical cycling of metals and influence the bioavailability of metal nutrients and contaminants. Harnessing these processes also holds great promise for a range of biotechnological applications including bioremediation, metal-recovery, and the biosynthesis of novel functional nanomaterials.

Here, we will discuss how the microbial reduction of a range of metals, including Cu, Fe, Pd, Au, and Ag, can be harnessed for a range of biotechnological applications, from metal-recovery to fine chemical synthesis. We will explore mechanistic insights into the reduction pathways involved and how these processes can be exploited to control the properties of a range of bionanomaterials. The impact of solution chemistry controls on the biosynthesis of high-value nanomaterials will also be discussed as well as the optimization of these systems for potential scale-up.

## Phototrophic iron oxidation under complex geochemical conditions

Bryce, C[1], Nikeleit, V.[2], Byrne, J.[1] and Kappler, A.[2]

1 School of Earth Sciences, University of Bristol, UK

2 Department of Geosciences, University of Tuebingen, Germany

---

Anoxygenic phototrophs capable of oxidizing Fe(II) to Fe(III) are thought to have been the Earth's earliest Fe(II)-oxidizing microbes, possibly even fueling the Earth's earliest biosphere. However, the microorganisms capable of this process typically have very flexible metabolisms and can use carbon, sulfur or hydrogen compounds as alternatives to Fe(II) oxidation. This metabolic flexibility (i.e. ability to use a wide range of different substrates) makes it difficult to determine the extent to which anoxygenic phototrophs actively contribute to iron cycling in modern environments where more energetically favorable substrates are also available. In a series of laboratory incubation experiments with model marine and freshwater anoxygenic phototrophs, we demonstrate that the presence of organic co-substrates in particular does not impede Fe(II) oxidation. Indeed, utilization of Fe(II) and organic compounds occurs simultaneously in numerous anoxygenic phototrophs and can even enhance rates of both Fe(II) oxidation and organic consumption. In further *in situ* studies in a seasonally stratified lake in Germany, however, we observe that the presence of organic compounds can act to mask the contribution of anoxygenic phototrophs to Fe(II) oxidation due to the promotion of Fe(III)-reducing bacteria, which lowers measurable Fe(II) oxidation rates via a cryptic iron cycle. Together these results suggest an under-estimation of the role of anoxygenic phototrophs in iron cycling in natural, geochemically complex, environments.

# A new way for microorganisms mediated by minerals to capture solar energy

Lu, A.H.[1]

[1]Beijing Key Laboratory of Mineral Environmental Function, School of Earth and Space Sciences, Peking University, 100871 Beijing, People's Republic of China

Corresponding author: ahlu@pku.edu.cn (Lu A.H.)

---

In nature, semiconducting minerals can be excited by solar photons, resulting in the transition of electrons from the valence band to the conduction band, as well as the formation of photo-holes and photoelectrons [1]. Semiconducting minerals with visible light responsiveness are widely distributed in the euphotic zone of offshore and estuary. The highly active photoelectrons generated by these semiconducting minerals under sunlight can function as an important energy source at the Earth's surface, complementing solar photons and valence electrons. This novel energy source might promote the microbially driven cycling of elements in the euphotic zone of the hydrosphere. Under light irradiation, semiconducting minerals, like goethite, rutile, and sphalerite, have been reported to generate photoelectrons, effectively supporting the growth of chemoautotrophic *Acidithiobacillus ferrooxidans*, heterotrophic Alcaligenes faecalis, and influencing the structure of microbial communities in natural settings. A notable disparity exists in the minimum energy threshold by microorganisms in complex aquatic environments and under the controlled conditions of pure culture systems in the laboratory. This discrepancy is primarily attributed to the capacity of microorganisms in natural environments, belonging to diverse metabolic categories, to maximize energy utilization by establishing syntrophic relationships. Especially in oligotrophic and low-energy aquatic habitats, microorganisms of different species, driven by energy constraints, are compelled to fully harness free energy released during catabolic reactions. Through diverse forms of close cooperation, these microorganisms form a syntrophic relationship with low energy demand and thus become the dominant species in the community. Within a complex system consisted of semiconducting minerals and microorganisms under sunlight, mineral photoelectrons have been demonstrated to enhance the growth of non-photosynthetic microorganisms. The energy of highly active photo-holes produced by semiconducting minerals under sunlight irradiation may also promote the metabolism of non-photosynthetic microorganisms. It has been found that *Shewanella oneidensis* MR-1 generates electrons from lactate metabolism and utilizes them to fill photoexcited holes in hematite under simulated sunlight. The generated photoelectrons from hematite can effectively reduce Cr(VI), resulting in the enhanced reduction efficiency of Cr(VI) and the tolerance of S. *oneidensis* MR-1 to Cr. This study illustrates how electroactive microorganisms and semiconducting minerals can synergistically convert light energy and drive the element cycle.

*References:*

[1] Lu A et al. (2019) Proc Natl Acad Sci 116: 9741-9746

# Geochemical and microbiological reactions controlling siderite in redox active soils

Chen, Z.[1,2], Perez, J.P.H.[1], Trivedi, C.B.[1], Stammeier, J.A.[1], Gislason, S.R.[3] and Benning, L.G.[1,2]

[1]GFZ German Research Center for Geosciences, Telegrafenberg, 14473 Potsdam, Germany

[2]Department of Earth Sciences, Freie Universität Berlin, 12249 Berlin, Germany

[3]Institute of Earth Sciences, University of Iceland, 102 Reykjavik, Iceland

---

A large proportion of global carbon is stored in northern, high-latitude permafrost soils [1]. Such carbon is usually associated with reactive iron minerals known as a 'rusty sink' and these play an important role in the carbon dynamics across many Arctic landscapes [2]. As the global temperature rises and the permafrost thaws, soils are also facing dramatic seasonal water level fluctuations. In Iceland, this leads to more intense chemical weathering of the host basaltic rocks. In the resulting soils, the interplay between iron mineral (trans)formations and organic carbon (OC) decomposition and cycling changes seasonally through waterlogging – a process that is invariably affected also by microbial activity. Studies to date have shown that following such seasonal redox fluctuations, more OC is degraded and released as a result of the recrystallisation of iron (hydr)oxides [3,4]. Among these iron phases, to note is the natural formation of siderite – an iron (II) carbonate – that precipitates from the high contents of dissolved ferrous iron and inorganic carbon in such soils. Siderite has been inferred to be a potential reservoir for $CO_2$ sequestration [5, 6], yet the formation and stability of siderite in these soils is poorly understood.

In order to study the conditions favorable for such siderite formation, we evaluated the chemical, mineralogical and biological variations in a seasonally waterlogged soil profile, characterized by a fluctuating vertical redox gradient. Our bulk and molecular scale results indicate that in the redox transition zone the Fe species, OC composition and microbial diversity were clearly distinct compared to any of the other horizons. Bulk powder X-ray diffraction analyses confirmed the presence of siderite in the redox transition zone. Using various chemical extraction methods, we determined that the total iron content in this zone was about 34 wt.%, which was 2-4 times higher than in all other horizons, and that a higher percentage of low-molecular-weight OC (up to 84%) indicate the larger extent of OC degradation. In addition, we combined bulk infrared spectroscopy and synchrotron radiation X-ray absorption spectroscopy to evaluate the variations, structural changes and interactions in both OC and Fe phases. Finally, by analysing the microbial diversity through 16S rRNA gene sequencing we could infer the relevance of specific microorganisms (e.g., Fe cyclers and fermentative bacteria) and their potential role in carbon and iron cycling in our soil profile. Taken together, our results provide, for the first time, a new perspective on the formation of natural siderite forming in soils under seasonal redox fluctuation. This is important because understanding how such seasonal processes affect iron and carbon cycling is critical for predicting greenhouse gas emissions from sub-Arctic soils in a future warming climate.

*References:*

[1] Kramer M and Chadwick O (2018) Nat Clim Change 8:1104–1108
[2] Lalonde K et al. (2012) Nature 483: 198-200
[3] Bhattacharyya A et al. (2018) Environ Sci Techno 52: 14129–14139
[4] Dong H et al. (2023) Nat Rev Earth Environ 4: 659-673
[5] Gislason S et al. (2010) Int J Greenhouse Gas Control 4: 537-545
[6] Linke T et al. (2024) Geochim Cosmochim Acta 370: 66-77

# On the occurrence of Carboniferous MnFe-oxide stromatolites from the Merdani Formation (Merzouga, Morocco)

Bernardini, S.[1], Abbassi, A.[1], Della Ventura, G.[1], Cipollari, P.[1], Boukili, B.[2], Cavallo, A.[3], Sodo, A.[1], Cosentino, D.[1]

[1]Department of Sciences, University of Roma Tre, Rome, Italy, simone.bernardini@uniroma3.it

[2]Department of Earth Sciences, University Mohammed V, Rabat, Morocco

[3]CERTEMA S.c.a.r.l., Cinigiano, Italy

---

Understanding the origin and the evolution of life on Earth and other planets is of paramount interest to humanity. The unambiguous evidence for the earliest appearance of life on Earth (~3.4 Ga) is found in stromatolites from the Pilbara Craton (Australia). Stromatolites form from the interaction between benthic microbial communities and detrital or chemical sediments; thus, they are precious archives for mineral-microbe interactions and environmental conditions through geological time.

Mn and Fe are the most abundant and biologically-relevant metal species in the Universe. A fundamental property of these metals is their high sensitivity to redox conditions and microbial activity. For instance, the solubility of Mn is much higher than that of Fe for $6 < pH < 8$, at $Eh < 600$ mV. Therefore, the redox-driven separation between these two metals can be used to investigate the evolution of seawater conditions over geological time. Moreover, bacteria and fungi may catalyze the formation of disordered and poorly crystalline Mn-oxides with a high average Mn oxidation state (above 3.5) [1]. Therefore, MnFe-bearing stromatolites have the potential to record both biological processes and environmental (redox) conditions and thus allow reconstructing past microbial habitats. While MnFe-carbonate stromatolites have been described from several localities around the world (*e.g.,* Southern Brazil and China [2,3], among others) marine MnFe-oxide stromatolites are extremely rare in the geological record (*e.g.,* Precambrian rocks from Botswana [4]).

Here we describe for the first time the occurrence of Middle Mississippian MnFe-oxide stromatolites from the Merdani Formation in the area of Merzouga (Morocco). According to literature [5], these sedimentary rocks mark the late Visean transgression and the development of a shallow-water marine environment where the formation of ferruginous crusts have been observed; these mineralizations have been studied here. The samples were analysed by combining Optical Microscopy (OM), Field Emission Scanning Electron Microscopy coupled with an X-ray Wavelength Dispersive System (FE-SEM-WDS), Powder X-Ray Diffraction, Infra-Red and Raman spectroscopies, and Inductively Coupled Plasma Mass Spectrometry. We show that these mineralizations consist of poorly crystalline birnessite and todorokite, two oxides recognized to be the primary products of microbially-mediated Mn oxidation [1]. OM, FE-SEM-WDS and Raman imaging shows that they preserve the morphological and chemical imprint of microbial populations: µm-sized cell-shaped spheroidal structures, often filled by clay minerals, resembling the cell envelopes are embedded in a filamentous matrix, which constitutes the scaffold of the whole mineralization. Our findings thus show that Mn oxides have the great potential to preserve their biological imprint over geological time (at least up to ~300 Ma), a consideration that has important implications also in investigating extreme environments or extraterrestrial life.

*References:*

[1] Tebo BM et al. (2004) Annu. Rev. Earth Planet. Sci. 32, 287–328

[2] Callefo F et al. (2022) Front. Earth Sci. 10, 804194

[3] Zhang Y et al. (2021) J. Palaeogeogr. 10, 1–26

[4] Litherland M and Malan SP (1973). J. geol. Soc. 29, 543–544

[5] Benharref M et al. (2014) Notes et memoires du service geologique du Maroc, 553 bis

# Geochemical and Microbiological Contribution to Speciation and Mineralogy of Antimony in Subsurface Environment

Kwon, M.J.[1], Zhang, Y.[1], Jang Y., Park, S.[1], Boyanov, M.I.[2,3], O'Loughlin E.J.[2], and Kenneth, K.M.[2]

[1]Department of Earth and Environmental Sciences, Korea University, Seoul, S. Korea, manjaekwon@korea.ac.kr

[2]Biosciences Division, Argonne National Laboratory, Lemont, IL USA

[3]Bulgarian Academy of Sciences, Institute of Chemical Engineering, Sofia, Bulgaria

---

The environmental behavior of antimony (Sb) has recently received greater attention due to the increasing global use of Sb in a wide range of industrial applications (e.g., flame retardants, batteries, catalysts, alloys) [1]. Elevated amounts of Sb have been found globally in many areas including mine, refinery, and military shooting range sites. The mobility and toxicity of Sb largely depend on its speciation, which is strongly influenced by its oxidation state, commonly presented as Sb(V) or Sb(III) in natural environments. It is generally believed that Sb(III) is more toxic than Sb(V), but Sb(V) can be more mobile in anoxic conditions. However, Sb(V) can be immobilized through adsorption by host phases such as Fe(III) oxides, which are later subjected to microbial Fe(III) reduction under anaerobic conditions. Despite these general views, our understanding on Sb speciation mediated by complex geochemical and microbiological processes in subsurface environments is still lacking. Therefore, it is crucial to study the biogeochemical processes impacting Sb redox transformations to understand the behavior of Sb in natural environments.

In this presentation, we will discuss our recent findings based on laboratory observations using field samples, as well as microcosm reactor studies: 1) Anaerobic microbial Sb(V) reduction by Sb-respiring pure strain YZ-1 isolated from Sb-contaminated soil [2], 2) Distribution and speciation of Sb and toxic metal(loid)s near an antimony refinery and their effects on indigenous microorganisms [3], 3) Sb speciation and mineralogy in soil near Sb mine and military shooting range sites, 4) Leachability or solubility of Sb from poorly crystalline Sb(V)-coprecipitated ferrihydrite and the more crystalline tripuhyite ($FeSbO_4$) during microbial Fe(III) and/or Sb(V) reduction, and 5) Effects of phosphate on the fate of Sb(V) adsorbed onto ferrihydrite under Fe(III)-reducing and/or sulfidogenic environment. These studies provide fundamental and critical information regarding complex Sb biogeochemistry for the improved management of Sb in natural and engineered systems.

*References:*

[1] Zhang et al. (2022) J Hazard Mat 431:128607
[2] Zhang et al. (2024) J Hazard Mat 465:133240
[3] Park et al. (2021) J Hazard Mat 403:123625

## Microbial interactions with nuclear waste glass

Thorpe, C.L.[1], Crawford, R.[1], Manifold, G.[1], Boothman, C.[2], Morris, K.[2], Lloyd, J.R.[2], Corkhill, C.L.[3] and Hand, R.J.[1]

[1]Immobilization Science Laboratory, Department of Materials Science and Engineering, University of Sheffield. Sir Robert Hadfield Building, Mappin Street, Sheffield, S1 3JD. clare.thorpe@sheffield.ac.uk.
[2] Williamson Research Centre, Department of Earth and Environmental Science, University of Manchester, Oxford Road, M13 9QQ.
[3]School of Earth Science, University of Bristol, Bristol, BS8 1RL.

---

Vitrification is used in many countries to immobilise high activity waste liquors and is increasingly considered for low and intermediate activity waste streams [1]. Radioactive elements are chemically incorporated in the glass structure and, therefore, will be released at the same rate that the glass dissolves meaning understanding the long-term behaviour of glassy material is vital when constructing the safety case for its storage and eventual subsurface disposal. Most studies to understand glass dissolution rates and mechanisms have been conducted at elevated temperatures and under sterile conditions [1]. However, as microbes have been found in the deepest subsurface environments explored their presence in every geological disposal scenario must be assumed.

It is well known that microorganisms can affect the rate of silicate mineral and silicate glass dissolution [2,3] with the majority of studies showing enhanced dissolution rates in the presence of active bacteria [4,5] whilst few studies infer that biofilm growth and associated bio-mineralization may be protective [6]. Vitrified radioactive waste can contain many elements desirable to microorganisms such as P and redox active metals such as Fe, Cr and U. Here, both laboratory and field studies combine to offer insight into glass corrosion in the presence of subsurface microorganisms and the fate of radionuclides released. Under laboratory conditions, the dissolution of complex and simple borosilicate glasses (surrogates vitrified waste glasses) containing P and Fe stimulated and altered the nearby microbial community. Fe(III) was reduced at the glass surface changing the structure and mineralogy of glass alteration layers. The influence of microbial respiration on the dissolution rate was dependent on both the glass composition and the geochemistry of the surrounding solution. Meanwhile ongoing field experiment aim to identify and characterise the microbial communities that colonise the interface between nuclear waste type glasses and their environment to ascertain their potential role in near surface and deep geological disposal facilities.

*References:*

[1] Thorpe CL et al. (2021) NPJ Mat Degrad
[2] Bennett PC et al. (2001) Geomicro J 18:1: 3-19.
[3] Weaver JL et al (2021) NPJ Mat Degrad 5:11.
[4] Buss HL et al. (2007) Chem Geol 240:326-342
[5] Stranghoener M et al. (2018) Frontiers in Microbiol 9: 1252
[6] Aouad G et al (2006) AGU Fall Meeting 2006

## Bi-Te-S biomineralization in the Volyn biota (Ukraine)

Franz, G.[1], Wirth, R.[2], Schreiber, A.[2], Khomenko, V.[3]

[1]Institut für Angew. Geowissenschaften, Technische Universität, Berlin, Germany; gefra548@gmail.com

[2]Deutsches GeoForschungsZentrum GFZ, Telegrafenberg 14473 Potsdam, Germany

[3]Institute of Geochemistry, Mineralogy and Ore Formation, Kyiv, Ukraine

---

The Volyn biota represent an ancient subsurface lithautotrophic microecosystem [1]. The fossils are exceptionally well preserved in 3D due to their occurrence in cavities of pegmatites of the 1.8-1.7 Ga old Korosten Pluton in NW Ukraine, which experienced no diagenesis, metamorphism or deformation. The fossilization occurred during influx of HF-bearing fluids from the granitic source into the miarolitic cavities, producing a µm-wide rim of Al-silicate minerals. Some of the fossils were interpreted as biofilms, others show similarities to filamentous fungi-like organisms, supported by the presence of chitosan, others are interpreted as methanogenic organisms.

Nanometer-sized particles, interpreted as biominaralisation, were found in three texturally different positions in filamentous and bulbous fossils: (i) randomly oriented, (ii) concentrated near a central channel in filamentous objects, and (iii) aligned in groups of several crystals.

Randomly oriented nano-inclusions with a size of approximately 50 to 100 nm occur in the central part of the fossils, excluding their origin as post-mortem inclusions. Their composition is variable in the samples, but all are characterized by Bi-Te-S, close to Bi(S,Te) or $Bi_4(S,Te)_3$.

In one object, they occur in a central channel, characteristic for some of the filamentous fossils. These nanoparticles are up to approximately 200 nm large, concentrated in aggregates, and the variable composition is Bi-Cu-Te-S (Fe, Si, Pb). Electron diffraction patterns of these mosaic crystals indicate an orthorhombic phase a = 7.70 Å, b = 10.4 Å, c = 6.75 Å, consistent with $Cu_3BiS_3$.

In a bulbous fossil object, the nano-sized biominerals are arranged in groups of several crystals. Their composition is dominantly Bi-Te-Pb. These crystals are connected by a filament of amorphous material, a few nanometer wide, and similar filamentous extensions from the nanocrystals were observed. These features indicate a possible function of the biominerals, whereas the randomly oriented particles might be the result of detoxification of Te.

*References:*

[1] Franz et al. (2022) BioGeosc 20:1901-1924

## Conundrum of anhydrite formation at surface conditions

Wehmann, N.[1], Lenting, C.[1], Stawski, T.M.[2] , Agudo Jácome, L.[2], Heim, C.[1], and Jahn, S.[1]

[1]Institut für Geologie und Mineralogie, Universität zu Köln, Zülpicher Straße 49b, 50674 Köln, Germany, c.lenting@uni-koeln.de

[2]Bundesanstalt für Materialforschung und -prüfung (BAM), Department for Materials Engineering, Unter den Eichen 87, 12205 Berlin, Germany

---

Three calcium sulfates, gypsum ($CaSO_4 \cdot 2H_2O$), bassanite ($CaSO_4 \cdot 0.5H_2O$), and anhydrite ($CaSO_4$), comprise the essential evaporite minerals for the evolution of hyper-arid surface environments on Earth and Mars [1,2]. However, the formation mechanisms for these minerals, specifically for anhydrite at surface conditions, are not well understood besides their crucial role for the interpretation of the paleo-environmental conditions during landscape formation.

To date, there exists no model that can reliably predict anhydrite formation at earth's surface conditions. While thermodynamics favour its formation, it is hardly achieved on laboratory time scales at conditions fitting either the Atacama Desert on Earth, or the surface of Mars.
Considering recent transmission election analyses [3] advocating for a complex, non-classical nucleation mechanism for all calcium sulphates, we present an analysis of natural samples from different facies of the Atacama Desert, i.e. aeolian deposits, (sub-)surface nodules and selenites, to identify key features that promote the nucleation and growth of anhydrite under planetary surface conditions.
Additionally, alternative pathways for anhydrite nucleation facilitated by metabolic products of biological organisms (e.g. fungi, lichen, cyanobacteria) found in soils of the Atacama [4] will be discussed.

*References:*

[1] Voigt et al. (2020) Glob Planet Change 148:103077
[2] Vaniman et al. (2018) Am Min 103(7):1011–1020
[3] Stawski et al. (2016) J Phys Chem C 124(15):8411-8422
[4] Knief et al. (2020) Glob Planet Change 148:103077

## Nanoscale biosignatures in native copper from the Wadi Tayin dunite, Oman

Tenuta, S.[1,2], Evans, K.A.[1], Reddy, S.R.[1,2], Rickard, W.D.A.[2], Saxey, D.W.[2]

[1] School of Earth and Planetary Sciences, Curtin University, GPO Box U1985, Perth, WA 6845, Australia, stefano.tenuta@postgrad.curtin.edu.au

[2] Geoscience Atom Probe Facility, John de Laeter Centre, Curtin University, GPO Box U1985, Perth, WA 6845, Australia

---

Hydration of ultramafic rocks (serpentinization) commonly oxidises iron to form ferric iron in magnetite and serpentine, and produces $H_2$(aq), and ultra-reducing conditions [1]. The $H_2$(aq) can react with dissolved $CO_2$ or carbonate to form organic acids [2]. Based on these observations, it has been proposed that serpentinization may have promoted the initiation of life [3], but many details, including the role of metal catalysts, remain unclear. We used Atom Probe Tomography (APT) and Time of Flight-Secondary Ion Mass Spectroscopy (ToF-SIMS), to provide nanoscale reconstructions of element distribution and investigate the spatial association between metals and carbon-bearing compounds in a sample from the Wadi Tayin ophiolite, Oman.

The ToF-SIMS ion maps show that CN-bearing complexes are enriched within native-Cu and precursor partially reacted chalcopyrite. APT analyses reveal Ag segregation along grain boundaries in native-Cu. These observations provide new insights into (i) the nanoscale nitrogen cycle; the previously undocumented association of Cu, partially reacted chalcopyrite, and CN-compounds suggests that N may be involved in redox processes during serpentinization. (ii) metal redistribution during potentially bio-mediated serpentinization-related alloy formation; Ag is not soluble in Cu metal at temperatures compatible with the stability field of lizardite [4], so the Ag-rich interface may record a biological influence. (iii) the details of redox reactions during serpentinization; the association of Cu, partially reacted chalcopyrite, and CN-compounds suggests that Cu originally hosted by chalcopyrite may have acted as an electron acceptor for biotic or abiotic processes that formed the CN-compounds. Our observations document, to the best of our knowledge, a previously unreported association between Cu and organic matter and provide insights into the redox reactions that may have initiated life on Earth.

*References*

[1] Alt JC and Shanks WCI (1998) J Geophys Res 103: 9917–9929

[2] Templeton A et al. (2021) J Geophys Res 126

[3] Cardace D and Hoehler TM (2009) Northeast Nat 16: 272–294

[4] Evans BW (2004) Int. Geol. Rev. 46(6): 479–506

## Metabolically-versatile Hg methylators: their implications and origins

Moreau, J.W.[1]; Lin, H.[2]; Gionfriddo, C.M.[3]; Moody, E.R.R.[4]; and Williams, T.A.[5]

[1]School of Geographical and Earth Sciences, University of Glasgow, UK

[2]Centre for Microbiome Research, Queensland University of Technology, AUS

[3]Centre for Freshwater Ecosystems, LaTrobe University, AUS

[4]School of Earth Sciences, University of Bristol, UK

[5]School of Biological Sciences, University of Bristol, UK

---

Recent work has shown that not only anaerobes can methylate mercury. These studies illustrate the role of metabolically versatile microbes across a range of redox potentials [1-4]. If mercury is being appreciably methylated under low oxygen (but not anoxic) conditions at the global scale, then we need to consider the implications for 1) greater complexity in biogeochemical mercury cycling than previously assessed, 2) links between Hg cycling and the redox speciation of other elements (especially nitrogen and sulphur), and 3) potential effects of climate change on Hg bioavailability. Here we present metagenomic and geochemical lines of evidence for metabolic versatility among marine mercury methylators, and consider the links between Hg and other key elemental cycles that may be impacted by climate change. For example, production of methylmercury in seawater would likely be enhanced by organic matter loading but also by amplification of marine redox gradients. We also consider terrestrial Hg methylation and the potential for climate change to impact Hg mobility and MeHg formation in wetlands, either directly or indirectly.

We conclude with analysis of the evolution of this mysterious metabolic function (Hg methylation), and propose a testable hypothesis for its origin. We compare the evolution of genes for Hg methylation and demethylation, to arrive at a putative explanation for the currently observed and seemingly random phylogenetic distribution of both capabilities.

*References:*

[1] Gionfriddo et al. (2016), *Nature microbiology* 1, 1-12.
[2] McDaniel et al. (2020), *Msystems* 5, e00299-20.
[3] Lin et al. (2021), *The ISME journal* 15, 1810-1825.
[4] Vigneron et al. (2021), *npj Biofilms and Microbiomes* 7, 83.

## Deciphering functional group controls on $CaCO_3$ nucleation using sulfated glycomaterials and insights for natural systems

Dove, P.M.[1,2,3], Knight, B.M.[1,2], Mondal, R.[2], Vaissier Welborn, V.[2], Gallagher, C.M.B.[2], Schulz, M.[2], Edgar, K.J.[2,4], and De Yoreo, J.J.[5,6]

[1] Department of Geosciences, Virginia Tech, Blacksburg, VA 24061, USA

[2] Department of Chemistry, Virginia Tech, Blacksburg, VA 24061, USA

[3] Department of Materials Science and Engineering, Virginia Tech, Blacksburg, VA 24061, USA

[4] Department of Sustainable Biomaterials, Macromolecules Innovation Institute, GlycoMIP Materials Innovation Platform, Virginia Tech, Blacksburg, VA 24061, USA

[5] Physical Sciences Division, Physical and Computational Sciences Directorate, Pacific Northwest National Laboratory, Richland, WA 99352 USA

[6] Department of Materials Science and Engineering, University of Washington, Seattle, WA 98195, USA

---

Advances in structural biology show that polysaccharides (e.g., chitin) and negatively charged proteoglycans (due to carboxyl, sulfate, and phosphate groups) are widely associated with animal and microbial life. These glycomaterials exhibit remarkable structural diversity that varies from simple monosaccharides to highly derivatized forms as well as extensively branched glycoproteins. Although acidic proteins have received decades of attention from the biomineralization community, glycomaterials found in the organic matrices at sites of calcification likely play greater roles than currently recognized.

Recent studies of biological crystallization reveal that sulfated glycomaterials, including heparin-related macromolecules, are widely associated with sites of biological crystallization in phylogenetically diverse animals. Heparin is the most charge-dense of known biomolecules and provides an excellent model for probing sulfate activity in biological and synthetic settings. However, there is little understanding of how heparin and the many other sulfated polysaccharides influence mineralization beyond qualitative observations [1,2]. Instead, carboxyl groups have been the focus.

Using advances in biopolymer synthesis, we test the hypothesis that sulfate density and position can be tuned to regulate the thermodynamics and kinetics of $CaCO_3$ nucleation. We find the rate of $CaCO_3$ nucleation is regulated by a systematic dependence on sulfate density that is determined by the interfacial energy to calcite crystallization ($\gamma_{cal}$ ). The measurements show a general trend whereby the influence of sulfate groups on nucleation is equivalent to that of carboxyls. We predict this is due to functional groups imparting similar effects on water structure at the polysaccharide-solution interface during crystallization. MD simulations and isothermal calorimetry measurements support this explanation by showing that $Ca^{2+}$-sulfate-polysaccharide interactions are solvent-separated and driven by changes in water structure, respectively. The findings reiterate the importance of establishing solvation properties and short-range interactions at macromolecule-solution interfaces in natural systems.

*References:*

[1] Knight BM et al. (2023) Biomacromolecules 24: 1078 - 1102
[2] Knight BM et al. (submitted)

## Determination of Great Barrier Reef Ca–C–O mineralogy and trace element systematics using synchrotron X-ray techniques

Missen, O.P.[1], Mills, S.J.[2], Villalobos-Portillo, E.E.[3] and Castillo-Michel, H.[4]

[1]Centre for Ore Deposit and Earth Sciences, University of Tasmania, Hobart, Tas. 7001, Australia. Email: owen.missen@utas.edu.au

[2]iRocks Fine Minerals and Crystals, PO Box 830460, Richardson, TX 75083, USA

[3]ALBA Synchrotron, Cerdanyola del Valles, Barcelona E-08290, Spain

[4]European Synchrotron Radiation Facility, Grenoble, Cedex 9, F-38043 France

---

The Great Barrier Reef (GBR), found off Australia's northeast coast, is the biggest and most complex reef ecosystem in the world. It represents 10 percent of the world's coral reef ecosystems by area. In this study, synchrotron micro X-ray fluorescence microscopy (µXFM) and micro X-ray absorption near-edge spectroscopy (µXANES) were performed at the ID21 beamline of the European Synchrotron Radiation Facility [1] to analyse trace element and mineralogical distributions in GBR corals [2-3]. Due to warmer seas leading to coral bleaching and the impact of human pollution from mining and agriculture, more than half of the coral in the GBR has been lost. Understanding the changes in mineral structure of the corals during the bleaching process is essential to find solutions against it.

This study is focused on the correlation between the mineralogical and geochemical characteristics of sediments and (mineralised) corals from the Low Isles reef near Port Douglas, Queensland. By characterizing the minerals present in the corals, we show how susceptible certain corals are to acidification from rising sea temperatures. Some oxalates such as the rare mineral weddellite $[Ca(C_2O_4)\cdot(2.5\text{-}x)H_2O]$ are less resilient to change than aragonite or high-Mg calcite. µXFM synchrotron mapping helped us to identify the distribution and concentration of elements from Si to Ca which were used as target elements to see differences between the Ca K-edge µXANES signals. These differences in XANES signals correspond to varying oxalate, carbonate (and phosphate) mineralogy, allowing us to use standards to determine whether spectra on given mineralised zones were formed by carbonates, oxalates or a mixture of the two. Differences between trace phosphorus and potassium hot-spots from bleached and non-bleached corals show that contamination, likely from fertilizer run-off from land-based agriculture, results in changes to the trace element signatures in coral.

*References:*

[1] Cotte M et al. (2017) J Anal Atom Spec 32: 477-493.
[2] Mills SJ et al. (2021) ESRF Dataset 10.15151/ESRF-ES-555094780
[3] Mills SJ et al. (2022) ESRF Dataset 10.15151/ESRF-ES-661815595

## Durability assessment of microbially-induced calcite precipitation

La Bella, M.[1], Noiriel, C.[2], Schroer, L.[3], Cnudde, V.[3,4] and Naillon, A.[1]

[1] Université Grenoble Alpes, CNRS, Grenoble INP, 3SR, F-38000, Grenoble, France, michela.labella@3sr-grenoble.fr

[2]Géosciences Environnement Toulouse, Observatoire Midi-Pyrénées, Universite Paul Sabatier, CNRS, IRD, CNES, Universite de Toulouse, 31400 Toulouse, France

[3]Department of Geology, Ghent University Krijgslaan 281/s8, 9000, Ghent, Belgium

[4]Department of Earth Sciences, Utrecht University, Princetonlaan 8a, 3584 CB, Utrech, Netherlands

---

Microbially-induced calcite precipitation (MICP) is a technique that exploits the ureolytic activity of specific bacteria (i.e. *Sporosarcina Pasteurii*) to create the conditions to precipitate $CaCO_3$ . MICP can be used to transform non-cohesive granular materials into cohesive media, creating $CaCO_3$ crystal bridges between the grains [1]. This application of MICP presents the advantage of being more environmentally friendly than the commonly used soil-reinforcement techniques. The mechanical properties of biocemented sand obtained through MICP have been extensively characterized at the macroscale and microscale. X-ray microtomography measurements and triaxial tests on biocemented samples permitted to understand that their macroscopic mechanical response mostly depends on the micromechanical properties of the cohesive contacts [2] [3]. In the optic of engineering applications of MICP, the durability of biocementation becomes a key point. One of the biggest concerns is represented by the exposure to weakly acid environments such as superficial and underground waters that may trigger the dissolution of $CaCO_3$ crystals. A first attempt to evaluate the durability of MICP under the effect of acidic solutions was done by exposing specimens of biocemented sand to acidic solutions (pH 6.6) and characterizing them *post-mortem* with triaxial tests and imaging techniques [4]. This permitted to demonstrate that the dissolution reduces the size of $CaCO_3$ crystals resulting in the damage of the contacts between the sand grains, and consequently decreases the strength of the material.

We have performed *in situ* X-ray synchrotron and laboratory µ-tomography measurements on biocemented sand columns obtained by MICP to characterize the $CaCO_3$ dissolution process in order to understand the evolution of the mechanical properties. Our multiscale approach, from 7µm voxel size down to 0.65µm, aimed at:

identify the possible presence of preferential $CaCO_3$ dissolution paths that would create inhomogeneities throughout the sample;

evaluate the kinetics of dissolution of bio-mediated $CaCO_3$ at different acidic pH values and compute the evolution of the cemented contact surface area responsible for the mechanical reinforcement of granular materials.

Thanks to this approach it was possible to observe the presence of preferential dissolution paths along the biocemented sand columns, especially for lower pHs and higher flow rates, that could be linked to the variation of permeability throughout the sample. Moreover, the dissolution of the bio-mediated $CaCO_3$ occurred faster compared to the previously calculated dissolution rates of geological $CaCO_3$, suggesting different reactivities.

These findings will be used successively as input parameters in discrete element models (DEM) developed by our team [5] to predict the evolution of the mechanical properties of biocemented sand in the long term.

*References:*

[1] Terzis D and Laloui L. (2019) Geomech Energy Environ 19: 100-116
[2] Dadda A et al. (2019) Int J Numer Anal Methods Geomech 43: 568-577
[3] Sarkis M et al. (2023) Acta Geotech 19: 1555-1570
[4] Geindreau C et al. (2022) Int J Geomech 22
[5] Sarkis et al. (2022) Comput Geotech 149: 104860

## Copper oxidation zone at Ľubietová (Slovakia) as a combination of ore weathering and biologically-induced mineralization

Majzlan, J.M.[1], Chovan, M.[2], Števko, M.[3], Jeleň, S.[3], Milovská, S.[3] and Milovský, R.[3]

[1]Institute of Geosciences, University of Jena, Germany

[2]Department of Mineralogy, Petrology, and Economic Geology, Comenius University, Bratislava, Slovakia

[3]Institute of Earth Sciences, Slovak Academy of Sciences, Bratislava and Banská Bystrica, Slovakia

---

The oxidation zone in Ľubietová is famous for its large crystals of libethenite and pseudomalachite (copper phosphates) and malachite. The source of copper is disseminated chalcopyrite in Permian meta-arcoses, localized in silicified tectonic zones. The reason as to why this oxidation zone is so exceptionally developed in comparison to other, geographically near occurrences, was studied in this work.

Hydrogen isotopes in malachite and libethenite showed that the secondary minerals formed from meteoric fluids at temperatures comparable to surface temperatures. These data exclude contribution of hydrothermal fluid for the formation of the oxidation zone, which could have been anticipated on the basis of the exceptional development of the crystals of secondary minerals. Carbon isotopes in malachite ($\delta^{13}C_{PDB}$ –19 to –17 ‰) document input of biologically-derived carbon from the surface, perhaps from the soils.

Bulk geochemical data showed that the marginal portions of the oxidation zone are enriched respective to the surrounding rocks in phosphate only by a factor of three. Therefore, phosphate could have been supplied by dissolution of rock forming minerals such as apatite from the host rocks. The oxygen isotopes in the apatite are light ($\delta^{18}O$ –0.6 to +3.2 ‰), comparable to isotopes in high grade metamorphic or igneous rocks. On the other hand, the oxygen isotopes in the secondary phosphate minerals are distinctly heavier (+7.0 to +15.5 ‰), suggesting that they were formed from biologically derived phosphate that interacted with meteoric water.

The studied oxidation zone formed during the times of intense weathering and tectonic quiescence. Geological evidence (kaolin crusts) witnesses that the oxidation zone was preserved by burial under thick strata of Neogene volcanic rocks. Biological activity was a substantial contributor to this oxidation zone.

## Bioremediation: learning from bio-geo processes in extreme environments

Onnis, P.[1*], Kirk, R.[2], Rehmanji M.[2], Falagan, C.[3], Ramos, V.[2], Jennings, E.[2], Newsome, L[2], Gandy, C.[4], Jarvis, A.[4], Rollinson, G.[2], Medas., D.[1], De Giudici G.[1], Hudson-Edwards, K.A.[2]

[1*] Department of Chemical and Geological Sciences, University of Cagliari, Monserrato, Italy.

patrizia.onnis@unica.it

[2] Environment and Sustainability Institute and Camborne School of Mines, University of Exeter, Penryn Campus, United Kingdom.

[3] School of Biological Sciences, King Henry Building, King Henry 1st St., University of Portsmouth, Portsmouth, United Kingdom.

[4] School of Engineering, Newcastle University, Newcastle Upon Tyne, United Kingdom.

---

Worldwide, legacy mine wastes can pose a hazard to human health and the ecosystem. Historical practices of waste disposal did not take the potential dispersion of contaminants and the generation of extreme environments into account. These practices caused bio-geo interactions with extreme microorganism survival and enhanced changes to the environments. These key bio-geo interactions can unlock bio-mining and bio-accumulation applications for environmental monitoring and remediation and boost bio-applications to critical raw material exploitation. Although research is on the right path to unravel such knowledge, much is yet to be explored. This contribution will present learning outcomes from extreme environments generated by the leaching of coal mining wastes at Seaham Beach in the UK. Beach sediments, composed mostly of pyrite, jarosite, and traces of alumina-silicates and dolomite, showed ecotoxic metal(loid) concentrations above environmental guideline values (As 220 mg/kg, Pb 150 mg/kg, Zn 260 mg/kg, and V 350 mg/kg). Acidic water pools (pH ~ 3) covered the beach in contact with a dolostone outcrop and hosted average concentrations of the mentioned metal(loid)s at <0.2 mg/L, with the exception of V, which reached 1 mg/L. Ongoing investigations suggest the presence of oxidative bacteria and fungi hyphae. Scanning electronic microscopy on minerals and biofilms, highlighted the interaction of roots with dolomite microscale crystals and of potential bacterial cells within jarosite-like phases. Open questions are the role of the microorganisms in pyrite oxidation kinetics, the mechanisms of formation of jarosite, and the possibility of pH buffering by dolomite observed at a macroscale (outcrop) and in the fungi hyphae. Notable is the capacity of the microorganisms to adapt to such extreme environments and their potential influence on mineral kinetic through biomineralisation processes.

## Skeletal disorder in laying hens: a study at macro and microscale of hen bone structure and composition

Cappelli, C.[1], Rodríguez-Navarro, A. B.[1], Álvarez-Lloret, P.[2], Enrich, T.[1], Duclos, M. J.[3] and Gautron J.[3]

[1] Departamento de Mineralogía y Petrología, Universidad de Granada, Granada, Spain, chiaracappelli@ugr.es

[2] Departamento de Geología, Universidad de Oviedo, Oviedo, Spain

[3] INRAE, Université de Tours, BOA, Nouzilly, France

---

The regulation of bone mineral formation and dissolution in vertebrates is extremely important to maintain the functionality of bone as a source of Ca and P essential for many cellular processes and the mineralization of other tissues [1]. Different bone pathologies (e.g., osteoporosis, osteogenesis imperfecta) result from the unbalance between bone formation and resorption rates (i.e., bone remodelling alteration). In this context, skeletal disorders in laying hens are a major concern for the egg industry [2]. The remodelling of hen bones is coupled with the daily mobilization of Ca to form eggshells, involving the displacement of approximately 2 grams of this element each day (equivalent to 10% of total body calcium) [3]. Despite the comprehensive understanding of the Ca cycle during eggshell mineralization, there remains insufficient information regarding the impact of composition, structural organization, and the interaction between the bone mineral phase and the organic matrix on the dissolution/precipitation processes and the mechanical properties of chicken bones.
The first step to understand the bone /eggshell (de)mineralization coupled process is to investigate the structural and compositional properties of bones during hen laying cycle. To this end, a systematic study of the properties of hen bones from the macro to the microscopic scale has been performed on tibiae samples collected at relevant stages over an extended production period (90 weeks). These preliminary data are crucial to reveal possible factors influencing bone dissolution and will help to perform targeted experiments to provide insights into the mechanisms leading to the decrease of bone quality. These findings have important implications for the egg industry, which is seeking increasingly sustainable production. Additionally, these results hold value in terms of advancing techniques and methodologies for investigating biominerals.

This study was supported by the DSM Nutritional Products France SAS and DSM nutritional products Europe, research contract C9371-A2/32001198/02, and the Marie Skłodowska-Curie Actions – Postdoctoral Fellowship, grant 101064255.

*References:*

[1] Seeman E and Delmas P D (2006) NEJM 354(21): 2250-2261
[2] Rodriguez-Navarro A B et al. (2018) J Struct Biol 201(1): 36-45
[3] Gautron J et al. (2021) BMC Mol Cell Biol, 22(1): 11

## Heavy Metal Adsorption from Mining Tailings Leachate Using Shell-Based Adsorbent: Characterization and Kinetic/Isotherm Studies

Fernández-González, A.[1], Ayala-Espina J.[2] and Fernández-Pérez, B.[2]

[1]Department of Geology, University of Oviesdo. C/ Jesus Arias de Velasco s/n 33005 Oviedo (Spain) mafernandez@uniovi.es

[2]Department of Materials Science andMetallurgical Engineering, University of Oviedo, 33004 Oviedo (Spain)

---

This research aims to identify the ideal conditions for utilizing waste mollusk shells (WS) in extracting heavy metals from three leachates originating from mining and metallurgical processes. Initially, the study examines the impact of various parameters including pH, contact duration, initial metal concentration, adsorbent quantity, and the co-presence of ions on the adsorption of $Cu^{2+}$, $Cd^{2+}$, $Zn^{2+}$, and $Ni^{2+}$ in synthetic solutions.

The uptake of metals was observed to correlate with the initial pH of the solution, with removal efficiency increasing as pH levels rose, reaching peak affinity within the range of pH 5–6. Additionally, greater removal efficiency was observed at lower metal concentrations compared to higher concentrations. Competitive adsorption experiments with bimetallic solutions revealed that the sorbent's adsorption capacity was limited in the presence of other ions, resulting in suppressed uptake of heavy metals compared to individual adsorption scenarios.

Among the metals studied, $Cu^{2+}$ demonstrated the highest inhibition on the removal of $Cd^{2+}$, $Zn^{2+}$, and $Ni^{2+}$. The Langmuir isotherm was found to be the most suitable model for describing the experimental data for $Cu^{2+}$, $Cd^{2+}$, and $Zn^{2+}$, whereas the Freundlich isotherm provided the best fit for $Ni^{2+}$. The data indicated maximum adsorption capacities ($a_{max}$) of 526.32 mg/g for $Zn^{2+}$, 555.56 mg/g for $Cd^{2+}$, and 769.23 mg/g for $Cu^{2+}$. Sorption kinetics data were best represented by the pseudo-second-order kinetic model.

The results obtained in the tests with three mining and metallurgical leachates showed that WS were effective in simultaneously removing several heavy metals ions such as Cu, Ni, Zn, Cd, Ni, As and Se.

# High concentrations of $Mg^{2+}$ decelerates the abiotic decomposition of ATP at elevated temperatures

Moeller, C.[1], Testemale, D.[2], Kokh, M.[1,3], Schmidt, C.[4], Guyot, F.[5], and Wilke, M.[1]

[1]Institut für Geowissenschaften, Universität Potsdam, Karl-Liebknecht-Straße 24/25, 14476 Potsdam, Ger.

[2]Néel Institute, Univ. Grenoble Alpes, CNRS 38000 Grenoble, Fr.

[3]Institut für Mineralogie, Universität Münster, Corrensstraße 24, 48149 Münster, Ger.

[4]Helmholtz-Zentrum Potsdam, Deutsches GeoForschungsZentrum GFZ, Telegrafenberg, 14473 Potsdam, Ger.

[5]IMPMC Muséum National d'Histoire Naturelle, 4 place Jussieu, 75005 Paris, Fr.

---

Extremophiles, microorganisms that thrive under extreme physical and chemical conditions have expanded our understanding of the potential for life beyond known boundaries. Diverse biotas are growing for example in hot springs, deep oceanic sediments, hyperacidic/hypersaline lakes, or in hydrothermal vent systems on the ocean floor [1]. The current temperature and pressure thresholds for life were set by studying two cultivated strains of archaea isolated from ocean floor hydrothermal vents. *Methanopyrus Kandleri sp.* demonstrates cell growth up to 122 °C at 20 MPa [2] while *Thermococcus Piezophilus sp*. thrives up to 125 MPa at a temperature range of 60-95 °C [3]. To survive and replicate under these physical extremes, extremophiles adapted by retrieving ions from the abiotic environment and by modifications of biochemical mechanisms to sustain vital processes like metabolism. One vital biochemical mechanism is the enzymatic hydrolysis of adenosine triphosphate (ATP) to adenosine diphosphate (ADP) which plays an important role in virtually every known metabolic pathway. However, this mechanism is counteracted by the abiotic decomposition of ATP through a non-enzymatic hydrolysis reaction. In cellular environments, the most prevalent form of ATP exists in complexes with $Mg^{2+}$ ions.

The application of in-situ Raman spectroscopy and high-pressure apertures, namely hydrothermal diamond anvil cells and autoclave with sapphire reaction cells, enabled us to determine hydrolysis rate constants for ATP in the presence of increasing $MgCl_2$ concentrations and temperatures of 80, 100 and 120 °C. Our first results indicate that the hydrolysis of ATP decelerates by 25% when reaching equimolarity of ATP and $MgCl_2$. At 80 °C, an increase of $MgCl_2$ does not further alter the reaction velocity. Increasing the temperature to 120 °C while increasing the concentration $MgCl_2$ to four times of the concentration of ATP results in a 50% decrease of the hydrolysis rate. The comparison of peak shifts in the Raman spectra and thermodynamic modelling of the ATP system showed an enhanced complexation of ATP with $Mg^{2+}$ when increasing the temperature. These new insights of the key metabolite ATP provide us another aspect to metabolic pathways of extremophiles.

*References:*

[1] Merino et al. (2019) xxx
[2] Takai et al. (2008) xxx
[3] Dalmasso et al. (2016) xxx

## The fate of Arsenic in the Carletti Spring System (Viterbo, Italy): a XAS speciation study

Montegrossi, G., Venturi S., Baroni T., Casentini B., Fazi S., Costagliola P., Rimondi V., Piacentini A., Mazzoni C. and Di Benedetto, F.

[1]Istituto Geoscienze e Georisorse, CNR, Firenze

[2]Dipartimento di Scienze della Terra, Università di Firenze

[3]Istituto di Ricerca sulle Acque, CNR, Roma

[4]Dipartimento di Biologia e Biotecnologie, Università di Roma "La Sapienza"

[5]Dipartimento di Fisica e Scienze della Terra, Università di Ferrara

---

A study aimed at unravelling arsenic (As) speciation in the carbonate sediments and the total suspended particulate (TSP) occurring at the Carletti spring system (CSS), part of the larger Bullicame (Viterbo, Central Italy) system, by means of XAS spectroscopy, has been undertaken.
In the CSS, As occurs as a geogenic anomaly, its mobility and speciation being likely affected by inorganic and/or microbiological processes. The determination of As speciation in the encrustation and TSP, highly diluted samples, is essential to validate the models on the fate of As in this "natural laboratory".

8 rock and 8 TSP samples were collected in the CSS, following relevant changes in temperature, distance from the spring and physicochemical features of the water/TSP/rock interfaces. All solid samples were analysed, without manipulation, by means of X-ray Absorption Spectroscopy at the As K edge in fluorescence mode and at low temperature (range 77-20 K). Experiments on rock and TSP samples were carried out at two beamlines (BM08 and BM26, respectively) at the ESRF facility.

The main results point to an almost constant As(III) over total As ratio over the whole spring system in the rock samples, As(III) being about 30% of the total Arsenic. Detailed investigation concerned with subsamples discriminated by colour (with reference to different abundances and speciation of co-localised microbiologic populations), finding no apparent changes in As speciation. TSP samples, analysed with a specific procedure due to their ultra-diluted nature, appear also constant and slightly enriched in As(III) with respect to the corresponding rocky samples. These data have to be compared to a water environment, which increases its oxidising potential and its pH while increasing the distance from the spring, as testified from the change of the As(III)/total As ratio from an initial 70% down to a final 40%.

This complex set of experimental results will be discussed on the light of two possible interpretive schemes, i.e. a kinetically constrained precipitation mechanism, and a microbiologically constrained change of As speciation, taking also into account of laboratory reference systems where the inorganic and biotic uptake of As(III) and As(V) were reproduced.

# Rare Earth Elements concentration in riverbed biominerals: Potential tool for Bio-Based Extraction

Sedda, L.[1*], Naitza, S.[1], Fancello, D[1]., Medas, D[1]., Musu, E[1]., Onnis, P.[1], Podda, F[1]. and De Giudici, G.[1]

[1] Department of Chemical and Geological Sciences, University of Cagliari, 09124 Cagliari, Italy. lorenzo.sedda@unica.it

---

Rare earth elements (REEs) are pivotal to developing modern technologies, and their demand is continuously increasing. Abandoned mines with mining dumps connected with mining activity could represent secondary sources of rare earth elements and critical raw materials. The Montevecchio mine in Sardinia (Italy) has a long history of base metal mining (lead and zinc), spanning almost 150 years, and recent studies have identified the presence of REEs in the mining dumps in the area [1]. This study investigated REE concentration in the Montevecchio mine dumps (Cantieri Sanna) and explored the potential of REE bioaccumulation by microorganisms along the riverbed biofilms.
A sampling campaign was conducted on the mine tailings and white patinas outcropping along the stream Roia Cani flowing through waste dumps and contaminated by Zn and other metals. The focus was on riverbed biofilms that, due to cyanobacterial activity, lead to the formation of hydrozincite white patinas. REE concentrations were measured by inductively coupled plasma mass spectrometry (ICP-MS) after acid digestion of the samples.
REE concentrations in the Montevecchio mine tailings were around 600 mg/kg. REE concentration in the river water was around 7 µg/L. The biogenic hydrozincite (with traces of zincite) showed REE concentrations up to 2800 mg/kg, indicating a significant bioaccumulation process. Noteworthy, these white patinas appear like those formed in the Rio Naracauli (Ingurtosu mine), in the same mining district, and described in some scientific works [2-5]. Further microbiological studies are underway to identify the strains driving the process.
The results of this study demonstrate that the Montevecchio mine waste dumps are a potential secondary source of REEs. Bioaccumulation processes could offer a potential method to extract REEs from these waste dumps more sustainably than traditional separation methods, which often involve using environmentally harmful chemical reagents.

**Keywords:** Bioaccumulation, Tailings, Montevecchio mine, Sardinia, Critical Raw Materials

*References:*

[1] Sedda L, De Giudici G, Fancello D, Podda F and Naitza S (2023) Minerals *14*(1), 3.
[2] Medas D, Cidu R, Lattanzi P, Podda F, Wanty R B and De Giudici G (2012) Applied geochemistry *27*(9), 1814-1820.
[3] Wanty R B, Podda F, De Giudici G, Cidu R and Lattanzi P (2013) Chemical geology 337, 1-10.
[4] De Giudici G, Wanty R B, Podda F, Kimball B A, Verplanck P L, Lattanzi P, Cidu R and Medas D (2014) *Chemical Geology 384*, 110-119.
[5] Medas D, Lattanzi P, Podda F, Meneghini C, Trapananti A, Sprocati A, Casu M A, Musu E and De Giudici G *(2014) Environ Sci Pollut Res 21, 6775–6782*

## Mineralogical controls on the persistence and preservation of DNA

Singh, V.V.[1], Kimber, R.L.[1,2], Kumar, N.[1,3], and Kraemer, S.M.[1]

[1]Department of Environmental Geosciences, University of Vienna, Austria

[2]Department of Earth and Environmental Sciences, University of Manchester, UK, richard.kimber@manchester.ac.uk

[3]Department of Environmental Sciences, University of Wageningen, Netherlands

---

Environmental nucleic acids are increasingly employed in a diverse range of technologies, including biomonitoring, (paleo)ecology, evolutionary anthropology, and viral monitoring. For these technologies to reach their full potential, a detailed understanding of the fate of nucleic acids in environmental systems is critical. Interactions at mineral surfaces play an important role in controlling the stability and fate of nucleic acids in the environment. For example, adsorption of DNA to mineral surfaces can protect against enzymatic hydrolysis,[1] leading to long-term preservation of genetic information. In contrast, adsorption of RNA to certain minerals can induce hydrolysis and speed up degradation.[2] However, the mechanisms and geochemical factors that underpin these processes remain poorly understood, limiting our understanding of the persistence of environmental DNA and RNA.

Here, we explore various mineralogical and geochemical controls on the adsorption of DNA to (bio)mineral surfaces and their impact on the DNA stability and preservation. We performed a series of controlled batch experiments to study adsorption kinetics and isotherms of DNA on a range of environmentally relevant minerals, including iron oxides, clays, and hydroxylapatite, under varying pH. We then studied the degradation of mineral-bound DNA using DNase I as a model nucleases enzyme to understand the effect of adsorption to minerals on DNA protection. The impact of DNA polymer length on its adsorption and protection at mineral surfaces was also investigated.

*References:*

[1] Romanowski G et al. (1991) Appl Environ Microbiol **57**(4):1057-1061.
[2] Zhang K et al. (2023) Environ Sci Technol **57**(22):8280-8288.

# Bioprospecting for Sustainable Mineral Management in Arsenic-Rich Environments

Tomlinson, N.O.,[1,2,3] Schofield, P.F.,[2] Jungblut, A.D.,[2] Hodson, M.E.[3] and Santos, A.L.[2]

[1] neda.tomlinson@nhm.ac.uk

[2] Natural History Museum, London

[3] Department of Environment and Geography, University of York

---

Introduction - Metals are a finite resource, and it is becoming increasingly important to extract metals from novel resources such as stockpiled low grade mining materials ore or mine waste. Biomining is a sustainable and economically viable metal extraction method and is already being used to produce up to 20% of the world's copper [1]. In essence, biomining utilises a consortium of microorganisms to solubilise the target metal into a leach solution ready for downstream processing. A further challenge is posed by the presence of the toxic metalloid arsenic (As) in potential ores and mine wastes leading to a decrease in biomining efficiency [2] and additional waste management considerations. The finding of As-tolerant microorganisms that can be used to selectively remove arsenic during mineral processing would allow effective biomining of currently untouchable materials.

Objectives - We want to understand how the microbial population dynamics in As-contaminated former mining environments are influenced by mineralogy and geochemistry. Using this knowledge we will isolate arsenic-tolerant bacteria, establish their biogeochemical mechanisms of interaction and assess their potential for bioleaching As-rich ore deposits and legacy mine waste.

Methods - Samples were collected in triplicate from an As-contaminated, legacy calcining site in Cornwall, UK. Their mineralogy and geochemistry were characterised using X-Ray Diffraction (XRD), Inductively Coupled Plasma-Mass Spectrometry (ICP-MS) and Scanning Electron Microscopy (SEM). The microbial population was characterised by metabarcoding and next generation sequencing (NGS). Isolation of microorganisms was achieved using BG11 and Basal Salts/Trace elements media, with and without As-supplements.

Results - The arsenic concentrations in soils close to the calciner were up to and above 1 wt% and generally similar to values previously reported [3]. Arsenic concentrations in mineral growths within calciner structures are as high as 30 wt%. The mineralogy of the soils is dominated by quartz, muscovite, and chlorite, with the most commonly identified As-mineral being arsenolite ($As_2O_3$). As-rich mineral growths from within the calciner have been identified as gypsum and pharmacolite. Culturing successfully isolated several distinct morphologies grown on arsenic-supplemented media. An endolithic growth found in the calciner mineral samples has also been successfully cultured in the laboratory. NGS of these cultured populations is the next step to learn more about the organisms that can be grown in the presence of arsenic, *ex situ*. The endolithic community in particular provides an exciting chance to understand population dynamics in As-rich environments.

References –
[1] Johnson BD et al (2023) Biomining Technologies 1-14
[2] Diaz JA et al. (2018) Minerals 8(5):2015
[3] Camm GS et al. (2004) J Geochem Expl 82: 1-15

# The effect of pressure on sulfur stability in silicate melts

Thomas, R.W.[1], Wood, B.J.[1]

[1]Department of Earth Sciences, University of Oxford,

Richard.Thomas@earth.ox.ac.uk; Bernie.Wood@earth.ox.ac.uk

---

In silicate melts sulfur occurs predominantly as sulfide ($S^{2-}$) or sulfate ($S^{6+}$). Recent experiments at 1-atm pressure [1,2] have provided a comprehensive picture of the temperature and compositional effects on sulfur speciation over the temperature range 1200-1500°C. The effects of pressure on speciation can only be estimated from observed pressure effects on FeS solubility, however, which requires several assumptions. In order to determine the effect of pressure on sulfide capacity ($logC_{S^{2-}} = log\ log\ S_{(melt)}(wt\%) + 0.5\ log\ log\ \left(\frac{fO_2}{fS_2}\right)$ ). We performed experiments at 1400°C, and at 1 bar to 2.5 GPa with $f(S_2)$ controlled by mixtures of Ag and $Ag_2S$ and oxygen fugacity controlled at the CCO buffer. Results show that $S^{2-}$ concentrations increase non-linearly with decreasing pressure across all compositions investigated (Fig 1a). A plateau or *'hump'* in sulfide capacity ($LogC_s$) appears to occur between 1 bar and 5 kbar, as suggested by O'Neill [1], indicating a low partial molar volume of $S^{2-}$ in this range. The plateau is only present in melts that contain 0-9 wt% FeO, however; melts with 20 wt% FeO show a monotonic increase in $LogC_s$ with decreasing pressure (Fig 1b). In addition, the volume change accompanying replacement of $O^{2-}$ in the melt by $S^{2-}$ is composition-dependent. For the compositions containing 0-9% FeO this is 10-11 $cm^3\ mol^{-1}$ similar to the difference in volume between CaO and CaS, while for silicate melts with 20 wt% FeO, ΔV is 6 $cm^3\ mol^{-1}$ corresponding to the difference between FeO and FeS. These observations may indicate that $S^{2-}$ anions change coordination environment with both pressure and composition.

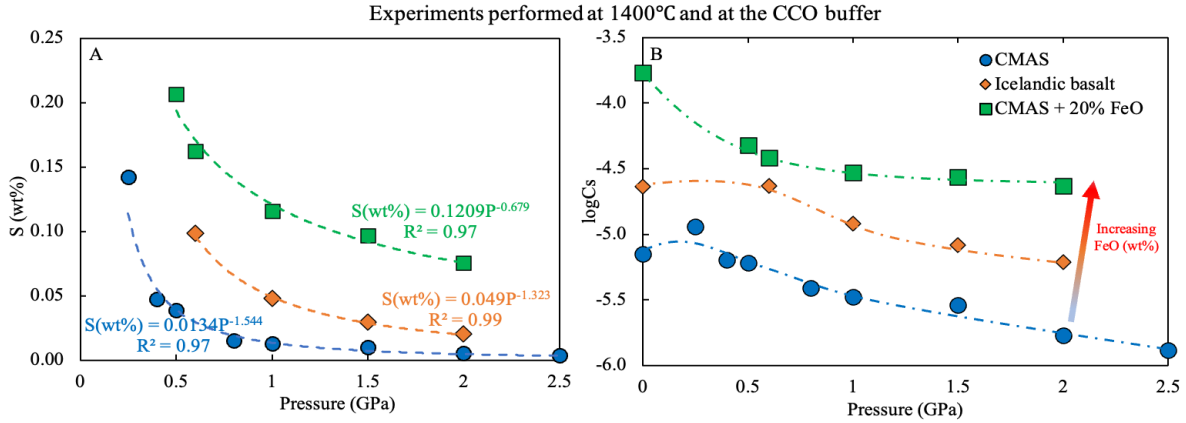


We have also performed experiments aimed at determining the partial molar volume of sulfate in silicate melts. These were intended to test the hypothesis of Matjuschkin et al [3] who suggested that there is a strong pressure effect on the $f(O_2)$-dependence of the crossover from $S^{2-}$ to $S^{6+}$ stability. We encountered long equilibration times, however, indicating that diffusion of $S^{6+}$ is much slower than that of $S^{2-}$, contrary to the findings of [4] who find negligible difference. Diffusion experiments have therefore been performed for $S^{2-}$ and $S^{6+}$ in basaltic melts as a function of T (1200-1500°C), and P (0.5-2 GPa). We find that $S^{6+}$ diffuses significantly more slowly than $S^{2-}$. $S^{6+}$ diffusion is also slower than that of $H_2O$ and $CO_2$, limiting its diffusive fractionation into bubbles formed during decompression of silica-rich melts.

*References:*

[1] O'Neill (2022) Magma Redox Geochemistry Chapter 10
[2] Boulliung and Wood (2023) Contrib Min Pet 178:56
[3] Matjuschkin et al. (2016) Contrib Min Pet 171(7):66
[4] Baker and Rutherford (1996) Contrib Min Pet 123:335-344

## The effect of water on chlorine solubility in basalts

Rusiecka, M.K.[1*] and Wood, B.J.[1]

[1] Department of Earth Sciences, University of Oxford, South Parks Road, OX1 3AN Oxford UK

[*]corresponding author monika.rusiecka@earth.ox.ac.uk

---

Chlorine, the fourth most abundant volatile in natural silicate melts after $H_2O$, $CO_2$, and sulphur species, plays a pivotal role in a variety of geochemical processes. It has, for example, been found that chlorine is, on a molar basis, more efficient at lowering liquidus temperatures than $H_2O$. Moreover, chlorine acts as a major ligand facilitating the transfer of economically important metals from melts into separating aqueous fluids, as a precursor to the formation of ore deposits. The release of magmatic chlorine may, however, also have adverse effects. Volcanic emissions containing chlorine play a role in ozone destruction, in acidification of natural waters and in elevating the risk of heavy metal pollution.

In this study, we investigate the influence of water on chlorine solubility in basalt using a synthetic starting material with the composition of basalt from Reykjanes Ridge, Iceland. Water was introduced in varying quantities as $Al(OH)_3$. Experiments were conducted under water-undersaturated conditions at 15 kb and 1300°C, as well as at 5 and 10 kb and 1200°C. Chlorine was introduced using a mixture of AgI and AgCl mixed in a known proportion with the silicate starting material, enabling precise control of chlorine fugacity. Graphite capsules were employed, with $Ag_2CO_3$ serving as a source of $CO_2$ to maintain the oxygen fugacity close to the CCO buffer.
Our results demonstrate a significant increase in chlorine content, at fixed chlorine fugacity, as $H_2O$ concentration in the melt increases. The effect corresponds to a 1.5-fold increase in Cl between 0 and 6 wt% $H_2O$ contents at each pressure. Similarly, chlorine content increases by approximately 1.3-fold between 15 and 5 kb at fixed $H_2O$ concentration. Quantifying the effects of water on chlorine solubility provides insights into the relationship between melt composition and brine separation. We further calculate the activity of NaCl in basaltic melt from Etna volcano, Italy, employing thermodynamic formulations and experimental data from the literature ([1], [2]). Our analysis shows that addition of water increases chlorine solubility and decreases activity of NaCl by dilution of all the components. Additionally, calculating the activity of NaCl presents a promising approach for estimating chlorine fugacities in experiments on fluid/melt partitioning, where chlorine fugacity was not controlled explicitly.

*References:*

[1] Stelling et al. (2008) Chem Geol 256(3-4):102:110
[2] Alletti et al. (2009) Chem Geol 263(1-4):37-50

# Speciation equilibria of $H_2O$, HCl, and NaCl in low-density magmatic-hydrothermal fluids

Salomone, F.[1], Dolejš, D.[1]

[1]Institute of Earth and Environmental Sciences, University of Freiburg, Germany
federica.salomone@minpet.uni-freiburg.de

---

Behaviour and speciation of $H_2O$, HCl and NaCl in hydrothermal fluids exerts strong control on acidity generation, acidic alteration, metal complexation, and ore-deposit formation. We critically evaluate existing thermodynamic models for speciation of $H_2O$, HCl and NaCl over wide range of magmatic and hydrothermal conditions: The approaches include: (i) density models using semi-empirical logarithmic correlations with water density [1]; (ii) electrostatic models [2], [3]; (iii) virial expansion models [4]; (iv) hydration models based on stepwise hydration of solute [5], and (v) various statistical-mechanical models, e.g. [6]. These models consistently predict $H_2O$ and HCl ionization up to 400 °C and above 30 MPa, with density models most accurately reproducing the experimental data. However, at high temperature or low pressures the predictions from individual models increasingly diverge and become discrepant, partly owing to theoretical limitations. We develop a new equation of state for the thermodynamic properties of aqueous species that accounts for intrinsic properties and solute-solvent interactions (hydration sphere compression etc.). Furthermore, we optimize functional forms for several thermodynamic properties such as heat capacity and hydration compression. The new model has been parameterized for dissociation of $H_2O$, HCl and NaCl, and these effects evaluated along several geologically relevant fluid-flow paths: (i) fluid ascent path during metamorphic devolatilization at 20 °C $km^{-1}$; (ii) lateral flow and cooling of magmatic fluid (at 200 MPa); (iii) vertical flow and cooling of magmatic fluid; (iv) adiabatic flow and cooling of magmatic fluid, all starting at 700 °C and 200 MPa (7.5 km). Model simulations highlight the effect of pressure and fluid density on solute ionization. Metamorphic fluids have significantly dissociated solutes, by four orders of magnitude in comparison to upper-crustal magmatic fluids. This demonstrates capability of high-pressure fluids to transport solute as ionic species. Fluids exsolved from upper-crustal magmatic sources have essentially identical behaviour upon cooling during lateral dispersion or vertical flow. They progressively reach dissociation of their solutes upon cooling, with significant generation of acidity starting at 400 °C. For fluids rising adiabatically, the decreasing density exerts the dominant control on their ionization behaviour. As the fluid expands, solute species remain completely associated. Significant dissociation and acidity generation can only be achieved during cooling and fluid contraction or condensation. The strongly contrasting behaviour of solute in fluids following distinct thermal gradients (host rock vs. adiabatic rise) shows that alteration and mineralization processes may have very variable efficiency between slowly vs. fast moving hydrothermal fluids.

*References:*

[1] Marshall W L and Franck E U (1981) J Phys Chem Ref Data 10: 295-304
[2] Tanger IV J C, Helgeson H C (1988) Am J Sci 288: 19-98
[3] Shock E L et al. (1992) J Chem Soc Faraday Trans 88: 803-826
[4] Akinfiev N N and Diamond L W (2003) Geochim Cosmochim Acta 67: 613-627
[5] Djamali E and Cobble J W (2009) J Phys Chem 113: 2398-2403
[6] Lvov S N et al. (2018) J Molecul Liq 270: 62-73

## The Volatility of Hg at Magmatic Temperatures

Boulliung, J., Wood, B.J. and Mather T.A.

Department of Earth Sciences, University of Oxford, OX1 3AN, U.K.

Mercury is a volatile element whose behaviour at high temperatures is difficult to measure experimentally but which is nevertheless environmentally important due to its toxicity and geologically important as a potential indicator of large-scale volcanism. A currently popular hypothesis is that 'spikes' in Hg concentration in the sedimentary record are definitive evidence of Large Igneous Province volcanism even, in some cases, in the absence of coeval lavas. In order to examine this hypothesis more closely we have been attempting to quantify the volatility of Hg in silicate melts and to compare its behaviour to that of other volatile elements.

Given that Hg is generally present at the ppb level in volcanic rocks, we started by doping basalts with several hundred ppm of Hg as HgO and performing conventional 1 atm experiments on Pt wire loops. All Hg was lost during heating to the solidus. We therefore switched to using sealed silica glass tubes that can contain a significant $P_{Hg}$. Our starting material was a natural basalt doped with about 500 ppm each of Cd, Cs, Cu, Ga, Ge, In, Pb, Rb, Sb, Sn, Zn, Li and Ag and 50ppm of Tl. This starting material was fused to form a glass which was ground and then doped with 93ppm Hg as HgO. The composition of the glass was checked by solution ICP-MS prior to commencing the experiments.

100mg of starting material as placed in a small alumina crucible which was inserted in the sealed end of a glass tube of 10mm O.D., 8mm I.D. and ~90mm length. The tube was evacuated to a pressure of ~$2x10^{-5}$ bar and sealed. Tubes were then heated in a vertical furnace at 1250, 1300 and 1400°C for times of 5 to 1440 minutes. After quenching, the product glass was ground and analysed with a mercury analyser. Chips of glass were saved for analysis with the electron microprobe and laser Ablation ICP-MS. As expected, almost all Hg was lost almost immediately from the melt generating an essentially constant partial pressure of Hg in the gas of ~0.14 bar. Hg contents in the melt generally declined rapidly with time, although in some cases there is evidence of redeposition on the glass during quenching. At 1400°C the Hg content of the glass declines to 38ppb within 60 minutes and remains essentially at this level out to 300 minutes. The corresponding 'plateau' level at 1300°C is ~110ppb. These concentrations are similar to those found in natural igneous rocks.

All of the other trace elements added are much less volatile than Hg. We found that behaviour of some volatile elements mirrored that of Hg but is much less extreme. Many elements declined gradually in concentration, however, eventually reaching about 50 % of the initial concentration (Cu, Ag, Zn, Sn, Pb, Ni, Co, Cr, V). Since Ni and Co have low volatility we presume that this behaviour reflects interactions with the crucible rather than volatility. Elements showing more obviously volatile behaviour are Tl, Cd and In.

# Decoding the $H_2O$ degassing mechanism as a trigger for the explosive eruption of the Lower Laacher See phonolite

Marks, P.L. and Nowak, M.

Department of Geosciences, Eberhard Karls University Tübingen, Germany; Patricia.Marks@uni-tuebingen.de

---

The Laacher See volcano is one of the youngest volcanoes in Germany with its last eruption 13,006 ±9 years BP[1]. About 6.3 km³ of hydrous phonolitic magma was explosively erupted by phreatomagmatic and Plinian eruptions in less than 10 days[2]. The eruption behavior of such volcanic systems is determined by the degassing mechanism of $H_2O$ fluid from the supersaturated hydrous silicate melt during ascent. The number of fluid vesicles per unit volume of silicate melt (*VND* in $mm^{-3}$) is a suitable parameter used to quantify the efficiency of fluid-melt separation. According to the nucleation theory, the *VND* increases strongly with decompression rate[3] and is thus used for quantifying magma ascent velocity. Recently and specifically for phonolitic melts, the process of spinodal decomposition has been proposed, which manifests in the independence of *VND* from the decompression rate[4].

To characterize the degassing behavior of the sodium-rich lower Laacher See phonolite, systematic decompression experiments were conducted in the internally heated pressure vessel. The melts were hydrated with 5.7 or 5.0 wt% $H_2O$ at 200 MPa and 1523 K for 96 h and then continuously decompressed at 1323 K with 0.064 – 1.7 MPa/s to final pressures between 110 MPa and 30 MPa. By reaching the final pressure, the samples were rapidly quenched to room temperature to preserve the vesicle textures and the residual $H_2O$ contents in the melts and to minimize vesicle shrinkage during cooling. The *VND*s and the spatial distribution of the vesicles, as well as the $H_2O$ contents in the decompressed melts were analyzed with quantitative image analysis, transmission light microscopy, and FTIR-spectroscopy.

Upon reaching sufficient supersaturation pressure of > 80 MPa, all samples exhibit homogeneously dispersed and micrometer-sized vesicles in the sample center. The results consistently show that the initial *VND* is independent of the decompression rate, with high log*VND*s of 4.1 to 5.6 causing very fast near equilibrium adjustment of $H_2O$ concentration of the melt by degassing. Further decompression of the vesiculated melts leads to vesicle coalescence, resulting in a significant reduction of *VND* by orders of magnitude.

These observations are consistent with that of Allabar and Nowak (2018), who determined a decompression rate independent log*VND* of ~5.2 ± 0.5 for hydrous potassium-rich phonolitic melt of the AD79 Vesuvius white pumice composition. From this, a trend emerges that at least for hydrated phonolitic melts, spinodal decomposition plays a crucial role in the $H_2O$ degassing behavior of the melt and thus in the explosive eruption behavior of the volcanic systems.

*References:*

[1] Allabar A and Nowak M (2018) EPSL 501: 192-201
[2] Reinig F et al. (2021) Nature 595: 66-69
[3] Toramaru A (2006) J Volcanol Geotherm Res 154: 303-316
[4] Wörner G and Schmincke HU (1984) J Petrol 25: 805-835

# On the paragenesis of quartz and native copper in the continental flood basalts of Western Volyn (Ukraine)

Batsevych, N.V.[1], Naumko, I.M.[2], Vovk, O.P.[3], Beletska, Yu.A.[4], Triska, N.T.[5]

[1, 2, 4, 5]Institute of Geology and Geochemistry of Combustible Minerals of the NAS of Ukraine, 3-a Naukova St., Lviv 79060, Ukraine, natalja_bats@ukr,net

[2]Lesya Ukrainka Volyn National University, 13 Voli Av., Lutsk 43025, Ukraine

---

The fundamental and applied significance of quartz in potentially copper-bearing volcanic rocks of the Ediacaran continental flood basalts of Western Volyn is determined by its consistent association with native copper. This characteristic paragenesis has been documented by us, following our predecessors, who, starting from work [1], pointed to the close connection of native copper with quartz and almost invariably observed the release of silica during its formation from hydrothermal solutions. Numerous researchers interpret these processes similarly, even today. Therefore, the purpose of our precise quartz investigations was to find the answer: where did such a large volume of hydrothermal solutions originate in order to evenly penetrate throughout the thicker layers of continental flood basalts in Western Volyn?

Quartz for research was extracted from geodes found in the basalts of the active Polytsi quarry, situated in the central region of the native outcrops of Western Volyn traps. The mineral occurs in the form of solid masses, grains, and growths. Druses and geodes are frequently encountered, with crystals ranging in size from a few mm to 1.5 centimeters along the main crystallographic axis. The color of quartz varies.

The crystal morphology of quartz is relatively simple. It exhibits basic forms such as the hexagonal prism m {10$\bar{1}$0}, along with two rhombohedra: the positive r {10$\bar{1}$1} and the negative z {01$\bar{1}$1}. The faces of the rhombohedra are shiny and typically equally developed. The prisms are generally short in most sizes. The crystal habit ranges from hexagonal-dipyramidal to hexagonal-prismatic.

Thermobarogeochemical studies have identified families of fluid inclusions, predominantly composed of gas-liquid phases, including both essentially gaseous and essentially liquid inclusions, within the planes of healed cracks in quartz. Relatively high homogenization temperatures of up to 370°C have been determined, falling within the operational temperature range of mesothermal processes (200–300°C).

Chemical mass spectrometry data revealed a high content of $H_2O$, $CO_2$, and $N_2$ in the relict fluids present in the defects within the studied basalts. Considering the presence of granophyre injections with $SiO_2$ content ranging from 63.72 to 77 wt.%, the question arises: how did such a significant amount of hydrothermal fluids penetrate the basalts to form quartz and uniformly alter the entire thickness of the trap formation? Water plays a pivotal role in the genesis, differentiation, ascent, and eventual eruption of magma. Previous research [3] has focused on the evolution of $H_2O$ and $CO_2$ saturation conditions for residual melt within the magmatic system crystallizing at 0.7 GPa. During crystallization, the maximum solubility of water gradually increases from ~10.2 to ~12.0 wt.%, while the solubility of $CO_2$ decreases from ~0.53 to ~0.36 wt.%. These findings suggest that the formation of quartz occurred as a result of fluid-liquefaction interaction [2] during the final stages of the evolution of a single magmatic process, following the separation of residual solutions enriched with silicic acid and saturated with water.

*References:*

[1] Lazarenko Ye et al. (1960) Mineralogy of Igneous Complexes of Western Volyn: 510

[2] Naumko I et al. (2016) Rep of the NASU 9: 69–78. DOI: https: //dx.doi.org// 10.15407/dopovidi2016.09.069.

[3] Petrelli M et al. (2018) Nature Communications 9 (1): 770. doi:10.1038/s41467-018-02987-6.

# Petro-geochemical and environmental significance of $SO_2$ emissions during a basaltic eruption in Central America: the case-study of the December 29th, 2013 eruption of the San Miguel volcano, El Salvador

Hernández De la Cruz, A.[1,2], Gimeno, D.[1], Conde Jacobo, V.[3], Olmos Guevara,R.[2], Barahona Escoto, F.[2], Hernández Martínez,M.[2] and Novembre,D.[4]

[1]Departament de Mineralogia, Petrologia i Geologia Aplicada, Facultat de Ciències de la Terra, Universitat de Barcelona. C/ Martí i Franquès s/n, 08028, Barcelona (España) d.gimeno.torrente@gmail.com domingo.gimeno@ub.edu

[2]Grupo de Investigaciones Vulcanológicas de la Universidad de El Salvador, San Salvador, El Salvador, C. A. agustin.hernandez@ues.edu.sv

[3]Department of Radio and Space Science, Chalmers University of Technology, 41296 Gothenburg, Sweden,

[4]Novembre, D. Dipartimento di Ingegneria e Geologia, Università degli Studi "G.D'Annunzio", Via dei Vestini 30, 66013 Chieti, Italy

---

The San Miguel or Chaparrastique volcano is placed at the east of El Salvador republic, Central America, and is a medium size (1.500 m of vertical development) basaltic-andesite basaltic stratovolcano representative of a large number of similar active arc volcanoes outcropping in the frontal pacific coast from the Tacaná volcano in Mexico-Guatemala border sector till La Yeguada volcano in Panamá. This volcanic front is related to the subduction of the Cocos plate under the Caribean one. The eruption of December 29th of 2013 (VEI-2) can be considered representative of a large number of similar eruptions that emitted ash clouds to the atmosphere; in this case from east to west, along some 90 km along most of the El Salvador.

The results of a detailed daily monitoring of $SO_2$ emission (with mobile stations) for a month and a half immediately after the VEI-2 eruption of December 29, 2013 of the San Miguel or Chaparrastique Volcano (El Salvador) are presented. In addition, a complete set of pristine ash samples where samples along the transect of dispersion, and were texturally, chemically and mineralogically characterized.

These data turn out to be higher at times of maximum emission (almost double in some cases) than those previously published from a small network of permanent stations and show the existence of several degassing cycles. It starts from pre-eruptive base values estimated at just over 300 t $SO_2$/day, to maximum peak values that reach 4,300 and 2,000 t $SO_2$/day in the first and second cycles, respectively [1]. We can conclude that available values of $SO_2$ emissions in the days prior to the eruption showed a poor predictive behaviour in terms of eruption forecast. On other hand, Textural and microchemical SEM-EDS studies showed a widespread presence of calcium sulphate crystals, both as a epitaxial growth and (even more prominent, larger ones phenocryst-like) included in the vitreous mesostase of individual pyroclasts.

Taking into account all these data, our current interpretation is that these calcium sulphate crystals were not formed only by direct sublimation within the eruptive column but that it might also correspond to the precipitation of anhydrite as a magmatic phase. This fact exists in other volcanoes [2] and this interpretation allows for the explanation of SO2 emission cycles at open conduct as a result of cycles of breakdown of these anhydrite phenocrysts and sudden gas leakage of the produced gas via the crater of the volcano. This might be followed by precipitation and successive breakdown of anhydrite in successive cycles or decreasing importance, until some kind of equilibria was achieved.

*References:*

[1] Hernández de la Cruz, A. et al, (2024) Geogaceta (in press)

[2] Luhr, J.F. (2008) JVGR 175:394-407

# Control of effusive and explosive eruptions of Ciomadul volcano: constraints by apatite composition

Hajdu Krisztina[1,2], Lukács Réka[2,3], Popa Razvan-Gabriel[4], Allaz Julien Marius[4], Pánczél-Oelberg Emese[1], Cserép Barbara[1,2], Bachmann Olivier[4], Pál-Molnár Elemér[5], Seghedi Ioan[6], Harangi Szabolcs[1,2]

[1] Eötvös Loránd University, Institute of Geography and Earth Sciences, Department of Petrology and Geochemistry, Budapest, Hungary email: tsunamisucks@gmail.com; [2] HUN-REN-ELTE Volcanology Research Group, Budapest, Hungary ; [3] HUN-REN Research Centre for Astronomy and Earth Sciences, Institute for Geological and Geochemical Research, Budapest, Hungary; [4] Department of Earth Sciences, Institute of Geochemistry and Petrology ETH Zürich, Zürich, Switzerland; [5] Department of Mineralogy, Geochemistry and Petrology, University of Szeged, Szeged, Hungary; [6] Institute of Geodynamics Sabba S. Ştefanescu, Romanian Academy, Bucharest, Romania

---

The Ciomadul Volcanic Complex, Eastern Carpathians, Romania is the youngest volcano in the Carpathian-Pannonian region, where volcanic activity occurred between 160 ka and 30 ka. It is a typical long-dormant volcano, where active stages were divided by several 10's kyr quiescence. Geophysical studies indicate that it is still underlain by a potentially active magma storage. Two main stages of volcanism are distinguished that are separated by ca. 40 kyr dormancy: the first eruptive episode from 160 ka to 95 ka was characterized by lava dome extrusions, followed by a mixed explosive and extrusive eruptive stage from 56 to 30 ka. Bulk rock composition, however, remained high-K dacitic and homogeneous. The dacitic volcanic products are composed of plagioclase, amphibole, biotite as well as accessory apatite, titanite, Fe-Ti oxides, zircon and allanite. Olivine, clino- and orthopyroxenes as well as quartz and K-feldspars occur occasionally. In this study, we focus on the apatite, particularly the variation in volatile content with an aim to reveal how it reflects the eruption type control. We analyzed the chemical composition of apatite microphenocrysts and inclusions enclosed by amphibole and biotite phenocrysts from lava dome rocks and pumices of both eruptive stages. We focus on the halogen contents (Cl, F), while the OH-content was calculated based on stoichiometry. The MgO content of the apatite was used to follow the behavior of the halogens during the magma differentiation, where higher amount of MgO represents the less evolved magma. We also analyzed the composition of the host amphibole crystals next to apatite inclusions to constrain the conditions of the apatite crystallization during the magma evolution.

The apatite data are plotted on a xCl/xOH vs xF/xOH diagram, where a breakpoint indicates the change of water-saturation state in the magma reservoir, due to the different behavior of Cl and F in water-saturated versus unsaturated states. F remains in the melt during water-saturation state, as it does in water-undersaturated conditions. In contrast, Cl shows similar incompatible behavior in water-undersaturated state, yet in water-(over)saturated conditions it partitions to the gas phase, so its content in the melt (and in apatite's crystal lattice) is buffered or decreased.

We conclude that effusive eruptions occurred when the magma reached water-(over)saturated state at constant Cl-content. In this case, the eruption triggering recharge event was not able to return the magma to water-undersaturated condition. On the contrary, the explosive events were characterized by magmas becoming water-undersaturated. In the case of the three oldest explosive eruptions the water-saturated felsic magma in the magma storage was returned to water-undersaturated state before the explosive eruptions by the mafic recharge material. Host amphibole compositions represent mostly low-temperature crystal mush, whereas occasionally high-temperature recharge and hybrid magma phases occur [1,2]. Notably, all apatite inclusions having water-saturated compositions are found in the low-Mg amphiboles derived from the felsic crystal mush magma, meanwhile apatite with water-undersaturated composition can be found in all the amphibole groups, and show no systematic distribution between recharge or hybrid magma or pre-eruptive state.

In accordance with the results of previous studies our apatite focused study also confirms the role of mafic magma recharge in the petrogenesis of the Ciomadul volcano.

This study belongs to the K135179 NKFIH-OTKA research project.

*References:*

[1] Cserép et al. (2023) Contributions to Mineralogy and Petrology 178:96

[2] Kiss et al. (2014) Contributions to Mineralogy and Petrology 167:986

# Potentially harmful elements released by volcanic ash of the 2021 Tajogaite eruption (Cumbre Vieja, La Palma Island, Spain): Implications for human health

Ruggieri, F.[1], Forte, G.[1], Bocca, B.[1], Casentini, B.[2], Petrangeli, A.B.[2], Salatino, A.[2], and Gimeno,D.[3]

[1]Department of Environment and Health, Istituto Superiore di Sanita, ` Rome, Italy.

[2]Water Research Institute (IRSA-CNR), National Research Council, Monterotondo, Italy

[3]Departament de Mineralogia, Petrologia i Geologia Aplicada, Facultat de Ciències de la Terra, Universitat de Barcelona. C/ Martí i Franquès s/n, 08028, Barcelona (España) d.gimeno.torrente@gmail.com domingo.gimeno@ub.edu

---

This study [1] assesses the potential impacts on human health of volcanic ash emitted during the 2021 Tajogaite eruption (La Palma Island, Spain). Ash samples were physically and chemically characterized and leaching tests (with deionized water and acidic solution). The tests were performed according to the IVHHN protocols to elucidate i) the leachable elements that may affect water quality and represent a potential threat for livestock and humans through drinking water supply; and ii) the bioaccessible fraction of toxicants able to be solubilized from ash surfaces if ashes are incidentally ingested by children. Fieldwork was conducted in the affected regions of La Palma Island on November and December 2021 while eruption was ongoing. The ash samples were collected as pristine as possible, but some cases natural leaching by rain was started. Concentrations of major elements (Si, Ca, Mg, Na, Ti, Mn, Fe, P, K and Al) in volcanic ashes were determined by wavelength dispersion X-ray fluorescence (WDXRF, Panalytical, Axios PW 4400/40 sequential spectrophotometer), and trace elements (As, Ag, Au, Ba, Cd, Ce, Co, Cr, Cu, Hg, In, Mo, Ni, Pb, S, Se, W, Zn, and Zr) by inductively coupled plasma optical emission spectrometry (ICP-OES, Agilent 5800) and inductively coupled plasma mass spectrometry (iCAP-Q ICP-MS, Thermo Fisher). In addition, the ash samples were texturally and microchemically studied by SEM (FEI QUANTA-250) under low vacuum conditions coupled with SDD EDS detectors (Thermo Fisher UltraDry - Pathfinder Alpine). Anions such as fluoride (F), sulfate ($SO_4$), chloride (Cl), phosphate ($PO_4$), and bromide (Br) were determined by IC chromatography (DIONEX DX 120, Thermo Fischer) on filtered undiluted water samples SEM images have been acquired with Secondary Electron detectors (SE) for topographical information, and with Backscattered Electron detectors (BSE) for semi-quantitative microchemical (average atomic number) analysis.

The most abundant readily water-soluble compounds were $SO_4$, F, Cl, Na, Ca, Ba, Mg, and Zn. Fluoride and chloride (up to 1085 and 1347 mg/kg) showed higher values in distal ash samples than closer ones. The potential F availability assessed from water leachates may suggest important environmental and health implications. In addition, long-term health hazard due to a long–term weathering of tephra deposits should be possible as confirmed by the greater amount of F extracted by acidic solution. Concentration of other trace elements (e.g., As, V, Mn, Mo, Cr, Fe, Se, Ti, Pb) were low compared to global medians and within the range globally assessed. Indicative calculation of hazard for water supply showed that F concentration may exceed both the recommended value (1 mg/L) for irrigation purpose and the health- based drinking water limits of 1.5 mg/L (for humans) and 2 mg/L (for livestock). If the predicted concentrations in water were compared with the toxicologically dose, F showed a potential health-risk for children through drinking water. The indicative health-risk characterization via accidental ash ingestion showed that the direct exposure does not represent a primary source of F daily intake for children. This important outcome confirmed F as element with the greatest health threat during Tajogaite 2021 eruption.

*References:*

[1] Ruggieri et al. (2023) Science of the Total Environment 509: 167103

## Sulphur speciation in magmatic fluids: facts and artefacts

Farsang, S.[1*] and Zajacz, Z.[1]

[1]University of Geneva, Switzerland (*stefan.farsang@unige.ch)

The speciation of sulphur in magmatic fluids released from ascending arc magmas affects magma redox, climate, and magmatic-hydrothermal ore deposit formation. Previous experimental work on sulphur speciation in high-pressure/temperature geologic fluids led to contrasting speciation models. For instance, $S^{6+}$ species were suggested to dominate at oxidising conditions [1,2] and $S_2^-$ and $S_3^-$ sulphur radical species at intermediate redox conditions [3,4].

To study the speciation of sulphur in magmatic fluids, we first trapped pre-equilibrated sulphur-bearing aqueous fluids as synthetic fluid inclusions (SFI) at $T$ = 750, 875, and 1000°C and $P$ = 200 MPa, and up to eight different oxygen fugacities at each temperature ranging from -1 to +2.5 log units relative to the Ni-NiO buffer. Fluid entrapment was conducted in a prototype externally heated molybdenum-hafnium carbide vessel apparatus with hydrogen membrane simultaneously allowing for rapid quenching and flexible, precise, and accurate redox control [5]. Following the synthesis, we reheated the SFI to their entrapment temperature in a microscope heating stage and analysed them by *in situ* Raman spectroscopy, employing laser excitations with 405 and 532 nm wavelengths.

Our experimental innovations allowed for the quantification of different sulphur-bearing aqueous species at previously inaccessible temperature and oxygen fugacity conditions. We found that $H_2S$, $HS^-$ and $SO_2$ are the only major sulphur species in magmatic fluids, while the previous interpretation of $S^{6+}$ and sulphur radical species as major sulphur species is due to different experimental artefacts, including the Raman resonance effect [6]. Furthermore, we show the effect of temperature and fluid salinity on sulphur speciation and assess the role of sulphur species in magma redox and ore deposit formation.

*References:*

[1] Binder B and Keppler H (2011) EPSL 301:190–198
[2] Ni H and Keppler H (2012) American Mineralogist 97:1348–1353
[3] Pokrovski G S and Dubrovinsky L S (2011) Science 331:1052-1054
[4] Pokrovski G S and Dubessy J (2015) EPSL 411:298–309
[5] Zajacz Z and Alex A (2022) American Mineralogist 107:692-702
[6] Farsang et al (2023) American Mineralogist 108:2234-2243

# Vibrational properties of oxidized sulfur species in hydrothermal fluids from ab initio molecular dynamics simulations and Raman spectroscopy

Jahn, S.[1], Schmidt, C.[2]

[1]Institute of Geology and Mineralogy, University of Cologne, Zülpicher Straße 49b, 50674 Köln, Germany (s.jahn@uni-koeln.de)

[2]GFZ German Research Center for Geosciences, Telegrafenberg, 14473 Potsdam, Germany (Christian.Schmidt@gfz-potsdam.de)

---

Sulfur species are important ligands and transport agents for metals in hydrothermal fluids. They are also indicators of the redox state and *pH* of such fluids. Especially oxidized sulfur species such as $SO_4^{2-}$ and $HSO_4^-$ ions or $H_2SO_4$ and $SO_2$ molecules have characteristic vibrational modes that are accessible even under high pressure and high temperature conditions using Raman spectroscopy, which makes this analytical method suitable for studying fluid properties under a wide range of geologically relevant conditions, e.g., in fluid or melt inclusions and in hydrothermal diamond anvil cell experiments.

However, a quantitative interpretation of Raman spectra and analysis of sulfur species abundances requires a good understanding of the vibrational mode frequencies and Raman susceptibilities, as well as their change with pressure, temperature, fluid composition and *pH*. *Ab initio* molecular dynamics (AIMD) simulations have provided unique insights into fluid speciation and supported the interpretation of various types of experimental spectra. Here, we present results of a joint AIMD simulation and *in situ* Raman spectroscopy study of $H_2SO_4$ and $NaHSO_4$ solutions up to temperatures of 1000 K and pressures of 1 GPa.

The experimental spectra show interesting behaviour, such as an asymmetric shape of several Raman bands and a strong decrease in the $\nu_S(SO_3)$ Raman scattering efficiency of $HSO_4^-$(aq) in $H_2SO_4$ fluids towards high temperatures, which have not been explained yet. The major difference between the AIMD simulations of $H_2SO_4$ and $NaHSO_4$ solutions, which were performed at 1000 K in a wide range of densities, is that the $HSO_4^-$ species in the $NaHSO_4$ solutions are relatively stable over the time scale of the simulation, while frequent proton hopping is observed in the $H_2SO_4$ solutions. In the case of the $HSO_4^-$(aq) molecule, this leads to increasing $\nu_{as}(SO_3)$ and $\nu_S$(S–OH) band intensities relative to that of $\nu_S(SO_3)$. Analysis of the vibrational properties of the simulated species was performed using the mode-projection approach [1]. Individual contributions to the total vibrational spectra could be identified and assigned to bands in the Raman spectra. Implications of these observations on the interpretation of *in situ* Raman spectra at high pressures and temperatures and varying *pH* will be discussed.

*References:*

[1] Spiekermann G et al. (2011) J Chem Phys 136:154501

# Unraveling metasomatic agent in the upper mantle xenoliths – via 3D Raman mapping of complex inclusions: a case study from the Styrian Basin (W-Carpathian Pannonian Region)

Myovela, J.L.[1,2,5], Aradi, L.E.3[3,4], Spránitz, T.[3,5], Hegedűs, M.[6], Taracsák Z.[7], Konečný, P.[8], Kovács, J.[1,9] and Berkesi, M*.[3,5]

[1]University of Pécs, Department of Geology and Meteorology, Hungary

[2]University of Dodoma, Department of Geology, Tanzania

[3]Lithosphere Fluid Research Lab, Eötvös Loránd University, Hungary

[4]Archaeometry Laboratory, National Archaeological Institute, Hungarian National Museum, Hungary

5HUN-REN Institute of Earth Physics and Space Science (EPSS), MTA FI Lendület FluidsByDepth Research Group, Hungary, *berkesi.marta@epss.hun-ren.hu

[6]Department of Materials Physics, Eötvös Loránd University, Hungary

[7]Department of Earth Sciences, University of Cambridge, Downing Street, Cambridge, United Kingdom

[8]State Geological Institute of Dionýz Štúr, Slovakia

[9]Environmental Analytical and Geoanalytical Research Group, Szentágothai Research Centre, University of Pécs, Hungary

---

The Styrian Basin, located in the transition zone between the Pannonian Basin and the Eastern Alps, is thought to have formed above a lithospheric wedge which had been affected by subduction. The Late Miocene-Pliocene alkali basalts sampled the subcontinental lithospheric mantle beneath the basin, bringing mantle xenoliths to the surface [1]. These xenoliths are amphibole-rich, indicating extensive modal metasomatism at mantle depth. We aim to enhance our understanding of fluid and melt-related processes in these xenoliths via inclusion studies. Of the studied xenoliths, one category contains co-entrapped fluid and melt inclusions, while the other contains only fluid inclusions (FI). We performed 3D confocal Raman mapping, Focused Ion Beam-Scanning Electron Microscopy, Electron Microprobe Analysis, and Scanning Electron Microscope with Energy Dispersive Spectroscopy. Our objectives are to 1) gain insights into the nature of metasomatic agents based on fluid and melt inclusions and 2) explore the applicability of 3D Raman mapping on inclusions. The studied inclusions are primary (fluid inclusions) and pseudosecondary (fluid and melt inclusions), occurring in orthopyroxene, clinopyroxene and amphibole. The FI are irregular to negative crystal-shaped (3-100 µm), whereas melt inclusions (MI) are glass-rich with rounded to negative crystal shapes (4-15 µm).

3D Raman mapping on these inclusions has revealed complex phase assemblages comprising fluid and solid phases (magnesite, silicate glass, pyrite, talc, anhydrite, and nahcolite). The fluid is dominated by $CO_2$ (up to 98.4 mol%) and $H_2O$ (up to 50.8 mol%). The silicate glass in the MI is $H_2O$-bearing (up to 3.3 wt%) and shows an evolved composition (i.e., trachyandesitic composition with $SiO_2$ between 54.31-60.65 wt%) relative to the host basalt of the studied xenoliths. We revealed pargasitic amphiboles in $SiO_2$-rich glass in the MI that co-entrapped with the $CO_2$-$H_2O$-rich fluid phase, suggesting that an immiscible $SiO_2$-rich melt and $CO_2$-$H_2O$-rich fluid as a potential metasomatic agent that could have been circulating in the mantle wedge above a subducted slab. Moreover, this study revealed that the laser-induced heating effect could overestimate sulfides in the 3D Raman models, while silicate glass could be underrepresented due to its low Raman scattering properties. Nevertheless, 3D Raman mapping remains a potential tool for deciphering intricate phase assemblages in inclusions.

This research was supported by the NKFIH_FK research fund nr. 132418 to M. Berkesi. Part of this research was funded by the Doctoral School of Earth Sciences of the University of Pécs.

*References:*

[1] Aradi et al., 2017; Tectonics, 36, 2987–3011.

## Halogen impact on Raman water bands at high pressure and the implications for salinity estimations in fluid inclusions

Grützner, T.[1,2,3] and Bureau, H.[1]

[1]Institut de Minéralogie, de Physique des Matériaux et de Cosmochimie, Sorbonne Université Paris, France.

[2]Research School of Earth Sciences, Australian National University, Canberra, Australia.

[3]Institut für Geowissenschaften, Goethe-Universität Frankfurt, Germany.

---

Halogens play a pivotal role as volatile elements, significantly impacting geodynamic processes. In crustal hydrothermal fluids, halogen complexes (e.g., in saline fluids, brines, or molten salts) serve as major agents for metal transport in ore-forming processes related to hydrothermal systems [1]. Samples of such fluids can be found entrapped as inclusions in minerals like quartz [2,3] or olivine [4] in magmatic and metamorphic rocks. Raman spectroscopy has been employed for decades to determine the salinity of fluid inclusions, especially those too small for other common techniques like microthermometry [2,4,5].

We present a new experimental dataset on the impact of the halogens chlorine, bromine and iodine on the Raman water bands concerning pressure and their concentration at room temperature. These experiments were conducted at ambient temperature, with variations in halogen concentration and pressure ranging from 0 to 1.4 GPa.

The strength of the Raman water band shift change increases with the ionic size from chlorine, over bromine, to iodine. Our experiments further demonstrate that increased pressure diminishes the impact of the halogen shift change to a varying extent for each of the three halogens. This finding can have significant implications for the salinity calculation of fluid inclusions in minerals such as quartz or olivine. Particularly in the low salinity range, the concentration can be markedly underestimated if the pressure effect is neglected.

*References:*

[1] Aiuppa A et al. (2009) Chem Geol 263:1-18.
[2] Brooks HL et al. (2019) Lithos 332-333:120-134.
[3] Pankrushina EA et al. (2020) Proceedings of the 10th All-Russian Youth Scientific Conference pp. 175-183.
[4] Kawamoto T et al. (2013) Proc. Nat. Acad. Sci. USA 110:9663-9668.
[5] Moncada D and Bodnar RJ (2012) PACROFI-XI Conference pp. 67.

# The origin of deep $CO_2$-rich fluids in the Pannonian Basin: combined stable isotope study on fluid inclusions and dissolved gases in groundwaters

Spránitz, T.[1], Lange, T.P [1,2,3,4], Hencz, M.[1], Porkoláb, K.[1], Kővágó, Á.[2,4,5], Gelencsér, O.[2,3], Créon, L.[6], Palcsu, L.[7], Tóth, Á.[8], Erőss, E.[9], Rouchon, V.[10], Szabó, Cs.[1,2], Kovács, I.J.[4], Török, K. [11], Berkesi, M.[1]

[1] MTA-EPSS FluidsByDepth Lendület Research Group, HUN-REN Institute of Earth Physics and Space Science, Csatkai Endre utca 6-8, Sopron 9400, Hungary; spranitz.tamas@epss.hun-ren.hu

[2] Lithosphere Fluid Research Lab, ELTE Eötvös Loránd University, Hungary;

[3] Doctoral School of Environmental Sciences, ELTE Eötvös Loránd University, Budapest 1117, Hungary;

[4] MTA-EPSS Lendület Pannon Lit$H_2$Oscope Research Group, HUN-REN Institute of Earth Physics and Space Science, Sopron, Hungary;

[5] Doctoral School of Earth Sciences, ELTE Eötvös Loránd University, Hungary;

[6] CAMECA, 29 Quai des Gresillons, Gennevilliers 92230, France;

[7] Isotope Climatology and Env Research Centre, HUN-REN Institute for Nuclear Research (ATOMKI), , Hungary;

[8] Copernicus Inst of Sustainable Devel, Utrecht Univ, Princetonlaan 8a, 3584 CB, Utrecht, The Netherlands

[9] József and Erzsébet Tóth Endowed Hydrogeology Chair, ELTE Eötvös Loránd University, Hungary;

[10] IFP Energies Nouvelles, Rond-point de l'Echangeur de Solaize BP 3, Solaize 69360, France

[11] Supervisory Authority for Regulatory Affairs, Budapest, Hungary

---

Stable isotope composition of $CO_2$ is a powerful tool to trace lithosphere scale fluid processes like Earth's degassing and global carbon cycling. Fluid inclusions (FI) encapsulating $CO_2$-rich fluids provide direct evidence on paleofluid migration events that took place at different levels of the deep lithosphere. On the other hand, deep fluid signature can also be detected in dissolved gases of much shallower-seated groundwaters, indicating the lithosphere scale connection of deep and shallow fluids. We present here preliminary results of the ongoing project FluidsByDepth, which aims to give contributions to the understanding of non-volcanic natural $CO_2$ degassing in the central Pannonian Basin. A comparative study has been carried out by determining the carbon and noble gas composition of deep lithospheric fluid as well as shallow groundwater's dissolved gases in the Bakony-Balaton Highland Volcanic Field, Hungary.

A detailed characterization and thus careful selection of FI permitted the filtering out of late-stage fluid inclusions, which was also supported by the results on previous studies made on the same xenoliths in the sample series. Moreover, groundwater was sampled considering the geohydrologic flow directions and hence was made at discharge areas.

Stable isotope compositions of FI were estimated both by crushing technique and Raman spectroscopy. One further goal of this study is to test the applicability to calculate $\delta^{13}C$-$CO_2$ isotope compositions of fluids based on in situ Raman spectroscopic measurements. We applied this method on fluid inclusions in xenoliths, including harzburgite, lherzolite, websterite, mafic-, felsic and metapelitic granulites, which sampled both the upper mantle and the lower to upper crust. In total 129 individual FI were selected in different host minerals, such as clinopyroxene, orthopyroxene, olivine, plagioclase and garnet.

The $\delta^2H$ and $\delta^{18}O$ stable isotopic ratio of the sampled groundwaters indicate meteoric origin and show no sign of an additional deep basin (metamorphic, magmatic) contribution. In contrast, the $\delta^{13}C$ isotopic ratio of the dissolved $CO_2$ gases shows a narrow range (-5.2 – -9.6) and suggests mantle origin with slight organic sedimentary overprint. Stable isotopic ratios of dissolved helium also clearly indicate mantle origin for specific domains of the volcanic area.

Our results highlight the indirect role of preceding monogenetic upwelling channels as well as their relation to groundwater discharge areas in recent mantle degassing, which could be important contribution to deep carbon cycle.

# Pfaffenbergite and "phase 430" new minerals in crystallized melt inclusions

Lorenzon, S.[1*], Ferrero, S.[2], Borriello, R.[1,3], Mugnaioli, E.[1], Borghini, A.[4], Fuchs, R.[5], Wirth, R.[6], Schreiber, A.[6] and Grew, E.S.[7]

[1]Department of Earth Sciences, University of Pisa, Via Santa Maria 53, I-56126 Pisa (Italy)

*Corresponding author: sofia.lorenzon@dst.unipi.it

[2]Department of Chemical and Geological Sciences, University of Cagliari, Blocco A, Cittadella Universitaria, I-09042 Monserrato (Italy)

[3]Department of Environmental Sciences, Informatics and Statistics, Ca' Foscari University of Venice, Via Torino 155, I-30172 Mestre (VE) (Italy)

[4]Faculty of Geology, Geophysics and Environmental Protection, AGH University of Kraków, 30-059 Krakow (Poland)

[5]Institute of Geosciences, University of Potsdam, Karl-Liebknecht-Straße 24/25, D-14476 Potsdam (Germany)

[6]Helmholtz-Zentrum Potsdam, Deutsches GeoForschungsZentrum (GFZ), Telegrafenberg, D-14473 Potsdam (Germany)

[7]School of Earth and Climate Sciences, University of Maine, Orono, Maine 04469 (USA)

---

Crystallized melt inclusions are key objects for investigating genetic processes and petrologic evolution in a wide range of geological settings. In the last decades, the study of primary melt and fluid inclusions (MIs and FIs) in garnets from high-grade and ultra-high-grade metamorphic rocks has provided information about the role of crustal material involved in volatile cycles at depths up to ~150 km [1]. Such MIs can be described as aggregates of micrometric crystals, occasionally still containing residual glass. Most MIs in garnet have a granitoid chemical composition [1, 2]. In addition to common mineral phases, such as quartz, K-feldspar, plagioclase and micas, other exotic and rather rare minerals were found, e.g., kokchetavite and kumdykolite, polymorphs of K-feldspar and albite, respectively [3]. However, given the nanometric to micrometric size of these crystals, it was often impossible to determine their crystal structure using conventional X-ray diffraction methods. Therefore, these mineral phases have been mainly identified by micro-Raman spectroscopy.

Here, we present a crystallographic study of two new mineral phases found in nanogranitoids hosted in several garnets in eclogites from Pfaffenberg [4], in the Saxon Granulite Complex and from Saidenbach Reservoir in the Erzgebirge (Bohemian Massif, Germany). Their crystal structures have been solved ab-initio and refined through three-dimensional electron diffraction (3DED) data, collected by a TEM [5]. One of these minerals has been recently approved by IMA-CNMNC with the name "Pfaffenbergite" (previously known as "phase 412") [6]. This mineral has ideal formula $KNa_3(Al_4Si_{12})O_{32}$ and crystallizes in space group *P6/mcc*. Pfaffenbergite is the Na-analogue of wodegongjieite ($KCa_3(Al_7Si_9)O_{32}$, [7]), a mineral recently found in inclusions within corundum in chromitites from Luobusa ophiolite (Tibet, China). The second mineral, "phase 430", has ideal formula $K_2Ca_3(Al_8Si_{34})O_{84}$ and space group *P6/mcc*. "Phase 430" consists of a feldspathoid-like tetrahedral framework with a completely new topology.

*References:*

[1] Nicoli G and Ferrero S (2021) Geosci Front 12: 101188
[2] Cesare B et al. (2015) Lithos 239: 186-216
[3] Ferrero S et al. (2016) Contrib Mineral Petrol 171:3
[4] Borghini A et al. (2024) Eur J Mineral 36: 279-300
[5] Gemmi M et al. (2019) ACS Cent Sci 5: 1315-1329
[6] Bosi F (2024), official communication about IMA No. 2023-105 (February 4th 2024)
[7] Mugnaioli E et al. (2022) Mineral Mag 86(6): 975-987

# The evolution of large ilmenite-hosted melt inclusions: evidence of spinodal and binodal dissociation of kimberlitic carbonated silicate melt

Büttner, S.H.[1], Marima, E.[1,2], A. Rocholl[3]

[1]Department of Geology; Rhodes University, South Africa, s.buttner@ru.ac.za

[2]Centre of Exploration Targeting, School of Earth Sciences, The University of Western Australia, Perth, Australia

[3]Deutsches GeoForschungsZentrum, Potsdam, Germany

---

Ilmenite megacrysts from the 89 Ma Monastery kimberlite in South Africa contain up to 7 mm-sized primary melt inclusions (MIs) [1, 2] containing mainly calcite and Mg-rich silicate matrix (SM) material, and accessory secondary ilmenite, perovskite, spinel, kassite/cafetite, phlogopite, garnet, apatite, and serpentine. The accessory phases commonly form 100-1000 µm thin semi-coherent and, in some places, zoned domains along the MI interface to the host ilmenite. The interior of melt inclusions is occupied by variable proportions of calcite and SM. Raman spectroscopy indicates that the SM commonly contains sub-SEM scale serpentine, but high-Mg silicate glass is preserved in some samples [1]. SIMS analysis of glass shows variable volatile contents of up to 9.8 wt% $CO_2$ and 10.3 wt% $H_2O$.

In carbonate-rich MIs, calcite forms large coherent domains that occupy most of the inclusions, forming a small number (1-3) of large crystals. Within the less abundant SM, small (<5 µm to >50 µm) calcite domains form an emulsion-type pattern with increasing calcite size towards the large coherent calcite domains. Other Ca-rich phases, such as Ca-Fe-Ti-rich garnet, are surrounded by thin SM seams that are calcite-free. Coherent domains of calcite-free SM rarely exceed ~100 µm in size. This pattern is consistent with carbonate-silicate melt segregation achieved by nucleation and growth of carbonate droplets. By contrast, in MIs containing low proportions of calcite, the SM forms large coherent domains separated from equally coherent calcite domains. In one sample, ROM264, calcite and the SM are separated by a ~300-500 µm thick zone of interconnected meandering and intertwined channels that consist of either calcite or Fe-Mg-rich silicate similar to the SM. These patterns are consistent with the spinodal segregation of an initially homogenous carbonated silicate melt.

In neither the SM nor the carbonate, Ti, P or K are abundant. This suggests that the crystallisation of kassite, perovskite, phlogopite, garnet, and minor apatite preceded melt segregation and quenching, and depleted the primary melt of these elements. This is consistent with trace element depletion of the SM melt during rapid perovskite growth in similar olivine-hosted MIs from the Monastery kimberlite [2]. Thereafter, Ca carbonate and Mg-Fe-Si-$H_2O$ components segregated by nucleation and growth of carbonate melt droplets or calcite, or by spinodal silicate-carbonate melt separation. The residual silicate melt, depleted in Ca, Ti, K and trace elements, had a composition close to Fe-rich (5-15 wt% FeO) serpentine, which in most cases formed as a (likely metastable) quench product or during the subsequent devitrification of glass. Where glass is preserved, it may still contain substantial amounts of $CO_2$.

The evolution of melt batches contained in primary ilmenite-hosted MIs [1] strongly suggests the presence of a carbonated silicate melt in the subcontinental lithospheric mantle of the Kaapvaal Craton, which crystallised, differentiated, and quenched during and after its ascent to the emplacement level close to the surface.

*References:*

[1] Büttner et al. (2023) Gondwana Res 115:81-97

[2] Howarth and Büttner (2019) Gondwana Res 68:116-126

# Innovative methodology for exploration of marine hydrocarbon deposits according to geological predictive criteria and mineralogical-thermobarogeochemical prospecting signs (using the example of the Black Sea)

Yanko, V. [1], Naumko, I.[2], Kadurin, V. [3], Zinchuk, I. [4], Dikol, O. [5], and Kadurin, S. [6]

[1,3,5,6] Department of Marine Geology, Hydrogeology, Engineering Geology and Paleontology, Odessa I.I. Mechnikov National University, 2 Shampansky Lane, Odessa 65015, valyan@onu.edu.ua

2,4 Institute of Geology and Geochemistry of Combustible Minerals NAS of Ukraine, 3-a Naukova St., Lviv 79060, Ukraine

---

In geology, progress is determined by a change in the main paradigm. In the theory of oil and gas formation, we understand the transition from organic theory to inorganic concept to be a paradigm shift. The latter implies the generation of hydrocarbons at great depths in the course of the Earth's core and mantle hydrogen degassing with subsequent transportation of deep fluids (along “degassing pipes”) to reservoir rocks as a special case of oil and gas polygenesis in the Earth’s mantle.

The great importance of this concept is the inexhaustibility of hydrocarbon deposits, since regeneration of hydrocarbon substances occurs despite their exploitation. It is clearly evident in the exploitation of oil and gas fields in large hydrocarbon provinces, such as the Persian Gulf countries.

The proposed methodology is based on the following principles: (1) Necessity and sufficiency; (2) Ranking of information; (3) Direction of information interpretation; and (4) Superposition of informative ranks: geophysical, structural-geological, gas-geochemical, mineralogical-thermobarogeochemical, micropaleontological, and isotopic, providing multidisciplinary interpretation of geological and geophysical information [1]. The mineralogical-thermobarogeochemical rank, which relays genetic information preserved in the form of persistent typomorphic features, both in fluid inclusions and in the crystalline structure of clayey layered minerals, is of paramount importance for identifying the exits of “degassing pipes” on the seabed. The most convincing indication of the influx of hydrocarbon flows from the subsurface were obtained from the study of gas-liquid inclusions in minerals from deep (2500-3000 m) parametric wells.

Microscopic observations of calcite from veins in Jurassic limestone of parametric well 2 on the Pradneprovskaya structure of the Black Sea shelf [2] identified gas-liquid inclusions with a ratio of aqueous solution (L) and gas phase (G) of 80 to 20. Mass spectrometry recorded stable high content of hydrocarbons within “degassing pipes”: $CH_4$ and homologues of CnH2n+2 (> 85 vol%), $CO_2$ and N (insignificant), and gas saturation (up to 1.0 Pa). Unlike the Jurassic limestone, the Cretaceous limestone is dominated by low saturation of $CO_2$ (65 vol%) over $CH_4$ and its homologues. Thus, the content of reduced gases decreased, while oxidized gases increased.

Subvertical inflow of fluids from deep horizons is also confirmed by high CH4 and significant gas saturation of samples from other prospective areas: Desantnaya, Karkynitskaya, and Stormovaya..

Therefore, mineralogical and thermobarogeochemical indicators are reliable typomorphic features that support evidence of vertical migration of fluids in exploring prospective oil and gas-bearing rock complexes of the northwestern shelf of the Black Sea [3].

*References:*

[1] Chepizhko O et al (2020) Herald of ONU. Geogr and Geol Sci 25,2(37): 289–309

[2] Yanko et al. (2024) Marine Environmental Research 193: 106285

[3] Naumko I (2020) Geophys. Journal 42(4): 72–96

# Immiscible fluids and melts trapped in garnet from pyroxenite-veined garnet peridotites related to metasomatism by basaltic melts

Čopjaková, R.[1], Kubeš, M.[1,2], Talacko, J.[1], Kotková, J.[1,2]

[1]Department of Geological Sciences, Masaryk University, Kotlářská 2, 611 37, Brno, Czech Republic / copjakova@sci.muni.cz

[2]Czech Geological Survey, Klárov 3, 118 21, Prague 1, Czech Republic

---

Multiphase solid inclusions (MSI) in garnet peridotites in the Gföhl Unit of the Moldanubian Zone, Bohemian Massif, provide direct constraints on metasomatic processes in the mantle beneath the Central European Variscides. Here, we present results of a detailed study on two contrasting types of MSI coexisting in garnet in two pyroxenite-veined garnet peridotite bodies Pd1 and Pd2 hosted by Gföhl gneisses and located about 40 km apart.

Both types of MSI are primary and preferentially concentrated in garnet cores. Tiny MSI with equant polygonal shape composed of oxides (rutile, ilmenite, spinel) along with silicates (amphibole, orthopyroxene, olivine and clinopyroxene) are common in both areas. These oxidic MSI (hereafter MSI-ox) are rarely decrepitated. The MSI of the second type are larger and intensively decrepitated, surrounded by haloes and trails of small inclusions, with obvious recrystallization of the host garnet. In Pd1, these MSI are composed mainly of silicates (amphibole, orthopyroxene, phlogopite) ± spinel and pentlandite (referred as silicate MSI = MSI-sil). By contrast, carbonates (magnesite>dolomite) commonly occur along with silicates (amphibole, orthopyroxene, clinopyroxene, phlogopite) and minor spinel, apatite and pentlandite (hereafter carbonate-silicate MSI = MSI-carsil) in Pd2 body. Ti-bearing oxides are completely absent in MSI-sil and MSI-carsil.

Post-trapping processes can partially modify chemical composition of the former fluids [1]. These processes were commonly observed in larger MSI with irregular contours and re-entrant angles and they included 1) non-equilibrium dissolution and precipitation of the host garnet resulting in partial enrichment of MSI-carsil in Cr and Ti; 2) chemical interaction between the host garnet and MSI-ox producing locally a symplectite rim of step-daughter minerals; 3) diffusion-controlled exchange of Fe and Mg between the MSI-ox and host garnet in Pd1 resulting in increase of $X_{Mg}$ in the MSI; 4) loss of material, especially water from MSI-sil and $CO_2$ and $N_2$ from MSI-carsil, during decrepitation events.

Despite the partial modifications of fluids during post-trapping processes, the study of MSI provided a valuable insight into complex metasomatic processes in mantle and chemical and physical character of metasomatizing medium. In both peridotite bodies, lherzolite metasomatism relates to percolation of primitive basaltic melts, now preserved as abundant garnet pyroxenite veins. The percolating basaltic melts were hydrous, $CO_2$-bearing, with important admixture of crustal component (high Cs, Rb, Ba, Pb, U, Li, + REE contents in Pd2). Immiscible, dense Ti-Mg-Fe-rich oxide melt and solute-rich aqueous fluid (Pd1) and dense Ti-Mg-Fe-rich oxide melt along with high-density silicate-carbonate fluid (Pd2) likely separated from the basaltic melt upon cooling and were trapped in garnet.

*References:*

[1] Frezzotti ML and Ferrando S 2015 Am Mineral 100:352-377

## A protocol to interpret magmatic processes recorded by melt inclusions

Esposito, R.[1]

[1] Dipartimento di Scienze dell'Ambiente e della Terra, Università di Milano Bicocca, Italy

---

One drop at the time, melt inclusions (MI) trapped in phenocrysts help to unveil magmatic processes at the microscale in a magma reservoir before an eruption. Thus, MI are studied to understand magma evolution during magma differentiations[1]. Researchers have studied MI to x-ray the plumbing system below a volcano or to constrain magma dynamics. In fact, pressure (depths) control the amount of volatile dissolved in silicate melt if magma is volatile-saturated. Magma dynamics, in turn, have implications for volcanic hazards. In addition, MI are able to record the composition of magmatic volatile phases (MVP[2]) at sub-volcanic depths giving information about the genesis of ore deposits. Lastly, one drop at the time MI may record the pre-eruptive volatiles to evaluate volatile global budget of the Earth and other extra-terrestrial bodies as the Moon. In any dataset relative to MI hosted in single crystals or in single samples, one can observe variable concentrations of major/minor/trace elements and volatiles. This variability of MI compositions can be explained either by microanalytical issues, or by post entrapment modification, or by magmatic processes as MI are trapped at different times during the evolution of a magma.

The work presented here is based on some recent works[1,3]. I present a method that could help to select MI which may be the best candidates to record reliably the composition of a melt representing a specific time and a specific space associated to the evolution of a magma below a volcano. The proposed protocol consists of four stages: 1-sample preparation aiming to study multiple MI study in the same crystals, 2-petrography of MI aiming to assess their relative age, 3-comparing composition of MI with that of bulk rocks and thermodynamical modeling, 4-interpretation of MI composition based on stage 2 and 3. Applying this protocol helped to assess mixing processes[3] and interpreting pre-eruptive volatile contents associated to single eruptions…one drop at the time.

*References:*

[1] Esposito R (2021) Mineralogical Association of Canada, Special Publication 49: 163-194

[2] Candela P A (1990) Ore-bearing Granite Systems, 11-20.

[3] Esposito R et al. (2023) Lithos *456*, 107301

# TEM study of a lower mantle mineral inclusion suite in a super-deep diamond

Ogunjobi, C.[1], Singerling, S.[1], Schreiber, A.[2], Bulanova, G.[3] and Brenker, F. E.[1]

[1]Schwiete Cosmochemistry Laboratory, Goethe University, 60438 Frankfurt, Germany
*cecily.ogunjobi@stud.uni-frankfurt.de, [2]GFZ, Potsdam, [3]University of Bristol, UK.

---

*Introduction*. The super-deep diamond P11 Machado hosts a unique mineral inclusion assemblage of olivine, diopside, enstatite, ferropericlase and $CaSiO_3$-walstromite. The coexistence of these minerals in the centre of a gem-quality diamond suggests a lower mantle (LM) origin, as the minerals are considered to be a forbidden assemblage in the upper mantle (UM) (e.g. [1]). Hence, this paragenesis must be linked to retrograde phase transitions [2] due to decreasing pressure during ascent of the diamond host [3, 4]. Inclusions of ferropericlase, enstatite and olivine, present in P11 and stable at UM-pressures, suggest a retrogression from ferropericlase and bridgmanite [3, 4]. Diopside can form through low pressure reactions between bridgmanite and $CaSiO_3$-perovskite or its lower pressure modification breyite [3, 4]. Breyite was found as inclusion in P11 as well. This study aims to examine this rare suite of micro-inclusions with respect to their micro- and nano-structural characteristics, including crystal defects, like dislocations, stacking disorder and twinning, as well as chemical heterogeneities, such as exsolution and precipitations.

*Methods.* Prior to the application of the main technique, (transmission electron microscopy (TEM)), scanning electron microscopy (SEM) images of the inclusion cloud within P11 were acquired. Electron transparent thin films of the micro-inclusions were prepared by the focused ion beam (FIB) technique. TEM work was performed on the ThermoScientific Talos F200X G2 located at the Schwiete Cosmochemistry Laboratory – SCL, Goethe University, Frankfurt am Main, Germany. This TEM is equipped with a ChemiSTEM Energy dispersive X-ray spectroscopy (EDX) system, with four plate detectors, allowing for rapid quantitative chemical analyses with low detection limits. Images were acquired with bright field (BF)-, dark field (DF)- and high-angle annular dark-field (HAADF)-detectors. Crystal structures of the mineral inclusions were analysed using selected area electron diffraction (SAED) and the high-resolution scanning TEM (HRSTEM) mode.

*Results.* The inclusions are located as an inclusion cloud in the centre of diamond P11, with µm-sized ferropericlase grains being dispersed throughout the cloud centre. Diopside is Fe-bearing and shows structural and chemical heterogeneities. Dislocation features are prevalent in a polycrystalline region (as indicated by SAED patterns) showing higher Ca-contents compared with adjacent regions. HRSTEM images display Moiré-patterns and areas characterized by irregular atomic arrangements occurring between well-ordered lattice planes. Less than 10 S-enriched grains (size ~70 nm) occur homogenously throughout the diopside. The enstatite contains homogenously distributed Fe and Ni. A 1 µm sized region within the enstatite is, however, structurally heterogeneous and chemically enriched in Fe, C and Ca. Breyite shows widespread stacking disorders.

*Discussion and Outlook.* The mineral assemblage in diamond P11 corroborates its lower mantle origin. Geochemical and structural heterogeneities hint towards the formation conditions and the retrograde transition from high-pressure phases [2] to the low-pressure polymorphs during diamond exhumation [4, 5]. TEM analyses of ferropericlase and breyite will be implemented as well as further examination of diopside and enstatite. This study is the first detailed investigation of the structural characteristics of a full assemblage of minerals originally formed and trapped in the lower mantle and will help to distinguish between different depths of origin for similar inclusions in super-deep diamonds.

*References:*

[1] Liu L (2002) Contrib Mineral Petrol 144: 16-21, [2] Irifune T and Tsuchiya T (2007) Mineral physics 2: 33-62 [3] Harte B and Harris J W (1994) Mineral Mag A 58: 384-385, [4] Stachel T et al. (2000) Contrib Mineral Petrol 140: 16-27, [5] Harte B et al. (1998) Mineral Mag A 62: 575-576.

# Confocal µ-XANES as a tool to analyse Fe oxidation state in heterogeneous samples: The case of melt inclusions in olivine from Hekla volcano

Wilke, M.[1], Botcharnikov, R.[2], Garrevoet, J.[3], Portnyagin, M.[4], Klimm, K.[5], Krasheninnikov, S.[1,6], Almeev, R.[6], Moune, S.[7], Falkenberg, G.[3]

[1]Institut für Geowissenschaften, Universität Potsdam, Germany,

[2]Institut für Geowissenschaften, Johannes-Gutenberg Universität Mainz, Germany,

[3]Deutsches Elektronen-Synchrotron, DESY, Hamburg, Germany,

[4]GEOMAR Helmholtz-Zentrum für Ozeanforschung, Kiel, Germany,

[5]Institut für Geowissenschaften, Goethe Universität Frankfurt, Germany,

[6]Institut für Mineralogie, Leibniz Universität Hannover, Germany,

[7]Observatoire de Physique du Globe de Clermont-Ferrand, Université Clermont Auvergne, France

e-mail: wilkem@uni-potsdam.de

---

Here we present a confocal Fe K-edge µ-XANES method for the analysis of Fe oxidation state in melt inclusions of one-side polished samples, potentially applicable to any heterogeneous sample. The method was applied to the analysis of natural melt inclusions trapped in forsteritic to fayalitic olivine crystals of the Hekla volcano, Iceland. The new technique allows for an analysis of small volumes with high spatial 3D resolution of <100 µm$^3$. Using a confocal setup, the probed volume is restricted to that just beneath the surface of the exposed object. This protocol avoids contamination of the signal by the host mineral and minimizes self-absorption effects. The technique has been re-calibrated and tested on a set of experimental glasses with a wide range of $Fe^{3+}/\sum Fe$ ratios. The measurements on the melt inclusion series of the Hekla volcano reveal a trend in $Fe^{3+}/\sum Fe$ from 0.17 in basaltic up to 0.45 in dacitic melts, whereas magnetite-ilmenite pairs testify redox conditions with $Fe^{3+}/\sum Fe \leq 0.20$ (close to FMQ, Fayalite-Magnetite-Quartz redox equilibrium) along the entire range of Hekla melt compositions. This discrepancy indicates that the oxidized nature of the glass in these melt inclusions could be related to post-entrapment diffusive hydrogen loss from the inclusions and associated oxidation of Fe in the melt. This process may take place at any temperature above the glass transition. The $Fe^{3+}/\sum Fe$ ratio in the silica-rich melts is particularly susceptible to this process due to their low FeO content. Such observations should be critically evaluated before petrological interpretation.

# Hydrocarbons in the Ivittuut cryolite body, SW Greenland

Szreter, A.[1,2], Finch, A.A.[1] and Friis, H.[2]

[1]School of Earth and Environmental Sciences, University of St Andrews, St Andrews, United Kingdom, aas37@st-andrews.ac.uk

[2]Natural History Museum, University of Oslo, Oslo, Norway

---

The Ivittuut cryolite body was formed by $F^-$- and $CO_3^{2-}$-rich, $H_2O$-poor peralkaline melts or fluids in the continental rift setting of the Mid-Proterozoic Gardar province (SW Greenland). The intrusion consists of a massive cryolite body on top of a small granite pipe (300 m in diameter). Cryolite ($Na_3AlF_6$) in Ivittuut is normally colourless to white but also occurs in black and purple varieties. The source and petrogenetic meaning of these colours, and the genesis of the deposit, remain unresolved.

No mineralogical explanation has been proposed for the purple colour, while it was suggested that the black colour is caused by radiation damage [1] or impurities [2]. In the present study, cryolite of the three colours was examined by a combination of compositional and spectroscopic methods, supported by thermal treatment.

All colour varieties turn white on thermal treatment (purple cryolite at 300 °C, black at 400 °C). Lifetime photoluminescence revealed that the purple colour relates to a structural defect, as in purple fluorite [3], but a structural defect alone cannot account for black colour. Compositional studies did not identify sufficient radioactive elements to support radiation damage as the source of the black colour. However, scanning electron microscopy revealed µm-scale, rounded inclusions, some of which 'exploded' during the experiment. Thermogravimetry coupled with mass spectrometry demonstrated release of C and $CO_2$ from black cryolite, correlated with 2 % mass loss. In the Raman spectra, peaks at 1360 and 1615 $cm^{-1}$ consistent with hydrocarbons appear with variable intensity. The presence of hydrocarbons in the top part of the deposit, in the black cryolite variety, is concluded.

*References:*

[1] Pauly H (1977) Bull Geol Soc Den 26(1):95-101
[2] Bøgvad R (1940) Med fra Dan Geol For 9:561-564
[3] Horsburgh N et al. (2023) Phys Chem Min 50(2):15

# Co-existing fenitizing fluids and carbonatite melts derived from ultramafic lamprophyres

Ezad, I.S.[1], Chattopadhyay, S.[1,2], Shcheka, S.S.[1], Foley, S.F.[1,3] and Tuimati, S.[4]

[1] School of Natural Sciences, Macquarie University, Sydney, Australia

[2] King Fahd University of Petroleum and Minerals, Dhahran 31261, Saudi Arabia

[3] Research School of Earth Sciences, Australian National University, Canberra, Australia

[4] Department of Earth Sciences, University of Milan, Milan, Italy

---

Fenites are an enigmatic group of rocks formed by high-temperature metasomatism of country rocks adjacent to carbonatite and alkaline igneous intrusions by aqueous fluids. The geological process of fenitization is thought to result from multiple pulses of alkali-rich aqueous fluids expelled from cooling carbonatitic and/or alkaline melts [1-3]. These fenitizing fluids may play an important and unrecognised role in upgrading the Rare Earth Element (REE) contents of carbonatities and have the potential to be used as exploration tools in the search for REE deposits [3]. Descriptions of fenites and their potential utility as exploration tools is currently limited, with insufficient experimental constraints on the compositions and processes of fluid expulsion from carbonatite and alkaline magmatic systems.

We have conducted high-pressure experiments on an ultramafic lamprophyre (aillikite) at conditions in which carbonatite melts are expected to occur; depths between 25 – 90km (~0.5 – 2.5 GPa) and temperatures of 850 - 1100°C. Alkali-poor carbonatite melts were generated in all experiments at temperatures above 900°C, but co-existed with immiscible alkali-rich aqueous fluids. We determined compositions for the dissolved solutes and fluids, establishing that K is the major alkali element present in these fluids. The expulsion of K from carbonatite melts at depth may explain the lack of K-rich, and predominance of Na-rich, carbonatites in the geological record and the propensity for fenite aureoles to be dominated by K-rich phases including phlogopite and feldspar [4]. We find no evidence in our experiments of co-existing immiscible carbonatite and silicate melts.

*References:*

[1] Morogan (1994) Terra Nova 6, 166-167
[2] Le Bas (2008) Can. Mineral. 46, 915-932
[3] Elliot et al. (2017) Ore Geol. Rev. 93, 38-59
[4] Gittins, J. et al. (1975) Geol. Mag. 112, 503-507.

# The distribution and generation of Archean to Recent carbonatites

Gibson, S.A.[1], McKenzie, D.[2] and Lebedev, S.[3]

[1]Dept of Earth Sciences, University of Cambridge, UK

---

Carbonatites play an important role in the deep cycling of carbon from Earth's mantle to its surface. Nevertheless, the physio-chemical framework that generates these $CO_2$-rich melts has been contentious for more than 60 yrs (e.g. Bailey, 1964 [1]). This primarily reflects the diverse tectonic settings where carbonatites occur: large igneous provinces; continental rifts and major extensional terranes; syn-to post-collisional settings; and ocean islands. The small volumes of these exotic melts, however, make them ideal probes of conditions in their directly underlying source regions. By combining locations of carbonatites with new global maps of lithospheric thickness, derived from seismic tomography, we show that those emplaced on the continents following Pangea break-up (i.e. <200 Ma) occur above the margins of thick cratonic lithosphere (e.g. adjacent to S. Atlantic and Indian Oceans or in N. America & Greenland. Figure 1), and also in regions where once thick lithosphere has undergone stretching (e.g. E. Asia). While the cratonic mantle modulates the carbon flux from Earth's convecting mantle to its surface and a major sink (C=6 ±3 x $10^{18}$ kg; Gibson & McKenzie, 2023 [2]), our work shows that at least in Phanerozoic times the outflux of C primarily occurs above craton margins.

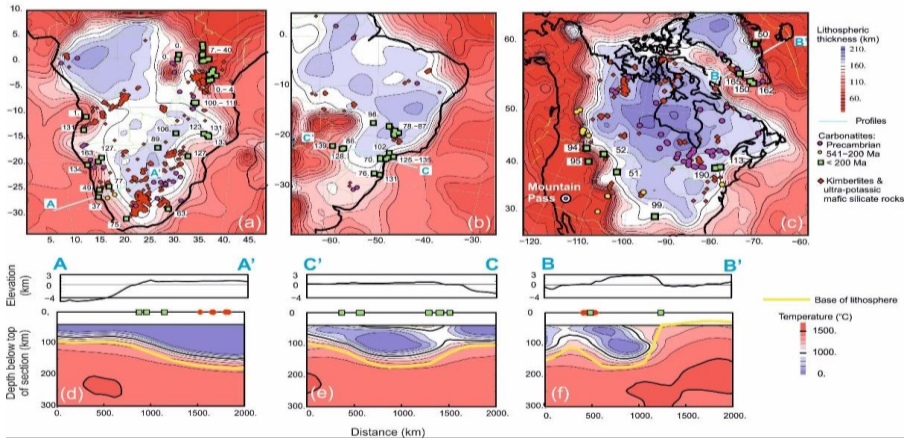


Figure 1. Lithospheric thickness maps & profiles showing distributions of carbonatites and kimberlites.

Only a few carbonatites have high $^3He/^4He$ ratios indicative of a primordial mantle component but $\delta^{11}B$ and $\delta^{34}S$ isotopes indicate the presence of recycled crustal components in mainly Phanerozoic carbonatites. These and other carbonate-peridotite derived melts are likely to remain interconnected at small melt fractions, be expelled from the asthenosphere and move upwards into the lithosphere. But their migration is too slow, and the volumes too small, to perturb the temperature, and the upwelling melt will solidify at a depth where the steady-state geotherm is at the carbonated peridotite solidus, i.e. at depths of 65-100 km. Our thermal modelling shows that lateral and vertical heat conduction on rifted craton margins, or rapid stretching of cratonic lithosphere, can mobilise metasomatised carbonated peridotite at the temperatures (950 to 1250 $^oC$) and pressures (2 to 3 GPa) required to form primary carbonatites or their parental alkali silicate melts. Importantly, our models show that heat conduction from either upwelling mantle plumes or ambient mantle on cratonic margins may sufficiently modify the temperature of the lithospheric mantle to cause melting of carbonated peridotite, settling the long-standing debate on the role of rifting and heating in the generation of Archean to Recent carbonatites.

*References:*

[1] Bailey, D.K., 1964. J. Geophys. Res., 69: 1103–1111.

[2] Gibson, S.A. & McKenzie, D., 2023. Earth Planet. Sci. Letts., 602: 117946.

## Distribution of hydrous carbonate liquid in dunite: an experimental study

Fumagalli, P.[1], Capizzi, L.[1], Ildefonse, B.[2], Tumiati S.[1] and Poli S.[1]

[1]Dipartimento di Scienze della Terra A. Desio, University of Milan, Italy patrizia.fumagalli@unimi.it

[2]Géosciences Montpellier, Université de Montpellier, CNRS, Montpellier, France

---

It is widely accepted that carbonate melts are important metasomatic agents within the Earth mantle. Their physical properties control their mobility from the source region to shallower depths, contributing to the long-term carbon cycle. Grain-scale distribution of partial melts is essential to the understanding of mass transport properties in these magmatic systems. Previous experiments assess the geometry and connectivity of intergranular liquids through measurements of dihedral angles (θ). Carbonate melts in contact with olivine develop θ of around 28° - 30° [1, 2], smaller than values for silicate melts in contact with any other silicate mineral. This suggests that, even at very low melt fraction, low density and viscosity carbonate liquids remain interconnected in a dunite matrix, making them extremely mobile at mantle conditions. Although natural carbonatitic melts are complex chemical systems with C–O–H species as major component, previous works have mainly investigated anhydrous model systems. The aim of this study is to explore texturally equilibrated geometries of volatile-rich carbonate melts in a dunite matrix as a function of time and water content.

Piston-cylinder experiments were run at 2.5 GPa, 1200°C from 3 to 306 hours, juxtaposing a pre-sintered dunite rod, made of sieved (<64 μm) San Carlos olivine, annealed at 0.8 GPa and 1200°C, to a hydrous carbonate source (with 5 or 30 wt.% added water) of dolomitic composition. Polyhedral olivine grains show well-developed triple junctions and evidence of crystal growth. Hydrous carbonatitic fraction is organized both as melt pockets along olivine grain boundaries and, in long lasting runs, as interconnected channels. The volume of liquid fraction infiltrated into the dunite matrix decreases from 10 vol.% to 2 vol.% as run duration increases and it is lower in experiments performed at higher water content. The addition of water into a carbonatitic melt shifts the apparent dihedral angle toward values significantly higher as compared with silicate and anhydrous carbonatitic melts. Dihedral angles evolve with time, ranging from ~ 31° at 3 hours run duration, to ~ 41° at 300 hours and reach almost 50° in runs with the highest water content (30 wt. %).

The evolution of wetting angles mimics sintering processes of the solid matrix [3] and can be the frame in which channelization can be explored. These results provide new insights into the mobility and interconnectivity of carbonatitic liquids in the Earth's mantle. The experimental approach using synthetic dunite and hydrous carbonatitic melts sheds light on the influence of water and challenges previous assumptions about the wetting behaviour of carbonatitic liquids.

*References:*

[1] Hunter and McEnzie (1989) EPSL 92:347-356
[2] Watson et al. (1990) in *Continental Mantle (ed. M.A. Menzies), Clarendon Press, Oxford*, 111-124
[3] German et al. (2009) J Mater Sci 44: 1-39

# Bromine partitioning between olivine, orthopyroxene and silicate melt at MORB and OIB source conditions

Joachim-Mrosko, B.[1], Clay, P.[2], Pawley, A.[3], Burgess, R.[3], Ballentine, C.J.[4] and Busemann, H.[5]

[1]University of Innsbruck, Institute of Mineralogy and Petrography, bastian.joachim@uibk.ac.at

[2]University of Ottawa, Department of Earth & Environmental Sciences

[3] The University of Manchester, Department of Earth and Environmental Sciences

[4]University of Oxford, Department of Earth Sciences

[5]ETH Zürich, Institute of Geochemistry and Petrology

---

The volatile and incompatible behaviour of the heavy halogens, chlorine, bromine and iodine, makes them excellent tracers for volatile transport processes in the Earth's mantle. Knowledge of the budget and distribution of bromine and iodine in the Earth's mantle is, however, very limited due to their extremely low abundances in the major phases of the Earth's upper mantle and a lack of well-defined partition coefficients that describe their behaviour during partial melting in mid-ocean ridge basalt (MORB) and ocean island basalt (OIB) source regions.

We performed high-pressure-high-temperature experiments at 1.0 and 2.3 GPa and between 1573-1873 K to partially melt an Fe-free peridotite-analogue at Earth's upper mantle conditions that was doped with heavy halogens Cl, Br and I. Microprobe analyses of the analytical run products reveal that they contain olivines and/or orthopyroxenes that are embedded in a glassy matrix, which represents a quenched silicate melt. With expected Br concentrations in olivine and orthopyroxene being below 1 ppm, a direct conventional analysis of Br concentrations is not possible due to a lack of well-defined standard materials and detection limits of most analytical methods that are above the expected Br concentrations in the minerals. In this study, the neutron-irradiation noble gas mass spectrometry (NI-NGMS) technique [1] was coupled with a UV-laser ablation technique, which allowed us for the first time to determine extremely small amounts of bromine in individual, nominally anhydrous minerals.

First results show that bromine behaves indeed very incompatible with partition coefficients between olivine/orthopyroxene and silicate melt being well below $10^{-3}$ at MORB and OIB source regions. For example, $D_{Br}^{fo/melt}$ = 4.5 ± 1.6 ×? $10^{-4}$ at 1773 K and 1 GPa, and $D_{Br}^{opx/melt}$ = 1.3 ± 1.0 ×? $10^{-5}$ at 1873 K and 2.3 GPa.

This implies that olivine is due to its large modal abundance potentially the most important carrier mineral for bromine in the Earth's upper mantle while orthopyroxene plays only a minor role. A combination of our newly determined partition coefficients with already known bromine bulk rock concentrations in MORBs and OIBs [2] will allow us to significantly improve our knowledge about the budget and distribution of bromine in the Earth's mantle and its recycling through subduction of oceanic lithosphere.

*References:*

[1] Johnson LH et al. (2000) Geochim Cosmochim Acta 64: 717-732

[2] Kendrick MA et al. (2017) Nat Geosci 10: 222-228

## Boron isotope fractionation in subducted oceanic crust

Xu, J.D.[1,2], Marschall, H.R.[1,2], Gerdes, A.[1,2], Schmidt, A.[1,2] and John, T[3].

[1] FIERCE (Frankfurt Isotope & Element Research Center), Goethe-Universität Frankfurt, Germany
xu@em.uni-frankfurt.de; marschall@em.uni-frankfurt.de

[2] Institut für Geowissenschaften, Goethe-Universität Frankfurt, Germany

[3] Department of Earth Sciences, Freie Universtät Berlin, Germany

---

Subducted oceanic crust plays an important role in controlling the chemical budget of the crust and mantle and produces abundant arc magmas. A key tracer for unravelling subduction-zone processes is the trace-element boron and its isotope ratio ($^{11}B/^{10}B$) with its potential to allow us quantify mass transfer processes at convergent margins and to distinguish among contrasting mass-transfer and magma-genesis models. Current models predict a strong decrease of $\delta^{11}B$ values in the subducting crust with progressive dehydration to values much below that of the depleted mantle (appr. -7 ‰). Yet, to date it is unclear to which degree these fractionation models accurately describe the processes operating in dehydrating slabs or if they indeed under- or overestimate the degree of B isotope fractionation.

The best samples to test the fractionation models are oceanic eclogites. Oceanic eclogites represent fragments of oceanic crust that have been through a subduction zone and were subsequently exhumed and exposed. A range of geochemical signatures in oceanic eclogites have been studied in the past to unravel the fluid-rock interaction processes that occur before, during and after this complex subduction-exhumation path.

We have analyzed elemental abundances and boron isotopic compositions of sets of oceanic high-pressure metamorphic rocks (blueschists and eclogites) from the Zambezi Belt (Zambia), the Cabo Ortegal complex (Spain), the Raspas Complex (Ecuador), Syros Island (Greece), and the Tian Shan (China). All of these samples have been demonstrated to represent subducted oceanic crust. Whole-rock B/Pr ratios were used to trace the progress of dehydration. The boron isotopic composition (expressed as $\delta^{11}B$) of almost all analysed samples from all of these localities is in the range of approximately -10 ‰ to +5 ‰, i.e. from values close to that of fresh MORB and the mantle to that of typical altered oceanic crust. Also, the sample set shows no correlation between $\delta^{11}B$ values and B/Pr, whereas current theoretical fractionation models predict a strong decrease in $\delta^{11}B$ with decreasing B/Pr. Our results, thus, demonstrate that B isotope fractionation in subducted oceanic crust is much smaller than predicted. We suggest that this discrepancy can be resolved by accepting high pH values of high-pressure hydrous fluids released during dehydration, which show a much smaller boron isotope fractionation in equilibrium with B-bearing silicates.

# Sources of sulphur in pyrite-rich eclogite and omphacitite xenoliths from the Navajo Volcanic Field (USA)

Pohlner, J.E.[1], Aulbach, S.[1], Stern, R.A.[2], Schulze, D.J.[3], and Helmstaedt, H.[4]

[1]Institut für Geowissenschaften and Frankfurt Isotope and Element Research Center (FIERCE), Goethe-Universität Frankfurt, Altenhöferallee 1, 60438 Frankfurt am Main, Germany (pohlner@em.uni-frankfurt.de)

[2]Department of Earth & Atmospheric Sciences, University of Alberta, Edmonton, Canada

[3]Department of Earth Sciences and Department of Chemical and Physical Sciences, University of Toronto, Mississauga, Canada

[4]Department of Geological Sciences and Geological Engineering, Queen's University, Kingston, Canada

---

Mass transfer of sulphur from slab to mantle wedge substantially influences the volatile and redox budget of the mantle, but more constraints on the sources, speciation, and isotopic composition of sulphur are needed to better characterise this process. While tectonically exhumed oceanic eclogites generally sample forearc depth only, eclogite xenoliths are usually derived from high-temperature (>800°C) regimes. An exception of subarc slab-derived xenoliths are the eclogites and omphacitites of the Navajo Volcanic Field (NVF), which record peak P-T conditions around 4 GPa and 600°C. They contain abundant (up to 2 vol%), well-preserved pyrite, which we analysed by secondary ionisation mass spectrometry.

Pyrite in the NVF samples is texturally variable, ranging from often euhedral <100 µm inclusions in garnet and omphacite to anhedral crystals several mm in size. Zonation in reflected light is common. The overall range of $\delta^{34}S$ values is large (–16 to +18‰), but values between +1 and +4‰ dominate, and extreme values are mostly confined to pyrite inclusions in garnet and omphacite as well as matrix pyrite cores. Most of the pyrite crystallised from an eclogite facies metasomatic fluid that also added Na and Si to the eclogites, variably transforming them into omphacitites. The sulphur in this fluid seems to be isotopically well homogenised and may be derived from a single source lithology. By contrast, the pre-metasomatic sulphides formed from a variety of sources and/or processes, possibly involving microbial reactions and/or seawater sulphate before subduction, and/or prograde metamorphic fluids that re-mobilised these components from other oceanic rocks.

# The speciation of sulfur in silicate melts between 1250 and 1050 °C

Gorojovsky, L. R.[1] and Wood, B. J.[1]

[1] Department of Earth Sciences, University of Oxford, South Parks Road, Oxford OX1 3AN, UK, Lauren.gorojovsky@earth.ox.ac.uk

---

The oxygen fugacities recorded by volcanic liquids and their source rocks are of great importance to Earth history, controlling and recording the compositions of C-O-H-S gases released to the evolving atmosphere and the distribution of economically valuable metals (e.g. Cu, Sn, Te, Pt) between the Earth's mantle and crust. Since sulfur can exist in oxidised and reduced forms in both the melt and vapor (e.g. $SO_4^{2-}$ and $S^{2-}$ in melt, and $SO_2$ and $H_2S$ in vapour, respectively), it has a significant impact on the redox state of magmatic systems [1]. Understanding these processes thus requires accurate knowledge of how the speciation of sulfur changes with $fO_2$, temperature, and melt composition. The solubilities of sulfate and sulfide (defined as $C_{S^{6+}}$ and $C_{S^{2-}}$, respectively) in silicate melts have thus far been characterised from 1600 to 1200 °C [2-5]. Extrapolation of the sulfate capacity to temperatures below 1200 °C indicates that there may be a non-linear dependence on reciprocal temperature. To test this, we have experimentally determined the solubility of sulfate and sulfide in silicate melts from 1250 down to 1050 °C. Natural and synthetic experimental compositions were brought into equilibrium over 1-3 days using gas mixtures of air, $SO_2$, CO, and $CO_2$ to control $fO_2$ and $fS_2$ under ambient pressure conditions. Major elements and S contents were determined on the quenched glasses by electron microprobe. The sulfate and sulfide capacities were fit with respective melt components and temperatures to equations derived from reciprocal solution theory [2]. Our results are consistent with those of previous work where temperatures overlap.

Combining the two models allows the speciation of sulfur ($S^{6+}/S^{2-}$) to be estimated as a function of $fO_2$, melt composition, and temperature. By expanding on existing models, our work now enables the determination of $S^{6+}/S^{2-}$ ratios in glasses with liquidus temperatures down to 1050 °C. These conditions are especially relevant for magmas originating from subduction zones where mixes of both $S^{2-}$ and $S^{6+}$ species are expected to occur and accordingly the effects of volatile degassing and differentiation on magma redox state is uncertain [6].

*References:*

[1] Fincham, C. J. B. and Richardson F. D. (1954) Proc. R. Soc. Lond. 223 (1152), 40–62.
[2] O'Neill, H. St. C. and Mavrogenes, J. A. (2002) J Petrol 43, 1049-1087
[3] O'Neill, H. St. C. and Mavrogenes, J. A. (2022) GCA, 334, 368-382
[4] Boulliung, J. and Wood B. J. (2022) GCA, 336, 150 - 164
[5] Boulliung, J. and Wood B. J. (2023) Contrib Mineral Petrol, 178 (8), 56
[6] Ding, S. Plank, T. Wallace, P. J. Rasmussen, D. J. (2023) G3 24 (3)

# A key role for paragonite mica in the recycling of volatiles and fluid-mobile elements in subduction zones

De Hoog, J.C.M.[1], Harris, B.H.[1] and Halama R.[2]

[1] School of GeoSciences, University of Edinburgh, UK; ceesjan.dehoog@ed.ac.uk

[2] Dept. of Earth Sciences, Keele University, UK (now at University of Halle, Germany)

White micas are major carriers of volatile and fluid-mobile elements (FME) in subducting crust. Phengite is the most common white mica in high pressure metabasites, and is stable in subducting mafic crust up to very high pressures and temperatures, and beyond the arc volcanic front. Thus, it can potentially carry volatiles into the deep mantle or may supply volatiles to the rear arc. The sodium-rich white mica paragonite is much less commonly reported in subduction-related metabasites and is generally not predicted to be stable according to thermodynamic phase-relation modelling.

However, here we present a study of 14 blueschists and eclogites collected from several high-pressure terranes and spanning a wide range of bulk $Na_2O$-$K_2O$ compositions, of which seven contain paragonite, co-existing with phengite in three samples (Fig. 1). Importantly, samples with <0.3 wt% $K_2O$ contain paragonite and no phengite, and most samples with >3 wt% $Na_2O$ contain paragonite ± phengite. Considering average MORB has 2.5 wt% $Na_2O$ and ca. 0.2 wt% $K_2O$, the dominant white mica in subducting unaltered oceanic crust is thus likely to be paragonite, not phengite. Altered oceanic crust has a wider range of compositions dependent on the type and temperature of alteration, but $Na_2O$-rich types are common, again favouring the formation of paragonite, with or without co-existing phengite depending on $K_2O$ content of the rock. Thus, considerable volumes of the subducted oceanic crust are predicted to have paragonite present.

It therefore appears that phase relation modelling overestimates the presence of phengite at the expense of paragonite, likely due to not properly predicting the muscovite component in paragonite. The common presence of phengite in high-pressure metabasites as sampled in high-pressure terranes may be related to interaction with sediment-derived K-rich fluids during exhumation. Paragonite has a more limited P-T stability field than phengite and breaks down in the slab beneath the fore or frontal arc. It contains high B and Sr (higher than co-existing phengite, if present), which will be released upon its breakdown. Thus, paragonite is a key mineral supplying FME to the sub-arc mantle wedge.

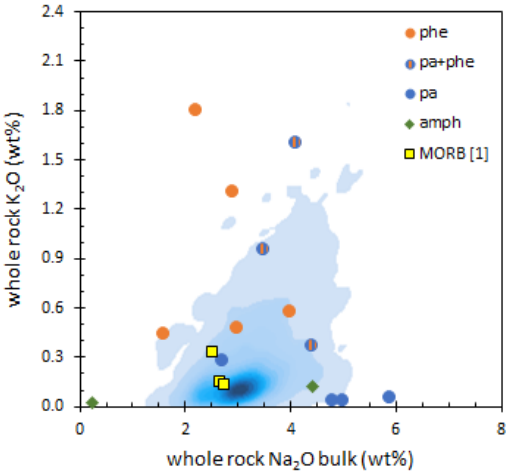


Fig. 1. White mica variety (phe = phengite, pa = paragonite) in high pressure metabasites in relation to their $Na_2O$-$K_2O$ contents. Samples indicated as *amph* (amphibole) contain no mica. Also indicated are compiled MORB estimates [1] and density contours of global ocean floor basalts compiled from PetDB (n=24120), of which 84% have <0.3 wt% $K_2O$.

*References:*

[1] Hernandez-Uribe et al. (2020) J Petr 61:egaa0806

# Fluid mobile elements and volatile behaviour during serpentinite dehydration

Asetre, J.H.[1], Alard, O.[1,2,3],Ezad, I.S.[1], and Foley, S.F.[1,2]

[1]School of Natural Sciences, Macquarie University, North Ryde, New South Wales, Australia; johannah.asetre@hdr.mq.edu.au

[2]Research School of Earth Sciences, Australian National University, Acton, ACT, Australia

[3]Géosciences Montpellier, Université de Montpellier, Place Eugène Bataillon, Montpellier, France

---

Geochemical exchanges occurring along subduction zones remobilize life-essential elements (e.g. C, H, O, S, F, Cl) between the exospheres and the deep earth. The cycling of volatiles from the seafloor to subduction depths are a product of key metamorphic reactions, as initiated by the dehydration of the plunging slab. Central to this dynamic process is the dehydration journey of serpentinites ($Mg_3Si_2O_5(OH)_4$), capable of storing and delivering key volatiles, fluid-mobile elements (FMEs), and high-field strength elements (HFSEs) back to the mantle wedge and/or the surface, or sequester them further down to the deep mantle. However, deserpentinization reactions and the composition of subduction-derived fluids remain unconstrained today. How efficient are these reactions in releasing fluids? Do these reactions release oxidized or reduced fluids? Is S significantly extracted from slab components, and if so, at which stage does this occur? Do water and halogens enhance element transfer? All these questions remain highly debated in the literature [1-6].

By employing Raman spectroscopy and mass spectrometry techniques, we investigate the storage and mobility of the halogens and other trace elements as a function of serpentine dehydration at various depths. Results from high-pressure experiments highlight the structural breakdown mechanisms of serpentine into olivine and the key element fractionations in this system. Preliminary analyses on serpentinites and metaperidotites from the Cerro del Almirez massif (Spain) and Cima di Gagnone and Alpe Arami massifs (Switzerland) offer insights into the element storage (FMEs, HFSEs) and $\delta^{34}S$ isotopic trends which can help infer the nature of sulfur released from the subducting mantle. Indeed, volatile release and retention in the plunging slab is a complex and protracted process that merits further investigation.

*References:*

[1] Benard, A et al. (2017) Geochimica et Cosmochimica Acta 199:324-350
[2] Evans, KA & Frost, BR (2020) Journal of Petrology 62(1):1-32
[3] Kendrick, MA et al. (2018) Geochimica et Cosmochimica Acta 235:285-304
[4] Marchesi C et al. (2013) Lithos 178:128-142
[5] Pettke, T and Bretscher, A (2022) Earth Science Reviews 225:103896
[6] Piccoli, F et al. (2019) Sci Rep 9:19573

## Redox dehydration in subduction zones

Padrón-Navarta J.A.

[1]Instituto Andaluz de Ciencias de la Tierra (IACT). CSIC-Universidad de Granada, Avda. de las Palmeras, 4, 18100. Armilla, Granada (España). albero.padrom@csic.es

---

Dehydration reactions occurring in subducting slabs govern the transport of volatiles in subduction zones and trigger significant chemical and mechanical instabilities, shaping one of the Earth's most active environments. These reactions are primarily influenced by dynamic changes in temperature (T) and pressure (P) associated with the subducting slab. Some crucial dehydration reactions, particularly those linked to hydrated mantle rocks (serpentinites), release a substantial volume of fluids over a narrow temperature range, introducing singularities in fluid extraction mechanisms. Despite being conceptually straightforward to model from a thermodynamic perspective, these reactions involve numerous poorly constrained dynamic parameters under natural conditions, including kinetics, porosity generation, permeability, generated strain rates, differential stresses, and mineral-reaction mechanisms. As a result, they have become the focus of intensive and multidisciplinary research.

Among all these parameters, changes in oxygen fugacity ($fO_2$) have not traditionally been explored in addressing the dynamics of dehydration reactions and consequently in interpreting mineral isograds related to these reactions in the field. The primary reason to support this view lies in the conventional petrological belief that $fO_2$ in natural settings is invariably controlled internally by the mineral assemblage (i.e., rock-buffered $fO_2$), and therefore is not a variable parameter. Nevertheless, when fluids are introduced and under specific conditions, there exists the potential to significantly alter the inherent $fO_2$ through the infiltration of external fluids with contrasting $fO_2$.

Illustrative natural examples will be presented to demonstrate the external regulation of $fO_2$ observed in high-pressure rocks experiencing the dehydration of serpentinite within exhumed paleo-subduction zones. This external modulation is facilitated by the hydraulic interconnection of fluids originating from other lithologies, notably metapelites and metacarbonates, owing to enhanced permeability generated during the initial stages of dehydration. When these external fluids exhibit a high redox-reducing capacity (e.g., $CH_2$-$CO_2$-$H_2S$ bearing fluids), their infiltration can catalyze the kinetics of dehydration and the local precipitation of carbonates. More significantly, it has the potential to significantly modify the oxygen fugacity and the levels of redox-sensitive elements (such as sulphur) in deserpentinization fluids, thereby carrying substantial implications for our understanding of chemical recycling and the redox dynamics within subduction zones.

## Recycled Carbonate-Bearing Silicate Sediments in the Sources of Circum-Mediterranean K-Rich Lavas: Evidence from Mg-Zn Isotopic Decoupling

Zi-Tan Shu[1,2], Sheng-Ao Liu[1], Dejan Prelević[3, 4], Yu Wang[5], Stephen F. Foley[2], Vladica Cvetković[4], Shuguang Li[1]

[1]State Key Laboratory of Geological Processes and Mineral Resources, China University of Geosciences, Beijing 100083, China. Email address: zitan.shu@mq.edu.au

[2]School of Natural Sciences, Macquarie University, North Ryde, New South Wales, Australia.

[3]Institute of Geological Sciences, University of Mainz, Becherweg 21, D-55099 Mainz, Germany.

[4]University of Belgrade, Faculty of Mining and Geology, Đušina 7, 11000 Belgrade, Serbia.

[5]State Key Laboratory of Isotope Geochemistry, Guangzhou Institute of Geochemistry, Chinese Academy of Sciences, Guangzhou 510640, China.

---

The high flux of subaerial volcanic $CO_2$ emissions around the circum-Mediterranean region requires the involvement of an unusually carbon-rich reservoir, but the origin of this is still unclear. Here we aim to resolve this problem by analysing Mg and Zn isotopes for the widely distributed mafic potassic to ultrapotassic lavas in this region. These K-rich lavas have lower $\delta^{26}Mg$ but similar $\delta^{66}Zn$ compared to mid-ocean ridge basalts (MORB). No known magmatic processes can explain the isotopic data, which must therefore be characteristics of the mantle sources. Recycled carbonate sediments are capable of explaining the low $\delta^{26}Mg$, but they typically also have high $\delta^{66}Zn$. Thus, the low $\delta^{26}Mg$ but unfractionated $\delta^{66}Zn$ of these K-rich lavas define "Mg-Zn isotopic decoupling" which has not yet been observed for other types of mantle-derived lavas. The carbonate-bearing silicate sediments analysed here possess low $\delta^{26}Mg$ and MORB-like $\delta^{66}Zn$, which can account for the Mg-Zn isotopic decoupling. Therefore, the nature of recycled materials (carbonates vs. carbonate-bearing silicate sediments) in the mantle can be distinguished by the coupling or decoupling of Mg and Zn isotopes of mantle-derived magmas. The input flux of carbon from the sediments to the lithospheric mantle is estimated to be ~8.1 million tons per year (Mt/yr), and ~22.4 Mt/yr of $CO_2$ emissions are predicted, which fit well with the observed output flux of 20.1 ± 13.4 Mt/yr. Our results demonstrate that recycled crustal carbon stored in the lithospheric mantle is an important source for the extensive subaerial volcanic $CO_2$ emissions in the circum-Mediterranean region.

# Reaction experiments constrain the products of crust-mantle interaction during the subduction of the continental crust

Borghini, A.[1], Borghini, G.[2], Ferrero, S.[3], Toffolo, L.[2]

[1]Faculty of Geology, Geophysics and Environmental Protection, AGH University of Kraków, 30-059 Kraków, Poland (borghini@agh.edu.pl).

2Dipartimento di Scienze della Terra "Ardito Desio", Università di Milano Statale, 20133 Milano, Italy

[3]Dipartimento di Scienze Chimiche e Geologiche, Università di Cagliari, 09042 Monserrato, Italy

---

Melts and fluids released by the subducted plate are responsible for the crust-mantle interaction and elements transfer to the mantle. An example of this process during the subduction of the continental crust was reported in the Granulitgebirge, Bohemian Massif [1]. Here primary granitic melt inclusions of a crustal origin are trapped in garnets of eclogite lenses embedded in garnet peridotite bodies. These inclusions were used to constrain the composition of the melt and the conditions at which crust-mantle interaction took place. The granitic melt most likely interacted with a mafic/ultramafic layer already present in the peridotite to produce the eclogites hosting it now at 2.2 GPa and 1000°C. However, the nature of the protolith is still unknown because of lack of mineralogical relicts.

In this study we performed reaction experiments to define the role of crustal melt-mantle interaction in generating garnet-bearing rocks at the conditions at which metasomatism took place in the Granulitgebirge. Reaction experiments were carried at 1.5, 2.2 and 2.9 GPa and equilibrated at 1100°C, after an initial stage at 1300°C for 1 hour. Starting materials are homogeneous mixtures of synthetic glass with the same composition of the granitic melt ($SiO_2$ = 70.95 wt%, $Al_2O_3$ = 16.84 wt%, $Na_2O$ = 5.43 wt%, $K_2O$ = 5.06 wt%) measured in the inclusions in the Granulitgebirge eclogites and two mantle protoliths. A fertile lherzolite pre-synthesized starting from a gel and a pyroxenite made by clinopyroxene and Al-rich spinel separated from a mantle mafic rock (bulk XMg = 0.74; [2]). Initial melt:rock weight proportion is 1:9, in order to simulate a rock-dominated metasomatic reaction.

The reaction lherzolite-granitic melt at 2.2 GPa results in melt consumption and crystallization of orthopyroxene-rich garnet-bearing websterite with traces of phlogopite. At 1.5 GPa the same reaction does not include garnet and produce opx-rich websterite with few amount of phlogopite + pargasitic amphibole. In the metasomatized peridotites, clinopyroxenes have higher Al and Na and lower Cr contents and garnet have higher grossular with respect to the pristine mantle phases. The reactions spinel clinopyroxenite-granitic melt completely consumed spinel and produced garnet and new clinopyroxene coexisting with an andesitic residual melt. New clinopyroxene has higher $X_{Mg}$ (0.84-0.89) and Na at lower Ti contents. At 1.5 GPa a coarse poikilitic grain (around 1 mm in size) of garnet developed suggesting very fast crystallization rate likely promoted by high amount of Al-rich reacted melt. Modal abundance of garnet, as well as its grossular content, increase with pressure and decrease with temperature, according to the reaction spinel + $cpx_1$ + granitic glass → garnet + $cpx_2$ + andesitic reacted glass. Interestingly the garnets resulting from this last batch of reaction experiments have composition similar to those in the Granulitgebirge eclogites. On contrary, clinopyroxenes crystallized by reacted melt are Al-rich diopside with low jadeite contents (Jd < 0.14), much lower than clinopyroxenes in eclogites. Our study suggests that Granulitgebirge eclogites might originate from the interaction between granitic melts and a pristine mafic rock during the subduction of the continental crust.

*References:*

[1] Borghini A et al. (2020) J Metamorph Geol 38, 207-234

[2] Borghini G et al. (2016) J Pet 54:4, 625-653

# Quantification of global $H_2O$ transport capacity in subduction zones by hydrous phases and nominally anhydrous minerals

Gies, N.B.[1], Hermann, J.[1] and Konrad-Schmolke, M.[2]

[1] Institute of Geological Sciences, University of Bern, Baltzerstrasse 1+3, 3012 Bern, Switzerland, nils.gies@unibe.ch

[2] Department of Earth Sciences, University of Gothenburg, Guldhedsgatan 5a, 41320 Gothenburg, Sweden

---

Numerous geological, petrological, and geophysical processes depend on the abundance, distribution, and transport of $H_2O$ between the Earth's surface and its interior. $H_2O$ transport in subduction zones from the surface to the Earth's interior can be accomplished by minerals containing OH in their structure. The stability of hydrous phases depends primarily on the chemical composition, initial hydration intensity and thermal structure of the subducting plate. The hydrated lithospheric mantle in cold subduction zones is especially important for $H_2O$ recycling into the deeper mantle because hydrous phases are stable to much greater depth. Additionally, $H_2O$ can be incorporated into nominally anhydrous minerals (NAMs), which equilibrate with a fluid during the breakdown reactions of hydrous phases. Because in most NAMs the transport capacity increases with increasing pressure and temperature, special attention needs to be paid to deep dehydration events.

To investigate the transport capacity of hydrous phases and NAMs we combined the subduction model on hydrous phases presented in Gies et al. (2024) [1] with a $H_2O$ partition in NAMs model. The model uses a global set of 56 subduction zone thermal patterns (Syracuse et al., 2010 [2]) in a gridded two-dimensional thermodynamic forward model, taking the migration of fluids within the slab into account. The model uses a combination of MATLAB and Perple_X, which uses Gibbs energy minimization to calculate modes of stable phases and amounts of coexisting fluid. On top of these first results, we are simulating the partitioning of $H_2O$ into NAMs based on representative FTIR measurements and literature estimates for each rock type and the most important phases in the subducting slab to compute the global $H_2O$ transport capacity. For example, by considering 600 ppm of $H_2O$ in CPX in the oceanic crust the global H2O transport into the deeper mantle in hydrous phases is exceeded. Finally, the new combined model, allows to benchmark the sensitivity of initial hydration on the transport capacity in hydrous phases and NAMs in exemplary hot, cold, and intermediate subduction zones.

Our results show:

1) The amount of subducted $H_2O$ beyond sub arc depth in hydrous phases strongly depends on the depth and intensity of the initial slab mantle hydration.
2) Hydrous phases are highly sensitive to the thermal patterns in a subduction zone, in contrast $H_2O$ transport in NAMs, is depended on the composition and increases with increasing pressure (and temperature).
3) NAMs are important for the global deep-water cycle, especially in hot subduction zones and thus could have played a major role in Earth's history when Earth was hotter.

*References:*

[1] Gies, N. B., Konrad-Schmolke, M., & Hermann, J. (2024). Modeling the global water cycle—The effect of Mg-sursassite and phase A on deep slab dehydration and the global subduction zone water budget. *Geochemistry, Geophysics, Geosystems*, 25, e2024GC011507. https://doi.org/10.1029/2024GC011507

[2] Syracuse, E. M., van Keken, P. E., & Abers, G. A. (2010). The global range of subduction zone thermal models. *Physics of the Earth and Planetary Interiors*, 183(1-2), 73-90. https://doi.org/10.1016/j.pepi.2010.02.004

# Investigating the diffusion of noble gases in the polymorphs of $SiO_2$: the decisive role of the structure

Figowy, S.[1], Mohn, C.E.[2] and Caracas, R.[3]

[1]Centre for Planetary Habitability (PHAB), University of Oslo, Oslo 0371, Norway (sarafig@uio.no)

[2]Department of Chemistry and Center for Materials Science and Nanotechnology, University of Oslo, Oslo 0371, Norway

[3]Institut de Physique du Globe de Paris, Université Paris Cité, CNRS, 1 rue Jussieu, 75005 Paris, France

---

A better understanding of the diffusion of noble gases in minerals is crucial for many geochemical applications [1]. It is essential to constrain diffusion in abundant minerals such as $SiO_2$, a major phase in crustal materials of the slab, in which trace amounts of noble gases can be incorporated via diffusion from neighbouring phases, or trapped after the crystallization of a volatile-rich melt. Its simple composition makes it a good proxy for the investigation of the diffusion of noble gases from crustal conditions to the depths of the lower mantle.

We model the diffusion coefficients of He, Ne, Ar and Kr in quartz, coesite (4-coordinated Si), stishovite, $CaCl_2$-type and seifertite (6-coordinated Si). Diffusion coefficients are computed by long *ab initio* molecular dynamics runs using the VASP software. We also use the nudged elastic band approach [2] as a complementary method to estimate the activation energy of rare events such as the very slow diffusion of He and Ne in seifertite.
Results show that the diffusion rates and paths of noble gases depend on the local environment around the diffusing atom, the noble gas nature, temperature and pressure [3]. In structures showing an octahedrally coordinated Si, the diffusion is highly anisotropic with the noble gas atoms migrating along the *z*-axis. For He, the denser the structure, the slower the diffusion. Diffusion rate globally decreases with the increasing size of the noble gases. However, the transport of He and Ne is controlled by the structure of the crystal, with Ne diffusing faster than He in very dense phases such as seifertite due to local repulsive effects. We show that a faster diffusion rate for Ne is also observed in various compounds depending on temperature, pressure and the local environment of diffusion. We also predict the diffusion loss of noble gases over geological timescales, showing that the ratio between noble gases may be impacted by $SiO_2$ phase transitions.

*References:*

[1] Baxter E F (2010) Rev Mineral Geochem 72 (1): 509–557
[2] Jónsson H et al. (1998) Classical Quantum Dyn Condensed Phase Simulat 385-404
[3] Figowy S et al. (2024) Earth. Planet. Sci. Lett 633: 118637

# Formation of hydrocarbons favored by high pressure at subduction zone conditions

Daniel, I.[1], Huang, J.[1,2] and Sverjensky D.A.[2]

[1]Universite Claude Bernard Lyon1, LGL-TPE, UMR 5276, CNRS, Ens de Lyon, Universite Jean Monnet Saint-Etienne, Villeurbanne, 69622, France

[2]Dept. of Earth & Planetary Sciences, Johns Hopkins University, Baltimore, MD 21218, United States of America

---

Subduction zones have a pivotal role for carbon transport to the deep Earth. At the surface or subsurface of subducted slabs, where temperature is moderate, carbon-bearing minerals react with water. Carbonates are readily dissolved in water and form abundant aqueous bicarbonate and carbonate under oxidizing conditions, as observed in rocks, fluid inclusions and experiments. However, the reactivity of organics in aqueous fluids, or reactions conducive to the formation of fluid hydrocarbons during subduction are still poorly understood, probably because the theory of a deep abiotic origin of hydrocarbons developed and detailed by Gold [1] has been highly controversial and discouraged investigations. Over the recent years, field and petrographic studies have provided evidence of the existence of immiscible hydrocarbon fluids in deep subducted rocks. For example, $CH_4$-$H_2$-rich fluid inclusions were detected in ultramafic rocks from the Lanzo Massif, western Italy [2], the Appalachian belt, northern Vermont [3], the Tianshan, northwestern China [4], suggesting that the formation of hydrocarbons is favored by pressures (P) greater than about 1 –2 GPa even at 400 °C. In deep (P ≥ 3.2 GPa) subducted metapelites exhumed at the Lago di Cignana (western Alps), the reduction of carboxylate was suggested during the formation of hydrocarbon fluid inclusions in diamond-forming rocks [5].

Here we report on the role of pressure influencing the formation of hydrocarbons, starting with 0.5 M Ca-acetate solutions as a carboxylate model. Experiments were performed in a diamond anvil cell coupled to *in situ* Raman spectroscopy, over a range of pressures (P) extending from 1.6 to 4.6 GPa at temperatures (T) between 300 and 350 °C [6]. Immiscible hydrocarbon fluid coexisting with aqueous carbonate or bicarbonate and crystals of calcite or aragonite formed under such P-T conditions. The quantity of immiscible hydrocarbons formed was enhanced at high pressure, and reached 65% of the carbon budget of the experiment. *In situ* Raman spectra of the co-existing aqueous solutions and analysis of the peak area ratios of acetate to $HCO_3^{2-}$ showed that pressure also increased the kinetics of hydrocarbon formation. Compared to previous experiments at 300 °C and 3 GPa with Na-acetate as the source of carbon, this study resulted in hydrocarbons enriched in methane and propane, with less isobutane. The hydrocarbon fluid became more reduced with increasing pressure. At 350 °C, isobutane transformed to one or more polyaromatic hydrocarbons in an immiscible fluid, that could be measured by UV Raman spectroscopy after quenching. Overall, our study supports the hypothesis that high pressures and high temperatures facilitate the possible occurrence of immiscible hydrocarbon fluids in the deep carbon cycle, in agreement with field studies.

*References:*

[1] Gold T (1992) Proc. Natl Acad Sci USA 89 : 6045-6049
[2] Vitale Brovarone A et al. (2020) Nat Commun 11: 1–11
[3] Boutier A et al. (2021) Lithos 396–397 : 106190
[4] Peng W et al. (2021) J Petrol 63 : egac070
[5] Frezzotti M.L. (2019) Nat Commun 10 : 4952
[6] Huang et al. (2023) Chem Geol 630: 121489

# The migration of methane-hydrogen-rich fluids may trigger seismic failure in subduction zones at forearc depths

Giuntoli F.[1], Menegon L.[2], Siron G.[3], Cognigni F.[4], Leroux L.[5], Compagnoni R.[6], Rossi M.[4], Vitale Brovarone A.,[1,7,8]

[1]Department of Biological, Geological, and Environmental Sciences, Università degli Studi di Bologna, Italy

[2]The Njord Centre, Department of Geosciences, University of Oslo, P.O. Box 1048 Blindern, Norway

[3]Département Géosciences, Université de Bourgogne-Franche-Comté, 16 route de Gray, 25030 Besançon, France

[4]Department of basic and applied sciences for engineering (SBAI), Università degli Studi di Roma La Sapienza

[5]Univ. Lille, CNRS, INRAE, Centrale Lille, UMR 8207, UMET, F-59000 Lille, France

[6]Dipartimento di Scienze della Terra, Università degli Studi di Torino, via Valperga Caluso 35, 10125 Torino, Italy

[7]Sorbonne Université, Muséum National d'Histoire Naturelle, UMR CNRS 7590, IRD, IMPMC, 75005 Paris, France

[8]Institute of Geosciences and Earth Resources, National Research Council of Italy, Pisa, Italy

---

Metamorphic fluids, faults, and shear zones are carriers of carbon from the deep Earth to shallower reservoirs. Some of these fluids are reduced and transport energy sources, like $H_2$ and light hydrocarbons. Mechanisms and pathways capable of transporting these deep energy sources towards shallower reservoirs remain unidentified.

It has been recently proposed that high-pressure genesis of abiotic hydrocarbon can lead to strain localization in subducted carbonate rocks[1]. In this study[2], we investigate omphacitite (i.e. omphacite-rich rock) adjacent to a high-pressure methane-rich fluid source from the Western Alps (Italy). In the field, omphacitite bands are up to 5 metres thick and tens of metres long and are adjacent to carbonate rocks affected by high-pressure reduction and methane-rich fluid production.

Hand specimens and thin sections display a brecciated structure, with omphacitite fragments ranging in size from a few microns to several centimetres, surrounded by a matrix of jadeite, omphacite, grossular, titanite, and graphite. X-ray compositional maps and cathodoluminescence images highlight oscillatory zoning and skeletal textures in jadeite, omphacite and garnet in the matrix, suggesting a fast matrix precipitation under plausible disequilibrium conditions. $CH_4$ and $H_2$ are found in fluid inclusions in the jadeite grains. This feature suggests a potential link between the genesis of $CH_4$ in the adjacent carbonate rocks and the brecciation event. Electron backscatter diffraction analysis was performed on omphacitite clasts close to their borders, where omphacite grain size varies between a few microns and a maximum of 100 microns. Those omphacite grains display no crystallographic preferred orientation, abundant low angle boundaries and low (< 5°) internal lattice distortion. We interpret these textures as formed by pervasive and diffuse micro-fracturing related to the brecciation occurring at high pore fluid pressure, reaching sub-lithostatic values. Thermodynamic modelling predicts that the production and accumulation of $CH_4$-$H_2$-rich aqueous fluids can produce fluid overpressure more easily than carbon-poor and $CO_2$-rich aqueous fluids.

This study provides evidence for the migration of deep Earth energy sources along tectonic discontinuities, and suggests causal relationships with brittle failure of hard rock types that may trigger seismic activity at forearc depths.

*This work is part of a project that has received funding from the European Research Council (ERC) under the European Union's Horizon 2020 research and innovation programme (No. 864045).*

*References:*

1. Giuntoli, F., et al., (2020) Sci Rep 10, 9848. https://doi.org/10.1038/s41598-020-66640-3
2. Giuntoli, F. et al. (2024) Nat Commun 15, 480. https://doi.org/10.1038/s41467-023-44641-w.

# Unravelling the redox conditions during deserpentinization through sulphide mineral assemblages

Cristóbal, L.S.[1], Padrón-Navarta, J.A.[1] and Garrido, C.J.[1]

[1]Instituto Andaluz de Ciencias de la Tierra (IACT). CSIC-Universidad de Granada, Avda. de las Palmeras, 4, 18100. Armilla, Granada (España). samuel.cristobal@csic.es

---

The origins of differences in oxidation state and volatile content between primitive arc magmas and mid-ocean ridges remain unclear. One hypothesis suggests fluids from subducted slabs oxidise the mantle wedge, with serpentinites playing a key role in terms of fluid generation [1]. However, the oxidising potential of fluids from serpentinite dehydration is still debated, as thermodynamic models predict elevated oxygen fugacity and the presence of sulphates, which are not consistently observed [2]. To investigate sulphur mobility and oxygen fugacity during serpentinite dehydration, we analysed sulphide mineral assemblages in serpentinites and metaperidotites from the Val Malenco region in the Alps. Val Malenco features substantial mantle exposure, which underwent exhumation, hydration at the seafloor, subduction-related regional metamorphism, and subsequent contact metamorphism due to the intrusion of the Bergell granodiorite. [3]. For this study, a 1.5-kilometer transect perpendicular to the Bergell intrusion (Alpe Zocca) was chosen to investigate the influence of increasing temperature on sulphur mineral assemblages and sulphide compositions. Along this transect, rocks can be classified based on their primary silicate mineral composition as follows: antigorite serpentinites (Atg-S); antigorite serpentinites with dusty clinopyroxene (Cpx-S); antigorite serpentinites with tremolite and olivine (Tr-S); partially reacted serpentinites (PR-S); olivine-talc metaperidotites (Ol-Tlc). Along the sampled transect, two primary reactions can be identified and mapped:

antigorite + diopside = olivine + tremolite + aqueous fluid (1)
antigorite = olivine + talc + aqueous fluid (2)

The combination of SEM and EMPA analyses enables the characterization of sulphide mineral assemblages, along with their major and minor compositions, along the temperature gradient delineated by contact metamorphism. The Cpx-S, and some of the Atg-S, record the lowest temperatures affected by the contact aureole, exhibiting a distinctive assemblage of oxides and sulphides including magnetite (Mt), pentlandite (Pn), heazlewoodite (Hzl), and awaruite (Awr), with an oxygen fugacity of approximately 4 log units below the FMQ buffer. The gradual increase in temperature recorded by Tr-S and Atg-S is accompanied by the presence of Mt, Pn, and pyrrhotite (Po) as the predominant sulphide-oxide assemblage. PR-S and Ol-Tlc-F are characterized by the progressive disappearance of antigorite, with sulphides evolving gradually from Mt, Pn, and Po, where Pn predominates, to a combination of Mt, Pn, Po, and in some instances, millerite (Mlr), reaching a maximum of approximately 1.5 log units above the FMQ buffer. Moreover, the sulphur content measured in the whole rock remains relatively constant along the transect. These observations suggest that during contact metamorphism, there is a progressive modification in serpentinite sulphide mineral assemblages, resulting in a gradual increase in both the oxygen fugacity ($fO_2$) and sulphur fugacity ($fS_2$) [4].

References:

[1] Evans Earth-Science Reviews, 113(1-2), 11-32 (2012). [2] Iacovino et al., Contributions to Mineralogy and Petrology, 175,1-21 (2020). [3] Trommsdorff and Connolly, Schweizerische Mineralogische und Petrographische Mitteilungen, 76,537-547, (1996) [4] Evans et al., Lithos, 278, 26-42, (2017).

# Decompression-driven crystallization of carbonate-silicate melts trapped in garnet in orogenic peridotite (NW Bohemian Massif)

Haifler, J.[1], Kotková, J.[2] and Čopjaková, R.[1]

[1] Department of Geological Sciences, Masaryk University, Kotlářská 2, 611 37 Brno, Czech Republic; haifler.j@mail.muni.cz

[2] Czech Geological Survey, Klárov 3, 118 21 Prague 1, Czech Republic

---

Orogenic garnet peridotites (lherzolite, harzburgite) in the crystalline basement of the NW Bohemian Massif contain multiphase solid inclusions (MSI) enclosed in the outer parts of garnet. The MSI reach ca. 25–40 µm in diameter and contain carbonate- and silicate-bearing mineral assemblages. They are interpreted as crystallization products of carbonate-silicate melts metasomatizing and interacting with their hosts [1, 2].

We applied conventional thermobarometry and thermodynamic modelling to investigate the evolution of the host peridotites and their trapped carbonate-silicate melts. The peak metamorphic conditions experienced by the host peridotites are estimated at ca. 1100°C and 4.5–5.5 GPa, based on Mg/Fe exchange equilibria, Al-in-Opx and Cr-in-Cpx thermobarometry. The carbonate-silicate melts originate from intrusion of garnet pyroxenite vein and further influx of volatiles involving CO2 and H2O into the hot mantle rocks, which promoted their partial melting. Subsequently, the melts evolved during their reactive infiltration into the hosts. These complex metasomatic processes triggered growth of the outer zone of the peridotite garnet, thus preserving the melt pools as inclusions. The melt entrapment is assumed to occur during an early stage of the near-isothermal peridotite exhumation path, at ca. 1000°C and 3.6–4.4 GPa.

Three carbonate-silicate assemblages occurring in the MSI were appropriate for application of the forward thermodynamic modelling (PT and PX($CO_2$) pseudosections) to evaluate the physico-chemical conditions of their (re)-equilibration. The amphibole-free mineral assemblage kinoshitalite (Ba-mica)/Ba-rich phlogopite + dolomite + magnesite + clinopyroxene + orthopyroxene + garnet + chromite provided the most robust estimates. It is stable at ca. 900-1000 °C and 1.8–2.2 GPa. The absence of olivine in the MSI corresponds to saturation of a system in a $CO_2$-rich fluid with $X(CO_2)\geq0.6$. A Monte Carlo-based verification method confirmed the robustness of the modelled stability field despite the relatively high uncertainties in the observed mineral modes (and consequently, in the estimated bulk compositions of the MSI). Two amphibole-bearing mineral assemblages in the MSI were successfully reproduced when identical P-T-$X(CO)_2$ conditions were applied. The position of the stability fields of interest in the P-T diagram agrees with a position of a near-isobaric segment of experimental solidus of carbonated and hydrated peridotite [3]. The lower solubility of silicates at the solidus, inferred from the reference experimental data, as well as concentric fabric of some MSI implies sequential crystallization with silicates followed by carbonates. The late differentiated melt was dolomitic. Our results suggest that the carbonated solidus ledge is a relatively narrow boundary in the lithospheric mantle capable of an abrupt immobilization of molten carbonates. We estimated that about 6 ppm of carbon is stored in the investigated peridotites as carbonates in the MSI.

*References:*

[1] Kotková J et al. (2021) Lithos 398-399:106309
[2] Haifler J et al. (2024) Contrib Miner Petrol 179:31
[3] Pintér Z et al. (2021) Lithos 396-397: 106224

# High-pressure metasomatism and carbonation of metaserpentinites during deformation at the subduction interface

López Sánchez-Vizcaíno, V.[1], Padrón-Navarta, J.A.[2], Menzel, M.D.[2] and Garrido, C.J.[2]

[1]Departamento de Geología, Universidad de Jaén, 23700 Linares, Spain. vlopez@ujaen.es

[2]Instituto Andaluz de Ciencias de la Tierra (IACT), CSIC-Universidad de Granada, Armilla, Granada, Spain.

---

The study of exposed paleosubduction metamorphic suites is revealing an increasing number of cases where carbonation of metaserpentinites and formation of magnesite-bearing rocks along the slab interface has occurred as a result of fluid-rock interactions under high-pressure conditions concurrent with tectonic mixing, deformation and recrystallisation. Subsequently, these hybrid metasomatic lithologies may undergo decarbonation reactions under prograde or retrograde conditions, which may influence the fluxes and cycling of C and other volatiles at convergent margins.

Here we study the Cerro Blanco ultramafic massif (Nevado-Filábride Complex, Betic Cordillera, southern Spain), which records high-pressure alpine subduction metamorphism as evidenced by the transition from antigorite serpentinite to chlorite-harzburgite due to high-pressure deserpentinisation. In this massif, decimetre-thick veins of coarse magnesite-amphibole-chlorite-magnetite aggregates are evidence of chlorite-harzburgite carbonation reactions. Such carbonation can be explained by thermodynamic models in which the infiltration of external $CO_2$ fluids derived from meta-sediments reproduces the formation of magnesite at high-pressure conditions. However, the modelling based on current high-pressure aqueous geochemistry databases predicts insufficient Ca solubility at these conditions, suggesting that the high amounts of amphibole observed may be due to locally Ca-enriched chlorite-harzburgite compositions.

Subsequent tectonic detachment and exhumation of the massif is recorded along a 60 m thick, very heterogeneous mylonite zone that includes strongly deformed marble layers, chlorite-harzburgite lenses (in some cases completely transformed into retrograde serpentinite) and transposed magnesite-bearing boudins. Combined field, EDS-SEM and EPMA data from a detailed sampling of a cross-section of this mylonite zone show that the chlorite-harzburgite magnesite veins were intensely reworked and re-equilibrated during mylonite formation. Thermodynamic modelling of these changes suggests that mineralogical and chemical re-equilibration for the resulting differently mixed hybrid bulk compositions occurred at temperatures between 550 and 600 °C. Simultaneous isothermal decompression and infiltration of $H_2O$-rich fluids induced a magnesite breakdown reaction (magnesite + amphibole + $H_2O$-rich fluid = dolomite + antigorite + $CO_2$-bearing fluid). Our results demonstrate that carbonated serpentinites are a sensitive archive of fluid flow both during prograde metamorphism and exhumation processes and act as a trap-and-release mechanism that modulates carbon fluxes in subduction zones.

Research funded by RUSTED project PID2022-136471N-B-C21 & C22 funded by MICIN/AEI/10.13039/501100011033 and FEDER program

## The continental subduction factory as a precursor to long-term volatile storage in the lithosphere

Aulbach, S.[1]

[1]Goethe University Frankfurt, Altenhöferallee 1, 60438 Frankfurt am Main, s.aulbach@em.uni-frankfurt.de

---

The transport of carbon and sulphur from the exosphere to the mantle via subduction, and their long-term storage in the mantle, versus re-entry into the atmosphere via arc magmatism, remain poorly constrained, also because this pivotal environment is rarely accessed. Subcontinental lithospheric mantle (SCLM) represents a potentially important sink and source of volatiles [1], with immense uncertainties regarding its storage capacity. Lithospheric mantle is initially stabilised by extraction of sufficient volumes of melt to increase its viscosity. This is accompanied extraction of volatile elements, which are incompatible but plausibly reintroduced via subduction. The effect of continental subduction on the volatile inventory of the overlying mantle wedge may be gauged by tectonically exhumed peridotite.

The Ulten Zone tectonic mélange (eastern Italian Alps) is a Variscan example where older SCLM was enriched in hydrous minerals and carbonates during residence in the hot mantle wedge and subsequent down-dragging to high-pressure conditions and cooling [2]. Radiogenic isotopes document a continental crustal imprint involving fluid with variable $H_2O/CO_2$ ratio and showing significant differences between different groups of peridotite lenses [e.g., 3]. This highlights that extrapolations from sparsely sampled peridotite outcrops may not be representative. Sulphides, in particular pentlandite, are ubiquitous and, depending on degree of prior melt depletion, at least in part reintroduced with a fluid or melt carrying sulphur with a minor sulphate fraction [4], attesting to redox interactions that likely involve Fe oxidation. In contrast, carbonates were largely deposited via redox-neutral carbonation reactions. If these findings are representative of continental collisions, which effectively shut down convergence and stabilise the SCLM, then huge swaths of Earth's continents affected by orogenies may be underlain by volatile-enriched SCLM, bearing in mind that this tectonic setting is affected by substantial crust-mantle decoupling.

*References:*

[1] Gibson SA and McKenzie D (2023) Earth Planet Sci Lett 602:117946
[2] Godard G et al. (1996) Tectonophys 259:313-341
[3] Gudelius D et al. (2022) Geology 50:163-167
[4] Consuma G et al. (2021) Geochim Cosmochim Acta 306:143-170

# The redox state of marble-cake mantle: clues from deeply recycled C-bearing crustal materials

Malaspina, N.[1], Langenhorst, F.[2], Pollok, K.[2], Cerantola, V.[1], Murri, M.[3], Longa, C.[1], Bersani, D.[4] and Montanini A.[5]

[1]Department of Earth and Environmental Sciences, University of Milano-Bicocca, Piazza della Scienza 4, 20126, Milano, Italy (nadia.malaspina@unimib.it)

[2]Institut für Geowissenschafte, Friedrich-Schiller-Universität Jena, Lessingstraße 14, 07743, Jena, Germany

[3]Department of Earth and Environmental Sciences, University of Pavia, Via A. Ferrata 1, 27100, Pavia, Italy

[4]Department of Mathematics, Physics and e Informatics Sciences, University of Parma, Parco Area delle Scienze 7/A, 43124, Parma, Italy

[5]Department of Chemistry, Life Sciences and Environmental Sustainability, University of Parma, Parco Area delle Scienze 157a, 43100 Parma, Italy

---

Fossil subduction zones are key locations to study the deepest geochemical cycles of C, O, S and H. In non-cratonic areas C-bearing mantle rocks were reported for the orogenic peridotite massif of Beni Bousera (Moroccan Rif belt) [1], where graphite occurs in garnet pyroxenite layers as pseudomorphs after diamond. Montanini et al. [2] found high-temperature graphite as flakes in garnet pyroxenite layers from the External Ligurides (Northern Apennine, Italy). Both sample sets show sulphides in equilibrium with carbon. These pyroxenite layers are proxies of deep recycling of subducted crust and may have formed by melt–rock reactions induced by C-S-related redox processes. We analysed the redox state of garnets and clinopyroxenes associated with C and S, related to a liquid segregated from the melting of a recycled eclogite. Transmission Electron Microscopy coupled with Electron Energy-Loss Spectroscopy and synchrotron micro-Mossbauer analyses were performed to check the $Fe^{3+}/Fe^{2+}$ distribution heterogeneities, in relation to its partitioning among mineral phases and/or to the occurrence of fluid fluxes at different redox conditions.

Our results indicate a strong partitioning between garnet and clinopyroxene at high temperature in samples from Beni Bousera, with $Fe^{3+}/\Sigma Fe$ in clinopyroxene reaching up to 0.30, vs garnets with values up to 0.07. Interestingly, graphite-bearing clinopyroxenites from External Ligurides show two generations of clinopyroxene. The first included in garnet has higher values of $Fe^{3+}/\Sigma Fe$ with respect to high temperature clinopyroxenes in the rock matrix (0.23-0.38 vs max 0.08). Garnet shows homogeneous values (up to 0.07). This variation in clinopyroxenes therefore records a variation of redox conditions, likely related to the interaction and evolution of C-S-bearing liquids, corresponding to ΔFMQ (Fayalite-Magnetite-Quartz buffer) from -0.25 to -5. These values correspond to redox conditions slightly above the CCO (Carbon-$CO_2$ buffer) to below the CCO, indicating a variation in the carbon speciation.

*References:*

[1] Pearson et al. (1994) Nature 338: 60-62
[2] Montanini et al. (2010) Geol Soc London, Special Publ 337: 87-105

# Crustal recycling into the mantle: evidence from HSE and Os isotope compositions of Ligurian garnet pyroxenites (N Apennine, Italy)

Montanini, A.[1], Luguet, A.[2], Van Acken, [2, 3], Tribuzio, R.[4]

[1]Dip. Scienze Chimiche, Vita e Sost. Ambientale, University of Parma, Italy (alessandra.montanini@unipr.it)

[2] Institute fuer Geowissenschaften, University of Bonn, Germany

[3]School of Earth Sciences, University College Dublin, Ireland

[4] Dip. *Scienze* della Terra e dell'Ambiente, University of Pavia, Italy

---

Pyroxenites derived from crustal recycling represent a major form of mantle heterogeneity. It is widely believed that they play a crucial role in magma genesis, contributing to the radiogenic Os signature of oceanic basalt sources. Here, we present HSE (Highly Siderophile Elements: Os, Ir, Pt, Pd, Re) compositions and $^{187}Os/^{188}Os$ fingerprint of a well-characterized suite of recycled pyroxenites (garnet clinopyroxenites and websterites) enclosed in mantle bodies from northern Apennine ophiolites [1,2]. The pyroxenites exhibit deeply fractionated HSE patterns, variably depleted in Os and Ir, and enriched in Pt, Pd and Re compared with host peridotites. Present-day $^{187}Os/^{188}Os$ ratios vary from moderately to highly radiogenic in the pyroxenites (0.154-2.475), corresponding to $\gamma_{Os}$ of +17 to +1810, similar to mantle pyroxenites from other suites [3,4,5,6]. The model calculations, based on bulk rock HSE compositions, indicate that the garnet clinopyroxenites are not consistent with residues after melting of oceanic crust. Instead, they reflect sulfur saturation and Base Metal Sulfide (BMS) crystallization from partial melts of eclogites derived from MORB-type gabbroic protoliths. HSE distribution and Os isotopic signature of the websterites, along with their sulfide mineralogy, suggest a hybrid origin involving contributions from both peridotitic and eclogite-derived components. The highly radiogenic Os isotope signature of the garnet clinopyroxenites reflects a long-term history characterized by high Re/Os ratios and derivation from old mafic protoliths (>1.0 Ga), followed by a relatively recent evolution, which includes a Mesozoic event of partial melting/crystallization in the presence of garnet, constrained by Nd-Hf isotope systematics [2]. The spatially associated host peridotites exhibit nearly flat chondrite-normalized HSE patterns and near-chondritic Se/Te and Pd/Ir ratios, coupled with $^{187}Os/^{188}Os$ ratios of 0.126 and 0.136. These characteristics are consistent with a history of depletion in incompatible HSE such as Pd and Re, followed by BMS addition during a melt percolation event. Such refertilization may have occurred through interaction with eclogite-derived melts under high-pressure conditions, as supported by the slightly suprachondritic $^{187}Os/^{188}Os$ value. Alternatively, refertilization could have been caused by asthenospheric melts related to rifting during the exhumation of the entire mantle section.

*References:*

[1] Montanini A et al. (2012) EPSL 351-352: 171–181
[2] Montanini A and Tribuzio R (2015) Geology 43: 911-914.
[3] Luguet A et al., 2008 Science 319: 453-456.
[4 Pearson DG and Nowell GM (2014) J.Petrol. 45: 439–455
[5] Van Acken D et al. (2010) Geochim. Cosmochim. Acta 74: 661–683
[6] Ackermann L et al. (2016) Lithos 256-257: 197-210

## Insights into molecular hydrogen solubility in $SiO_2$ polymorphs from redox-buffered experiments at subduction conditions

Toffolo, L.[1], Tumiati, S.[1], Confortini, G.[1], and Fumagalli P.[1]

[1]Dipartimento di Scienze della Terra "Ardito Desio", University of Milan (Italy).

---

The incorporation of hydrogen into various nominally anhydrous rock-forming minerals is well-established. While the focus on hydrogen solubility has dominantly centered on the formation of hydroxyl groups, emerging evidence suggests that the diffusion of molecular hydrogen ($H_2$) also plays a significant role in the Earth's interior. Specifically, the mobility of $H_2$ can impact the δD signature of mantle minerals and contribute to redox reactions, potentially influencing the equilibria among minerals, fluids, and melts. In this context, subduction zones emerge as a crucial region for hydrogen production. However, the processes of hydrogen incorporation and release, as well as the potential minerals involved, remain unclear.

To address this gap, we explored the solubility of $H_2$ in $SiO_2$ polymorphs under a range of P-T-redox state conditions relevant to subduction settings (1–9.6 GPa, 500–900 °C, ΔFMQ ~0 to ~–5.7) running piston-cylinder and multi-anvil experiments buffered using the double capsule technique. In each experiment the inner capsule was filled with a mixture of powdered ultrapure quartz sand (Sigma-Aldrich), previously calcinated at 1000 °C, and ultrapure water, while the outer capsule contained water and a mineral assemblage capable of buffering the hydrogen fugacity. After each run, a capsule-piercing device directed the quenched fluids from the inner capsules to a quadrupole mass spectrometer.

The quenched fluids exhibited significant $H_2$ concentrations, reaching a maximum of ~33 mol% for quartz at 2 GPa, 700 °C, and ΔFMQ ~–5.7. Hydrogen concentration decreased under more oxidized conditions, higher temperatures, and lower pressures. No detectable hydrogen was found in the fluid from the experiment in the stishovite stability field. Remarkably, the measured $H_2$ concentrations surpassed those predicted by thermodynamic modeling for an aqueous fluid at the investigated P-T-redox state conditions by up to two orders of magnitude. Using single quartz crystals as a starting material rather than powder did not alter the $H_2/SiO_2$ molar ratio, ruling out surface effects. Thus, we support the hypothesis that $H_2$ is soluble in quartz and coesite crystal lattice (up to ~4000 μg $H_2$/g SiO2), with bulk diffusion mechanisms consistent with observed reversible hydrogen release upon cooling and/or depressurization. The transition to a denser octahedrally coordinated structure appears to hamper this process.

Our experiments suggest that, at conditions encountered in subduction zones, quartz and coesite can act as sinks for molecular hydrogen, with important amounts of $H_2$ dissolved even at the relatively oxidized conditions of ΔFMQ ~–1.6. As the process is largely reversible, changes in P-T-redox state may induce a release of hydrogen at depth, potentially perturbing the redox state of subduction channel rocks and, ultimately, the mantle wedge.

# Volatile storage and melting processes in the thermal boundary layer and lower lithosphere beneath continents

Foley, S.F.[1,2], Chen, C.F.[1,3], Ezad, I.S.[1] and Jacob, D.E.[2]

[1] School of Natural Sciences, Macquarie University, Sydney, NSW, Australia. Stephen.foley@mq.edu.au.

[2] Research School of Earth Sciences, Australian National University, Canberra, AT 2601, Australia

[3] School of Earth Sciences, China University of Geosciences, Wuhan 430074, China

---

The incompatible volatile components $H_2O$ and carbon have been gradually accumulated and stored at the base of continental lithosphere over time. Water is transported in melts that recrystallize as discrete hydrous pyroxenite dykes which may be rich in phlogopite, amphibole, clinopyroxene, apatite and oxide minerals, whereas carbon is stored as carbonate or diamond/graphite, depending on the oxidation state. The transition from asthenosphere to lithosphere is not sudden (although commonly depicted as such) but is a thermal boundary layer (TBL) approximately 20-50km thick in which the age of dykes shows a general increase upwards. Re-melting may thus involve dykes with locally variable rock types, ages, and oxidation states: hydrous pyroxenites and peridotites are intimately juxtaposed, and rocks with carbonates and diamond/graphite may also melt independently close to each other. Although the oxidation state of the mantle generally decreases with increasing depth, it varies greatly over short distances within the TBL and lower lithosphere. Carbonates may be derived mostly from oxidised melts of subducted sediments [1], whereas diamond/graphite may additionally be derived from reduced melts originating deeper in the mantle [2].

Experiments on peridotite with mixed volatiles have delineated a range of possible melts from carbonatite to alkaline silicate, but it is usually not explained where the volatiles come from. An increasing number of experiments on hydrous pyroxenites and other likely TBL dyke lithologies are now available, which show that they all melt at temperatures below that of “damp” peridotite and also store their own volatiles [3]. Amphiboles and phlogopite melt rapidly, producing high degrees of melting in hydrous dykes where adjacent peridotite may remain unmelted. Erosion of the TBL from below by edge-driven convection, lateral advection, or regional downwelling in the asthenosphere leads to melting, which includes oxidation of diamond/graphite to form carbonate-rich melts. This melting does not need extra heat input from a plume. Melting of this complex mixture of lithologies frees transition metals, which are sequestered predominantly in hydrous minerals [3], and transports them together with sulfur in carbonate-rich melts [4]. The types of melt formed close to the base of the lithosphere may vary as a function of time at one location due to the changes in oxidation state and dyke rock types that were formed at different times in Earth history. Reduced melts and diamonds were more common in the Proterozoic TBL and lower lithosphere, whereas oxidised melts and carbonates became dominant in the Phanerozoic. This is demonstrated by copper isotopes which indicate reduced sources containing metal for Proterozoic lamproites, but carbonate-rich conditions at least 2.5 log units $fO_2$ higher by the late Neoproterozoic [5].

[1] Chen CF et al. (2023) Nature 620, 576-581.
[2] Foley SF et al. (2024) Nat Sci Rev (in press)
[3] Ezad IS et al. (2024) Min Dep 59, 227-236.
[4] Ezad IS et al. (2024) Sci Adv (in press)
[5] Chen CF et al. (2024) Nat Comm (in press)

# A new machine learning single-crystal barometer and thermometer for peridotitic garnet

O'Sullivan, G.J.[1], Janney, P.E.[2], Higgins, O.[1], Tomlinson, E.[1]

[1]Department of Geology, Trinity College Dublin, Ireland

[2]Department of Geological Sciences, University of Cape Town, South Africa

---

Xenoliths and xenocrysts from the sub-cratonic lithospheric mantle record the thermal conditions of the mantle at the time of emplacement, allowing us to understand the thermal, chemical and structural evolution of the mantle through Earth history. Such PT estimates are also central to understanding diamond formation, fertility, and exploration. And further, they are critical to understanding changes in water content, redox conditions, and mineralogy or lithology with depth. Single crystal estimates of pressure and temperature from garnet are particularly desirable, as garnet xenocrysts are present in most pipes, are resistant to surface weathering and transport processes, and occur in both fertile and depleted peridotite compositions. However, while Ni-in-Grt thermometry [1] is an excellent tool for accurately estimating peridotitic garnet T, a single crystal garnet barometer remains elusive as the Cr-in-Grt barometer provides only minimum pressure estimates, from all but the most depleted peridotite compositions.

Here, we demonstrate a new barometer for peridotitic garnet based on machine learning applied to a natural dataset of harzburgite, wehrlite and lherzolite xenoliths. We first calculate PT for >1500 garnet peridotite xenoliths using established two-phase exchange thermometers and barometers. We then calibrate the garnet major element geochemistry in these xenoliths to those pressures and temperatures to successfully generate a new single-crystal barometer and thermometer, which can be applied to peridotitic garnet in kimberlite separate and alluvium. Our models have no skew or bias vs existing thermobarometer combinations and provide temperature estimates that compare favourably with Ni-in-Grt estimates. As our method is calibrated to a large natural dataset it covers the full natural range of garnet compositions, pressures, and temperatures. Off-craton, orogenic, and xenoliths from thinned crust are included to ensure that the model can be applied to any detrital peridotitic garnet and to cover the full compositional range of natural peridotitic garnet. Our barometer is applicable from c. 2 – 6 GPa, and our thermometer from c. 750 °C to 1350 °C. The mean absolute errors of our models vs the test dataset Grt-Opx pressures and temperatures are 4.5 Kbar and 60 °C, respectively. We consider this level of performance to be more than sufficient to construct geotherms for the sub-continental and sub-cratonic lithosphere using only garnet separate or detritus. We show the use and utility of our models in several short case studies, demonstrating how such data can help constrain lithospheric thickness and stratigraphy.

*Reference:*

[1] Griffin W.L et al. (1989) Contrib. to Min. and Petrol. 103: 199-202

# Oxidation state and metasomatism of the lithospheric mantle beneath Letlhakane, Botswana: Insights into effects of metasomatism on the Re-Os system

Rakipov, A. [1,2,*], Woodland, A.B. [1,2], Heckel, C. [1,2] and Luguet, A.[3]

[1]Institut für Geowissenschaften, Johann Wolfgang-Goethe-Universität, Frankfurt am Main, Germany

[2]Frankfurt Isotope and Element Research Center (FIERCE), Goethe-Universität, Frankfurt am Main, Germany

[3]Institut für Geowissenschaften, Universität Bonn, Germany

*E-Mail: a.rakipov@stud.uni-frankfurt.de

---

The metasomatized lithospheric mantle is a palimpsest, documenting various interactions involving fluids and melts that have occurred since its formation [1]. Unravelling this complex record is key to constrain the evolution of the thick roots underlying ancient cratons. Here, we combine the first oxygen fugacity (ΔlogfO2(FMQ)) estimates of peridotite xenoliths from Letlhakane, Zimbabwe Craton, Botswana, with their trace element compositions and previously published whole rock Re-Os ages [2] in order to better investigate the style of metasomatism.

Our suite comprises eleven peridotites including garnet (GP), garnet-phlogopite (GPP), spinel (SP), and phlogopite peridotites (PP). They originate from depths of ~ 85 to 180 km, with temperatures ranging from 720 to 1380°C. Our suite's $\Delta\log fO_2$(FMQ) ranges over 2 log units from FMQ-2.5 to FMQ-0.8, generally displaying relatively oxidizing conditions. Trace element concentrations of olivine, orthopyroxene, clinopyroxene, and garnet imply various metasomatic interactions: i) silicate/kimberlitic melt, ii) carbonatitic fluid, iii) silicate melt with carbonatitic component, and iv) Phlogopite-Ilmenite-Clinopyroxene (PIC). We indicate the existence of oxidising agents (beyond the EMOG/EMOD stability) in the case of silicate melt that may have contributed to the carbonate conversion of diamond or graphite (at > 140 km). A more reducing agent (carbonatitic fluid) is apparent between 140 and 120 km. At shallower depths (above 110 km) we observe the influence of oxidising silicate melts. Our shallowest sample (~85 km) is characterized by chemical depletion and reduced $\Delta\log fO_2$(FMQ), which may indicate that the metasomatic agents were unable to reach this level in the lithosphere.

We established a link with published whole rock Re-Os ages, HSE-patterns, and Ti-Eu Systematics, which indicate the metasomatic style: melt- and fluid-overprinted or depleted. Depleted or fluid-overprinted samples both indicate reliable Re-Os $T_{RD}$ model ages for craton formation or stabilization between 2.5 and 2.7 Ga. The fluid-metasomatism, which caused oxidation and garnet to phlogopite transition has a negligible effect on Base Metal Sulphides (BMS). On the other hand, Re-Os ages differ between oxidized and melt-metasomatized samples. We argue the influence of a melt overprint on the whole rock Re-Os system. Our deepest sample, MB1, at 180 km, exhibits multi-phase melt-related signatures, consistent with the disturbance of the Re-Os system. The whole rock Re-Os age of 952 Ma is consistent with previous observations of an accretion event at ~1.0 Ga [3;4]. Such oxidising silicate melts might have accelerated mild carbonate redox melting [5] by destabilizing diamond. At shallower depths, this results in mild metasomatism, which disturbs the Re-Os system to a lesser extent. Thus, such metasomatism reveals mixing-ages between craton formation (2.5 to 2.7 Ga) and primary melt metasomatism (~1.0 Ga). We propose a three-stage evolution of the lithospheric mantle beneath this part of the Zimbabwe Craton.

*References:*

[1] O'Reilly S and Griffin W (2013) LNESS 1: 471–533

[2] Luguet A et al.. (2015) Geochim Cosmochim 164: 441–463

[3] Richardson S et al. (1990) Nature 346: 6279

[4] Aulbach S et al. (2017) Lithos 268-271: 364-382

[5] Foley S (2011) J Petrol 52: 7-8

# Slip system-controlled segregation of minor and trace elements in olivine low-angle grain boundaries

Dimitriou, D.[1*], Reddy, S.[1,2], Evans, K.[1], Fougerouse, D.[1,2], Saxey, D.[2], Tacchetto, T.[1]

[1]School of Earth and Planetary Sciences, Curtin University, Perth, WA, Australia.

[2]Geoscience Atom Probe, John de Laeter Centre, Curtin University, Perth, WA, Australia.

*Corresponding author: dimitrios.dimitriou@curtin.edu.au

---

Olivine comprises up to 70% of the Earth's upper mantle, hence it plays a crucial role in the geochemical and geodynamic processes in the Earth's interior [1]. A feature that requires more study is the olivine low angle grain boundaries (LAGBs). They may act as reservoirs for minor and trace elements [2], and can influence mantle processes and properties, such as diffusion and seismic anisotropy [3,4]. This study explores how different slip systems in a naturally deformed olivine affect the partition of minor and trace elements to LAGBs. Furthermore, we are studying the potential connection between the evolution of slip systems and elemental segregation.

The studied olivine grains are from a mantle xenolith from Gerrei in Sardinia, Italy. We investigate two tilt LAGBs with the same misorientation angle of 4° and different slip systems, [100](010) (A-type) and [100](001) (E-type). Electron backscatter diffraction (EBSD) was used to locate and characterise suitable grain boundaries. Transmission electron microscopy (TEM) was used to and observe dislocations along the selected grain boundaries. Finally, atom probe tomography (APT) was utilised to obtain three-dimensional geochemical data.

Our preliminary TEM results show that the A-type LAGB shows distinct dislocations in regular intervals. In comparison, E-type LAGBs do not present this feature and are instead more uniform. APT results show that both LAGBs act as a reservoir for incompatible minor and trace elements. Enrichment in most minor elements, such as Al, Ca, Na, and Ti, was observed. Trace elements (e.g. Co, Cr, and P) show a considerably increased concentration of up to twice the bulk concentration. The enrichment along the [100](010) follows the dislocation arrays, compared to a more disorganised and uniform distribution along the [100](001), with both slip systems showing increased enrichments on boundary kinks.

The homogenous elemental distribution that is associated with E-type slip system is shown by the TEM images and the dislocations observed on the A-type slip system TEM images largely align with the increased segregation areas shown by APT. Despite the very different appearance of the two LAGBs, they both show similar concentration of minor and trace elements. This, potentially, shows that geochemical segregation only plays a minor role, if any, in the transition of slip systems from A-type to E-type.

The results of this study increase our understanding of olivine and have larger implications for controls on upper mantle processes. The expanded knowledge on olivine LAGBs can be utilised to improve the interpretation of mantle-related geochemical and structural data and to better model its behaviour.

*References:*

[1] Ismail W B and Mainprice D (1998) Tectonophysics 296 (1): 145–157
[2] Tacchetto T et al. (2021) Contributions to Mineralogy and Petrology 176 (7): 59
[3] Dohmen R and Milke R (2010) Reviews in Mineralogy and Geochemistry 72 (1): 921–970
[4] Jackson I et al. (2002) Journal of Geophysical Research: Solid Earth B12: ECV 5-1- ECV5-16

## Quantifying the melting conditions of Archean mantle peridotites

Kaekane, J.B.[1], Hoare, B.C. and Tomlinson, E.L.[1]

[1]Geology, School of Natural Sciences, Trinity College Dublin, Dublin, Dublin 2, Ireland.

---

Archean cratons are underlain by ultramafic lithospheric roots that are sometimes thick and cool enough to extend into the diamond stability field. The properties of these cratonic mantle roots have been determined through petrological studies on mantle xenoliths and further complemented by geophysical observations. However, the depth and setting at which melting took place is poorly constrained. For instance, both low-pressure and high-pressure depths of melting have been invoked for the Kaapvaal craton. This is due in part to the effects of subsolidus re-equilibration during cooling, and to variable silica addition which obscures primary indicators of melting conditions.

Nonetheless, spinel/clinopyroxene exsolution lamellae in orthopyroxene is a feature that is observed in a selection of spinel-harzburgite xenoliths from the 84 Ma Kimberly kimberlite, Kaapvaal craton. Previous studies have established that at high temperatures, orthopyroxene can accommodate high concentrations of Al and Ca, which upon slow cooling of at least ~500°C to the modern geotherm exsolves Al-Ca bearing phases, to garnet at high pressure and spinel + clinopyroxene at lower pressure. Therefore, the aim of this study is to determine the initial P-T conditions of orthopyroxene formation in such samples by reversing the slow cooling process - reflected currently as exsolution lamellae - back in time to high temperature conditions when exsolutions were dissolved in the host orthopyroxene (precursor). Through phase equilibrium modelling of this precursor orthopyroxene in the system NCFMASTOCr, the depth of orthopyroxene formation will be resolved at the solidus. Trace element data will be used to elucidate the phases present at the time of this orthopyroxene formation and comparison of formation P-T conditions with the equilibration P-T conditions will reveal the overall cooling P-T path. The equilibration P-T conditions will be assessed utilizing exchange thermobarometers and/or complemented with composition isopleth thermobarometry. Our work will also provide constraints on the conditions of silica enrichment and the origin of the enriching agent, shedding light on a key process affecting the Kaapvaal cratonic lithosphere.

## The melting behaviour of fertile and depleted peridotite at high pressures

Melai, C.[1]; Walter, M.J.[2]; Yang, J.[2], Rinaldi, M.[1] and Tomlinson, E.[1]

[1] Geology, School of Natural Sciences, Trinity College Dublin, Dublin, Dublin 2, Ireland. (melaic@tcd.ie)

[2] Earth and Planets Laboratory, Carnegie Institution for Science, Washington, DC20015, USA

---

High-pressure and high-temperature melting experiments underpin our knowledge of mantle melting processes. This information is critical for elucidating the conditions of melting in modern mantle plumes, the generation of komatiites (particularly prevalent during the Archean), as well as impact melting and the dynamics of magma ocean processes in the early Earth. Experimental datasets for fertile peridotite composition are generally limited to pressures below 7 GPa[1]. Building upon the work of Walter (1998), this study significantly expands the previously investigated pressure range for melting of fertile peridotite KR4003 up to 12 GPa by means of multianvil experiments. The aim is to additionally investigate poorly constrained aspects of melting phase relations such as the behaviour of orthopyroxene (opx) above the solidus (e.g. the compositional effect of its transition from orth- to clino-enstatite), the depth over which peritectic opx forms above the solidus and the stability and proportion of garnet in the residue across the melting range. This work on bracketing of the melting behaviour of a dry garnet peridotite composition allows the investigation of the influence of pressure on its melting behaviour and its potential role in komatiite melt formation. Depleted initial $^{176}Hf/^{177}Hf$ compositions of both cratonic peridotite and komatiite lavas require them to be derived from a depleted mantle source[2,3,4,5]. Thus, to broaden the scope and allow the investigation of komatiite generation, we are also investigating the melting phase relations of a synthetic depleted peridotite produced by mixing high-quality oxide powders. The melting behaviour of this composition is investigated from 4 to 12GPa in 2 GPa increments.

This research faces significant technical challenges. Achieving the narrow temperature window between the solidus and liquidus necessary for successful experiments proves challenging, even with meticulous efforts to minimize thermal gradients within the multi-anvil assembly. Furthermore, employing graphite capsules, as utilized by Walter (1998), is not feasible at high pressures due to transformation of graphite to diamond. This transformation can lead to loss of the melt into the porous space created during diamond formation, hindering proper retrieval and analysis. Additionally, the melt loss does not ensure equilibrium in the experimental run, making the recovered samples unusable.

For the successful runs, the chemical composition of the coexisting phases was analyzed by means of electron-probe microanalyzer (EPMA) and phase proportions were calculated by least squares mass balance from the measured phase compositions at each pressure and temperature point. The resulting data were than implemented in the thermodynamic modelling of the KNCFMASTOCr system to improve the calibration of the melt model.

*References:*

[1] Walter, M. J. (1998), *Journal of Petrology*, 39(1), 29-60

[2] Lazarov, M., Brey, G. P. & Weyer, S. (2012), *Lithos* 154**,** 193–209

[3] Lazarov, M., Brey, G. P. & Weyer, S. (2009), *Earth Planet. Sci. Lett.* 279, 1–10 (2009).

[4] Blichert-Toft, J. & Puchtel, I. S. (2010), *Earth Planet. Sci. Lett.* 297**,** 598–606 (2010).

[5] Blichert-Toft, J., Arndt, N. T., Wilson, A. & Coetzee, G (2015), *Am. Mineral.* 100**,** 2396–2411 (2015).

## Petrogenesis and indicator mineral chemistry of the K-richterite- and leucite-bearing diamondiferous Kareevlei Kaapvaal lamproite

Qashani, Z.[1], Hashibi, S.[1], Howarth G. H.[1], Janney, P. E.[1], le Roux, P.[1] and Robey, J.[2]

[1] Department of Geological Sciences, University of Cape Town, Rondebosch 7701, South Africa

[2] Rockwise Consultants, Kimberley 8300, South Africa

---

Kareevlei is the first diamond mine to be hosted in a K-richterite- and leucite-bearing Kaapvaal lamproite (formerly termed Group II kimberlite). To constrain the petrogenesis and lithospheric setting of the Kareevlei Kaapvaal lamproites, we present petrography, groundmass mineral compositions, bulk-rock major and trace element concentrations, and Sr–Nd isotopes for 13 coherent-textured samples, along with garnet indicator mineral compositions and Ni-in-garnet thermobarometry.

Two distinct mineralogical varieties of Kaapvaal lamproites are identified: (1) phlogopite-diopside olivine lamproites and (2) leucite-richterite olivine lamproites. Phlogopite macrocryst and microcryst laths have two distinct core populations, interpreted as xenocrysts from phlogopite peridotites and MARIDs, whereas rims represent crystallisation from the magma. The leucite-richterite lamproites are characterised by higher bulk-rock $SiO_2$, $Al_2O_3$, and $Na_2O$, and lower MgO contents compared to the phlogopite-diopside lamproites. The two mineralogical varieties have distinct incompatible trace element concentrations, with the leucite-richterite samples having lower concentrations of light REEs (LREE: La = 656–828; Ce = 518–597; Nd = 234–261 times chondrite) compared to the phlogopite-diopside samples (La = 1125–1391; Ce = 817–1029; Nd = 333–415 times chondrite). Additionally, these two groups exhibit clear separation in trace element ratios, with higher La/Sm and Gd/Yb in the phlogopite-diopside lamproites, which is interpreted to represent formation by lower degrees of partial melting relative to the leucite-richterite lamproites. However, both lamproite varieties have similar $^{87}Sr/^{86}Sr_i$ and $^{143}Nd/^{144}Nd_i$ ratios, suggesting derivation from an isotopically homogeneous source in the subcontinental lithospheric mantle (SCLM).
The indicator mineral suite at Kareevlei comprises, in decreasing abundances, oxides (predominantly ilmenite and chromite), garnet, corundum, and rare clinopyroxene. Garnets are largely eclogitic (59%) with only smaller proportions of peridotitic G9 (19%) and G10 (8%) garnets observed. Peridotitic garnet thermobarometry indicates a paleogeotherm with an estimated surface heat flux of ~44.3–44.9 mW/m$^2$ and an estimated lithospheric thickness of ~187–195 km, which is within error of the nearby highly diamondiferous Finsch Kaapvaal lamproite (cf. 192 ± 6 km). Single mineral garnet thermobarometry suggests that most peridotitic garnets at Kareevlei were sampled by the lamproite at relatively shallow depths above the diamond stability field. The dominance of eclogitic garnet and the absence of peridotitic garnet that equilibrated within diamond stability suggests that the high-value diamonds extracted from Kareevlei are predominantly eclogitic in origin.

## The origin of melilitites: an experimental study

Poli, S.[1] and Melluso, L.[2]

[1]Dipartimento di Scienze della Terra, Università di Milano.

[2] Dipartimento di Scienze della Terra, Università di Napoli Federico II.

---

Melilitites are ultramafic magmas characterized by normative $Ca_2SiO_4$, larnite, high FeO* and $TiO_2$. Melilitite primitive lavas (Mg# 67-77) occurs in ocean island as well in alkaline volcanic districts on rifted continental crust. Liquids compositionally close to melilitites were experimentally reproduced in the model system CaO-MgO-$Al2O_3$-$SiO_2$-$CO_2$ at 3.2-3.3 GPa, approx. 1500 °C [1], at relatively high melt proportions. In complex compositions, MORB-eclogite derived, carbonated, partial melts reacted with a fertile peridotite were proposed at the origin of melilitites [2]. The experimental reconstruction of phase relationships on the liquidus of carbonated natural melilitites reveal that clinopyroxene and olivine or garnet are stable phases [3,4], suggesting that carbonated wehrlites are potential sources for the genesis of melilitites.

Here, we explore phase relationships on the high pressure melting of a model wehrlite, initially composed of a mechanical mixture of San Carlos olivine, diopside, aegirine, dolomite, rutile and kyanite. Starting materials were loaded in graphite capsules, inserted in sealed platinum capsules. Vitreous carbon spheres and synthetic diamond grains were adopted for liquid traps.
A first set of experiments performed at 3.2 GPa from 950 to 1450 °C reveal that the solidus for the model wehrlite composition is located at temperatures in the order of 1050 °C. In all experiments, an orthopyroxene-rich layer, with polygonal microstructure, forms at contact with aggregates resulting from quenched liquids, its thickness increasing with increasing temperature, i.e., increasing melt fraction. Estimates of liquid composition are melilititic at 1150-1200 °C, with $TiO_2$ approx. 2.5 wt.% on a volatile free basis.

A second set of sandwich experiments is devoted to verifying the modification and equilibration of liquids produced by a natural aphyric melilitite from Alaotra district (central-northern Madagascar) interbedded with wehrlite.

Currently available experiments suggest that the melting reaction producing a melilitite liquid is dolomite + olivine + clinopyroxene + garnet = orthopyroxene + liquid. This is feasible only if the primary phase field of orthopyroxene on the liquidus surface extends on the Ca-rich portion of the volume forsterite-enstatite-nepheline-larnite in the presence of $CO_2$.

*References:*

[1] Gudfinnsson GH and Presnall DC (2005). J Petrol 46: 1645-1659.
[2] Mallik A and Dasgupta R (2014) Geochem Geophys Geosyst 15: 1533–1557
[3] Brey GP and Ryabchikov ID (1994) N Jahr Miner Monat 10: 449-463
[4] Tatsumi Y et al. (1999) J Petrol 40: 497-509

# Olivine in ultramafic lamprophyres from the Delitzsch carbonatite complex, Saxony, records metasomatic activity in the Central European lithospheric mantle

Hellers, M.*[1], Bussweiler, Y.[1], Kühle, T.[1], Wombacher, F.[1], Möckel, F.[2], Münker, C.[1]

*Presenting author

[1] Institute of Geology and Mineralogy, University of Cologne

[2] Wismut GmbH, Chemnitz

mheller3@uni-koeln.de

---

Olivine is capable of recording mantle and igneous processes across a diverse range of mafic and ultramafic lithologies. Its prevalent occurrence in rift-related ultramafic magmas offers great potential to document melting and metasomatism in the sub-continental lithospheric mantle. Here, we investigate olivine in ultramafic lamprophyres of the Cretaceous Delitzsch carbonatite complex, Germany [1]. We present comprehensive analyses of major and trace element mineral compositions of alnöites obtained from drill-cores using electron-probe microanalysis (EPMA) and laser ablation inductively coupled plasma mass spectrometry (LA-ICPMS). Olivine grains with normal and reversed zonation represent the most abundant phenocrysts in the analysed samples. No evidence for mantle-derived olivine xenocrysts is found, as evidenced by relatively high Ca and relatively low Ni contents in the olivine cores. The majority of olivines exhibit complex zonation, providing evidence for multi-stage igneous processes. The cores of these olivines display the highest Fo# and Ni contents, along with low Ni/Mg and Mn/Fe ratios. In an inner zone, magma differentiation is recorded by a decrease in Fo#, Ni contents, and an increase in Ni/Mg. Interaction with a separate magma led to the development of an outer rim marked by higher Ca and Ti contents and an increase in Fo# and Mn/Fe. We interpret the olivine cores and inner rims as representing xenocrysts (antecrysts) that crystallized from an earlier magma pulse with a characteristic signature of continental rift magmatism [2,3]. The low and variable Mn/Fe and Ni/Mg of these olivine cores indicates the presence of phlogopite in a heterogeneous mantle source [3] and is supported by reports of mantle-derived xenocrystic phlogopite in similar ultramafic lamprophyres from the Delitzsch carbonatite complex [1]. The outer rims have a geochemical signature of intraplate magmatism [2,3] and likely developed during entrainment of the olivine xenocrysts in the alnöitic melt. Our results demonstrate the complex growth history of olivine in alnöites from the Delitzsch carbonatite complex. The composition of the olivines provides insights into the interaction and differentiation of multiple magma pulses originating from heterogeneous metasomatized mantle sources. This study contributes to our understanding of the intricate history of multiple generations of magma that interacted with the Central European sub-continental lithosphere.

*References:*

[1] Krüger et al. (2013) Chem Geol 353: 140-150

[2] Foley et al. (2013) EPSL 363: 181-191

**[3] Veter et al. (2017) Lithos 292-293: 81-95**

## $^{182}W$, $^{142}Nd$, and Pb isotopes indicate entrainment of Hadean recycled crust within the Deccan-Réunion plume

Pakulla, J.J[1].*, Tusch, J.[1], Hasenstab-Dübeler, E.[1], Ravindran, A.[1], Jansen, M.W.[1], Leitzke, F.P.[1,2], Gadpallu, P.[3], Duraiswami, R.A.[3], Münker, C.[1]

[1]Universität zu Köln, Institut für Geologie und Mineralogie, 50674 Köln, Germany

[2] Universidade Federal de Pelotas, Depto. de Engenharia Geológica, Centro de Engenharias, 96010-540, Pelotas, Brazil

[3] Savitribai Phule Pune University, Department of Geology, 411007 Pune, India

---

Short-lived radiogenic isotopes such as $^{182}W$ and $^{142}Nd$ have become important tools in assessing the geodynamics and chemical processes that occurred during the Hadean/Archean as well as in the lower mantle tapped by plume-related magmatism. In that regard, it has been suggested that $^{182}W$ deficits found in Ocean Island Basalts (OIBs) are either derived from core-mantle interaction or involvement of (recycled) ancient material that experienced early silicate differentiation [1,2,3,4]. The latter process has been further invoked by variations of $^{142}Nd$ for some OIBs [e.g. 2, 3, 5].
At the Deccan-Réunion hotspot system, $^{182}W$-$^{142}Nd$-$^{3}He$ systematics of modern and cretaceous (~66 Ma) samples indicate, similar to other OIBs, a complex combination of core-derived and Hadean/Archean recycled crustal material as indicated by a reported correlation between $^{182}W$ and $^{142}Nd$ [3].
Here we provide new $^{182}W$, $^{142}Nd$, as well as Pb isotope data for samples from Réunion and the Deccan Large Igneous Province (DLIP) to further decipher the origin of $^{182}W$ and $^{142}Nd$ anomalies in mantle plume-derived magmas. Our samples range in $\mu^{182}W$ from -12 ± 2.3 to values overlapping modern mantle compositions. DLIP samples can be divided into 2 groups based on trace elements, $^{182}W$, and Pb isotopes. One lower mantle-derived group displays higher $^{182}W$ deficits than Réunion OIB and one lithosphere-contaminated sample suite overlaps with Réunion OIB in $\mu^{182}W$. We did not identify any $^{142}Nd$ anomalies in the DLIP and Réunion samples studied. Thus, while $^{142}Nd$ and $^{182}W$ anomalies may co-exist in the Deccan-Réunion plume, our data show evidence that they are not correlated. Most importantly, due to a co-variation of $^{182}W$ and Pb isotopes, we suggest that the negative $\mu^{182}W$ anomalies in the Deccan-Réunion plume are rather derived from recycled Hadean/Archean mafic crust than core-mantle interaction.

*References:*

[1] Mundl et al. (2017), Science, 356
[2] Peters et al. (2018), Nature, 555
[3] Peters et al. (2021), G-Cubed, 22
[4] Tusch et al. (2022), PNAS, 119
[5] Horan et al. (2018), EPSL, 484

# Sheared peridotites: linking deformation and hydrous metasomatism to the onset of craton destabilization

Heckel, C.[1,2], Woodland, A.B.[1,2], Gibson, S.A.[3], Linckens, J.[1,4], Withers, A.C.[5], Seitz, H.-M.[1,2] and Ludwig, T.[6]

[1]Institut für Geowissenschaften, Goethe-University Frankfurt, Germany – woodland@em.uni-frankfurt.de

[2]Frankfurt Isotope and Element Research Center (FIERCE), Goethe-University Frankfurt, Germany

[3]Department of Earth Sciences, University of Cambridge, UK

[4]Tata Steel, R&D, 1970 CA Ijmuiden, The Netherlands

[5]Bayrisches Geoinstitut, University Bayreuth, Germany

[6]Institut für Geowissenschaften, Ruprechts-Karls-University Heidelberg, Germany

---

Kimberlite-hosted sheared peridotite xenoliths are highly deformed and, due to their bimodal grain size distribution (coarse-grained porphyroclasts vs. fine-grained neoblasts), provide snapshots of short-lived processes in the cratonic mantle concomitant with their entrainment.

We combine measured $H_2O$ contents of olivine, orthopyroxene (opx) and clinopyroxene (cpx) with analysed olivine fabrics from 22 well-characterized sheared peridotite xenoliths [1, 2] in order to investigate the connection of $H_2O$-rich metasomatism and deformation. The mantle xenoliths derive from kimberlite clusters at Kimberley and northern Lesotho on the Kaapvaal craton. They consist of olivine, opx ± cpx ± garnet ± spinel. They may be classified into (i) low-, (ii) moderate- and (iii) high-T sheared peridotites [2] with PT equilibrium conditions (porphyroclastic cores) of (i) 850 – 1000°C and 3 – 4.5 GPa, (ii) 1200 – 1300°C and 5 – 5.5 GPa and (iii) 1350 – 1450°C and 5.5 – 6.5 GPa, respectively. All groups are geochemically depleted with Mg# in olivine ranging from 91 to 94.

Heckel et al. [1, 2] showed that the peridotites were affected by multiple metasomatic events preserved in the porphyroclastic cores ("old"), porphyroclastic rims ("young") and neoblasts ("youngest"). Comparison of olivine fabrics and $H_2O$ concentrations in olivine, opx and cpx give further insights into their evolution. $H_2O$-dependent olivine crystallographic preferred orientations (CPO) (bimodal, B-, C-, E-type fabric) imply the presence of an $H_2O$-rich agent during deformation [3, 4]. $H_2O$ concentrations in opx and cpx are in agreement with hydrous deformation conditions. However, measured $H_2O$ concentrations in olivine give contrary results: those in low-T sheared peridotites are consistent with hydration, but olivines in *most* moderate- and high-T sheared peridotites are almost dry. Partition coefficients indicate disequilibrium of pyroxenes and olivine.

Once formed, olivine fabrics require high strain to be overprinted [5] and the contrary results from the fabrics and $H_2O$ concentrations of olivines in the sheared Kaapvaal peridotites record either two different events or changing deformation conditions. We propose that the olivine fabrics in the moderate- and high-T sheared peridotites developed during an older (hydrous) deformation event caused by melts similar to megacryst-forming magmas – related to early kimberlite magmatism. Subsequent events (proto-kimberlite pulses) caused further metasomatism and deformation (i.e. a metasomatism-deformation cycle; [1]). A subsequent melt with low $H_2O$ fugacity could have dehydrated the olivine immediately before the final kimberlite pulse that brought the peridotite xenoliths to the surface. The consequence of this pervasive magmatism and metasomatism is rheological weakening, thermal perturbation and mixing of the lower lithospheric mantle beneath the Kaapvaal craton [2].

*References:*

[1] Heckel C et al. (2022) J Petrol 63: 1-24
[2] Heckel C et al. (2023) J Petrol 64: 1-29
[3] Jung H et al. (2006) Tectonophysics 421: 1-22
[4] Wallis D et al. (2019) EPSL: 51-61
[5] Boneh Y and Skemer P (2014) EPSL: 213-222

## Complex metasomatic history and exhumation-driven refertilization of subcontinental lithospheric mantle beneath Central Europe

Kubeš, M.[1,2], Čopjaková, R.[1], Kotková, J.[1,2], Ackerman, L.[2,3], Haifler, J.[1], Škoda, R.[1]

[1]Department of Geological Sciences, Masaryk University, Kotlářská 2, 611 37, Brno, Czech Republic

[2]Czech Geological Survey, Klárov 3, 118 21, Prague 1, Czech Republic / martin.kubes@geology.cz

[3]Institute of Geology of the Czech Academy of Sciences, Rozvojová 269, 165 00, Prague 6, Czech Republic

---

The high-grade Gföhl Unit of the Moldanubian Zone (Bohemian Massif) hosts diverse orogenic peridotite types derived from different mantle domains [1, 2]. Moreover, these mantle rocks experienced metasomatic overprint mainly due to percolation of transient basaltic melts from which abundant garnet-bearing pyroxenite veins crystallized [3]. The studied pyroxenite-veined garnet peridotites (PVGP) associated with high and ultra-high pressure (HP-UHP) crustal assemblages in the Gföhl Unit provide insights into complex metasomatic history and mantle refertilization beneath the Variscan orogenic root in Central Europe.

The PVGP association records an extensive refertilization of the originally refractory subcontinental lithospheric mantle (SCLM). This resulted from reactive percolation of depleted MORB mantle-like (DMM) melts produced by decompression partial melting of the asthenosphere at exhumation related to lithospheric thinning [4]. The transformation of an original refractory protolith (likely harzburgite) to fertile lherzolite is documented by conspicuous LREE depletion, Sr–Nd isotopic signatures ($^{87}Sr/^{86}Sr_{338} \leq 0.7028$; $\varepsilon Nd_{338}$ 7.3), high bulk CaO and $Al_2O_3$ contents reflecting relatively high modal amount of clinopyroxene (up to 9 vol%) of lherzolite. Trace element chemistry of clinopyroxene (e.g. high Ti/Eu and Ti/Nb) and garnet (elevated ∑REE, Zr, Ti) along with whole-rock positive correlation between fluid-immobile incompatible elements (Zr, Yb, Sc, V) also record the SCLM refertilization.

The percolation of DMM-like basaltic melts ($^{87}Sr/^{86}Sr_{338}$ 0.7025–0.7029; $\varepsilon Nd_{338} \leq 7.9$) in wall-rock peridotite triggered various metasomatic reactions involving: (i) stealth metasomatism, recorded by extensive clinopyroxene and garnet crystallization in lherzolite, (ii) cryptic metasomatism, reflected by lower Mg# values of orthopyroxene and olivine in lherzolite, and (iii) modal metasomatism, resulting in crystallization of amphibole and phlogopite in lherzolite adjacent to the veins. The modal compositional imaging coupled with elemental distribution maps of the peridotite-pyroxenite interface revealed the main ways of migration of silicate melts through the upper mantle and strong element fractionation controlled by differentiation of the basaltic melt. Accordingly, we demonstrate that DMM-like melt can significantly fractionate during the reactive percolation, leading to the segregation of volatile-rich melt fractions that can migrate through large volumes of wall-rock peridotites and produce chromatographic SCLM enrichment in highly incompatible elements.

*References:*

[1] Kubeš M et al. (2022) Lithos 422:106726
[2] Medaris JG et al. (2005) Lithos 82:1-23
[3] Svojtka M et al. (2016) J Petrol 57:897-920
[4] Kubeš M et al. (submitted) J Petrol

## The thickness of the Archean Kaapvaal cratonic lithosphere at 1.6 Ga

Qashani, Z.[1], O'Sullivan, G. J.[1], Janney P. E.[2], and Tomlinson E. L.[1]

[1] Geology, School of Natural Sciences, Trinity College Dublin, Dublin, Dublin 2, Ireland. qashaniz@tcd.ie
[2] Department of Geological Sciences, University of Cape Town, Rondebosch 7701, South Africa

---

The present-day cratonic lithosphere is characterised by strong geochemically depleted, rigid, isostatically buoyant, and viscous cratonic keels that extend to 200 – 250 km depth. These characteristics are the result of high degrees of partial melting which has been linked to high temperatures in the underlying convecting mantle during the Archean. Re-Os isotope studies (e.g., Pearson et al., 2021; Carlson et al. 1999) have confirmed that the lithosphere of the Kaapvaal craton remained stable to a depth of at least ~200 km since the Archean up to at least the time of peridotite sampling by Cretaceous kimberlites. Dating of mantle xenoliths and diamond inclusions have also indicated that ~150 – 200 km thick lithosphere existed beneath the Kaapvaal craton in southern Africa (e.g., Boyd et al., 1985). More recently, diamond stability and low temperatures of diamond inclusions require that the lithosphere was thicker (ca. 300 km) at the time of diamond formation, predominantly in the Archaean and early Proterozoic, to provide insulation from the hotter mantle and crust (e.g., Hoare et al., 2022). However, most of the xenoliths studied from the Kaapvaal craton were exhumed by Phanerozoic and Cretaceous kimberlites and, therefore, the direction and magnitude of variations in the thickness of cratonic lithosphere through geologic time remain unclear.

This study reconstructs the thickness of the lithosphere beneath the western Kaapvaal craton using xenoliths exhumed by 1.6 Ga Zero kimberlite, and garnet and clinopyroxene from kimberlite concentrate from the Kuruman cluster, which represents the earliest known sampling of the Kaapvaal lithosphere. Our approach encompasses (1) determination of equilibrium pressures and temperatures (P-T) of xenoliths from Zero; (2) determination of P-T for pyrope garnet in kimberlite concentrate from Zero and other members of the Kuruman cluster (i.e., Elson and White Ladies) using a new machine learning single crystal barometer and the Ni-in-garnet thermometer; and (3) calculation of the local geothermal gradient of the lithosphere (thickness is defined by the point at which the geotherm calculated based on P-T data crosses the mantle adiabat). Ultimately, thickness information when combined or compared with younger xenoliths across the Kaapvaal craton will give a snapshot of changes in the thickness of the lithosphere over time. As well as the thermal evolution of the lithosphere since Archean. Our findings will be discussed in relation to mechanisms for craton formation and causes of changes in lithospheric thickness.

*References:*

Carlson, R.W., Pearson, D.G., Boyd, F.R., Shirey, S.B., Irvine, G., Menzies, A.H., and Gurney, J.J., 1999. In The JB Dawson Volume—Proceedings of the Seventh International Kimberlite Conference, Cape Town. Red Roof Design, Cape Town (pp. 99-108).

Boyd, F.R., Gurney, J.J. and Richardson, S.H., 1985. Nature, 315(6018), pp.387-389.

Hoare, B.C., Tomlinson, E.L. and Kamber, B.S., 2022. Earth and Planetary Science Letters, 597, p.117796.

Pearson, D.G., Scott, J.M., Liu, J., Schaeffer, A., Wang, L.H., van Hunen, J., Szilas, K., Chacko, T. and Kelemen, P.B., 2021. Nature, 596(7871), pp.199-210.

# An improved thermodynamic model for the melting evolution of a peridotite up to 12 GPa

Rinaldi, M.R.[1], Green, E.C.R. [2], Melai, C. [1] and Tomlinson, E.L.,[1]

[1] Geology, School of Natural Sciences, Trinity College Dublin, Dublin, Dublin 2, Ireland. rinaldim@tcd.ie

[2] School of Geography, Earth and Atmospheric Sciences, University of Melbourne, Melbourne

---

Since petrological phase equilibrium modelling was developed, it has provided key information on the evolution of a multitude of magmatic settings. Its flexibility to investigate a broader range of bulk compositions and environmental conditions, interpolating between sparse experiments, has led to a better understanding of plume and impact melting, as well as the magmatic processes under hot mantle conditions in the Archean and the generation of komatiites. Still, the lack of experimental constraints in the literature on anhydrous compositions set the modelling upper-pressure limit at 6 GPa, restraining the calculations at the shallow part of the upper mantle and preventing a further investigation of deep magmatic systems. Therefore, the potential of a modelling approach was limited at relatively low pressures, and a modification and extension to the high pressure of the thermodynamic models of Tomlinson and Holland (2021) [1] was needed.

In this work, an improvement and extension in the calibration of the melt and the main anhydrous magmatic minerals have been developed using recent experimental data in the KNCFMASTOCr system. The new database, with 12 GPa as a pressure upper limit, allows the thermodynamic calculation of magmatic processes down to a depth of ~360 km in the terrestrial upper mantle. Specifically, the new calibration consists of (i) a new melt model for > 6 GPa, (ii) new end members for existing high-pressure phases (e.g., majorite), and (iii) refining low-pressure models for clinopyroxene, orthopyroxene, garnet, and spinel.

We demonstrate the application of the new database by applying it to komatiite generation. Komatiites are high Mg (≥ 18 wt.%) magmatic rocks that erupted primarily in the Archaean, favoured by hotter mantle conditions than today. This feature is widely considered the result of long and extensive melting processes, even though the geological settings where these processes took place are still discussed. We will investigate the variation in melt composition at different pressure-temperature conditions, validating the model against experimental data and comparing it to natural komatiites for a better understanding of mantle melting during the Archaean.

*References:*

[1] Tomlinson EL and Holland TJB (2021) J Petrol 62: 1-23

## Compositional effects of komatiite-peridotite reaction

Tomlinson, E.L.[1], Rinaldi, M.[1] and Melai, C.[1]

[1]Geology, School of Natural Sciences, Trinity College Dublin, Dublin, Dublin 2, Ireland. tomlinse@tcd.ie

The Archaean lithosphere is dominated by harzburgite with uniformly high Mg# (>92) and is widely considered to have formed as the residue after protracted, high degree (35-50%) mantle melting[1]. Komatiites are produced by very high degree peridotite melting that consumes orthopyroxene and olivine and were predominantly erupted in the Archean, observations that, at least qualitatively, complement the highly refractory nature of Archean peridotites. However, a simple melt-residue relationship is undermined by observations that (i) both komatiite and cratonic peridotite have depleted initial Hf-isotope compostions; and (ii) komatiite extends to both higher and lower silica than experimental melts of fertile peridotite. Therefore, the relationship between komatiite and the cratonic lithosphere is enigmatic.

At very high pressure, komatiite liquid is so compressible that it has similar density to solid peridotite, but at <13 GPa komatiite melt escapes and ascends through the overlying mantle, during which time it may react. Reaction of komatiite with earlier depleted peridotite in a mantle upwelling may account for the variable silica composition of both peridotite and komatiite melt and is potentially the missing link in the residue-melt relationship. Melt-rock reaction may also explain the lack of chemical stratification observed in the cratonic lithosphere and the absence of temporal trends in the $Al_2O_3/TiO_2$ evolution of komatiites.

In this contribution we use an updated version the thermodynamic model for peridotite in the system KNCFMASTOCr system to model the phase relations of a number of natural komatiites and demonstrate that many lack a multiple saturation point, suggesting that they may have undergone fractionation and/or reaction during ascent. In addition, we use the updated model to investigate the effect of komatiite-peridotite reaction on the compositions of both melt and residue for melts produced at 4-10 GPa. We compare our findings to natural komatiite and peridotites from the Archaean lithosphere.

## H storage and speciation within the deep Earth

Bolfan-Casanova N.[1]

[1]Laboratoire Magmas et Volcans, CNRS, UCA, IRD, Clermont-Ferrand, France

Hydrogen, incorporated as hydroxyl, has long been recognized to be an ubiquituous trace component of most mantle minerals [1]. Xenoliths from the cratonic keels host up to 200-250 hundreds of parts per million by weight of water (ppm wt $H_2O$). While in the convecting mantle, the water content measured in Mid Ocean Ridge Basalts (MORBs) also points out to a few hundreds of ppm wt $H_2O$ in their source at about 100 km depth. Deeper, the low seismic velocities atop the transition zone are unanimously interpreted as due to melting, especially dehydration melting, due to the high water content in the material ascending from the transition zone (estimates range from 0.2 to 1 wt% $H_2O$ see [2]). For the rest of the deeper part of the Earth, the lower mantle, there are very few constraints on the actual water content and the water storage ranges from 0.6 to 3 ocean masses depending on the storage in the main mineral bridgmanite, which is very controversial.

Because the Earth's mantle gets more and more reducing with increasing pressure [3], the speciation of H is expected to change as a function of depth, going from $H_2O$ and $OH^-$ under oxidizing conditions to $H_2$ under reducing conditions. And indeed, recently, we have discovered $H_2$ in natural omphacite from eclogite xenoliths brought up by kimberlites [4], in agreement with previous experimental observations [5]. Due to the difficulty in detecting $H_2$, with spectroscopy, it is possible that the H storage of the mantle has therefore been largely under-estimated in previous studies of mantle xenoliths.

Since the fractionation between minerals and $H_2O$ fluid is very different from that between minerals and $H_2$ fluid we expect that incorporation of $H_2$ in minerals will change the magnitude and possibly the sign of D/H fractionation at depth. Indeed, at equilibrium, the fractionation between hydrated, or rather hydroxylated, minerals (such as micas, chlorites, amphiboles and serpentines) and water is generally negative, indicating that deuterium is depleted in the mineral relative to the fluid during fractionation: the mineral is enriched in the "light" isotope. While in the presence of $H_2$, the fractionation between the mineral and the fluid is positive [6]. Thus, assessing the speciation of Hydrogen in the deep Earth appears a necessary pre-requisite to understanding the deep water cycle from the point of view of isotopes.

*References:*

[1] Bell DR and Rossman GR (1992) Science, 255: 1391-1397
[2] Andrault and Bolfan-Casanova N (2022) Phys Earth Planet Int 322
[3] Frost DJ and McCammon C (2008) Ann Rev Earth Planet Sci 36: 389-420
[4] Moine B et al. (2020) Nature Communications 11: 10
[5] Yang X and Keppler H (2016) Geochem Perspect Lett 2: 160
[6] Richet et al. (1977) Ann Rev Earth Planet Sci 5: 65-110

# Latest advances in hydrogen analysis in Nominally Anhydrous Minerals and Diamonds with ERDA

Bureau, H.[1], Khodja, H.[2], Estève I.[1]

[1]Institut de Mineralogie, de Physique des Materiaux et de Cosmochimie, Sorbonne Universite, CNRS UMR 7590, Paris, France

[2]Universite Paris-Saclay, CEA, CNRS, NIMBE, LEEL, Gif-sur-Yvette, France

---

Elastic Recoil Detection Analysis (ERDA) is now recognized as a reference method for the quantitative analysis of hydrogen (and water) in geological materials such as diamonds, garnets and accessory minerals such as staurolite or magnetites [1-4]. This method is based on the detection of recoil H nuclei produced by elastic collisions induced by a 2.7 - 3 MeV $^4He^+$ beam. Analyses are usually conducted by rapidly scanning a µm-focused beam on large areas of about 200x200 $\mu m^2$ (to prevent H loss), for 1 to 2h per sample. Three detectors are simultaneously employed: an ERDA detector to record H nuclei, an annular detector to record backscattered particles and an x-ray detector to record particle induced x rays. The sample holder is tilted in order to obtain a low grazing angle of 15° with respect to the sample surface allowing ejection of H nuclei from the analysed surface. Well-known reference materials are used to calibrate the backscattered detector solid angle at a normal incidence. The ERDA detector solid angle is calibrated in tilted geometry by using a Kapton standard and well-known glasses. During the course of the ERDA measurement, the backscattered spectrum provides precise estimation of the deposited charge on the sample, therefore permitting H quantification. The detection limit is calculated to be 5 to 6 ppm by weight H with an uncertainty of 8 to 15 % depending on the samples.

We will present the latest advances in ERDA to quantitatively analyse hydrogen (and water) in nominally anhydrous minerals, glasses and metals relevant to the depths of the Earth. Emphasis will be placed on specific preparations using cryogenic methods intended to avoid any loss of H in specific samples such as natural diamonds or for particularly fragile samples such as inclusions trapped in mantle minerals, or minerals and glasses from high pressure and high temperature experiments. When samples are too small to be analysed with ERDA, e.g. fibrous diamonds [1] or extra-terrestrial magnetites [4], it is also crucial to propose a method capable to characterize the hydrogen (and water) contents of reference samples to calibrate other methods more appropriate in terms of spatial resolution. The example of nanoSIMS analysis will be discussed. A few recent results about hydrogen in mantle minerals and their consequences for the deep water cycle will be also presented.

*References:*

[1] Vangu D., Bureau H., Khodja H., Charrondière M., Estève I., Béneut K., Remusat L., Gaillou E., P. Cartigny, Boulliard J.C. (2023) Diamond and Related Materials 136, 110007.

[2] Mosenfelder J.L., von der Handt A., Withers A.C., Bureau H., Raepsaet C., Rossman G. R. (2022) Coupled American Mineralogist, Volume 107, pages 587–602.

[3] S Azevedo-Vannson, L Remusat, H Bureau, et al. Rapid Commun Mass Spectrom. 2022;36(17): e9331. doi:10.1002/rcm.9331

[4] J. Aléon, S. Mostefaoui, H. Bureau, D.vangu, H. Khodja et al. (2024) Meteoritics and Planetary Sciences 1-15 doi: 10.1111/maps.14139.Smith R et al. (2012) Rev in Econ Geol 17: 1-12

# Hydrogen defect evolution in natural diamonds and implications for the preservation of primordial hydrogen

Day, M.C.[1], Pamato, M.G.[1*], Jollands, M.C. [2], Novella, D.[1], Nestola, F [1]., and Dovesi, R [3]

[1]Dipartimento di Geoscienze, Universita degli Studi di Padova, Via Gradenigo 6, I-35131, Padova, Italy

[2]Gemological Institute of America (GIA), 50 W 47th St., New York, NY 10036, USA

[3]Accademia delle Scienze di Torino, Via Accademia delle Scienze 6, 10123, Torino, Italy

**Corresponding Author***: Maxwell C. Day (maxwell.day@unipd.it)

---

Hydrogen (H), after nitrogen (N), is the most common impurity in natural diamonds reaching concentrations up to thousands of at. ppm. Both impurities provide important geochemical information regarding the mantle substrates and fluid/melt associated with diamond formation. It is important to understand the type of defects in which impurities like N and H are hosted in the diamond structure as this allows for classification diamonds and determination of their residence time/temperature in the mantle. This is done by interpretation of the distinct signal that each N/H-defect produces in the infrared (IR) spectra of diamonds measured using Fourier Transform IR spectrometry. Alternatively, computational methods developed in recent years can be used to improve our understanding of the origin and evolution of such defects.

The mechanisms by which N atoms substitute for carbon and migrate through diamond to form a variety of different defects is well-understood, with the most common N-defects being single substitutional N (C-centers), $N_2$ dimers (A-centers) and $VN_4$ defects (B-centers). Our understanding of H in diamond, on the other hand, is much more restricted as it is largely based on only a handful of H-related peaks observed in the IR spectra of *Type IaA* (A-centers) and *IaB* (B-centers) diamonds. The most common H-related peaks, located at 3107 and 3236 $cm^{-1}$ correspond to the C-H stretching modes of the $VN_3H$ and $VN_4H$ defects (V = carbon vacancy), respectively [1,2]. These defects are assumed to form from trapping of interstitial H ($H_i$) by $VN_3$ and $VN_4$ which suggests that after incorporation, H remains interstitial during much of the diamond's residence time in the mantle. To gain a better understanding of H incorporation, we report a comprehensive and up-to-date compilation of observed and computed hydrogen (H)-related peaks for different V-N-H defects. This unique compilation of data revealed an extremely large number of peaks in the C-H stretching region of some *type Ib* (C-centers) diamonds suggesting $H_i$ may be trapped much earlier during residence or even during diamond growth [3]. Our results suggest that H in the diamond forming media or $H_i$ is trapped during or shortly after diamond growth and that the most common H-defects in *Type IaA and IaB* diamonds (e.g. $VN_3H$) likely form by combination of simpler V-N-H defects (e.g. NH) rather than by trapping of $H_i$ by highly aggregated defects like $VN_3$. These new findings have important implications for the ability of diamonds to preserve the original (potentially primordial) H isotopic composition and thus may serve as a proxy for the origin of water on Earth.

*References:*

[1] Goss J P *et al*. (2014) J. Phys. Condens. Matter 26: 145801.
[2] Keat T J *et al*. (2024) Diamond Rel. Mat. 141: 110661.
[3] Day M C *et al.* (2024) Diamond Rel. Mat. 143: 110866.

## The spectroscopy of hydride in perovskites

Palfey, W.R.[1], Hwang, S.J.[2], Goddard, W.A. III[3], and Rossman, G.R.[1]

[1]Division of Geological and Planetary Sciences, California Institute of Technology

[2]Division of Chemistry and Chemical Engineering, California Institute of Technology

[3]Materials and Process Simulation Center (MSC), California Institute of Technology

---

With only a handful of exceptions, the study of hydrogen in nominally anhydrous silicate and oxide mantle phases has focused primarily on $OH^-$ groups. This speciation of hydrogen is well established and makes intuitive sense in the context of oxide-based minerals. However, insights from materials science research have revealed that an alternate form of hydrogen is stable in crystalline oxides: the hydride ion ($H^-$). Under highly reducing conditions, hydrogen may bond directly to cation species, taking on a negative charge and directly substituting for $O^{2-}$. These substitutions are highly favorable in the (Ca,Sr,Ba)$TiO_3$ family of perovskites, where up to 20% of all $O^{2-}$ ions can be replaced with $H^-$, with significant implications for material properties[1]-[4]. Given that these Ti-based materials are structural analogues to bridgemanite and davemaoite (the 1st and 3rd most abundant mantle phases, respectively), it is natural to wonder whether hydride could be a component of perovskites in the deep earth, potentially representing a large, "hidden" reservoir for hydrogen. Nonetheless, many aspects of hydride incorporation in perovskites have yet to be thoroughly investigated. This includes detection of $H^-$ via methods like infrared (IR) spectroscopy, which are suitable for *in-situ* high pressure experiments and analysis of diamond inclusion samples. Without these analytical capabilities, hydride's importance in the mantle cannot be assessed.

In this presentation, we report our work to characterize the H- ion in titanate perovskite materials through a combination of computational and experimental techniques. We have successfully documented vibrational modes attributed to hydride incorporation in perovskites via infrared spectroscopy and find that the spectral signatures of $H^-$ can be easy to overlook and difficult to identify. This stands in direct contrast to the more widely studied and characterized $OH^-$ modes. Complimentary information provided by density functional theory (DFT) calculations and $^1H$ nuclear magnetic resonance (NMR) spectroscopy is shown to be essential in interpreting and contextualizing these infrared features. Based on our findings from analogue titanate perovskites, we also propose possible mechanisms through which hydride may be incorporated into silicate perovskites and simulate their spectra via DFT. This work represents the preliminary steps toward more advanced studies of $H^-$ in silicate perovskites, which could include hydride's solubility in the lower mantle and its effect on bulk material properties. If hydride proves to be a viable constituent of lower mantle silicates, then current models of the deep earth hydrogen budget will need to be fundamentally revised to account for this new component.

*References:*

[1] T. Sakaguchi *et al.*, *Inorg. Chem.* **51**, 11371–11376 (2012).
[2] Y. Kobayashi *et al.*, *Nature Mater.* **11**, 507–511 (2012).
[3] R. Aleksis *et al.*, *Phys. Chem. Chem. Phys.* **24**, 28164–28173 (2022).
[4] T. Gao *et al.*, *Adv Elect Materials*. **9**, 2300068 (2023).

# High resolution transmission electron microscopy of a defect in hydrous forsterite

Miyajima, N.[1], Purevjav, N.[1] and Withers, A.C.[1]

[1]Bayerisches Geoinstitut, Universität Bayreuth, D-95440, Germany, Nobuyoshi.Miyajima@uni-bayreuth.de

Water is stored in hydrous and nominally anhydrous minerals (NAMs) mainly as hydroxyl groups and hydrous defects, respectively, and is transported into the deep Earth via plate tectonics. Hydrogen in NAMs can play important roles in geophysical properties in the Earth. Olivine is the most abundant NAM in the upper mantle, and has a larger capacity to contain hydrogen under high pressure conditions, e.g., up to about 10,000 ppm at 12 GPa and 1250 °C. The site distributions of hydrogen and the related disordered olivine structure are under the spotlight because they control the mobility of elements such as hydrogen, magnesium and silicon. As a result, cation diffusion plays a role in the rheology of the upper mantle. With saturation of hydrogen contents, some hydrous phases in the humite group can be crystallized as nanometer-sized lamellae, visible only in transmission electron microscopy (e.g., Khisina et al. [1]). To understand the mechanisms of hydrogen substitution in olivine, we report a defect in hydrous forsterite.

Forsterite was examined using transmission electron microscopy (TEM). To avoid high-energy beam irradiation damage in the thin foil preparation, the sample powders made from single crystals of forsterite and olivine were directly loaded on TEM grids with ethanol solvent. Additionally, energy-dispersive X-ray spectroscopy (EDS) analysis in scanning TEM was conducted to identify any chemical differences within the forsterite fragments in the sample powers.

High resolution transmission electron microscopy (HRTEM) of a hydrous forsterite containing about 2000 ppm wt. $H_2O$ revealed a cryptic contrast on the projected image along the [010] zone axis. The fast Fourier transformed patterns of the HRTEM images and selected area electron diffraction (SAED) patterns show diffuse scattering and superlattice diffraction spots between the Bragg spots of the forsterite structure, which implies evidence of a short-range ordering of elements, i.e., crystal defect cluster in the structure. The defects detected might be related to hydrogen substitution mechanisms on the cation sites of Mg and/or Si in forsterite. The low-magnification bright-field and dark-field TEM images with a reflection of $\boldsymbol{g}$ = 004 also display a dusty diffraction contrast, but no chemical difference in the EDS analysis was detected. In comparison, a hydrous Fe-bearing olivine containing about 2000 ppm wt. $H_2O$ and 10 % fayalite component was also investigated in HRTEM using the same TEM system. The olivine displayed neither similar cryptic contrast nor diffuse scattering/superlattice spots in HRTEM and SAED pattern, respectively.

A cryptic crystal defect in hydrous forsterite was visualized in HRTEM. The defective hydrous forsterite is an intermediate candidate to provide the missing link between isolated local defects (ILD) and condensed extended defects (CED) (in the terminology of Matsyuk and Langer, [2]) in the transformation between forsterite and hydrous minerals under high pressure conditions.

*References:*

[1] Khisina N.R., Wirth, R., Andrut, M., and Ukhanov, A.V. (2001) Phys. Chem. Miner. 28:291-301.
[2] Matsyuk, S.S., and Langer, K. (2004) Contrib Mineral Petr 147: 413-437.

## The coesite-stishovite transition of hydrous, Al-bearing $SiO_2$: An in situ synchrotron X-ray study

Koch-Müller, M.[1], Lathe, C.[1,2], Wunder B.[1], Appelt, O.[1], Bhat, S.[2], Farla, R.[2], Roddatis, V.[1], Schreiber, A.[1], Wirth, R.[1]

[1] Deutsches GeoForschungsZentrum GFZ, Telegrafenberg 14473 Potsdam, Germany, mkoch@gfz-potsdam.de

[2] DESY, Deutsches Elektronen Synchrotron, Notkestrasse 85, 22607 Hamburg, Germany

---

Seismic discontinuities in the depth range of 230-350 km (termed X-discontinuities) are linked to the phase transition of coesite (coe) to stishovite (sti) [1] which may occur in the oceanic subducted crust. It is assumed that the transition is sharp because $SiO_2$ is thought to be a near pure component in the recycled basalt [2].

However, it is well-known that coe and sti can incorporate significant amounts of Al and H in their structures by various substitutions [e.g. 3]. The intension of this study was to determine if Al and H incorporations have an influence on the P, T position of the coe-sti phase boundary, in analogy to the compositional-induced shift of the sti to post-sti transition [4].

We examined the transformation of coe to sti in the presence of 1 wt. % $Al_2O_3$ and water in excess by means of in situ X-ray diffraction measurements with the large-volume press at the synchrotron PETRA III, Hamburg.

Compared to the pure $SiO_2$ system the coe-sti transition in hydrous Al-bearing $SiO_2$ is shifted parallel to Ono et al. [5] by about 0.7 GPa to lower pressures. Additionally, we observed in the recovered samples of our experiments much less sti than expected from the in situ experiments. The hydrous Al-bearing sti of our experiments partly transformed back to coe, with an unusual high Al- and H-content.
Thus, conventional quench experiments would lead to erroneous results of the coe-sti transiton in the Al, H bearing $SiO_2$-system.

*References:*

[1] Williams Q and Revenaugh J (2005) Geology 33:1-4.
[2] Zhang J et al. (1996) Phys Chem Min 23:1-10.
[3] Chen M et al. (2024) Solid Earth 15:215-227.
[4] Bolfan-Casanova N et al. (2009) Phys Earth Plan Int 174:77-80.
[5] Ono S et al. (2017) Phys Earth Plan Int 264:1-6.

## Spin transition links water and ferric iron in Earth's lower mantle

Buchen, J.B.[1,2,3], Pardo, O.S.[2], Dobrosavljevic, V.V.[2], Sturhahn, W.[2], Ishii, T.[1], Chariton, S.[4], Greenberg, E.[4], Toellner, T.S.[5] and Jackson, J.M.[2]

[1]Bayerisches Geoinstitut, Universität Bayreuth, Bayreuth, Germany, EU; johannes.buchen@uni-bayreuth.de

[2]Seismological Laboratory, California Institute of Technology, Pasadena, CA, USA

[3]Department of Earth Sciences, University of Oxford, Oxford, England, UK

[4]GSECARS, The University of Chicago, Chicago, IL, USA

[5]Advanced Photon Source, Argonne National Laboratory, Argonne, IL, USA

---

Ocean island basalts (OIB) and other magmas erupted at hotspots tend to have higher $H_2O$ contents than mid-ocean ridge basalts (MORB) [1]. Since hotspots are believed to be rooted in Earth's lower mantle, significant amounts of water or $H_2O$ might be stored in minerals and melts of the lower mantle. The $H_2O$ content of hotspot magmas correlates with their $Fe^{3+}/\Sigma Fe$ ratio in several locations [2], indicating a potential connection between $H_2O$ and ferric iron.

At pressures and temperatures of the lower mantle, $H_2O$ may be stored in high-pressure oxyhydroxide phases, which can be described as solid solutions between $MgSiO_2(OH)_2$ (phase H), δ-AlOOH (δ-phase), and ε-FeOOH (ε-phase). In experiments, oxyhydroxide solid solutions have been found to form in equilibrium with bridgmanite [3], further substantiating their potential role as $H_2O$ host phases. High-pressure oxyhydroxides containing ferric iron undergo a spin transition at pressures of the lower mantle [4,5]. How this spin transition affects the stability of oxyhydroxide phases as well as the phase equilibria that control $H_2O$ storage, however, remains unexplored. We performed a series of high-pressure experiments on samples of δ-(Al,Fe)OOH, including high-pressure and high-temperature X-ray diffraction (XRD) and high-pressure nuclear resonant inelastic X-ray scattering (NRIXS) experiments, to constrain the changes in energy associated with the spin transition of ferric iron in high-pressure oxyhydroxides. Based on our and previous [6] experimental results, we constructed a thermodynamic model to evaluate the impact of the spin transition on phase equilibria.

According to our analysis, the spin transition of ferric iron in high-pressure oxyhydroxide phases may reduce the thermodynamic activity of $H_2O$ in a coexisting hydrous melt by several orders of magnitude. This reduction in the $H_2O$ activity implies that the spin transition significantly reduces the amount of $H_2O$ that would be required to form an $Fe^{3+}$-bearing oxyhydroxide phase. Alternatively, if the $H_2O$ activity is buffered at a nearly constant value, the spin transition will shift the dehydration reaction of an $Fe^{3+}$-bearing oxyhydroxide phase to higher temperatures. By stabilising $Fe^{3+}$-bearing oxyhydroxides at lower $H_2O$ activities and to higher temperatures, the spin transition of ferric iron may facilitate the storage of $H_2O$ in the lower mantle. The resulting geochemical association of $H_2O$ with ferric iron might be sampled by deep-rooted plumes and reflected in their magmas.

*References:*

[1] Hirschmann M M (2006) Annu Rev Earth Planet Sci 34:629–653
[2] Brounce M et al. (2017) Proc Natl Acad Sci USA 114:8997–9002
[3] Walter M J et al. (2015) Chem Geo 418:16–29
[4] Ohira I et al. (2019) Am Mineral 104:1273–1284
[5] Strozewski B et al. (2023) J Geophys Res Solid Earth 128:e2022JB026291
[6] Ohira I et al. (2021) Sci Rep 11:12036

## Water partitioning between nominally anhydrous minerals and hydrous minerals, and the role of water in subducting slabs

Ohtani, E.[1] and Ishii, I.[2]

[1]Department of Earth Science, Tohoku University, eohtani@tohoku.ac.jp

[2]Institute for Planetary Materials, Okayama University

---

We have investigated the water partitioning between nominally anhydrous minerals and hydrous minerals under the water-undersaturated conditions. Our experiments revealed that water is strongly preferred to hydrous phases resulting in formation of nearly dry nominally anhydrous minerals such as olivine (<1 ppm), wadsleyite (<300ppm), and bridgmanite (<1ppm) under the water-undersaturated conditions [1, 2]. Aluminum is strongly partitioned to both aluminous phase D and phase δ-H solid solution resulting in alumina depletion in coexisting bridgmanite.

Rheology and deformation of dry olivine and its phase transformation kinetics have been applied to large deformations of subducting slabs in the mantle transition zone [3] and origin of the deep seismicity [4]. Geophysical and mineral physics data together with our experiments revealed that subducting slabs are under the wet conditions, and water is stored mainly in hydrous minerals and coexisting nominally anhydrous minerals are essentially dry. Therefore, the dry transformation kinetics of olivine and its high-pressure polymorphs can be applied even to wet slabs under water-undersaturated conditions. Our results also revealed that dry anhydrous minerals could exist in wet slabs at the top of the lower mantle. Some of the deep earthquakes occurred at the depths exceeding 660 km may be caused by dehydration of hydrous minerals such as superhydrous phase B and phase D which are stable at the top of the lower mantle. The dry nature of bridgmanite coexisting with hydrous minerals suggests that the major water carriers in the lower mantle are hydrous minerals, and bridgmanite cannot be the water reservoir and can result in dry rheology of the wet lower mantle.

*References:*

[1] Ishii T and Ohtani E (2021) Nat Geosci 14:526-530
[2] Ishii T et al. (2022), Earth Planet Sci Let 583:117441
[3] Mohiuddin A et al., Nature Geosci.(2020) 13:170–174
[4] Kirby SH et al. (1996) Rev. Geophys. 34, 261–306

# The importance of carbon to the formation and composition of silicates during mantle metasomatism

Rinaldi, M.R.[1], Mikhail, S.[2], Sverjensky, D.A.[3] and Kalita, J.[2]

[1] Geology, School of Natural Sciences, Trinity College Dublin, Dublin, Ireland. rinaldim@tcd.ie

[2] School of Earth and Environmental Sciences, University of St. Andrew, UK

[3] Department of Earth and Planetary Sciences, Johns Hopkins University, USA

---

Mineral and fluid inclusions in mantle diamonds provide otherwise inaccessible information concerning the nature of mantle metasomatism and the role of fluids in the mass transfer of material through the Earth's interior. We explore the role of carbon concentration during fluid-rock metasomatism in generating the range of garnet and clinopyroxene compositions observed in diamonds from the sub-continental lithospheric mantle. We use the Deep Earth Water model to predict the results of metasomatism between silicic, carbonatitic and peridotitic fluids and common mantle rocks (peridotites, eclogites and pyroxenites) at 5 GPa, 1000 ◦C, across a range of redox conditions ($\log fO_2$ = − 2 to − 4 ΔFMQ), and a wide range of initial carbon concentrations in the metasomatic fluids.

Our results show that the predicted compositions of metasomatic garnets and clinopyroxenes are controlled by the initial geochemistry of fluids and rocks, with subsequent mineral-specific geochemical evolution following definable reaction pathways. Model carbon-rich metasomatic fluids that can form diamond (initial C-content > 5.00 molal) result in Mg-rich garnets and clinopyroxenes typical of peridotitic, eclogitic, and websteritic inclusions in diamonds. However, model carbon-poor metasomatic fluids that do not form diamond result in Mg-poor, Ca-rich garnets and clinopyroxenes. Such garnets and clinopyroxenes do nevertheless occur as inclusions in diamonds. In our models, the abundance of carbon in the fluids controls the behaviour of the bivalent ions through the formation of aqueous Mg-Ca-Fe-C complexes, which directly govern the composition of garnets and clinopyroxenes precipitated during the metasomatic processes. As the C-rich initial fluids can form the higher Mg-eclogitic, peridotitic, and websteritic inclusions in diamonds, these inclusions can be syngenetic (metasomatic) or possibly protogenetic. However, in our models, the relatively Mg-poor, Ca- and Fe-rich eclogitic garnet and clinopyroxene inclusions found in mantle diamonds formed from C-poor fluids that do not precipitate diamond. These inclusions most likely reflect a metasomatic event prior to being incorporated into their host diamonds, or they could represent protolith-based protogenetic geochemistry. Therefore, the paragenetic groups used to classify diamonds should not be considered a genetic classification, as the role of fluid geochemistry appears to be more important than the one played by host rock geochemistry [1].

*References:*

[1] Rinaldi M., Mikhail S., Sverjensky D.A. and Kalita J. (2023) GCA 356: 105 - 115

# Phase relations in the system $MgO-CO_2-H_2O$: dehydration of brucite and melting of brucite and magnesite in subduction zones

Sieber, M.J.[1,2], Reichmann, H-J[2] , Farla, R.[3] , Koch-Müller, M. [2]

[1]University of Potsdam, Institute for Geosciences and melanie.sieber@uni-potsdam.de

[2]GFZ German Research Centre for Geosciences

[3]Deutsches Elektronen-Synchrotron DESY

---

The fates of carbon and hydrogen in the mantle are intimately linked to each other. For instance, within the subducting slab, hydrous minerals transport water into the mantle and the condition under which hydrous minerals release $H_2O$ effect not only the distribution and cycle of $H_2O$ in the mantle but also enhance the dissolution of carbonates. Further, it is undisputed that the presence of $H_2O$-bearing fluids reduces the melting point and initiates partial melting of carbonate-bearing rocks.

We examined the stability of brucite ($Mg(OH)_2$), studied as a prototype for hydrous and layered minerals, and elucidated the behaviour of Mg-carbonate (magnesite; $MgCO_3$) in the presence of a hydrous fluid between 1 and 12 GPa.
Two experimental approaches were applied: In situ energy dispersive X-ray diffraction (EDXRD) experiments in the 'Aster-15' 3 x 5 MN six-ram multi-anvil press at the P61B end-station at the 'Deutsches Elektronen-Synchrotron' was used to monitor changes in the mineral assemblage as function of pressure and temperature. In addition, the falling sphere method was applied and textures of quenched products were investigated by scanning electron microscopy. In all experiments, the magnesite/fluid-ratio was kept constant by using a mixture of natural magnesite powder ($Mg_{9.9}Fe_{0.1}Ca_{0.03}(CO_3)_{10}$ from Brumado, Brazil) and 16 wt% laboratory-grade brucite as starting material establishing ~5 wt% $H_2O$ in the capsule after dehydration of brucite. Using EDXRD, the onset of dehydration and melting are indicated by rapid changes in the peak intensity of solids during heating. Starting materials were loaded in diamond cylinders enclosed on top and bottom by Pt-lids. The ductile behavior of platinum enclosed and sealed the diamond cylinder under compression and upon heating.

Experiments show that brucite dehydrates forming periclase and $H_2O$ up to about 4 GPa and 1400 K. This incongruent dehydration reaction has a positive Clapeyron slope. Between 4 and 10 GPa brucite is stable up to about 1423 K. A negative Clapeyron slope is found for the incongruent melting of brucite above 10 GPa.
In the presence of periclase and an aqueous fluid, magnesite is stable up to e.g. 1473 K at 1.6 GPa and 1673 K at 3.5 GPa. Between 6 to 9 GPa, magnesite is stable with periclase and a supercritical fluid up to 1923-1948 K. Compared to the anhydrous system, adding about 5 wt% $H_2O$ lowers the stability of magnesite by ~100 K for pressures below 6.5 GPa. For pressures above 6.5 GPa, the liquidus of the anhydrous and hydrous system diverges strongly with increasing pressure.

The observed phase transitions provide insights into the fate of magnesite-bearing rocks in subduction zones, particularly when they are infiltrated by fluids released due to the breakdown of hydrous minerals (e.g. brucite). Our findings show that magnesite remains stable under typical subduction zone gradients even when infiltrated by hydrous fluids. Therefore, we conclude that magnesite can be subducted down to and beyond sub-arc depths.

## Using quartz to constrain the formation conditions of pegmatites

Bermanec, M.[1], Pettke, T.[1] and Hermann J.[1], Nils Gies[1]

[1]Institute of Geological Sciences, University of Bern, Baltzerstrasse 1+3, Bern, Switzerland; Corresponding email: marko.bermanec@gmail.com

---

Studying fluid evolution is crucial for understanding the formation of pegmatites as it provides insights into the geological processes, mineral formation mechanisms, and the deposition of scientifically and economically relevant minerals. This case study investigates the genesis of pegmatites in the Misox valley, European central Alps [1] and on Elba Island [2], to unravel their formation mechanisms using a multidisciplinary approach. The study integrates careful petrography, petrology, fluid inclusion microthermometry, and the major to trace element composition analyses of pegmatite-forming minerals and hydrothermal fluids. By examining samples from pegmatites formed by partial melting of crustal lithologies such as paragneisses and orthogneisses in the Central Alps, the research sheds light on the complex processes underlying pegmatite formation, comparing it to a classic model of pegmatite formation from residual S-type granitic melts from Elba Island.

A novel aspect of this work involves an extensive dataset derived from Fourier-transform infrared spectroscopy (FTIR) mapping of quartz from pegmatite miarolitic cavities. These FTIR maps characterize $H_2O$ incorporation in quartz crystals across different structural sites and correlate it with variable trace element composition, as revealed by texturally well-controlled laser ablation inductively coupled plasma mass spectrometry (LA-ICP-MS) spot measurements. Quartz crystals from both localities exhibit distinct zoning patterns, with core-rim zoning observed in both samples but significantly more complex zonation patterns in Misox samples. In Rosina, a core-rim zonation is present for Li, Al, and $H_2O$, with higher concentrations in the cores compared to the rims. Boron exhibits an oscillatory zoning pattern within the same crystals. In Misox, all elements exhibit lower concentrations in the cores, with higher concentrations occurring in complex zonation at the tips of the crystals. In Rosina, the concentrations of Li, B, Al, and Ti in quartz range from 11 to 454, 1 to 250, 43 to 1780, and 0.16 to 12 µg/g, respectively. In Misox, the concentrations range from 0.5 to 100, 0.05 to 11, 4.5 to 764, and 0.02 to 5.7 µg/g for Li, B, Al, and Ti, respectively. The quantification of $H_2O$ was performed according to the method described in [3] with an in-house software SpecXY [4]. Concentrations of $H_2O$ reach up to 50 µg/g in the cores of Rosina quartz, falling to around 15 µg/g at the rim of the crystals. In Misox, the concentration of $H_2O$ in quartz reaches up to 40 µg/g at the tips of the crystals, while the cores rarely have over 10 µg/g. Furthermore, individual fluid inclusions were measured by LA-ICP-MS to determine the fluid solute loads. Pegmatite formation conditions are constrained with several methods including two feldspar thermometry, Ti-In-Quartz thermometry, and solidi calculations of S-type granitic magma.

The multi-method analytical approach to studying quartz, coupled with the classic petrological analyses of vein mineralization and host rocks holds significant promise as a valuable method of tracing fluid evolution during magmatic – hydrothermal transition and contributes to the fields of pegmatite research and the understanding of water incorporation mechanisms in magmatic-hydrothermal quartz. The findings show that FTIR can be efficiently used to track the conditions of late-stage hydrothermal mineralization processes in pegmatitic and other hydrothermal systems.

*References:*

[1] Stroppini A (2019) Schweizer Strahler 3:2-19
[2] Altieri A et al (2023) Min Mag 87(1):130-142
[3] Stalder R (2021) Eur J Mineral 33:145-163

## Hydrogen concentrations and petrophysical properties of an exceptionally fresh tectonically exhumed oceanic mantle lithosphere sliver

Demouchy, S.[1], Barou, F.[2] , Ishikawa, A.[3], Gardés E.[1], and Tommasi A.[2]

[1]Laboratoire Magmas et Volcans, Université Clermont Auvergne, CNRS, IRD & OPGC, France, sylvie.demouchy@uca.fr

[2]Geosciences Montpellier, CNRS & Université de Montpellier, Montpellier, France

[3]Tokyo Institute of Technology, School of Sciences, Japan

---

We characterize and quantify the microstructure, hydrogen concentrations, and seismic properties of a tectonically exhumed – very fresh – sliver of oceanic lithospheric mantle outcropping in the Moa Island (Leti archipelago, Timor-Tanimbar region). The 18 studied spinel peridotites (lherzolites and harzburgites) display variable degrees of olivine recrystallization (6.9-31.3 %), recorded by growth of strain-free neoblasts onto the pre-existing deformed (coarse-porphyroclastic) microstructure. Occurrence of clinopyroxenes with interstitial (cuspate) shapes and crystal-preferred orientations (CPOs) uncorrelated with the olivine CPO implies post-deformation crystallization by reactive melt percolation. The olivine CPO has dominantly axial-[010] or [100](010) patterns, similar to those usually observed in peridotitic xenoliths from oceanic mantle lithosphere. Seismic properties are calculated based on the modal compositions and CPO data for all samples. Increase in the olivine recrystallized fraction decreased the seismic anisotropy, since dynamic recrystallization produced some dispersion of the CPO but did not change the pattern acquired during the asthenospheric deformation. Average seismic velocities (mean Vp=7.9 km.s$^{-1}$; mean Vs=4.5 km.s$^{-1}$) and anisotropy (mean maximum S wave polarization anisotropy = 4.5%) are estimated by considering coherent orientation of the foliation and lineation of all samples. The nominally anhydrous minerals contain small amounts of hydrogen (olivine: 18 ppm $H_2O$ by weight; orthopyroxene: 58-175 ppm $H_2O$ wt and clinopyroxenes: 244-288 ppm $H_2O$ wt), which yields an average bulk water content of 50 ppm $H_2O$ wt for the Moa spinel-bearing peridotites, in agreement with previous estimates for the oceanic mantle lithosphere based on peridotitic xenoliths. This is the first direct measurement of the hydrogen concentrations in peridotites from an oceanic mantle lithosphere not modified by extensive serpentinization or magmatic extraction. As previously reported, no correlation between CPO patterns and hydrogen concentrations is found.

# SpecXY – an open-source tool for working with spatial spectroscopic data

Gies, N.B.[1], Hermann, J.[1], Lanari, P.[1]

[1]Institut für Geologie, Baltzerstrasse 1+3, 3012 Bern, Switzerland

---

Spectroscopic techniques such as Fourier Transform Infrared Spectroscopy (FTIR) or Raman are important tools to estimate volatile contents in minerals. In recent years there has been a shift away from using exclusively single-spot analysis towards using a combination of multiple single point measurements or even multi-dimensional maps. These combined measurements help to reveal patterns in a sample that would not be revealed by single point measurements. Filtering and extracting signal information from multiple combined spectra can help improve the signal-to-noise ratio and therefore the accuracy of the data. However, the amount of data and information in the dataset increases significantly when maps are used instead of single spot analysis. Combining multi-layered numerical datasets - bringing together different types of information (e.g., obtained using different instruments, grain orientations or measurement settings) - expands the ability to explore and investigate individual samples in much greater detail.

To explore these large datasets, we will present SpecXY, a user-friendly and open-source software solution for preparing, manipulating, exploring, extracting, and comparing large (spatially resolved) spectral datasets. SpecXY can be used to visualise and classify spectra, perform peak deconvolution, and correlate spectral data with chemical data (e.g., from EMPA, LA-ICP-MS) or other numerical data.

SpecXY consists of three main modules for processing spectroscopic data. The first module SpecMaps is designed for the investigation of spatially resolved spectroscopic data and allows various maps to be generated. This module provides a quick and efficient way to compare signals between different areas and extract average spectra for further calculations. It can be used to visualise and classify spectra, perform peak deconvolution from pixel spectra, and to correlate spectral data with chemical data (e.g. from EMPA and/or LA-ICP-MS) or other numerical data of the same area. SpecMaps can handle any data type containing a map of wavenumber energy frequency wavelength and intensity. The second module SpecDB is designed as a spectra database with the ability to perform manipulations, advanced peak deconvolution, calculations (e.g. $H_2O$ quantification), match unknown spectra or visualise and compare important features in selected spectra. The third module GeoCPlot allows to classify data and helps to visualise numerical data in classified correlation matrices.

The simple graphical user interfaces makes SpecXY accessible to all users with basic computer skills. Advanced users with an understanding of MATLAB programming can adapt, customise and extend SpecXY due to its modular and function-based program structure.

# Three dimensional distribution of hydrogen distribution in corundum resolved using photoluminescence lifetime imaging

Jollands, M.C.[1], Jones, D.J.[2] and Jin S.[3]

[1] Gemological Institute of America, 50 W. 47th St, New York, NY 10036, USA

[2] Gemological Institute of America, Suite 101, 303 Meadowlands Parkway, Secaucus, NJ 07094, USA

[3] Gemological Institute of America, 5355 Armada Dr, Carlsbad, CA 92008, USA

---

Mapping hydrogen distributions in experimental and natural samples generally requires samples to be sectioned into slabs and polished. This naturally means that some features will be lost. Here, we present a method whereby the distribution of H in corundum is determined using confocal photoluminescence lifetime imaging.

The method is summarized as follows. Divalent cations into corundum, in some cases, are charge compensated by electron holes. These holes often contribute to the colour of natural and synthetic crystals. These holes quench the photoluminescence of $Cr^{3+}$, which is present in all natural corundum, and detectable in all synthetic corundum that we have studied so far. This quenching is associated with a shorter luminescence lifetime. A higher concentration of holes means a shorter average $Cr^{3+}$ - hole distance, therefore more intense quenching. The addition of H into such crystals may be associated with the removal of these holes. Therefore, the addition of H reduces the quenching of $Cr^{3+}$, and increases its luminescence lifetime. The luminescence lifetime of $Cr^{3+}$ can be mapped using a confocal system, therefore allowing a three dimensional map of hole concentration to be constructed.

Simulations of the quenching through Forster resonance energy transfer allows a relationship between $Cr^{3+}$ lifetime, hole concentration and H concentration to be determined, therefore allowing the data to be converted into a 3D map of H concentration. At this point, the data remain semi-quantitative, and the method is only currently suitable for some experimental samples using specific types of simple synthetic corundum, but future developments in understanding may allow this to be used in more complex systems.

## Water in the continental lithosphere: insights from inclusions in diamonds

Curtolo, A.[1,*], Novella, D.[1], Bolfan-Casanova, N.[2], Day, M.C.[1], Pamato, M.G.[1], Nestola, F.[1] and Harris, J.W.[3]

[1]Dipartimento di Geoscienze, Università degli Studi di Padova, Padova, Italy

[2]Laboratoire Magmas et Volcans, CNRS, IRD, OPGC, Université Clermont Auvergne, Clermont-Ferrand, France

[3]School of Geographical and Earth Sciences, University of Glasgow, G12 8QQ Glasgow, UK

[*]Corresponding author: andrea.curtolo.2@phd.unipd.it

---

Diamonds contain mineral inclusions from otherwise inaccessible regions of the mantle that are trapped during diamond formation and are protected from subsequent interactions with the surrounding environment. Consequently, mineral inclusions in diamonds have been used in many studies to investigate the geochemistry and petrology of the interior of our planet.

Recently, studies have focused on measuring the $H_2O$ concentration of nominally anhydrous mineral (NAMs) inclusions in lithospheric diamonds to investigate the presence of $H_2O$ in that part of the mantle and evaluate the potential effect water has on rheology and cratonic stabilization. These studies revealed that, in general, and irrespective of paragenesis, inclusions have null or very low $H_2O$ concentrations (< 50 ppm wt.). These findings are in contrast with $H_2O$ concentrations obtained from xenoliths where concentrations can range from 100 to 1000 ppm wt. or more in certain eclogitic samples [1]. Recent studies [1, 2] highlight the important effect of metasomatism in modifying the $H_2O$ concentration of NAMs in xenoliths, possibly leading to overestimation of the $H_2O$ content of the cratonic lithosphere. Thus, the study of NAMs inclusions in diamonds might be key to assessing the original $H_2O$ concentration of the lithosphere allowing for accurate modelling of its physico-chemical properties.

Currently, studies determining the $H_2O$ content of NAMs inclusions in diamonds are still relatively scarce and those published focus largely no peridotitic mineral inclusions in diamonds from the Siberian craton. In addition, almost no data are available regarding the $H_2O$ content of eclogitic inclusions (in particular omphacites), despite their high-water storage capacity [3, 4] and high $H_2O$ contents reported by natural samples [5, 6].

Here we present data on the $H_2O$ content of 117 NAMs inclusions in diamonds (more than the entire available literature) using Fourier Transform Infra-Red (FTIR) spectroscopy and with an emphasis towards eclogitic inclusions and in particular omphacites from African kimberlites. The new data are compared with analogous data from mantle xenoliths and in the context of their paragenesis. From this data important implications are made about the viscosity of the lithosphere, the long-term stability of cratons, and the $H_2O$ content of the continental lithosphere.

*References:*

[1] Peslier AH et al. (2017) Space Sci Rev 212:743-810
[2] Wang YF et al. (2021) Geochim Cosmochim Ac 292:382-408
[3] Bromiley GD et al. (2004) Am Mineral 89:941-949
[4] Bromiley GD and Keppler H (2004) Contrib Mineral Petrol 147:189-200
[5] Skogby H (2006) Rev Mineral Geochem 62:155-167
[6] Moine B et al. (2020) Nat Commun 11:3604

## Data-driven discovery in mineralogy: Mineral evolution, mineral ecology, and Edward Grew's legacy

Hazen, Robert M.[1]

[1]Earth and Planets Laboratory, Carnegie Institution for Science, Washington DC 20015 USA

---

The story of Earth is a 4.5-billion-year saga of dramatic transformations, driven by physical, chemical, and biological processes. The co-evolution of life and rocks unfolded in an irreversible sequence of evolutionary stages [1-3]. Each stage re-sculpted our planet's surface, while introducing new planetary processes and phenomena. This grand and intertwined tale of Earth's living and non-living spheres is coming into ever-sharper focus, thanks to advances in "mineral informatics"—a field that employs large and growing mineral data resources to tell the deep-time stories of our evolving planet [4-6].

Minerals are remarkably information rich, holding dozens of trace and minor elements, scores of stable isotopes, solid and fluid inclusions, chemical zoning, twinning, exsolution, countless defects, and a host of optical, magnetic, electrical, and other properties. Every mineral specimen is a time capsule waiting to be opened—waiting to tell its story. This lecture will explore some of the advanced data analytical and visualization methods that are shining new light on the old field of mineralogy.

An important part of the legacy of Edward Grew is the application of rigorously curated mineral data to a wide range of fundamental mineralogical problems, including analysis and predictions of the diversity and distribution of the minerals of Li, Be, and B [3,7-11].

*References:*

[1] Hazen R, et al. (2008) Am Min 93:1693-1720
[2] Hazen R, Grew E, et al. (2011) Am Min 96:953-963
[3] Grew E and Hazen R (2014) Am Min 99:999-1021
[4] Morrison S, et al. (2017) Am Min 102:1588-1596
[5] Hazen R, Grew E, et al. (2019) China Engineering 5:397-405
[6] Prabhu A, et al. (2023) Am Min 108:1242-1257
[7] Grew E, et al. (2011) Origins Life Evol. Biosphere 41:307-316
[8] Hazen R, Grew E, et al. (2015) Canadian Min 53:295-323
[9] Grew E, et al. (2016) Canadian Min 54:125-143
[10] Grew E, et al. (2017) Am Min 102:612-619
[11] Grew E, et al. (2019) European J Min 31:755-774

# Titanium in ultra-high-pressure rocks: Implications of the new minerals wenjiite, $Ti_5Si_3$, maurogemmiite, $Ti_{10}Fe_3O_3$, paulrobinsonite,$Ti_8Fe_4O_2$, and TiFe

Grew, E.[1*], Xiong, F.[2], Mugnaioli, E.[3], Xu, X.[2], Yang, J.[4], Wirth, R.[5], Franke, P.[6], and Yates, M.[1]

[1]University of Maine, Orono, Maine, 04469 U.S.A., esgrew@maine.edu, corresponding author, *presenter

[2]Center for Advanced Research on the Mantle, Chinese Academy of Geological Sciences, Beijing 100037, China

[3]Department of Earth Sciences, University of Pisa, Via S. Maria 53, 56126 Pisa, Italy

[4]School of Earth Sciences and Engineering, Nanjing University, Nanjing, 210023, China

[5]Helmholtz Centre Potsdam, GFZ, Section 3.5, Telegrafenberg, C 120, D-14473 Potsdam, Germany

[6]Karlsruhe Institute of Technology, IAM-AWP, D-76021 Karlsruhe, Germany.

---

A fragment 0.8 mm across extracted from chromitite no. 31 in the Luobusa ophiolite has an unparalleled mineralogical diversity – 11 species occurring in three mineralogically distinct zones: (1) a core of Ti-Fe-Si alloys, surrounded by (2), a rim of α-Ti isolating the alloy core from (3), which is a partial rim dominated by aluminosilicate phases. The alloy core consists of (1) Ti grains in part overgrown by maurogemmiite (Mmi)[1] and paulrobinsonite (Prbs)[1] and (2) a vermicular intergrowth of TiFe and osbornite, Ti(N,C) (Obn), in equal proportions to give $Ti_2Fe(N,C)$ for the precursor. The 20-70 μm thick α-Ti rim is separated from the outermost zone by a wenjiite (Wnj) border ~10 μm thick. This zone consists of ~45 modal% coesite (Coe), ~15% kyanite, ~40% amorphous aluminosilicate containing significant Ti, Mg and Na; native Fe, qingsongite, BN (Qsg), Obn and $TiO_2$-II (α-$PbO_2$ structure) are present in trace amounts [2, 3]. Nitrogen and C isotopes in Obn have a mantle signature, whereas the bulk composition and the presence of B in the outermost zone suggest a crustal precursor [3]. As Coe is interpreted to form pseudomorphs of stishovite (Sti) [2], the outermost zone is inferred to have crystallized first at 12 GPa, 1300 °C, then at 7 GPa, 1300 °C [2].

We suggest a scenario whereby a fragment of pelitic rock originating in the crust became attached to a fragment of Ti-Fe alloy of mantle origin at depth and reacted with it during burial and exhumation. The mantle signature suggests that N originated in the alloy core and subsequently migrated to form Obn and Qsg in the aluminosilicate rim. The presence of Ni in the Fe-bearing minerals of the alloy core suggests affinity with Ni-bearing base metal alloys also extracted from chromitite no. 31 [4].

The genesis of the fragment can be considered in terms of the Ti-Fe-Si-O system and the phases Ti, Coe, Wnj, and $TiO_2$. At the *P-T* conditions inferred for the fragment, β-Ti is stable instead of α-Ti [5]. As β-Ti incorporates more Fe than α-Ti [6], conversion of β-Ti to α-Ti during exhumation could have released Fe, some of which was incorporated in Mmi and Prbs. Despite the simplifications involved in applying experimental results at $P$ = 0.1 MPa reported in [7], we suggest that the join Wnj+$TiO_2$-II is stable in lieu of β-Ti + Coe; that is, the Wnj border formed by the reaction $3SiO_2 + 8Ti \rightarrow Ti_5Si_3 + 3TiO_2$. At $P$ = 0.1 MPa and $T$ = 1300 °C, we calculate that Wnj requires $\log a_{O2} < -21.9$; cf. –10.7 for Fe/wüstite. Such highly reducing conditions are rarely observed in rocks exposed at the Earth's surface, whence the uniqueness of the Ti-rich assemblage in the fragment from chromitite in the Luobusa ophiolite.

*References:*

[1] CNMNC Newsletter 73, European J Mineral 35: 397-402 (2023)
[2] Yang J et al (2007) Geology 10:875–878
[3] Dobrzinetskaya L et al (2014) Am Mineral 99:764–772
[4] Bai W et al (2000) Canad Mineral 38:585-598
[5] Tonkov E Yu & Ponyatovsky E G (2005) Phase Transformations of Elements under High Pressures CRC Press
[6] Okamoto H (1996) J Phase Equilibria 17:368-369
[7] Goldstein J I et al (1995) J. Am Ceram Soc 78:913-922

## Magnesioqingheiite, a new member of the alluaudite supergroup of minerals

Cámara, F.[1], Chopin, C.[2] and Deldicque, D.[2]

[1]Università degli Studi di Milano, Milano, Italy

[2]Ecole normale supérieure – CNRS – Université PSL, Paris, France

---

Magnesioqingheiite, ideally $Na_2Mg(MgAl)(PO_4)_3$, a new member of the alluaudite supergroup, occurs in quartz segregations concordant with the foliation of the surrounding garnet–albite gneiss and quartz–phengite schist of the Stockhorn series, on the western ridge of the Stockhorn, Zermatt valley, Valais, Switzerland, which is also the type locality of bearthite [1]. In the holotype, the new mineral occurs as the main primary phosphate, along with lazulite and apatite, as a prismatic grey phase with high refringence and very low birefringence. In this sample bearthite is rare and occurs as micrometre-size inclusions in primary apatite. Magnesioqingheiite is monoclinic, $P2_1/n$, $a$ 11.7248(3), $b$ 12.31465(19), $c$ 6.38859(13) Å, β 114.226(3)°, $V$ 841.20(3) Å$^3$, $Z$ 4, and therefore belongs to the wyllieite group in the alluaudite supergroup. It is biaxial (–), with $n$ 1.643, and $\Delta n$ 0.006. The empirical formula is $^{A(2)'}Na_{1.01}\ ^{A(1)}(Fe_{0.45}Ca_{0.10}Sr_{0.01}Mn_{0.01}Na_{0.43})_{\Sigma 1.00}\ ^{M(1)}(Mg_{0.71}Fe_{0.29})_{\Sigma 1.00}\ ^{M(2)}(Mg_{1.47}Al_{0.53})_{\Sigma 2.00}\ (P_{0.99}O_4)_3$. It has therefore Mg and Al occupying the $M$(2a) and $M$(2b) sites and Na occupying the $A$(2)' and $A$(1a) sites as in qingheiite, but Mg dominant at $M$(1), instead of $Mn^{2+}$ in qingheiite and $Fe^{2+}$ in ferroqingheiite. It is therefore the Mg-analogue of qingheiite, hence the naming, conforming to the nomenclature proposed by [2], based on the $M$ sites and ignoring complications in the channel sites. Nevertheless, $Fe^{2+}$ being very dominant (80%) at the $A$(1b) site (<$A$(1b)–O> = 2.215 Å), the actual composition of the new mineral is best written doubling the formula as $^{A(2)'}Na_2{}^{A(1a)}Na^{A(1b)}Fe^{2+}{}^{M(1)}Mg_2{}^{M(2a)}Mg_2{}^{M(2b)}(MgAl)\ (PO_4)_6$, $Z$ 2, which emphasizes the double occupancy at $M$(2b), imposed by the presence of a divalent $A$(1b) cation instead of Na and by the multiplicity of $A$(1b) being half that of $M$(2b). These findings may call for a revisiting of the naming scheme for the wyllieite group in the alluaudite supergroup.

*References:*

[1] Chopin C et al. (1993) Schweiz Mineral. Petrogr Mitt 73: 1–9

[2] Hatert F (2019) Eur J Mineral 31: 807–822

# $Fe^{3+}GeO_6H_5$ and $Fe^{3+}SnO_6H_5$: hints of novel H behaviour in perovskite-related structures

Welch, M.D.[1], Najorka, J.[1] and Kleppe A.K.[2]

[1]Natural History Museum, London SW7 5BD, UK m.welch@nhm.ac.uk

[2]Diamond Light Source Ltd, Harwell Science and Innovation Campus, Didcot, Oxfordshire, UK

---

Frameworks comprising corner-linked $M^{n+}O_6$ octahedra ($n$ = 1 – 5), in which all oxygen atoms form OH groups, occur as rare secondary minerals associated with Pb-Fe-Mn ore deposits. Several have also been synthesized. The structures are perovskite-like but lack an *A* cavity cation and, as such, are related topologically to $ReO_3$-type phases [1]. The combination of an empty *A* site and extensive hydrogen bonding results in highly rotated octahedra and very compressible structures, e.g. bulk moduli of 40-80 GPa. Most are stannates of divalent metals $M Sn(OH)_6$ (*M* = Mg, Ca, Mn, Fe, Co, Ni, Zn). Other compositions include $In(OH)_3$, $Ga(OH)_3$, $Fe(OH)_3$, $NaSb(OH)_6$ and $FeGe(OH)_6$. The synthetic high-pressure silicate $MgSi(OH)_6$ is considered to have a significant role in the transport of $H_2O$ into the Earth's deep mantle at subduction zones [2].

A study of the mineral jeanbandyite $Fe^{3+}SnO_6H_5$, the partially deprotonated and oxidised analogue of natanite $FeSn(OH)_6$, indicated that novel H behaviour may occur [3]. The discovery in 2023 of the Ge-analogue of jeanbandyite $Fe^{3+}GeO_6H_5$ suggests that such stoichiometric partially deprotonated states could be common, although they may be easily overlooked. $Fe^{3+}GeO_6H_5$ originates from partial deprotonation of stottite $FeGe(OH)_6$ and oxidation of $Fe^{2+}$ to $Fe^{3+}$. Jeanbandyite and $Fe^{3+}GeO_6H_5$ are the only $ReO_3$-type protonated frameworks with a combination of 3+ and 4+ cations.

In this presentation the crystal chemistry of $Fe^{3+}GeO_6H_5$ and $Fe^{3+}SnO_6H_5$ will be described with reference to $Fe^{2+}Ge(OH)_6$ and $Fe^{2+}Sn(OH)_6$. Crystallographic and spectroscopic data will be presented that illustrate the distinctiveness and novelty of these structures.

A static model in which five of the six oxygen atoms form hydroxyl groups and one is unprotonated is not crystal chemically reasonable as this single oxygen is very under-bonded, i.e. writing the formulae as $Fe^{2+}GeO(OH)_5$ and $Fe^{2+}SnO(OH)_5$ is misleading. A provisional model is proposed in which 5 H are shared between all 6 oxygen atoms, so that each oxygen is, on average, associated with ⅚ H. Thus, the formal bond-valence sum of oxygen is satisfied: $^{VI}Fe^{3+}$-O + $^{VI}$Ge-O + ⅚ H-O = 0.50 *vu* + 0.67 *vu* + 0.83 *vu* = 2.00 *vu*. Hence, we write the formulae as $Fe^{3+}GeO_6H_5$ and $Fe^{3+}SnO_6H_5$. The behaviour of H at the local level, which may be dynamic, and interaction with oxygen remain to be determined. It is now recognised that $ReO_3$-type protonated frameworks, such as those described here, are relevant materials for electrolytic fuel cells on account of their promise as photocatalysts [4].

*References:*

[1] Evans et al. (2020) Nature Review Materials 5: 196-213
[2] Welch et al. (2024) Amer Min 109:255-264
[3] Welch and Kampf (2017) Min Mag 81:297-303
[4] Gao et al. (2018) Am Chem Soc: Sust Chem Eng 6: 781-786.

# 3D electron diffraction for the crystallo-chemical characterization of micrometric and sub-micrometric mineral phases in mantle inclusions

Mugnaioli, E.[1], Grew, E.[2], Wirth, R.[3], Ferrero, S.[4], Lorenzon, S.[1], Borriello, R.[1,5], Xiong, F.[6,7], Xu, X.[6,7], Yang, J.[8], Borghini A.[9]

[1]Department of Earth Sciences, University of Pisa, 56126 Pisa (Italy); enrico.mugnaioli@unipi.it

[2]School of Earth and Climate Sciences, University of Maine, Orono, 04469 Maine (USA)

[3]Helmholtz Centre Potsdam - GFZ German Research Centre for Geosciences, 14473 Potsdam (Germany)

[4]Dipartimento di Scienze Chimiche e Geologiche, University of Cagliari, 09042 Monserrato (Italy)

[5]Depart. of Environmental Sciences, Informatics and Statistics, Ca' Foscari Univ. of Venice, 30172 Mestre (Italy)

[6]Center for Advanced Research on the Mantle (CARMA), Chinese Acad. Geological Sci., 100037 Beijing (China)

[7]Southern Marine Science and Engineering Guangdong Laboratory, 511458 Guangzhou (China)

[8]School of Earth Sciences and Engineering, Nanjing University, 210023 Nanjing (China)

[9]Faculty of Geology, Geophysics and Environmental Protection, AGH Univ. of Kraków, 30-059 Kraków (Poland)

---

In the last fifteen years, electron diffraction has found increasing applications for the structural determination and refinement of micro-crystalline and sub-microcrystalline phases. This advancement was boosted by the development of protocols for the acquisition of three-dimensional data [1] and of algorithms able to model dynamical scattering [2]. Despite a structural residual generally in a range of 10-15%, fine structural details in inorganic compounds can confidently be refined. Moreover, electron diffraction is very sensitive to hydrogen atoms and chirality. The growing interest in three-dimensional electron diffraction (3DED) is testified by the appearance of dedicated electron diffractometers and by its extensive use in material sciences and organic chemistry. However, its application for mineralogical studies is still limited to only a few laboratories, mostly operating in Europe.

Examples of the successful application of 3DED include the identification of new minerals in micrometric inclusions in corundum from the Luobusa ophiolite (Tibet, China) and in garnet from the Pfaffenberg peridotite body (Bohemian Massif, Germany). The new minerals from Luobusa are ultra-reduced intermetallic compounds such as zhiqinite, $TiSi_2$, badengzhuite, TiP, wenjiite, $Ti_{10}(Si,P,\square)_7$ and kangjinlaite, $Ti_{11}(Si,P)_{10}$, which together with wodegongjieite were identified in a single FIB lamella of just 10 x 5 µm [3-5]. A new complex oxide, jianmuite, was also identified, both in Luobusa inclusions and in the matrix of the Allende meteorite [6]. Pfaffenberg inclusions consist of biotite, omphacitic clinopyroxene, kumdykolite and two recurrent phases unconventionally labelled 'phase 412' and 'phase 430' by their Raman main peak at 412 and 430 $cm^{-1}$, respectively [7]. 'Phase 412' was recently solved and refined by 3DED, then approved by CNMNC with the name pfaffenbergite [8]. Remarkably, kumdykolite and pfaffenbergite represent rare polymorphs of common K-Na-Ca feldspars.

Inclusions in the Luobusa ophiolite and Pfaffenberg peridotites formed in poorly understood chemical environments and T-P conditions. Proper understanding cannot be achieved solely by bulk chemical analyses but requires detailed crystallographic determination of all the mineral phases present.

*References:*

[1] Gemmi M et al. (2019) ACS Cet. Sci. 5: 1315-1329
[2] Brázda P et al. (2019) Science 364: 667-669
[3] Xiong et al. (2020) Eur. J. Mineral. 32, 557-574
[4] Mugnaioli E et al. (2022) Mineral. Mag. 86, 975-987
[5] Xiong F et al. (2023) Am. Mineral. 108: 197-210
[6] Bosi F et al. (2023) CNMNC Newsletter 75, Eur. J. Mineral. 35, 891-895
[7] Borghini A et al. (2024) Eur. J. Mineral. 36: 279-300
[8] Bosi F (2024), official communication about IMA No. 2023-105 (February 4th 2024)

# Eudialyte decomposition and the formation of a cuspidine-wöhlerite skarn associated with the Sierra La Vasca complex, Mexico

Mitchell, R.H.[1] and Rodriguez Vega, A.[2]

[1]Department of Geology, Lakehead University, Thunder Bay, ON, Canada/rmitchel@lakeheadu.ca.

[2]Escuela Ingenieria "Lic.Adolfo Lopez Mateos", Universidad Autonoma de Coahuila, Mexico.

---

The Tertiary Sierra La Vasca intrusive complex is a part of the Mexican Eastern Alkaline Province and is considered to be an extension of the Texas-New Mexico Trans-Pecos alkaline magmatic province. Although the geology of the complex is as yet not well-characterized, it consists predominantly of diverse alkaline syenites forming a large near-circular pluton with a radius of about 5 km. All rocks of the Sierra La Vasca complex are alkaline-to-peralkaline and are a rare example of oversaturated peralkaline magmatism characterized by eudialyte; in this case Nb-poor eudialyte-kentbrooksite solid solutions.

A consequence of the intrusion of the alkaline rocks into the diverse Cretaceous carbonate country rocks is the development of a halo of mineralogically complex skarns. This study is focussed on a small eudialyte-rich vein and accompanying skarn which illustrate the unusual skarn-forming thermal and metasomatic effects of Zr mobilization. The material investigated consists of a eudialyte-rich vein (2 cm) and adjacent (6 cm) skarn and country rock marble. Although small this material is a microcosm of the more extensive skarn assemblages associated with the complex. The eudialyte vein consists of 1-2 mm subhedral-to-anhedral fresh eudialyte crystals set in a matrix of quartz, albite, potassium feldspar, and aegirine with minor calcium catapleiite, calcite and britholite. Towards the skarn contact fresh eudialyte is replaced by a complex fine grained assemblage of altered eudialyte, with the dominant replacing minerals being cuspidine, wöhlerite and Mn-bearing wollastonite with minor Y-bearing britholite. Adjacent to this region is a zone consisting of cuspidine, götzenite, wöhlerite, pectolite and minor thorogummite interspersed with irregular areas of kimzeyite, Zr-bearing andradite and wollastonite. The following thin zone consists of wollastonite plus apatite which is transitional to irregular zones consisting of complex intergrowths of wollastonite, diopside, cuspidine, fluorite, apatite and calcite. The contact is with a calcite marble formed by recrystallization of a limestone lacking any silicates.

The skarn-forming vein is essentially a peralkaline granite modally enriched in eudialyte by flow differentiation. This vein was probably emplaced at temperatures close to the granitic magmatic-to-hydrothermal transition. Skarn formation was the result of alteration of eudialyte by deuteric F-and REE-bearing hydrothermal fluids with subsequent transport of Zr- Si- and REE into the country rock carbonates. These metasomatic reactions generated the complex Zr-bearing calc-silicate assemblage

# Extreme chemical disequilibrium patterns in hydrothermal vein minerals – a case study from Columbian emeralds

Franz, G.[1], Khomenko, V.[2] Schiperski, F.[1], Gernert, U.[3], and Nissen, J.[3]

[1]Institut für Angew. Geowissenschaften, Technische Universität, Berlin, Germany; gefra548@gmail.com

[2]Institute of Geochemistry, Mineralogy and Ore Formation, Kyiv, Ukraine

[3]Zentraleinrichtung Elektronenmikroskopie, Technische Universität, Berlin, Germany

---

Chemical zoning in metamorphic and igneous minerals has been shown to be a very powerful tool for reconstruction of pressure-temperature-time condition of growth of minerals. Vein minerals have also been the focus because of their common occurrence with economically interesting mineralizations. Columbian emeralds formed in veins in low-grade metamorphic black shales; they are known as highly-prized gemstones and have been studied extensively over the years. We present data about their growth phenomena, from combined element distribution mappings with µ-XRF and the electron microprobe EMPA in oriented thin sections, and from scanning electron microscopy SEM.

External growth phenomena are small indentations on the basal plane (0001), which are interpreted as an expression of skeletal growth along the *c*-axis of the beryl, and rare sceptre growth. Chemical zoning shows very unusual patterns with sector zoning, which is however variable for different elements in different crystals. Sector boundaries are in some instances straight, or curved, or serrate. Stripes in the sectors were observed with alternating chemical composition. Most unusual are chemical patterns produced by the substitution Al+□(channel) = Mg+Na, with straight borders and in variable angles to the *c*-axis. In the root zone of the crystals, cone-shaped structures extend in *c*-direction from a homogeneous zone.

Freely grown crystals, such as beryls in open veins are often characterized by dissolution-formed etch pits. Columbian emeralds show also such etch pits, with different shapes (rectangular, diamond-shaped), originating from point- as well as line-defects, typically arranged in chains, parallel and oblique to the c-axis, what has not been observed in pegmatitic beryls. These chains of etch pits point to screw-dislocation arrays and are another indication for rapid growth of the crystals. In summary, both features of growth and dissolution phenomena point to extreme disequilibrium.

## Mechanisms of uranium incorporation into garnet

Marschall, H.R.[1,2], Ackermann, C.[1,2], Millonig, L.J.[1,2], Kutzschbach, M.[3], Walters, J.B.[1,2,4], Schmidt, A.[1,2], Woodland, A.B.[1,2], and Hezel D.C.[1,2]

[1]Institut für Geowissenschaften, Goethe Universität, Frankfurt am Main, Germany

[2]FIERCE, Goethe Universität, Frankfurt am Main, Germany, marschall@fierce.uni-frankfurt.de

[3]Institut für Angewandte Geowissenschaften, Technische Universität Berlin, Germany

[4]Institut für Geologie, Universität Bern, Switzerland

---

The garnet supergroup with its general formula $X_3Y_2T_3\Phi_{12}$ has 32 approved species, one of which – elbrusite – contains U as a major component [1]. However, U-rich garnet is exceedingly rare and typical garnets found in natural rocks contain only trace levels of U. Generally, 1–50 µg/g are observed in andraditic garnet, but even 1–100 ng/g as typical for natural almandine–pyrope is sufficient for LA-ICPMS U–Pb dating at a geologically meaningful level of precision [e.g., 2,3]. This opens up the opportunity to establish this method as a powerful petrochronometer. However, limited knowledge of the mechanisms and systematics of U incorporation into garnet hamper the processes of sample selection and data interpretation for garnet petrochronology.

Garnet commonly contains di- and tri-valent cations in its X- and Y-site, respectively. The substitution of ions of a higher valence states thus requires charge balance. Incorporation of $Ti^{4+}$ into the Y-site is charge balanced either through coupled substitution with a divalent cation, producing the morimotoite species, $Ca_3(TiFe^{2+})[Si_3O_{12}]$, or by coupled substitution with trivalent Fe for Si on the tetrahedral T-site, leading to the schorlomite species, $Ca_3Ti_2[Fe^{3+}{}_2SiO_{12}]$. Uranium in the octahedral Y-site in elbrusite is hexavalent and requires even more charge balance, which is achieved by complete occupation of the tetrahedral site by trivalent Fe, hence $Ca_3(U^{6+}{}_{0.5}Zr_{1.5})[Fe^{3+}{}_3O_{12}]$ or possibly divalent Fe, hence $Ca_3(U^{6+}Zr)[Fe^{3+}{}_2Fe^{2+}O_{12}]$. Theoretical calculations have demonstrated that tetravalent U incorporation is strongly favoured on the dodecahedral X site, again charge balanced by tetrahedral $Fe^{3+}$, which has applications for the fixation of actinides in YIG (yttrium-iron garnet) for nuclear waste disposal [4].

Here we present the results of a detailed investigation of a range of andraditic garnets from hydrothermal (skarn) and alkaline magmatic settings that included major and trace-element mapping (including U) of individual grains and U-Pb dating. Mössbauer spectroscopic analyses were conducted to determine the oxidation state (di- and tri-valent) and coordination environment (X, Y and T) of Fe in the crystals. Our results suggest that the elbrusite substitution does not operate at the trace-element level of U in natura garnet. Instead, the incorporation of tetravalent U into the dodecahedral X-site seems to dominate, charge balanced through tetrahedral $Fe^{3+}$ and/or through divalent cations in the Y-site, leading to the theoretical species $(U^{4+}Ca_2)Fe^{3+}{}_2[Fe^{3+}{}_2SiO_{12}]$ and $(U^{4+}Ca_2)Fe^{2+}{}_2[Si_3O_{12}]$, respectively. Strong oscillatory zoning was observed in many samples with a covariation of U, Th and the light REE (but not Zr), demonstrating that incorporation of the lanthanides and actinides may be controlled by the same crystal chemical mechanisms. Some samples additionally show strong sector zoning in U (and Th and Ce) with a 20–50 % enrichment of U In the {211} sectors compared to the {110} sectors, demonstrating a control of crystal growth rate on U incorporation.

*References:*

[1] Grew ES (2007) Am Min 98: 785–811
[2] Millonig LJ, et al. (2020) Earth Planet Sci Lett, 552: 116589
[3] Shu Q, et al. (2024) Contr Min Pet, in press
[4] Rák ZS et al. (2011) Pys Rev B 84: 155128

## Garnet in low-temperature metamorphic rocks: far from simple, far from cubic

Cesare, B.[1], Mugnaioli, E.[2], Tacchetto, T.[3], Lorenzon, S.[2], Biagioni, C.[2], Nestola, F.[1], Campomenosi, N.[4], and Della Ventura, G.[5]

[1]University of Padova, Geosciences Department, Padova, Italy (bernardo.cesare@unipd.it)

[2]University of Pisa, Earth Sciences Department, Pisa, Italy

[3]Curtin University, School of Earth and Planetary Science, Perth, Australia.

[4]University of Genova, DISTAV Department, Genova, Italy

[5]University of Roma Tre, Department of Sciences, Roma, Italy

---

Since the first report on the tetragonal structure of common (OH- and andradite-free) garnet in metamorphic rocks [1], many new occurrences have been discovered.

Non-cubic anhydrous garnets are widespread in low-temperature metamorphic terranes worldwide, including the world-renowned blueschists from the Franciscan Complex (USA), Syros (Greece) and Aosta Valley (Italy), and the phyllites from the iconic Barrow garnet zone of Scotland.
These garnets share compositional features such as grossular >20% and pyrope <7%, which are common in both metabasites and metapelites metamorphosed at T < ≈500 °C.

The non-isotropic nature of these garnets determines a very weak birefringence, which is generally overlooked, yet it can be easily detected by polychromatic polarization microscopy on conventional 30-µm thin sections. Similarly, this deviation from an isotropic behaviour can be observed by Raman microspectroscopy using crossed-polarized geometry.
Optically, the birefringence pattern suggests the presence of twelve growth sectors (twins) arranged in a dodecahedron, displaying sector quartets with three crystallographic orientations having optical axes swapped by 90°.

Preliminary single-crystal XRD and HRTEM investigations have demonstrated that these anisotropic garnets have a pseudocubic tetragonal structure with a minimal (≈ 1/1000) difference between the a,b and c axes.

Due to the minimal departure from the cubic cell, conventional EBSD orientation analysis could not discriminate the orthogonal orientation of <c> axes in the optically different sectors. However, EBSD revealed consistent, small (<1°) structural disorientations coincident with the rhythmic Ca-Fe compositional variations, similar to what is observed in zircon growth zoning.
This presentation will report the new results obtained from FPA-FTIR, HRTEM, single-crystal XRD and synchrotron micro-XAS investigations, aiming to better constrain the crystallographic structure of tetragonal garnets as well as their OH- content, thereby providing a better understanding of the origin of their departure from a cubic structure.

*References:*
[1] Cesare B et al. (2019) Sci Rep 9, 14672.

# A Single-Crystal UV/Vis Spectroscopic Investigation of $^{VIII}Fe^{2+} + {}^{VI}Fe^{3+} \rightarrow {}^{VIII}Fe^{3+} + {}^{VI}Fe^{2+}$ Intervalence Charge Transfer in Aluminosilicate Garnets

Geiger, C.A.[1] and Taran, M.N.[2]

[1]Chemistry and Physics of Materials, University of Salzburg, Jakob Haringer Str. 2a, A-5020 Salzburg and Institute for Mineralogy and Crystallography, University of Vienna, Vienna, Austria, charles.geiger@univie.ac.at

[2]M.P. Semenenko Institute of Geochemistry and Mineralogy and Ore Formation, National Academy of Sciences of Ukraine, Palladin Ave. 34, 03680 Kyiv-142, Ukraine

---

The single-crystal UV/Vis/NIR absorption spectra of two different almandine-rich, spessartine-rich and grossular-rich garnets, as well as a single almandine-pyrope garnet, were measured. Absorption was observed from roughly 15000 to 30000 $cm^{-1}$. The spectra were deconvoluted and a very broad band with FWHM values ranging from 4000 to 9000 $cm^{-1}$ and having a maximum located between about 21000 and 22000 $cm^{-1}$ in the visible region could be fit. Various narrow spin-forbidden bands occur on this broad absorption feature. The intensity of the broad band depends greatly on garnet composition and is strongest in a nearly end-member composition almandine and weakest in a very grossular-rich iron-poor crystal. This band is assigned to intervalence charge transfer (IVCT) of the type $\{Fe^{2+}\} + [Fe^{3+}] \rightarrow \{Fe^{3+}\} + [Fe^{2+}]$.

Photon-induced electron transfer occurs through an overlap of *d* orbitals of $Fe^{2+}$ and $Fe^{3+}$ in their respective coordination polyhedra that share edges, namely the triangular dodecahedron and the octahedron of the garnet crystal structure. The two different Fe cations should have markedly different energy potentials and this results in asymmetric IVCT behavior. This, together with the relatively long $Fe^{2+}$-$Fe^{3+}$ distances (greater than 3.2 Å) in garnet, leads to the high energy of the $Fe^{2+} + Fe^{3+} \rightarrow Fe^{3+} + Fe^{2+}$ IVCT compared to that observed in other oxide and silicate structures. The latter two groups often have iron cations in octahedra or quasi-octahedral coordination. The IVCT is observed in the spectra of different composition garnets that grew under dissimilar *P-T-X* conditions. The resulting absorption band greatly affects color because it is centered in the blue region of the electromagnetic spectrum. It remains to be determined why IVCT is observed in the spectra of some garnets but to a much lesser degree or not at all in the spectra of other crystals. An understanding of various physical properties (e.g., IVCT, color, magnetism, paramagnetic NMR resonances) of garnet is increasing, but a better description of the precise electron behavior controlling them is needed.

# Boron-rich fluids in a highly evolved niobium-yttrium-fluorine (NYF) type pegmatite

Anderson, A.J.[1], Scott, M.[2], Wise, M.A.[3] and Boucher, B.M.[4]

[1]Department of Geology, Saint Mary's University, Halifax, NS, Canada B3H 3C3 Alan.Anderson@smu.ca

[2]Department of Earth Sciences, St. Francis Xavier University, Antigonish, NS, Canada B2G 2W5

[3]Department of Mineral Sciences, NMNH, Smithsonian Institution, Washington DC, USA 20560

[4]Department of Earth Sciences, University of New Brunswick, Fredericton, NB, Canada E3B 5A3

---

The Zapot pegmatite, Mineral County, Nevada, is a multi-zoned niobium-yttrium-fluorine (NYF) type pegmatite emplaced in a quartz monzonite intrusion in the western part of the Gillis range. Compared to other amazonite-bearing pegmatites, the Zapot pegmatite is enriched in lithium and rubidium as indicated by the presence of zinnwaldite, lepidolite, and low K/Rb (7.5) microcline. Miarolitic cavities, or pockets, are common in the intermediate amazonite-topaz zone of the pegmatite and to a lesser extent in the perthite wall zone. The composition of pocket fluids and the conditions of pocket formation was investigated using primary and pseudo-secondary fluid inclusions in quartz. Pocket quartz crystals collected for this study have an irregular smoky quartz core and an overgrowth of colourless quartz. The average of Li, Al, Ti, and Ge concentration in the smoky quartz core and colourless quartz overgrowth are respectively, 8.4, 84.2, 4.1, 3.7 ppm, and 0.41, 2.8, 0.7, 1.4 ppm. Pseudo-secondary fluid inclusion assemblages occur in healed microfractures within the smoky quartz core. At room temperature most pseudo-secondary fluid inclusions contain sassolite ($H_3BO_3$) and stibioclaudetite ($AsSbO_3$) daughter minerals and a small vapour bubble ($T_hLV \rightarrow L$ = 120 to 180 °C). Many fluid inclusions in the core and overgrowth are intersected by long, needle-like crystals of topaz. Freezing point depression measurements of eighty-three pseudo-secondary inclusions yield salinities ranging between 2.7 and 4.26 mass% NaCl equivalent. Laser ablation inductively coupled mass spectrometry (LA-ICP-MS) analyses show that the dominant solutes in the inclusion fluids are Na and K with minor concentrations of Li, B, As, Cs, Sb and Pb. Although tourmaline and other boron-bearing minerals are uncommon in the Zapot pegmatite [1], the late-stage pocket-forming fluids are boron-rich (7.0 ± 0.8 mass% $H_3BO_3$) as indicated by the common occurrence of sassolite in the fluid inclusions. The enrichment of Li, B, As and Cs in fluid inclusions from the Zapot pegmatite mirrors the trace element signature of fluids in some highly evolved lithium-cesium-tantalum (LCT) type pegmatites and demonstrates the effective partitioning of these elements into the magmatic volatile phase during NYF pegmatite crystallization.

*References:*

[1] Foord E.E. et al. (1999) Min Rec 30(4):277-292

# Bond-valence constraints for tourmalines with Li and various *X*-site occupancy

Bačík P.[1] and Ertl, A.[2,3]

[1]Comenius University in Bratislava, Ilkovičova 6, 842 15, Bratislava, Slovak Republic, peter.bacik@uniba.sk

[2]Mineralogisch-Petrographische Abt., Naturhistorisches Museum, Burgring 7, 1010 Wien, Austria

[3]Institut für Mineralogie und Kristallographie, Universität Wien, Josef-Holaubek-Platz 2, 1090 Wien, Austria

---

Among the Li-bearing end members of the tourmaline supergroup, we can find Na-dominant members with either $Li_{1.5}Al_{1.5}$ or $Al_2Li$ *Y*-site occupancy, Ca-dominant members with $Li_2Al$ occupancy and X-site vacant tourmalines with either $Al_2Li$ or $Al_{2.5}Li_{0.5}$ occupancy. However, as it is visible from the fractional occupancies in some cases, it is evident that end-member formulae are different from the possible short-range structural arrangements. The possibility of stable arrangements and their combination with the various *X*-site occupancy was tested on arrangements with $AlMn^{2+}Li$, $AlFe^{2+}Li$, $Al_2Li$, $Al_3$, $AlLi_2$ and $Li_3$ *Y*-site occupancy.

A theoretical bond-topological model for each arrangement was calculated and refined to fit with the structural data from natural samples. From the bond-valence perspective, both $AlMn^{2+}Li$ and $AlFe^{2+}Li$ are perfectly reasonable and can be stable with $^{X}$Na and both $^{W}$F and $^{W}$OH occupancy. Similarly, $Al_2Li$ and $Al_3$ can be stable, but increased bond-valence sum (BVS) on O1 and O2 anions should be balanced by $^{W}$O as in darrellhenryite (or $^{V}$O as in olenite), *X*-site vacancies as in rossmanite, or both of them as in alumino-oxy-rossmanite. In contrast, a decrease in BVS on O1 and O2 of $AlLi_2$ arrangement suggests that Ca is necessary to compensate as in fluor-liddicoatite.

The decrease in BVS on O1 and O2 in the $Li_3$ arrangement is too large for a divalent substituent at the *X*-site and would require a trivalent cation at *X*. However, this is highly unlikely in natural compositions; only trivalent lanthanoids from $La^{3+}$ to $Gd^{3+}$ with bond lengths similar to $Ca^{2+}$ could occupy the *X* site [1], but their content in Li-rich environments is usually very limited.

Acknowledgement: This research was funded in parts by the Slovak Research and Development Agency under contract APVV-18-0065 (PB), project VEGA 1/0189/23 (PB) and Austrian Science Fund (FWF) project P35585 to AE.

*References:*

[1] Bačík P. and Fridrichová J. (2021) Am Mineral 106: 851-861

## On the limitation of Li in tourmalines with Na and vacancies at the *X* site

Ertl, A.[1,2] and Bačík P.[3]

[1]Mineralogisch-Petrographische Abt., Naturhistorisches Museum, Burgring 7, 1010 Wien, Austria
andreas.ertl@a1.net

[2]Institut für Mineralogie und Kristallographie, Universität Wien, Josef-Holaubek-Platz 2, 1090 Wien, Austria

[3]Comenius University in Bratislava, Ilkovičova 6, 842 15, Bratislava, Slovak Republic

---

Aluminum-rich tourmaline can contain significant amounts of Li. Natural and synthetic samples were used to investigate which Li-containing short-range orders can occur in Li-bearing Al-rich tourmalines. The investigated samples exhibit lattice parameters with a = 15.72-15.84 Å, c = 7.07-7.10 Å. Synthetic Al-rich and Li-bearing tourmalines with no F, but with $^{[4]}$B and $^{[4]}$Al are of special interest, because they contain no Ca, only Na and vacancies at the *X* site and mainly Al and Li at the *Y* site [1]. Since these tourmalines (synthesized by David London) do not have such a complex composition, relationships are easier to recognize.

Stable short-range orders of Al-rich tourmalines containing Na at the *X* site with the *Z* site fully occupied by Al can have the following *Y*-site occupancy: $AlMn^{2+}Li$, $AlFe^{2+}Li$, $Al_2Li$, $Al_3$. Stable short-range orders of Al-rich tourmalines with a vacant *X* site can have similar *Y*-site occupancies. In such short-range orders, there can be substitutions of Si by Al/B. Additionally, the *W* site can be occupied by O or OH/F. No short-range orders with $Li_2Al$ at the *Y* site exist for such tourmalines.

The combination of these different short-range orders makes it clear that the Li content in such a tourmaline containing only Na and vacancies at the *X* site can only be in the range of 0–1 apfu Li. Therefore, the Li content for such tourmalines is limited to 1.0 apfu and cannot be exceeded.

Acknowledgement: This research was funded in parts by the Austrian Science Fund (FWF) project P35585 to AE.

*References:*

[1] Ertl A et al. (2012) Am Mineral 97: 1591-1597

## Metamorphic and detrital tourmaline in the Archean meta-turbidites of the Beartooth Mountains, MT-WY, USA: Evidence for lithologically diverse Mesoarchean crust

Henry, D.J.[1], Mogk, D.W.[2], Mueller, P.A.[3], Loocke, M.[1] and Dutrow, B.L.[1]

[1]Department of Geology & Geophysics, Louisiana State Univ., Baton Rouge, LA, USA
[2]Department of Earth Sciences, Montana State Univ., Bozeman, MT, USA
[3]Department of Geological Sciences, Univ. of Florida, Madison, WI, USA

---

The Archean Jardine Metasedimentary Sequence (JMS) of the western Beartooth Mountains, northern Wyoming Province, MT-WY, USA, contains multiple tourmaline (tur) grains with metamorphic overgrowths that nucleated on detrital tur cores. The tur overgrowths preserve information about the prograde metamorphic history. Detrital tur core compositions constrain the lithologic character of the upper continental crust prior to deposition of the sequence. The JMS preserves sedimentary structures typical of turbidite sequences that suggest a mid-to-distal submarine fan on an active continental margin. The JMS turbidites were deposited after 2.9 Ga (youngest detrital zircon in the JMS) and before intrusion of cross-cutting granitic plutons at 2.8 Ga. U-Pb ages of JMS detrital zircons (2.9 to 3.6 Ga) and Sm-Nd depleted mantle model ages (3.2-4.0 Ga) suggest an ancient provenance for the protoliths. Medium-grade, low-pressure metamorphism (550-600°C, 3-4 kbar) of JMS metapelitic rocks is characterized by a diagnostic assemblage of staurolite-andalusite-biotite and  occurred between 2.8 and 2.9 Ga.

Synchronous metamorphic tur overgrowths exhibit compositional asymmetry closest to the detrital core along the *+c* and *-c* poles. Representative compositions are $(Na_{0.74}\square_{0.25}Ca_{0.01})(Mg_{1.42}Fe_{1.14}Al_{0.32}Ti_{0.03}Cr_{0.01})(Al_{6.00})Si_{6.00}(BO_3)_3O_3([OH]_{0.69}O_{0.31}F_{0.07})$ at *+c* and $(Na_{0.75}\square_{0.13}Ca_{0.08}Sr_{0.02})(Mg_{1.44}Fe_{1.31}Ti_{0.23}Zn_{0.01})(Al_{5.81}Mg_{0.19}Cr_{0.01})Si_{6.00}(BO_3)_3O_3([OH]_{0.66}O_{0.27}F_{0.07})$ at *-c*. These compositional differences are temperature dependent and, based on tur thermometer calibrations, tur began to crystallize at ~350°C. With progressive metamorphism, the overgrowth compositions converge to a composition of $(Na_{0.44}\square_{0.44}Ca_{0.10})(Mg_{1.65}Fe_{0.82}Al_{0.43}Ti_{0.09}Cr_{0.01}Zn_{0.01})(Al_{6.00})(Si_{5.90}Al_{0.10})(BO_3)_3O_3([OH]_{0.83}O_{0.17})$ at peak thermal metamorphic conditions (550-600°C).

Detrital tur core compositions provide important insights into potential protoliths of the clastic material. Detrital cores are distinguished from metamorphic overgrowths by textural features such as rounding, different mineral inclusion suites, and distinct discontinuities in chemical composition (commonly observable with BSE imaging). Application of AFM, CFM and other tur provenance discriminant diagrams suggests lithologic sources of the detrital cores included peraluminous granitic rocks, weakly fractionated and oxidized granitic rocks, aluminous metapelites, Al-poor and $Fe^{3+}$-rich metapsammites, magnesian metasediments, and calc-silicate rocks. Thus, the crust formed and exposed at the surface during the 2.9-3.6 Ga interval contained a wide range of more evolved compositions than typically assumed for Mesoarchean and older crust. The JMS appears to be allochthonous relative to the proximal Beartooth Block (BB), implying provenance for detrital tur is not local from the BB, but from other distal source(s) of heterogeneous, evolved lithologies.

This study of ancient tur-bearing metasediments is meant to be a tribute to the multidimensional studies of Edward Grew across Earth's time and compositional realms.

# Chromium-bearing tourmalines from the Jack Hills, Western Australia: Implications for Cr mobility

Dutrow, B.L.[1], Henry, D.J.[1], Cavosie, A.J.[2], Valley, J.W.[3] and Loocke, M.[1]

[1]Department of Geology & Geophysics, Louisiana State University, Baton Rouge, LA, USA

[2]School of Earth and Planetary Sciences, Curtin University, Perth, Australia

[3]Department of Geoscience, University of Wisconsin, Madison, WI, USA

---

The contributions of Edward S. Grew to petrologic mineralogy span the Universe. From his studies of new minerals in meteorites, such as chopinite, to those of ancient continents, such as boralsilite, he has enriched our field across space and time. Although his contributions are expansive, perhaps he is best known for his work on light elements encapsulated by many papers and *Elements'* issues. It is fitting to honor Dr. Grew with this study of tourmaline supergroup minerals in an unusual setting.

A metaconglomerate sample (01JH42) from the Jack Hills, Western Australia, consists of deformed and flattened quartz clasts with Cr-bearing muscovite defining a pervasive fabric. Trace detrital minerals in the sample include: chromite ($Chr_{39.3}Hc_{24.2}Zchr_{15.6}Ghn_{9.9}$), zircon, rutile, monazite and rare garnet ($Alm_{61.4}Gr_{19.5}Sps_{8.6}Py_{7.7}And_{1.5}Uv_{.12}$); pyrite and chalcopyrite are also observed. Within a micaceous layer, there are two ca. 150 micrometer tourmaline grains with an orientation perpendicular to the *c* axis within the foliation. The tourmaline grains are concentrically zoned with well-formed, chemically distinct rims surrounding at least one additional zone. These features suggest multiple growth episodes. Neither grain displays a detrital core. Based on cross-cutting textural features of the growth zones and the chemical discontinuities, both grains appear to have undergone dissolution and reprecipitation in the tourmaline cores.
Tourmalines are Mg-rich dravites, $X_{Mg}$ = 0.71 – 0.92, with a few analyses consistent with magnesio-foitite and oxy-dravite species. Notably, the tourmalines contain $Cr^{3+}$, ranging from 0.16 to 0.52 apfu; $V^{3+}$, from 0.01 to 0.03 apfu; and up to 0.17 F apfu. Chromium contents vary throughout the grain but increase in the outer rims. Iron is < 0.74 apfu, and $X_{Ca}$ ranges from 0.1 – 0.3. An average ordered tourmaline formula for the outer zone most likely in equilibrium with the matrix minerals is: $(Na_{0.5}Ca_{0.2}\square_{0.3})(Mg_{2.13}Fe_{0.39}Cr_{0.34}Al_{0.06}Ti_{.05}V_{0.3})Al_6(BO_3)_3(Si_{5.8}Al_{0.2})O_{18}(OH_3)(OH_{0.7}O_{0.2}F_{.1})$. The inner zone has greater X-site vacancy ($\square$), $Al^{[Y]}$ and $OH^{[W]}$, with correspondingly less $Ca^{[X]}$, $Cr^{[Y]}$, and $F^{[W]}$. Muscovite contains up to 0.28 apfu Cr, with higher Cr contents in micas adjacent to the spinels. An average muscovite composition near the tourmaline is $(K_{1.39}\square_{0.57}Na_{0.1}Ba_{0.01})(Al_{3.59}\square_{1.87}Mg_{.25}Cr_{0.19}Fe_{0.1}Ti_{.04}V_{.01})(Si_{6.23}Al_{1.67})O_{20}(OH_{3.9}F_{.1})$.

Based on the concentric zoning, tourmalines are suggested to be metamorphic in origin. Boron is likely derived from the breakdown of clay minerals or micas, in pulses, with increasing temperature and/or availability of constituents in the fluid phase. The presence of chromium throughout the tourmaline and in chromium-richer zones suggests that Cr was mobile during tourmaline growth in a low-Na fluid. Chromite grains within the sample may have provided the chromium. These data provide the first high-quality chemical analyses of tourmaline in the metaconglomeritic rocks of the Jack Hills area.

# New insights into the origin and metamorphic evolution of the Waldheim prismatine granulite (Saxon Granulite Complex) from pseudosection modeling, B isotopes and nanogranitoids

Rötzler, J.[1], Grew, E.S.[2], Ferrero, S.[3]*, Borghini, A.[4], Meixner, A.[5], Wilke, M.[6] and Yates, M.G.[2]

[1]GFZ German Research Centre for Geosciences, 14473 Potsdam, Germany

[2]University of Maine, Orono, Maine 04469 USA

[3]Università degli Studi di Cagliari, 09042 Monserrato, Italy (silvio.ferrero@unica.it) *presenter

[4]AGH University of Kraków, 30-059 Kraków, Poland

[5]University of Bremen, 28334 Bremen, Germany

[6]University of Potsdam, 14476 Potsdam, Germany

---

The prismatine granulite found at the type locality of prismatine in the Saxon Granulite Complex (SGC), European Variscan belt, has a diverse mineralogy dominated by sodic Pl, with Grt, Ky, Crn, Spr, Sil, Bt, Kfs, Rt, and dravitic Tur as minor constituents. The most striking feature of the migmatitic rock is the presence of prismatine (Prm), which forms large prisms, rarely up to 5 cm in length, as well as aggregates and occurs preferentially in irregular domains of leucocratic neosome. Mineral abbreviations according to Warr [1].

Thermodynamic modelling at $aH_2O = 0.3$ indicates equilibration of the peak assemblage Grt+Ky+Rt+Ab+L at ~2.3 GPa and 1050°C. Textural features are ambiguous about the involvement of Tur in the peak assemblage but do not preclude it. The modelled peak P-T conditions are slightly above the upper thermal stability limit of dravite as defined in experiments [2]. As low $H_2O$ activity stabilizes Tur to higher T whereas $B_2O_3$ lowers the solidus T, the melt inclusion-bearing Tur may well have been part of the peak assemblage. The analysed Grt core composition has slightly lower pyrope contents than the calculated one, which is possibly an indirect evidence that the natural system contained a phase higher in $X_{Mg}$ such as Tur. The absence of Omp, which the model predicts at ~ 2.3 GPa and ~ 1000°C, imposes an upper P limit on the metamorphism. Prm growth occurred late during near-isothermal decompression, as evidenced by overgrowths of Prm on Tur and Sil, as well as the intimate association of Prm with Sil and Bt. Whole rock B isotope analysis of the Prm granulite gave $\delta^{11}B = -8.93 \pm 0.02‰$, which together with $\delta^{18}O = +7.67‰$ previously reported, is consistent with the Prm granulite body and the surrounding felsic granulites both having a magmatic origin. More likely B was introduced prior to burial rather than during burial or exhumation.

Inclusions of primary nanogranitoids ≤50 µm in diameter were found in Grt, Prm and Tur, thereby constraining their formation to suprasolidus conditions. In Prm, the inclusions mainly contain kumdykolite (Kdy, orthorhombic $NaAlSi_3O_8$) + Crs/Trd or (rarely) Qz + kokchetavite (Kct, hexagonal $KAlSi_3O_8$) + Bt/Phl + white mica ± $CO_2$. In Grt the inclusions contain instead Kdy + Bt + Qz/Crs ± phase 430 (a novel phase currently under investigation). In tourmaline the inclusions can either be crystallized to Crs/Qz + Kdy + white mica ± Kct or glassy with a shrinkage bubble. We can thus infer that prismatine trapped a granitic melt with a significant amount of $H_2O$, likely at shallower crustal levels in the late stages of rock evolution, whereas Grt (and possibly also Tur) likely crystallized earlier at significantly higher pressures, trapping a silicate melt poorer in both K and $H_2O$.

*References:*

[1] Warr (2021) Min Mag 85: 291–320

[2] Werding and Schreyer (1996) Rev Min Geochem 33: 117-163

# A potentially new tourmaline with tetrahedrally coordinated boron

Cempírek, J.[1], Skřápková, L.[1], Jonsson, E.[2]

[1]Department of Geological Sciences, Faculty of Science, Masaryk University, Kotlářská 2, 611 37 Brno, Czech Republic (email: jcemp@sci.muni.cz)

[2]Geological Survey of Sweden, Department of Mineral Resources, Box 670, SE-751 28 Uppsala, Sweden

---

Tourmaline with tetrahedrally coordinated boron, ideally $Na(Al_3)Al_6(Si_4B_2)(BO_3)_3O_{18}(OH)_3(O)$, is a potentially new tourmaline species from B-rich granitic pegmatite, in the Sahatany Valley, central Madagascar. It crystallised during a late stage of open pocket crystallisation in a highly fractionated granitic pegmatite dike of lithium-caesium-tantalum-enriched type (LCT-type) of likely Pan-African age. Pink crystals of the tourmaline are in part rimmed by, or intergrown with fibrous prisms in parallel growth of yellowish-brown tourmaline, and are associated with behierite, quartz and K-feldspar.

The tourmaline forms euhedral crystals ca. 5-10 mm in diameter, pink with a vitreous to transparent lustre, conchoidal fracture and white streak. It has the Mohs hardness of ca. 7, the calculated density of 3.038 g.cm$^{-3}$ and is uniaxial with ω = 1.659(2), ε = 1.639(2) at 589.3 nm white LED light, pleochroism is light grey in the omega direction and colourless in the epsilon direction.

The tourmaline has trigonal symmetry, space group *R3m*, *a* = 15.6509(8) Å, *b* = 15.6509(8) Å, *c* = 7.0406(5) Å, *V* = 1493.55 (19) Å$^3$ and *Z* = 3. The crystal structure was refined to $R_1$ = 1.99 % using 2192 unique reflections collected with Mo*K*α X-ray source. The structure was refined using the SHELXL-2013 program [1] with employing neutral scattering factors. Occupancies of X-, Y-, Z- and T-cation sites were refined as free variables. Occupancies of X-, Y-, and T- sites were refined using two major elements located in the respective sites, i.e., Na vs Ca at the X-site, Al vs Li at the Y-site, and Si vs B at the T-site. The hydrogen atoms were located in a residual electron-density map. The H1 and H3 site isotropic displacement parameters were constrained to be equal to 1.2 times of that of the O1 and O3 site; their distances from the donor oxygen atoms were constrained to 1.02(5) and 0.98(5) Å, respectively.

The empirical formula of the potentially new tourmaline was calculated on the basis of Y+Z+T+B = 18 (apfu) and ($OH^-$+$F^-$+$Cl^-$+$O^{2-}$) = 4 apfu. The structural refinement showed full occupancies of the Y-, Z-, and T-sites, resulting in the final empirical formula:
$^{X}(Na_{0.573}Ca_{0.220}\square_{0.207})_{\Sigma 1.000}{}^{Y}(Al_{2.760}Li_{0.187}Mn_{0.051}Ti_{0.002})_{\Sigma 3.000}{}^{Z}(Al_{6.000})^{T}(Si_{4.526}B_{1.419}Al_{0.055})_{\Sigma 6.000}{}^{B}(B_{3.000})O_{27}$
$^{V}(OH_{2.857}O_{0.143})^{W}(O_{0.974}F_{0.026})$

The ideal formula of the potentially new tourmaline conforms to both the dominant-valency and dominant-constituent rules [2]. The dominant end-member approach [3] provided an identical result. Based on the analysis, the structural formula contains 57.3 mol. % of the end-member (limited by the 0.573 apfu Na at the X-site).

The closest end-member compositions of valid tourmaline species are olenite, alumino-oxy-rossmanite, and darrellhenryite, related by the substitutions: $^{T}Si^{4+} + {}^{V}O^{2-} \rightarrow {}^{T}B^{3+} + {}^{V}OH^-$ accompanied by the disorder exchange $^{V}O^{2-} + {}^{W}OH^- \rightarrow {}^{V}OH^- + {}^{W}O^{2-}$; $^{X}\square + {}^{T}Si^{4+} + {}^{T}Al^{3+} \rightarrow {}^{X}Na^+ + 2({}^{T}B^{3+})$; and $^{Y}Li^+ + 2({}^{T}Si^{4+}) \rightarrow {}^{Y}Al^{3+} + 2({}^{T}B^{3+})$, respectively.

*References:*

[1] Sheldrick GM (2015) Acta Crystalogr 71:3-8
[2] Bosi F et al (2019) Minerals 9:591
[3] Hawthorne F (2023) Min Mag 87:494-504

## Rubinite from Hatrurim Complex, Israel

Galuskin, E.V.[1], Galuskina, I.O.[1], Kusz, J.[2] and Vapnik Ye.[3]

[1]Institute of Earth Sciences, University of Silesia, Będzińska 60, 41-200 Sosnowiec, Poland, evgeny.galuskin@us.edu.pl

[2]Faculty of Science and Technology, University of Silesia, 75. Pułku Piechoty 1, 41-500 Chorzów, Poland

[3]Department of Geological and Environmental Sciences, Ben-Gurion University of the Negev, P.O.B. 653, Beer-Sheva 84105, Israel

---

Gehlenite hornfelses and paralavas of the pyrometamorphic Hatrurim Complex are characterized by a wide development of garnets of the schorlomite-andradite series. Two new garnets: priscillagrewite-(Y), $(Ca_2Y)Zr_2Al_3O_{12}$, Daba-Siwaqa, Jordania [1] and midbarite, $Ca_3Mg_2(V_2Si)O_{12}$, Hatrurim Basin, Israel [2] were discovered in the Complex pyrometamorphic rocks. Priscillagrewite-(Y) belongs to the bitikleite group, while midbarite defines a new group in the garnet supergroup with the cation charge at the Z = 14 [3]. In gehlenite paralava bearing native iron from the Hatrurim Basin, an unusual Fe-free uvarovite containing significant impurities of the hutcheonite and goldmanite end-members was described [4]. Rubinite, a $Ti^{3+}$-garnet known from meteorites [5], was found in the phosphide-bearing breccia of the Hatrurim Basin. Rubinite is confined to small xenoliths, represented by altered carbonate rocks cemented by pseudowollastonite-gehlenite paralava. Xenoliths composed of hydrogrossular, hydrosilicates (tacharanite, tobermorite, and awfillite), and calcite were previously presented by high-temperature, predominantly gehlenite-hatrurite fine-grained clinker rock. Barringerite, murashkoite, osbornite, paqueite, perovskite, baghdadite, cuspidine, fluorapatite, and pseudowollastonite are high-temperature minerals that are relics in these xenoliths. Rubinite with a mean empirical formula $Ca_3(Ti^{3+}_{1.13}Al_{0.42}Ti^{4+}_{0.36}Mg_{0.10})_{\Sigma 2.01}(Si_{2.71}Al_{0.29})_{\Sigma 3.0}O_{12}$ forms thin rims on pseudowollastonite that crystallized at temperature above 1200°C. Paqueite, $Ca_3Ti^{4+}(Ti^{4+}_{0.71}Si_{0.29}Al_{2.00})_{\Sigma 3.00}Si_2O_{14}$, is confined to the contact zone between the altered xenolith and paralava, where rare rubinite crystals with Ti-bearing grossular core are noted.
A structure refinement of a 15 μm-sized rubinite crystal ($a$ = 12.0193(4) Å) confirmed the incorporation of $Ti^{4+}$ at tetrahedral site: $Ca_3(Ti^{3+}_{0.90}Al_{0.55}Ti^{4+}_{0.35}Mg_{0.20})_{\Sigma 2.0}(Si_{2.70}Ti^{4+}_{0.15}Al_{0.15})_{\Sigma 3.0}O_{12}$. Rubinite serves as an indicator of super-reduced conditions and is the first $Ti^{3+}$-silicate discovered *in situ* on the Earth.
Investigations were supported by the National Science Center (NCN) of Poland, grant 2021/41/B/ST10/00130.

*References:*
[1] Galuskina I et al. (2021) Am Mineral 106: 641-649
[2] Galuskina I et al. (2024) Eur J Mineral 36: 1-4
[3] Grew ES et al. (2013) Am Mineral 98: 785-811
[4] Futrzyński J et al. (2023) Lithosphere 215: 1-15
[5] Ma C and Beckett JR (2016) 47th Lun and Plan Sci Conf: 1595

## Niobium garnets

Galuskina, I.O.[1], Galuskin, E.V.[1], Vapnik, Ye.[2]

[1]Institute of Earth Sciences, University of Silesia, Będzińska 60, 41-200 Sosnowiec, Poland, irina.galuskina@us.edu.pl

[2]Department of Geological and Environmental Sciences, Ben-Gurion University of the Negev, P.O.B. 653, Beer-Sheva 84105, Israel

---

In literature there are several mentions on Nb content in garnets, but only garnets from carbonatites with marked Nb content deserve attention [1], [2], [3]. The highest contents are noted in morimoite –1.30 wt.% $Nb_2O_5$ (ailikite, Kandalaksha) and 0.44 wt.% $Nb_2O_5$ (monchiquite, Turij Mys) in the Kola Alkaline Carbonatite Province, Russia [3]. Kimzeyite with high Nb content described from carbonatite eluvium of the Loluni crater, Tanzania is worthy of special attention. The highest content of $Nb_2O_5$ is 10.09 wt.% [4]. The crystal chemical formula of the described Nb-garnet is as follows:
$(Ca_{2.95}Mn^{2+}_{0.02}Nd^{3+}_{0.02}Ce^{3+}_{0.02}La^{3+}_{0.01})_{\Sigma 3.02}(Zr_{1.33}Nb^{5+}_{0.48}Ti^{4+}_{0.11}Y^{3+}_{0.03}Mg_{0.07})_{2.02}(Fe^{3+}_{1.37}Al_{0.97}Si_{0.61})_{\Sigma 2.95}O_{12}$.
There are two main end-members: kimzeyite (43%) and a potentially new garnet $Ca_3NbZrR^{3+}_2O_{12}$ (48%) in the composition, where $R^{3+}$ is predominantly $Fe^{3+}$ and insignificantly $Al$. The potentially new Nb-garnet from Tanzania belongs to the bitikleite group [5].

Recently, in gehlenite-wollastonite-Ti-bearing andradite paralava from the Negev Desert, Israel, andradite with high $Nb_2O_5$ content was found. The studied garnets show zonation. $Nb_2O_5$ contents vary from 1.5 to 13.54 wt.% in one sample (1) and from 2 to 15.89 wt.% in second one (2). The crystal chemical formulas of garnet with the highest $Nb_2O_5$ contents in these cases look as follows:
(1) $(Ca_{2.94}Mn_{0.06})_{\Sigma 3}(Fe^{3+}_{1.30}Nb^{5+}_{0.56}Mn^{2+}_{0.07}Mg_{0.03}Fe^{2+}_{0.02}Ti^{4+}_{0.02})_{\Sigma 2}(Si_{1.75}Fe^{3+}_{0.91}Al_{0.23}V^{5+}_{0.11})_{\Sigma 3}O_{12}$;
(2) $Ca_{3.00}(Fe^{3+}_{0.88}Nb^{5+}_{0.66}Mn^{2+}_{0.36}Mg_{0.05}Ti^{4+}_{0.05})_{\Sigma 2}(Si_{1.90}Fe^{3+}_{0.83}Al_{0.20}V^{5+}_{0.07})_{\Sigma 3}O_{12}$.
In the case of Nb-garnets from Israel, the definition of the end-members is ambiguous. If the end-member in the formula (1) can be easily defined and there is one Nb-end-member $Ca_3(Nb^{5+}_{1.5}Fe^{3+}_{0.5})_{\Sigma 2}Fe^{3+}_3O_{12}$, the content of which in the formula is 37%. Then the formula (2), with higher content of divalent cations at the Y site, has two possible the end-members definitions. The first option yields two Nb-garnet end-members: $Ca_3(Nb^{5+}_{1.5}Fe^{3+}_{0.5})_{\Sigma 2}R^{3+}_3O_{12}$ (35%), where $R^{3+}$ is predominantly $Fe^{3+}$, and the next one: $Ca_3(Nb^{5+}_{0.67}Mn^{2+}_{1.33})Si_3O_{12}$ (22%). The second option yields: $Ca_3(Nb^{5+}_{1.67}Mn^{2+}_{0.33})R^{3+}_3O_{12}$ (34%) and $Ca_3(Nb^{5+}_{0.67}Mn^{2+}_{1.33})Si_3O_{12}$ (13%). In the Raman spectra of the studied Nb-garnet a band at 580 $cm^{-1}$ corresponds to the vibrations of $Nb^{5+}O_6$ octahedra. All the stated above indicate that there may be two new mineral species in the bitikleite and garnet groups [5].

Investigations were supported by the National Science Center (NCN) of Poland, grant 2021/41/B/ST10/00130.

*References:*

[1] Chakhmouradian AR and McCammon CA (2005) Phys Chem Minerals 32: 277–289

[2] Samal AK et al. ( 2021) Minerals 11: 756

[3] Vozniak AA et al. (2023) Mineralogy and Petrology 117:553–571

[4] Zaitsev AN et al. (2010) MinMag 74(5): 803–820

[5] Grew ES et al. (2013) AmMin 98: 785-811

## Coesite and florencite hidden in garnet and revealed by micro-Raman spectroscopy

Ghignone, S.,[1] Borghini, A.[2], Boero, F.,[1] Prencipe, M.,[1] Bruno, M.,[1,3] Gilio, M.,[4,5] Scaramuzzo, E.,[6] Manzotti, P.[7]

[1]Department of Earth Science, University of Turin, 10125 Torino, Italy

[2]Faculty of Geology, Geophysics and Environmental Protection, AGH University of Kraków, 30-059 Kraków, Poland (borghini@agh.edu.pl) *presenter.

[3]Center for Nanostructured Interfaces and Surfaces (NIS), University of Turin, 10135 Torino, Italy

[4]Department of Earth and Environmental Sciences, University of Pavia, 27100 Pavia, Italy

[5]Institut für Geowissenschaften, Universität Hamburg, D-20146 Hamburg, Germany

[6]Department of Science and High Technology, University of Insubria, 22100 Como, Italy

[7]Department of Geological Sciences, Stockholm University, 10691 Stockholm, Sweden

---

Mineral inclusions represent useful tools to obtain information on host and hosting rock genetic processes, pressure (P) and temperature (T) evolution and storage of elements of economic interest (e.g., rare earth elements (REE)) that otherwise might be lost. Micro-Raman spectroscopy is an powerful technique to investigate inclusions and confidently recognize mineral phases of microscopic size (≤ 1 μm) and polymorphs.

Here we present the first occurrence of coesite and florencite [$REEAl_3(PO_4)_2(OH)_6$] in garnets from oceanic metasediments exposed in two key localities in the Western Alps and we provide the first florencite reference spectrum. The studied metasediments are from the Monviso Massif [1,2] and Susa Valley [2,3] both part of the Internal Piedmont Zone. They contain inclusions-bearing and almandine-rich zoned garnets. Inclusions were identified in different garnet domains and, beside the two $SiO_2$ polymorphs (quartz and coesite) and florencite, they also comprise kyanite, jadeite, chloritoid, amorphous carbon, rutile, monazite, pseudomorphed lawsonite, xenotime and zircon.

Pristine coesite occurs as 10-60 μm monocrystalline grains with either well-developed facets or mostly rounded shape. The Raman spectra show the characteristic vibrational modes of coesite, with a slight shift to higher wavenumbers in fully enclosed grains. The main band is located at 522 $cm^{-1}$ (instead of 521 $cm^{-1}$), and the secondary bands are at 426, 270, and 178 $cm^{-1}$. Locally, coesite inclusions are partially re-equilibrated in polycrystalline aggregates of quartz and are surrounded by radial cracks developed due to the sharp volume increase at the coesite-quartz transition.

Ce-rich florencite occurs in garnets as ≤ 10 μm crystals exhibiting well-developed facets with idiomorphic to hypidiomorphic or subrounded shapes. This phase was identified based on chemical composition as a reference Raman spectrum was not available. Through the combination of experimental measurements and theoretical calculations we were able to define the Raman spectrum of florencite and to assign the different Raman signals to specific vibrational modes. Interestingly at ab initio level measured and computational Raman spectra show a remarkable coincidence.

The occurrence of coesite and florencite inclusions in garnet provides different but precious information. Coesite is an ultra-high pressure index mineral which proves the burial of oceanic material at mantle depth (> 100km). Florencite is a REE-reservoir: further studies will constrain its poorly known stability field and shed light on REE transport and storage during deep subduction.

*References:*

[1] Ghignone S et al. (2023a) Am Min 108(7):1368-1375

[2] Ghignone S et al. (2023b) J Raman Spectr 55(3):394-405

[3] Ghignone S et al. (2024) Lithos, 472-473:107575

## Garnet, not always the archetypal cubic mineral

Lorenzon, S.[1*], Mugnaioli, E.[1], Biagioni, C.[1], Nestola, F.[2] and Cesare, B.[2]

[1]Department of Earth Sciences, University of Pisa, Via Santa Maria 53, I-56126, Pisa (Italy)

[2]Department of Geosciences, University of Padua, Via Giovanni Gradenigo 6, I-35131, Padua (Italy)

*Corresponding author: sofia.lorenzon@dst.unipi.it

---

Garnet is one of the most widespread minerals in the Earth, growing in rocks with composition from ultramafic to felsic (e.g. mantle peridotites, metamorphic rocks and granulites) and occurring as detrital mineral in sediments [1]. Its broad *P-T* stability field (*T* up to 2000 °C and *P* ~25 GPa) allows garnet crystallization from the Crust to the deep Mantle, at depths up to ~660 km [2,3]. These characteristics, along with its chemical variability and peculiar resistance, make garnet a key mineral in Earth Sciences to investigate the history and evolution of many geological environments.
Garnet is considered the archetypal cubic mineral, crystallizing in the *Ia-3d* space group and appearing optically isotropic under cross polarized light [4]. However, rare occurrences of garnets showing optical birefringence are reported [5,6,7]. These "uncommon" samples are characterized by specific chemistry, i.e. hydrogrossular ($Ca_3Al_2(SiO_4)_{3-x}(H_4O_4)_x$) and "grandite" (solid solution between grossular and andradite ($Ca_3(Al,Fe^{3+})_2(SiO_4)_3$)) compositions [5,6,7]. In these cases, the optical anisotropy is explained as a consequence of symmetry reduction, from cubic to tetragonal, possibly due to cation ordering or to the presence of a significant hydrogarnet component, or it is attributed to externally-imposed or internal lattice strain [5,6,7].

Recent findings of sector-zoned birefringent garnets with almandine-grossular, $(Fe^{2+},Ca)_3Al_2(SiO_4)_3$, composition in blueschist- and greenschist-facies metamorphosed rocks from several worldwide localities (e.g. Farinole, Cazadero, Jenner and eastern Italian Alps) have suggested that optically anisotropic, not-cubic garnets could be more widespread than commonly assumed [8]. In detail, Cesare et al. [8] propose that garnets could initially grow tetragonal in low-*T* (<450 °C) geological contexts, with possible consequences on the role of garnet as investigative-process tool in these environments. However, the cause of birefringence in these samples is not clear and a more detailed investigation is required.

Here, we present a series of crystallographic studies on sector-zoned birefringent and non-hydrated garnets, using both X-ray and electron diffraction data. Data were collected on low-*T* garnets in metamorphosed rocks from Cazadero (California, USA) and Farinole (Corsica, France). Our data suggest the birefringence is due to a reduction of symmetry from cubic to tetragonal systems connected with twinning or exsolution.

*References:*

[1] Baxter EF et al. (2013) Elements 9: 415-419
[2] Ringwood AE (1991) Geochim Cosmochim Acta 55: 2083-2110
[3] Wood BJ et al. (2013) Elements 9: 421-426
[4] Grew ES et al. (2013) Am Min 98: 785-810
[5] Allen FM and Buseck PR (1988) Am Min 73: 568-584
[6] Antao SM (2013) Powder Diffr 28(4): 281-288
[7] Xu H et al. (2023) Am Min 108: 572-583
[8] Cesare B et al. (2019) Sci Rep 9: 14672

## Minerals as a case study of a bounded (as opposed to open-ended) evolutionary system – Mineralogical Society Hallimond Lecture

Hazen, Robert M.[1]

[1]Earth and Planets Laboratory, Carnegie Science, Washington DC 20015 USA

---

Minerals, which display dramatic increases in diversity and complexity through more than 4.5 billion years of Earth's evolution, provide a quintessential example of an abiotic evolving system [1-4]. Quantitative studies of mineral evolution rely on large and robust mineralogical data resources, coupled with advanced analytical and visualization methods. These resources enable us to probe fundamental questions about the nature of the mineral kingdom, for example, to what extent are mineral systems limited in their potential diversity (i.e., "bounded") versus unrestricted ("open-ended")? A recent framework that unifies behaviours of both biotic and abiotic evolving systems posits that all such systems are characterized by combinatorial richness subject to selection [5]. In the case of minerals, combinatorial richness derives from the possible combinations of chemical elements coupled with permutations of their formulas' coefficients. Observed mineral species, which are selected for persistence through deep time, represent a miniscule fraction of all possible element configurations. Furthermore, this model predicts that as planetary systems evolve, stable minerals become an ever-smaller fraction of the "possibility space." A postulate is that "functional information," defined as the negative $\log_2$ of that fraction [6], must increase as a system evolves. We have tested this hypothesis for minerals by estimating the fraction of all possible chemical formulas observed from one stage of mineral evolution to the next, based on numbers of different essential elements and the maximum chemical formula complexity at each of 9 chronological stages of mineral evolution. We find a monotonic increase in mineral functional information through these 9 stages—a result consistent with the hypothesis [7]. Furthermore, analysis of the chemical formulas of minerals demonstrates that modern Earth may be approaching the maximum limit of functional information for natural mineral systems—a result demonstrating that mineral evolution is not open ended.

*References:*

[1] Hazen R, et al. (2008) *Am Min* **93**:1693-1720

[2] Hazen R (2019) *Am Min* **104**: 810-816

[3] Hazen R & Morrison S (2022) *Am Min* **107**:1262-127

[4] Hazen R et al. (2023) In L Bindi & G Cruciani [eds], *Celebrating the International Year of Mineralogy*. NY: Springer, pp. 15-37

[5] Hazen R et al. (2007) *PNAS*, **104**:574-581

[6] Wong M et al. (2023) *PNAS*, **120**:e2310223120

[7] Hazen R & Wong M (2024) *PNAS Nexus*, https://doi.org/10.1093/pnasnexus/pgae248

## A datasharing ecosystem for everyday datasets

Hezel, D.C.

[1]Institut für Geowissenschaften, Goethe-Universität Frankfurt, Frankfurt am Main, Germany
dominik.hezel@em.uni-frankfurt.de

---

We regularly require basic or everyday datasets such as element masses, decay constants, compositions of reference material, electron binding energies, isotope compositions – or simply some example datasets for teaching. Such datasets are then collated by many researchers, resulting in unnecessary doubling of time and effort, or adequate dataset are not found (in time), incomplete, or for some reason unsatisfactory. Further, individual data in a dataset might become outdated or revised.

Here I suggest a lightweight data sharing ecosystem to solve this problem. This ecosystem consists of the following parts: 1) a GitHub repository that stores such everyday datasets. 2) a webpage through which anyone can contribute, i.e., upload additional datasets, thereby adding to a growing collection of datasets. 3) each uploaded dataset requires an ORCID authentication that automatically links the dataset with the person who uploaded it. Each uploaded dataset requires additional metadata such as a title, the data source, or usage licence, to make the dataset as compatible with the FAIR (Findable, Accessible, Interoperable, Reusable) criteria as possible. 4) The datasets are versioned, so any dataset remains identifiable even after an update of it. 5) A table of contents of the entire repository is automatically produced and accessible for searching. 6) The entire ecosystem is embedded in a webpage that facilitates new dataset uploads, provides instructions and how-tos, provides a webform to search the table of contents, and so on. 7) Importantly, each user remains in control of his or her uploaded datasets through her or his ORCID authentication. This means, every user can update or retract his or her datasets conveniently through a webpage. It is, however, also possible to make datasets permanent. This is then indicated as part of the mandatory metadata. 8) One of the most important parts is an accompanying python package that allows direct access, use, or download of all datasets. This means, after a simple import of this python module, each dataset can be loaded using the get_data() function provided with this package. So, no download from the repository is required, although as well possible. All datasets are readily usable in an e.g., Jupyter Notebook. The python package further provides functions to manipulate, plot and generally work with the datasets. In principle, the datasets can be used with only the python package and no knowledge of the GitHub backend or dataset upload part.

The above-described functionalities have all been programmed using python and are fully working. Some tweaking is, however, still required to make it a stable program but should be completed in the next weeks. The webpage has been programmed with python and deployed using streamlit. The data-sharing platform – called mag4 – will start with a couple dozens of datasets, and it is intended to find a first set of supporters to start with an even larger number of datasets.

Individual datasets have been used to produce helpful web-apps, e.g., to identify peak-overlaps for the electron microprobe or quickly find isotope properties. Further additions such as a dataset validator could be added, or persistent identifiers (PIDs; e.g., a doi) for individual datasets. Everyone is invited to support this effort.

# Factors of development of lithodynamic processes in the coastal zone of the north-western Black Sea region (Ukraine)

Melnyk E.V.[1], Granova A.K.[1], Volynska V.O.[1]

[1]Institute of Geological Sciences of the National Academy of Sciences of Ukraine, Kiev, Ukraine, e-mail: 20vita15@ukr.net

---

Lithologic factor. The formation of the coastal zone is influenced by: composition of rocks, their ability to erode and conditions of occurrence. The abrasion-overbank is composed of loose Pleistocene rocks (loams, sandy loam, sand, clay). Sands and sandy loam are at the base of the cliff. They contribute to rapid erosion and collapse of the overlying strata with the formation of wave-surge niches. The composition of rocks of the underwater slope is important. For the northwestern Black Sea region, these are Pleistocene loess-like rocks. In the southwest of the region, Upper Pleistocene loesses are eroding on the slope. The underwater slope of the abrasion and rockfall bank is represented by loess-like rocks of the Lower Pleistocene with horizons of red-colored buried soils of heavy composition. In addition, dark gray and black silt of the Old Black Sea horizon is abraded on the slope. The composition of loose rocks of the cliff and submarine slope contributestointensiveabrasionprocess.

Hydrodynamic factor. This is the main factor of lithodynamic processes in the coastal zone. It is determined by the wave regime, coastal-marine currents, sea level and ice regime. The coastal zone is characterized by an average wave regime, which causes a high intensity of relief and sediment recycling in this zone. The distribution of waves by direction is subordinate to the wind regime. Waves with a north-westerly direction are characteristic of the open sea. In the coastal zone, waves of north and south directions are more common. The specific features of currents in the coastal zone are subordinated to the wind-wave regime. The speed of coastal-marine currents decreases with distance from the coast. This explains the decrease of underwater slope relief deformation with depth. The ice regime has a weak influence on the morphology and dynamics of the coastal zone. In the cold period, the sea coast is mostly ice-free and sea waves intensively affect the shores.

Wind factor. It ensures hydrodynamic processes in the coastal zone and the development of aeolian processes on the embankments. These processes have a marked influence on the development of accumulative forms, the redistribution of sediment on the surface of the embankments, and the transport of material into the sea or estuary. They ensure changes in the height and width of coastal accumulative forms and saturation of the longshore drift of sediment. Studies have confirmed that aeolian transport mainly involves 0.1-0.5 mm fractions.

In the northwestern Black Sea coastal zone receives sedimentary material from cliffs and benches. Abrasion landforms are composed of clayey rocks, absolutely dominated by siltstone and pelite fractions. The main amount of sedimentary material is carried as suspension into the open sea. On the underwater slope, pelitic and silty-pelitic muds are exposed - the Kalamite and Vityazev layers. There is a steady tendency to shift the coastline towards the sea. This is explained by the insignificant content of beach-forming material in the abraded rocks, the steady tendency of the territory to sink (5 m during the Holocene), eustatic sea level rise (0.2 mm per year), and the conditions of wind and hydrological regimes. The main factor of litho- and morphodynamic processes in the coastal zone of the northwestern Black Sea coast is hydrodynamic.

## Predicting unknown mineral occurrences with Mineral Association Analysis and improving our understanding of mineralogy

Prabhu, A.[1], Morrison, S.M.[1], Eleish, A.[1], Fox, P.[2], Golden, J.[1], Downs, R.T.[3], Perry, S.[4], Burns, P.C.[4], Ralph, J.[5], and Hazen R.M.[1]

[1]Carnegie Institution for Science, Washington, DC, USA

[2]Rensselaer Polytechnic Institute, Troy, NY, USA

[3]University of Arizona, Tucson, AZ, USA

[4]Notre Dame University, Notre Dame, IN, USA

[4]Mindat.org, UK.

---

Abstract: Minerals are the oldest surviving materials from the formation of our solar system. They are time capsules that store and provide information about the evolution of Earth and other planetary bodies. In addition to being a cornerstone of geoscience research, minerals also have economic, industrial, and commercial importance in many sectors of society. One of the fundamental questions in mineralogy and geosciences in general is “Where to find minerals?”. Due to the complex and intertwined nature of natural systems, it has been hard to predict the occurrences of minerals. However, with increase in the volume and accuracy of mineral data and rise of mineral informatics, data science and analytics methods can be developed to answer this fundamental question in mineralogy.

In this contribution, we present “mineral association analysis”, a method to: 1) Predict the mineral inventory for any existing locality. 2) Predict previous unknown localities for any given mineral. Mineral association analysis is a machine learning method that uses association rule learning to find interesting patterns based on mineral occurrence data [1]. Using mineral association analysis, we have been able to predict locations of critical minerals, such as minerals with Li- and Th-bearing phases, predict the mineral inventory of mars analogue sites, and even understand how mineralization and mineral associations changed through deep time [2].

*References:*

[1] Prabhu, A., Morrison, S. M., Eleish, A., Narkar, S., Fox, P. A., Golden, J. J., ... & Hazen, R. (2019, December). Predicting unknown mineral localities based on mineral associations. In AGU Fall Meeting Abstracts (Vol. 2019, pp. EP23D-2286).

[2] Morrison, S. M., Prabhu, A., Eleish, A., Hazen, R. M., Golden, J. J., Downs, R. T., ... & Fox, P. (2023). Predicting new mineral occurrences and planetary analog environments via mineral association analysis. PNAS nexus, 2(5), pgad110.

# Using Machine Learning for automatic rock classification

Tamanna Tamanna[1], Dominik C. Hezel[1], Nishtha Srivastava[1,2], Johannes Faber[2,3]

[1]Institute of Geosciences, Goethe University,Altenhöferallee 1, 60438 Frankfurt am Main, Germany
tamanna@uni-frankfurt.de

[2]Frankfurt Institute for Advanced Studies, Frankfurt am Main, 60438, Germany

[3]Institute of Theoretical Physics, Goethe University, Max-von-Laue-Strasse 1, 60438 Frankfurt am Main, Germany

---

**Introduction:** The application of Machine Learning (ML) in Geochemistry is a promising new tool for analysing large volumes of geochemical data to e.g., assist in revealing the origin of ore deposits [1], discriminate among different tectonic environments [2], or lithology classification [3]. Here we utilise ML to classify igneous rocks on the basis of 10 major and minor elements ($SiO_2$, $TiO_2$, $Al_2O_3$, FeOT, MgO, MnO, CaO, $Na_2O$, $K_2O$, and $P_2O_5$). We use the widely applied TAS plot (**T**otal **A**lkalis: $Na_2O + K_2O$ vs. **S**ilica: $SiO_2$) as a well defined framework to test this new approach. If successful, ML rock classification opens new options, e.g., classifying rocks for which no silica was analysed, as is often the case with solution-based techniques.
**Methods:** We start with a supervised ML technique represented as a neural network (NN) model. Using python and the tensorflow library the NN model was created and trained on an idealised dataset with fake data to learn distinguishing the rock types in the TAS plot. The fake data consist of 2500 random data points for smaller fields, with a gradual increase to 5500 data points for larger fields in the TAS plot. Further, 3 different sets of fake data were created: data points (a) were allowed on the borders between individual rock types, (b) were not allowed on the borders, and (c) had to be 10% away from the borders. The additional major/minor element oxide compositions for all 17 rock types were taken from existing literature and databases [4 and references therein].
**Results and Discussion:** The model was tested on real data from the GeoROC [5] and PetDB [6] databases. We first classified the fake dataset on the basis of the 10 major and minor elements and achieved an accuracy of 99.4% for case (a) and 100% for both (b) and (c). The 0.6% misclassification for (a) was due to data points on the shared borders of the rock fields. The accuracy dropped to 52% and 72%, respectively, when applied to the entirety of the GeoROC and PetDB datasets. An average of about 46.5% of the GeoROC data were misclassified, i.e., lie outside the respective fields on the TAS plot for which these have been classified. The misclassified data were identified and removed from the original GeoROC data. These filtered data were then retested on the fake data trained model leading to an improvement in the model's accuracy to 99.57%. In the next step, we will assess the extent to which other element oxides as well as the trace elements contribute to the classification of rocks.

*References:*

[1] Sun et al., (2022) Ore Geology Reviews 142.
[2] Petrilli et al., (2016) Contributions to Mineralogy and Petrology 171.
[3] Wu et al., (2021) Natural Resources Research 30.
[4] DIGIS Team, 2021, "GEOROC Compilation: Rock Types".
[5] https://georoc.eu/ ; [6] https://search.earthchem.org

# MinPlot 2.0: A new tool for formula recalculation, visualization, and comparison of large mineral compositional datasets

Walters, J.B.[1] and Gies, N.[1]

[1]University of Bern, Institute for Geological Sciences, Bern, Switzerland

Jesse.walters@unibe.ch

---

Collection and visualization of mineral chemical data are essential to mineralogical and petrological studies. Increasing access to microbeam techniques allows for the production of large mineral chemical datasets; however, commonly used spreadsheet-based approaches to mineral formula recalculation typically lack visualization tools and are inefficient for large datasets. Here we update MinPlot [1], a command-line based MATLAB program, to a stand-alone program with a new graphical user interface (GUI). MinPlot 2.0 provides a quick and simple way to recalculate mineral formulae and create publication-ready plots of chemical data. Functions for mineral formula recalculation are provided for a wide range of common rock-forming and accessory minerals; however, the user can also add their own recalculation functions and associated plots. Recalculation functions have been streamlined to improve calculation time for large datasets. In addition, the user may provide $Fe^{3+}/Fe^{2+}$, $Mn^{3+}/Mn^{2+}$, and $H_2O$ contents or have these values estimated automatically. Analytical uncertainty based on counting statistics can be propagated by a Monte Carlo simulation into mineral formulae and endmember fractions.

Importantly, the new GUI based approach allows for plotting of multiple datasets, which can be organized and plotted by sample name, rock type, metamorphic grade, textural location (e.g. core or rim), and other category of metadata. If provided, X-Y positions can be used to plot mineral compositional transects. Data can also be color-coded based on mineral chemistry (e.g. $X_{Mg}$) and plotted spatially, even on top of calibrated optical or electron back scattered images. Data can also be plotted on multi-dimension correlation diagrams, allowing the user to easily and quickly investigate relationships between chemical variables in large datasets. New types of plots can also be added by the user within the framework of the program.

The transition to a GUI-based standalone program means that a MATLAB license is not needed. The source code for mineral formula recalculation and plotting functions are provided. As a result, MinPlot 2.0 is both open-source and freely available to the scientific community. Data and metadata are automatically compiled and exported, allowing the user to easily provide mineral compositional data files for publication and storage in online databases. Combined, MinPlot 2.0 is designed to be consistent with FAIR (Findability, Accessibility, Interoperability, and Reuse of digital assets) principles for scientific data management.

*References:*

[1] Walters JB (2022) Mineralogia 53:51-66

# mineralML: Leveraging Machine Learning for Probabilistic Classification in Earth and Planetary Minerals

Shi, S.[1], Wieser, P.[2], Toth, N.[3], Antoshechkina, P.[4], Lehnert, K.[1]

[1] Columbia University, Lamont-Doherty Earth Observatory, Geoinformatics

[2] University of California, Berkeley, Department of Earth and Planetary Science

[3] University of Cambridge, Department of Earth Science

[4] California Institute of Technology, Division of Geological and Planetary Sciences

---

Explorations of mineral compositions have proliferated with the growing accessibility of geochemical data repositories and computational methods. The generation and continued maintenance of mineral data in these data repositories requires significant human intervention. One major problem is that minerals may be misclassified (i.e., compiled datasets of clinopyroxenes may contain amphiboles), and compilations may contain low-quality electron microscopy (EPMA/EDS) analyses (low totals, low cation sums, poor correspondence to mineral stoichiometry). There are currently no community quality standards for mineral data. To address this, we create an open-source Python package called mineralML (mineral classification using Machine Learning). mineralML classifies common mineral phases based on electron microscopy oxide data, with functions for calculating stoichiometries and crystallographic sites based on this classification. We streamline data cleaning and processing to allow for the rapid transition to classified mineral phase, for detecting phases and generating mineral maps, and for the identification of misclassified phases or low-quality data.

Allocating a mineral classification based on multivariate oxide data alone is surprisingly challenging. We explore and develop machine learning workflows with a training dataset of 86k analyses of 17 common mineral phases, compiled from literature. Supervised learning with variational inference in Bayesian neural networks allows for the successful classification, with confidence intervals, of validation data (~1 million analyses) with 95% accuracy. Misclassifications of the neural network reveal where published classifications may be dubious and prompt further reexamination. We pair this with unsupervised learning, through dimensionality reduction with autoencoders and density-based clustering, presents the opportunity to classify minerals with little *a priori* information. Autoencoder-derived latent spaces offer useful visualizations of the relationships between mineral phases and demonstrate similar trends to the observations made with neural networks.

Both workflows are applied to datasets of mineral analyses from PetDB [1], GEOROC [1], and LEPR [2] to evaluate model performance and show potential for integration into data processing routines for mineral phase segregation and classification, with meaningful visualizations. Now that a successful machine learning framework has been identified to separate mineral groups, we plan to expand it to extraterrestrial minerals to examine whether similar relationships between minerals hold.

*References:*

[1] Lehnert, K., Su, Y., Langmuir, C., Sarbas, B., & Nohl, U. (2000). A global geochemical database structure for rocks. *Geochem. Geophys. Geosyst.* 1, doi:10.1029/1999GC000026.

[2] Hirschmann, M.M., Ghiorso, M.S., Davis, F.A., Gordon, S.M., Mukherjee, S., Grove, T.L., Krawczynski, M., Medard, E., Till, C.B. (2012). Library of Experimental Phase Relations (LEPR): A database and Web portal for experimental magmatic phase equilibria data. *Geochem. Geophys. Geosyst. 9*(3), doi.org/10.1029/1999GC000026.

[3] https://astromat.org.

## Using average mineral properties to study trends through mineral evolution

Bermanec, Marko.[1], Hazen, Robert M.[2], Ma, Xiaogang[3]

[1]Institute of Geology, University of Bern, Baltzerstrasse 1+3, Bern, Switzerland; Corresponding email: marko.bermanec@gmail.com
[2]Earth and Planets Laboratory, Carnegie Institution for Science, 5251 Broad Branch Road NW, Washington DC 20015, USA
[3]Department of Computer Science, University of Idaho, 875 Perimeter Dr., Moscow ID 83844, USA

---

Understanding mineral evolution requires not only decoding individual mineral origins and transformations but also discerning broader patterns and trends within mineralogical systems. Tracking average and statistical trends of mineral properties and formation conditions [1] such as symmetry index [2], Mohs hardness [3], structural and chemical complexity [4] etc. is crucial for unravelling Earth's geological history and predicting future mineralogical changes.

Average trends offer insights into overall compositional, structural, and textural characteristics of mineral assemblages over time. They help identify dominant geological processes, environmental conditions, and tectonic settings influencing mineral formation and alteration. Additionally, average trends aid in recognizing key mineralogical signatures associated with specific geological epochs or events, facilitating the reconstruction of past Earth environments.

Statistical trends complement average analyses by revealing variability, distribution patterns, and outliers within mineralogical datasets. Techniques such as frequency distributions and clustering algorithms elucidate mineral species diversity, abundances, and interrelationships. Documenting statistical trends identifies anomalous occurrences, rare mineralogical associations, and indicators of extreme geological processes or environmental conditions, enhancing interpretation robustness.

The presence of hydrogen (H) profoundly influences the symmetry of minerals. By occupying non-centrosymmetric crystallographic sites or forming hydrogen bonds with other elements, hydrogen alters structural arrangements within mineral lattices, which can lead to reductions in crystallographic symmetry, while impacting mineral properties and behaviors. Regarding mineral rarity, the oldest known ages of minerals often correlate with their formation in unique geological environments characterized by specific paragenetic modes. Minerals formed under unusual conditions or in extreme environments tend to exhibit greater rarity due to the limited occurrence of the geological processes conducive to their formation, thereby contributing disproportionately to Earth's mineralogical diversity. It is found that older paragenetic modes tend to form more common minerals and that these minerals have, on average, a greater number of possible modes of formation compared to minerals formed by younger paragenetic modes.

Tracking average and statistical trends has practical implications for mineral exploration, resource assessment, environmental monitoring, and planetary science. It aids in identifying prospective areas for mineral exploration, assessing economic viability, and mitigating environmental risks associated with mining. Moreover, insights into Earth's mineral evolution inform space exploration missions and astrobiological investigations.

*References:*

[1] Hazen RM and Morrison SM (2022) Am Min 107(7):1262-1287
[2] Bermanec M et al (2024) Geosci. Data J 11(1):69-85
[3] Bermanec M et al. (2023) Minerals 13(8): 1089
[4] Krivovichev SV et al. (2022) Min Mag 86(2): 183-204

## Lithodynamic processes on the north-western shelf of the Black Sea of Ukraine

Granova A.K.[1], Melnik E.V.[1], Volynska V.O.[1]

[1]Institute of Geological Sciences of the National Academy of Sciences of Ukraine, Kiev, Ukraine, e-mail: 20vita15@ukr.net

---

The lithodynamic connections between the coastal and shelf zones during the Upper Pleistocene-Holocene in the area from the mouth of the Dniester estuary to the Danube delta and the adjacent part of the shelf were traced. The research was based on mineralogical analysis. The main focus was on the quantitative and qualitative composition of the heavy fraction.

The results of the studies allowed us to distinguish three lithodynamic zones: the upper zone - from the beach to a depth of 10 m, the middle zone - to a depth of 30-35 m (the boundary between the outer and inner shelf) and the lower zone to the outer shelf edge. There are significant differences in relief, direction and intensity of hydrodynamic processes between the zones. Therefore, we consider the inner and outer shelf as different lithodynamic zones. The sedimentation processes on the inner shelf are influenced by compensating currents. The outer shelf is dominated by gravity-passive sedimentation.

Sea level rise was very rapid at the beginning of the Novoevxinsky stage. This hindered the stabilisation of the coastline and the formation of accumulative bodies. Between the first and second stages of the New Euxine transgression (bolling), shoreline stabilisation was recorded at 30-32 m. This level was also characteristic of the Uzunlar and Suroga basins, when powerful accumulations of alluvium and deltaic sediments were formed. During the Allerød and Early Holocene, the north-western sector of the Black Sea formed thick and extended accumulation formations in the overlying coastal zone. The structure of Holocene sediments indicates a landward shift of the accumulations to the Atlantic optimum. As a result of rapid sea-level rise and intensive coastal abrasion during the Atlantic period, a significant volume of terrestrial material was transported to the submarine part of the coastal zone. Coastal abrasion decreased in post-Atlantic time and a powerful submarine rampart was formed at the site of the first wave crash. With the formation of the rampart and the longshore sediment flow, the Danube Estuary begins to fill rapidly. The sand ridges are increasingly shifting seaward and overlying the young muddy sediments. The mineralogical composition of the sand ridges differs from the mineralogical composition of the hard sediment of the Danube. This confirms that the formation of the sand ridges is due to the input of material from the longshore drift of sediment. At this time, modern lithodynamic zones with characteristic depositional environments were formed.

## Characterizing Earth's biosignatures via mineral network analysis

Morrison, S.M.[1], Prabhu, A.[1], Hazen. R.M.[1], Wong, M.L.[1] and Eleish, A.[1]

[1]Earth and Planets Laboratory, Carnegie Institution for Science, 5241 Broad Branch Rd NW, Washington, DC 20015 USA; *smorrison@carnegiescience.edu

---

Determining the habitability of planets remains a fundamental question in science and society. In this study, we harness network theory to explore the unique patterns exhibited by minerals and their mineralizing environments in both biotic and abiotic contexts throughout the evolution of Earth and other terrestrial bodies in our solar system [1-. By examining mineralogical networks across diverse planetary systems, including early solar system bodies, the early Hadean Earth (closely related to modern-day Mars), plate tectonics, and modern Earth, we gain valuable insights into Earth's history and the factors that have shaped the development and sustainability of life. Our investigation reveals distinct characteristics within biotic networks, setting them apart from their abiotic counterparts.

This research significantly advances our understanding of the intricate interplay between Earth and life. Network analysis offers deeper insights into the connections between minerals and living systems, providing invaluable perspectives on the emergence and co-evolution of life on our planet. Moreover, our findings contribute to identifying and characterizing planetary biosignatures, essential for the search for extraterrestrial life. Recognizing these unique patterns within biotic networks lays the groundwork for developing targeted exploration strategies for detecting potential biosignatures and interpreting the complexities of planetary environments.

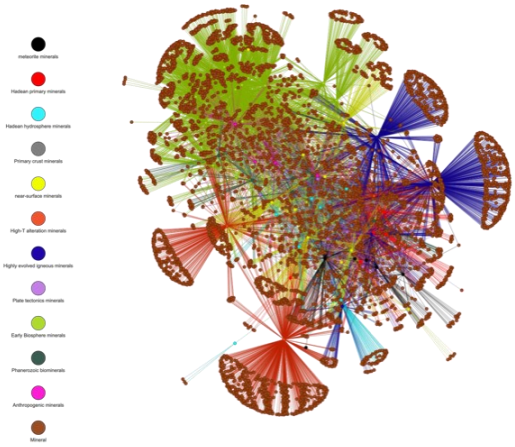

Figure 1. A network representation of the relationships between all known mineral species and their modes of formation in our solar system. Brown nodes represent mineral species. Colored nodes represent paragenetic modes (modes of mineralization). Links demonstrate that a mineral is known to form in the linked paragenetic

Our innovative network analysis of minerals and mineralizing environments sheds new light on the relationships between Earth and life. By delving into the intricate connections within biotic and abiotic systems, we deepen our understanding of Earth's dynamic history and enhance our knowledge of potential habitats for life beyond our planet.

**References:**

[1] Morrison SM, Liu C, Eleish A, Prabhu A, Li C, Ralph J, Downs RT, Golden JJ, Fox P, Hummer DR, Meyer MB, Hazen RM (2017) Network analysis of mineralogical systems. American Mineralogist, 102, 1588-1596, https://doi.org/10.2138/am-2017-6104CCBYNCND

[2] Morrison SM, Prabhu A, Hazen RM (2023) Exploration of the Biological Influence in Earth's Mineralogical Networks, Geological Society of America Abstracts with Programs. Vol. 55, No. 6, 2023, doi: 10.1130/abs/2023AM-394193

[3] Morrison, S.M., Prabhu, A. and Hazen, R. (2023) Is Earth's biological influence recorded in its mineralogical networks? AGU23.

## The German National Research Data Infrastructure for the Earth System Sciences (NFDI4Earth)

Bernard L.[1], Braesicke P[2]., Bertelmann R.[3], Frickenhaus S.[4], Gödde H.[3], Keßler C.[5], Lorenz S.[6], Mahecha M.[7], Marschall H.R.[8], Hezel D.C.[8], Nagel W.E.[1], Reichstein M.[9], Sester M.[10], Thiemann H.[11], Weiland C.[12], Wytzisk-Arens A.[13], Xu J.D.[8*], NFDI Consortium Earth System Sciences

[1] Technische Universität Dresden, Germany

[2] Karlsruhe Institute of Technology

[3] Helmholtz Centre Potsdam

[4] Alfred Wegener Institute Helmholtz Centre for Polar and Marine Research

[5] Bochum University of Applied Sciences

[6] GEOMAR Helmholtz-Zentrum für Ozeanforschung Kiel

[7] Universität Leipzig

[8] Goethe-Universität Frankfurt, Germany

[9] Max-Planck-Institut für Biogeochemie

[10] Leibniz Universität Hannover

[11] German Climate Computing Center DKRZ

[12] Leibniz Institution for Biodiversity and Earth System Research

[13] Bochum University for Applied Sciences

* xu@em.uni-frankfurt.de

---

The NFDI4Earth (https://www.nfdi4earth.de/) – the German National Research Data Infrastructure for the Earth System Sciences (ESS) – addresses the digital needs of Earth System Science (ESS) researchers. The ESS comprises many disciplines and communities, all with the common goal of better understanding the subsystems of the Earth system and their interactions. The connections between different sub-disciplines and scientific approaches can be significantly strengthened through common research data management (RDM) and knowledge extraction, ultimately leading to a new quality of science.

The NFDI4Earth aims to offer researchers a FAIR (Findable Accessible Interoperable Reusable), simple, coherent, efficient, open and – whenever possible – unrestricted gateway to Earth system data as well as scientific data management and data analysis services. Setting up the NFDI4Earth services is a user-driven process and widely supported by the German Earth System Science community with currently over 60 partners from universities, research institutions, infrastructure providers and authorities.

The web-based entry point to the NFDI4Earth services – called OneStop4All – together with a user support network serve ESS researchers with access to data repositories, educational materials, collaborative and analysis tools, as well as RDM services. Besides, there are Pilots, Incubator Lab, Interest Groups and Acedemy in NFDI4Earth, which focus on the community support of ESS. No matter if you are a student, professional, service provider or top scientist, we have offers for you and hope that you can join us or find/provide the required information for your objectives in our services.

Reference:
https://zenodo.org/records/5718944

## Geochemical Modelling Beyond Mars – from Asteroid Belt to Kuiper Belt

Yoosefdoost, A.[1], Bakhshoodeh, R.[2] and Santos, R.M.[1]

[1] School of Engineering, University of Guelph, Guelph, Ontario, Canada; santosr@uoguelph.ca

[2] Department of Civil, Environmental and Mining Engineering, University of Western Australia, Perth, Australia.

---

Space geochemical modelling is a powerful tool for supporting cosmochemistry in studying the geochemistry of visited astronomical objects and predicting the geochemical conditions on more obscure planets and moons. Geochemical models can assist in simulating the evolution of the atmosphere, crust, and interior of planets or moons and the geochemical conditions of their surface or subsurface.[1] However, despite the number of studies on the Moon and other celestial bodies as far as Mars, the number of geochemical modelling studies conducted on celestial objects from the Asteroid Belt to the Kuiper Belt is sparse and hence not well known or summarized. Therefore, this work focused on such studies to provide a vision of what has been done thus far by analysing, categorizing and providing the critical points of the research's objectives, the explored geochemical modelling aspects and findings. The approach began by generating a list of 180 celestial objects and selecting a comprehensive set of keywords and phrases for identifying relevant studies about geochemical modelling for celestial bodies. The study applied bibliometric analysis techniques, including a novel approach consisting of combining Bibliometrix and custom-developed data analysis tools to enhance the relevance of identified publications for target keywords, to identify influential publications, authors, and journals in this field.

The analysis identified Saturn's moons Enceladus and Titan, Jupiter's moon Europa, and Ceres as the most studied celestial objects involving geochemical modelling. For instance, on Ceres, the review identified studies that leveraged geochemical modelling (of silicate chemistry, ocean chemistry, ammonia reactions, and thermal evolution) to study the body's structure, composition, and potential for a subsurface ocean,[2] and additionally investigated how such investigations contribute to the study of the early solar system and its potential for hosting alien life. Geochemical modelling has also been central to a proposed model for Ceres' internal evolution that incorporates geochemical aspects such as the redistribution of potassium and the freezing of the ocean and to the conceptual study of the potential formation of organic compounds and the influence of environmental parameters on their speciation and abundance in the Ceres' subsurface ocean.[3] By exploring studies with novel solutions that leverage geochemical modelling and the utilization of available resources, this project showcases solutions for reducing the barriers to exploring distant space corners of the solar system to answer ambitious questions, from probing the potential for harbouring alien life to assessing the habitability of worlds beyond our own in addition to increasing the understanding of the chemical composition, processes, and evolutionary narratives of celestial bodies in such least accessible borders.

*References:*

[1] Johnson PV (2019) Icarus 321:857-865
[2] Castillo-Rogez JC and McCord TB (2010) Icarus 205:443-459
[3] Diab J (2023) Icarus 391:115339

## Mineral species and mineral substances according to the IMA-CNMNC

Bosi, F.

Department of Earth Sciences, Sapienza University of Rome, Piazzale A. Moro, 5, I-00185 Rome, Italy
Email: ferdinando.bosi@uniroma1.it

Minerals constitute rocks, which in turn constitute planets and all extraterrestrial solid bodies. Minerals are thus the fundamental building blocks of our planet, and their study is of primary importance to Earth Sciences.

It is important to establish a distinction between “mineral species” and “mineral substances.” The Commission on New Minerals, Nomenclature, and Classification (CNMNC) of the International Mineralogical Association (IMA) considers them as distinct entities. Mineral species are ideal entities, whereas mineral substances are real entities. As the mineral species is not an entity existing per se in nature, but rather the result of an agreement around certain conventions, the problem is not to recognize this or that natural species, but rather to establish criteria and definitions that can be come universally accepted. To represent these entities accurately, specific mineral formulae are required, such as the ideal formula and the empirical (real) formula.

The CNMNC identifies mineral species using a name and an ideal formula. The latter typically represents a compositional extreme. However, exceptions may exist due to historical or crystal-chemical factors. The empirical formula, which should ultimately lead to the ideal formula, usually reflects the chemical variability resulting from atomic substitutions within the mineral species' structure.

The number of mineral substances is vast and likely incalculable, encompassing all chemically homogeneous solid phases (including crystalline, quasicrystalline and amorphous substances) formed through geological processes across the universe. In contrast, the current number of recognized mineral species exceeds 6050, meticulously documented in “The New IMA List of Minerals - A Work in Progress.” The CNMNC regularly approves new mineral species, with over a hundred species accepted annually, accounting for more than 80% of proposed species.
This contribution will discuss the difference between mineral species and mineral substance, along with the formulae that best represent them.

# Two new super-reduced phases from Luobusa chromitite: jianmuite, $ZrTi^{4+}Ti^{3+}_5Al_3O_{16}$, and a $Ti^{3+}$-rich calcium amphibole, $\square Ca_2(Mg_2Ti^{3+}_3)(Si_5Al_3)O_{22}(OH)_2$

Borriello, R.[1-2]*, Xiong, F.[3], Ma, C.[4], Lorenzon, S.[2], Mugnaioli, E.[2], Yang, J.[5], Xu, X.[3] and Grew, E.S.[6]

[1]Department of Environmental Sciences, Informatics and Statistics, Ca' Foscari University of Venice, Via Torino 155, 30172 Mestre (VE), Italy

[2]Department of Earth Sciences, University of Pisa, Via S. Maria 53, 56126 Pisa, Italy

[3]Center for Advanced Research on the Mantle, Chinese Academy of Geological Sciences, Beijing 100037, China

[4]Division of Geological and Planetary Sciences, California Institute of Technology, Pasadena, California 91125, USA

[5]School of Earth Sciences and Engineering, Nanjing University, Nanjing, 210023, China

[6]School of Earth and Climate Sciences, University of Maine, Orono, Maine 04469, USA

*Corresponding author: roberto.borriello@unive.it

---

Corundum from the Cr-11 chromitite orebody in the Luobusa ophiolite near Kangjinla (Tibet, China) [1] contain a great variety of ultra-reduced inclusions (URIs, i.e. phases without oxygen, e.g. phosphides, silicides, nitride) and super-reduced inclusions (SRIs, i.e. phases with oxygen, but also with metals in an unusual, reduced state, e.g. $Ti^{3+}$). Given the micrometric to sub-micrometric size of these inclusions, their chemical and structural characterization is only possible by using advanced analytical protocols that involve a focused ion beam (FIB) and transmission electron microscope (TEM). In particular, three-dimensional electron diffraction (3DED) [2] combined with programs for the dynamical refinement (i.e., structural refinement that takes into account dynamical scattering) [3] constitute powerful tools to solve the structure of crystal phases that are too small for conventional single-crystal X-ray diffraction methods. In this work, we present two new phases found as SRIs in a FIB lamella from a corundum grain extracted from the Cr-11 orebody.

Jianmuite, ideally $ZrTi^{4+}Ti^{3+}_5Al_3O_{16}$ [4], is a Zr-Ti-Al-oxide similar in chemistry and paragenesis to carmeltazite, $ZrAl_2Ti^{3+}_4O_{11}$ [5], but with a space group *I*-4, *a* = 10.3675(10) Å, *c* = 9.1825(10) Å. Remarkably, this mineral was also found among refractory phases in the matrix of the Allende meteorite, a CV3 carbonaceous chondrite. In the same lamella, we also found another potential new mineral, with a structure consistent with the amphibole supergroup [6], but a novel composition with the ideal formula $\square Ca_2(Mg_2Ti^{3+}_3)(Si_5Al_3)O_{22}(OH)_2$. The charge arrangement is unique as is $Ti^{3+}$ being the dominant trivalent C cation (through the hypothetical homovalent substitution $^{C}Al^{3+} = {}^{C}Ti^{3+}$), so a new rootname and the prefix “titano-“ (never used so far in the amphibole supergroup) are needed. The occurrence of $Ti^{3+}$ in terrestrial minerals is petrologically significant as it constrains the redox conditions under which the $Ti^{3+}$-bearing minerals crystallized.

*References:*

[1] Xiong F et al. (2020) Eur J Mineral 32: 557-574
[2] Gemmi M et al. (2019) ACS Cet Sci 5: 1315-1329
[3] Brázda P et al. (2019) Science 364: 667-669
[4] Bosi F et al. (2023) CNMNC Newsletter 75, Eur J Mineral 35: 891-895
[5] Griffin W L et al. (2018) Minerals 8: 601
[6] Hawthorne F C et al. (2012) Am Mineral 97: 2031-2048

## Crystal chemistry of Belgian ardennites

Depret, M.[1], Hatert, F.[1], Blondieau, M.[2], Puccio, S.[3], Dal Bo, F.[1], Erambert, M.[4] and Bomal F.[1]

[1]Laboratory of Mineralogy B18, University of Liège, B-4000 Liège, Belgium (martin.depret@uliege.be)

[2]Val des Cloches 131, B-6927 Tellin, Belgium

[3]Rue des Fontaines 156, B-4041 Vottem, Belgium

[4]Department of Geosciences, University of Oslo, PO box 1047 Blindern, N-0316 Oslo, Norway

---

*Ardennite* is a rare Mn-rich aluminium silicate originally found in Salmchâteau, Stavelot Massif, Belgium, during the second half of the 19th Century. Samples were simultaneously investigated by A. von Lasaux and F. Pisani leading to some controversies between the two scientists as they initially considered the mineral as vanadium-bearing [1-3], and then as arsenic-rich [4]. Nowadays, two distinct species were defined: ardennite-(As) with the ideal formula $Mn^{2+}{}_4Al_4(AlMg)(AsO_4)(SiO_4)_2(Si_3O_{10})(OH)_6$ and with type-locality Salmchâteau (Belgium), and ardennite-(V) with the ideal formula $Mn^{2+}{}_4Al_4(AlMg)(VO_4)(SiO_4)_2(Si_3O_{10})(OH)_6$ and with type-locality Sparone (Piedmont, Italy [5]). During the past years, new occurrences of *ardennite* were discovered in the southern part of the Stavelot Massif, initiating the crystal-chemical investigation of eleven Belgian *ardennite* samples originated from various localities or mineralogical and petrographic associations.

Chemical compositions obtained from electron-microprobe analyses are in good agreement with single-crystal structure refinements. The $As^{5+} \leftrightarrow V^{5+}$ homovalent substitution on the *T*4 tetrahedral site explains the existence of a complete solid solution between ardennite-(As) and ardennite-(V), while the incorporation of $Si^{4+}$ and $P^{5+}$ seems to be more restricted. Solid solutions towards the potential new species "ardennite-(P)" and "ardennite-(Si)" therefore appear to be relatively limited although some samples show significant enrichments, with up to 0.28 $P^{5+}$ atoms per formula unit (apfu) and 0.74 $Si^{4+}$ apfu. An heterovalent substitution mechanism involving the *T*4 and *M*3 sites, $^{T4}Si^{4+} + {}^{M3}(Al, Fe)^{3+} \leftrightarrow {}^{T4}(As, V, P)^{5+} + {}^{M3}Mg^{2+}$, also clearly occurs. Due to the various multiplicities of the *M*3 and *T*4 sites, 4 and 2 respectively, a valency-imposed double-site occupancy on *M*3 is necessary to preserve charge-balance [6] in the ideal end-member formulae of ardennite-group minerals. Only a few satisfactory trends were observed between the chemical composition and the structural parameters of ardennites, probably due to an overall adjustment of the unit-cell. The unit-cell parameters tend to increase with the (Ca + Mg + Fe) contents of ardennites and a negative correlation has been observed between the bond length distortion coefficients on the *M*3 and *T*4 sites, that seems to be controlled by the position of the oxygen shared by both sites. Discussions concerning the nomenclature of the ardennite group are also presented.

*References:*

[1] von Lasaulx A (1872) Neues Jahrb für Min 1872: 930-934
[2] von Lasaulx A (1872) Verh naturh Ver preuss Rheinl Wesph 29: 189-192
[3] Pisani F (1872) CR Acad Sci Paris 75: 1542-1544
[4] Pisani F (1873) CR Acad Sci Paris 77: 329-333
[5] Barresi A A et al. (2007) Eur J Mineral 19: 581-587
[6] Hatert F and Burke E A J (2008) Can Mineral 46: 717-728

# “Ferroåkermanite" - a potentially new mineral from kirschsteinite-bearing paralava from Hatrurim Complex, Israel

Juroszek, R.[1], Krüger, B.[2], Galuskin, E.[1] and Vapnik Ye.[3]

[1]Institute of Earth Sciences, Faculty of Natural Sciences, University of Silesia in Katowice, Poland; rafal.juroszek@us.edu.pl

[2]Institute of Mineralogy and Petrography, University of Innsbruck, Austria

[3]Department of Geological and Environmental Sciences, Ben-Gurion University of Negev, Beer-Sheva, Israel

---

The melilite group consists of seven sorosilicate minerals in which åkermanite, $Ca_2MgSi_2O_7$, and gehlenite, $Ca_2Al(SiAl)O_7$ are the most widespread members that forming the solid-solution series [1]. The general formula of the melilite group is $X_2T1(T2)_2O_7$, where $X$ = □, Na, K, Ca, Ba, Sr; $T1$ = B, Be, Mg, $Fe^{2+}$, Zn, $Fe^{3+}$, Al, Si and $T2$ = Si, Al, B, Be [2]. A potentially new member of the melilite group - “ferroåkermanite”, ideally $Ca_2Fe^{2+}Si_2O_7$, was found in coarse-grained kirschsteinite-bearing paralava from the pyrometamorphic Hatrurim Complex in Israel. Together with wollastonite, rankinite, cuspidine, gehlenite, kirschsteinite, kalsilite, and fluorapatite, “ferroåkermanite” comprises the rock-forming assemblages. The potentially new mineral rarely forms transparent, light-yellow single subhedral crystals up to 40 µm in size, most common are aggregates and overgrowth with gehlenite. The empirical formula of “ferroåkermanite” calculated based on 14 O is present as $(Ca_{1.81}Na_{0.17}K_{0.03}Sr_{0.01})_{2.02}(Fe^{2+}_{0.56}Al_{0.35}Mg_{0.10})_{1.01}(Si_{1.81}Al_{0.19})_2O_7$. Moreover, obtained chemical data confirm the presence of “ferroåkermanite”-gehlenite solid solution in the studied specimen.

The crystal structure of “ferroåkermanite” was solved by direct methods using single-crystal XRD data, which yielded the tetragonal symmetry ($P$-$42_1m$): $a = b = 7.7528(7)$ Å, $c = 5.0186(5)$ Å, $V = 301.65(5)$ Å$^3$, Z = 2. “Ferroåkermanite” has a melilite-type structure with layers composed of disilicate $(Si_2O_7)^{6-}$ groups and $(Fe^{2+}O_4)^{6-}$ tetrahedra, connected by large eightfold-coordinated Ca atoms. The site population refinement of the tetrahedra converges at 0.504(18) Fe and 0.496(18) Mg (Al+Mg) and gives the mean distance of T1-O = 1.832(7) Å.

The Raman spectrum of “ferroåkermanite” exhibits the presence of the main vibrations related to $Fe^{2+}O_4$ tetrahedra and $Si_2O_7$ groups on the $T1$ and $T2$ sites. The most intense bands at 620 cm$^{-1}$ and 664 cm$^{-1}$ with shoulder at 702 cm$^{-1}$ are related to symmetric stretching ($\nu_s$) vibrations of $Fe^{2+}O_4$ and Si-O-Si modes of $Si_2O_7$, respectively. The presence of the Raman band at 836 cm$^{-1}$ assigned to symmetric stretching ($\nu_s$) vibrations of $AlO_4$ might indicate the partial substitution on $T1$.

The presence of rock-forming minerals like wollastonite, gehlenite or rankinite suggests that the paralava formed in high-temperature conditions. The presence of $Fe^{2+}$-bearing phases, kirschsteinite, “ferroåkermanite” indicates the reduced conditions related to lower oxygen fugacity.

*Acknowledgements:*
The project is co-financed by the Polish National Agency for Academic Exchange BPN/BAT/2023/1/00019/U/00001 and OeAD Project: Scientific & Technological Cooperation Austria-Poland, Project PL 11/2024, and partially supported by the National Science Center (NCN) of Poland Grant 2021/41/B/ST10/00130.

*References:*
[1] Sharma SK, Yoder Jr. HS, Matson DW (1988) Geochimica and Cosmochimica Acta 52:1961-1967.
[2] Bindi L, Bonazzi P, Fitton G (2001) European Journal of Mineralogy 13:121-125.

# Crystal chemistry and nomenclature of the triphylite group of phosphates

Hatert, F.[1], Lyalina, L.M.[2] and Selivanova, E.A.[2]

[1] Laboratory of Mineralogy, University of Liège B18, 4000 Liège, Belgium (fhatert@uliege.be)

[2] Geological Institute, Kola Science Center of the Russian Academy of Sciences, Apatity, 184209, Russia

Minerals of the triphylite group are phosphates that occur as primary phases in some rare-element granitic pegmatites. Their olivine-type crystal structure (space group *Pbnm*) is characterized by two chains of edge-sharing octahedra parallel to the *c* axis: the first chain is constituted by the *M*1 octahedra occupied by Li, Na, or vacancies, and the second chain is formed by the *M*2 sites occupied by Fe, Mn, and Mg [1]. The occupancy of the *M*1 position varies from 0 to 1 in Li-bearing species, and it approaches 1 in Na-bearing species. The structural formula of triphylite-type phosphates is $M1M2TO_4$, where *T* corresponds to $P^{5+}$ in tetrahedral coordination [1]. The cation ordering between *M*1 and *M*2, first defined for natrophilite [2], is the main crystal-chemical difference between triphylite-type phosphates and silicates of the forsterite-fayalite series, in which Fe and Mg are disordered over the two sites.

Oxidation of $Fe^{2+}$ to $Fe^{3+}$ and of $Mn^{2+}$ to $Mn^{3+}$ produces Li-vacancies at the *M*1 sites, which are necessary to maintain charge balance. This process is responsible for the so-called "Quensel-Mason" oxidation sequence, in which triphylite ($LiFe^{2+}PO_4$) and lithiophilite ($LiMn^{2+}PO_4$) progressively transform into heterosite ($Fe^{3+}PO_4$) and purpurite ($Mn^{3+}PO_4$) [3]. The alignment of the *M*1 octahedra along the *c* axis explains why the [001] direction becomes an easy and fast pathway for Li/Na leaching during the oxidation, or for Li/Na absorption when conditions lead to the reduction of Fe and Mn. This is the principle widely used Li-ion batteries based on olivine-type phosphates [4].

Based on new crystal-chemical data on natural samples [5], we present an IMA-CNMNC-accepted scheme for the classification and nomenclature of the triphylite group of minerals [6]. Besides the Li-bearing species of the triphylite-lithiophilite and heterosite-purpurite solid solutions, the group also contains the Na-bearing phosphates natrophilite ($NaMn^{2+}PO_4$) and karenwebberite ($NaFe^{2+}PO_4$) [7], as well as the Li-Mg-bearing phosphate simferite which has been redefined as $LiMgPO_4$. Ferrisicklerite and sicklerite correspond to intermediate phases in the triphylite-heterosite and lithiophilite-purpurite solid solutions, respectively. As a consequence, and according to the CNMNC dominant-constituent rule [8], they were discredited. A new mineral oxidation sequence is also defined, which modifies the traditional “Quensel-Mason” sequence by taking into account the different oxidation capacities of iron and manganese.

*References:*

[1] Losey A et al. (2004) Can Mineral 42: 1105-1115
[2] Moore P B (1972) Am Mineral 57: 1333-1344
[3] Quensel P (1937) Geol Fören Stockholm Förhand 59, 77-96.
[4] Yakubovich O et al. (2020) Minerals 10(6): 524
[5] Hatert F et al. (2012) Can Mineral 50: 843-854
[6] Lyalina L et al. (2023) Eur J Mineral 35: 427-437
[7] Vignola P et al. (2013) Am Mineral 98: 767-772
[8] Hatert F & Burke E A J (2008) Can Mineral 46: 717-728

## New data for undescribed uranyl minerals supporting the CURIES database

Olds, T.A., Spano, T.L., McDonnell, M., Smith, R., Niedziela, J.L., Miskowiec, A., Kapsimalis, R. and Shields, A.E.

---

Making accurate mineral identifications and assignments of vibrational spectra for uranyl minerals can be extremely difficult in the absence of supporting chemical or crystallographic data. This is particularly true for sulfates, which can exhibit nearly identical band positioning and splitting. Other artefacts, spectral broadening and admixtures of multiple minerals can confuse pattern matching algorithms employed by other identification software. The CURIES database, a Compendium of Uranyl Raman and Infrared Experimental Spectra, developed by scientists at Oak Ridge National Laboratory and the Carnegie Museum of Natural History, seeks to create a better search-match algorithm using insights gained from new uranium minerals. Crystallographic and Raman data are presented for three new uranyl minerals with unique spectral features that are helping to inform our development of the database.

# Cr - analogue of hydrocalumite – a potentially new mineral from the Negev Desert, Hatrurim Complex, Israel

Skrzyńska, K.[1], Stachowicz, M.[2], Juroszek, R.[1], Pakhomova, A.[3], Galuskina, I.[1], Vapnik, Y.[4], and Galuskin, E.[1]

[1]Faculty of Natural Sciences, University of Silesia in Katowice, Będzińska 60 Road, Sosnowiec, Poland/ corresponding author: katarzyna.skrzynska@us.edu.pl

[2]Department of Geochemistry, Mineralogy and Petrology, Faculty of Geology, University of Warsaw, Żwirki i Wigury 93,02-089, Warsaw, Poland

[3]European Synchrotron Radiation Facility, avenue des Martyrs, CS 40220, 38043 Grenoble Cedex 9, France.

[4]Department of Geological and Environmental Sciences, Ben-Gurion University of the Negev, POB 653, Beer-Sheva, Israel

---

A potentially new mineral ($Ca_4Cr_2OH_{12}Cl_2{\cdot}4H_2O$) with hydrocalumite-type structure was found in low-temperature altered rocks of pyrometamorphic Hatrurim Complex, Israel. It forms hexagonal plates and tabular crystals, rarely exceeding 60 µm in size with thickness up to 20 µm. lt was found as a layer of crystal aggregates on the specimens that contains mainly afwillite, minerals of ettringite-thaumasite series, and a mixture of calcium hydrosilicates. An accessory minerals: fluorapatite, hydrocalumite, baryte, gypsum and opaque spinels were identified. The Cr - analogue of hydrocalumite exhibits the attractive feature of light-induced colour change from bluish-violet to pinkish-violet colours depending on the type of lighting. The crystals of the potentially new mineral are brittle with perfect cleavage along {001}. They are translucent and characterized by vitreous lustre. In terms of optical properties, the crystals of this new phase are uniaxial, indicating a high symmetry. Based on electron microprobe analyses the following empirical formula can be written as: $(Ca_{3.94}Sr_{0.01})_{\sum 3.95}(Cr_{1.47}Al_{0.52}\ Fe_{0.05})_{\sum 2.05}(OH_{10.86}Cl_{1.14})_{\sum 12.00}[Cl_{1.99}(SO_4)_{0.01}]_{\sum 2}{\cdot}0.91H_2O$. The crystal structure was modelled based on merged X-ray diffraction data from an *in-house* diffractometer and synchrotron radiation facility. The structure was solved in the *R*-3*c* space group with unit cell parameters: $a$ = 5.7944(2) Å, $c$ = 46.70(4) Å and $V$ = 1357.7(10) Å$^3$. The final model converged to the $R_1$ = 0.0847. The structural investigation corroborated the lamellar double hydroxide (LDH)–type structure. The $Cr^{3+}$ and $Al^{3+}$ occupy the octahedral site coordinated by hydroxyl groups. The $Ca^{2+}$ is coordinated by six oxygens and one water molecule. The intercalated $Cl^-$ anions balance the charge of the layers.

Interestingly, the potentially new mineral surprisingly revealed trigonal symmetry, whereas most of the known structures of hydrocalumite crystalize in a monoclinic system [1]. Even more intriguing is the absence of a carbonate group in the interlayer space, confirmed by Raman spectroscopy.

The Raman spectrum is characterized by the most distinctive mode at 522 $cm^{-1}$, which is unique for this type of structure and is related to M – OH stretching vibrations [2, 3].

Acknowledgement: The investigations were supported by NCN of Poland, grant no. 2019/35/O/ST10/01015.

*References:*

[1] Mills S J et al. (2012) *Mineral. mag.* 76: 1289–1336.

[2] Frost R L et al. (2011) *J. Raman Spectrosc.* 42: 1163–1167.

[3] Yue Y et al. (2018) *Cement and Concrete Composites* 86: 306–314.

# The puzzle of an allanite-like epidote mineral from Malmkärra, Sweden: Toward the new (OH)-analogue of dollaseite-(Ce)

Taddei, A.[1], Bindi, L.[1], Bonazzi, P.[1], Casey, P.[2], Förster, H.-J.[3], Holtstam, D.[4] and Karlsson, A.[4]

[1]Dipartimento di Scienze della Terra, Università degli Studi di Firenze, Via G. La Pira 4, 50121, Firenze, Italy; alice.taddei@unifi.it

[2]Geological Survey of Sweden, Villavägen 18, SE-752 36, Uppsala, Sweden

[3]Helmholtz Centre Potsdam GFZ German Research Centre for Geosciences, Telegrafenberg, 14473 Potsdam, Germany

[4]Department of Geosciences, Swedish Museum of Natural History, Box 50007, SE-104 05, Stockholm, Sweden

---

A peculiar allanite-group mineral has been found in a REE-rich fragment of skarn from the Malmkärra iron mine, Norberg, Västmanland (Sweden), occurring in a Bastnäs-type deposit. The associated minerals are characteristic of this type of mineralization: calcite, dolomite, magnetite, lizardite, talc, fluorite, baryte, scheelite and gadolinite-(Nd), along with the newly discovered fluorbritholite-(Nd) [1].

Single-crystal X-ray diffraction, electron microprobe analyses, FT-IR and Mössbauer spectroscopy were applied to comprehensively study the mineral. Additionally, one crystal was subjected to annealing experiments at temperatures ranging from 500 to 700°C, in 50°C steps, and a second crystal was heated directly at 700°C. Each annealing experiment was performed in air for 48 hours. The examination of both structural and chemical data allowed to assign the following cationic populations: *A*1 = $Ca_{0.96}REE^{3+}_{0.03}Mn_{0.01}$; *A*2 = $REE^{3+}_{0.99}Ca_{0.01}$; *M*1 = $Mg_{0.40}Al_{0.32}Fe^{3+}_{0.26}Fe^{2+}_{0.02}$; *M*2 = $Al_{0.98}Fe^{3+}_{0.02}$; *M*3 = $Mg_{0.72}Fe^{2+}_{0.18}Fe^{3+}_{0.10}$; *T*1,2,3 = $Si_{2.93}Al_{0.07}$, yielding a total positive charge of 24.63. Given the occurrence of considerable amounts of divalent cations such as Mg and Fe (verified by Mössbauer data) at both *M*1 and *M*3, more than one monovalent anion per formula unit (pfu) is required to achieve charge balance. If *M*1 and *M*3 are dominated by divalent cations, as in dollaseite-group minerals [2], fluorine substitutes for oxygen at the O4 site to maintain charge neutrality. The present mineral, however, is devoid of fluorine, suggesting that there could be additional $H^+$ in order to achieve charge balance. A possible $O\cdots O$ contact showing a suitable distance for a hydrogen bond could be O10-O2, as discussed by Gatta et al. [3] and Liebscher [4], and it has been speculated that some natural epidote minerals could host more than one $OH^-$ pfu [5]. In the studied mineral, however, it was possible to locate only one independent proton, with O10 as donor and O4 as acceptor. The presence of additional $H^+$ could explain some of the many peaks observed in the OH region of the FT-IR spectra. After the heating of the sample, the intensity of all peaks decreased, in agreement with the partial deprotonation of $OH^-$ occurring concurrently with $Fe^{2+}$ oxidation. The interpretation of the FT-IR data is not yet confident, but we suggest that the Malmkärra mineral contains a fraction (40%) of a yet undescribed end-member, the (OH)-analogue of dollaseite-(Ce), in solid solution with dissakisite-(Ce) (32%) and ferriallanite-(Ce) (28%).

*References:*

[1] Holtstam D et al. (2023) Min Mag 87: 731-737
[2] Armbruster T et al. (2006) Eur J Mineral 18: 551-567
[3] Gatta GD et al. (2012) Phys Chem Miner 39: 1-15
[4] Liebscher A (2004) Rev Mineral Geochem 56: 125-170
[5] Varlamov DA et al. (2019) Geol Ore Depos 61: 827-842

## Zoning in cassiterite: Sectors or twins?

Drivenes, K.[1], Sørensen, B.E.[2], Antao, S.[3], Brownscombe, W.[4], Debuhr[2], Seltmann, R[4], Spratt, J.[4], and Thomas, R[5]

[1]Geological Survey of Norway, Leiv Erikssons veg 37, 7491 Trondheim, Norway. Kristian.drivenes@ngu.no

[2]Dept of Geoscience and Petroleum, Norwegian University of Science and Technology, Trondheim, Norway

[3]Department of Geoscience, University of Calgary, Calgary, Canada

[4]Natural History Museum, London, United Kingdom

[5]Im Waldwinkel 8, D-14662 Friesack, Germany

---

Distinct zoning patterns in cassiterite from a quartz-tourmaline rock in SW England can clearly be observed in the optical microscope. They appear in (near-) basal sections and are reminiscent of sector zoning found in other minerals such as zircon, titanite and clinopyroxene. The model for sector zoning in minerals involves contrasting incorporation and diffusion rates of elements between different forms and faces in a crystal. Cassiterite in our samples differs from the well-known examples in that there is no systematic chemical difference between the apparent sectors. The chemical zoning of detected trace elements (Ti, Fe, W, Nb) is either oscillatory or patchy, commonly relating to the color observed in plane polarized transmitted light. In particular, W (up to 1 wt% $WO_3$) is correlated with dark brown color in transmitted light. The other main trace element, Ti, is typically concentrated in the core and is oscillatory zoned, and may be up to 2.4 wt% $TiO_2$. The cathodoluminescence intensity shows a weak inverse relationship with Ti, and a distinct inverse relationship with Nb.

EBSD analyses of the grains showed no variation in c-axis orientation across the “sectors”, and very minor misorientation throughout grains with the pronounced zoning. Two EBSD patterns taken from two different “sectors” could not be distinguished from each other. Misorientation within a grain relative to a randomly selected point was less than 3°, and can be correlated to fine CL-zoning. This minor variation in orientation may be due to local defect-induced lattice strain. Cassiterite commonly develops elbow twins by reflection around [011]. This is also observed in our samples, but is not the cause of the sectors, since the c-axis orientation does not vary.

The apparent sectors observed in the optical microscope represent the growth traces of the pyramidal {h0l} plane or the {h00} prism plane. The 4-fold symmetry around the c-axis in cassiterite (tetragonal, 4/mmm) indicates that pyramidal and prism faces are symmetrically equivalents. This does not conform with the distinct variation in interference color ($\Delta n \approx 0.05$) between the “sectors”. In addition a grain cut normal to the c-axis showed a biaxial optical axial figure with 2V of ca 10-15°. We speculate that the “sectors” may be produced by either of the following, both hypothesizing that the observed phenomenon is twinning:
The observed mineral is not tetragonal. Very minor difference between the lengths of *a* and *b*, or possibly *β*, making the mineral orthorhombic or monoclinic, respectively. The differences must be very small, since the confidence index of the indexed patterns using a tetragonal crystal structure was around 0.9. Alternatively, the unit cell is tetragonal, but the symmetry of the crystal is orthorhombic or monoclinic

Nanoscale phases of another $SnO_2$ phase included in the mineral induce strain in certain crystallographic directions.

# End-member Hunter: A computer algorithm for assigning proper end-member formulae to minerals from their empirical formulae

Haifler, J.

[1] Department of Geological Sciences, Masaryk University, Kotlářská 2, 611 37 Brno, Czech Republic; haifler.j@mail.muni.cz

---

The Commission on the New Minerals, Nomenclature and Classification of the International Mineralogical Association has provided instructions that should be followed when identifying a mineral species from an empirical formula of a mineral. However, straightforward application of the preferred dominant-valency rule, as originally defined [1], in some cases resulted in charge-imbalanced mineral formulae. Therefore, the revised approach [2] to the application of this rule was introduced, which addressed this issue. This approach includes a so-called site-total-charge (STC) method, by means of which a dominant root-charge arrangement (RCA) is recognized amongst a dominant set of related root-charge arrangements as an initial step. Subsequently, a dominant-constituent rule is applied to find a chemical formula with corresponding RCA involving dominant elements (or element pair) on each crystallographic site. In contrast, an alternative approach, the application of dominant end-member rule, has been advocated by some authors, e.g. [3]. Regardless of the method chosen, assigning an end-member formula to a complex mineral with many different chemical components at a crystallographic site can be difficult. Finding the correct solution may require considering many potential solutions.

This contribution introduces a computer algorithm End-Member Hunter (EMH), which is coded in MATLAB. The algorithm consists of 2 main functions. Using first of them, a database of all possible stoichiometric chemical formulae applicable for a given set of constraints (number of crystallographic sites, stoichiometric coefficients, chemical constituent and their valences) is developed. The second function is designed to match user's empirical mineral formulae with a chemical end-member formula in the database. The results are obtained using the IMA-CNMNC-approved extended dominant-valency rule [1, 2] and the non-approved dominant end-member rule [3] for comparison. The mineral compositions are input via a generated template editable in Microsoft Excel. The algorithm has been tested successfully using the examples from [2] or the type compositions of several tourmaline-supergroup minerals approved in the last decade (oxy-schorl, fluor-liddicoatite, lucchesiit, princivalleite, celleriite, uvite, darrellhenryite…). The algorithm is available on the author's academic web site: is.muni.cz/auth/www/haifler.j/.

*References:*

[1] Hatert F and Burke E (2008) Can Min 46:717-728
[2] Bosi F et al. (2019) Mineral Mag 83:627-632
[3] Hawthorne F (2023) Mineral Mag 87: 494-504

## Allanite-(Y) from the Åskagen, Sweden

Skřápková, L.[1], Cempírek, J.[1] and Škoda, R.[1]

[1]Department of Geological Sciences, Faculty of Science, Masaryk University, Kotlářská 2, 611 37 Brno, Czech Republic (email: lenkas@sci.muni.cz)

---

Allanite-(Y), ideally $CaYAl_2Fe^{2+}(SiO_4)(Si_2O_7)O(OH)$, is a valid species with the type locality in the Åskagen pegmatite, Värmland, Sweden [1]. However, no structural characterisation of the material from the type locality has been done yet. The mineral has not been formally approved by IMA-CNMNC and published up to date.

The mineral occurs as an accessory phase in the blocky zone of the NYF granitic pegmatite near Åskagen, Värmland, Sweden. Allanite-(Y) form rims around altered crystals of thalénite-(Y). Allanite-(Y) replaced primary thalénite-(Y) during an episode of early post-magmatic hydrothermal activity. Other associated minerals are iimoriite-(Y) and allanite-(Nd).

We characterised samples from the type locality using electron microprobe analysis, single-crystal X-ray diffraction, Raman spectroscopy, and Mössbauer spectroscopy. Allanite-(Y) forms euhedral crystals with size up to 1 mm, black with a vitreous lustre, conchoidal fracture and greyish brown streak. Allanite-(Y) has the Mohs hardness of ca. 6, the calculated density of 3.948 $g.cm^{-3}$ and is biaxial (−) with $\alpha = 1.760(3)$, $\beta = 1.799(2)$ and $\gamma = 1.784(3)$ at 589 nm light, pleochroism is weak pale yellowish brown.

Allanite-(Y) has monoclinic symmetry, with the space group $P2_1/m$, $a$ = 8.8520(8) Å, $b$ = 5.6959(5) Å, $c$ = 10.0543(9) Å, $\beta$ = 115.510(2)°, $V$ = 457.52(7) Å$^3$ and $Z$ = 2. The allanite-(Y) structure was refined to $R_1$ = 3.83 % using 2202 unique reflections collected with Mo$K\alpha$ X-ray source using the SHELXL-2013 program [2]. For the refinement we employed neutral scattering factors for cations and ionized scattering factors for oxygens [3]. Occupancies of A1-, A2-, M1- and M3- cation sites were refined as free variables. Occupancies of A(2) and M(1,3) sites were refined using two major elements located in the respective sites, i.e., Nd vs Ca with fixed Y at the A2 site, and Al vs Fe at the M1, M3 sites. The hydrogen atom was located in a difference Fourier map.

The formula of allanite-(Y) was calculated on the basis of M+T = 6 (apfu), the amount of OH was calculated by charge balance. $Fe^{3+}$ was determined from the structure with respect to the results of Mössbauer spectroscopy. During the structural refinement, all sites evinced full occupancies with the resulting formula:
$^{A1}(Ca_{0.920}Mn_{0.073}Na_{0.007})_{\Sigma 1.000}{}^{A2}(Y_{0.322}Ca_{0.239}Nd_{0.111}Sm_{0.100}Gd_{0.091}Dy_{0.046}Ce_{0.027}\square_{0.018}Pr_{0.012}Tb_{0.014}Er_{0.009}Ho_{0.005}Yb_{0.004}La_{0.002})_{\Sigma 1.000}{}^{M1}(Al_{0.916}Fe^{3+}{}_{0.080}Ti_{0.004})_{\Sigma 1.000}{}^{M2}(Al_{1.000})^{M3}(Fe^{2+}{}_{0.922}Al^{3+}{}_{0.052}Mg_{0.025})_{\Sigma 0.999}{}^{T1}(Si_{1.000})^{T2}(Si_{1.000})^{T3}(Si_{0.956}Al_{0.044})_{\Sigma 1.000}O_{11.856}[(OH)_{1.000}]$.

Allanite-(Y) belongs to the allanite group of the epidote supergroup. The closest end-member compositions of valid allanite group species are allanite-(Ce), allanite-(La) and allanite-(Nd) related via the simple substitutional mechanism Y ↔ REE.

References:
[1] Armbruster et al. (2006) Eur J Min 18:551-567
[2] Sheldrick G. M. (2015) Acta Crystalogr 71:3-8
[3] Hovestreydt E. (1983) Acta Crystalogr 39:268-269

# Applying Correlative Microscopy in Solar System Science

Daly, L.[1,2,3]

[1]School of Geographical and Earth Sciences, University of Glasgow, Glasgow, UK, luke.daly@glasgow.ac.uk.

[2]Department of Materials, University of Oxford, Oxford, UK

[3]Australian Centre for Microscopy and Microanalysis, University of Sydney, Sydney, Australia.

---

Meteorites and rocks returned from the surfaces of planetary bodies are treasure troves of information regarding Solar System formation and evolution. These samples are also the key to address fundamental questions in Planetary Science e.g.: How do you build a habitable planet? Microanalytical techniques are ideal tools to investigate these materials. However, traditionally, these techniques have been applied in isolation. This means that broad-scale surveys are blind to the fine details while high-resolution techniques miss the big picture context. It is now possible to combine techniques to provide complete characterisation of rocks and provide more robust interpretations of the processes that resulted in their formation using correlative microscopy.

Correlative microanalysis involves progressive measurements of the same sample volume using multiple complementary techniques [1,2]. An example pipeline could include using X-ray computed tomography to investigate cm-mm scale textures in 3D [3,4], electron microscopy techniques to examine µm-nm scale structures and geochemistry [5], secondary ion mass spectrometry for *in-situ* isotope measurements [6] and atom probe tomography to obtain atomic scale information [7] (Figure 1). Ideally correlative microanalysis uses a data driven approach to inform where and what further higher-resolution measurements and sub-sampling is required to address the research question.

In this presentation we describe the correlative microscopy approach and demonstrate how it has been used to investigate planetary materials and provide novel insights from asteroid Itokawa [8], the Winchcombe CM carbonaceous chondrite meteorite [9,10] and Martian Nakhlite meteorites [11,12].

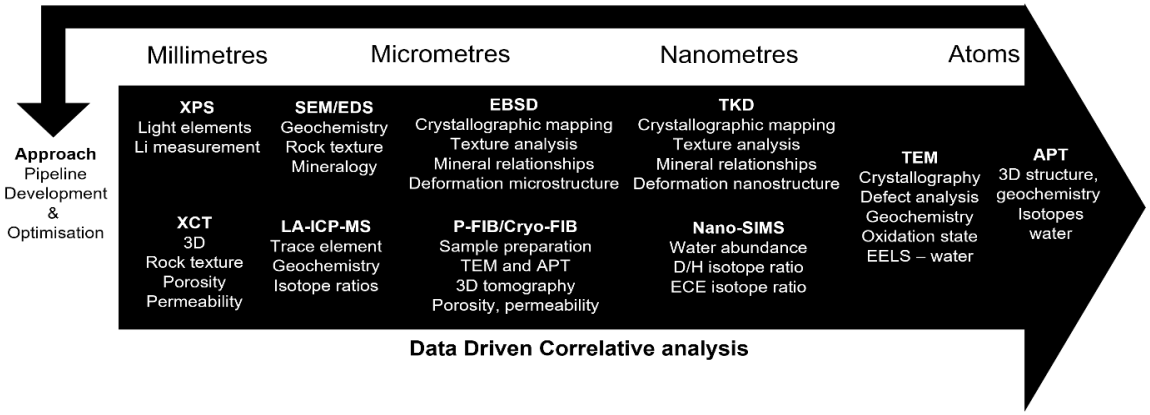


Figure 1. A data driven correlative microanalytical pipeline.

*Acknowledgements:* Science doesn't happen in a vacuum. I would like to thank all the wonderful researchers and citizen scientists I have collaborated with or interacted with over my career to date.

*References:* [1] Eswara S. et al. (2019) App. Phys. Rev. 6:021312; [2] Cognigni F. et al. (2023) J. Exp. Thero. Anal. 1(2):74-85; [3] Hanna R.D. & Ketcham R.A. (2017) Geochem. 77(4):547-572; [4] Martell J. et al., (2024) J. Geophys. Res. Planet. 129(2): e2023JE008222; [5] Lee M.R. (2010) Min. Mag. 74(1):1-27; [6] Hoppe P. (2002) New Astro. Rev. 46(8-10):589-595; [7] McCarroll I.E. et al., (2022) MRS Bull. 47(7):696-705; [8] Daly L. et al. (2021) Nat. Astro. 5(12):1275-1285; [9] King A.J. & Daly L. et al. (2022) Sci. Adv. 8(46):eabq3925; [10] Daly L. et al., (2024) Met. & Planet. Sci. in press.; [11] Daly L. et al., (2020) IOP Conf. Ser. 491(1):012008; [12] Martell J. et al. (2022) Sci. Adv. 8(19):eabn3044.

## 3D electron diffraction and nanotexture analysis of impactites.

Gemmi, M.[1], Parlanti, P.[1], Mugnaioli, E.[2], Campanale, F.[2,3] , Folco L.[2] and Veron M.[4]

[1]Electron Crystallography, Istituto Italiano di Tecnologia, Pontedera, Italy. mauro.gemmi@iit.it

[2]Dipartimento di Scienze della Terra, Università di Pisa, Pisa, Italy.

[3]Dipartimento di Scienze dell'Ambiente e Della Terra, Università degli Studi di Milano-Bicocca, Milan, Italy

[4] Université Grenoble Alpes, CNRS, Grenoble INP, SIMaP, F-38000 Grenoble, France.

---

We present a synergic study using 3D electron diffraction (3D ED) [1] and nanotexture analysis in a TEM to characterize small impact ejecta (usually spherulites of few hundred microns) with the aim to identify new mineralogical phases and to understand their formation mechanism/conditions. The method of analysis consists of: a FIB thin section preparation on an area of interests determined by SEM imaging and EDS analysis; identification of the crystal structures of the main phases through 3D ED, a single crystal diffraction technique on nanometric grains; texture and phase analysis using a scanning diffraction method known as PACOM (Precession Assisted Crystal Orientation Mapping) [2]. We applied this methodology to two sets of samples: impactite ejecta belonging to the Australasian tektite/microtektite strewn field and Fe-Ni oxide spherules generated by the impactor which created the Kamil crater (Egypt).

In the case of the Australasian ejecta 3D ED allowed the identification and structure solution of the $TIO_2$-II high pressure polymorph, which resulted to be a Zr-free srilankite endmember. The texture analysis indicates that $TiO_2$-II is usually surrounded by well-ordered rutile grains which retains a topotactic relation with the embedded $TiO_2$-II suggesting a partial transformation due to P-T wave during the impact.

In the case of the spherulites from Kamil crater it has been possible to depict a complex scenario in which a matrix of Fe-Ni oxides grains showing fine exsolutions of two different phases is permeated in the interstitial volume by a Si rich fluid which, in most of the cases, is amorphous. PACOM and HREM imaging revealed that the two exsolved Fe-Ni oxide phases have a trevorite (the Fe-rich component) and a bunsenite (the Ni-rich component) structure and that inside each micrometric grain they are coherent. The amorphous interstitial part usually separates into two components: $SiO_x$ amorphous droplets and a silicic component rich in Fe and P. This second component has been found both in an amorphous and in a crystalline form. When crystalline 3D ED identified it as olivine with a P content as high as 3%-4%at. The full crystallochemical characterization at the nanoscale depicts a formation model in which the Ni-Fe-P melt from the meteorite oxidizes and mixes with the melted quartzite from the target. The oxidized Fe Ni crystallizes in Fe-Ni oxides micrometric grains which, upon cooling, exsolve the two abovementioned phases. The remaining Fe with all the P enriches the silicic melt, which forms a glass that fills the interstitial void.

The combination of 3D ED with PACOM allows at the same time the discovery of new crystal phases present in micrometric planetary materials and to obtain a global crystallochemical view, which is essential for understanding the thermal history and for building a formation model of the retrieved sample. We envisage a crucial application of this methodology to any kind of planetary material coming from sample return missions.

*References:*

[1] Gemmi M et al. (2019) ACS Cent. Sci. 5:1315-1329.

[2] Viladot D. et al. (2013) Journal of Microscopy 252:23-34.

[3] Campanale F et al. (2024) Meteoritics & Planetary Science 59: 529-543.

## The functional chemistry of Ryugu organic matter investigated by high spatial resolution electron energy loss spectroscopy

Vollmer, C.[1], Lier, J.[1], Kepaptsoglou, D.[2], Mosberg, A. B.[2], and Ramasse Q. M.[2]

[1]Institut für Mineralogie, Universität Münster, cvoll_01@uni-muenster.de

[2]SuperSTEM Laboratory, Keckwick Lane, Daresbury, UK

---

The functional chemistry and molecular constitution of extraterrestrial organic matter (OM) is one of the major science goals of the Hayabusa 2 mission to asteroid Ryugu [e.g., 1]. OM is a complex material occurring in a wide range of extraterrestrial samples such as carbonaceous chondrites. Its morphological and chemical diversity is the result of processes in circumstellar and interstellar environments or the early solar nebula, as well as fluid-induced reactions on asteroids. Ryugu OM is of paramount importance in this respect, because in contrast to meteorites found on Earth, terrestrial alteration of Ryugu OM is virtually absent. Abundances of gypsum or ferrihydrite, typical minerals within aqueously altered chondrites, are extremely low [1]. Previous investigations on minimally processed Ryugu OM by high-spatial resolution techniques such as synchrotron-radiation spectroscopy or electron microscopy have shown that it consists of similar organic materials as found in other primitive meteorites [e.g., 2], but some observations demonstrate the heterogeneous nature of the OM. For example, aliphatic bonding dominates some regions of Ryugu OM [3], while other work has shown the presence of organic vesicles inside or around mineral grains or the presence of irregular “vermicular” OM [2]. This underlines the highly complex nature and diversity of Ryugu samples on a sub-µm scale and the need for further high spatial resolution work.

In this work, we investigated polished sections as well as pristine particles pressed into indium foils of Ryugu samples from both A and C chambers sampled at two different collection sites by electron energy loss spectroscopy (EELS) in a dedicated scanning transmission electron microscope (STEM). A Hitachi Ethos NX5000 Focused Ion Beam (FIB) instrument equipped with a low-energy argon polisher was used to create ultra-thin lamellae with minimal damage. We targeted OM-rich regions of interest on the surfaces of samples, but we also thinned OM located within the lamellae in deeper areas that were not exposed to air prior to lift-out. Ryugu OM was then analyzed on a Nion UltraSTEM100MC-HERMES at SuperSTEM, operated at 60 kV for low-dose conditions to reduce beam damage on carbon-based materials. The microscope is equipped with a unique monochromator design for high energy resolution (<< 0.1 eV) and a Nion IRIS spectrometer with an ultra-low noise Dectris ELA direct-electron detector, specifically optimized for EELS [4]. We investigated OM elemental abundances, fine-scale textures, and the energy loss near-edge structure (ELNES) at the carbon and nitrogen K-edges and the vibrational low-loss regime. OM occurs as large irregular or globular grains, but mainly as diffuse regions in association with ubiquitous magnetites and phyllosilicates that show distinct functional chemistry on a nm scale. Further results will be presented at the meeting.

*References:*

[1] Nakamura T et al. (2022) Science 10.1126/science.abn8671
[2] Yabuta H et al. (2023) Science 379, eabn9057
[3] Ito M et al. (2022) Nat Astron 6, 1163
[4] Vollmer C et al. (2024) Nat Comm 15, 778

# Rare-earth element distribution in particles from asteroid Bennu measured by high-energy synchrotron X-ray fluorescence.

Tkalcec, B.[1], DePauw, E.[2], Bazi, B.[2], Vekemans, B.[2], Tack, P.[2], Baert, T.[2], Herthogs, J.[2], Vincze, L.[2], Falkenberg, G.[3], Garrevoet, J.[3], Di Michiel, M.[4], Burghammer, M.[4], Connolly Jr., H. C.[5,6,7], Lauretta, D. S.[6], and Brenker, F. E.[1]

[1]Goethe University, Dept. of Geoscience, 60438 Frankfurt am Main, Germany. *tkalcec@em.uni-frankfurt.de.

[2]Ghent University, Dept. of Chemistry, 9000 Ghent, Belgium.

[3]Deutsches Elektronen-Synchrotron DESY, 22607 Hamburg, Germany.

[4]ESRF - The European Synchrotron Radiation Facility, 38000 Grenoble, France.

[5]Department of Geology, Rowan University, Glassboro, NJ, USA.

[6]Lunar and Planetary Laboratory, University of Arizona, Tucson, AZ, USA.

[7]Department of Earth and Planetary Science, American Museum of Natural History, New York, NY, USA.

---

*Introduction:* The distribution and enrichment of rare-earth elements (REEs) in extraterrestrial materials can provide valuable insight into the process of aqueous alteration on their parent body and, thus, the presence and behaviour of fluids in the early Solar System. Here we present the first high-energy synchrotron X-ray fluorescence (SXRF) analyses of rock samples collected from the surface region of the hydrated, carbonaceous asteroid (101955) Bennu by NASA's OSIRIS-REx mission [1]. This study focuses on the REE concentrations of Ca-phosphates in the Bennu sample [2] because such material, e.g., apatite, can contain abundant REE-bearing phases in extraterrestrial material [3].

*Methods:* Three Bennu rock fragments (from OREX-800045-101), 350–500 µm in size, were analysed by SXRF at the European Synchrotron Radiation Facility (ESRF) in Grenoble, France [4], and the Deutsches Elektronen-Synchrotron (DESY, PETRA III) in Hamburg, Germany [5]. SXRF excitation energies of 21 keV (beamline P06 at DESY) and 90 keV (beamline ID15A at ESRF), applied with beam spot sizes of ~1 µm and ~500 nm, respectively, enabled (trace-)elemental information to be obtained from a wide range of elements (from Si to Pb, $14 \leq Z \leq 82$), including REEs. In addition to conventional 2D SXRF scans, 3D depth-resolved information was obtained by XRF computed tomography (XRF-CT) and absorption CT, rotating the sample over 360°. Finally, SXR diffraction (SXRD), performed at beamline ID13 (ESRF), was applied to confirm the identity of the Ca-phosphate phases.

*Results:* Our qualitative SXRF data reveal a relatively high abundance and strongly heterogeneous distribution of Ca-phosphates in the Bennu rock fragments. Quantified SXRF measurements of the Ca-phosphates reveal REE concentrations up to 500 times greater than mean chondritic CI levels [6], which is slightly higher than those reported for Ca-phosphates in asteroid Ryugu [3,7] and may indicate a greater degree of aqueous processing on Bennu.

*Acknowledgments:* This material is based upon work supported by NASA under Contract NNM10AA11C issued through the New Frontiers Program. We are grateful to the entire OSIRIS-REx Team for making the return of samples from Bennu possible. We acknowledge ESRF for provision of synchrotron radiation facilities with beamtime allocated for proposal ES-1018. We acknowledge DESY (Hamburg, Germany), a member of the Helmholtz Association HGF, for the provision of experimental facilities with beamtime allocated for proposal II-20230010 EC. Funding by the German Science Foundation – DFG (Grant BR 2015/37-1) is greatly acknowledged.

*References:*

[1] Lauretta, D. S. et al. (2022) Science, 377:285–291; [2] Barnes et al. (2024) 55th LPSC, Abstract #1532; [3] Tkalcec et al. (2024) MaPS, under review; [4] Boesenberg, U. et al. (2016) J. Synchrotron Radiat., 23(6):1550–1560; [5] Vaughan, G. B. M. et al. (2020) J. Synchrotron Radiat., 27:515–528; [6] Lodders, K. et al. (2021) Space Sci. Rev., 217:44-77; [7] Tack et al. (2022) EPS, 74:146.

# Water/rock interaction within primitive asteroids explored using the Solar System's oldest calcite, aragonite, and dolomite

Lee, M.R.[1], Griffin, S.[1]

[1]School of Geographical and Earth Sciences, University of Glasgow. Martin.Lee@Glasgow.ac.uk

The Mighei-like (CM) carbonaceous chondrites are fragments of water- and organic matter-rich C-complex asteroids, and those CM meteorites that fell to Earth early in its history may have been an important source of compounds that were essential for the origins of life [1]. The CM chondrites are rich in serpentine, which is commonly intergrown with a few volume per cent of carbonates (aragonite, calcite, dolomite). These minerals formed ~4563 million years ago (approximately 5 million years after the birth of the Solar System) accompanying radiogenic heating of asteroid interiors and concomitant melting of water-rich ices [2]. Here we explore the insights that carbonates provide into the mechanisms by which aqueous fluids interacted with asteroids, which ultimately determined how much water they could have delivered to the primordial Earth.

Our recent work using triple oxygen isotope analysis and clumped isotope thermometry has shown that dolomite in CM chondrites precipitated after coexisting calcite and at higher temperatures (~75-101 °C vs ~5-51 °C, respectively) [3]. Thus, the carbonates formed in a prograde system, with the calcite to dolomite transition likely being thermally controlled. Here we focus on understanding the relative timing and conditions of formation of aragonite and calcite using the Winchcombe CM chondrite, which fell in Gloucestershire on 28$^{th}$ February 2021 [4]. We used a 9.2 mm$^2$ size polished block (P30555) loaned by the Natural History Museum, London. All work was undertaken in the University of Glasgow GEMS facility. P30555 was initially imaged using a Zeiss Sigma field-emission Scanning Electron Microscope (SEM), then the mineralogy and microstructure of aragonite and calcite grains were characterised using an Oxford Instruments Symmetry Electron Backscatter Diffraction (EBSD) system attached to the Zeiss SEM.

The Winchcombe sample contains tens of micrometre size grains of aragonite and calcite, but no dolomite. The Ca-carbonate grains are monomineralic or bimineralic with the latter dominated by calcite. Most aragonite grains are polycrystalline, often with mild internal deformation, and are commonly twinned. Calcite grains are typically single crystals with lower deformation than the aragonite, and some are also twinned. Petrographic relationships in the bimineralic grains are ambiguous but suggest that calcite has replaced aragonite. This paragenesis would be consistent with the greater deformation of aragonite than calcite reflecting the impact of a meteorite into Winchcombe's parent asteroid between crystallization of the two minerals. The occurrence of unaltered aragonite grains within a few micrometres of pristine calcite grains can be explained by Winchcombe's parent asteroid having a very low intergranular permeability, and/or liquid water being present for only very short periods of time.

This work was funded by the UK Science and Technology Facilities Council via grant ST/W001128/1.

*References:*

[1] Alexander CMO'D. (2017) Phil. Trans. R. Soc. A 375, 20150384.
[2] Fujiya W et al. (2012) Nature Communications 3, 627.
[3] Clog M et al. (2024) Geochimica et Cosmochimica Acta, 369, pp. 1-16.
[4] King AJ and Daly L et al. (2022) Science Advances 8: eabq3925.

# Expanded Insights into Martian Mineralogy: Updated Analysis of Gale Crater's Mineral Composition via CheMin Crystal Chemical Investigations

Morrison, S.M.,[1] Downs, R.T.,[2] Bristow, T.F.,[3] Rampe, E.B.,[4] Blake, D.F.,[3] Vaniman, D.T.,[5] Achilles, C.N.,[6] Hazen, R.,[1] Eleish, A.[1] Prabhu, A.,[1] Ming, D.W.[4] Yen, A.S. [7] Treiman, A.H.[8], Morris, R.V.[4], Chipera, S.J.[10], Craig, P.I.[8], Tu,V.M.[4], Meusburger, J.M.[3] , Castle, N.[8], Sarrazin,P.C.[10] and Des Marais, D.J.[3]

[1]Earth and Planets Laboratory, Carnegie Institution for Science, 5241 Broad Branch Rd NW, Washington, DC 20015 USA; *smorrison@carnegiescience.edu

[2]University Of Arizona, Tucson, AZ

[3]NASA Ames Research Center, Moffett Field, CA

[4]NASA Johnson Space Center, Houston, TX

[5]Planetary Science Institute, Tucson, AZ

[6]NASA Goddard Space Flight Center, Greenbelt, MD

[7]Jet Propulsion Laboratory, Caltech, Pasadena, CA

[8]Lunar and Planetary Institute - USRA, Houston, TX

[9]Chesapeake Energy Corporation, Oklahoma City, OK

[10]SETI Institute, Mountain View, CA

---

This study presents mineral composition estimates of rock and sediment samples analyzed with the CheMin X-ray diffraction instrument onboard the NASA Mars Science Laboratory rover, Curiosity, in Gale Crater, Mars [1]. This study examines all samples analyzed by CheMin from the beginning of the mission until March 2024, with 40 distinct geologic and petrologic sites sampled, representing a large swath of the Gale crater stratigraphy. These samples are fluviolacustrine and aeolian in nature and include both drilled rock and loose sediment samples. Samples are analyzed with the CheMin instrument in order to identify the mineral phases, their abundance, and to refine their unit-cell parameters via Reitveld refinement [2]. To gain a greater understanding of the formational conditions and geologic history of Gale crater and the minerals found therein, the CheMin team developed crystal-chemical algorithms to estimate mineral composition based on the unit-cell parameters derived from the CheMin XRD patterns [1,3,4]. The mineral groups characterized include those found in major abundance by the CheMin instrument (i.e., feldspar, olivine, pyroxene, and spinel oxide.) In addition to estimating the composition of the major mineral phases observed in Gale crater, we place their compositions in stratigraphic context within Gale crater as well as provide a comparison to that of martian meteorites. This work is expanding our understanding of Gale crater, Mars, and the processes that formed the terrestrial bodies in our solar system.

**References**:

[1] Morrison et al. (2024) Minerals (Submitted)

[2] Blake et al. (2013) Science, 27, 341, 1239505

[3] Morrison et al. (2017) Am Min, 103(6): 848-856

[4] Morrison et al. (2017) Am Min, 103(6): 857-871

# Micro-mineralogical characterization of two Ryugu particles by advanced FIB-SEM, TEM and electron diffraction

Borriello, R.[1-2]*, Ferrari, M.[3], Folco, L.[2], Mugnaioli, E.[2] and Masotta, M.[2]

[1]Department of Environmental Sciences, Informatics and Statistics, Ca' Foscari University of Venice, Via Torino 155, 30172 Mestre (VE), Italy

[2]Department of Earth Sciences, University of Pisa, Via S. Maria 53, 56126 Pisa, Italy

[3]INAF-IAPS, Via del Fosso del Cavaliere 100, 00133 Rome, Italy

*Corresponding author: roberto.borriello@unive.it

---

Volatile-rich C-type asteroids are planetary bodies with primitive composition that are thought to represent the parent-bodies of carbonaceous chondrites [1], which in turn are the probable source of the volatile species delivered to the Earth during its accretion history [2]. The C-type asteroid (162173) Ryugu has been recently sampled by the JAXA/Hayabusa2 mission [3], providing samples of inestimable scientific value. However, given the rubble-pile nature of the asteroid, these samples are often fragile, porous and made of a heterogeneous material consisting of micrometric to nanometric minerals and amorphous phases. These features represent an analytical challenge that requires innovative instrumentation and techniques. In this work, we show the application of different techniques involving scanning electron microscope (SEM), focused ion beam (FIB) and transmission electron microscope (TEM) to two grains (A0198 and C0091) in order to achieve a petrographic and mineralogical characterization of the asteroid Ryugu and expand to our comprehension about planetary phenomena that affect the C-type asteroids.

SEM images show textures that suggest aqueous alteration and different cycles of hydration-dehydration, e.g. fibrous phases, phyllosilicate flakes, sulfide dissolution, veining, framboidal magnetite and structures similar to mud cracks. More in-depth TEM observations, obtained crossing chemical analyses by energy-dispersive X-ray spectroscopy (EDS) and structural analyses by three-dimensional electron diffraction (3DED) [4], show amorphous carbonaceous matter, Fe-Mg silicates (both anhydrous and hydrate, e.g. olivine and phyllosilicates), Fe-oxides (magnetite and/or maghemite), Fe-sulfides (pyrrhotite and a single grain of troilite), pentlandite, Zn-sulfide (possibly wurtzite), Cr-oxide (possibly eskolaite), manganochromite, Mn-bearing dolomite, apatite, Ca-Na-Mg-phosphates (possibly merrillite), unidentified Fe-Ni-phosphides and a fibrous Fe-S-O phase (possibly tochilinite).

This research highlighted the analytical potential of using sophisticated techniques to analyse challenging samples of scientific value and the importance of developing innovative analytical protocols from the sample preparation to the data collection and processing.

*References:*

[1] Johnson T V and Fanale F P (1973) J Geophys Res 78: 8507-8518

[2] Marty B (2012) Earth Planet Sci Lett 313–314: 56–66

[3] Watanabe S et al. (2019) Science 364: 268-272

[4] Gemmi M et al. (2019) ACS Cet Sci 5: 1315-1329

## Relict of an unknown process in the pre planetary nebula? Petrological & geochemical analysis of Inver-zoned Chondrules

Joseph, F.[1], Drozdovsky, I.[2], Junge, M.[1,3], Brau, J.[1], Kaliwoda, M.[1,3]

[1]Department of Earth and Environmental Sciences, Ludwig-Maximilians-Universität München, Theressienstrasse 41, D-80333 Munich, Germany

[2]Directorate of Human and Robotics Exploration, European Astronaut Center (EAC) – European Space Agency (ESA)

[3]Mineralogical State Collection Munich, (SNSB), Theressienstrasse 41, D-80333 Munich, Germany.

---

Chondrules are some of the oldest objects in our Solar System [1]. As such, they play an important role as messengers, providing new insights into the early processes of the Solar System and potentially understanding its formation. It is, therefore, crucial to study all detailed structures, especially those that are not well known, such as inverse-zoned chondrules (IZ Chondrules). In this work, we describe the chemical and structural composition of inverse-zoned chondrules using optical microscopy, EDX, BSE and Raman spectroscopy, revealing a new process in the early solar system [2]. IZ chondrules consist of an Mg-rich pyroxene core surrounded by a Fe-rich olivine rim. The olivines have a higher Fe content (Fa 39 - 41%) than those found in other chondrules. The core has a radially striated pyroxene chondrule with sometimes Mg-rich olivines (Fa34). These silicate spherules may have formed in the early stages of our solar system and do not show the typical constant cooling observed in chondrules [2]. The pyroxene core is most likely formed by rapid cooling of the early protoplanetary disk (500-2500 K/h) [3], which is later reheated to about 1600-1800 K to form the olivine shell [2].

*References:*

[1] Scott, A. E. (2003) *Chondrites and their components, Treatise on geochemistry, 1, 711.*

[2] Joseph, F. et al. (Submitted at 2023) Petrological and Geochemical Analysis of Inverse-zoned Chondrules, Meteoritics & Planetary Science.

[3] Libourel, G. and Portail, M. (2018) *Chondrules as direct thermochemical sensors of solar protoplanetary disk gas, Science advances, 4(7), eaar3321.*

# The microstructure of dolomite from asteroid Ryugu characterised by transmission electron microscopy and transmission Kikuchi diffraction

Lee, M.R.[1], Griffin, S.[1], Daly, L.[1], Fujiya, W.[2]

[1]School of Geographical and Earth Sciences, University of Glasgow. Martin.Lee@Glasgow.ac.uk

[2]Faculty of Science, Ibaraki University, 2-1-1 Bunkyo, Mito, Ibaraki 310-8512, Japan

---

In December 2020 the Japan Aerospace Exploration Agency (JAXA) Hayabusa2 spacecraft returned ~5.4 g of material from the near-Earth C-complex asteroid 162173 Ryugu [1]. Samples are fine-grained and rich in phyllosilicates (saponite, serpentine), with subordinate carbonates (calcite, dolomite, breunnerite), sulphides, and oxides. These minerals formed by aqueous alteration of their parent asteroid in response to radiogenic heating and concomitant melting of water-rich ices [2]. The timescale of water/rock interaction can be determined by $^{53}Mn$–$^{53}Cr$ dating of carbonate minerals, and initial results [3] suggest that Ryugu carbonates are older than in the CM group of aqueously altered carbonaceous chondrites [4]. As part of continuing work on chronologies of water/rock interaction, we have characterised the microstructure of dolomite in two polished blocks of Ryugu loaned by JAXA.

Ryugu dolomite is typically Mn- and Fe-rich, with a composition of $Ca_{46}Mg_{45}Fe_4Mn_6$ being obtained from grains in sample A0058 [5]. The carbon and oxygen isotopic compositions of carbonates in samples A0058 and C0002 show that calcite formed first during prograde alteration, with dolomite crystallizing later as the asteroid cooled [5]. We studied dolomite grains in Ryugu samples A0203 and C0022. They were first characterised by SEM and X-ray mapping, then ~100 nm thick wafers were extracted from selected grains using a FEI Helios xenon plasma Focused Ion beam (FIB) microscope. Bright-field images and selected area electron diffraction (SAED) patterns were acquired from the wafers using a FEI T20 transmission electron microscope (TEM). The wafers were then loaded into a pre-tilted holder and characterised using a Zeiss Sigma scanning electron microscope equipped with an Oxford Instruments 150 $mm^2$ energy dispersive X-ray spectroscopy detector and Symmetry electron backscatter diffraction (EBSD) system that was used for Transmission Kikuchi Diffraction (TKD).

TKD is very effective for characterising FIB-produced wafers of the Ryugu dolomite, and results are complementary to TEM/SAED. The TKD technique enables rapid mapping of minerals and their microstructures by automated indexing of the Kikuchi patterns, which can be combined with simultaneously collected EDS data. Samples A0203 and C0022 contain dolomite, magnetite, and phyllosilicates. The dolomite and magnetite could be readily characterised by both TEM/SAED and TKD, but the phyllosilicates did not generate Kikuchi patterns that could be indexed. Dolomite grains in A0203 are polycrystalline aggregates whose constituent crystals are subhedral and ~0.8–2 μm in size. TKD shows that most crystals are minimally internally deformed but can contain subgrains. C0022 dolomite grains are larger, up to ~9 μm, and also contain subgrains. The TEM and TKD results are consistent with dolomite grains growing in a porous matrix and having experienced minimal subsequent deformation.

This work was funded by the UK Science and Technology Facilities Council via grant ST/W001128/1.

*References:*

[1] Tachibana S et al. (2022) Science 375,1011-1016.
[2] Nakamura T et al. (2023) Science 379, eabn8671.
[3] McCain KA et al. (2023) Nature Astronomy 7, 309–317.
[4] Fujiya W et al. (2012) Nature Communications 3, 627.
[5] Fujiya W et al. (2023) Nature Geoscience 16, 675–682.

# Transmission electron microscopy of the fine-grained matrix in the observed meteorite fall Winchcombe

Lier J.[1], Vollmer C.[1], Risthaus L.[1], Kepaptsoglou D.[2], Ramasse Q. M.[2], Mosberg A. B.[2], El Hajraoui K.[2], Bays C. L.[3,4], Schofield P. F.[3], King A. J.[3]

[1]Institut für Mineralogie, Universität Münster, jlier@uni-muenster.de

[2]SuperSTEM Laboratory, Keckwick Lane, Daresbury, UK

[3]Planetary Materials Group, Natural History Museum, London, SW7 5BD, UK

[4]Royal Holloway University of London, Egham, UK

---

Samples of observed meteorite falls provide important constraints about the formation of the solar system and the alteration history of these primitive materials. They can also be compared to asteroid samples from the Hayabusa2 and OSIRIS-REx missions. The Mighei-type (CM) carbonaceous chondrites are breccias and so, contain a wide range of materials with different formation histories. These meteorites record the compositions of the earliest solids in the protoplanetary disk and the transformational history of the parent body [1]. The Winchcombe meteorite fell in the UK on 28$^{th}$ February 2021 and was classified as a CM2 chondrite [2]. The fall was observed by >1000 eyewitnesses and captured by the UK Fireball Alliance, who subsequently recovered the first material in under 12 hours. Due to its rapid collection, terrestrial alteration in Winchcombe was minimal [3]. The petrographic study of the meteorite revealed eight different lithologies and variable aqueous alteration extents from advanced (CM2.0–2.3) to mildly altered (CM2.6).

In this work, the petrography and mineralogy of Winchcombe was analysed by transmission electron microscopy (TEM) on three lamellae which originate from the matrix and lithology H [2], extracted using the focused ion beam (FIB) technique. High-angle annular darkfield (HAADF) and brightfield (BF) imaging as well as energy-dispersive X-ray spectroscopy (EDXS) and high-resolution TEM were applied using the ThermoFisher Scientific “Themis” TEM at the University of Münster. Our results confirm earlier studies demonstrating that the fine-grained matrix of Winchcombe is dominated by Mg-Fe-rich phyllosilicates of the serpentine group and tochilinite-cronstedtite intergrowths (TCIs) with variable alteration degrees. However, we also located primitive areas in investigated lamellae such as homogeneous amorphous silicates and GEMS-like particles (glass with embedded metal and sulphides), which can be regarded as the building blocks of an ideal CM 3.0 matrix [4]. One distinct GEMS-like domain shows rimmed Fe-rich metal and sulphide grains in a Mg-rich amorphous groundmass embedded in primitive organic matter, which likely shielded it from more severe alteration. Furthermore, Fe-Ni-sulphides such as pentlandite are mainly concentrated in the lamellae of the matrix. In addition to the sub-µm scale brecciated texture, the three lamellae show different alteration extents, further demonstrating the complex nature of this CM2 meteorite.

*References:*

[1] Suttle et al. (2021) Geochimica et Cosmochimica Acta 299: 219–256
[2] King et al. (2022) Sci. Adv. 8, eabq3925: 1-17
[3] Suttle et al. (2022) Meteoritics & Planetary Science: 1-25
[4] Leroux et al. (2015) Geochimica et Cosmochimica Acta 170: 247–265

# More than cool curiosities: using social media for mineral science communication to engage on geoscience topics

Anderson, E.B.[1,2]

[1]The Hunterian, University of Glasgow, Glasgow, G12 8QQ

[2]Royal Ontario Museum, 100 Queen's Park, Toronto, ON, Canada M5S 2C6

---

Minerals and the crystals they form have captured the interest of the public due to their visually appealing qualities, but the science behind them is less widely known. Using social media to do mineral science communication as well as geoscience communication allows scientists [1] and enthusiasts to relay knowledge in a digestible form to the public. This format of science communication is easily accessible to public audiences as well as widely available and easy to learn to those wishing to apply it themselves. It is an opportunity to take advantage of a medium that many of the public already engage in, in one form or another [2].

Geoscience facts can be relatively unknown to the public, yet that can mean there is ample opportunity to leverage social media to promote the discipline. Minerals, rocks, gems, and meteorites make great aesthetic visuals for use in social media posts and can be an anchor for a post to base scientific information around. Posts can include information on scientific work outside of geoscience facts alone, encompassing topics such as field work, laboratory and analytical work, or museum collections work.

Science communication in the form of social media can also weave in vital topics in the geosciences such as diversity in science, decolonization, and geoethics. These topics are important to share with the public as they offer a holistic view of the discipline as well as push beyond scientific discoveries. Not only can one communicate engaging scientific facts, one can expound upon the impact of the geosciences on society throughout history, as well as in the present and future [3]. Short form social media posts can convey a snapshot view of these far-reaching topics in a digestible manner to the public as well as engage fellow scientists on the broader impacts of the field.

Social media takes many forms, such as X (formerly Twitter), Facebook, Instagram, Mastodon, Bluesky, and YouTube, each with their own formats with different combinations of text, pictures, and videos. There are general best practices and tips, such as the use of alt text and hashtags [4], that can be applicable to multiple of these platforms to make posts more accessible and engaging. Text, photos, and videos are a common way to distribute science information but there can be further engagement through audience participation in quizzes and polls. Posts can be tailored to the specific audiences, like fellow scientists, mineral enthusiasts, or the broader public, in order to have the desired reach and impact.

*References:*

[1] Collins K et al. (2016) PLOS One 11: 1-10
[2] Boulianne S (2015) Information, Communication & Society 18: 524-538
[3] Bohle M. (2015) Geological Society London, Special Publications 419.1: 5-12
[4] Improving the Accessibility of Social Media in the Government (accessed March 26 2024) https://digital.gov/resources/improving-the-accessibility-of-social-media-in-government/

# Geo-education in Colombia enhanced by student chapters

Cramer, T.H.[1], Bonilla-Perez, A.[2] and Sanchez Novoa, D.F.C.[1]

[1]Universidad Nacional de Colombia, Bogotá, thcramer@unal.edu.co.

[2]Servicio geológico Colombiano, Bogota, Colombia

---

Colombia is a geologically very diverse country between the Atlantic (Caribbean) and Pacific Ocean, composed to the East by up-to 1.85 Ga felsic rocks as part of the Amazonian Craton, which constitutes the largest areas of this tropical country, but nearly without habitants. To the West, accretionary and subducting Pacific oceanic crust plates continue triggering the three main Andean Cordillera chains partially elevating >5000 m asl, expressing in volcanic, Earth-shakes and geomorphological features shaped at the surface by glacial to tropical humid clime-zones, causing additional geo-risks like landslides, inundations and desertification (not only) in this mountainous region where most of the 48 million habitants are living often in fast growing metropoles like Bogota. Various mineral deposits like gold, and locally emeralds, nickel, salt or construction materials besides carbon and petroleum are important sources of income and divisas, but are also increasingly admitted as threat to one of the biologically most diverse and richest regions of the World.

In spite of this wealth, challenges and risks, the knowledge about geological and mineralogical features is not widespread in society, which together with still high grades of informality give bases to speculation and erroneous views in public opinion and politics, also hampering knowledge-based decision making. On the other hand, increasing access of young people to schools and universities as well as high wages for geologists since 2000, when exploration geologists were searched desperately, induced also an increase in Earth-science students and programs at various traditional and new universities, with the negative side effect of actually unemployment rates of ~50% among geologists.

In this context, geo-sites, geoparks, geoarchaeology, geo-conservation, geo-education as well as environment protection are becoming increasingly popular among students, professionals and society in general, including important institutions like the Colombian Geological Survey (SGC). At the same time, not only research groups like our (GEGEMA https://sites.google.com/unal.edu.co/coleccionmineralunalbog-gegema) but also student groups and national chapters of international association like the SEG, EAAG or SGA (Society for Geology Applied to Mineral Deposits) in our case developed and proofed to be an important tool in connecting with society in general, schools, municipalities, mining communities, print media directly and often also using social reds like Facebook, Instagram and so on for teaching and learning mutually.

We present examples of work and capacitations mostly in the context of field trips to far-away zones like Choco, Amazonas and Orinoco regions, where we researched on mineral occurrences like coltan, cassiterite, wolframite, REE- and Li-bearing minerals, or PGE and nearly always gold. But also in big cities like Bogota and surroundings, Villa de Leyva or mining sites like Marmato, an emblematic gold producing zone in W-Colombia with a huge informal but traditional mining community where our students organized workshops with local people from children to their parents and administrative staff of the local environment protection offices. These activities are often transmitted or reported by local press and TV. It is interesting to see how due to private initiative a Mining Museum is built up as an expression of the efforts to not forget the significant mining history of many places, often with a pre-Columbian mining tradition.

# Crystal magic – Fascinating tourmaline crystals with fantastic inner worlds 20 years of optimization of a successful traveling exhibition

Rustemeyer, P.

Waldackerweg 10, 79194 Gundelfingen, Germany, Rustemeyer-gundelfingen@t-online.de

In thin sections (perpendicular to the c-axis) of dark tourmaline crystals, multicolored, detailed color zones and diverse patterns are common - often with an astonishingly aesthetic visual effect. Using more than 30,000 cuts, the “imagery” of the tourmaline discs has been largely deciphered and, in many cases, a relationship has been established with external morphological phenomena of tourmaline crystals. Many of the images in the tourmaline slices arise from a superposition of sector zoning, concentric growth zoning, delta features as a second color domain within a sector, splitting patterns according to different splitting principles, and healing patterns after fracture or corrosion events. If individual tourmaline crystals are cut into sets of slices, their often very complex three-dimensional architecture can be recognized and studied. The scientific and aesthetic results of this private research activity have been published in books and articles [1, 2, 3, 4].

In addition, the author designed the traveling exhibition “Crystal Magic – Fascinating Crystals with Fantastic Inner Worlds”, which has been a guest in 24 natural history museums since 2007. “Crystal Magic” combines artistic, aesthetic insights into the fantastic inner worlds of tourmaline crystals with the opportunity to immerse yourself in a holistic scientific view of the diverse phenomena of crystals and their formation. Art makes the visitors curious about science – and vice versa.

The aesthetics of many thin sections and crystals had to be made accessible using special methods, because many sections only contain very small but fantastically beautiful images. The black crystals must be exhibited in particularly soft light to make their shape visible. It has proven useful to work with high enlargements in addition to the original: large slides in light boxes make the structures of objects that are too small easy to recognize, and large-format macro photos present details of slices as fantastic landscapes or abstract paintings. Photos of perfectly illuminated crystals illustrate the phenomena and encourage you to find the right viewing angle for the originals in the display cases. A 2m large, luminous model of a sliced crystal impresses because the theme of the exhibition can be intuitively grasped from it. A film on a large screen was designed with an alternation of meditative sequences accompanied by music (for example with flights through tourmaline crystals) and little explanatory text - this film encourages you to look at the somewhat more detailed texts with the scientific explanations in the showcases.

Interactive offers for a closer look: an observation course with a worksheet for particularly interested visitors, a memory game, a cube puzzle with nine large cubes, crystal optical experiments, workshops for grinding and discovering by the participants, as well as a painting table with minimalistically designed coloring templates that let the creativity of some visitors blossom.

The exhibition content is constantly supplemented and expanded with new, attractive or even more informative crystals, thin sections, pictures and films. The response has been positive from experts and laypeople alike - which is reflected in the comments in the visitors' book and in the number of visitors.

*References:*

[1] Rustemeyer, P. (2003) Faszination Turmalin, Spektrum akad. Verl. 2003, 308p

[2] Rustemeyer, P. (2015) Turmalin – Fascinating Crystals with phantastic inner worlds, München 276p

[3] Rustemeyer, P. (2022) The Inner Architecture of Tourmaline Crystals as inferred from the morphology of color zones in thin slices, J. Geoscience 67: 103-128

[4] Rustemeyer, P. (2023) Fascinating Structures within Slices from Dark Tourmaline Crystals, Rocks and Minerals 98: 418 – 434

# Guided tours and projects for children and young people at the Museum Mineralogia Munich on the topic of "How was the moon actually formed and what can we learn from meteorites?

Kaliwoda, M.[1], Junge, M.[1], Hentschel, F. [1] and Schmahl, W.W.[1]

[1]Mineralogical State Collection Munich, Bavarian National History Museums (snsb) and kaliwoda@snsb.de

---

Most children and young people have a natural affinity for all things that do not come from Earth, which explains their interest in space, meteorites, asteroids, shooting stars, alien planets and our nearest celestial body, the moon. There are certainly many reasons for this strong interest. Even during guided tours and children's projects, it becomes clear how enthusiastic children and young people are about this topic.

On the one hand, there is curiosity and a desire to discover: children and young people have a natural thirst for knowledge, which needs to be encouraged. Space represents the unknown and children are often fascinated by things that lie beyond their everyday horizon of experience. Space also stands for adventure; it offers an infinite new "world". Images of space telescopes in particular reinforce this fantasy. Young people and children can even get a better idea of the moon, Mars or asteroids in space. There are also space missions and the International Space Station (ISS), which they are familiar with from television and the internet.

Guided tours or projects on the new special exhibition “Moon Impact - How the moon was formed!” at the Museum Mineralogia Munich will therefore address various questions: (1) How was the moon formed? (2) Are all moons or satellites formed in this way? (3) How do you imagine outer space? (4) How did minerals and rocks form on Earth or in space? (5) Why do we actually study the moon? (6) How does this benefit our knowledge of the Earth's structure? (7) What can we learn about meteorites and meteorite craters.

These are just some of the topics that are dealt with here. One of the tools for these projects is the new special exhibition, which includes lunar and Martian meteorites, many minerals and rocks, impact craters and their rocks as well as a wide range of illustrations and visual aids. Of course, the programmes are also interactive, so children and young people can touch different meteorites and discover, for example, that an iron meteorite is much heavier than a rock meteorite. The children are also particularly enthusiastic about the diversity of the rocks. So far, we have found that the programmes on the moon and meteorites have been very well received by children and, as already mentioned at the beginning, there is a great fascination among children and young people for the topic of space, which can be further strengthened by the programmes.

# Roots of removal: Kenyan basalt rock and mineral sculpture art and the carbon removals odyssey – The Mutuma Marangu Sculpture and Art Collection's *"TMMSAC" "RoR BRAMSA Movement"* Exhibition

Marangu, M.[1], Collinson, J.D.[2], Blackbourn, G.[3], Roobroeck, D.[4], Manga, M.[5], Kimani, F.[5], Santos, F.M.[6], Oroo, G.M.[1], Oendo, P.K.[1], Mbera, R.O.[1], Tabule Ogao, J.A.[1], Kombo, C.D.[1], Ong'esa, E.[1]

[1] The Mutuma Marangu Sculpture and Art Collection "TMMSAC", Nairobi, Kenya; mutu@888mail.net

[2] Retired Consultant, Newcastle-under-Lyme, Staffordshire, United Kingdom

[3] Consultant, Bo'ness, United Kingdom

[4] CO-REGEN and the International Institute of Tropical Agriculture, Nairobi, Kenya

[5] Olsuswa Energy, Nairobi, Kenya

[6] School of Engineering, University of Guelph, Guelph, Ontario, Canada

---

ROOTS OF REMOVAL *"RoR"*: KENYAN BASALT ROCK AND MINERAL SCULPTURE ART *"BRAMSA"* AND THE CARBON REMOVALS ODYSSEY, hereafter, *"RoR: BRAMSA Movement"*, an exhibition presented at the Nairobi National Museum in September 2023, coinciding with the first Africa Climate Summit, attempted to engage the wider public imagination and understanding of Carbon Capture and Storage, *"CCS"* and Enhanced Rock Weathering, *"ERW"* through the exploration of specific geology and mineralogy of seven sample Kenyan basalts and meta-basalts, comprising the RoR BRAMSA *"ORIGINAL 7"*, used as the basis for unique works by four ultra-contemporary Kenyan master sculptors. The RoR BRAMSA Movement exhibition, selected and assembled by the lead author, through TMMSAC, was seen by 13,800+ visitors of all ages, and was positively received by geological & climate science experts/novices, as well as sculptural art experts/novices alike.

TMMSAC consists of many hundreds of Kenyan rock and mineral sculptural works by six ultra-contemporary Kenyan master sculptors using a wide range of rock types, however, the sculptural works included in the RoR BRAMSA Movement exhibition were produced by the master sculptor authors, who all worked with basalts or meta-basalts. The MESO-level ORIGINAL 7 sample sculptures were displayed alongside MACRO-level geographical and MICRO-level geological and mineralogical details of the rocks from which they were sculpted. Field localities, mesoscopic textures, microscopic compositions, and textures illustrated by photo and electron-micrographs and compositions derived from XRF and XRD analyses were documented through photographs and plots.

Basalts are currently being widely evaluated for their potential as reservoirs for the removal of atmospheric $CO_2$ through both CCS and EWR processes. The abundance of basalts within Kenya makes the country a natural theatre to explore and draw attention to its potential for contributing to climate amelioration and carbon removal. Meta-basalts in the Archean basement outside the Kenya Rift may additionally provide material for testing rock weathering in fertile agricultural areas. Live laboratory examples were illustrated in the exhibition by a plant experiment provided by CO-REGEN and the International Institute of Tropical Agriculture. Basalts within and close to the rift are geologically young and continue to be extruded almost to the present day. These may have the potential for CCS, particularly if its viability could be established in coordination with ongoing geothermal power exploration which is being actively pursued in the floor of the northern part of the rift by Olsuswa Energy Limited.

The positive responses from this unique RoR BRAMSA Movement exhibition give optimism that the creative and imaginative combinations of arts and science may provide important ways in which greater awareness and knowledge of the issues and possible solutions of climate amelioration and carbon removals can be brought to a wider, non-technical audience.

## Finding the Smoking Gun: A cross-museum survey of pyrite

Royce, K.[1]

[1] School of Geography and the Environment, University of Oxford, South Parks Road, Oxford, OX1 3QY; kroyce@pm.me

---

Pyrite has accrued millennia's worth of scientific and cultural value. However, its noxious deterioration has long made it a challenge for collectors and museum professionals alike. In order to preserve pyrite—be it as single crystals or part of assemblages—we must first understand how pyrite deteriorates within indoor environments. Despite over a century of study, pyrite decay as it occurs in these conditions is still poorly understood. Most reports remain effectively anecdotal; sample numbers are limited and do not truly represent pyrite's diverse nature. Further, no known substantial longitudinal studies have been conducted. In order to acquire quantitative evidence of pyrite's long-term behaviour within the museum setting, a cross-museum study was conducted using specimens from four UK museums: Oxford University Museum of Natural History, National Museum Cardiff, National Museums Liverpool, and the Sedgwick Museum of Earth Science. Survey and colorimetric data provided sufficient evidence to infer the main causal factor governing pyrite decay: the total concentration of impurities, as determined by formation conditions. The formulation of this hypothesis evidences that mineral deterioration pathways can be determined through such methods, and allowed for the author to produce pragmatic recommendations for the future care of pyritic specimens. Actions utilising these findings are already underway at the four museums.

# An extensive powder diffraction study of 'hydrocerussite-type' mineral specimens in museum collections from the Mendip Hills area, Somerset, UK.

Rumsey, M.S.[1], Najorka, J.[1]

[1]Science Department, Natural History Museum, Cromwell Road, London, SW7 5BD

Corresponding author: *e-mail:m.rumsey@nhm.ac.uk*

---

The Mendip Hills area has been the source of several important mineralogical discoveries regarding lead oxychlorides and more recently lead hydroxycarbonates related to hydrocerussite. The mineral collections at the Natural History Museum in London cover both the chronological and locational discoveries of this region dating back to the 18th Century. In addition, the collection contains most of the type specimens of these discoveries, so is perfectly suited for a systematic review with reference materials to hand. The hydrocerussite [$Pb_3(CO_3)_2(OH)_2$] from the region shows the largest crystals of any geological deposit and the re-discovery of plumbonacrite [$Pb_5O(CO_3)_3(OH)_2$] (2012) and particularly the characterisation of somersetite [$Pb_8O(CO_3)_5(OH)_4$] (2018) [1] at the location suggests the likelihood for considerable misidentification within museum reference specimens, alongside the potential for undiscovered further related layered structures [2].

An extensive powder diffraction study was started to systematically review all the samples that visually contained 'hydrocerussite' in the collections from the area. During, the study a new, related phase was identified by its unique powder diffraction pattern, the structure was solved by single crystal diffraction and shown to have the most complex structure thus far identified with an idealised formula of [$Pb_{11}O(OH)_6(CO_3)_7$]. The potential new mineral is hexagonal, P63/mmc, with unit cell dimensions of a = 5.24512(4) Å and c = 56.4771(5) Å. The structure consists of hydrocerussite- and plumbonacrite-type blocks stacked along c, similar to the structure of somersetite. While the block stacking is alternating in somersetite, another hydrocerussite-type block is inserted in [$Pb_{11}O(OH)_6(CO_3)_7$], forming a stacking sequence of two hydrocerussite-type blocks and one plumbonacrite-type block in the c direction. Similar to other hydrocerussite-type minerals, stereochemically active lone electron pairs on $Pb^{2+}$ are accommodated between the blocks.

This presentation will cover the potential new mineral, the results of the systematic study to date, with a particular focus on the distribution of the occurrences of the different members of these related phases across geographical locations and chronological discoveries.

*References:*

[1] Siidra O et al. (2018) Min Mag 82(5):1211-1224
[2] Siidra O. et al (2018) Acta Cryst B74:182-195

# Seeking a Specific Mineral for Research? An Introduction to Mineral Specimen Data Infrastructure and MinExt for Darwin Core

Walcott, R.C.[1] and Norton, B.[2]

[1]Department of Natural Sciences, National Museums Scotland EH1 1JF, Edinburgh, UK.

---

There are millions of minerals in collections around the world. These collections not only contain physical evidence of thousands of different species, crystal habits and environmental associations, but also potentially harbour vast reserves of metadata for research. Unfortunately, the term 'potentially' is key here, as determining the exact locations of these specimens and their availability for research is currently an extremely arduous task. However, numerous developments are underway to solve this problem.

The vast majority of mineral specimens are housed in museums and university collections. These two institutions often differ in their management structure and the audiences they serve. Here, we focus on minerals in museum collections, as they often contain the largest, most diverse, and historically significant collections.

A notable feature of natural history museum collections is that they usually contain many more biological specimens, and thanks to funding aimed at addressing the biodiversity crisis, substantial strides have been made to make (biological) specimen data publicly accessible. However, infrastructure for mineral and geological collections has different needs, so progress has been slower in its development.

We outline some of the services available for museum specimens in general and address issues relating to mineralogical collections in particular. We present some projects and initiatives for customised mineral collection management systems, schemas and open searchable data portals. We finish with an introduction to the proposed Mineral Extension for Darwin Core [1] and its significance within the broader context. Finally, we invite feedback on our endeavours to enhance accessibility and understanding in mineralogical research and exploration.

*References:*

[1] https://www.tdwg.org/community/esp/mineralogy/

# GeoSpecify, a Collection Management Platform for Geological Objects

Beach, J. H. [1], Burri, T. [2] and Fitzsimons, G[1].

[1] Specify Collections Consortium, Biodiversity Institute, Univ. of Kansas, USA, beach@specifysoftware.org

[2] Naturhistorisches Museum Bern, Switzerland

---

Multidisciplinary natural history museums (NHMs) that include geological collections have a common problem. Whereas the biological departments can choose from an ample selection of Collection Management Systems (CMS) for the registration of biodiversity specimens, few of those CMS are capable of adequately supporting data curation for geological collection objects. To address their data processing needs, Earth Science departments have adapted other data platforms, or have tried to manage their holdings data using a generic data management system, like MS Access, FileMaker, directly in SQL, or with spreadsheets. These self-adapted solutions enabled basic cataloguing and description of geologic objects, but they were usually not accompanied by a software application with collection management logic or a user interface based on discipline data standards. For example, home-grown systems commonly use locally-defined descriptors that are not complete nor consistent with widely-accepted domain vocabularies. Also, earth collection scientists designing data processing platforms are usually not trained software engineers, and these adapted or local solutions have been variously constrained by limited extensibility, domain semantics, user interface capabilities, and particularly by the absence of ongoing software support and maintenance. Switzerland had these research informatics challenges where several large and small Swiss natural history museums were simultaneously searching for a more robust and supported CMS for geologic objects. The 2021 launch of an initiative of the Swiss Academy of Sciences named the “Swiss Natural History Collections Network” (SwissCollNet) [1] provided the opportunity for submitting a project proposal entitled “Integrating Geoscience Collections into Specify Software” aimed at developing a CMS capable of effectively handling data from geologic objects [2]. The proposal was submitted as a collaboration between the NHM’s of Basel, Bern, Geneva and Lausanne. Instead of a completely new development, the idea was to build on the knowledge and engineering of an established biological collections CMS, extending it for geologic objects. In late 2022, the SwissCollNet Program funded the effort among the four museums. The Specify Collections Consortium [3] was engaged as the project’s software engineering partner. Ben Norton (Taxonomic Databases Working Group, North Carolina) was also contracted to survey community data resources, information concepts and data standards relevant to geocollections curation. After two years of collaborative work, the open-source, web-based, GeoSpecify platform is nearing public release.

In our talk we will discuss general and specific challenges of extending the Specify biodiversity collections management system to support geological collections. We will highlight the expectations and user requirements set by the Swiss NHM’s, the elaboration of a geocollections data model, and current implementation activities to extend the existing database schema, business logic, and user interface of the Specify software platform.

*References:*

[1] https://swisscollnet.scnat.ch/en

[2] https://swisscollnet.scnat.ch/en/running_projects/mineralogy

[3] https://www.specifysoftware.org, https://github.com/specify

# Count Vargas Bedemar , J. W. v. Goethe and the Mineralogical Collection in Jena

Kreher-Hartmann, B.

Friedrich-Schiller-University Jena, Germany; birgit.kreher@uni-jena.de

---

The Mineralogical Collection of the University of Jena, in the middle of Germany, looks back on almost 250 years of history. It emerged in 1779 from a classical mineral cabinet of the 18th century. The first curator and professor of mineralogy at the University of Jena, Johann Georg Lenz (1745 – 1832) founded the "Societät für die gesammte Mineralogie zu Jena" in 1797. This foundation brought the collection an enormous increase in attention and thus also in objects [1]. In addition to the various groups of members, the structure of the society also included a president and a vice-president.

J.W. von Goethe (1749 - 1832) was very active as the third president of this society from 1804 until his death. Goethe is well known as a poet, but he was also very interested in nature. He was particularly interested in the formation of rocks and minerals and their properties. Goethe's private geoscientific collection grew to around 18,000 objects by the end of his life.

One day, he received a letter from a previously unknown novelist, Count Vargas Bedemar (1770 – 1847) from Denmark. Bedemar was not sparing in his praise for Goethe's publications, but he also told him about the trips he made for the Danish king to the Faroe Islands, Iceland and Greenland in search of raw materials and minerals. The loose contact became more intensive and Bedemar's persistent interest in Goethe's work earned him, among other things, the House Order of the Grand Duchy of Saxony-Weimar-Eisenach and the post of Vice President of the Jena Mineralogical Society.

The mineralogical collection in Jena was richly endowed during Bedemar's time as vice president. Between 1819 and 1827, he sent 8 gift suits to Jena [2]. All together more than 1000 objects, mainly minerals, including larger specimens. After he was employed by the Danish king in 1813 for geological exploration and the acquisition of raw materials, his travels took him mainly through the Nordic countries. And so many pieces came to Jena from Sweden, Bornholm, the Faroe Islands, Iceland and Greenland, but he also sent pieces from England and from a trip to Madeira, the Azores and the Canary Islands.

Interestingly, Bedemar was never in Jena and his interest in the Jena collection waned considerably after Goethe's death, although he then held the office of President of the Jena Society on a rotating basis and continued to do so until his death. But thanks to the minerals donated, including a small set of cut opals from Iceland, Count Vargas Bedemar, alias Carl Otto Grosse, is still an important person for the Jena collection today.

*References:*

[1] Kreher-Hartmann, B. (2006): Die Mineralogische Sammlung und Mineralogisches Museum der Friedrich-Schiller-Universität Jena. – Beiträge zur Geologie von Thüringen, N.F., Heft 13, 73 – 82.
[2] Kreher-Hartmann, B. (2014): Die Mineralogische Societät zu Jena – Beiträge aus den Sammlungen der Universität Jena, Band 3, 36 S.

# The historical Ungemach mineral collection at the University of Liège

Hatert, F.[1*], Bouvy, A.[1] and Warin, R.[2]

[1] Laboratory of Mineralogy, University of Liège B18, B-4000 Liège, Belgium

[2] Rue du Wérihet 33, B-4052 Beaufays, Belgium

[*]corresponding author: fhatert@uliege.be

---

The mineralogy museum of the University of Liège was constituted shortly after the foundation of the university, in 1817. Accumulated over the years by famous geologists and mineralogists Gustave Dewalque (1826-1905), André Dumont (1847-1920), Giuseppe Cesàro (1849-1939), and Henri Buttgenbach (1874-1964), the mineral samples were rare and of high historical value. In his description of the museum in 1938, Buttgenbach [1] lists a total of 32.000 samples, among which 21.000 minerals from the systematic international collection, 4.500 specimens from Belgium, 360 samples from Congo, and 6.000 minerals from the Ungemach collection.

During the second World War, a bombing raid by the German army provoked a terrible fire in the museum, that destroyed many samples, books, and mineralogy instruments. This tragical even was described in detail by J. D. H. Donnay [2], who states that "*The whole museum (except for a few pieces which were in the vault) and all the other facilities were burned the day the Germans left! It is a great disaster*". After this publication, the international mineralogical community was extremely generous, and many donations allowed to slowly reconstruct the collection which nowadays hosts approximately 23.000 mineral specimens.

Even if many mineral samples were indeed damaged by this fire, it appears that famous historical specimens are still preserved in the mineralogical collection of the Liège University, and we now realise that the description of Donnay [2] was certainly too dramatic, in order to stimulate international donations. The exquisite Ungemach collection, which was acquired by the university of Liège in 1938, was considered by the international mineralogical community as totally destroyed… but indeed, most of these samples are preserved since they were still stored in their wooden transportation boxes in 1944!

Nowadays, the Ungemach collection constitutes the most beautiful and rich part of the historical mineral samples belonging to the Liège University. Henri Léon Ungemach (1879-1936) was a mineralogist from Strasbourg, friend of Giuseppe Cesàro and student of Georges Friedel. From the 6.000 samples originally reported in his catalogue, 360 are preserved in the collection of the Natural History Museum of Strasbourg, and approximately 2.500 are still in our collection. Most historical European mineral localities are represented, but the most exceptional part of the collection is constituted by the sulfosalts, among which occur many specimens from the German classical ore deposits (Freiberg, Andreasberg, …) and from the Alsace mines (Sainte-Marie-aux-Mines, …).

*References:*

[1] Buttgenbach H. (1938) Le Musée de Minéralogie de l'Université de Liège. Vaillant-Carmanne, Liège, 41 p.
[2] Donnay J. D. H. (1945) Am. Mineral. 30: 81-83

## The role of natural history museums for the public awareness of the need of raw materials

Junge, M.[1,2], Kaliwoda, M.[1,2], Hentschel, F.[1,2], and Schmahl, W.W.[1,2]

[1]Mineralogical State Collection (SNSB-MSM), Germany, junge@snsb.de

[2]Department of Earth and Environmental Sciences, Ludwig Maximilian University of Munich, Germany

---

Public awareness of the importance of critical raw materials for our society has increased significantly in recent decades thanks to numerous media reports. These media reports may present questionable information about mining and the commodities market, which can lead to confusion. Geoscience and natural science museums offer an ideal environment for knowledge transfer about the connection between minerals and their application in our everyday lives. Due to the political and social development towards low-carbon energy production, topics related to raw materials are also becoming an important part of school education. Workshops for students in a museum, as an extracurricular activity, are very useful learning techniques to deepen the knowledge of the young generation. In addition to workshops, museums also use exhibitions on topics related to raw materials. One concept of these exhibitions is to visualize a direct connection between the mineral and the application. Museum educators usually have to be creative in order to include raw materials in exhibitions that at first glance have nothing to do with raw materials. These exhibitions can then reach new audiences who have the opportunity to learn about the importance of raw materials in our daily lives.

*References:*

[1] Smith R (2011) Min Dep 47:303-322
[2] Smith R and Jones P (2010) Econ Geol 105:443-798
[3] Smith R et al. (2012) Rev in Econ Geol 17: 1-12

# An Investigation of Material Changes Occurring within Mineral Collections

Royce, K.[1]

[1] School of Geography and the Environment, University of Oxford, South Parks Road, Oxford, OX1 3QY; kroyce@pm.me

---

According to the literature [1 and citations therein], at least 10% of currently identified mineral species are susceptible to deterioration within the museum setting. This primarily occurs through changes in hydration and oxidation state. There is a question, however, of whether such responses are overrepresented. Data for other reaction types are far fewer and generally more qualitative. Light-induced reactions are a poignant example: details such as illuminance, length of exposure, and distance from the illuminant are often missing, effectively making the reports little more than anecdotal. Physical examinations of mineralogical collections were thus deemed necessary to determine:

- whether there is agreement between the material changes experimentally reported and what occurs within collections, and
- whether there are any unreported species demonstrating deterioration within the museum context.

The systematic mineral collection at Oxford University Museum of Natural History (OUMNH) was surveyed to investigate the above. 13,716 specimens belonging to 1,049 species from all mineral groups, including silicates, were examined. Results suggest that the aforementioned reaction types are indeed prevalent in museum collections and are likely not overrepresented in the literature. However, museum collections may also contain more species susceptible to other reaction types (e.g., photo-induced) than recorded. The nature of museum storage makes these species difficult to identify, especially without repeated surveying. Yet of foremost importance is the susceptibility of minerals to physical forces. About a quarter of OUMNH mineral specimens have been affected by physical forces to some degree. All other potential reaction types occur in less than 10% of specimens. These results act as a reminder that—whilst it is indeed important to identify a species' susceptibility to temperature, moisture, light, and pollutants—one cannot ignore physical forces altogether.

*References:*

[1] Royce K (2023) *Assessing the Stability of Mineralogical Collections in Museums*. DOI: 10.5287/ora-d5dagxd4g

## Early 19th Century mineral collection: Robert Jameson's last stand

Walcott, R.C.[1]

[1]Department of Natural Sciences, National Museums Scotland EH1 1JF, Edinburgh, UK.

---

Robert Jameson (1774-1854) was a major figure in early 19th-century European mineralogy, particularly in the English and German-speaking worlds. Unfortunately, due to his inclination to adhere to outdated concepts such as Wernerism and the Natural System of mineral classification, not to mention losing important scientific collections such as James Hutton's, history hasn't always been kind to him. Nonetheless, he developed an impressive network of significant contacts, which he tapped into to build an extensive and renowned collection of minerals. His efforts and collection led to the foundation of the current National Museum of Scotland.

In the 170 years since his death, curatorial focus on other topics, moves, and neglect has resulted in information loss, leaving only the most skeletal knowledge of these early 19th-century collections remaining. Through a detailed data capture exercise, we have not only unearthed his last systematic collection but also a range of other histories and mysteries.

This presentation covers the techniques we used to gather data and reassemble his final collection. It has resulted in revealing important stages in the evolution of mineralogy as a science hidden within the collection as a whole.

# Alexearlite ($Hg^{2+}_3(MoO_4)S_2$): A new mineral with a novel chemistry and structure

Emproto, C.[1], Olds, T.A.[1], Kampf, A.R.[2] and Ma C.[3]

[1]Section of Minerals and Earth Sciences, Carnegie Museum of Natural History, Pittsburgh, Pennsylvania, USA

[2]Mineral Sciences Department, Natural History Museum of Los Angeles County, California, USA

[3]Division of Geological and Planetary Sciences, California Institute of Technology, California, USA

---

Alexearlite, ideally $Hg^{2+}_3(MoO_4)S_2$, is a new mercury molybdate mineral and the first known mercury mineral with essential site-defining molybdenum. The alexearlite type specimen was discovered in waste rock piles at the Lucky Boy mine in Piute County, Utah, USA. Mining in the late 19$^{th}$ century produced a small volume of mercury from processing tiemannite (HgSe). Alexearlite occurs at the Lucky Boy mine as transparent orange to yellowish-orange spear-like prisms within void spaces in tiemannite. The new mineral was also identified in association with corderoite in a cinnabar and quartz-rich matrix at the McDermitt mine in Humboldt County, Nevada, USA, where it occurs as dull cream-colored masses of fibrous crystals. Alexearlite is soft (hardness c. 3) and has a cream white streak. The empirical formulas for alexearlite from both the Lucky Boy mine ($Hg_{3.01}(Mo_{0.99}O_4)(S_{1.80}O_{0.20})$) and the McDermitt mine ($Hg_{3.00}(Mo_{0.95}O_4)(S_{1.77}O_{0.23})$) determined by electron microprobe (on the basis of S + O = 6) suggest a minor substitution of $O^{2-}$ for $S^{2-}$. The crystal structure of alexearlite is orthorhombic (*Pnma*) with *a* = 8.0624(5) Å, *b* = 6.9185(3) Å, and *c* = 13.0035(6) Å. The structure of alexearlite is novel among both natural and synthetic materials and consists of a complex framework of relatively strong Hg-S bonds and weak Hg-O bonds. The topology of the framework is dominated by the local coordination environments of the $Hg^{2+}$ atoms, which bind to S2- with average bond distances of 2.386 Å. The Hg-S bonds form corrugated hexagonal sheets that extend infinitely along [010]. Oxygen atoms of molybdate tetrahedra connect the corrugated Hg-S sheets along [100] and sit within pores of the Hg-S net that extend infinitely along the same direction. Interestingly, while there are many known natural and synthetic substances in the series $Hg_3(XO_4)(S/O)_2$ (where X = Cr, Mo, S, or W), alexearlite shares only limited structural components with other substances in this series. The topologies of the $Hg_3(XO_4)(S/O)_2$ series are diverse, and there exists potential for discovering novel structures in this system in both natural and synthetic materials. The name alexearlite honors Mr. Jayson Alexander (Alex) Earl (1997–2023), a mineralogist, mineral collector, and photographer who helped collect the type specimen.

# Sulphide to sulphate reactions: sulphur degassing and its effects on platinum group mineral enrichment, Rum layered intrusion, NW Scotland

Pentland, K.[1], Einsle, J.F.[2], Divers, M.[3]

[1]University of Glasgow, 2455292p@student.gla.ac.uk/kimberleypentland@outlook.com

[2]School of Geographical and Earth Sciences

[3]Glasgow G12 8QQ

---

The Rum layered intrusion is an example of a mafic-ultramafic layered intrusion formed in an open-system, similar to more renowned intrusions such as Bushveld, South Africa and Stillwater, USA. Though Rum is smaller in scale and enrichment rates, its significantly younger than the Archean Bushveld and Stillwater, having being intruded in the Palaeogene period 60.53±0.08. Rum is a fantastic analogue site to investigate the constraints on Platinum group minerals (PGM's) enrichment relating to sulphide/sulphate reactions and oxidation processes within open-system layered intrusions due to its lack of alteration by deformation and erosion [1, 2] .

Investigation into the formation of PGM's within layered intrusions is growing more important in recent years. Global demand for PGM's is increasing due to the minerals multiple applications and uses, often divided as catalyst (refining crude oil, production of fine/commodity chemicals etc.) and non-catalyst uses (industrial: electrical and machine uses, healthcare, jewellery etc.) [3]. PGM's are also a vital resource in the advancement of green technology which is vital to help reduce carbon emissions and reach global and national development goals [4] . Due to PGM's high affinity with sulphide minerals, investigations regarding the desulfurization and oxidation processes associated with PGM formation will aid overall understanding of layered intrusion formation and distribution of PGM's (regarding the in-situ vs fractional crystallisation debate) [1].

To develop understanding of sulphide/sulphate reactions within the rims of sulphide minerals in the PGM enriched chromite seam of Rum, this project investigates phases within the sulphide minerals using machine learning systems to analyse high and low count data, producing cluster maps and spectra plots highlighting elemental changes across minerals. Further work includes phase maps and spectra produced from SEM-eds mapping and 3D imaging of titanomagnetites using FIB microscopy techniques to aid understanding of the role of oxidation on sulphide/chromite reactions and degassing.

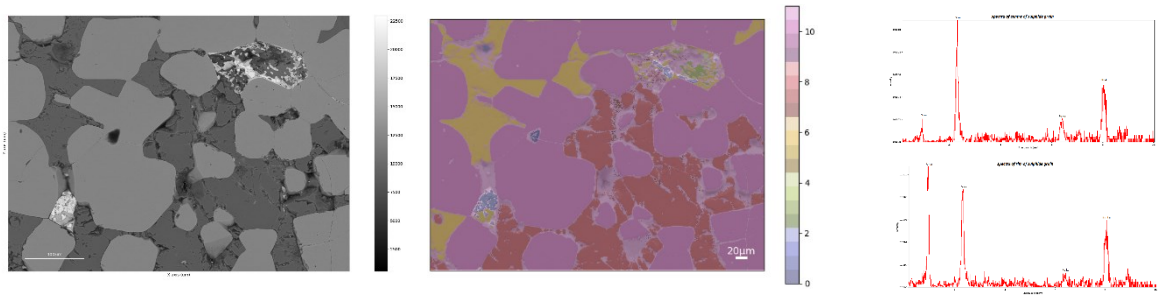


Left image showing BSE image of Rum sulphide. Centre image of Rum sulphide data post clustering. Spectra images highlight geochemical differences between sulphide centre and rims.

*References:*

[1] Latypov R et al (2013) Contributions to Mineralogy and Petrology, 166(1): 309–327.
[2] Hepworth L.N. et al. (2018) Journal of Petrology, 59(8): 1605–1642.
[3] Hughes A.E. et al. (2021) Resources, 10(93): 1-40.
[4] Rasmussen, K.D. et al. (2019) Environ. Sci. Technol, 53(19) :11541–11551.

# Age and evolution of the Raibl carbonate-hosted Zn-Pb deposit (NE Italy)

Velicogna M.[1], Beltrame M. [1], Barago N.[1], De Min A. [1], Lenaz D. [1], Nimis P.[2], Chiaradia M.[3] Venier M.[1], Chelle-Michou C. [4] and Tavazzani L.[4]

[1]Department of Mathematics, Informatics and Geosciences, University of Trieste (Italy); matteo.velicogna@units.it

[2]Department of Geosciences, University of Padova (Italy)

[3]Department of Earth Sciences, University of Geneva

[4]Department of Earth Sciences, ETH Zürich

---

The Triassic sedimentary sequences of the European Alps host more than 200 Zn-Pb deposits [1]. The majority of these deposits is located near the Periadriatic Line, an E-W striking fault of regional importance that divides the Austroalpine nappes in the north from the Southern Alps and Dinarides to the south. In the Eastern-Southern Alps, the ore reserves are localized in the area that includes the Bleiberg-Kreuth, Mežica, Raibl and Salafossa deposits [1], all hosted within Anisian to Norian limestone, dolostone and shale units [2].
The Raibl mining district is located in the Julian Alps near the village of Cave del Predil (Friuli Venezia Giulia, Italy), close to the borders with Slovenia and Austria. The deposit is hosted by the Carnian Schlern Dolomite (locally also known as Dolomia Metallifera), which is locally interlayered with a basinal lithology formed by coeval carbonatic-tuffaceous sediments (pseudo-Buchenstein or Acquatona Formation; [1, 2]).

The Raibl deposit is a low-temperature carbonate-hosted Zn-Pb deposit. The ore bodies are composed by different amounts of sphalerite, galena and iron sulphides, forming columns and veins and rarely stratiform bodies, generally, controlled by the main Triassic tectonic lines of the area. Other occurrences are represented by mineralized breccias filling fissures and old erosion cavities. The most common ore texture is dominated by colloform sphalerite (i.e. schalenblende), which mostly occurs as yellow or red bands hosting dendritic or crystallized galena. Gangue minerals are represented by dolomite, calcite a rarely barite. Based on the chemical features of sphalerite and geometry of the ore bodies, previous authors defined three main ore sectors, implying a connection between mineralization style, paleogeography and tectonics evolution [1, 3]. In particular, the episodic (re)activation of Triassic syngenetic faults is considered one of the main driver of the mineralization evolution, driving the circulation of metallogenic fluids, in a prolonged polyphasic remobilization and re-concentration of original sulphide ores. However, the actual timing and duration of the main mineralization stage(s) has largely remained unconstrained.

We present a large set of new in situ U-Pb ages of petrographically characterized hydrothermal gangue carbonates found in spatial association with the sulphide mineralization. The combination of petrographic observations with U-Pb geochronology results help define several generations of carbonates (pre-, syn- and post-ore) crystallized between 234.3 $\pm$ 5.7 Ma and 92 $\pm$ 10 Ma. Furthermore, by combining the radiometric ages of the sulphide-associated hydrothermal carbonates with the chemical and isotopic composition of the ore minerals, the new data effectively allow to link the mineralizing events with the activation (or re-activation) of the Triassic faults during the Mesozoic. The comparison with similar Alpine Zn-Pb mineral districts will be crucial to build a proper metallogenic model that encompasses all the coeval ore bodies occurring in the Alps

*References:*

[1] Omenetto P. (1979) Annales de la Société Géologique de Belgique 102:519-529
[2] Jadou F. et al. (2002) Mem. Soc. It. 57:29-43
[3] Brigo L. and Cerrato P. (1994) Sediment-hosted Zn-Pb ores 179-197

# Cation and anion ordering in synthetic lepidolites and lithian muscovites: Influence of the OH/F and Li/Al ratios on the mica formation studied by NMR spectroscopy and X-ray diffraction

Fechtelkord M.[1], Marler B.[2] and Sulcek L.[2]

[1]Ruhr-Universität Bochum, Institut für Geologie, Mineralogie und Geophysik, Bochum, Germany

[2]Ruhr-Universität Bochum, Institut für Geologie, Mineralogie und Geophysik, Bochum, Germany

---

A large number of lepidolites $K(Li_xAl_{3-x})[Si_{2x}Al_{4-2x}O_{10}](OH)_yF_{2-y}$ and Li-muscovites $K(Li_xAl_{2-x/3}\square_{1-2x/3})[Si_3AlO_{10}](OH)_yF_{2-y}$ were synthesised by a gelling method in combination with hydrothermal syntheses at a pressure of 2 kbar and a temperature of 873 K. The nominal composition ranged between $0.0 \le x \le 2.0$ and $0.0 \le y \le 2.0$, i.e., from polylithionite $K[Li_{2.0}Al][Si_{4.0}O_{10}](OH)_yF_{2-y}$ over trilithionite $K[Li_{1.5}Al_{1.5}][AlSi_{3.0}O_{10}](OH)_yF_{2-y}$ to muscovite $K[Al_{2.0}\square][AlSi_{3.0}O_{10}](OH)_yF_{2-y}$. $^1H$, $^{19}F$, $^{29}Si$, $^{27}Al$ Magic-Angle Spinning Nuclear Magnetic resonance (MAS NMR) and $^{27}Al$ Multiple-Quantum Magic-Angle Spinning (MQMAS) NMR spectroscopy has been performed to investigate the order/disorder state of Si and Al in the tetrahedral layers and of Li, Al, OH and F in the octahedral layer. The synthetic mica crystals are very small, ranging from 0.1 µm to 5 µm. With increasing Al content, the crystal sizes decrease. Rietveld structure analyses showed that nearly all samples consist of two mica polytypes (1M and $2M_1$) of varying proportions. In the case of lepidolites, the $1M/2M_1$-ratio depends on the Li/Al ratio of the reaction mixture. The refinement of the occupancy factors of octahedral sites shows that lepidolites ($1.5 \le x \le 2.0$) represent a solid solution series with polylithionite and trilithionite as the endmembers. In the case of the Li-muscovites ($0.0 \le x \le 1.5$) the $1M/2M_1$-ratio depends on the amount of impurity phases like eucryptite or sanidine depleting the reaction mixture of Li or Al. There is no solid solution between trilithionite and muscovite, instead, the Li-muscovite crystals consist of domains differing in the relative proportions of muscovite and trilithionite.

The overall composition of the synthesized micas which consist of two polytypes can be characterised by $^{29}Si$, $^1H$ and $^{19}F$ MAS NMR spectroscopy. The Si/Al ratio in the tetrahedral layers and thus the content of $^{[4]}Al$ was calculated by analysing the signal intensities of the $^{29}Si$ MAS NMR experiments. The Li content $x_{est}$ was calculated from the measured tetrahedral Si/Al ratio of the $^{29}Si$ MAS NMR signals. The $^{19}F$ and $^1H$ MAS NMR experiments reveal that F and OH are not distributed statistically but local structural preferences exist. F is attracted by Li-rich and OH by Al-rich environments. The $^{27}Al$ quadrupolar coupling constant which represents the anisotropy of the Al coordination is low for polylithionite with $C_Q$ = 1.5 MHz and increases to $C_Q$ = 3.8 MHz for trilithionite. For tetrahedral Al a smaller increase of $C_Q$ from 1.7 MHz to 2.8 MHz is observed. Advancing from trilithionite to muscovite both quadrupolar coupling constants decrease to 2.5 MHz for octahedral and 1.5 MHz for tetrahedral Al. In polylithionite there is the most isotropic environment for octahedral Al, there are only $Li_2Al$ sites coordinated by F in the octahedral sheets and O from the tetrahedral sheets which are regular containing only Si. The distortion and anisotropy for both Al in tetrahedral and octahedral sheets increases with rising Al content. The most anisotropic environment can be found in trilithionite, especially for octahedral Al [1].

$^{27}Al$-$^{27}Al$ double-quantum single-quantum magic-angle spinning (DQSQ) NMR data suggests a preference for $^{[4]}Al$ in the tetrahedral sheet to occupy positions close to the $^{[6]}Al$ of the octahedral sheets [2].

*References:*

[1] Sulcek L et al. (2023) Eur J Miner 35: 199-217

[2] Sulcek L et al. (2020) Mag Reson Chem 58: 1099-1108

# New pathway to enhance crop and vegetable yield and quality through the infrared emissive characteristics of minerals

Du Y.F.[1, 2], Ding H.R.[1, 2], Lu A.H.[1, 2]

[1]Beijing Key Laboratory of Mineral Environmental Function, School of Earth and Space Sciences, Peking University, 100871 Beijing, People's Republic of China

Lead author: yifeidu@stu.pku.edu.cn (Du Y.F.)

---

Natural minerals have good photoelectric effect, which minerals subjected to solar radiation can generate energy conversion and non-classical photosynthesis [1]. Through the study of infrared emission spectra and characteristics of carbonate minerals, carbonate minerals have good infrared radiation characteristics [2], and their synergistic interaction with polar water molecules can weaken the hydrogen bond strength of water and improve the efficiency of plant photosynthesis. In this study, we combined the photoelectric effect of natural minerals with the classical photosynthesis of plants and used carbonate mineral materials with natural infrared emission spectra to react and prepare plant irrigation water under sunlight. The lettuce hydroponic experiment, lettuce pot experiment and field experiments of peanuts, sweet potato and other vegetables were conducted. The impacts of the treated irrigation water on plant biomass, mineral element content and nutrient quality of plants were studied.

The comprehensive experiment results revealed that under identical nutrient level and field management conditions, irrigation with water after mineral light reaction not only significantly increased the biomass of lettuce leaves, peanut kernels and sweet potato roots, but also showed a synergic increase in the contents of K, Ca and Mg elements in plant tissues, and antioxidant substances such as total polyphenols, total flavonoids and carotenoids. In particular, the content of vitamin C has increased significantly. The explorations from hydroponics experiment and pot experiment to field experiment innovatively uses the infrared spectral effect of minerals emitted by sunlight radiation, expands a new way to improve the yield and quality of crops and vegetables. It also provides fresh perspectives for exploring and utilizing the synergistic mechanism and effect of the "solar radiation-mineral-organisms-water" in the earth system.

*References:*

[1] Lu A et al. (2019) Proc Natl Acad Sci 116(20): 9741-9746
[2] Zhu Y et al. (2020) Phys Chem Miner 47(3): 1-15

# Investigation of Microscale Pores in Terrestrial Mineral Coatings and Their Photoreactive Traits

Ge X.[1], Ding H.R.[1], Wang C.Q.[1], Lu A.H.[1]

[1] Beijing Key Laboratory of Mineral Environmental Function, School of Earth and Space Sciences, Peking University, China

Leading author: gexiao@pku.edu.cn (Ge X.)

---

Across diverse terrestrial settings, a film-like substance ranging from several tens to hundreds of micrometers thick frequently forms on the surface of rocks and soils, termed "rock varnish" or "mineral coating" [1,2]. These coatings, enriched with semiconductive minerals such as iron and manganese oxides, exhibit the ability to persistently capture and convert solar energy, playing a pivotal role in Earth's material cycles [3]. Yet, the intricate internal structure of mineral coatings remains insufficiently explored. Contrary to the simplistic and homogeneous layered structures previously attributed to mineral coatings, our research has unveiled a complex internal pore network, constituted by $TiO_2$ and clay minerals, for the first time.

The specimen was obtained from a site in Eastern China. SEM-EDS examinations of the procured specimens indicate that the mineral coating comprises elements like O, Si, Al, Ti, and Fe, which markedly diverge in composition from the substrate rock. Notably, we have uncovered the existence of microscale pores within the mineral coating, featuring diverse sizes and intricate configurations, for the first time. The pore surfaces are predominantly sheathed in a $TiO_2$-enriched film, with Ti concentrations reaching up to 73.8 wt%. Raman spectroscopic assessments corroborate the predominance of anatase and brookite as the principal forms of $TiO_2$. Advancements in FIB methodologies and HRTEM analyses have elucidated the tri-dimensional pore structure and mineral distribution.

Moreover, Raman spectroscopy has detected the co-presence of anatase and β-carotene within the mineral coating—the latter being a crucial photosynthetic pigment. Experimental simulations have verified that β-carotene, in concert with $TiO_2$, considerably extends the effective sunlight absorption spectrum and augments the photoelectric conversion efficiency.

When exposed to sunlight, the microscale pores within the mineral coating may serve as a "natural reaction chamber", facilitating the collaborative interplay between semiconductive minerals and photosynthetic pigments, and thereby enabling the conversion of solar energy into mineral photoelectron energy. This inquiry offers fresh insights into the genesis, evolution, and environmental interactivity of Earth's surface mineral coatings. It also bears prospective utility for the innovation of novel photocatalytic substances and the advancement of solar energy transformation methodologies.

*References:*

[1] Potter R and Rossman G (1977) Science 196:1446-1448
[2] Goldsmith Y et al. (2014) Geochim Cosmochim Ac 126:97-111
[3] Lu A et al. (2019) Proc Natl Acad Sci 116: 9741-9746

# The role of volatile elements in cancrinites from the Larvik Complex, Norway

Dehousse, C.[1*], Hatert, F.[1], Friis H.[2] and Dal Bo, F.[1]

[1] Laboratory of Mineralogy, University of Liège B18, B-4000 Liège, Belgium (ch.dehousse@gmail.com)

[2] Natural History Museum, University of Oslo, Blindern, 0318 Oslo, Norway

---

Minerals of the cancrinite group are microporous feldspathoids with hexagonal or trigonal symmetry, characterised by the presence of zeolitic cages and large channels in their structures. The diversity observed in this group is associated with numerous possibilities of incorporation within the channels, including cations ($Na^+$, $K^+$, $Ca^{2+}$), anions ($Cl^-$, $S^{2-}$, $F^-$), anionic groups ($CO_3^{2-}$, $SO_4^{2-}$, $OH^-$, $C_2O_4^{2-}$, $PO_4^{3-}$), and neutral molecules ($H_2O$, $CO_2$). These minerals are found in various geological environments, including silica-poor alkaline rocks, where they crystallise as primary phases and alteration products of nepheline and sodalite. Numerous crystal-chemical studies have been conducted both on natural and synthetic cancrinites [1]. However, despite a general consensus about the geometry of the aluminosilicate framework, different models often contradict each other when it comes to the extra-framework components [2].

The structure and chemical content of natural cancrinites were reinvestigated through the combination of various complementary analytical techniques, including electron probe microanalysis, single-crystal X-ray diffraction, and Fourier transform infrared spectroscopy. A total of thirty-five samples were investigated, among which representative cancrinites from various alkaline complexes stored in the Mineralogy collections of the Universities of Liège and Oslo, as well as new samples collected on the field in the Larvik Plutonic Complex (LPC) in Norway.

Our study highlighted the significant importance of infrared analysis in studying cancrinites, especially for evaluating the speciation of the carbon atom (i.e., $CO_3$, $C_2O_4$ or $CO_2$). It was possible to subdivide cancrinites *sensu stricto* into different categories based on their infrared spectra, and correlations were established between the vibrational frequencies of $CO_3$ groups and their environments within the channels. Electron-microprobe analyses allowed to study the Si/Al substitution mechanism, and to detect the presence of non-carbonaceous volatile elements. Particularly, sulphur and fluorine were detected in significant proportions in some samples.

A focused investigation of samples from the Saga 1/Sagåsen quarries in the Larvik Plutonic Complex shows that cancrinites are associated with saccharoidal albite and aegirine, in pegmatites transitioning from miaskitic to agpaitic regimes. Cancrinites crystallise in those rocks due to extensive late-stage hydrothermal alteration processes [3], and correlations between the volatile contents of cancrinites and their parageneses provide insights into the post-magmatic processes affecting the alkaline pegmatites of the LPC. The distribution of volatile elements within the structure of natural cancrinites was also discussed, suggesting their potential as petrogenetic indicators in different intrusive alkaline complexes, as previously mentioned by Pekov et al. [4].

*References:*

[1] Chukanov et al. (2021) Microporous Mesoporous Mater 323: 111098
[2] Shendrik et al. (2021) Crystals 11: 280
[3] Sunde et al. (2019) Nor J Geol 99: 93-111
[4] Pekov et al. (2011) Can Mineral 49: 1129-1150

# STRUPLO-24, a new version of the crystal-structure drawing program

Fischer, R.X.[1], Messner, T.[1]

[1]Fachbereich Geowissenschaften, Universität Bremen, 28359 Bremen, Germany, rfischer@uni-bremen.de.

---

STRUPLO [1] was one of the first programs drawing crystal structures in polyhedral representation. The old FORTRAN code was rewritten in Delphi with a graphical user interface [2]. Bonds were drawn as cylinders, atoms as spheres, and groups of atoms coordinated to a central atom as polyhedra. All structural elements, like atoms, bonds, or polyhedra, can be identified or modified online simply by using the mouse pointer. Tables of distances and angles can be generated. Typical drawings are shown in Fig. 1 which can be exported in bmp or jpg format.

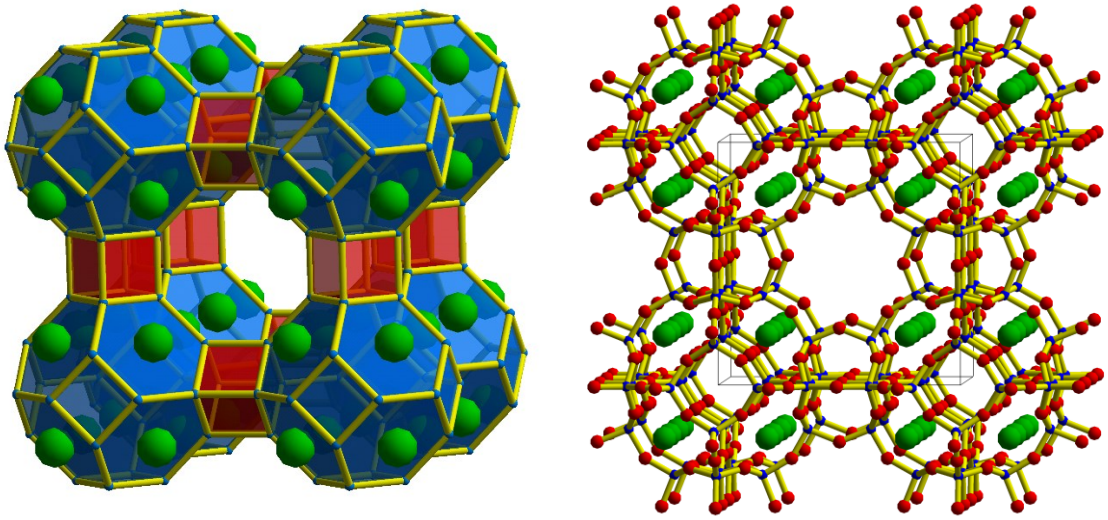

Fig. 1: Zeolite A [3] in two different representations. Left: semi-transparent cages with Na shown as green spheres. Right: Ball and stick model with green Na, blue Si/Al, and red O.

Meanwhile, many features have been added for the crystal-chemical evaluation of crystal structures. This is especially the calculation of parameters describing the geometrical influence of lone electron pairs (LEP) and the calculation of bond valences and bond-valence sums (BVS). STRUPLO calculates the vector (eccentricity parameter) describing the deviation of the central ion from the geometrical point of gravity of the peripheral ions which can be used to describe stereochemically active LEPs [4]. Bond valences and BVS parameters are calculated based on the algorithms derived by Brown [5].

*References:*

[1] Fischer RX (1985) J Appl Crystallogr 18:258-262
[2] Fischer RX and Messner T (2003) Abstract DMG meeting 2003 in Bochum
[3] Smith JV and Dowell LG (1968) Z Kristallogr 126: 135-142
[4] Wang X and Liebau F (2007) Acta Crystallogr B63:216-228
[5] Brown ID (2002) The chemical bond in inorganic chemistry: The bond valence model. Oxford Univ Press.

# Chemical composition of calcite of veinlets-impregnation mineralization of rock complexes of the Silesian cover of the northwestern part of the Ukrainian Carpathians

Zankovuch, H.O.[1], Naumko, I.M.[2], Kokhan, O.M.[3], Matviishyn, Z.H.[4].

[1, 2, 3, 4]Institute of Geology and Geochemistry of Combustible Minerals of the NAS of Ukraine, 3-a Naukova St., Lviv 79060, Ukraine, zankovuch@gmail.com

---

Calcite is the main mineral of the veinlets-impregnation mineralization of the Silesian Cover rock complexes of the northwestern part of the Ukrainian Carpathians, which is common in terrigenous sediments of Cretaceous-Paleogene age [1, 2].

Calcite forms spotted nested clusters, lenses and differently oriented veins (up to 55 mm) and veins, the thickness of which varies from microscopic to 2-3 cm, and in swells even more (calcite 1). Veins with partially or completely leached calcite and traces of sliding are often encountered. Calcite veins (calcite 2) are often found, which are also intersected by calcite longitudinal and transverse veins of different orientations (calcite 3). Calcite samples for the study were taken from natural outcrops and quarry walls.

The mineral is represented by crystalline-grained varieties. Large crystalline varieties (over 0.1 mm) predominate. Large calcite grains reach 4-6 mm. Polysynthetically twinned grains are often observed. Dense aggregates, druses, and sometimes well-cut crystals of rhombohedral and prismatic habit occur.

The color of calcite varies from colorless, transparent individuals to milky white opaque crystals colored in various light colors (gray, yellow).

We studied the chemical composition of all three types of calcite. According to the results of the research, all types of calcite contain magnesite-rodochrosite-siderite impurities and dissolved mechanical impurities $Fe_2O_3$ (0,16-1,26 wt%), $Al_2O_3$ (0,01-0,50 wt%) etc. If we exclude dissolved mechanical impurities and recalculate the carbonate part by 100%, we can see the following calcite composition: $CaCO_3$ – 96,46-98,79 %, $MgCO_3$ – 0,73-2,90 %, $MnCO_3$ – 0,11-1,61 %, $FeCO_3$ – 0,15-0,64 % (for calcite 1); $CaCO_3$ – 96,61-97,58 %, $MgCO_3$ – 1,59-1,81 %, $MnCO_3$ – 0,20-0,94 %, $FeCO_3$ – 0.41-0.87 % (for calcite 2); $CaCO_3$ – 97,44-97,58 %, $MgCO_3$ – 1,79 %, $MnCO_3$ – 0,22-0,46 %, $FeCO_3$ – 0,30-0,41 % (for calcite 3).

Crystallochemical formulas of calcite obtained by the oxygen method [3] of calculation:
$(Ca_{0,97\text{-}1,00}Mg_{0,01\text{-}0,04}Mn_{0\text{-}0,01}Fe_{0\text{-}0,01})C_{0,98\text{-}1,00}O_3$ (for calcite 1);
$(Ca_{0,99\text{-}1.01}Mg_{0,02\text{-}0,03}Mn_{0\text{-}0,01}Fe_{0\text{-}0,01})C_{0,98\text{-}0,99}O_3$ (for calcite 2);
$(Ca_{0.99\text{-}1.00}Mg_{0.03})C_{0.98\text{-}0.99}O_3$ (for calcite 3).

The above data shows that the carbonate part of calcite is replaced by small amounts of magnesium with very small amounts of manganese and iron. The difference in the chemical composition of all three types of calcite is insignificant or the same. This indicates a single source of mineralizing fluids.

*References:*

[1] Zankovuch H &Naumko I. (2015) Mineralogical Review. 2015. N 65. Issue 2. P. 126–140.
[2] Hnylko O. (2010) SSN 0869-0774. Geology and Geochemistry of Combustible Minerals. № 2 (151). P. 44–57.
[3] Bekesha S & Bilyk N. (2014) Calculation of mineral formulas: 510.

## Aleutian Arc Initiation: Tectonic and climatic implications

Hoernle, K.[1,2], Jicha, B.[3], Portnyagin, M.[1], Hauff, F.[1], Höfig, T.[4], Yogodzinski, G.[5], Timm, C.[1], Guillong, M.[6], Berndt, C.[1,2], Savelyev, D.[7], Bezard, R.[8], Baranov, B.[9]

[1]GEOMAR Helmholtz Center for Ocean Research Kiel, Germany (khoernle@geomar.de)

[2]Institute of Geosciences, Kiel University, Germany

[3]Department of Geoscience, University of Wisconsin-Madison, USA

[4] Projektträger Jülich, Forschungszentrum Jülich GmbH, Rostock, Germany

[5]School of Earth, Ocean, and Environment, University of South Carolina, Columbia, SC, USA

[6]Department of Earth Sciences, ETH, Zurich, Switzerland

[7]Institute of Volcanology and Seismology FEB RAS, Petropavlovsk-Kamchatsky, Russia

[8]Geochemistry and Isotope Geology Department, University of Göttingen, Göttingen, Germany

[9] Shirshov Institute of Oceanology, Russian Academy of Sciences, Moscow, Russia

---

The timing and cause of Aleutian subduction initiation remain enigmatic. Here we combine new geochronologic and geochemical data for samples from the western Aleutian Arc igneous basement with plate tectonic reconstructions to constrain Aleutian Arc initiation and the tectonic evolution of the northern and western Pacific. Zircon U-Pb and 40Ar/39Ar data from four locations spanning 750 km range from 55.6 to 46.2 Ma. The oldest Aleutian samples have similar incompatible element abundances to the oldest rocks (forearc basalts) from the Izu-Bonin-Marianas and Tonga arcs. Plate tectonic reconstructions in a mantle reference frame suggest that there was a change in absolute plate motion between 56 and 55 Ma from a WNW to a northerly direction, consistent with induced Aleutian Arc initiation. Aleutian subduction initiation is part of a ten-million-year period of major plate tectonic reorganization in the circum-Pacific that culminated with formation of the Hawaii-Emperor Bend. The new timing of Aleutian subduction initiation at ~56 Ma correlates with the Paleocene-Eocene Thermal Maximum (PETM). Therefore, a causal relationship is conceivable: either through the sudden release of large amounts of carbon due to a tectonic event, such as uplift of a large epicontinental seaway, or intrusion of arc magmas into organic-rich sediments on the seafloor.

# Palaeozoic continental growth: The Köli Nappe Complex, Swedish Caledonides: Iapetus Ocean arc magmatism, rifting and accretion to Baltica

Cuthbert, S.J.[1], Ziemniak, G.[2] and Walczak K.[1], Carter, I.[1,3]

[1] AGH University of Krakow, 30-059 Kraków, Poland simon.cuthbert@agh.edu.pl

[2] University of Wrocław, 50-204 Wrocław, Poland

[3] Uppsala University, Box 256, 751 05 Uppsala, Sweden

---

The Köli Nappe Complex (KNC) is a major volcano-sedimentary assemblage in the Upper Allochthon (UA) of the Scandinavian Caledonides, outcropping along >1000 km of this collisional orogen. The UA originated as outboard terranes within the Neoproterozoic to Devonian Iapetus Ocean basin [1]. This enormous lithotectonic assemblage was an important Palaeozoic crustal addition to the Baltica palaeocontinent. The tectonic environment and nature of the magma sources for the KNC are not yet well understood. We have addressed this using new whole-rock trace element and isotopic data from Västerbotten, Sweden. The KNC comprises (from lowest to highest) the Björkvattnet, Stikke, Atofjället and Krutfjellet Nappes. In each of these is a suite of metavolcanic rocks ("quartz ketatophyre" and "greenstone") and associated meta-intrusive rocks of latest Cambrian to early Ordovician age [2] that range in composition from basalt to rhyolite. In addition, the Björkvattnet, Stikke and Krutfjellet nappes contain early Silurian metabasalts, leucotonalites, gabbros and granites, representing a second major magmatic event (arc rifting?). Normalised trace element patterns of the Cambro-Ordovician metavolcanics show typical subduction-zone features in all the nappes; LIL enrichments *decrease* tectonostratigraphically upwards through the lower three nappes but are *greatest* in the uppermost (Krutfjellet) Nappe. Mafic varieties in the Björkvattnet Nappe are E-MORB but are N-MORB in the Stikke and Atofjället nappes. Intermediate and felsic rocks change up through the Björkvattnet, Stikke and Atofjället nappes from calc-alkaline to tholeiitic, while the Krutfjellet Nappe has some mature arc characteristics. Overall, the subduction influence appears to decrease up the nappe sequence, but the structurally highest Krutfjellet Nappe differs in exhibiting some continental crustal influence. εNd discriminates between the different nappes, decreasing structurally downwards, suggesting a greater continental crustal contribution in that direction. Again, the Krutfjellet Nappe reverses that trend, having negative εNd. If the nappes are structurally restored this suggests a westward (modern co-ordinates) decrease in subduction influence, but further west still lay an arc with continental basement – the Krutfjellet Nappe. Pb isotopes in the Björkvattnet and Stikke Nappe metavolcanites show a strong Grenvillian or Sveconorwegian influence in the mantle source. Pb isotopes in the Silurian intrusions of the Krutfjellet Nappe lack this. Overall, the KNC represents a major addition of juvenile, subduction-related, early Palaeozoic crust to Baltica, along with some recycled continental crust. These may have been accreted directly or by accretion to Laurentia and then tectonic transfer to Baltica during the Scandian collision. Pb isotopes for the Silurian plutonic rocks in the Krutfjellet Nappe suggest a major modification of their mantle source during rifting of the older arc / back-arc edifice immediately before tectonic accretion to Baltica.

*References:*

[1] Stephens, M (2020) Mem Geol Soc London 50: 549-575
[2] Carter I et al. (2023) J Geol Soc London 178: jgs2022-130
[3] Saalman K et al. (2021) J Geol Soc London 178: jgs2020-214

# Constraints on Iceland mantle sources from $\mu^{182}W$, Sr-Pb isotopes and trace elements

Kallnik, N.[0,1], Armstrong, C.[1], Pakulla, J.[1], Halldórsson, S.A.[2], Fischer-Gödde, M.[1], Hasenstab-Dübeler, E.[1], Münker, C.[1]

Corresponding author: niklas.kallnik@gmail.com

[1]Universität zu Köln, Institut für Geologie und Mineralogie, Zülpicher Str. 49, 50674 Köln, Germany
[2]Institute of Earth Sciences, University of Iceland, Sturlugata 7, 102 Reykjavík, Iceland

---

Ocean island basalts (OIB) provide important insights into the composition of Earth's interior, its structure, and dynamics as some of them sample deep-seated mantle material via mantle plumes. Recent discoveries of $\mu^{182}W$ deficits in modern ocean island basalts have spurred discussion about the possible existence of primordial reservoirs in Earth's mantle that differentiated during the first ~60 Ma of solar system history ($^{182}Hf \rightarrow {}^{182}W$, $T_{1/2}$ = 8.9 Ma [1]). Reservoirs that preserve $\mu^{182}W$ deficits may have formed by excessive incorporation of late accreted material [2], by core-mantle interaction [3], or recycling of Hadean proto-crust [4]. Even though, several OIB suites have been investigated in that regard, combined data of $\mu^{182}W$ and long-lived radiogenic isotopes remain scarce.

This study focuses on combined Sr-Pb-$\mu^{182}W$ compositions of neovolcanic to ~4 Ma old volcanic rocks from Southern Iceland, which is influenced by active-ridge and plume-related volcanism. In total, 19 mantle-derived tholeiitic basalts of varying MgO contents (2.55-10.19 wt.%), supplemented by two andesites, and one rhyolite were analysed for trace and high field strength elements (HFSE) using quadrupole-inductively coupled plasma-mass spectrometry (Q-ICP-MS) and for Sr and Pb isotopes by multi collector-ICP-MS. Preliminary results indicate the existence of at least two different mantle sources for the parental magmas of the analysed samples. More unradiogenic Sr and Pb isotope ratios in combination with canonical HFSE ratios such as Nb/Th as high as 27 suggest depleted upper mantle material as one of the sources. The second mantle source is characterized by more radiogenic Sr and Pb isotope compositions and Nb/Th ratios of ~10 akin to a more primitive, undegassed high $^{3}He/^{4}He$ mantle source as described by Jackson and Jellinek [5]. The latter group falls within the previously determined high-Pb endmember characterized by $\mu^{182}W$ values between 0 and -15 [3], while the high Nb/Th group shows compositions transitional between the high-Pb and low-Pb endmembers. Following measurements for W isotopes will be used to investigate whether these two subgroups display distinct $\mu^{182}W$ values. These data, in combination with long-lived isotope systems, can reveal potential compositional heterogeneities of the Iceland plume and its sources.

*References:*

[1] Vockenhuber C et al. (2004) Phys Rev Lett 93: 172501

[2] Marchi et al. (2017) Nature Geoscience 11: 77-81

[3] Mundl-Petermeier et al. (2019) Chemical Geology 525: 245-259

[4] Tusch et al. (2022) PNAS 119

[5] Jackson and Jellinek (2013) Geochem Geophys Geosyst 14: 2954–2976

## Significance of W isotope anomalies in early Earth rocks

Münker, C.[1], Fischer-Gödde, M.[1] , Tusch, J.[1] and Hoffmann, J.E.[2]

[1]University of Cologne, Germany, c.muenker@uni-koeln.de.

[2]Freie Universität Berlin, Germany

---

Most Archean rocks on Earth exhibit $^{182}W$ anomalies, which are mainly excesses and only in a few cases deficits. Two endmember models can explain these isotope anomalies: (1) variable contributions of late veneer components to the local ambient mantle sources and (2) relict signatures of early silicate differentiation, possibly formed during the magma ocean stage. We evaluate these endmember models using a combination of high precision $^{182}W$, $^{142}Nd$ and $^{100}Ru$ data measure for the same sample suites, comprising data from the Pilbara, Kaapvaal, and North Atlantic Craton. In their combination, the three approaches can unambiguously discriminate between the two endmember models. While $^{182}W$ patterns in the Pilbara Craton can entirely be explained by a missing late veneer model, such an approach fails to fully account for combined $^{182}W$, $^{142}Nd$ and $^{100}Ru$ patterns in the other two cratons. Rather, combined $^{182}W$, $^{142}Nd$ and $^{100}Ru$ patterns in rocks from the Isua region of the North Atlantic Craton require a combination of both processes. Isotope signatures in rocks from the Kaapvaal craton, on the other side, can entirely be explained by early silicate differentiation, as they present correlations between short- and long-lived radiogenic isotope signatures. Among possible candidates for these signatures of early silicate differentiation, recycled mafic-ultramafic restites from differentiated Hadean proto-crust are a viable endmember that can not only explain compositions of Kaapvaal Craton rocks, but also the endmember carrying the largest $^{182}W$ deficits in modern ocean island basalts.

The combined data from different Archean cratons have also far reaching implications for understanding the early history of the Earth-Moon system. The observation that missing late veneer can only partially account for $^{182}W$ patterns in Archean rocks requiries that early silicate differentiation on Earth must have commenced within the lifetime of $^{182}Hf$, placing these events within the first 70 Myrs of solar system history. Considering refined models for the late veneer that largely comprised CI/CM chondrite-like material, only ca. 50% of the ca. +25 ppm $^{182}W$ excess in the silicate Moon can be explained by missing late veneer. In accord with the lower W/Th of the lunar mantle, lunar core formation must therefore have fractionated Hf/W on the Moon. Hence, core formation therefore provides the most plausible explanation for the other half of the lunar $^{182}W$ excess and, by consequence, the Moon must have also formed during the lifetime of $^{182}Hf$, within the first 70 Myrs of the solar system.

# Mechanisms of pyrite formation in marine sediments and implications for isotope fractionation in the presence of trace elements

Rabone, J.[1], Blanchard, M.[1], Aufort, J.[2] and Le Pape, P.[2]

[1] Géosciences et Environnement Toulouse, CNRS, Université Toulouse 3, France, jeremy.rabone@get.omp.eu

[2] IMPMC, CNRS, Sorbonne Université, France

---

The elemental and isotopic compositions of sedimentary pyrites provide insights into the chemical evolution and redox state of the oceans over geological timescales. In particular, iron isotope ratios are proxies for the progressive increase in atmospheric oxygen during the Archean and Paleoproterozoic [1]. However, the interpretation of the isotopic signatures is subject to large uncertainties arising from the limited understanding of the mechanisms and kinetics of pyrite formation. Notably, the presence of other trace elements has been shown to modify significantly the nucleation and growth of pyrite, and presumably its precursors.

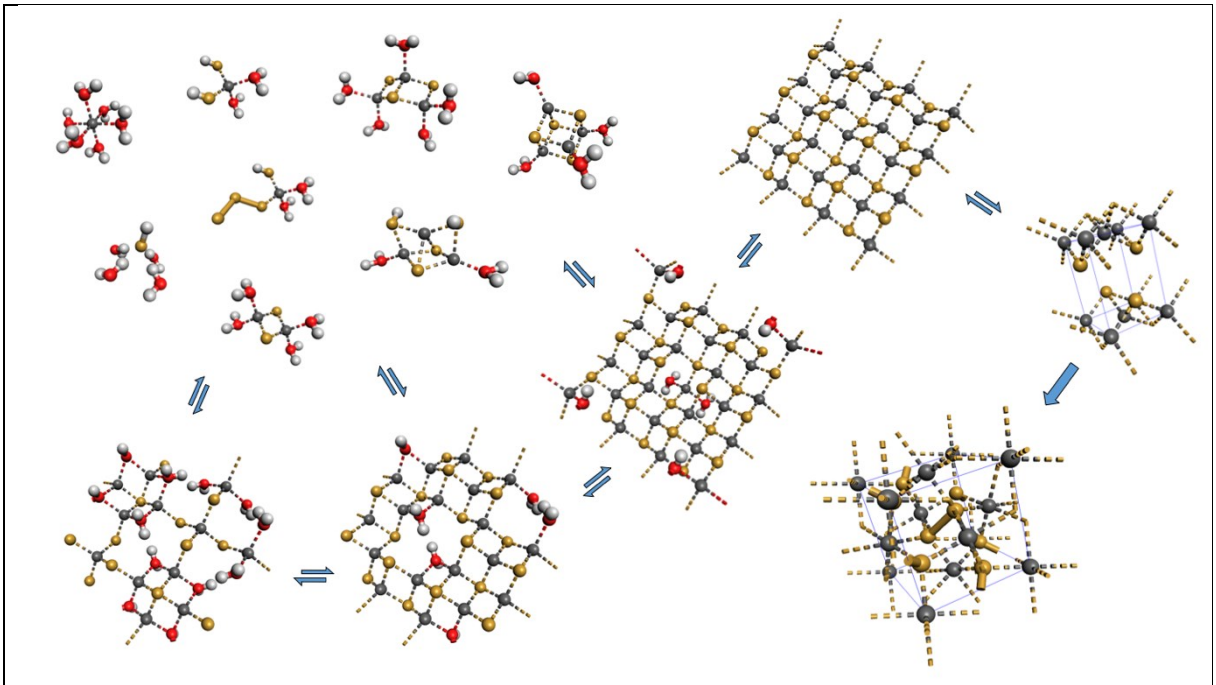

Schematic of pyrite formation via mackinawite by precipitation of aqueous iron-sulphur clusters.

The objective of this work, conducted in tandem with experimental approaches, is to identify the likely mechanisms involved in the growth of sedimentary pyrite and how these are affected by the presence of trace elements, such as nickel and arsenic. To this end, density functional calculations and molecular dynamics will be applied to build an understanding of how sedimentary pyrite is formed. A comprehensive study of the solid iron sulphide phases that might be implicated in these mechanisms, such as mackinawite and greigite as well as amorphous and partially deconstructed structures will tackle the problem from one perspective. A detailed study of iron-sulphide clusters in aqueous solution will identify the likely contributions of these species to the eventual pyrite. The distribution of iron isotopes between the various phases can be determined from fractionation factors based on the contribution to the free energies of the thermodynamic partition functions calculated using linear-response density functional calculations and molecular dynamics.

*References:*

[1] Rouxel O J, Bekker A, Edwards K J (2005) Science 307:1088-1091

# Geochemistry of the pre-Variscan Pedrógão Grande S-type granitic pluton, central Portugal

Andrade, L.[1], Carvalho, P. C. S.[1] and Santos, J. F.[1]

[1]GeoBioTec—GeoBioSciences, GeoTechnologies and GeoEngineering, Department of Geosciences, University of Aveiro, 3810-193 Aveiro, Portugal; paulacscarvalho@ua.pt

---

The Pedrógão Grande granitic pluton is located about 50 km south of Coimbra in central Portugal, outcrops in the Central Iberial Zone of the Iberian Massif and intrudes the Neoproterozoic/Cambrian Schist-Metagraywacke Complex. Seven samples were collected from the different facies of the pluton. Major and trace elements, including REE, were determined by ICP-AES and ICP-MS after a lithium metaborate/ tetraborate fusion at Actlabs, Canada. The Rb-Sr data were obtained by Thermal Ionization Mass Spectrometry at the University of Aveiro, Portugal.

The pluton presents various granitic facies, medium to coarse-grained texture is dominant, with local occurrences of porphyritic texture, but also of fine to medium-grained texture. In terms of mineral habit, texture is usually hypidiomorphic to xenomorphic. Modal compositions are characterized by quartz, plagioclase, K-feldspar, muscovite, scarce biotite (often chloritized), apatite, zircon, rutile and tourmaline.

The granitoid rock is a peraluminous (with A/CNK ranging from 1.26 to 1.63), silica-rich ($SiO_2$ > 71 %) and ferroan leucogranite, with calc-alkali to alkali-calcic signature. The granitoid is classified as a syn-collisional and S-type granite. ∑REE varies from 11.3 to 43.6 ppm and the REE patterns, normalized to the primitive mantle, show strong negative Eu anomalies (Eu/Eu* from 0.06 to 0.26) and weak LREE/HREE fractionation ($La_N/Lu_N$ between 2.95 and 5.23.

The Rb-Sr isotopic data was determined in five samples whole-rock samples from different facies. $^{87}Sr/^{86}Sr$ vs $^{87}Rb/^{86}Sr$ correlation gives an “isochron” corresponding to 542 ± 59 Ma, with $(^{87}Sr/^{86}Sr)_i$ ratios of 0.719 ± 0.032. The high value of MSWD (30) may cast doubts on the geochronological significance of the obtained “isochron”. However, results presented by other authors [1] [2] [3], based on both Rb-Sr and K-Ar methods, varied between 520 and 580 Ma. Therefore, the result obtained in this study is within the range of the set of data previously reported. Several other plutons located in the CIZ close to the Ossa Morena Zone were considered ante-Ordovician [4] [5] [6].

The Pedrogão Grande pluton is a highly fractionated granite, as evidenced by the low Eu/Eu* values, that require extensive fractionation of plagioclase, K-feldspar, or both and low ∑REE. The pluton may have been formed by fractional crystallization of a melt generated by anatexis of a metasedimentary source with a strong pelitic component during continental collision events. Considering the whole set of data, the Pedrógão Grande pluton is constituted of a peraluminous granite, with a crustal origin, that may be related to the Cadomian Orogeny.

*References:*

[1] Sherperd T and Oliveira J (1990) Joint Project Between BGS (UK) & DGGM (Portugal) – Final Report, 2 vols., 251 pp.

[2] Silva A, Romão J, Ribeiro A and Silva J (1996) Comunicações do Instituto Geológico e Mineiro, t. 82, 3-14.

[3] Pereira L and Macedo C (1983) Comun Serv Geolo Portugal, 69: 256-266.

[4] Pereira L (1987) Unpublished PhD Thesis, Univ. Coimbra, 331 pp.

[5] Reis A, Silva M and Antunes I (2010) Estudios Geológicos. 66 (1): 51-56. doi:10.3989/egeol.40142.096

[6] Gomes E Antunes I (2011) Abstract volume- VIII Congresso Ibérico de Geoquímica / XVII Semana de Geoquímica.

# Missing late veneer constrained by short-lived isotopes in the earliest rock record of South America

Leitzke, F.P.[1,2,3], Pakulla, J.J.[1], Tusch, J.[1], Ravindran, A.[1], Barbosa, R.G.[2], Zincone, S.A.[4], Hellers, M.[1], Martins, A.A.[3], Spreafico, R.R.[5], Yang, R.[1], Wombacher, F.[1], Barbosa, J.S.F.[6], Münker, C.[1]

[1] Institut für Geologie und Mineralogie, Universität zu Köln, 50674 Köln, Germany, felipe.leitzke@gmail.com

[2] Departamento de Engenharia Geológica, Universidade Federal de Pelotas, 96010-540, Pelotas, Brazil

[3] Laboratório de Geologia Isotópica, Universidade Federal do Rio Grande do Sul, 90650-001, Porto Alegre, Brazil

[4] Depto. de Geologia, Escola de Minas, Universidade Federal de Ouro Preto, 35400-000, Ouro Preto, Brazil

[5] Companhia Baiana de Pesquisa Mineral (CBPM), Salvador, 41745-002, Brazil

[6] Instituto de Geociências, Universidade Federal da Bahia, 40170-290, Salvador, Brazil

---

The chemical evolution of the early Earth is still a matter of debate. Oldest Archean rocks on Earth are present in greenstone belts and in the tonalite-trondhjemite-granodiorite (TTG) associations that form most cratons. Negative $\mu^{142}$Nd compositions were identified recently in Archean inliers of the Borborema Province at the border of the SFC [1] indicating the possible presence of a Hadean/Archean enriched component, However, that is in contrast to previously reported non-anomalous $\mu^{142}$Nd values of Archean rocks that are within the SFC boundary [2]. In that sense, we applied short-lived radiogenic isotopes ($^{142}$Nd and $^{182}$W) in combination with long-lived $^{143}$Nd and $^{176}$Hf isotope systems from a set of Eo- to Paleoarchean amphibolites, TTG gneisses, granites and a gabbroic rock from the northern segment of the São Francisco Craton (SFC) in eastern Brazil. This is still an understudied area regarding high-precision short-lived isotope systematics and our data covers rocks with ages that range from 3.3 to 3.65 Ga, providing further insight into Hadean/Archean geodynamic processes. In this study, we found positive $\mu^{182}$W values and $\mu^{142}$Nd similar to modern upper mantle, which coupled to long-lived data, suggest that the rock source was formed after the virtual extinction of $^{146}$Sm. Interpretation of the possible causes for the discovered anomalies range from a prolonged and heterogeneous depletion via metal segregation in the Hadean, disproportional later addition of meteoritic material to the Earth and/or early silicate differentiation and inefficient mixing on a yet not fully convective Earth. However, the combination of $\mu^{182}$W and $\mu^{142}$Nd in the same geological unit can be used to constrain a missing late veneer component in the source of the SFC Archean rocks, indicating the presence of a long-lasting Hadean component as already observed for other cratons worldwide.

*References:*

[1] Garcia, V.B. et al. (2023) GPL, 28:1-6

[2] Wainright, A. et al. (2018) Goldschmidt Abstracts

# Sulfur concentration and isotope composition in the (ultra)mafic rocks of the Central Sudetic Ophiolite, Poland

Woźniak W.[1], Elsheriff E.[1], Ciążela J.[1], Strauß H.[2]

[1]Institute of Geological Sciences, Polish Academy of Sciences

[2]Institut für Geologie und Paläontologie - Historische und Regionale Geologie, Westfälische Wilhelms-Universität Münster

---

Central Sudetic Ophiolite in southwestern Poland gives a unique insight into the geotectonic setting of the variscian orogenesis. Its constituents — Ślęża, Nowa Ruda, and Braszowice–Brzeźnica Massifs, all allow for access into a significant part of the ophiolitic sequence. One hundred forty-four rock samples were collected from those massifs, representing all (ultra)mafic lithologies, and studied for metal distribution (see Esherif et al. 2024, this issue). Here, we provide more detailed information on the sulfur concentrations and isotopes to understand the fundamental processes controlling the metal migration.

Sulfur content and $\delta^{34}S$ measurements were conducted at the Institute of Geology and Palaeontology of the University of Münster. We used CS ELTRA 580 with the combustion chamber and the IR detector to determine sulfur contents. Samples with >40 ppm S (n = 78) were deemed suitable for isotopic measurements. Those samples underwent the sulfur extraction process described by Canfield [1] and Rice [2]. ThermoFinnigan Delta Plus mass spectrometer was used for isotopic measurements.

Sulfide Sulfur(SS)/Total Sulfur(TS) ratio of ~0.8, suggesting that 80% of sulfur is hosted in sulfides and the rest in sulfates. TS values ranged from 5 to 5000 ppm, SS from 44 ppm to 3700 ppm, and $\delta^{34}S$ from −5,4‰ and +5,2‰, partially consistent with previous, less precise, local measurements (3000 ppm to 15000 ppm of Total Sulfur and $\delta^{34}S$ values between −1.8 ‰ and +6 ‰ [3]). In gabbro and basalts, samples with higher S contents typically show higher $\delta^{34}S$, implying a sulfur influx into those rocks in hydrothermal processes. However, diabase samples display lower $\delta^{34}S$ values (−5‰ to +2 ‰) than basalt (−2‰ to +5‰) or even gabbro (-5‰ to 4‰) but have higher average SS values (1119 ppm), compared to basalt (651 ppm) and gabbro (708 ppm).

Basalt and gabbro show lower sulfur contents, and all the rocks, including diabase, lowered isotopic signatures compared to other ophiolites [4][5], which may suggest sulfur depletion processes affected examined rocks' isotopic, chemical, and mineral composition. The high-temperature hydrothermal activity could have been followed by low-temperature leeching, potentially explaining the low sulfur content and $\delta^{34}S$ values found in the examined samples[6]. Additionally, microbial processes are suspected to have influenced the isotopic and chemical composition of some samples with very low $\delta^{34}S$ (–2‰) [7].

**References**:

**[1]**Canfield et al., 1986. The use of chromium reduction in the analysis of reduced inorganic sulfur in sediments and shales

**[2]**Rice et al., 1993. The analysis of forms of sulfur in ancient sediments and sedimentary rocks: comments and cautions. Chemical Geology 107, 83–95.

**[3]**Weber-Weller et Jędrysek, 1998, Sulphur isotope budget in the mafic member of the Ślęża ophiolite complex.

**[4]** Oeser et al., 2012. A profile of multiple sulfur isotopes through the Oman ophiolite

**[5]** Pedersen et al., 2017. A multiple sulfur isotope study through the volcanic section of the Troodos ophiolite

**[6]**Alt et al., 2007. Hydrothermal alteration and microbial sulfate reduction in peridotite and gabbro exposed by detachment faulting at the Mid-Atlantic Ridge, 15°20'N (ODP Leg 209): A sulfur and oxygen isotope study

[7]Rouxel et al. 2008 Sulfur isotope evidence for microbial sulfate reduction in alteredoceanic basalts at ODP Site 801